20 YEARS ARCHIVING AT IIS, AND ITS MAXIMUM UTILIZE OF ENVIRONMENT AND DISASTER MONITORING FROM SPACE

Takeuchi, W., Nemoto, T., Baruah, P. J., and Yasuoka, Y.

Institute of Industrial Science
University of Tokyo, Japan

wataru@iis.u-tokyo.ac.jp

ACRoRS
Asian Center for Research on Remote Sensing

11th CEReS Int. Sym. Remote Sens.
Dec. 13-14, 2005 @ Chiba-U, Japan

東京大学
THE UNIVERSITY OF TOKYO

ADEOS-II GLI Asia mosaic

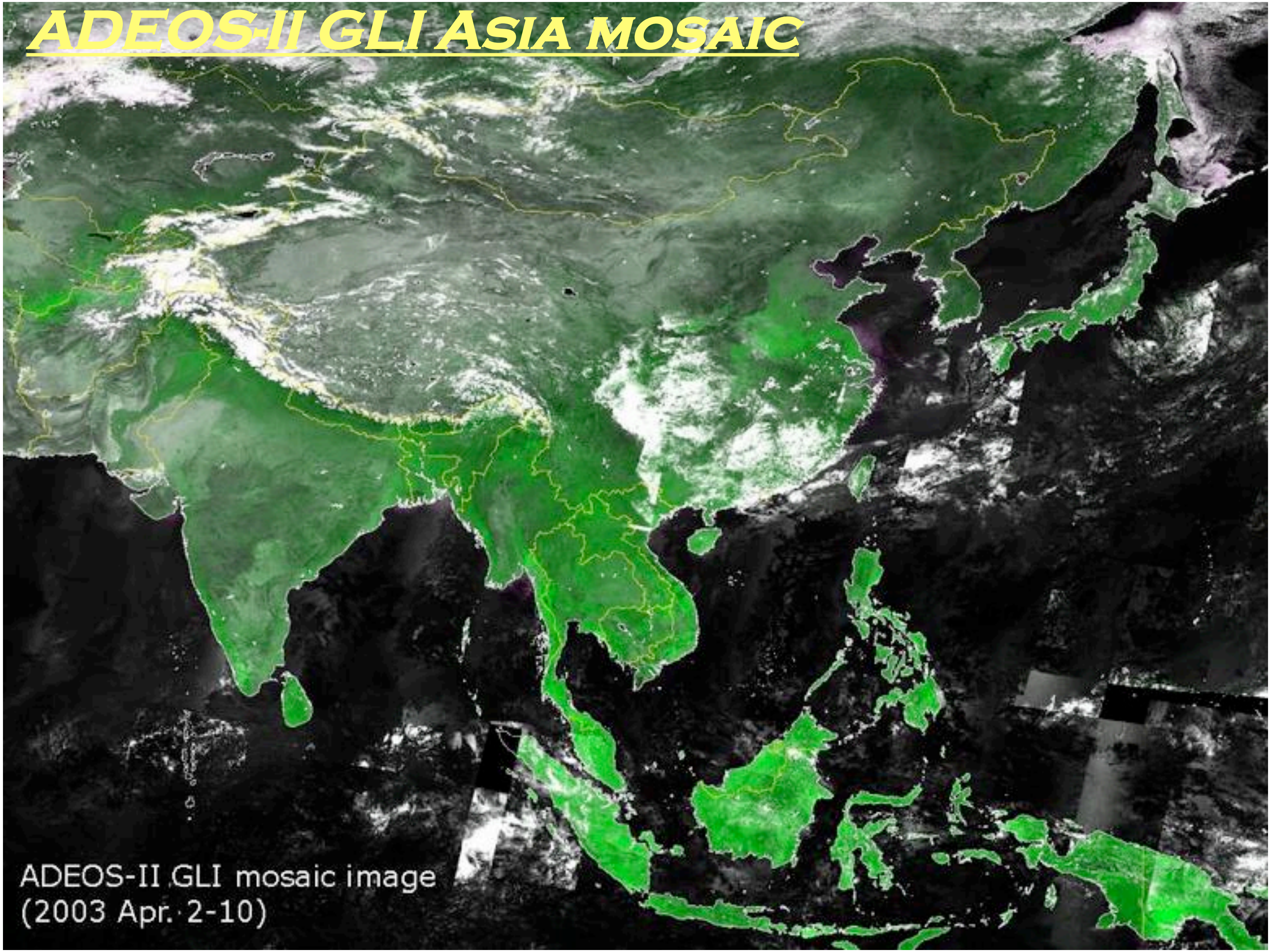

To meet the needs of users

- IIS and AIT have been receiving NOAA **AVHRR** and Aqua/Terra **MODIS** data at the direct receiving station.
- AVHRR since 1983
- MODIS since 2001
- Over 20 years of record is archived in data storage system.
- Network based (WWW or FTP) data distribution is in process.

Contribute to data utility promotion (especially for Asian countries)!!

MODIS antenna in Tokyo

MODIS antenna in Bangkok

Spatial coverage of MODIS and AVHRR

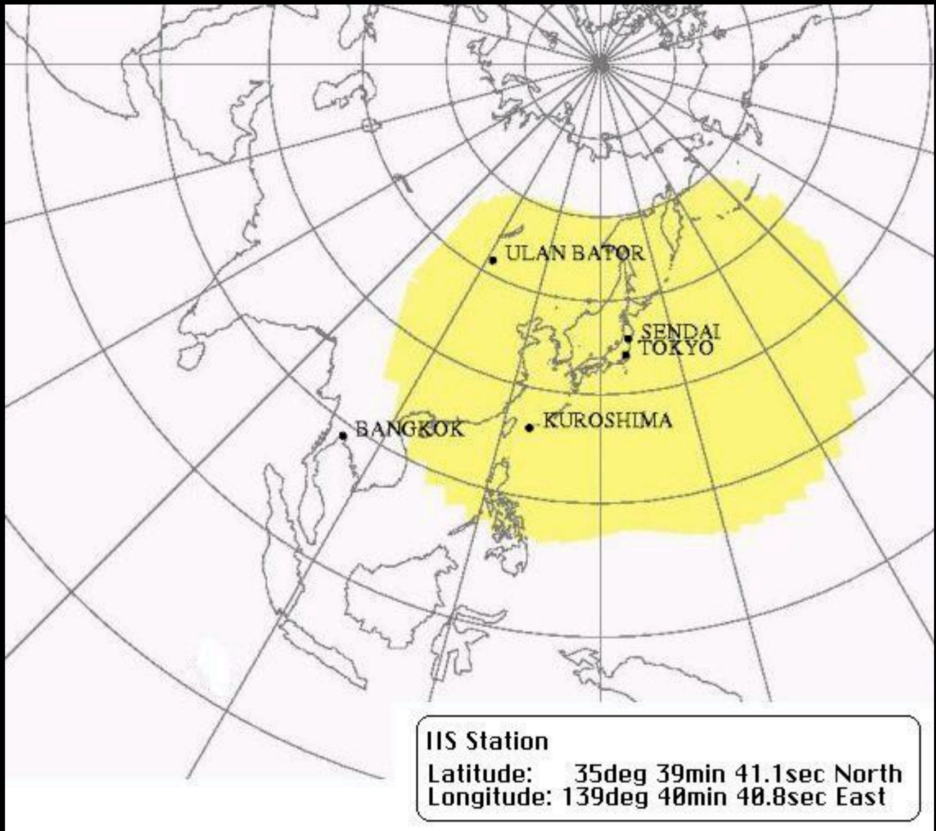

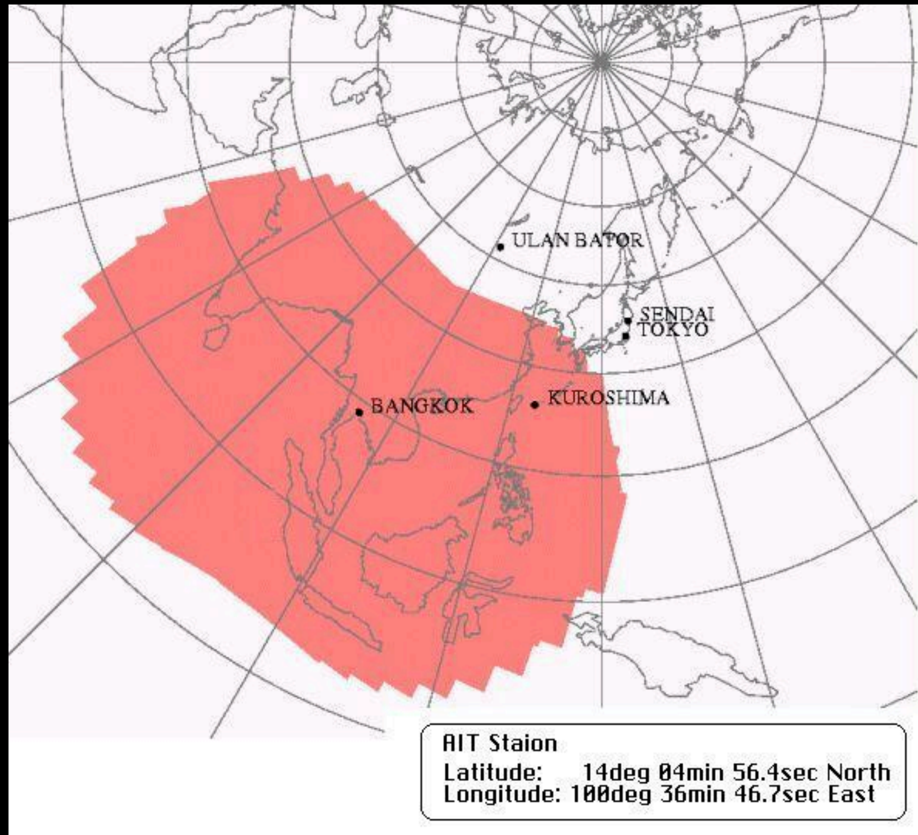

IIS, Tokyo
Since Oct. 1983

AIT, Bangkok
Since No.v 1997

Data transfer from Thai to Japan

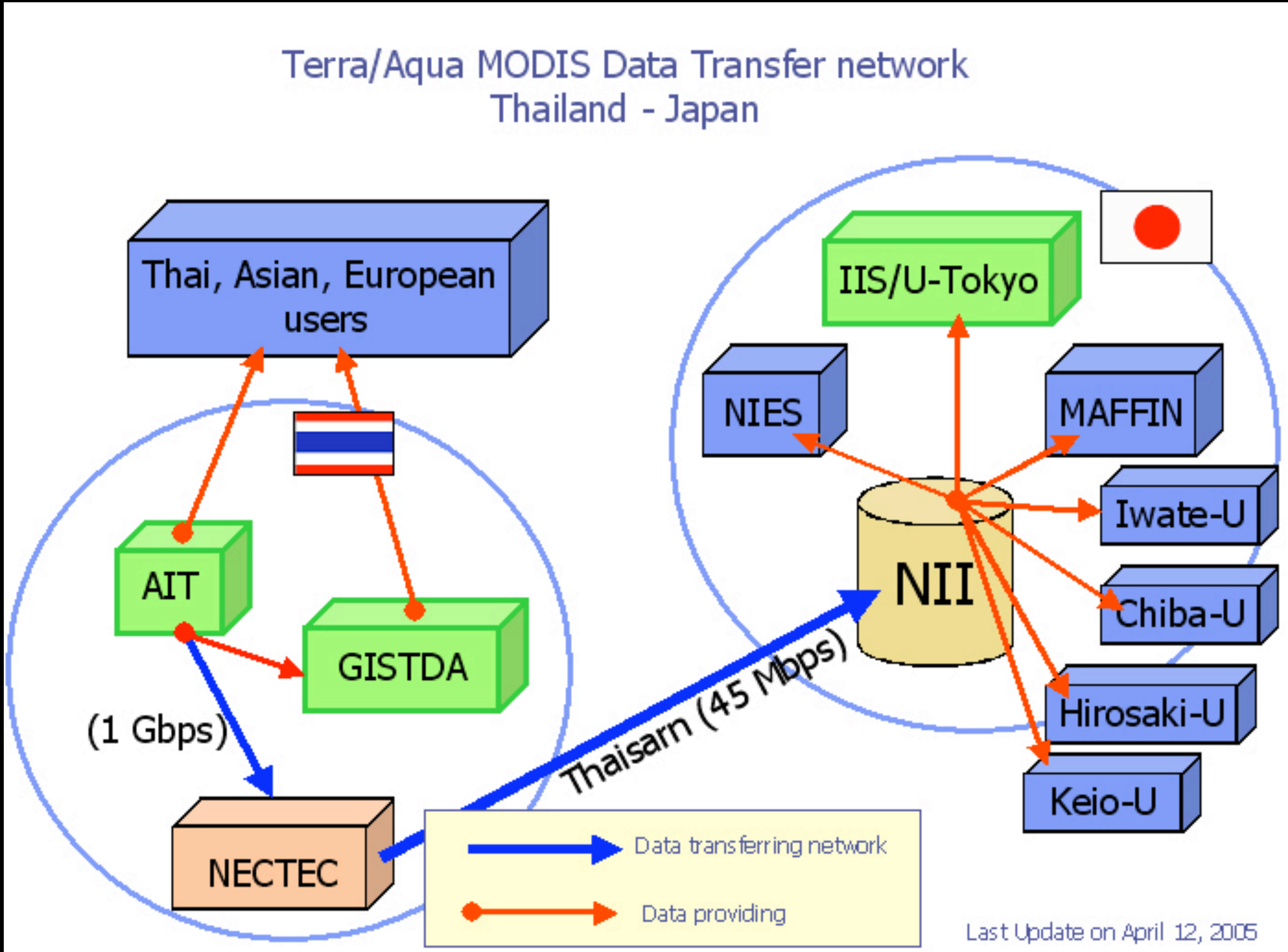

From data receiving to data distribution

1. Data receiving
   - NOAA AVHRR
   - Aqua/Terra MODIS
   - Dundee/England system
2. Data processing
   - Radiometric / geometric correction, Quick look image, cloud-free compositing
3. Data archive
   - Huge data storage system on tape archiving (-600TB)
4. Data distribution
   - Network-based (FTP and WWW) download

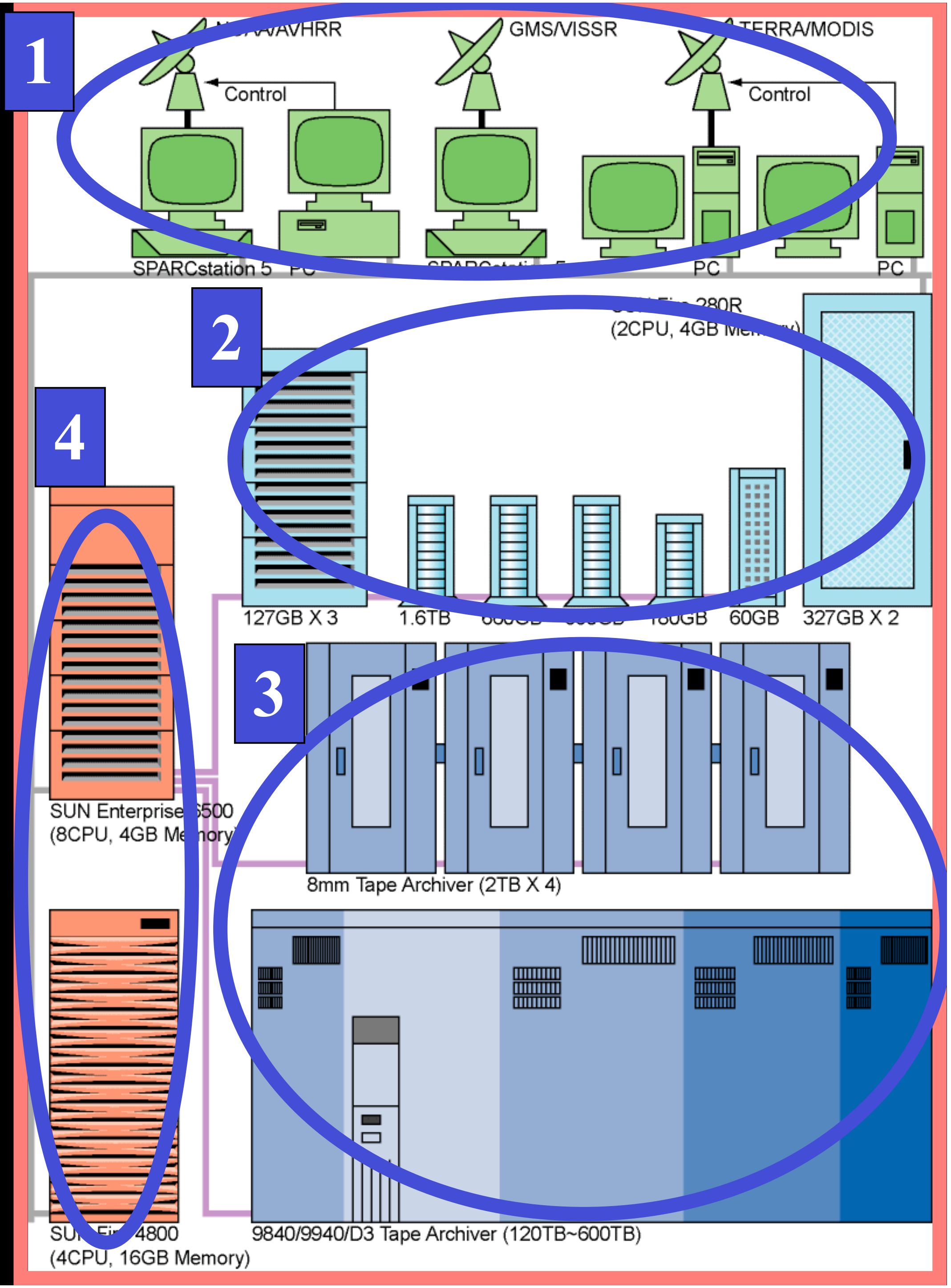

COMPUTER FACILITIES AT IIS

Air-conditioned server room

Antenna control machines

Linux (6)
Xserve (6)
RAID (20TB)
Solaris (1)

MODIS and AVHRR data processing, archiving and distributing

ONLINE DATA DISTRIBUTION SERVICE

WebMODIS (Aqua/Terra MODIS)

1  Online subsetting scene by scene

2 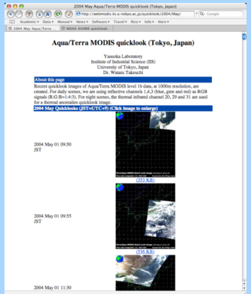 Rapid response by quicklook

3 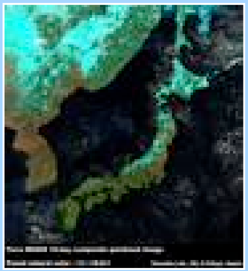 10 day cloud-free composite

WebPaNDA (NOAA AVHRR)

1  Online subsetting scene by scene

2 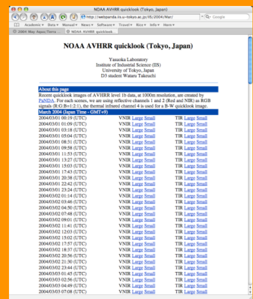 Rapid response by quicklook

3 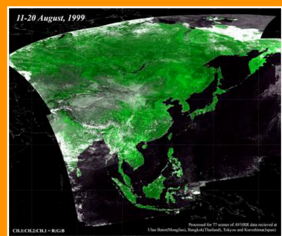

10 day cloud-free composite

MODIS processing system on WWW

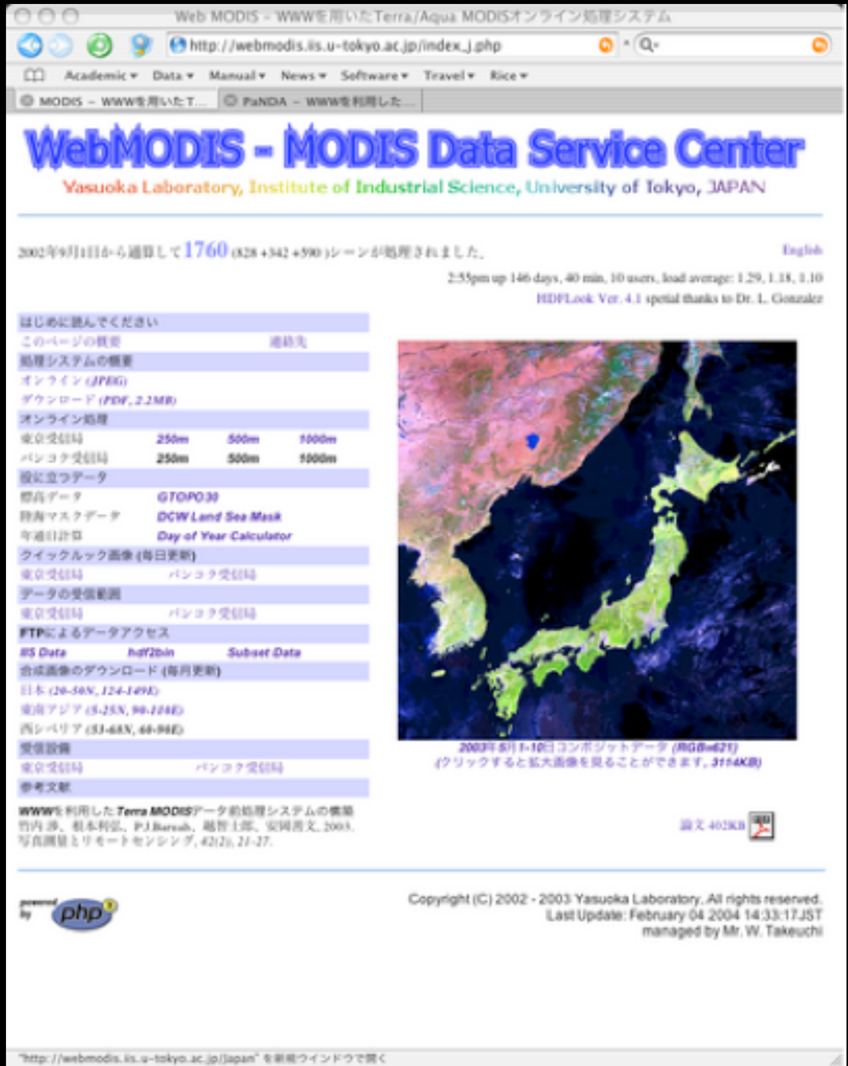

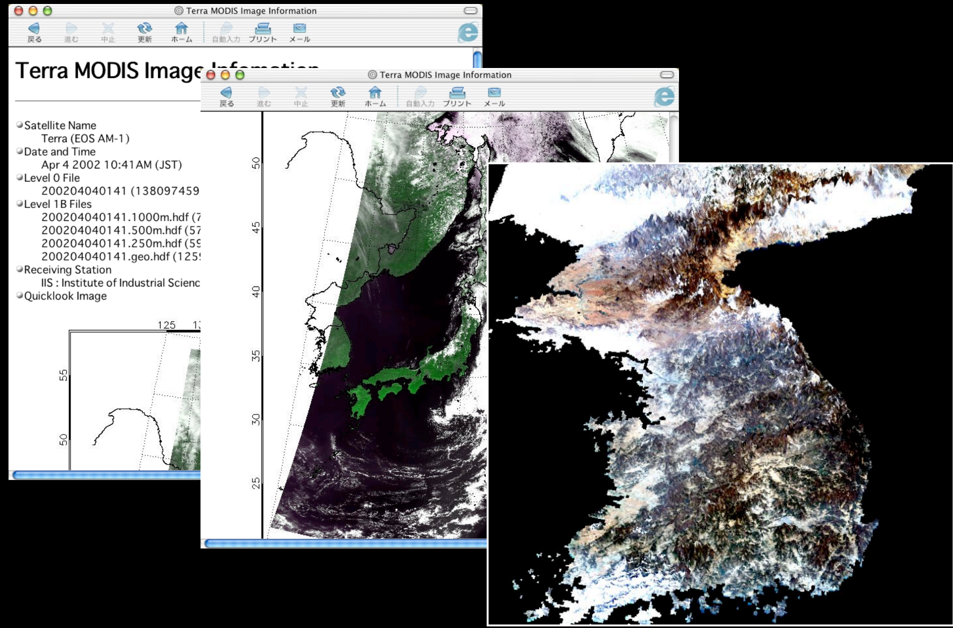

- Data search with mouth click
- Radio. / geo. Correc., spatial subset
- FTP download instruction via e-mail

4,000 scenes have been delivered in 3 yrs

WebMODIS website

http://webmodis.iis.u-tokyo.ac.jp/

AVHRR processing system on WWW

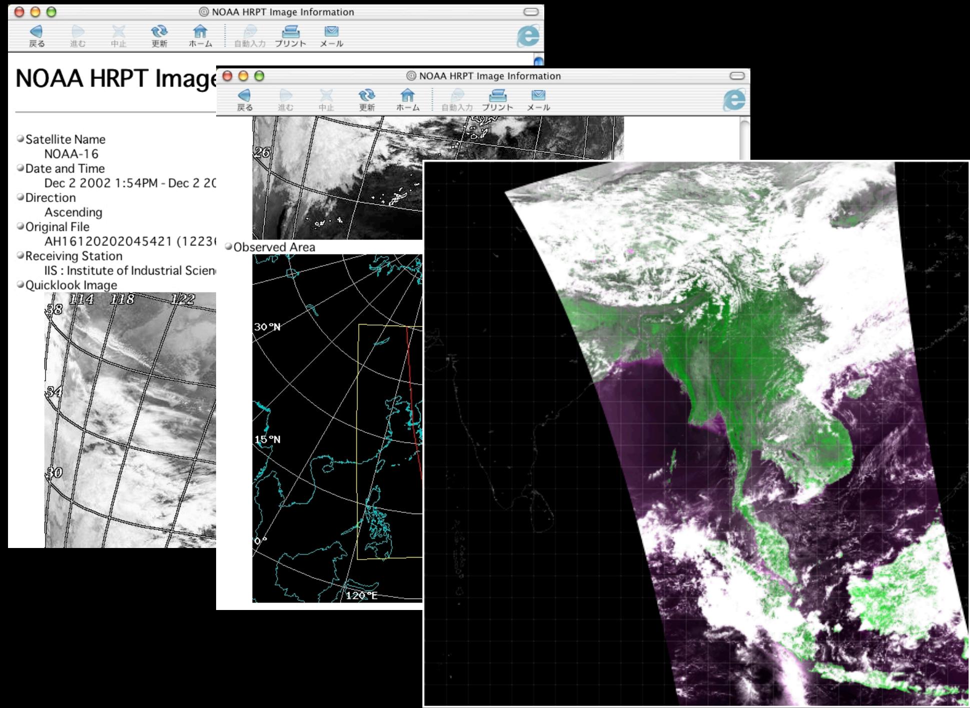

- Data search with mouth click
- Radio. / geo. Correc., spatial subset
- FTP download instruction via e-mail

16,500 scenes have been delivered in 3 yrs

WebPaNDA website

http://webpanda.iis.u-tokyo.ac.jp/

HARDWARE SYSTEM STRUCTURE

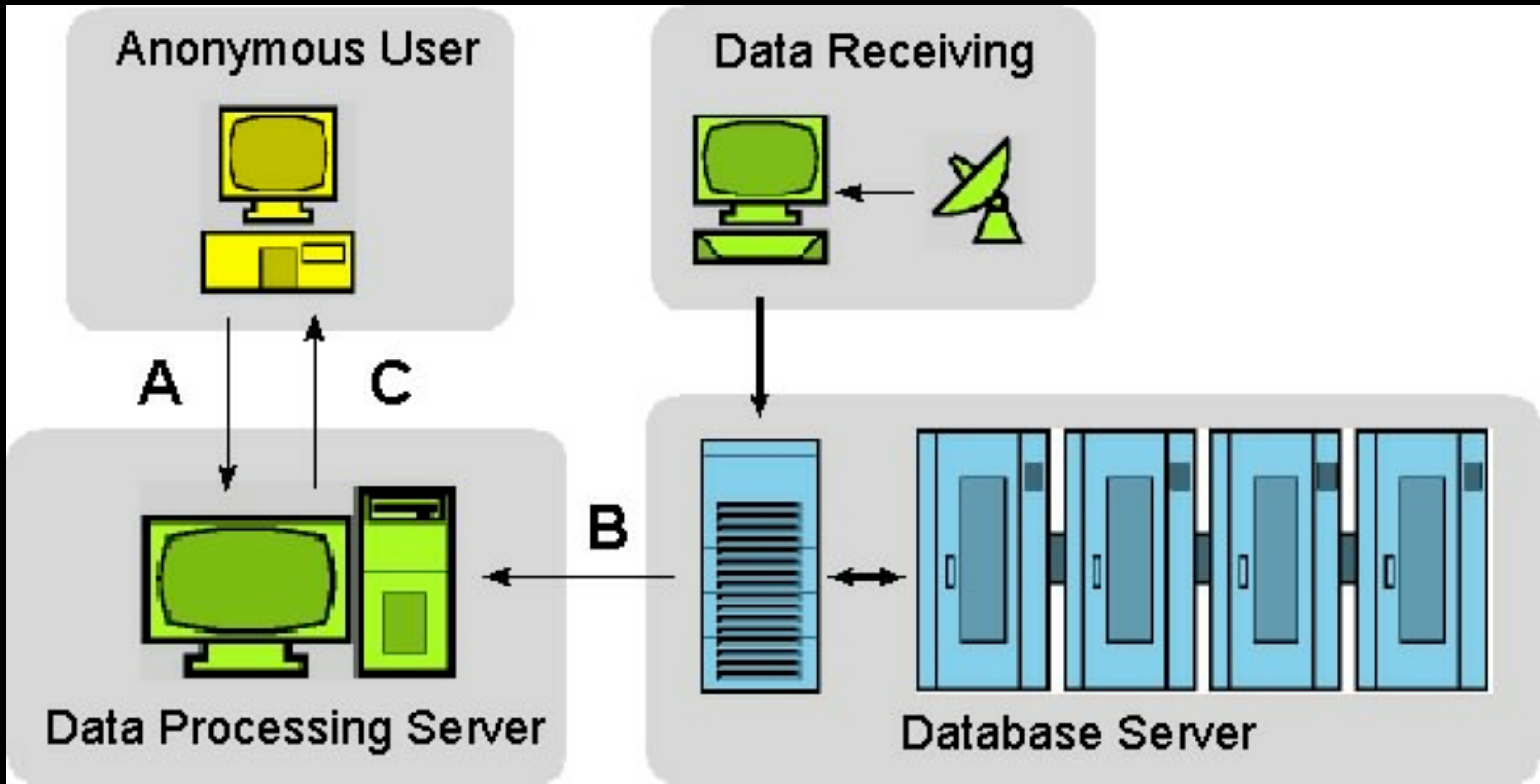

A) Input mapping parameters by anonymous users
B) Pre-processing of MODIS data
C) Deliver data via the FTP

NOTIFICATION VIA E-MAIL

From: webmaster@webmodis.iis.u-tokyo.ac.jp
Subject: **Your order is available**
Date: 2005年9月30日 17:26:41:JST
To: undisclosed-recipients:;

***** MODIS Processing System on WWW (Tokyo) *****

Your order 200202010120.1000m.hdf, submitted on 2005 Sep 30 17:22 (JST=UTC+9) is available for you to ftp copy.
You can pick up your data set via ftp://webmodis.iis.u-tokyo.ac.jp/IIS/1KM/20050930172211/

File Description:
200202010120_1KM.met
200202010120_1KM_QuickLook.jpg
200202010120_QKM_Aggr1KM_RefSB.hdf
200202010120_HKM_Aggr1KM_RefSB.hdf
200202010120_1KM_RefSB.hdf
200202010120_1KM_Emissive.hdf
200202010120_SensorAzimuth.hdf
200202010120_SensorZenith.hdf
200202010120_SolarAzimuth.hdf
200202010120_SolarZenith.hdf

NOTE: You must pick up your data within 72 hours of this notice.

*****

Thank you very much!
WebMODIS Developer: Dr. Wataru Takeuchi
E-mail: wataru@iis.u-tokyo.ac.jp

Users are notified how to download MODIS product from FTP via e-mail

Download MODIS product via FTP

```
lftp webmodis.iis.u-tokyo.ac.jp:/IIS/1KM/20050930172211> ls
-rw-r--r--   1 501      501          1107 Sep 30 08:22 200202010120_1KM.met
-rw-rw-r--   1 501      501     294996936 Sep 30 08:25 200202010120_1KM_Emissive.hdf
-rw-rw-r--   1 501      501       2533078 Sep 30 08:26 200202010120_1KM_QuickLook.jpg
-rw-rw-r--   1 501      501     276565630 Sep 30 08:23 200202010120_1KM_RefSB.hdf
-rw-rw-r--   1 501      501      92245381 Sep 30 08:23 200202010120_HKM_Aggr1KM_RefSB.hdf
-rw-rw-r--   1 501      501      36949303 Sep 30 08:22 200202010120_QKM_Aggr1KM_RefSB.hdf
-rw-rw-r--   1 501      501      18516459 Sep 30 08:25 200202010120_SensorAzimuth.hdf
-rw-rw-r--   1 501      501      18516457 Sep 30 08:25 200202010120_SensorZenith.hdf
-rw-rw-r--   1 501      501      18516457 Sep 30 08:25 200202010120_SolarAzimuth.hdf
-rw-rw-r--   1 501      501      18516455 Sep 30 08:25 200202010120_SolarZenith.hdf
lftp webmodis.iis.u-tokyo.ac.jp:/IIS/1KM/20050930172211>
```

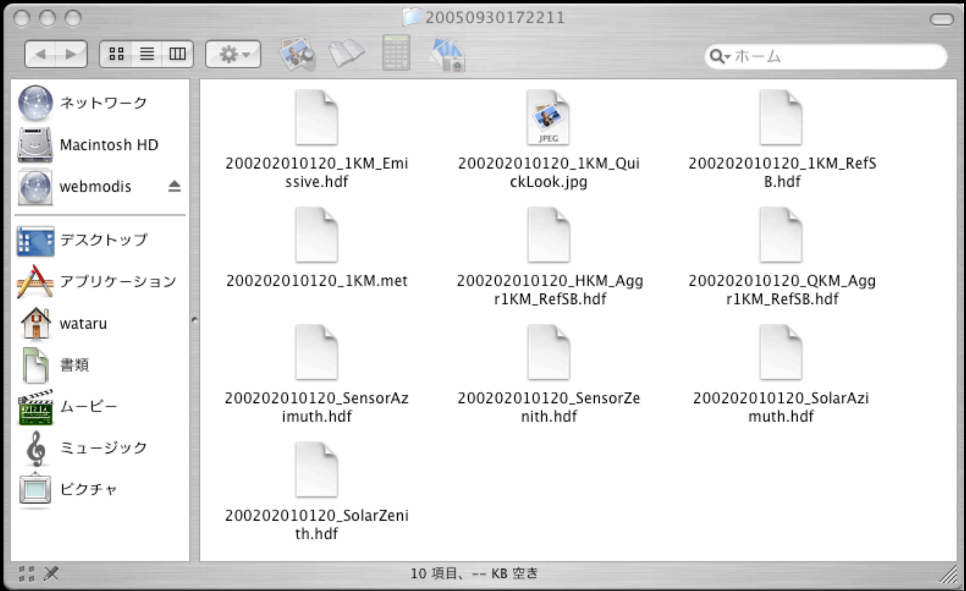

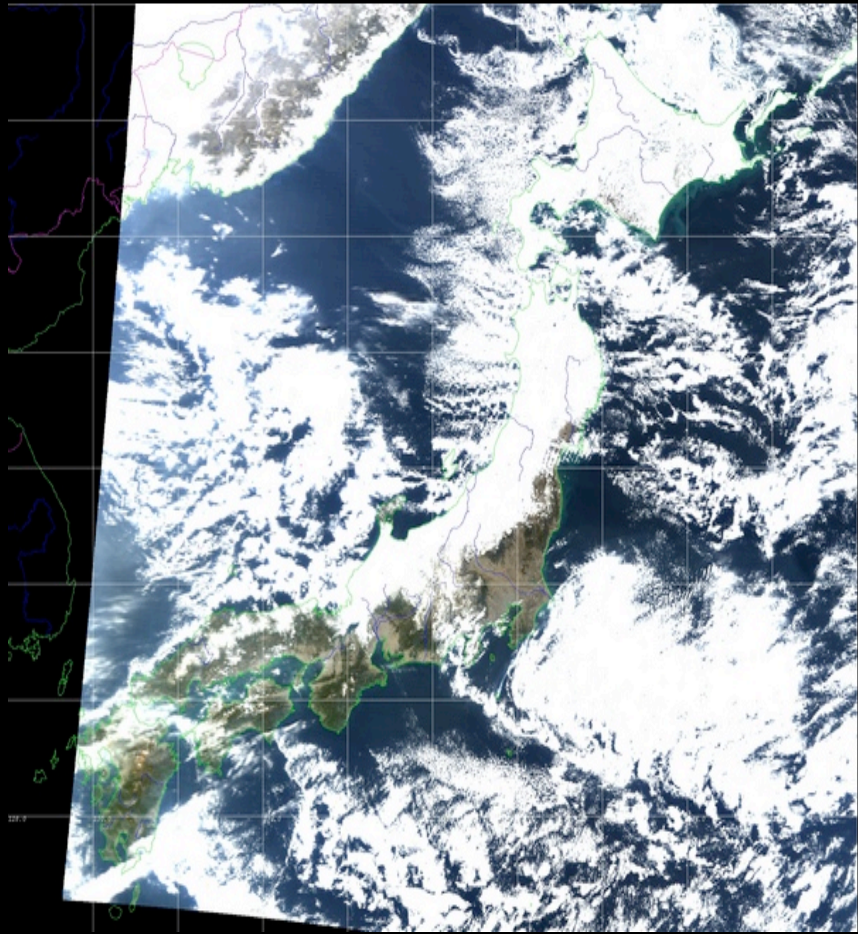

Geo-coded MODIS image
(200302010120 Terra)

ONLINE DATA DISTRIBUTION SERVICE

WebMODIS (Aqua/Terra MODIS)

1 

Online subsetting scene by scene

2 

Rapid response by quicklook

3 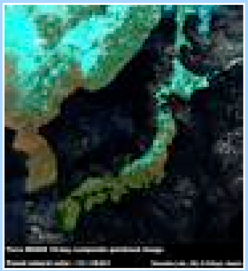

10 day cloud-free composite

WebPaNDA (NOAA AVHRR)

1 

Online subsetting scene by scene

2 

Rapid response by quicklook

3 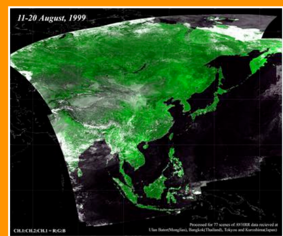

10 day cloud-free composite

L1B QUICKLOOK IMAGE OF MODIS AND AVHRR

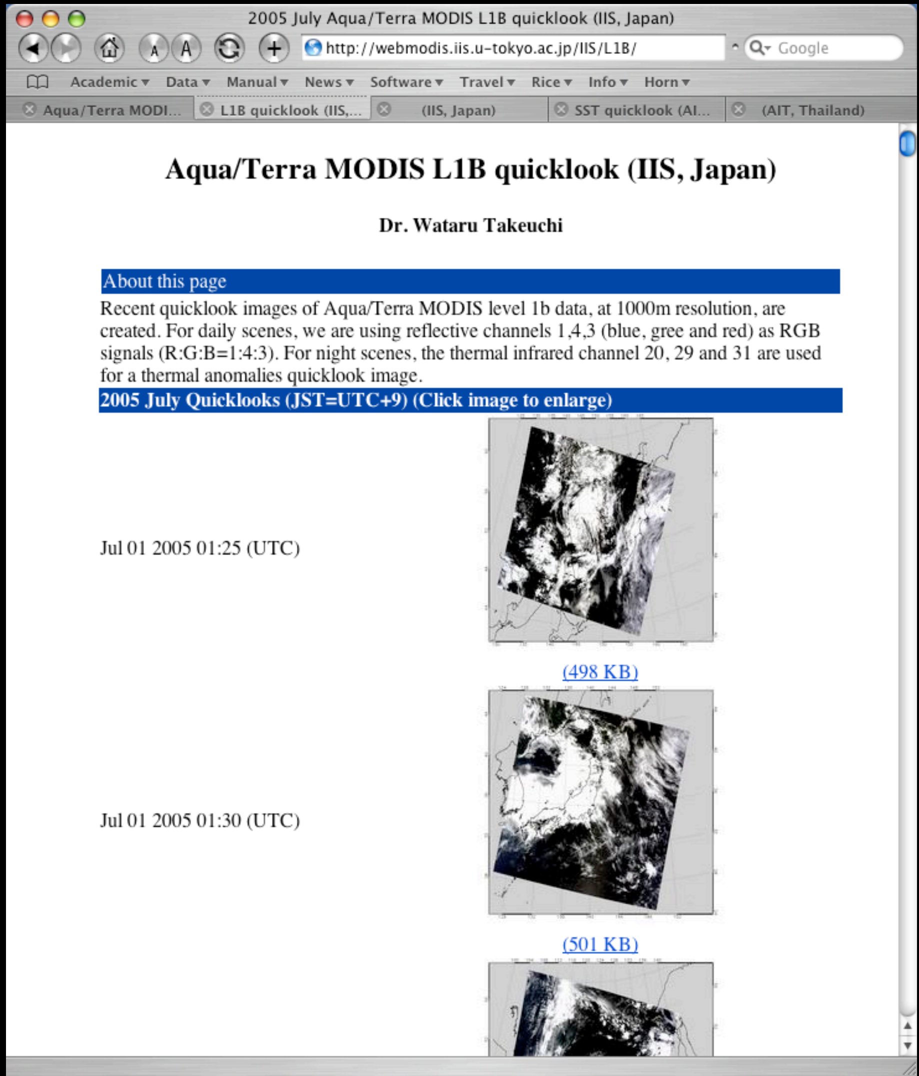

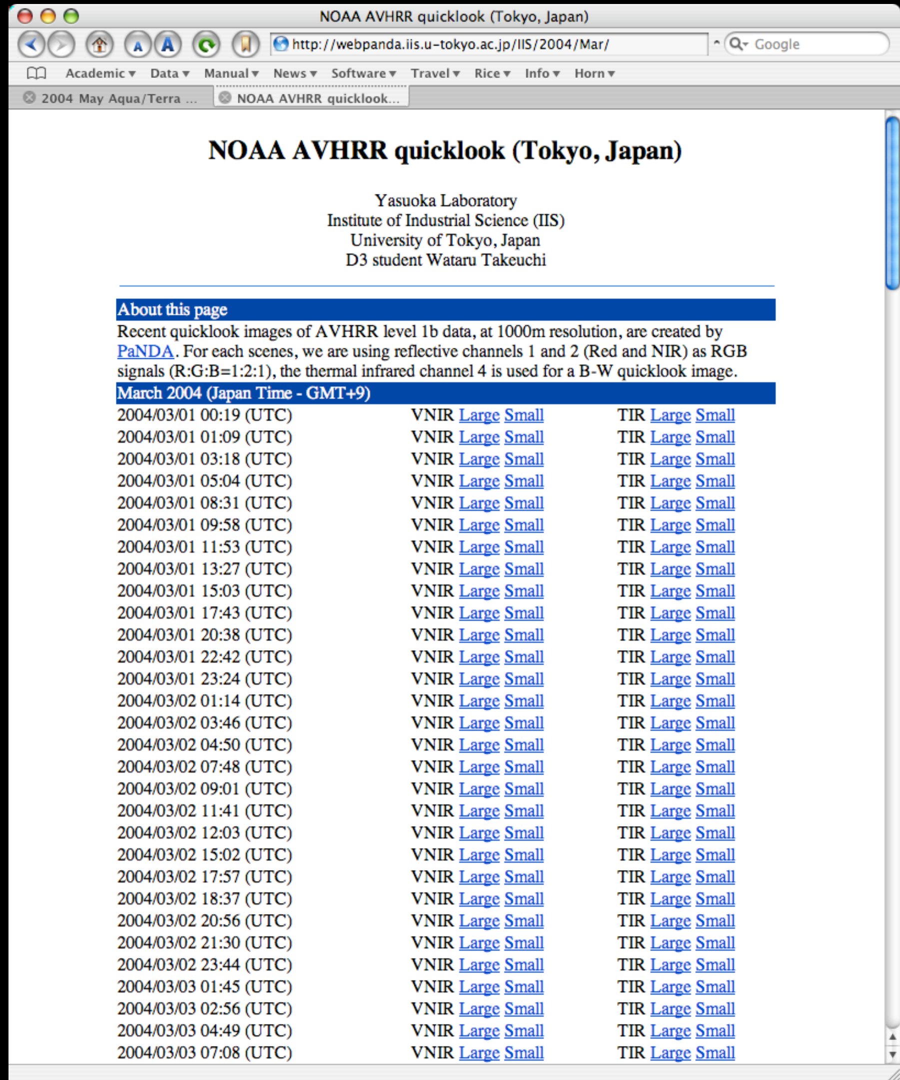

Terra / Aqua MODIS
http://webmodis.iis.u-tokyo.ac.jp/

NOAA / AVHRR
http://webpanda.iis.u-tokyo.ac.jp/

LEVEL2 PRODUCTS - SEA SURFACE TEMPERATURE

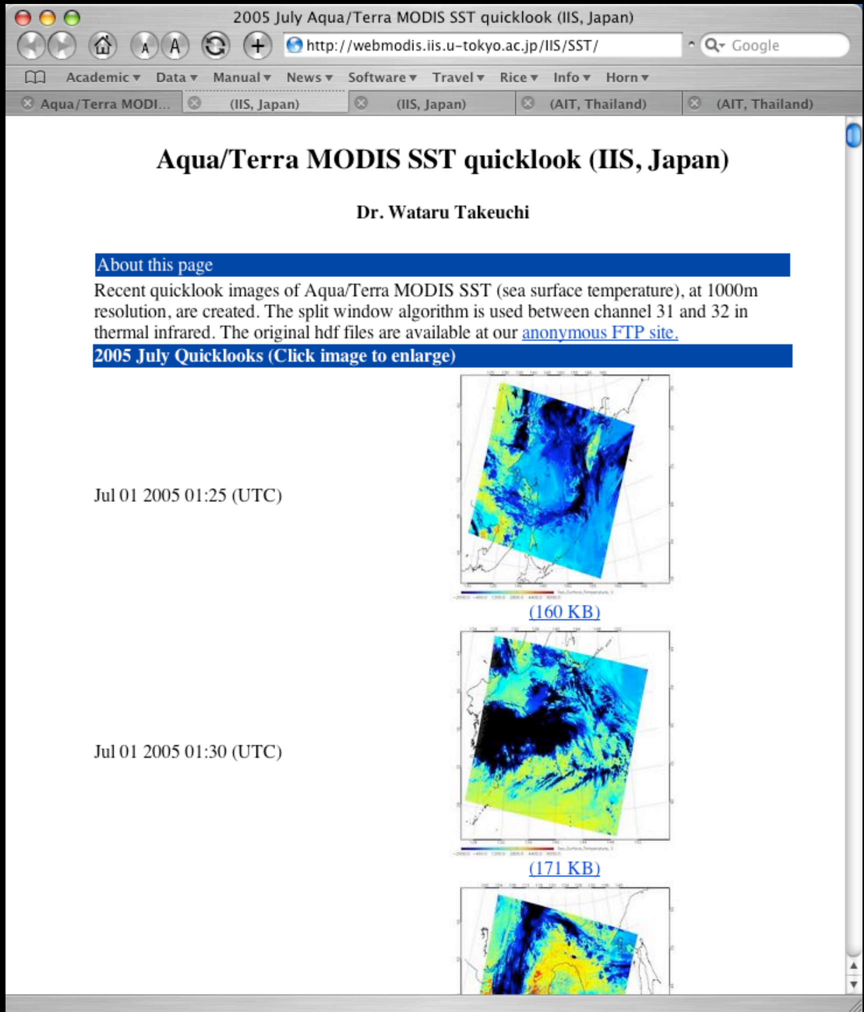

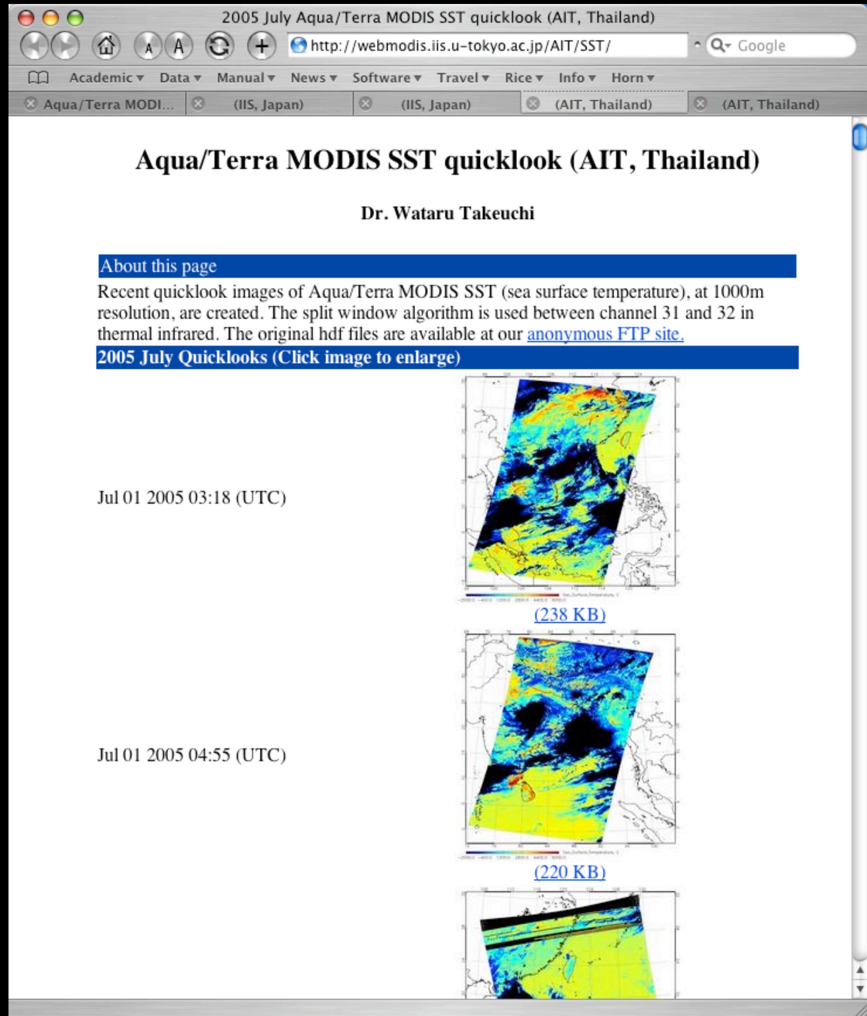

$$modis\_sst = c_1 + c_2 * T_{31} + c_3 * T_{3132} + c_4 * (\sec(\theta) - 1) * T_{3132} \qquad (18)$$

T_{31} is the band 31 brightness temperature (BT) (*cf.* AVHRR Channel 4)

T_{3132} is (Band32 - Band31) BT difference (*cf.* AVHRR (Channel 4 - Channel 5))

θ is the satellite zenith angle

[ATBD MOD28, 1999]

LEVEL2 PRODUCTS - PRECIPITABLE WATER VAPOR

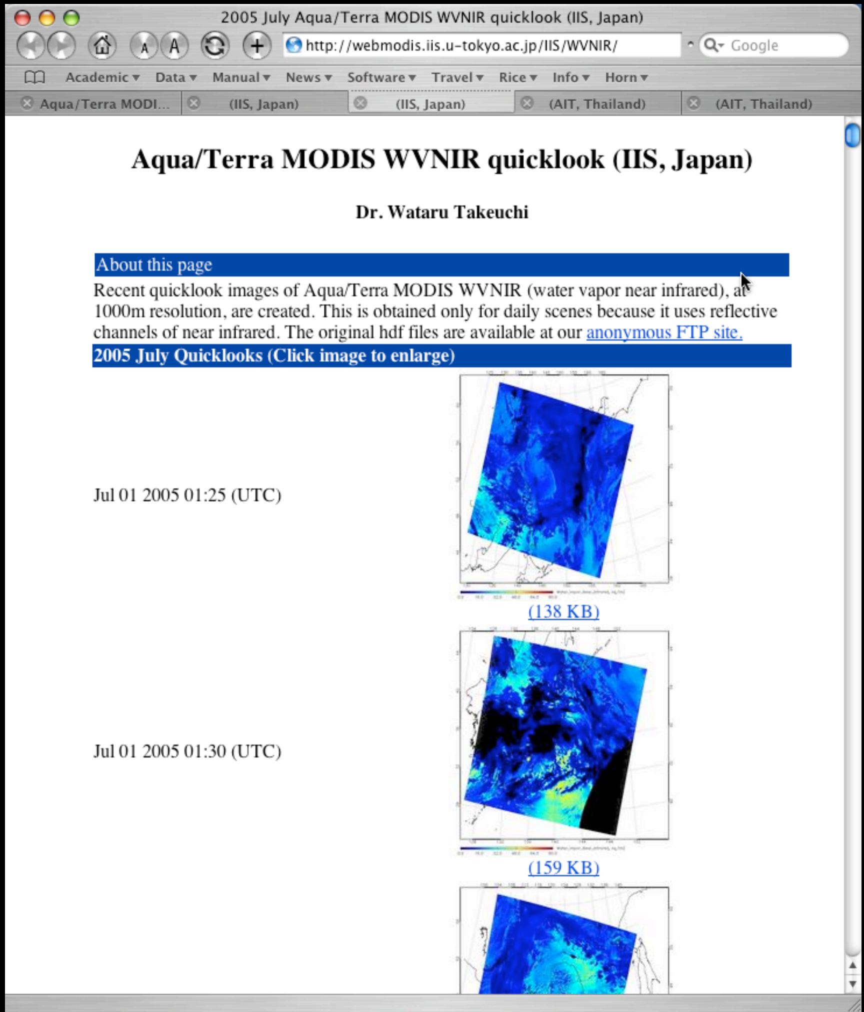

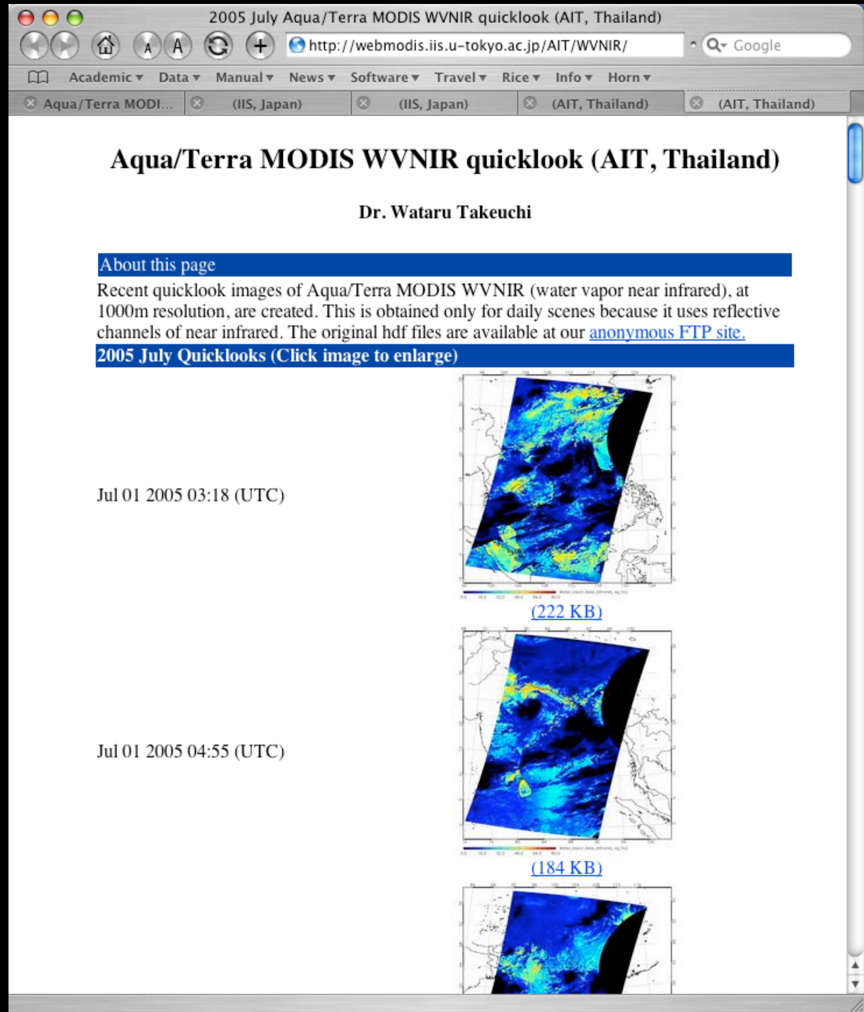

MODIS Channel #	Position (μm)	Width (μm)
2	0.865	0.040
5	1.240	0.020
17	0.905	0.030
18	0.936	0.010
19	0.940	0.050

[ATBD MOD05, 1998]

LEVEL2 PRODUCTS - ACTIVE FIRE MAPPING

# LAT(deg.)	LON(deg.)	REF2(%)	T22(K)	T31(K)	CONFIDENCE(%)
31.979397	117.255943	0.265969	320.278168	295.943878	57
31.939053	117.259239	0.270117	322.583588	293.936523	73
31.936943	117.271469	0.271943	328.083862	296.270966	90
31.835857	117.318924	0.251624	321.923523	294.569916	27
31.476776	118.412544	0.270130	313.733917	294.438507	55
29.819904	112.897804	0.246956	315.107361	293.052795	26
29.035807	117.113449	0.246717	319.720398	296.258667	79
29.025869	117.111214	0.238511	325.189270	296.320282	87
27.660099	117.370224	0.298122	318.211731	294.644928	74
27.657619	117.384056	0.234624	317.685730	295.485626	76
5.109268	103.068985	0.298627	312.639740	289.793518	61
4.576164	103.443192	0.250744	327.012390	299.084869	84
4.575822	103.436310	0.286776	321.617249	297.631409	77
4.573782	103.450356	0.246780	321.024261	299.349457	59
0.573904	101.991135	0.207827	315.481232	297.972137	57
0.443134	99.184494	0.241613	311.445862	293.728821	54
-0.312369	102.095795	0.273498	314.674988	298.178528	55
-2.259895	112.353577	0.241130	318.764923	293.268005	25
-2.262557	112.371567	0.294802	317.460693	292.818054	33
-2.264346	112.364517	0.288234	324.755310	293.879913	86
-1.376376	101.523788	0.294958	312.057800	297.570465	58
-2.887460	110.387360	0.217305	312.835907	297.008270	33
-2.889391	110.400452	0.233988	320.713898	297.075653	81
-2.881775	110.395081	0.224970	318.845215	296.634094	74
7.865060	81.378456	0.264071	324.977661	306.354187	87
7.410981	81.197235	0.277698	319.903687	304.062622	80
7.191035	81.660492	0.284265	332.174286	305.196381	94
7.189600	81.670547	0.276508	333.683136	305.870667	95
7.165615	81.122513	0.297655	322.248718	303.390198	83
22.539001	120.352409	-1.000000	311.410614	295.912994	75
22.548471	120.354294	-1.000000	307.343994	296.160004	53
-1.083907	103.410461	-1.000000	309.296814	293.002075	65
-0.692875	102.677574	-1.000000	305.995483	293.967926	40
-0.334271	101.513763	-1.000000	314.794373	293.160431	86
0.439169	101.129417	-1.000000	308.033295	292.837097	58
0.764716	100.830078	-1.000000	305.158203	293.217407	21
1.388330	101.071106	-1.000000	311.115051	293.835846	74
1.259210	100.037872	-1.000000	305.156036	293.286987	21
1.355377	100.582779	-1.000000	313.326233	294.357056	82

Active fire pixels on 2005/07/02

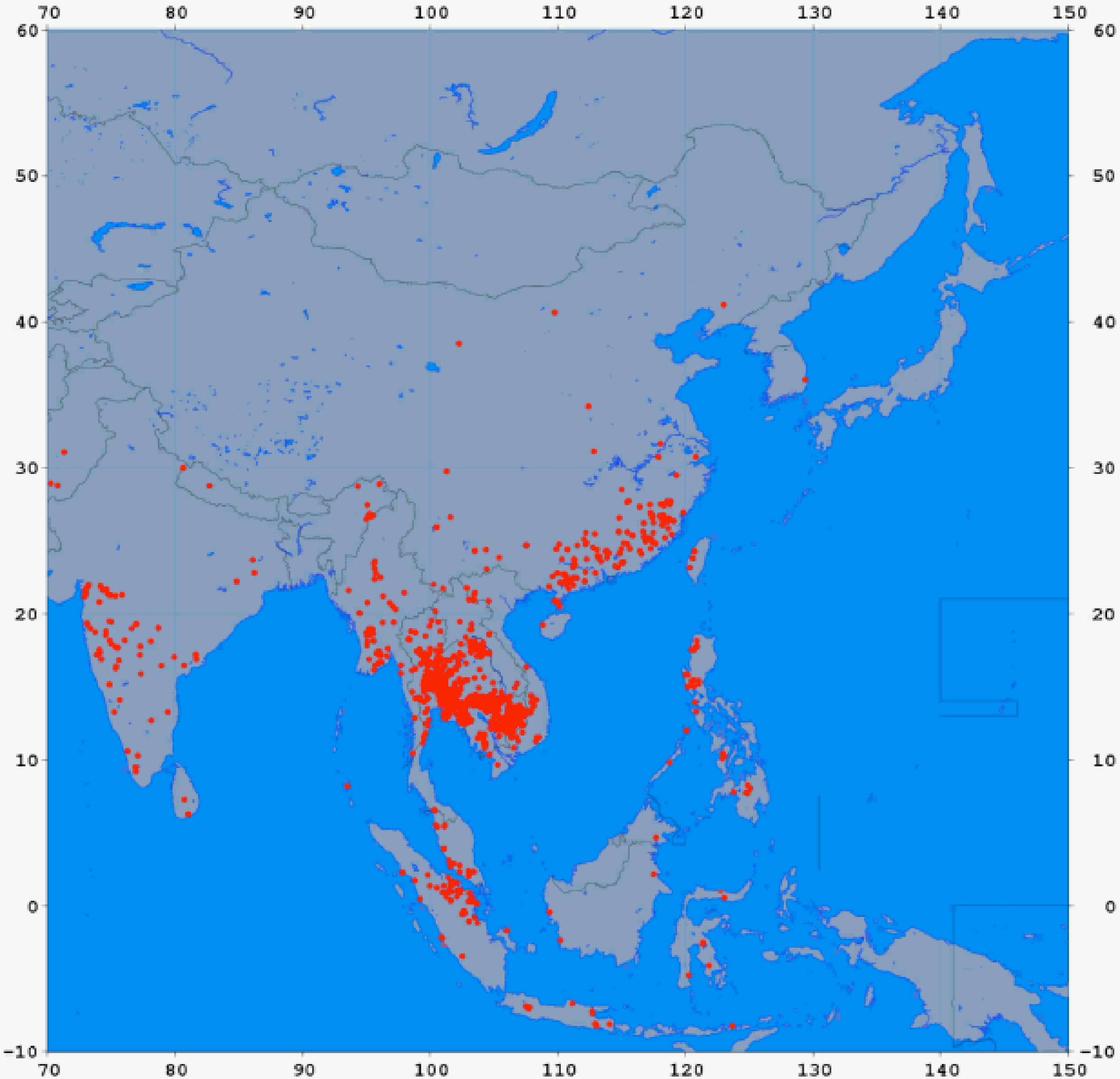

Aqua/Terra MODIS active fire map as of 2004/01/01-10 (C) Institute of Industrial Science, U-Tokyo

Sea ice monitoring in Ohotsuku sea

RGB=621

Middle-infrared channel (1.6μm) is effective to distinguish sea and land ice from clouds.

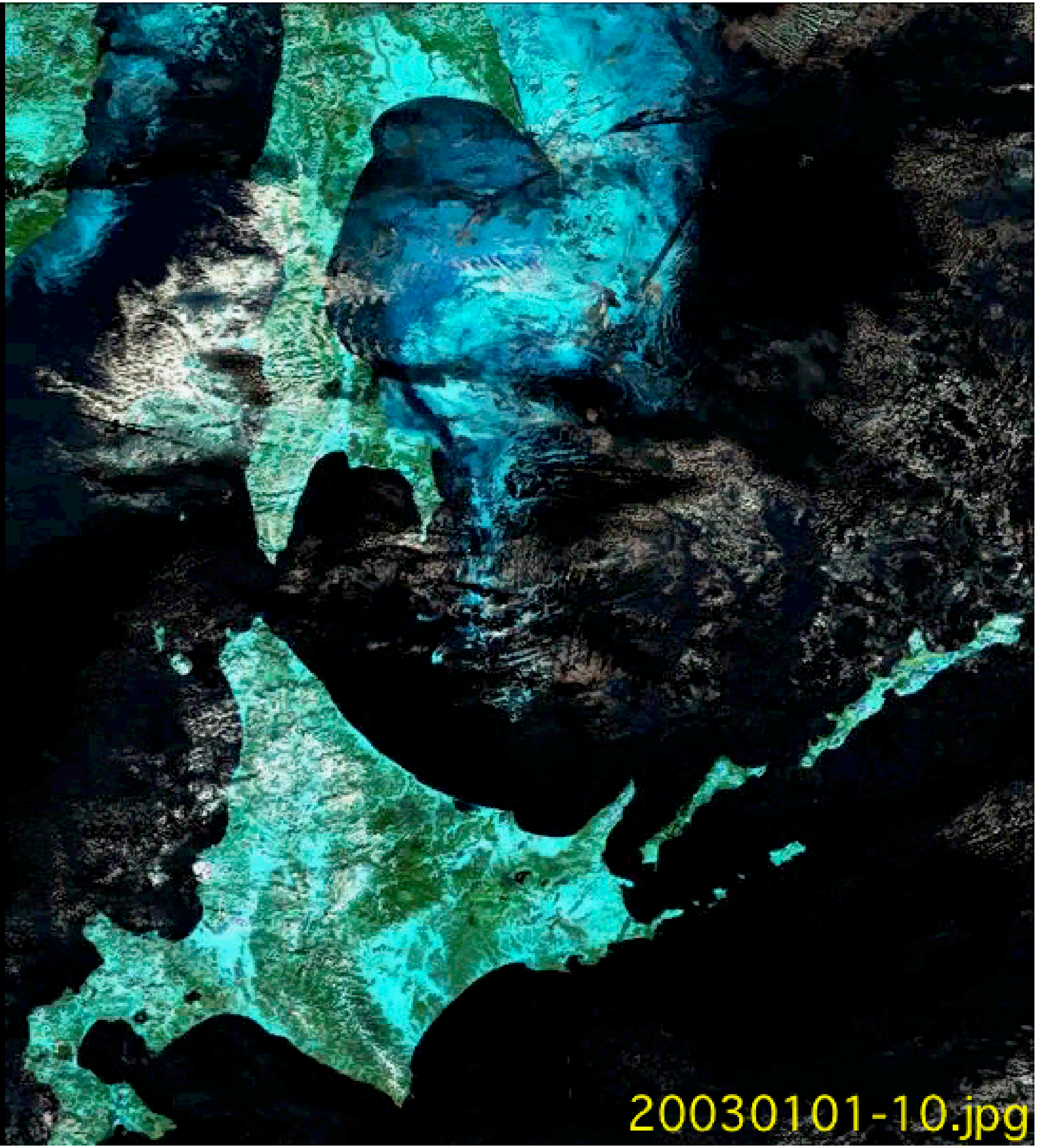

Yellow dust monitoring

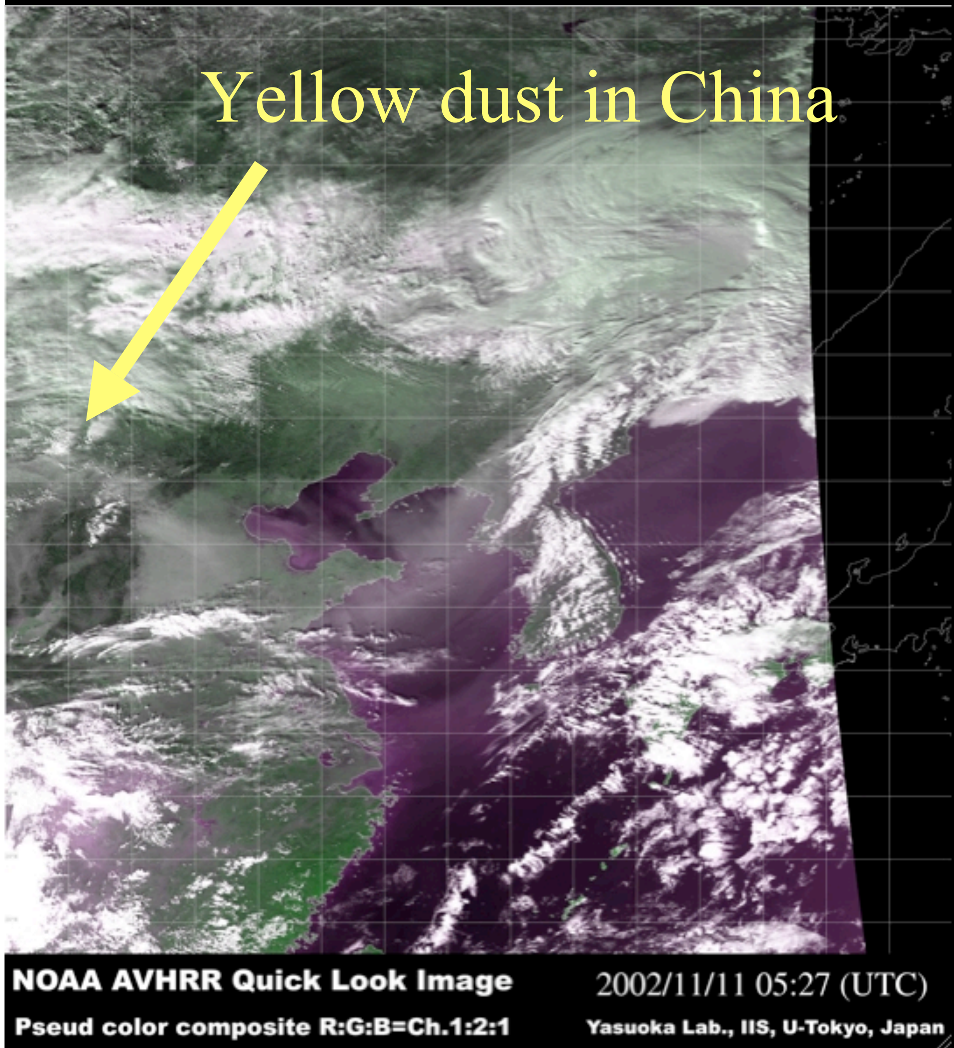

2002/11/11 14:27 (JST)

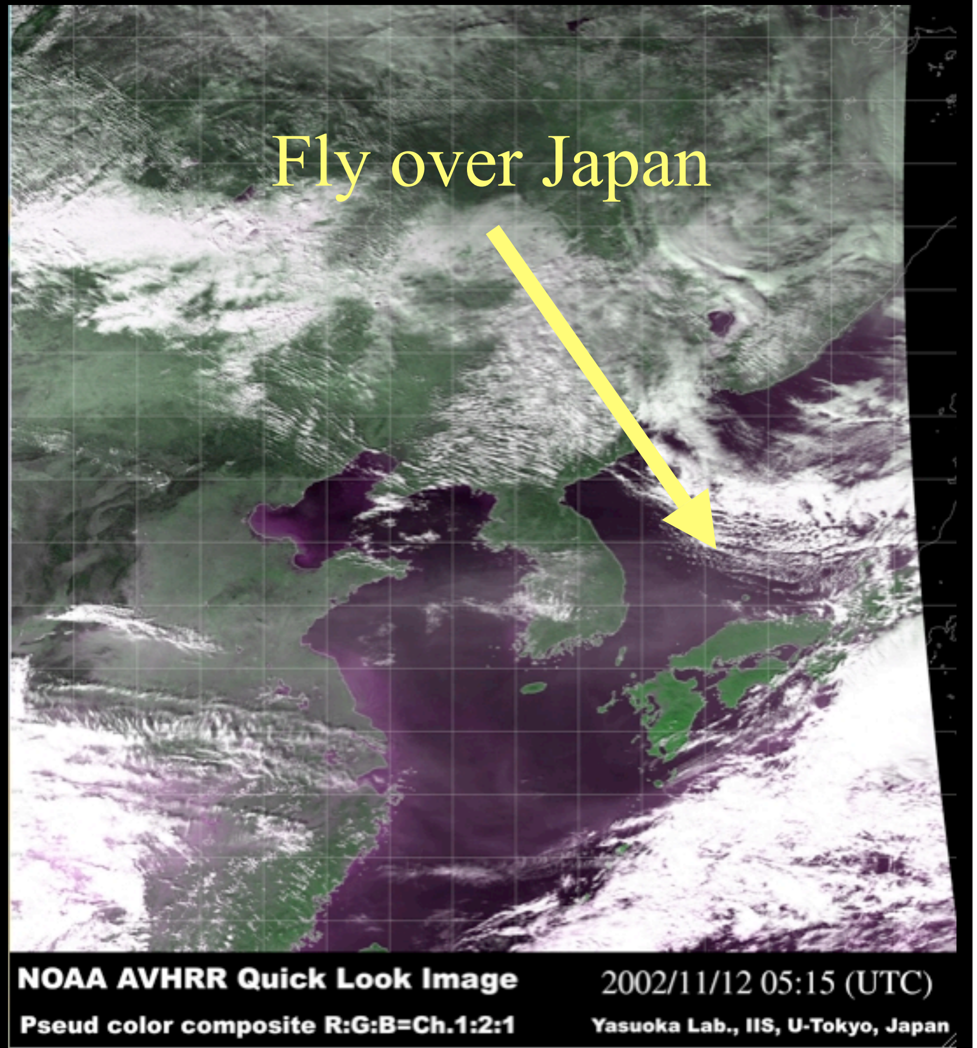

2002/11/12 14:15 (JST)

Tsunami tragedy from MODIS QKM

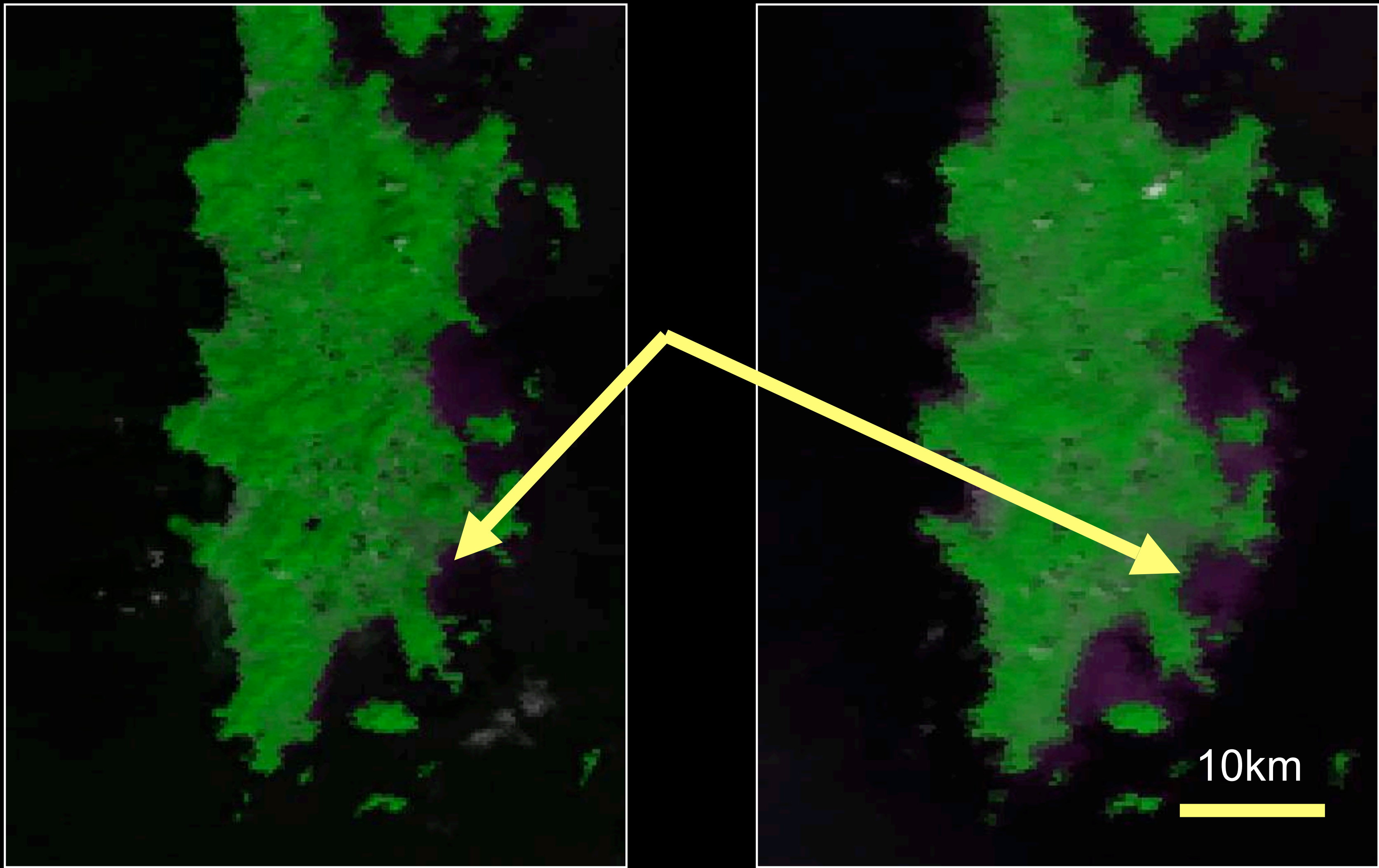

2002 Dec. 8th 4:10 (UTC)　　2004 Dec. 26th 3:35 (UTC)

Turbid water along the coastal line just after the tsunami occurrence

AVHRR FALSE COLOR (RGB=121)

10 day composite
Dec. 20 -31, 2001
NTMinS criteria
1km resolution

MODIS FALSE COLOR (RGB=621)

10 day composite
Dec. 20 -31, 2001
Min. blue criteria
500m resolution
Remarkable view

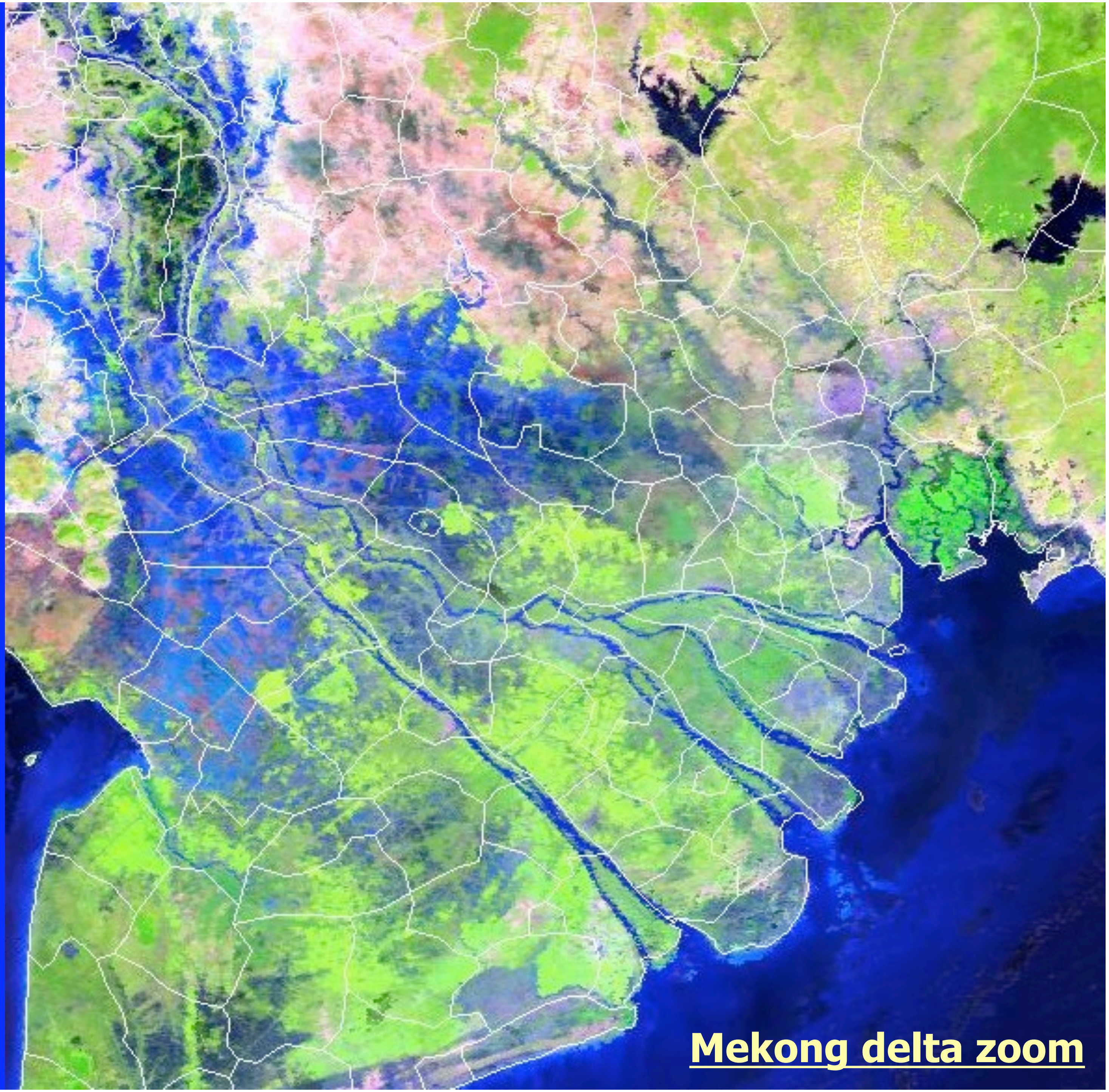

Mekong delta zoom

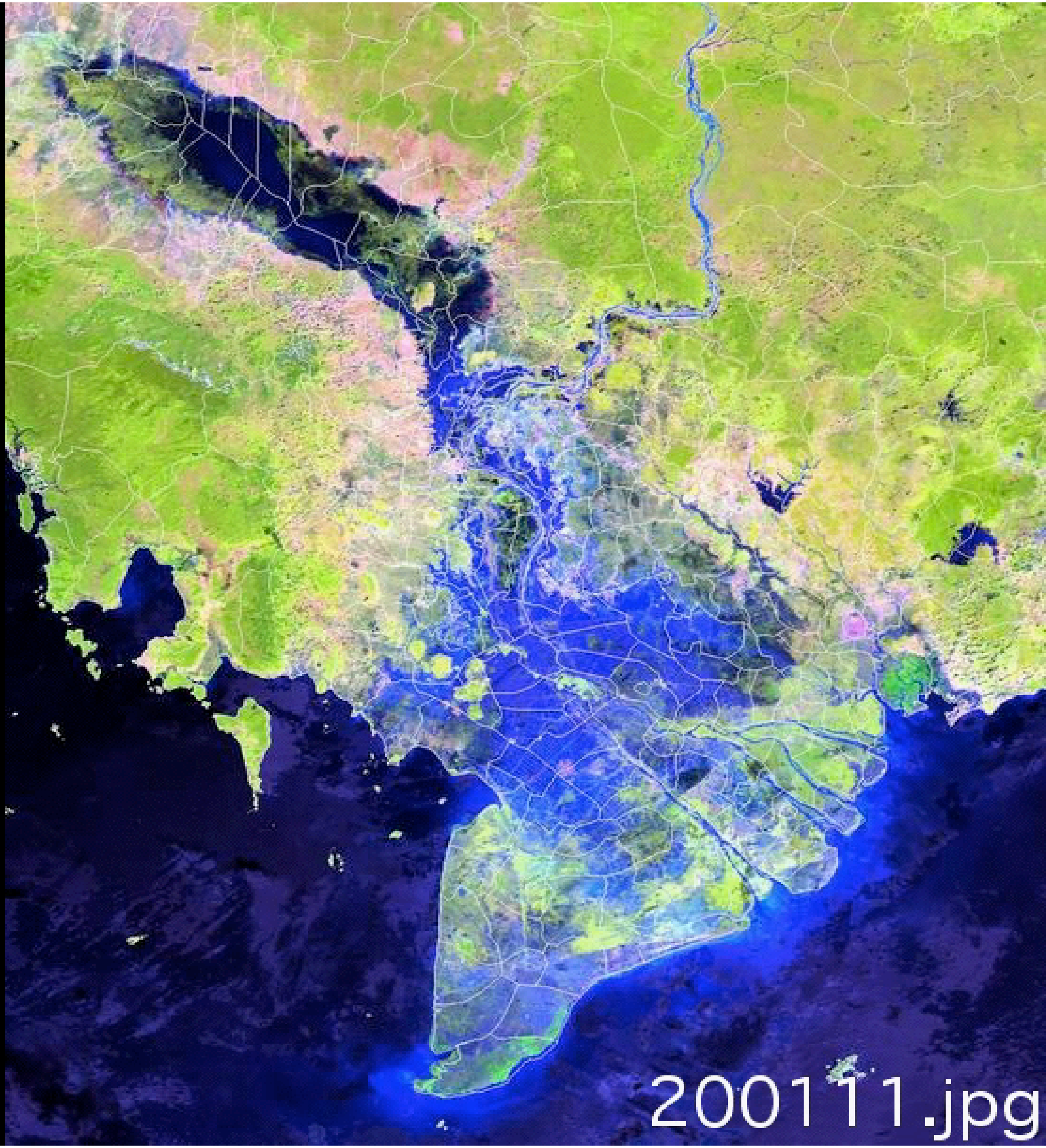
200111.jpg

RICE CULTIVATION OVER ASIA

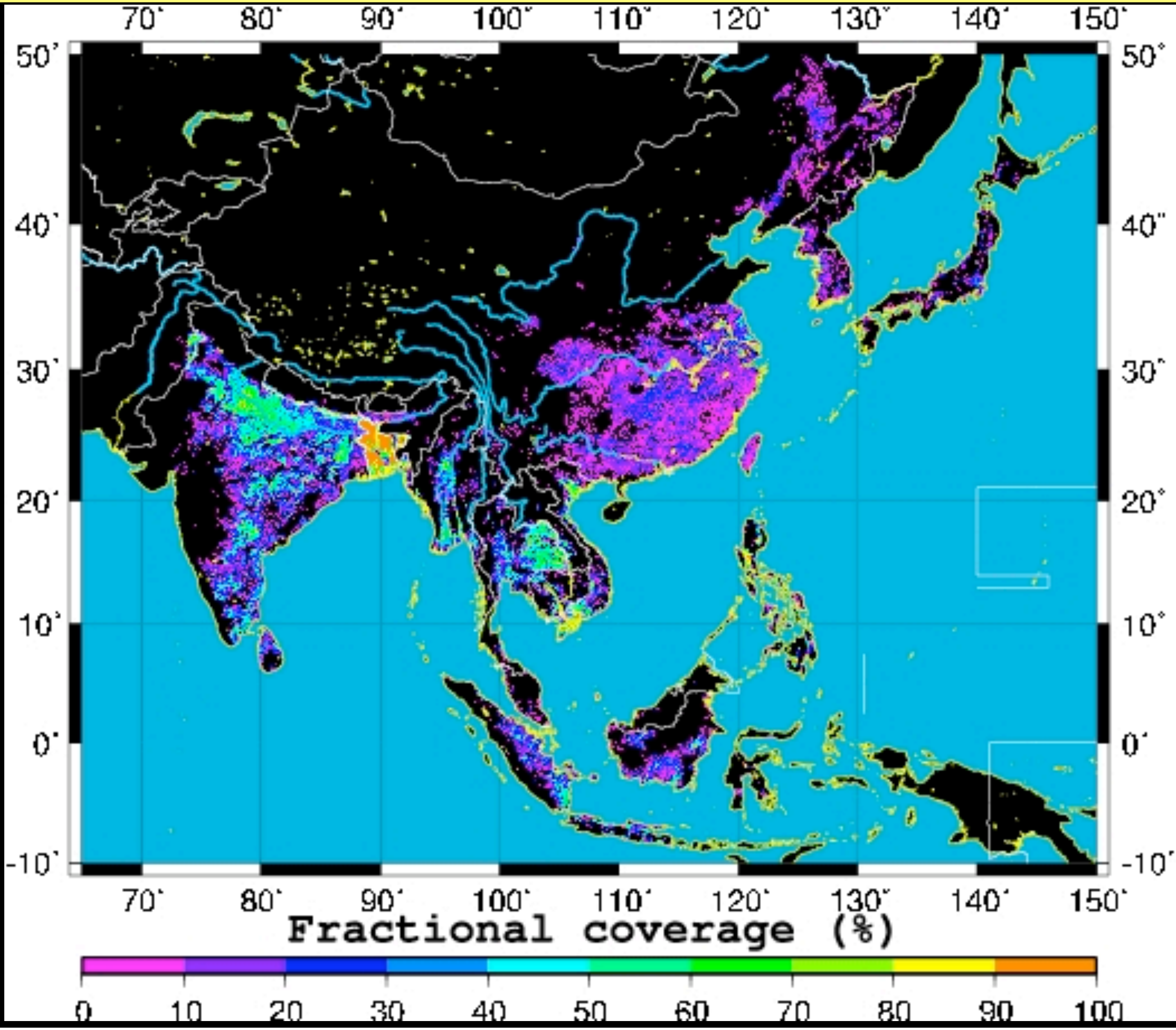

[Taekcuhi, 2005]

ONLINE DATA DISTRIBUTION SERVICE

WebMODIS (Aqua/Terra MODIS)

1 

Online subseting scene by scene

2 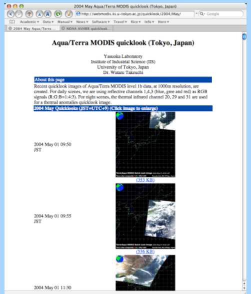

Rapid response by quicklook

3 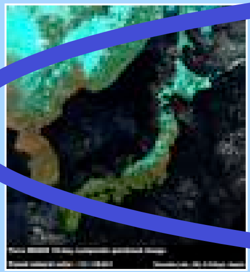

10 day cloud-free composite

WebPaNDA (NOAA AVHRR)

1 

Online subsetting scene by scene

2 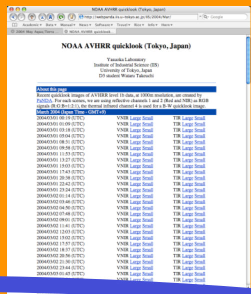

Rapid response by quicklook

3 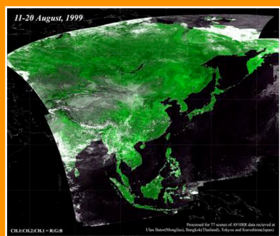

10 day cloud-free composite

ONLINE DATA LIST IN DETAIL

	Sensor	Period	Data type	Processing level	Media
1	NOAA AVHRR(Japan)	1983 Jan-	10day composite	reflectance, temp., NDVI, SST	anonymous FTP
2	NOAA AVHRR(Asia)	1997 Nov-	10day composite	reflectance, temp., NDVI, SST	anonymous FTP
3	Aqua/Terra MODIS(EAsia)	2001 May-	10day composite	reflectance, temp., NDXI, SST	anonymous FTP
4	Aqua/Terra MODIS(Asia)	2001 May-	10day composite	reflectance, temp., NDXI, SST	anonymous FTP

1

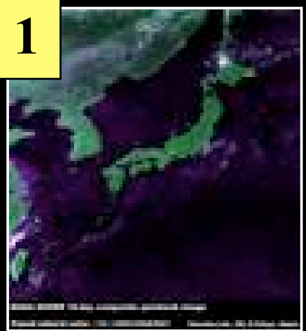

2

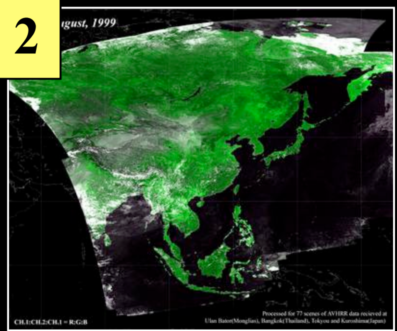

3

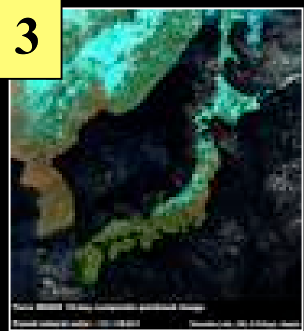

4

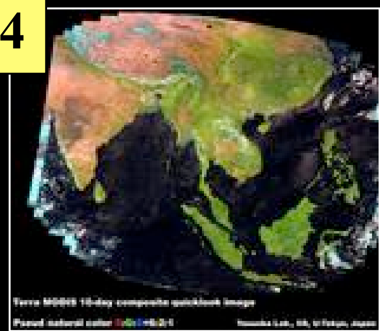

50N120E-20N150E 80N50E-20S170E 50N124E-30N146E 40N70E-10S130E

Compositing algorithm

- AVHRR - NDVI and thermal criteria followed by minimum scan angle method (NTMinS) [Lei, 2001]
  - NDVI of cloud is lower than normal pixel.
  - Thermal value of cloud is cooler than normal pixel.
  - The smaller scan angle is, the better the spatial resolution is.

  Reference:

  Lei, L., and Yokoyama, R., 2001. Development of AVHRR 10-day composite over the whole Asia (in Japanese with English abstract). *J. Remote Sens. Soc. Japan*, 21(2), 168-178.

- MODIS - Thermal criteria followed by minimum blue method (TMinB) [Takeuchi, 2004]
  - Blue channel is subject to atmospheric effects.
  - Cloud shadow is cooler than fine pixel.
  - Not only vegetation but also water and soil mixture are better represented.

  Reference:

  Takeuchi, W., and Yasuoka, Y., 2004. Development of compositing algorithms for MODIS data (in Japanese with English abstract). *J. Japan Photogramm. Remote Sens.*, 22-32, 42(4).

NOAA AVHRR CLOUD-FREE COMPOSITE

East Asia

Southeast Asia

Whole Asia

Ref. /
B. T.
(Ch.1-5)

NDVI

SST

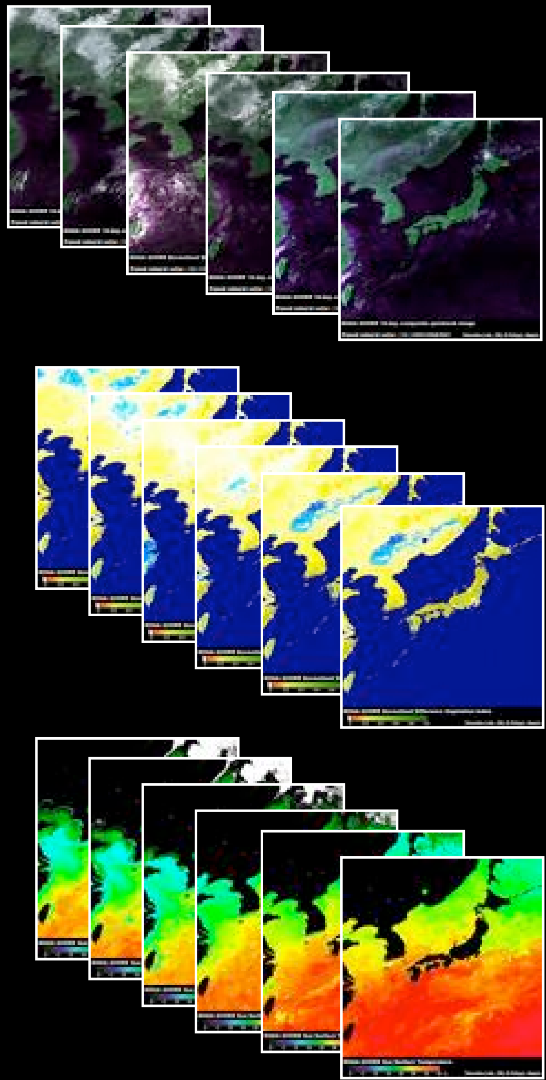

1983~2005

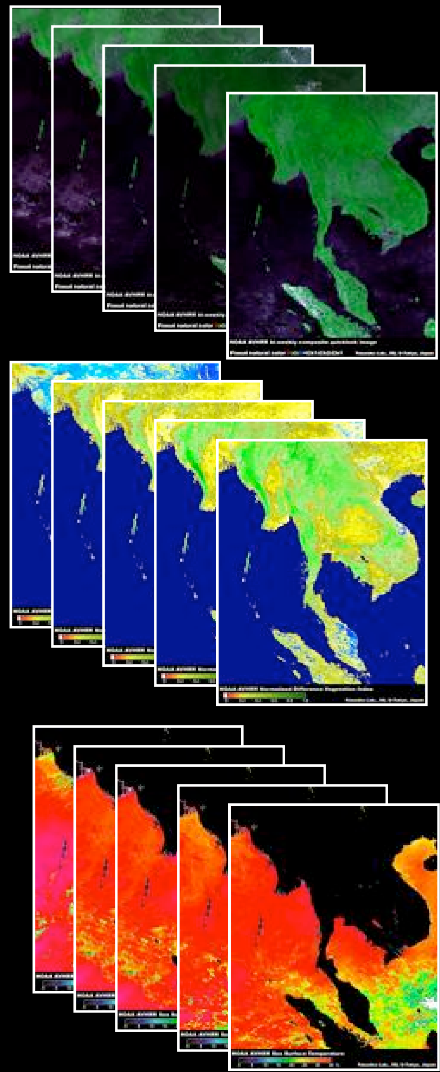

1997~2005

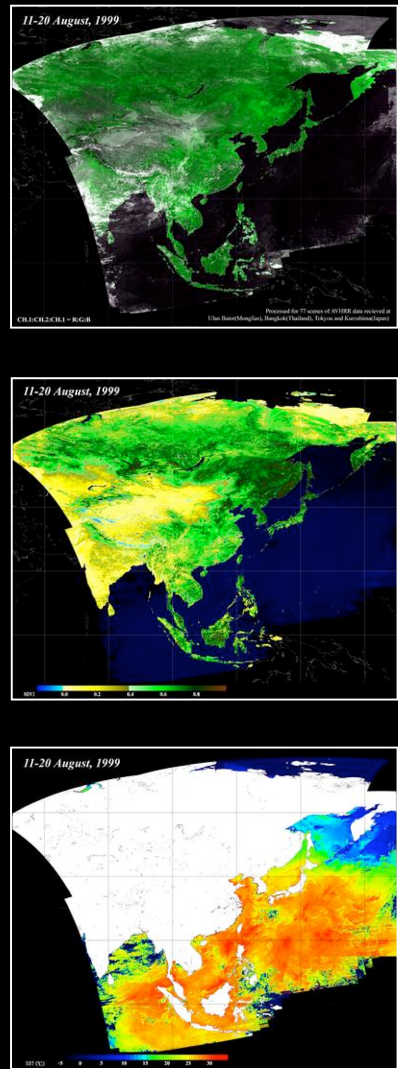

1998~1999

Aqua/Terra MODIS cloud-free composite

East Asia | Southeast Asia

Ref. /
B. T.
(Ch.1-7,31,32)

NDVI, NDSI,
NDWI

LST, SST

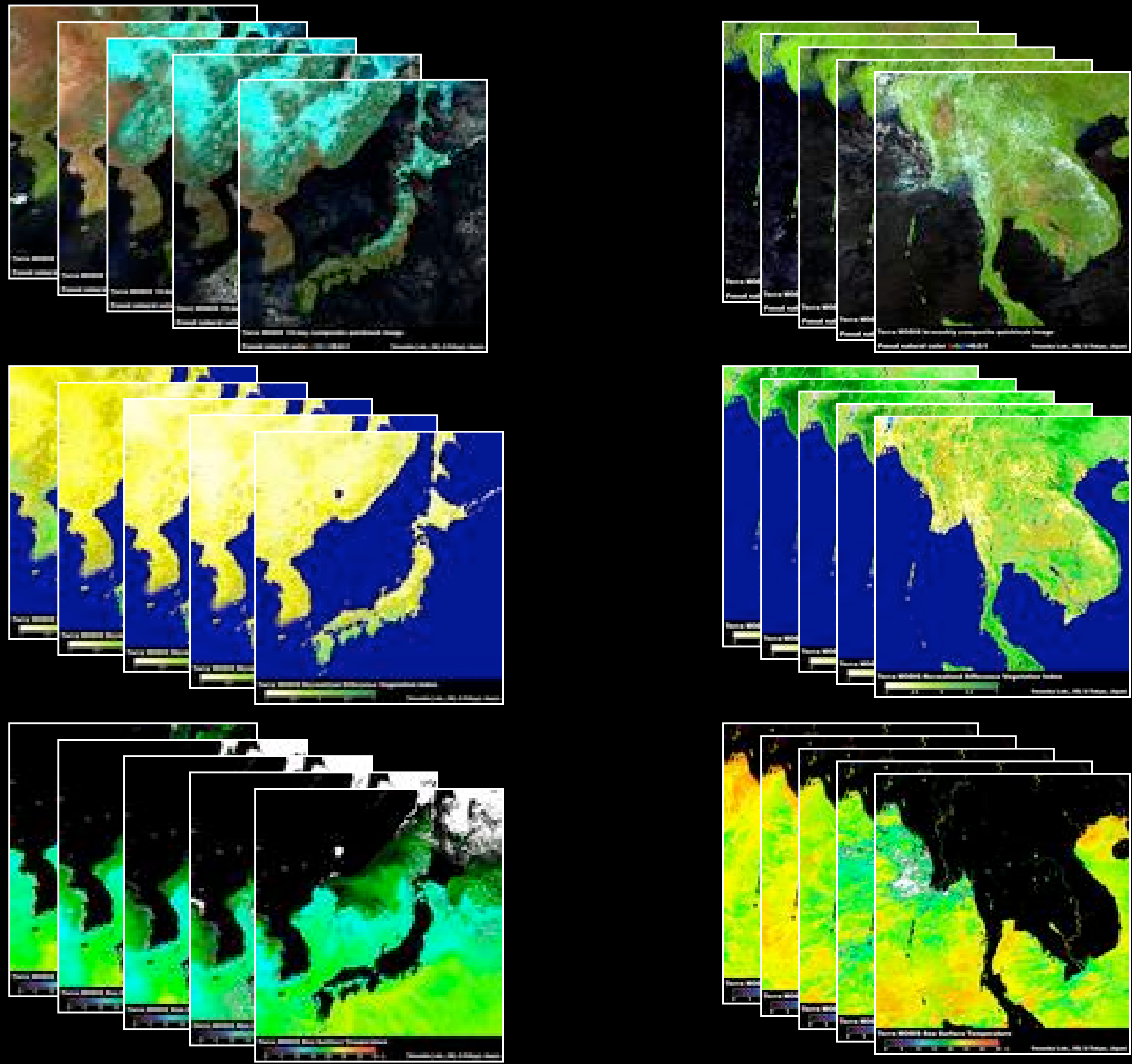

2001~2005 | 2001~2005

MODIS EAST ASIA MOSAICS

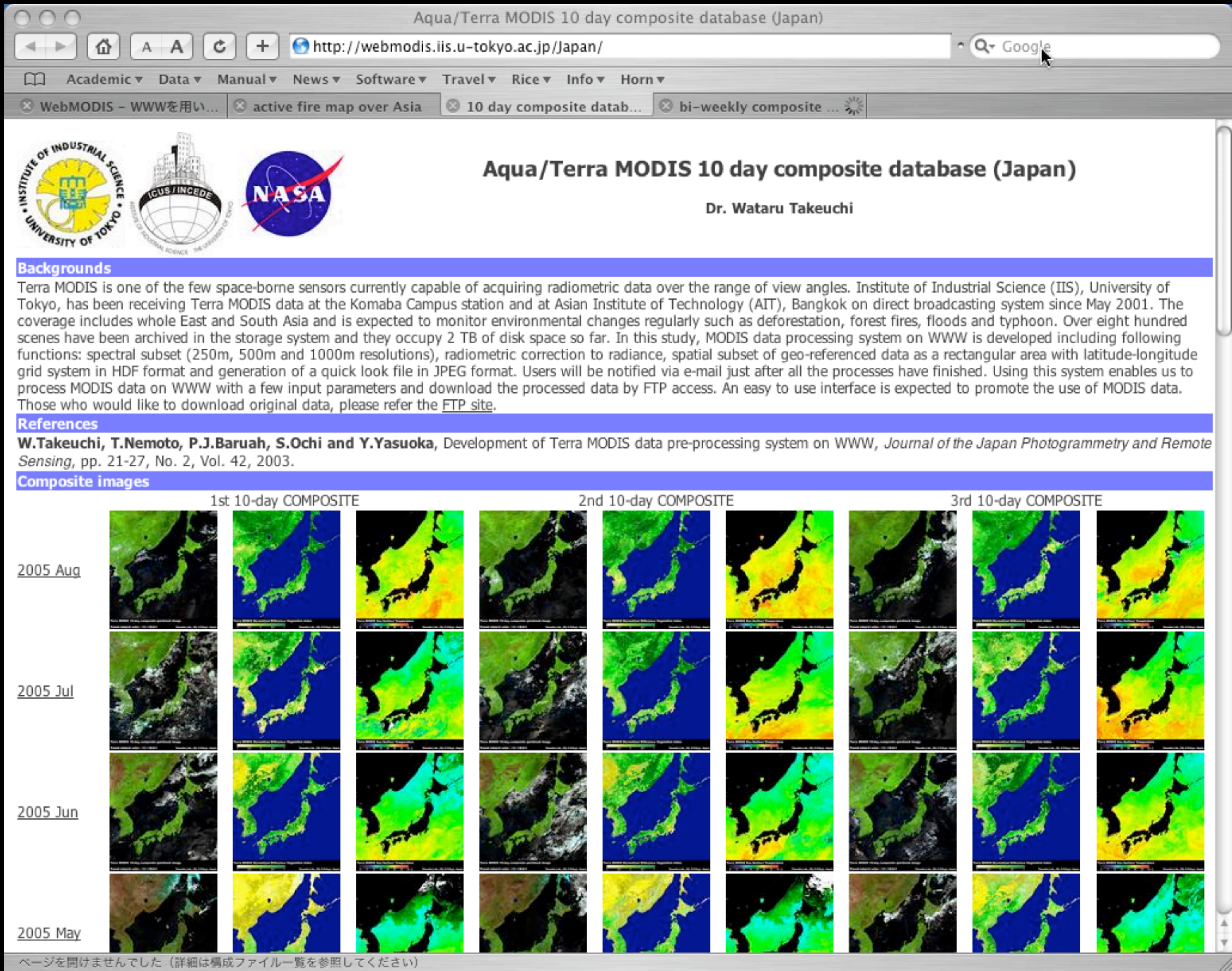

MODIS SE/S-ASIA MOSAICS

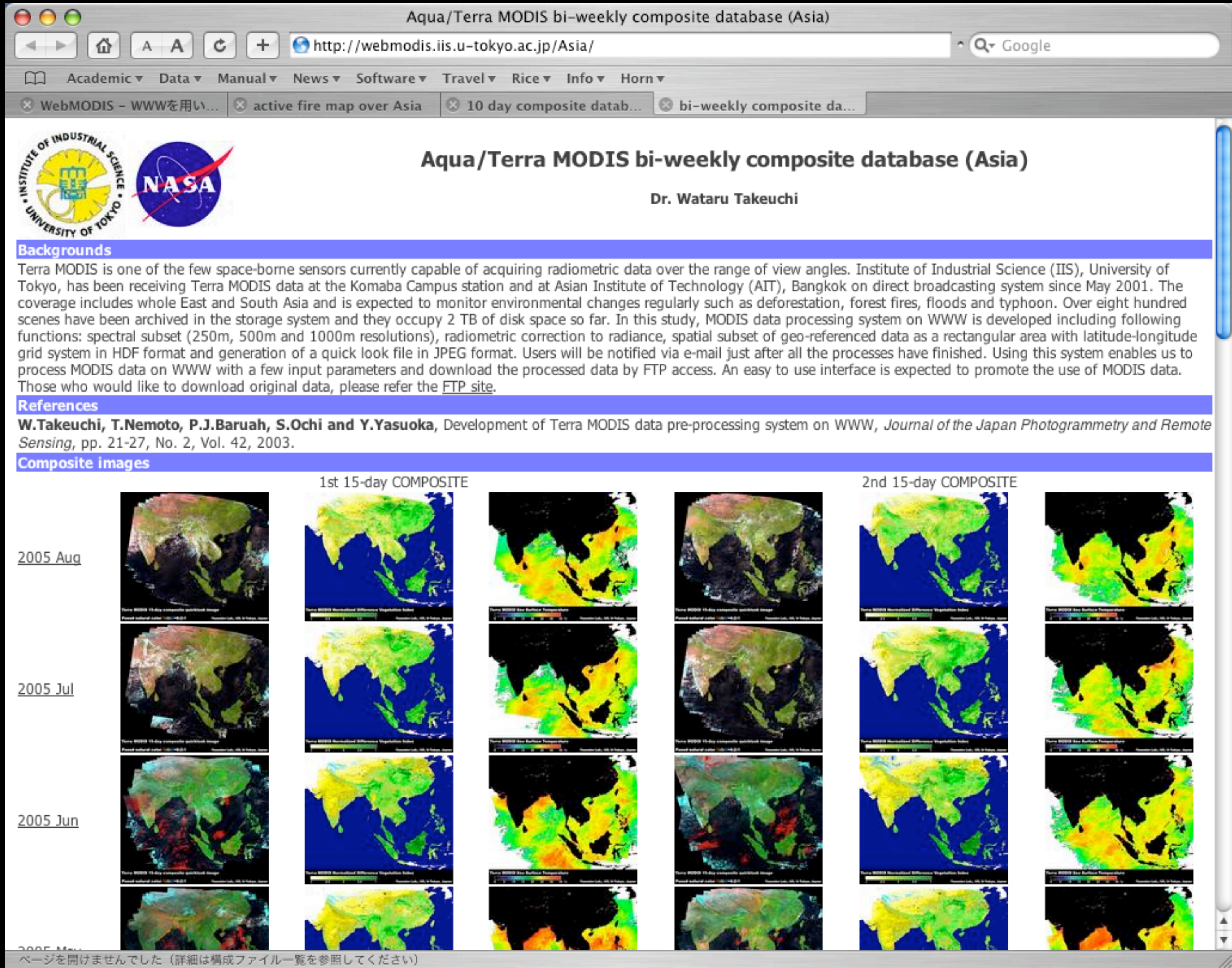

Online FAQ for users

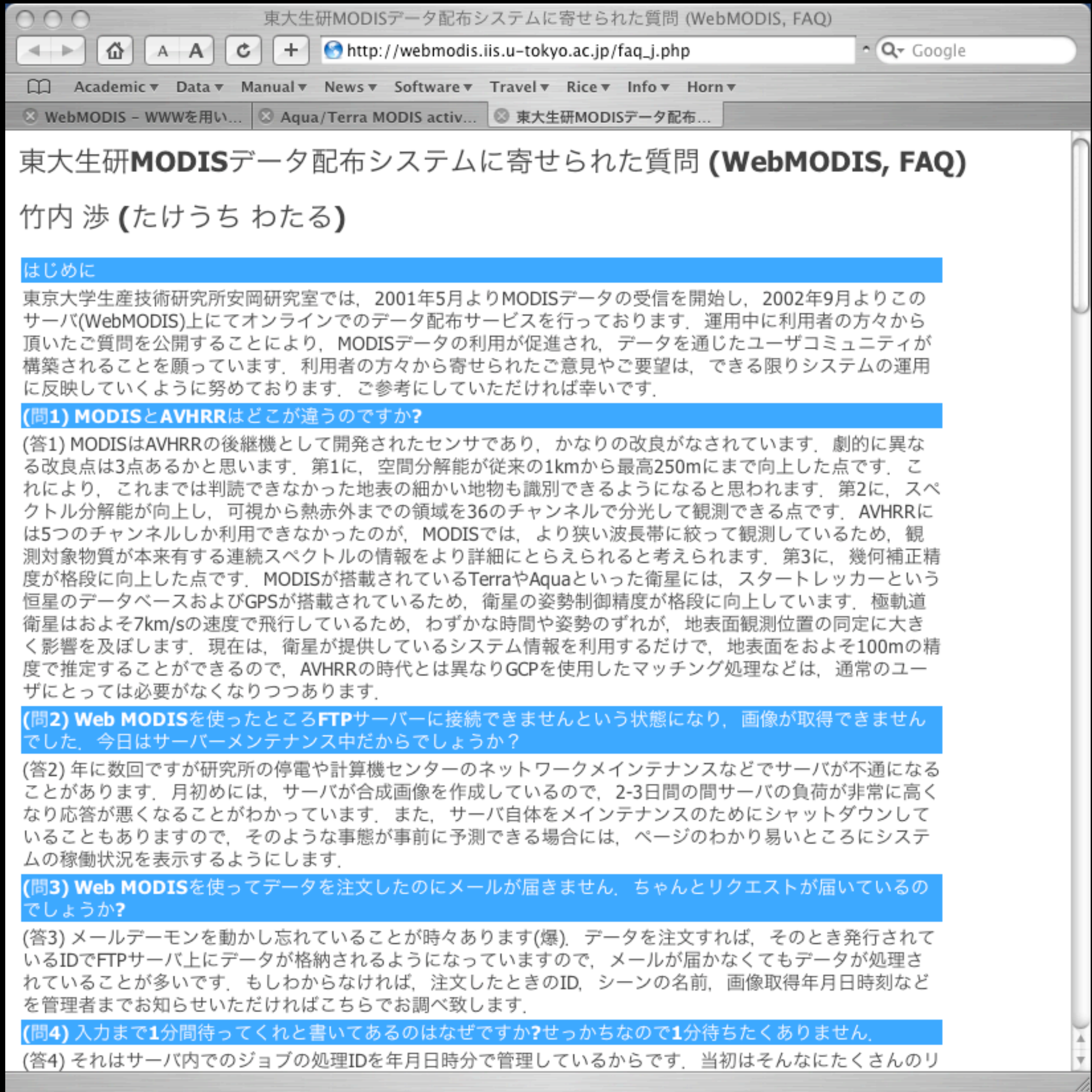

東大生研MODISデータ配布システムに寄せられた質問 (WebMODIS, FAQ)

http://webmodis.iis.u-tokyo.ac.jp/faq_j.php

Academic Data Manual News Software Travel Rice Info Horn

WebMODIS - WWWを用い… Aqua/Terra MODIS activ… 東大生研MODISデータ配布…

東大生研**MODIS**データ配布システムに寄せられた質問 **(WebMODIS, FAQ)**

竹内 渉 **(**たけうち わたる**)**

はじめに

東京大学生産技術研究所安岡研究室では，2001年5月よりMODISデータの受信を開始し，2002年9月よりこのサーバ(WebMODIS)上にてオンラインでのデータ配布サービスを行っております．運用中に利用者の方々から頂いたご質問を公開することにより，MODISデータの利用が促進され，データを通じたユーザコミュニティが構築されることを願っています．利用者の方々から寄せられたご意見やご要望は，できる限りシステムの運用に反映していくように努めております．ご参考にしていただければ幸いです．

(問1) MODISとAVHRRはどこが違うのですか?

(答1) MODISはAVHRRの後継機として開発されたセンサであり，かなりの改良がなされています．劇的に異なる改良点は3点あるかと思います．第1に，空間分解能が従来の1kmから最高250mにまで向上した点です．これにより，これまでは判読できなかった地表の細かい地物も識別できるようになると思われます．第2に，スペクトル分解能が向上し，可視から熱赤外までの領域を36のチャンネルで分光して観測できる点です．AVHRRには5つのチャンネルしか利用できなかったのが，MODISでは，より狭い波長帯に絞って観測しているため，観測対象物質が本来有する連続スペクトルの情報をより詳細にとらえられると考えられます．第3に，幾何補正精度が格段に向上した点です．MODISが搭載されているTerraやAquaといった衛星には，スタートレッカーという恒星のデータベースおよびGPSが搭載されているため，衛星の姿勢制御精度が格段に向上しています．極軌道衛星はおよそ7km/sの速度で飛行しているため，わずかな時間や姿勢のずれが，地表面観測位置の同定に大きく影響を及ぼします．現在は，衛星が提供しているシステム情報を利用するだけで，地表面をおよそ100mの精度で推定することができるので，AVHRRの時代とは異なりGCPを使用したマッチング処理などは，通常のユーザにとっては必要がなくなりつつあります．

(問2) Web MODISを使ったところ**FTP**サーバーに接続できませんという状態になり，画像が取得できませんでした．今日はサーバーメンテナンス中だからでしょうか？

(答2) 年に数回ですが研究所の停電や計算機センターのネットワークメインテナンスなどでサーバが不通になることがあります．月初めには，サーバが合成画像を作成しているので，2-3日間の間サーバの負荷が非常に高くなり応答が悪くなることがわかっています．また，サーバ自体をメインテナンスのためにシャットダウンしていることもありますので，そのような事態が事前に予測できる場合には，ページのわかり易いところにシステムの稼働状況を表示するようにします．

(問3) Web MODISを使ってデータを注文したのにメールが届きません．ちゃんとリクエストが届いているのでしょうか**?**

(答3) メールデーモンを動かし忘れていることが時々あります(爆)．データを注文すれば，そのとき発行されているIDでFTPサーバ上にデータが格納されるようになっていますので，メールが届かなくてもデータが処理されていることが多いです．もしわからなければ，注文したときのID，シーンの名前，画像取得年月日時刻などを管理者までお知らせいただければこちらでお調べ致します．

(問4) 入力まで**1**分間待ってくれと書いてあるのはなぜですか**?**せっかちなので**1**分待ちたくありません．

(答4) それはサーバ内でのジョブの処理IDを年月日時分で管理しているからです．当初はそんなにたくさんのリ

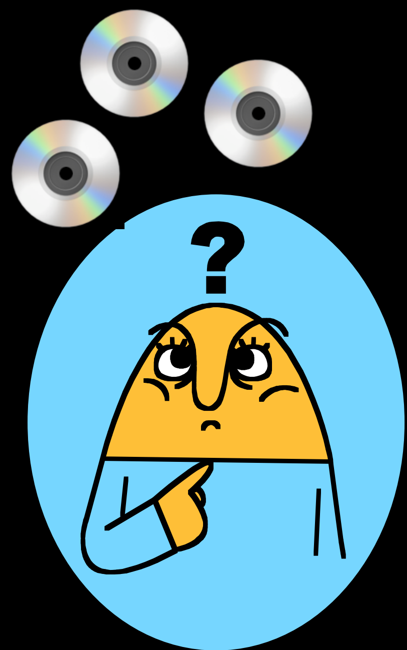

MODIS Sample Data CDROM

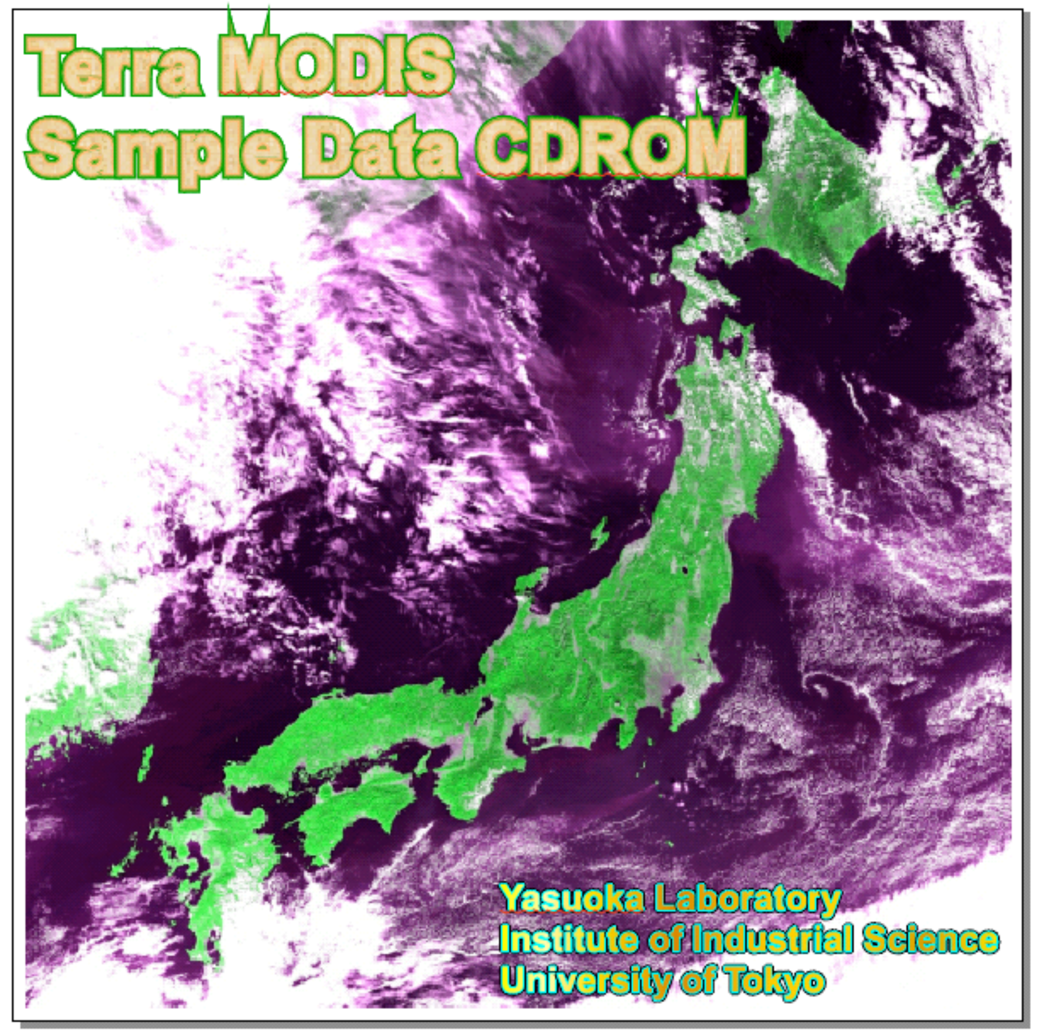

Received @ IIS, U-Tokyo
Oct. 15th, 2001 A.M. 11:00(JST)

- *250m - Ch.1-2*
- *500m - Ch.1-7*
- *1000m - Ch.1-36*

Freely available via the Internet

ftp://yasulab.iis.u-tokyo.ac.jp/

USAGE STATISTICS OF WWW

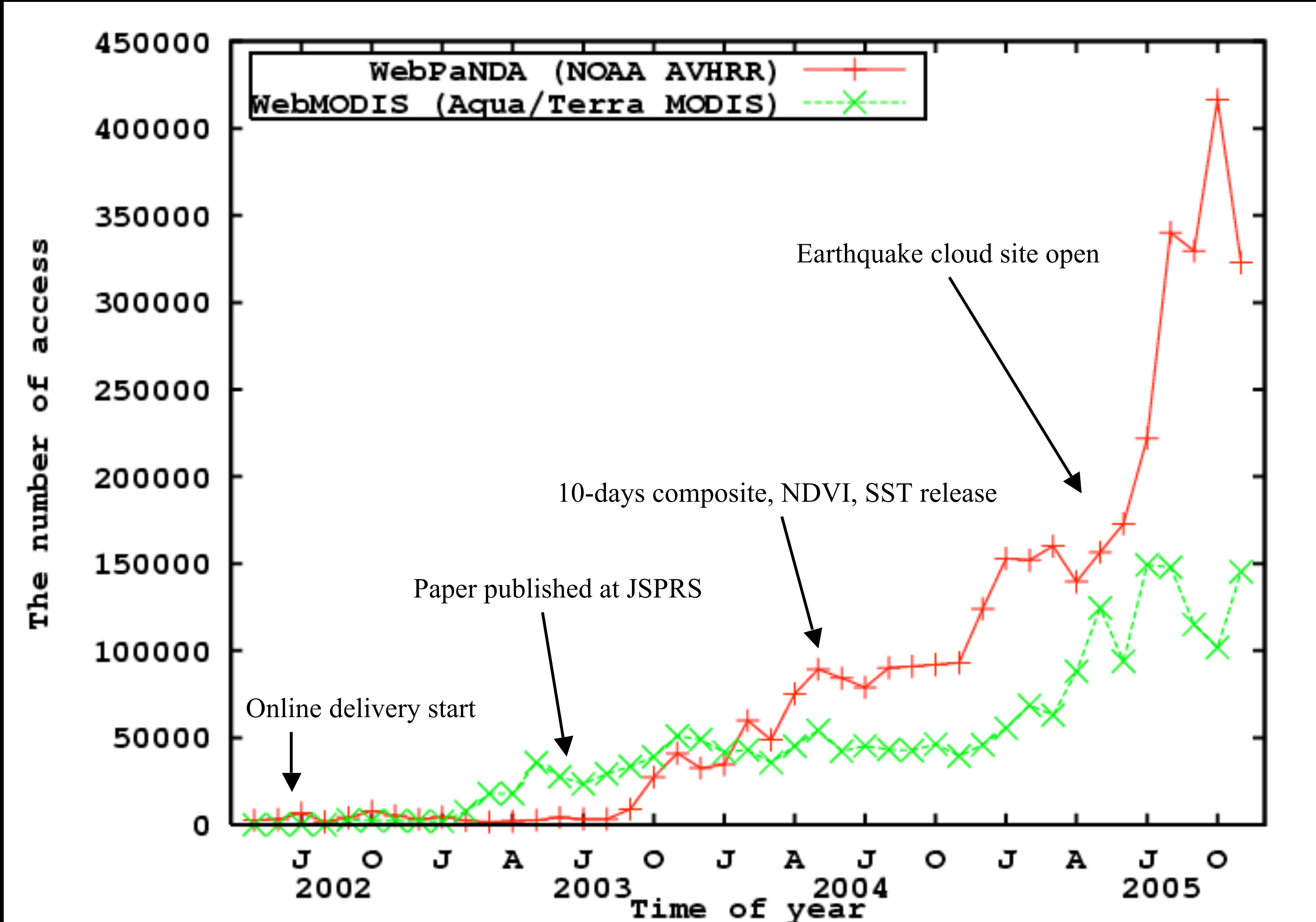

USAGE STATISTICS IN DETAIL

Server	Access
WebPaNDA (AVHRR)	Japan (47%, Kyoto-U, Tohoku-U, U-Tokyo, Nihon-U, JAXA, RESTEC)
	Private company (11%, both domestic and foreign country)
	Foreign country (22%, Thailand, Singapore, Korea, USA, Netherlands, Canada, Germany, France)
	Search engine (20%, google, yashoo)
WebMODIS (MODIS)	Japan (52%, Hiroshima-U, Kagoshima-U, JAXA, Tohoku-U, Kobe-U, U-Tokyo, RESTEC)
	Foreign country (19%, Thailand, Malaysia, Korea, France, Russia, USA, Taiwan)
	Private company (5%, both domestic and foreign contry)
	Search engine (24%, google, yahoo)

- **50 %** are from university or national institutes.
- 30 % are from foreign countries in **Asia**
- **20%** from Google or yahoo!!

Lessons learned from users

- A user to quick look system not always submits a job to deliver or download data
  - Data delivery request is not much; 300 scenes/300,000 access (AVHRR), 100 scenes/100,000 access (MODIS).
  - It does not always provide enough information on applications.
- **A system failure** hinders users' access on WWW
  - No idea how to submit a job on WWW or no response from the server.
  - WWW users are prone to give up with less efforts on data handling.
- System maintenance is a time-consuming job
  - Feedback or acknowledgement from users can be a strong motivation or incentive for system engineers.
  - Human resources is the most important point to keep up a system from a long term point of view.

Mission on DB station

- **Safety net** with multiple data receiving but not much connection to share know-how
  - 20 or mote NOAA AVHRR station in Japan; JMA, Tohoku-U, MAFFIN, Chiba-U, UT, Tokai-U
  - 5 or mote Aqua/Terra MODIS station in Japan; JAXA, Tokyo Info-U, UT, Tokai-U
- **Quick data delivery** is required for DB station from the users communities
  - MODIS are available from DAAC/GSFC at near real-tome (12-hrs Terra, 48-hrs Aqua)
  - AVHRR are not available at near real-time fashion on LAC.

Provide data smoothly and flexibly on users request

CONCLUDING REMARKS

- **Online** processing and delivering of AVHRR and MODIS data is introduced.
- Data distribution via WWW or FTP is developed at considerably **low cost** to make the use of open source software.
- Quick look image will be expected to work as a **rapid monitoring** system.
- Local data distributor should live up to the **needs or expectations** of local data users with a view to NPP/NPOESS era.

APPENDIX – USEFUL ONLINE DATA

DAAC NASA GSFC (MODIS data)

http://daac.gsfc.nasa.gov

Aqua / Terra MODIS processing system on WWW

http://webmodis.iis.u-tokyo.ac.jp/

NOAA/AVHRR processing system on WWW

http://webpanda.iis.u-tokyo.ac.jp/

MODIS cloud-free composite imagery

ftp://webmodis.iis.u-tokyo.ac.jp/

AVHRR cloud-free composite imagery

ftp://webpanda.iis.u-tokyo.ac.jp/


Thank you for attention!!
Photo at Phitsanulok (2004 Feb.)

CEOP Centralized Data System and integrated analysis tools

Kenji Taniguchi[1)], Toshihiro Nemoto[2)], Eiji Ikoma[3)], Masaki Yasukawa[2)], Toshio Koike[1)] and Masaru Kitsuregawa[2)]

1) Dept. of Civil Eng., Univ. of Tokyo
2) Institute of Industrial Science, Univ. of Tokyo
3) Center for Spatial Information Science, Univ. of Tokyo

11th CEReS International Symposium, 13th Dec. 2005

Outline

- Background
- Introduction of CEOP
- CEOP Centralized data system
- Integrated data analysis tools
- Future challenge of the CEOP centralized data system

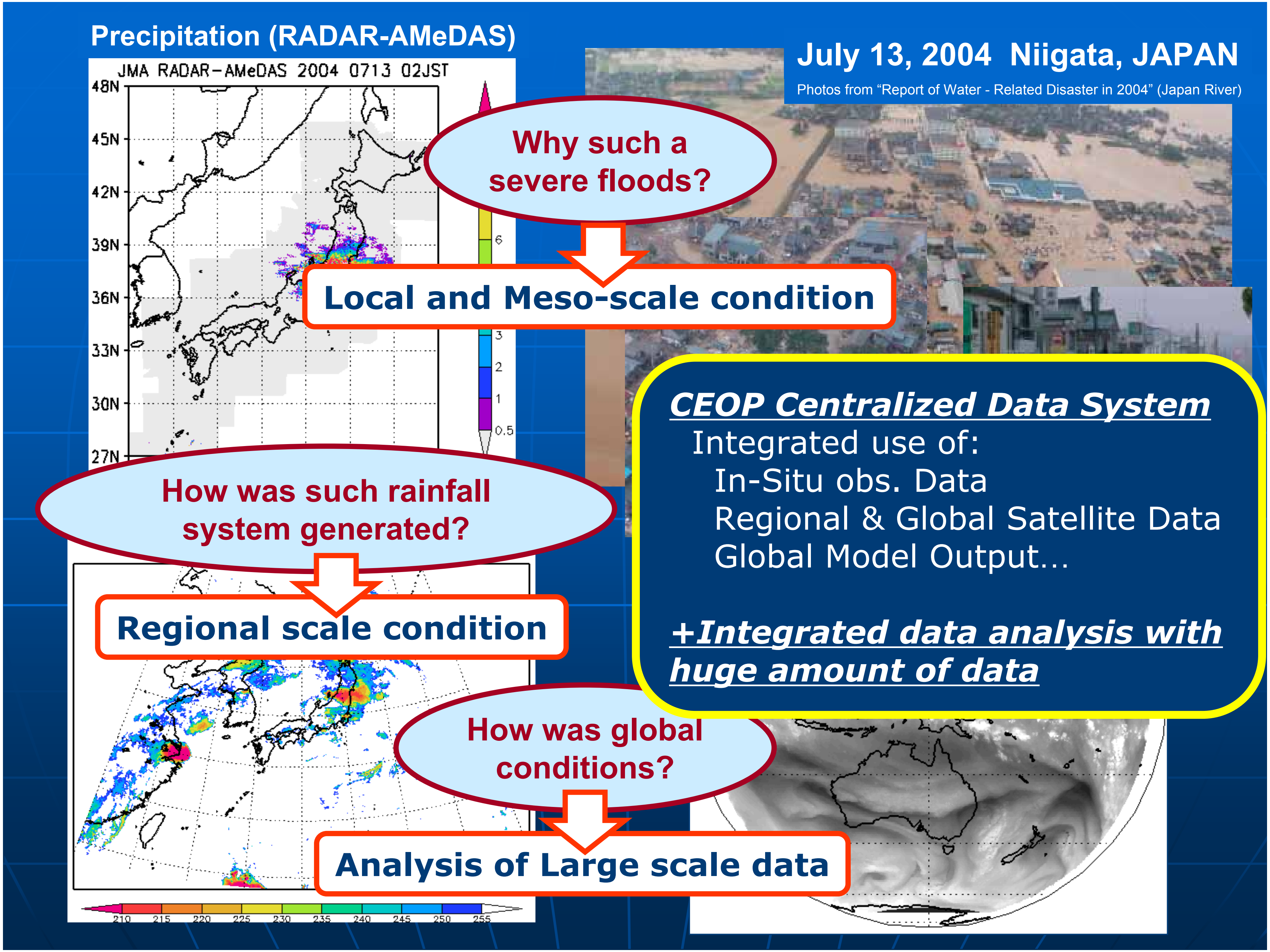
Precipitation (RADAR-AMeDAS)
JMA RADAR-AMeDAS 2004 0713 02JST
48N
45N
42N
39N
36N
33N
30N
27N
6
3
2
1
0.5
July 13, 2004 Niigata, JAPAN
Photos from “Report of Water - Related Disaster in 2004” (Japan River)
Why such a severe floods?
Local and Meso-scale condition
How was such rainfall system generated?
Regional scale condition
How was global conditions?
Analysis of Large scale data
CEOP Centralized Data System
Integrated use of:
In-Situ obs. Data
Regional & Global Satellite Data
Global Model Output…
+Integrated data analysis with huge amount of data
210
215
220
225
230
235
240
245
250
255

Coordinated Enhanced Observing Period
Three Unique Capabilities

A Prototype of the Global Water Cycle Observation System of Systems

International Cooperation for the Global Coverage

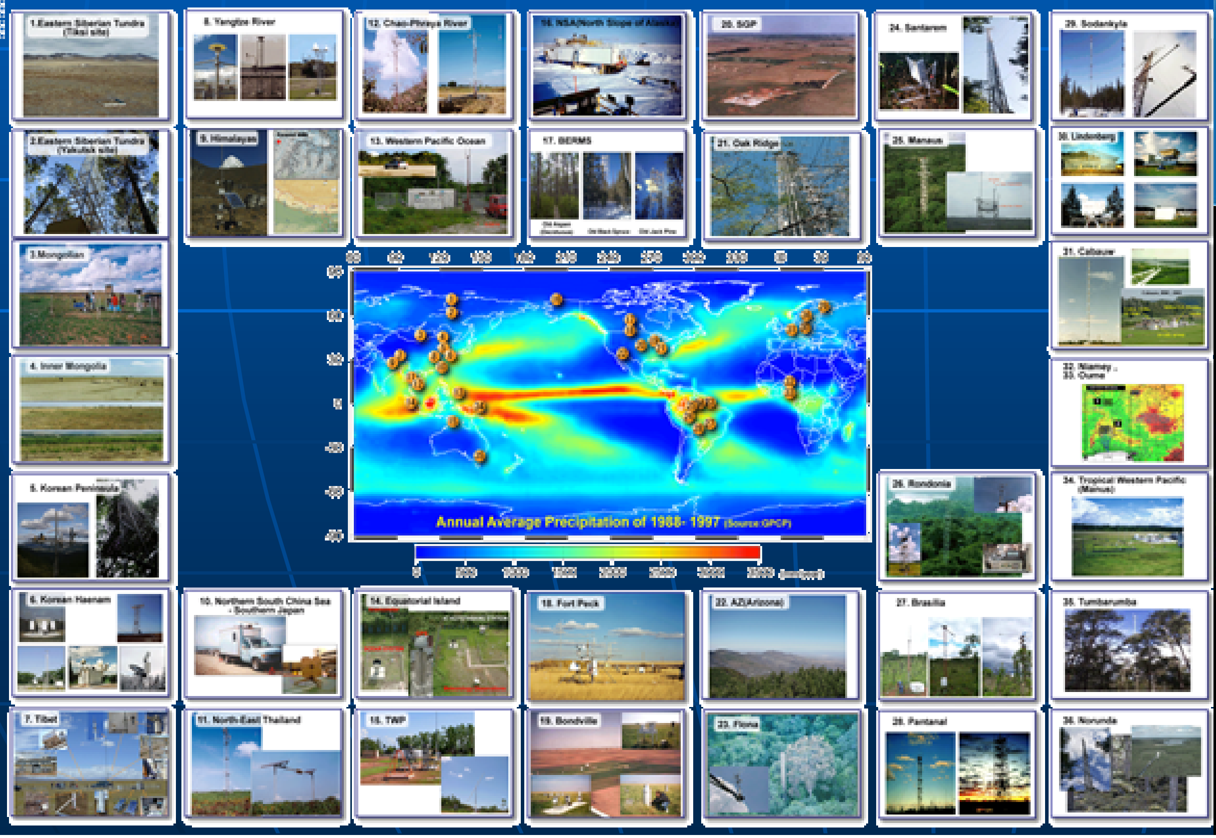

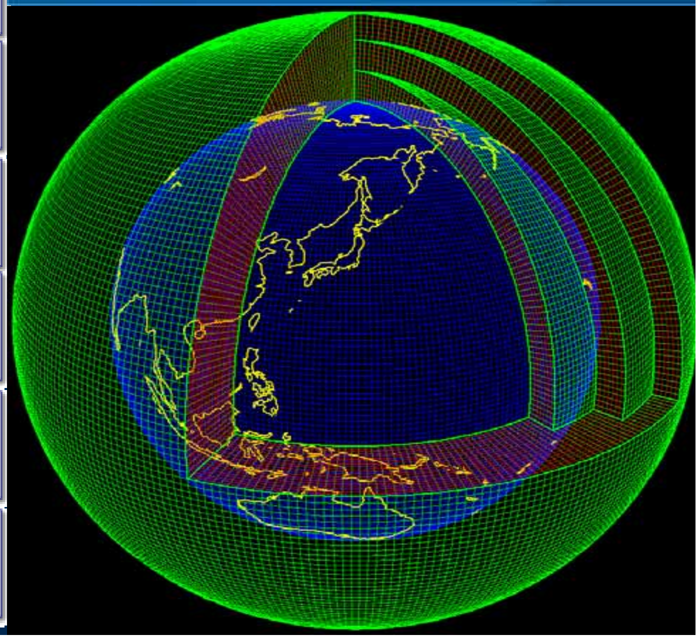

Coordinated Enhanced Observing Period
Three Unique Capabilities

A Well Organized Data Archive System

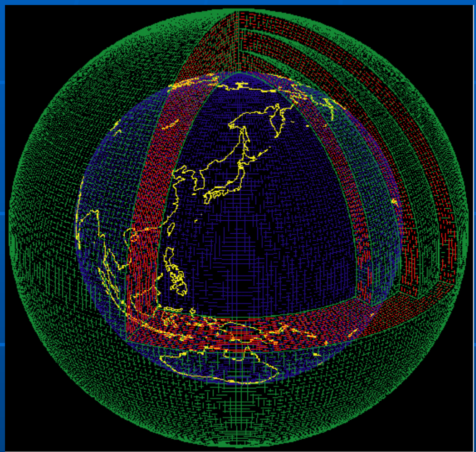

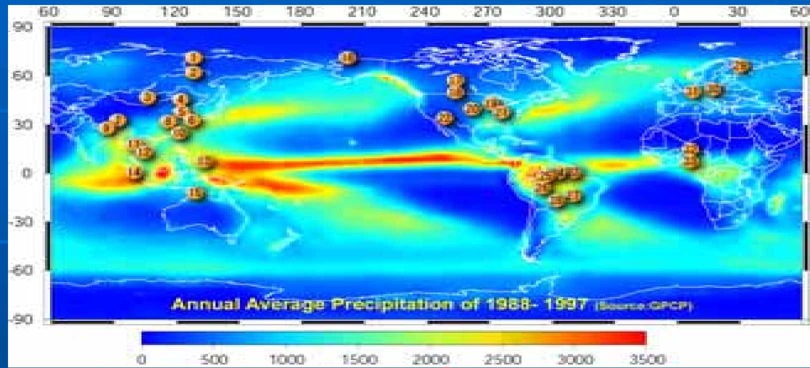

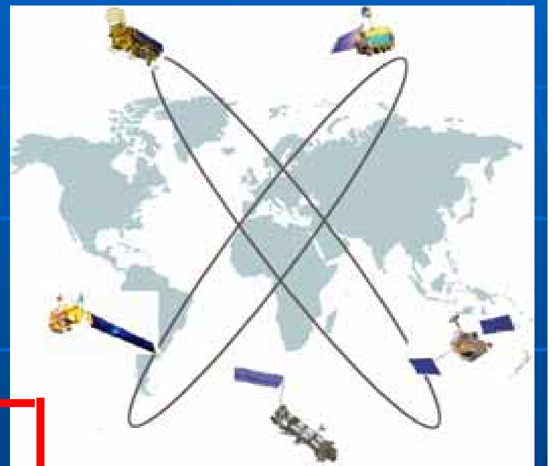

In-Situ Data Archiving Center at UCAR (University Corporation for Atmospheric Research) of USA

Model Output Data Archiving Center at the World Data Center for Climate, Max-Planck Institute for Meteorology of Germany

Data Integrating/Archiving Center at University of Tokyo and JAXA of Japan

Architecture of Centralized Data Integration System

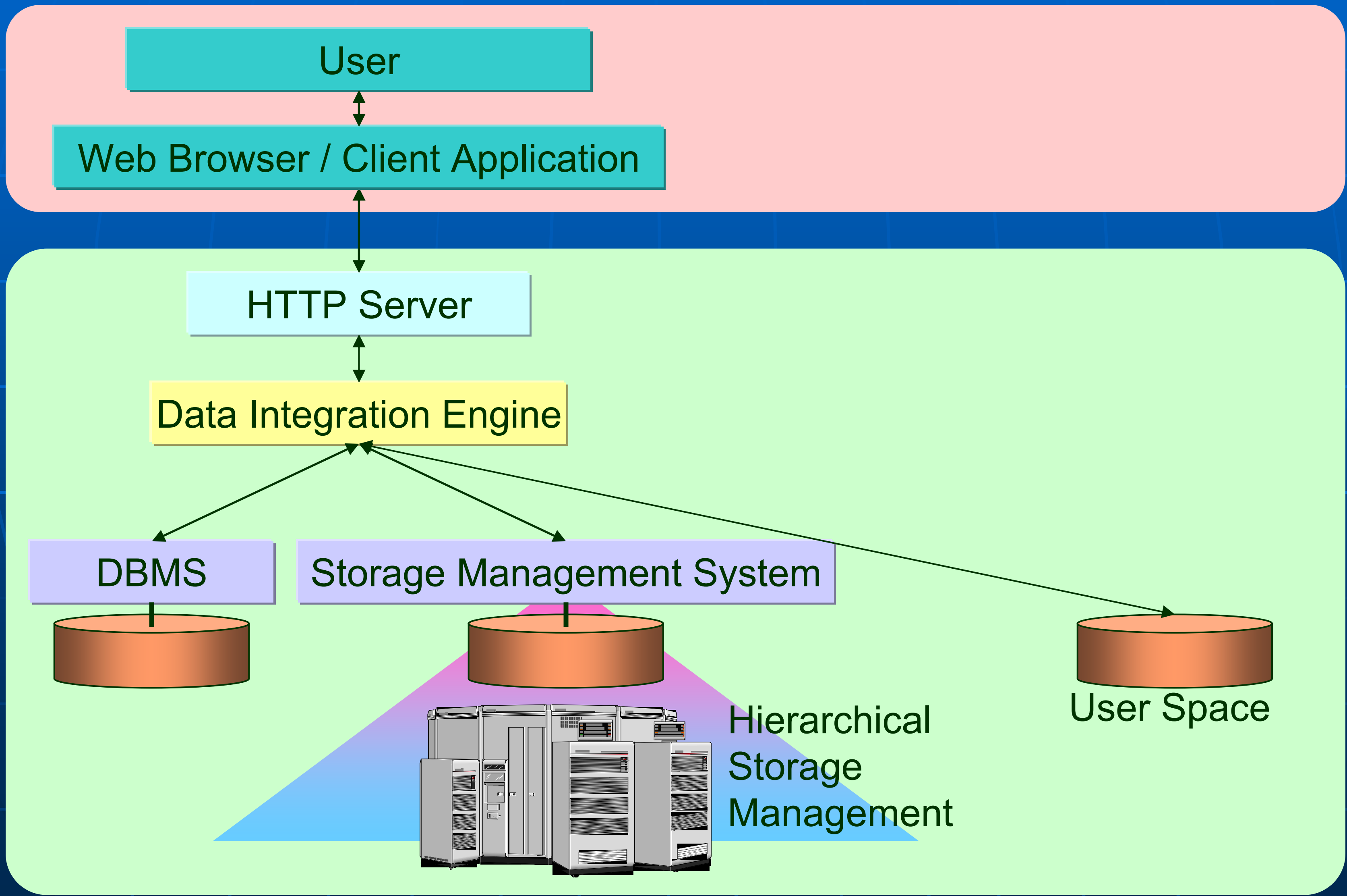

Request and Data Flow
- Retrieval -

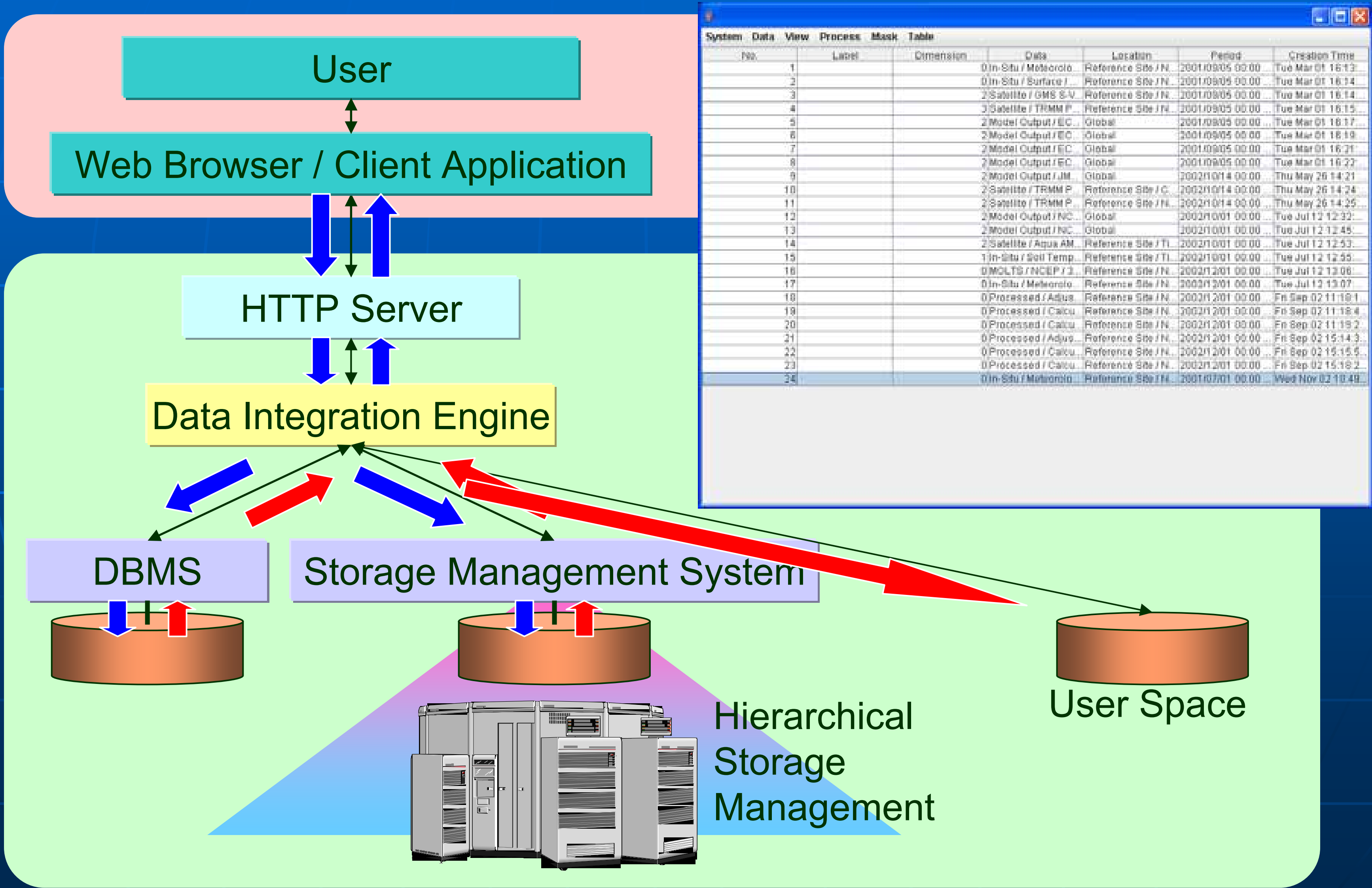

No.	Label	Dimension	Data	Location	Period	Creation Time
1		0	In-Situ / Meteorolo...	Reference Site / N...	2001/09/05 00:00 ...	Tue Mar 01 16:13:
2		0	In-Situ / Surface / ...	Reference Site / N...	2001/09/05 00:00 ...	Tue Mar 01 16:14
3		2	Satellite / GMS S-V...	Reference Site / N...	2001/09/05 00:00 ...	Tue Mar 01 16:14
4		3	Satellite / TRMM P...	Reference Site / N...	2001/09/05 00:00 ...	Tue Mar 01 16:15
5		2	Model Output / EC...	Global	2001/09/05 00:00 ...	Tue Mar 01 16:17
6		2	Model Output / EC...	Global	2001/09/05 00:00 ...	Tue Mar 01 16:19
7		2	Model Output / EC...	Global	2001/09/05 00:00	Tue Mar 01 16:21:
8		2	Model Output / EC...	Global	2001/09/05 00:00	Tue Mar 01 16:22:
9		2	Model Output / JM...	Global	2002/10/14 00:00	Thu May 26 14:21
10		2	Satellite / TRMM P...	Reference Site / C...	2002/10/14 00:00	Thu May 26 14:24
11		2	Satellite / TRMM P...	Reference Site / N...	2002/10/14 00:00 ...	Thu May 26 14:25
12		2	Model Output / NC...	Global	2002/10/01 00:00 ...	Tue Jul 12 12:32:...
13		2	Model Output / NC...	Global	2002/10/01 00:00 ...	Tue Jul 12 12:45:...
14		2	Satellite / Aqua AM...	Reference Site / Ti...	2002/10/01 00:00 ...	Tue Jul 12 12:53:...
15		1	In-Situ / Soil Temp...	Reference Site / Ti...	2002/10/01 00:00 ...	Tue Jul 12 12:55:...
16		0	MOLTS / NCEP / 3...	Reference Site / N...	2002/12/01 00:00 ...	Tue Jul 12 13:06:...
17		0	In-Situ / Meteorolo...	Reference Site / N...	2002/12/01 00:00 ...	Tue Jul 12 13:07
18		0	Processed / Adjus...	Reference Site / N...	2002/12/01 00:00 ...	Fri Sep 02 11:18:1
19		0	Processed / Calcu...	Reference Site / N...	2002/12/01 00:00 ...	Fri Sep 02 11:18:4
20		0	Processed / Calcu...	Reference Site / N...	2002/12/01 00:00 ...	Fri Sep 02 11:19:2
21		0	Processed / Adjus...	Reference Site / N...	2002/12/01 00:00 ...	Fri Sep 02 15:14:3...
22		0	Processed / Calcu...	Reference Site / N...	2002/12/01 00:00 ...	Fri Sep 02 15:15:5...
23		0	Processed / Calcu...	Reference Site / N...	2002/12/01 00:00 ...	Fri Sep 02 15:18:2...
24		0	In-Situ / Meteorolo...	Reference Site / N...	2001/07/01 00:00 ...	Wed Nov 02 10:49...

Request and Data Flow
- Visualization -

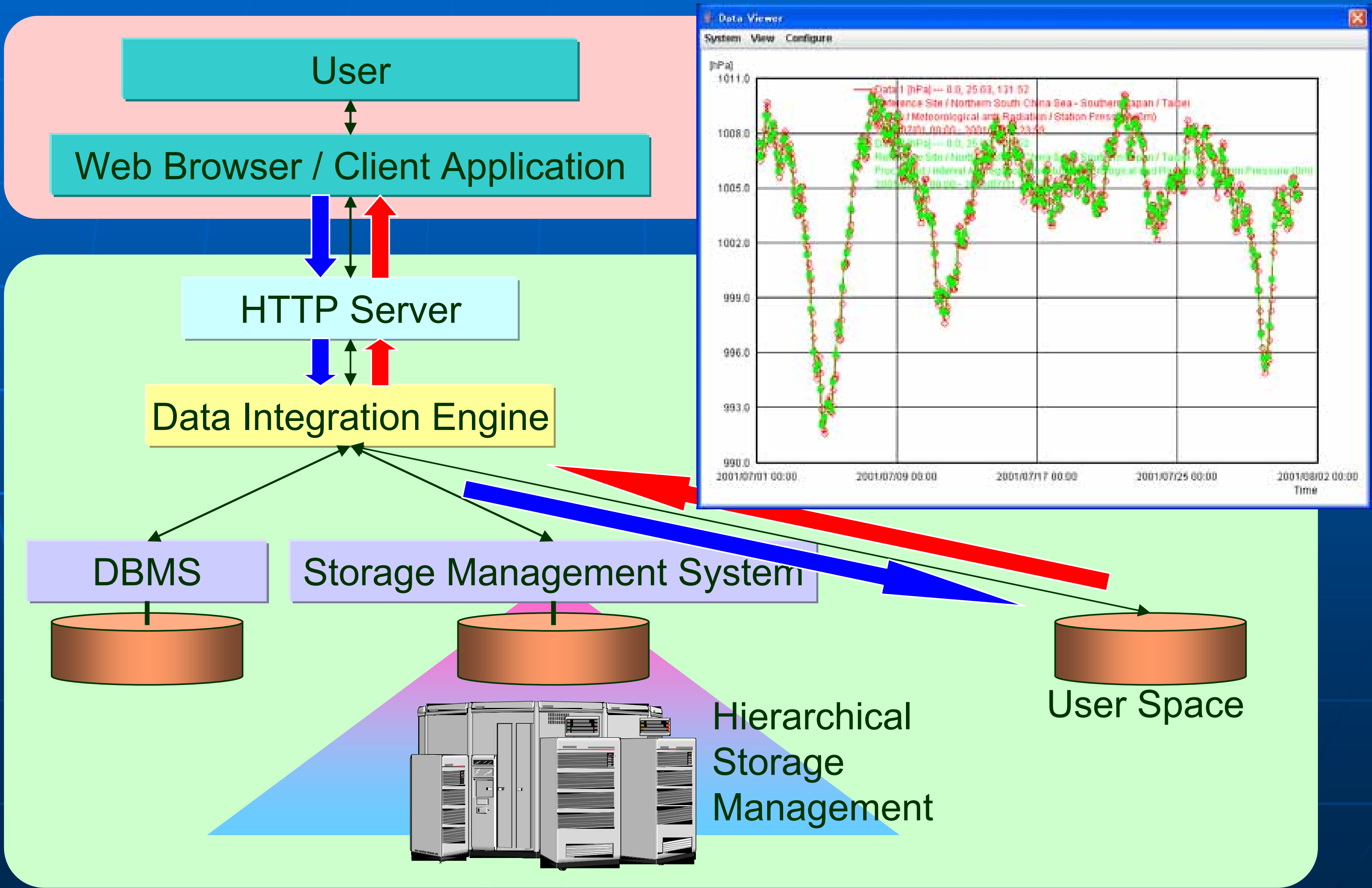

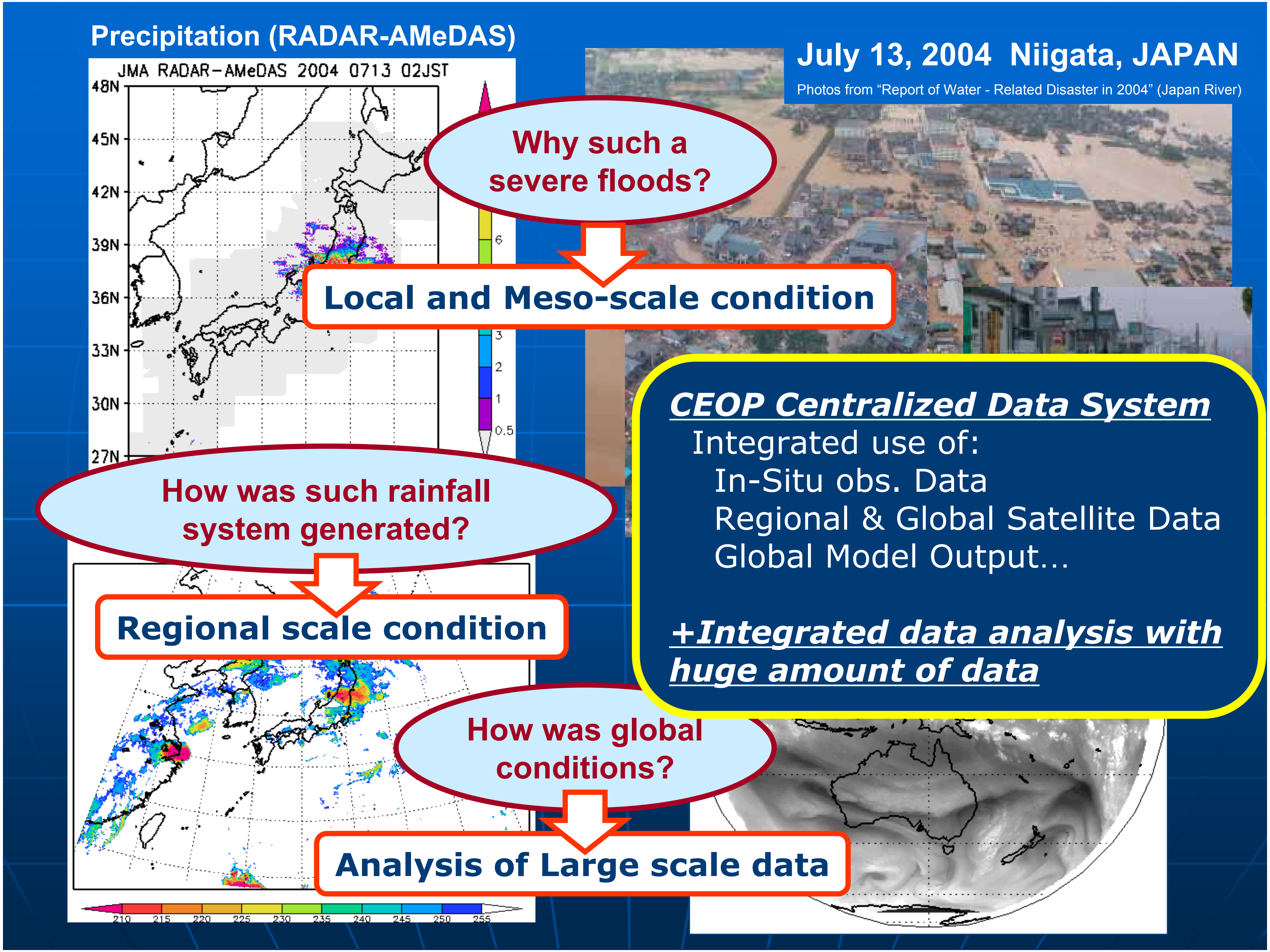
Precipitation (RADAR-AMeDAS)
JMA RADAR-AMeDAS 2004 0713 02JST
48N
45N
42N
39N
36N
33N
30N
27N
6
3
2
1
0.5
July 13, 2004 Niigata, JAPAN
Photos from "Report of Water - Related Disaster in 2004" (Japan River)
Why such a severe floods?
Local and Meso-scale condition
How was such rainfall system generated?
Regional scale condition
How was global conditions?
Analysis of Large scale data
CEOP Centralized Data System
Integrated use of:
In-Situ obs. Data
Regional & Global Satellite Data
Global Model Output…
+Integrated data analysis with huge amount of data
210
215
220
225
230
235
240
245
250
255

3D Data Visualization System at Univ. of Tokyo

Development of a 3D Data Visualization System

- Tool for mesoscale analysis
- Asia Area (10N-50N, 70E-150E)
- Cutting out arbitrary surface from 3D data
- Displaying multiple 3D data in virtual reality space
- Web interface with easy treatment

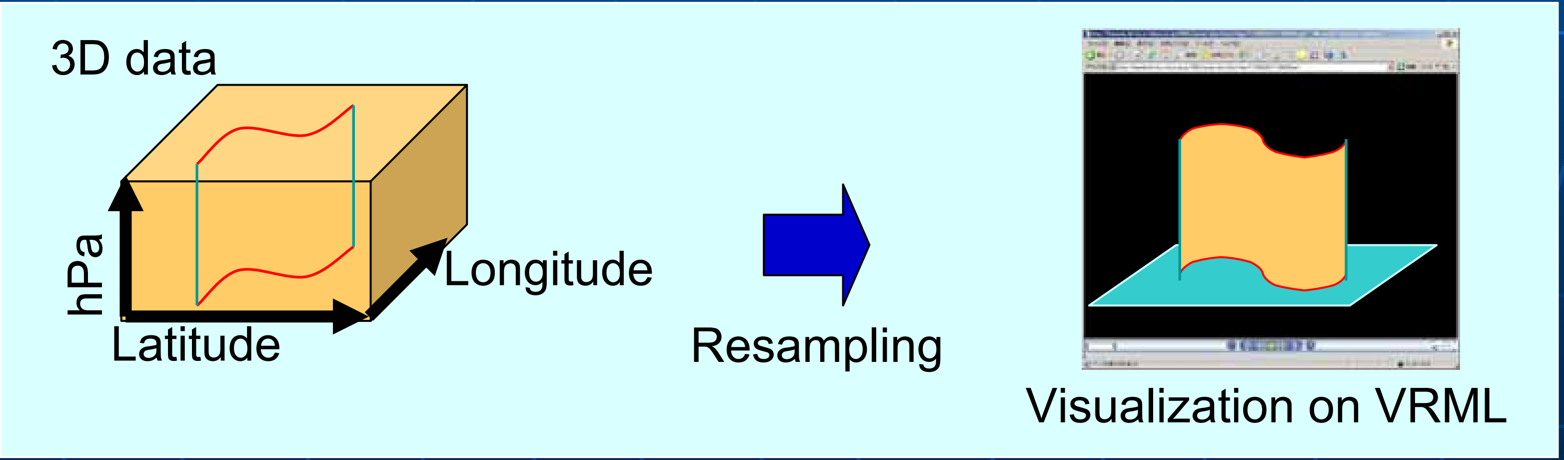

3D Data Visualization System at Univ. of Tokyo

Demonstration:

Heavy Rain in Niigata and Fukui in 2004

- ◆2004/07/09-2004/07/14
- ◆Water vapor [gm/kg_dry_air] of AIRS products
  - •AIRS (Atmospheric Infrared Sounder) on Aqua Satellite
  - •28 pressure levels
  - •Arbitrary surface (Shaded contour plot)
- ◆Geopotential height [m] of NCEP/NCAR reanalysis data
  - •17 pressure levels
  - •Contour line

3D Data Visualization System at Univ. of Tokyo

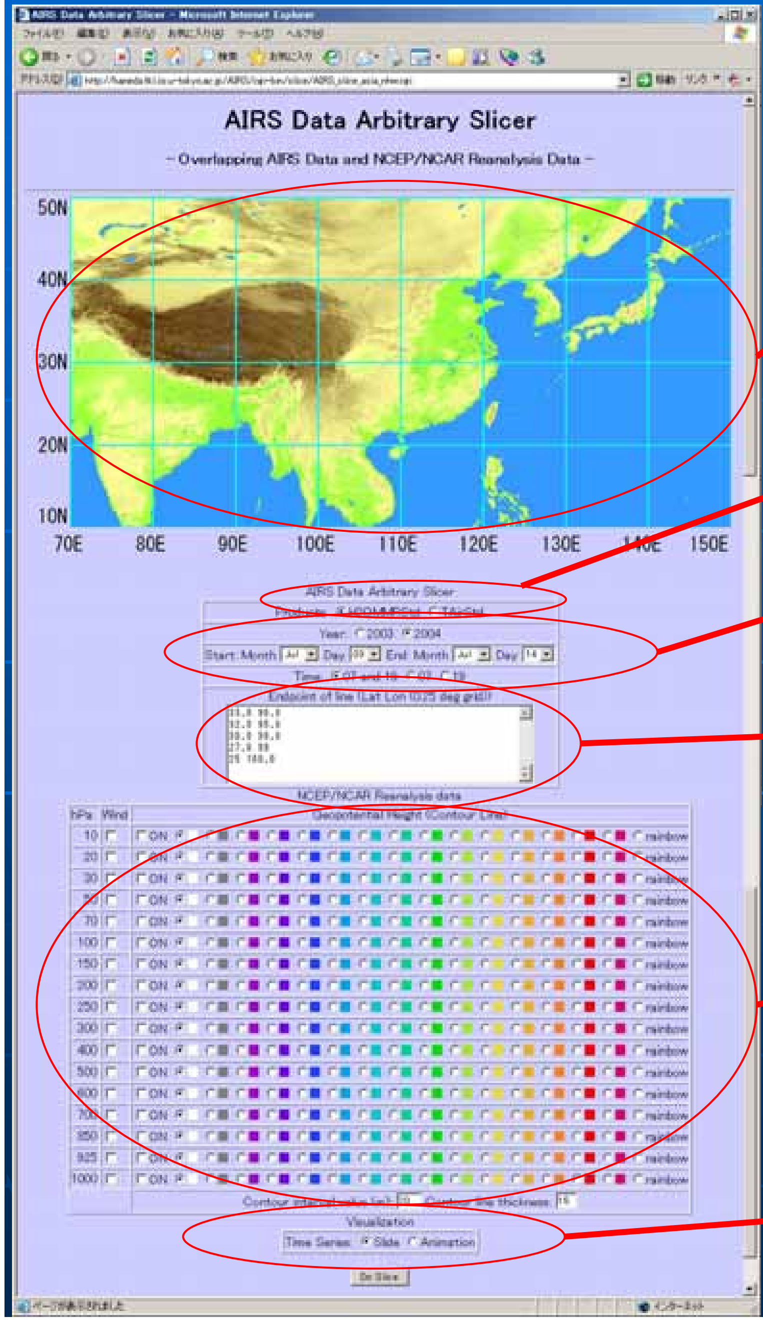

Data Selection Page

Coverage of this tool
(10N-50N, 70E-150E)

AIRS Products

Period

Points on arbitrary surface
(latitude, longitude)

NCEP/NCAR Reanalysis data
on each pressure level
(geopotential height, wind)

Visualization type
(slide or animation)

High dimensional Information Extraction
Using Integrated Data visualization and Analysis System

- Correlation Coefficient Analysis tool
- Spatial Filtering Analysis System

for Huge Volume Data of Water Cycle Change

Correlative Analysis System of Climate Anomalies

•PURPOSE=Search the correlation between the base time sequential data and other various kind,area,time of data.

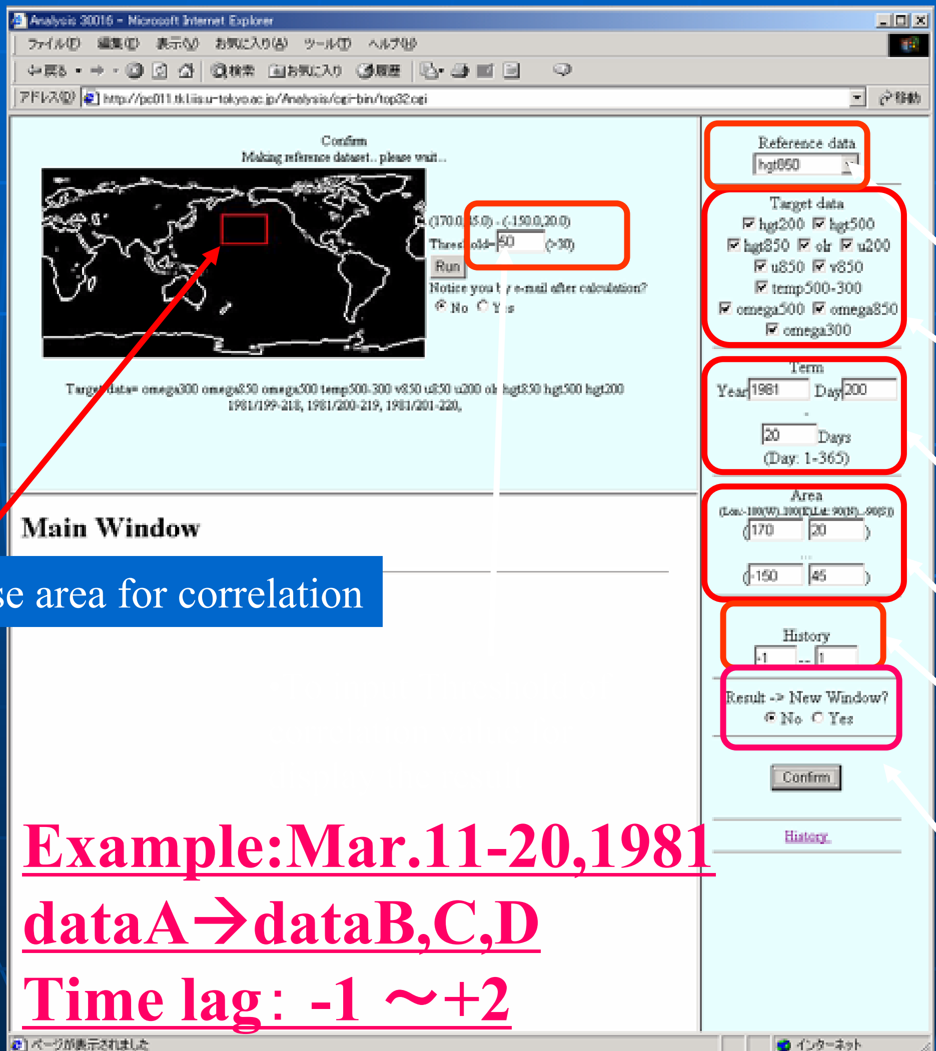

•Base area for correlation

Example:Mar.11-20,1981

dataA→dataB,C,D

Time lag：-1 ～+2

•Select Base data

•Select target data to analyze the correlation

•Define the period of correlation analysis(to cut-off the time sequential data)

•Define the area of base date

•Define the time lag

•After processing, whether the system notice to user by e-mail or not

Result (1)

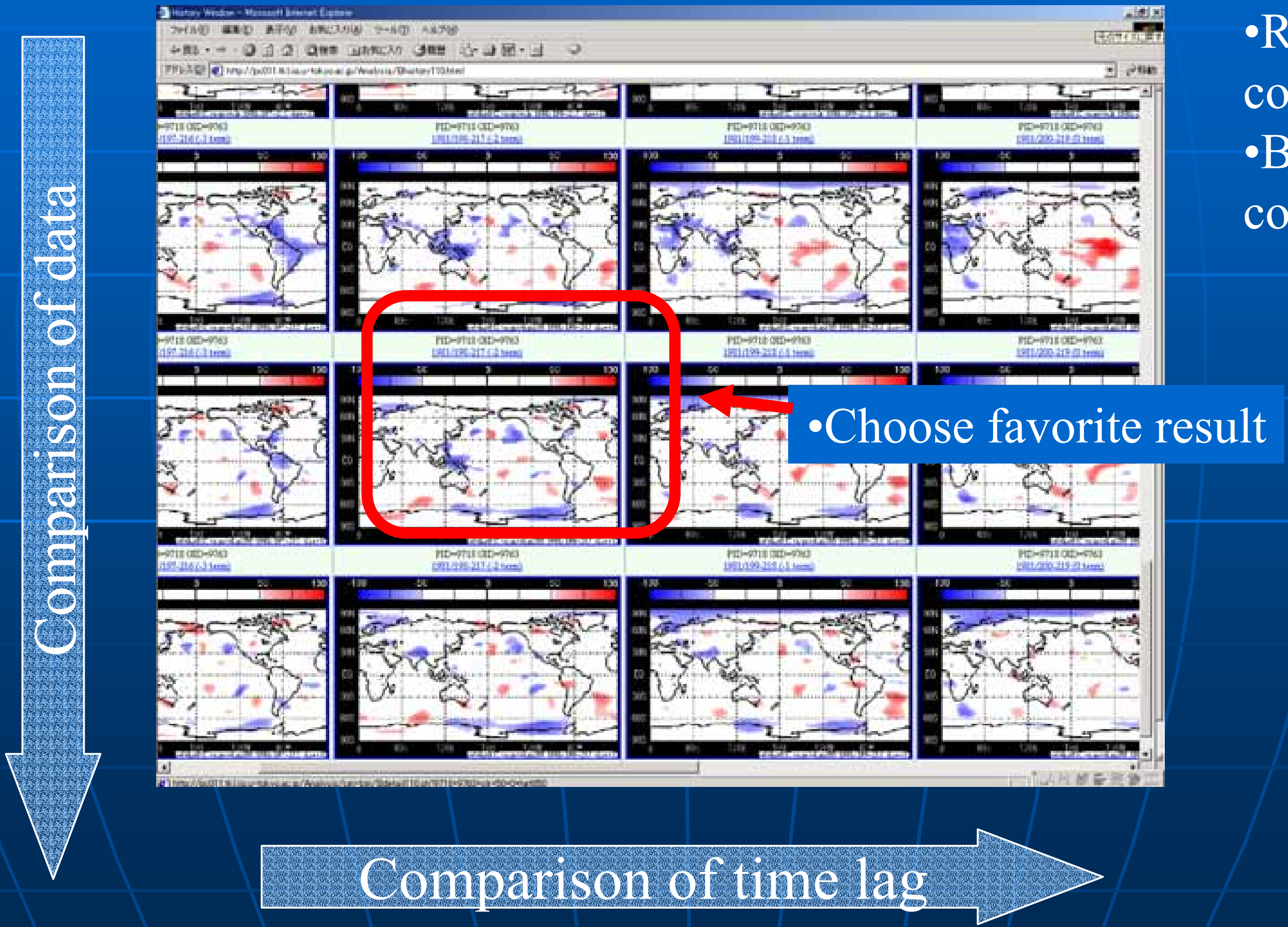

•Red: positive correlation
•Blue: negative correlation

Result(2)

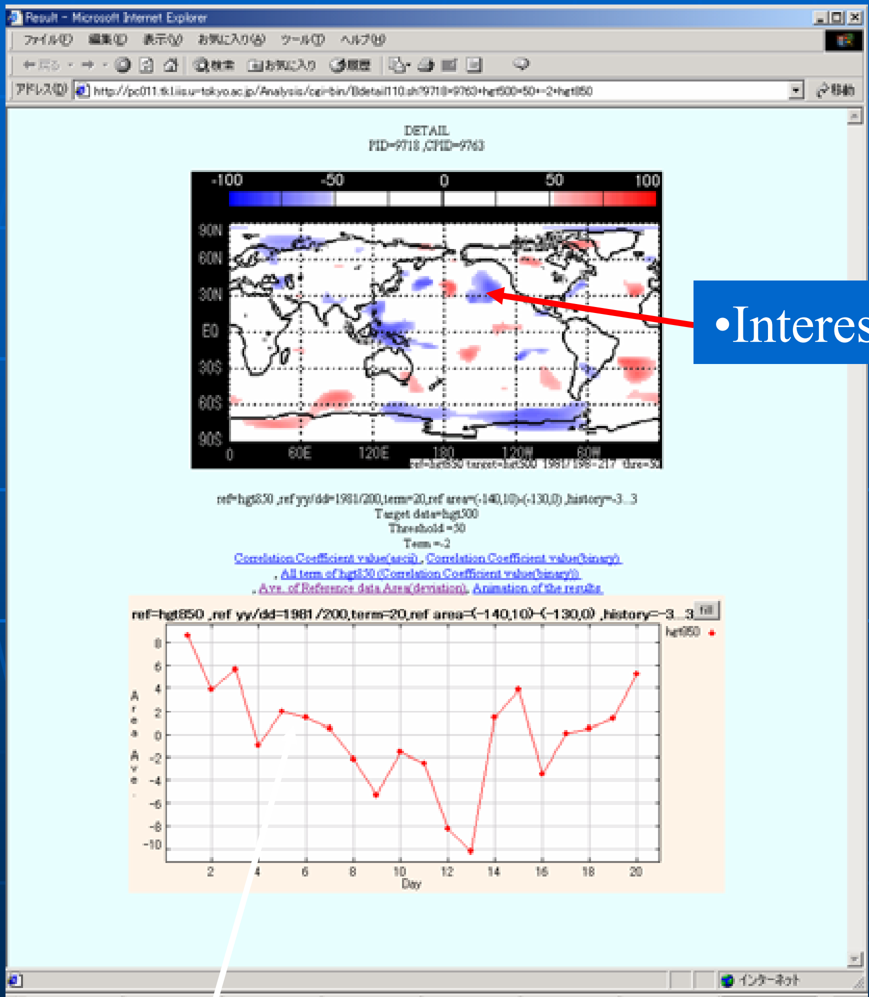

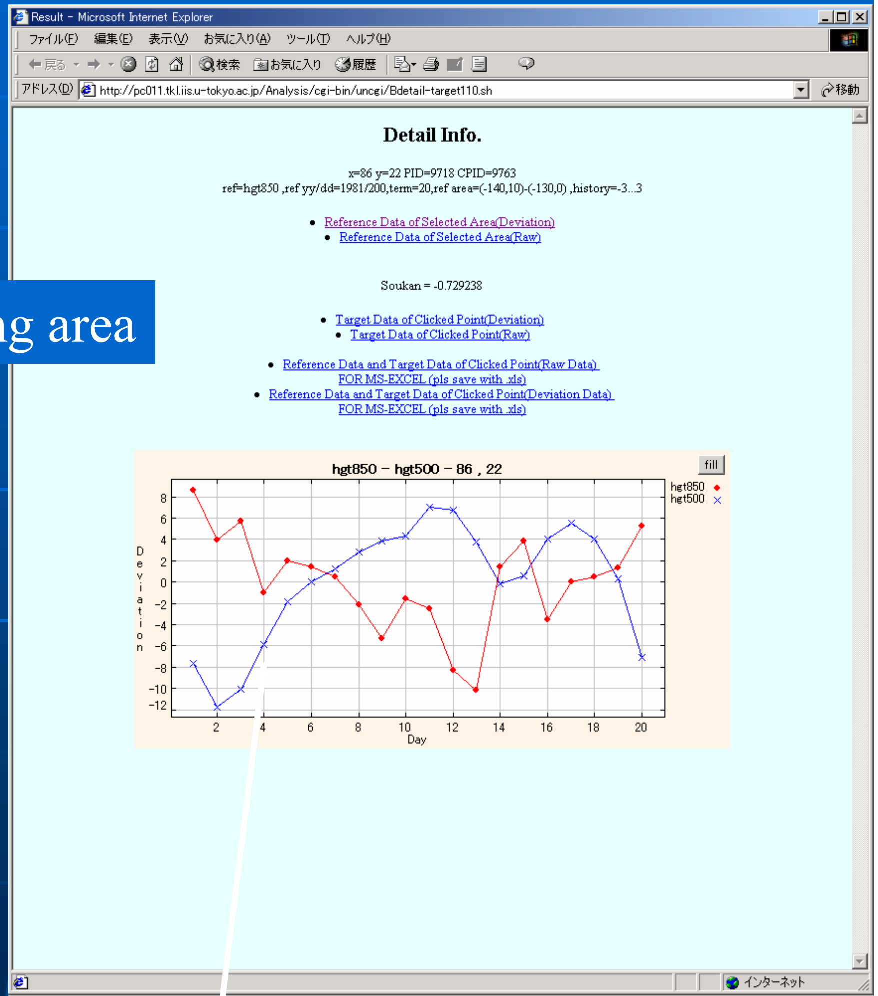

•Interesting area

•Time sequential info of clicked point

•Time sequential information of base data

Result(3)

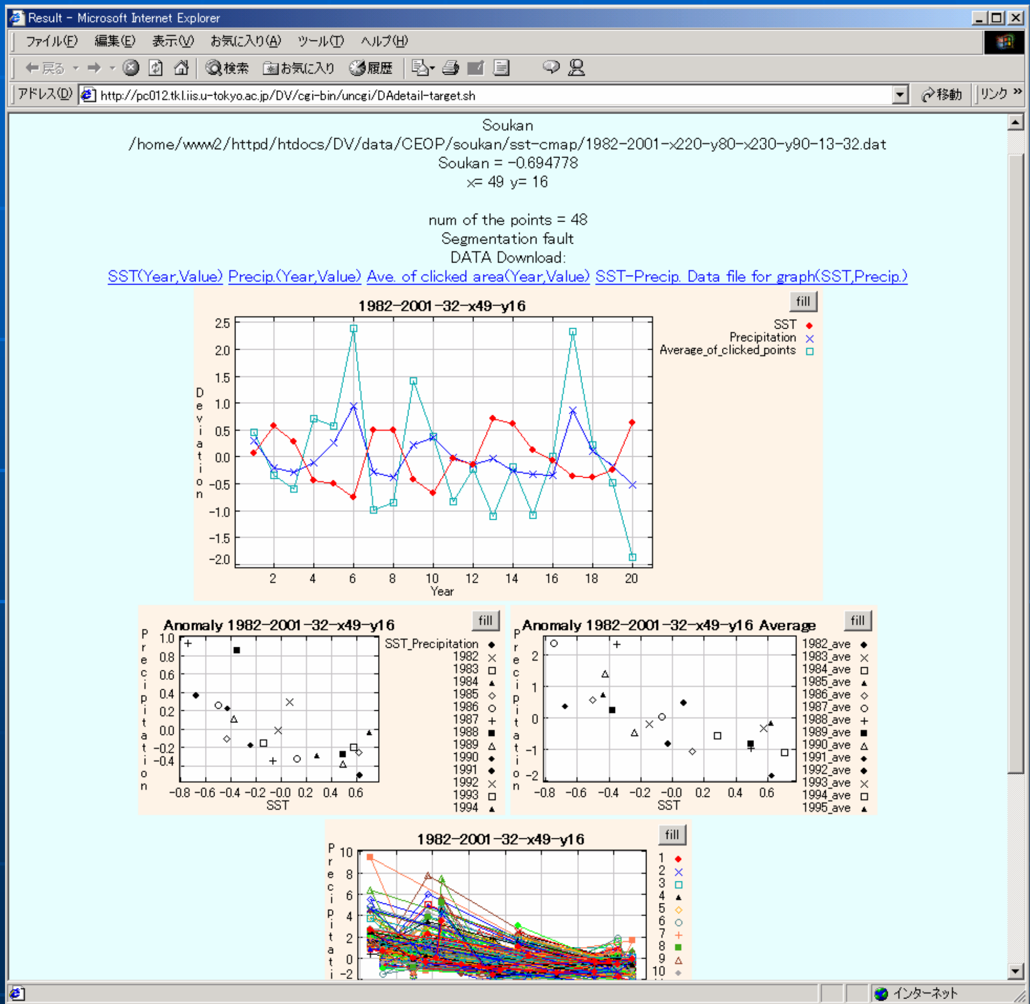

Result - Microsoft Internet Explorer
http://pc012.tkl.iis.u-tokyo.ac.jp/DV/cgi-bin/uncgi/DAdetail-target.sh
Soukan
/home/www2/httpd/htdocs/DV/data/CEOP/soukan/sst-cmap/1982-2001-x220-y80-x230-y90-13-32.dat
Soukan = -0.694778
x= 49 y= 16
num of the points = 48
Segmentation fault
DATA Download:
SST(Year,Value) Precip.(Year,Value) Ave. of clicked area(Year,Value) SST-Precip. Data file for graph(SST,Precip.)
1982-2001-32-x49-y16
SST
Precipitation
Average_of_clicked_points
Deviation
Year
Anomaly 1982-2001-32-x49-y16
SST_Precipitation
Anomaly 1982-2001-32-x49-y16 Average
Precipitation
SST
1982-2001-32-x49-y16

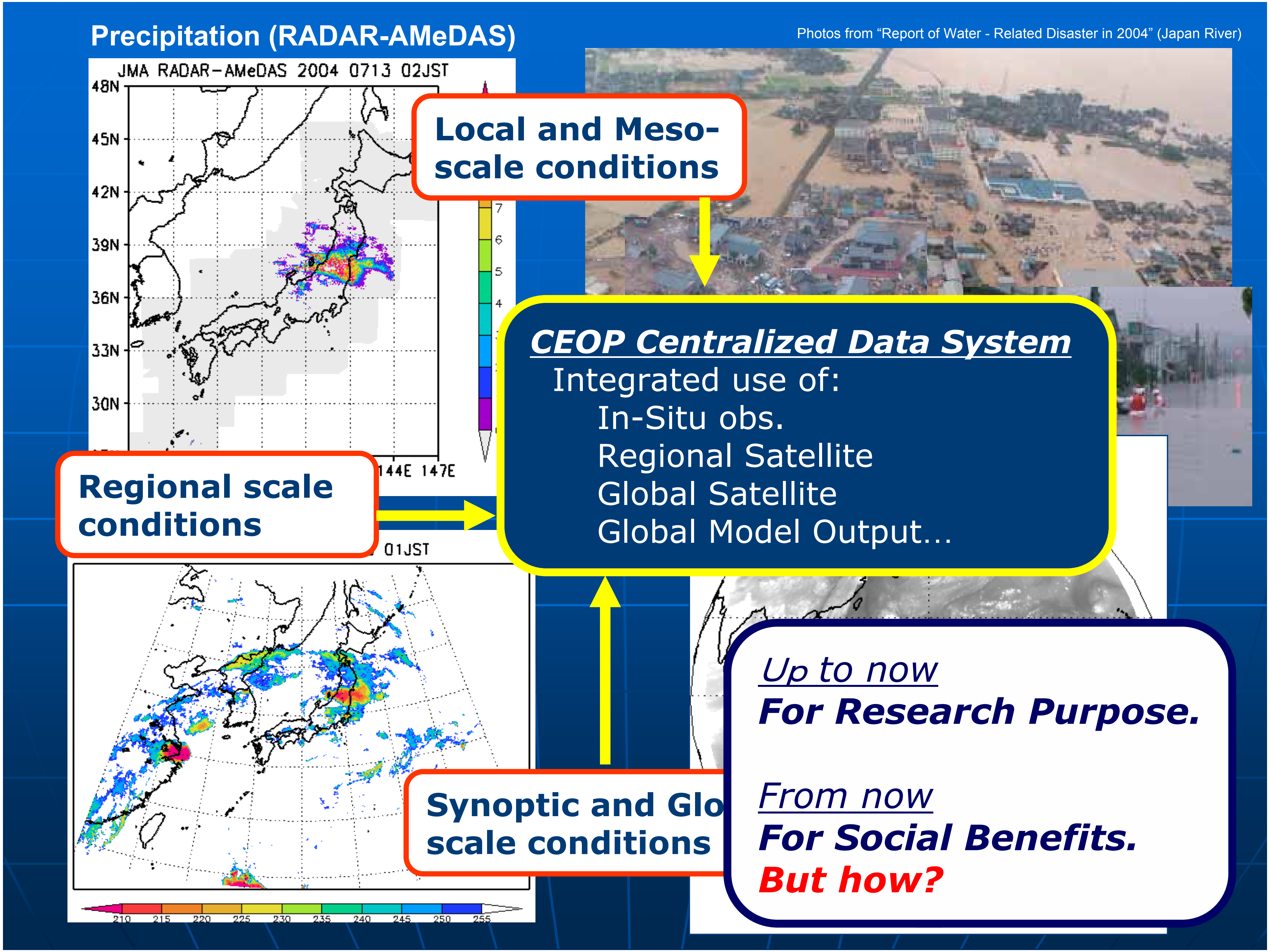
Precipitation (RADAR-AMeDAS)
Photos from "Report of Water - Related Disaster in 2004" (Japan River)
JMA RADAR-AMeDAS 2004 0713 02JST
48N
45N
42N
39N
36N
33N
30N
144E 147E
01JST
Local and Meso-scale conditions
Regional scale conditions
CEOP Centralized Data System
Integrated use of:
In-Situ obs.
Regional Satellite
Global Satellite
Global Model Output…
Synoptic and Glo
scale conditions
Up to now
For Research Purpose.
From now
For Social Benefits.
But how?
210 215 220 225 230 235 240 245 250 255

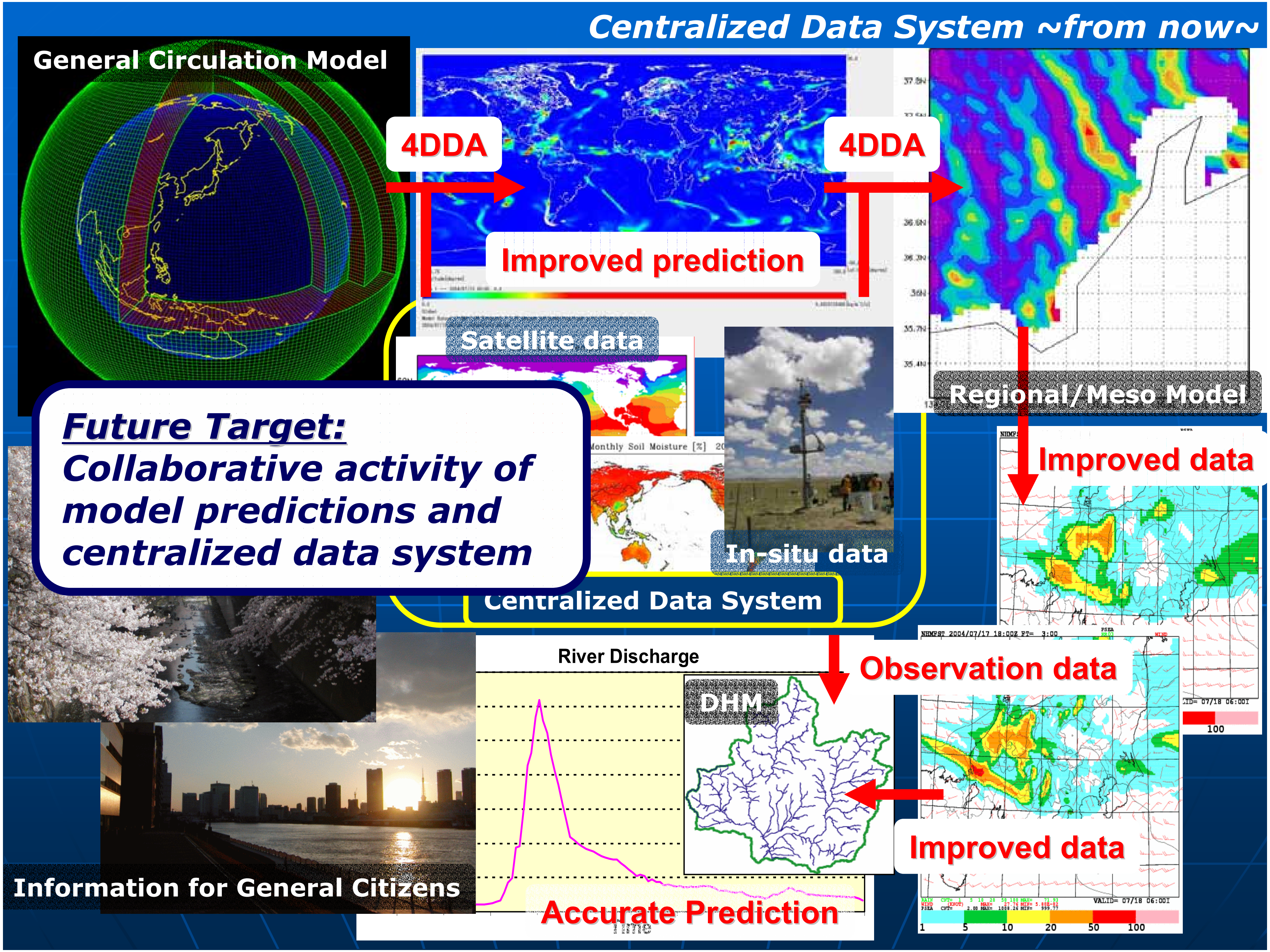

Centralized Data System ~from now~
General Circulation Model
4DDA
4DDA
Improved prediction
Satellite data
Monthly Soil Moisture [%]
In-situ data
Regional/Meso Model
Improved data
Future Target:
Collaborative activity of model predictions and centralized data system
Centralized Data System
River Discharge
DHM
Observation data
Improved data
Accurate Prediction
Information for General Citizens

Summary

- CEOP centralized data system realizes visualization and data analysis of multi-scale, various and huge amount of data (In-situ, satellite and model output).
- CEOP centralized data system has been developed mainly for research purposes. From now, such a data integration system should aim to social benefits.
- For that purpose, an ongoing challenge (cooperation of *meteorological/hydrological modeling and data management system*) is one possible prototype of next "***Multi-scale Data/Information Fusion***".

Thank You.

The 11th CEReS Int. Symp. On Remote Sensing, 13 Dec 2005

TRMM PR, its possibility and limitation for the global mapping of precipitation

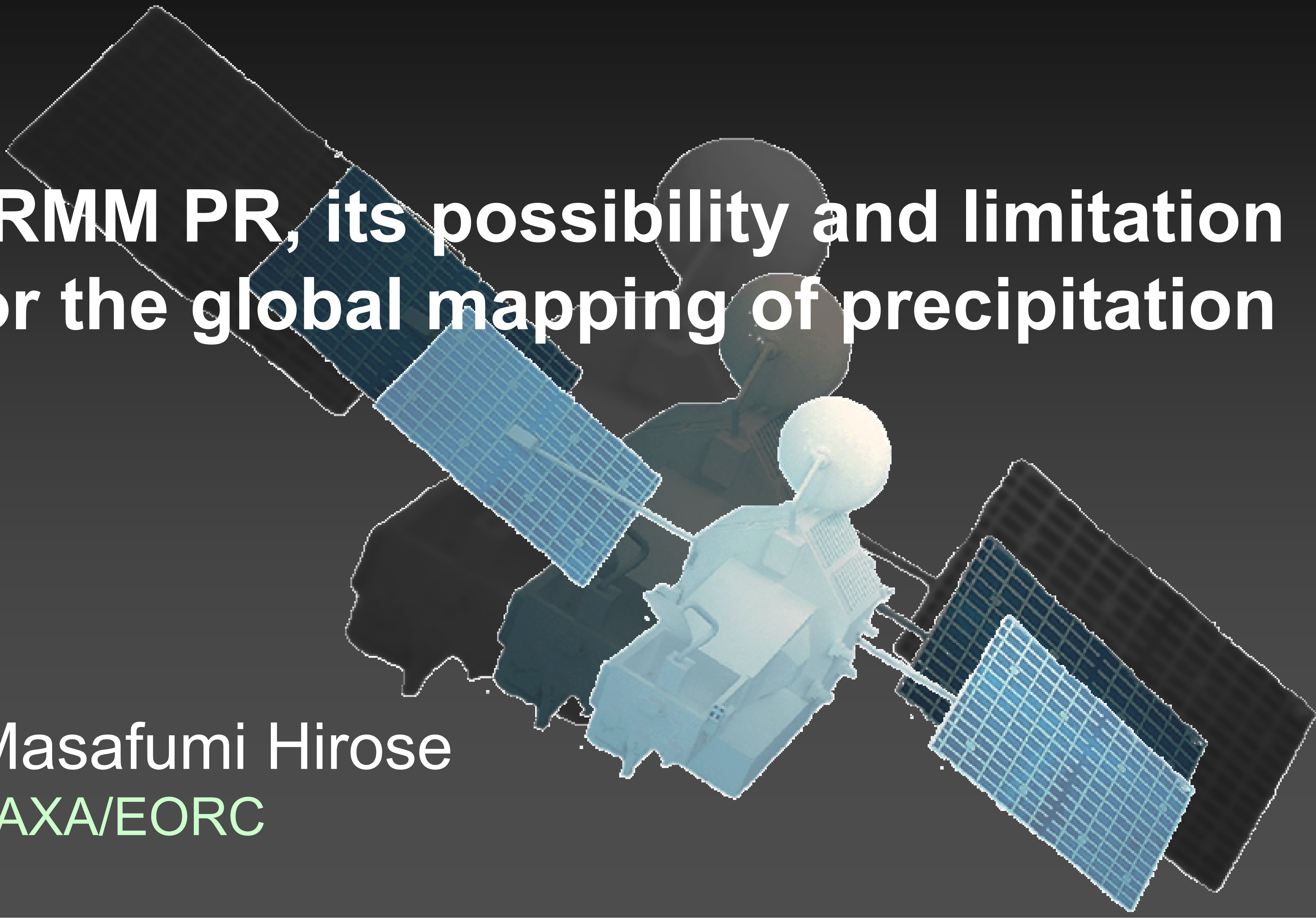

Masafumi Hirose
JAXA/EORC

Topics

0. What is TRMM PR?

1. The unique strengths of the observation

2. The sampling issue for the global mapping of precipitation

3. Spatiotemporal features of rainfall by 8-year data

4. Rainfall map in view of "Precipitation system climatology"

5. Remaining issues on the precipitation retrieval

0. What is TRMM PR?

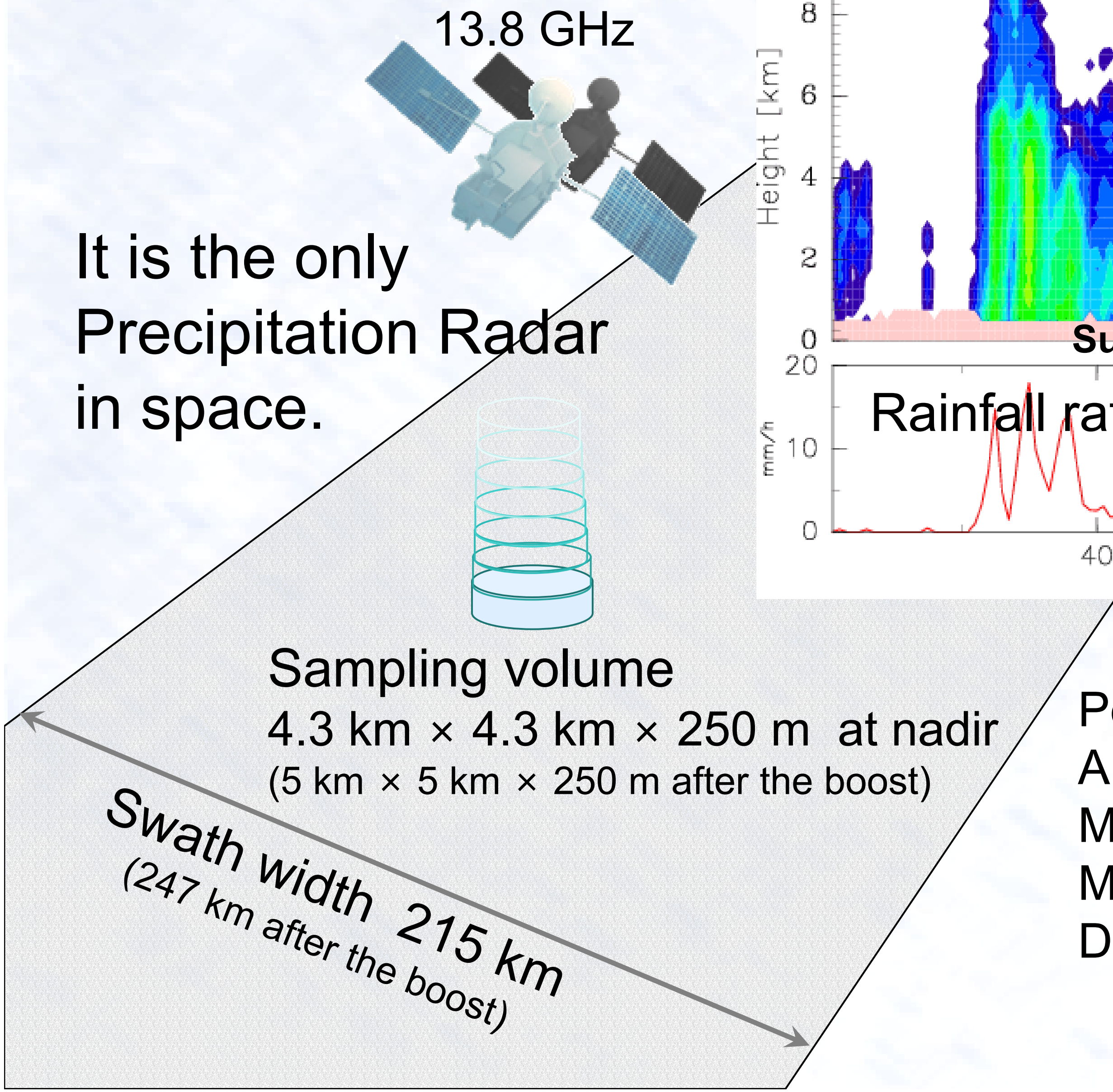

It is the only Precipitation Radar in space.

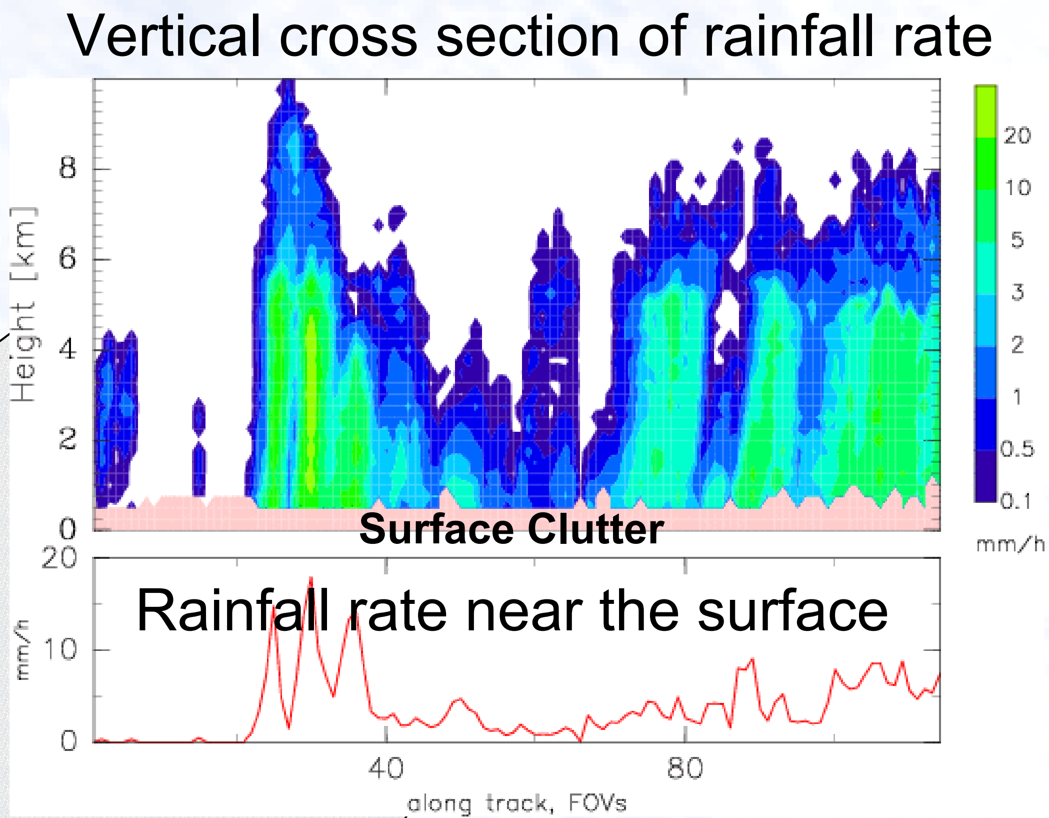

Period: 1997/12-, 8yrs

Area: 36S-36N

Main dataset: 2A25, v.6

Main data: Z, Rainfall rate

Datasize: 780 GB (compressed)

12.5 TB (original)

1. The unique strengths of the observation

• Global 3-D observation of precipitating echo

- provides homogeneous dataset over land and ocean

- improved the algorithm of the precipitation type required for specifying the drop-size distribution

- collected a number of precipitation profiles which is indispensable to the conventional retrievals by using remotely sensed proxies

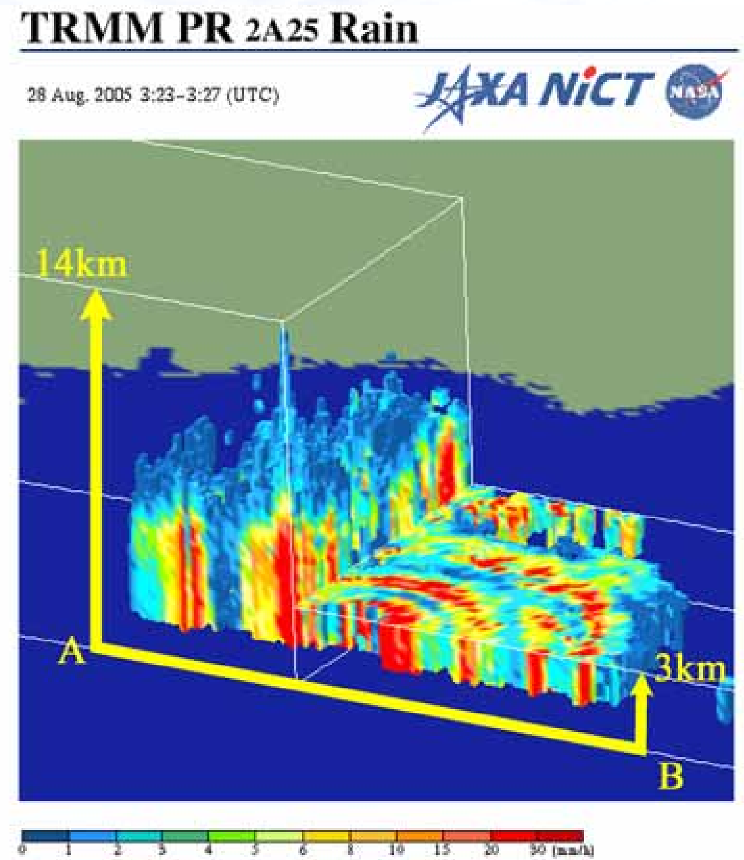

cont'd

- **Attenuation correction**

 - is developed by utilizing the path integrated attenuation

- **Non-sun-synchronous orbit**

 - makes the statistics more accurate by sampling various developing stages (i.e., the diurnal cycle) of convective activity

- **The combination of the multiple sensors on the same platform**

 - enabled us to examine data characteristics of the radar together with other sensors such as the microwave radiometer (TMI)

2. The sampling issue for the global mapping of precipitation

The number of samples over 0.1-deg-box during August 1998

1-10th 11-20th 21-31th 1-31th

0-6 LT

6-12 LT

12-18 LT

18-24 LT

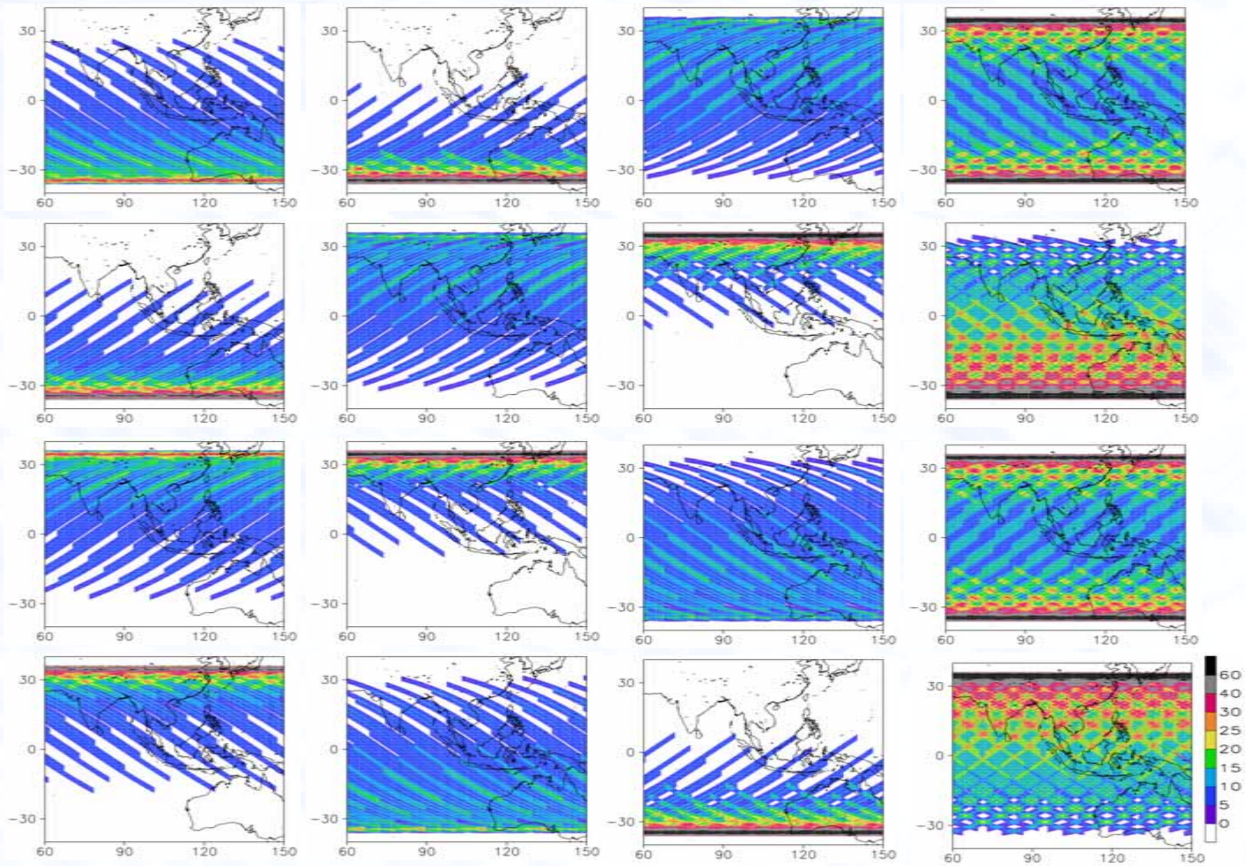

We are not data rich for any given month. The frequency is about 12 to 60 times per a month. The sampling bias should be kept in mind for one-month data.

Reduction of the uncertainty by using multiple-year data

A number of samples are required to understand the features of precipitation systems which exist in various spatiotemporal scales. The 8-year data is of great utility in the study of <u>regional and diurnal variations</u> of precipitation.

The sampling retains the local time bias for any given month.

The minimum number of hourly samples is significantly increased by using the eight-year data.

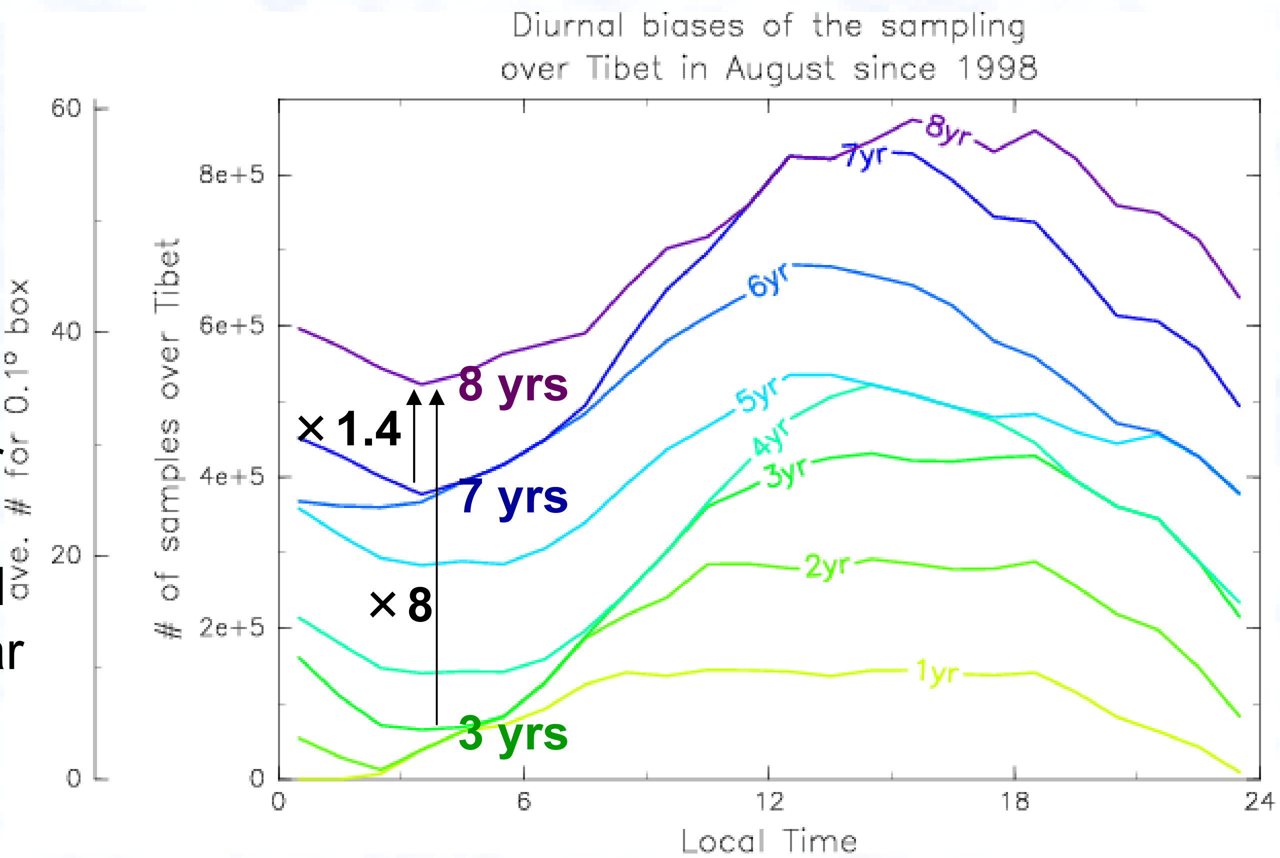

3. Spatiotemporal features of rainfall by 8-year data

Impact of long-term data accumulation

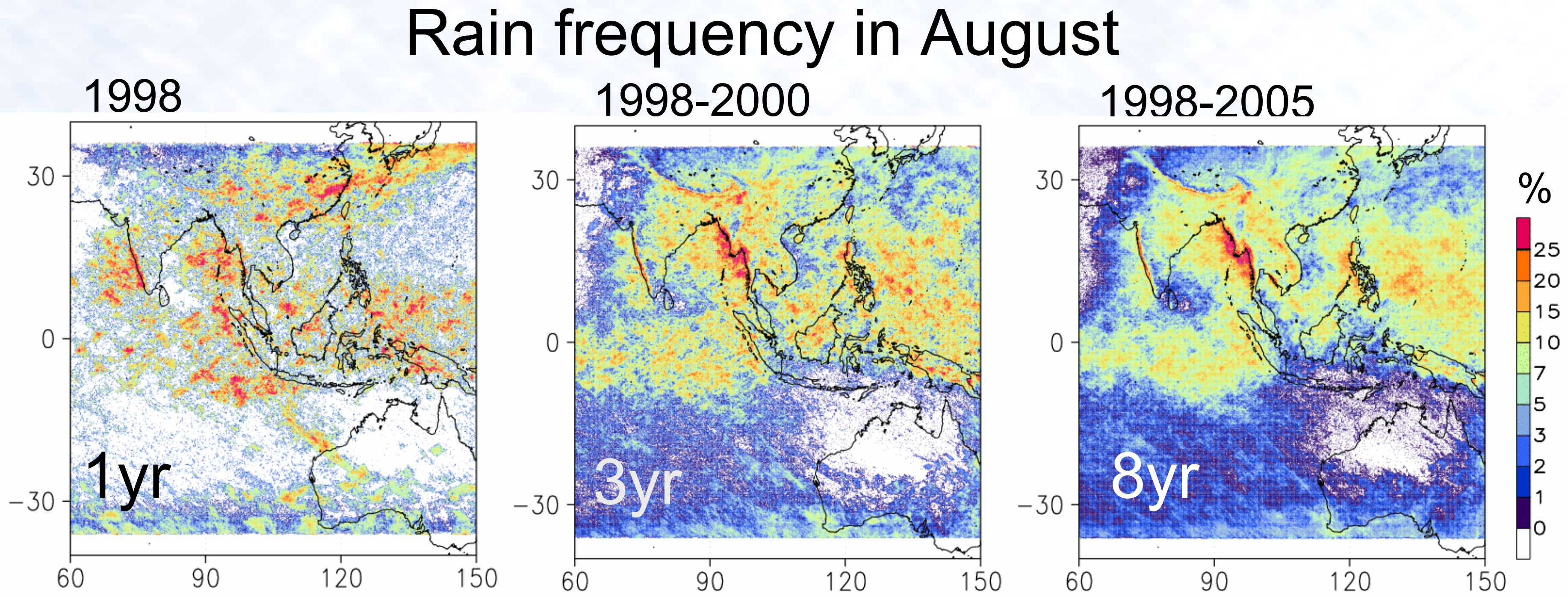

TRMM PR data are becoming climatologically significant and reliable data. The eight-year data accumulation has greatly benefited for global and regional understanding of precipitation systems, rare events, the intraseasonal variation, and so on.

Increased possibility in detection of the diurnal signature

Time of the maximum rainfall at each 0.2-degree grid for JJA

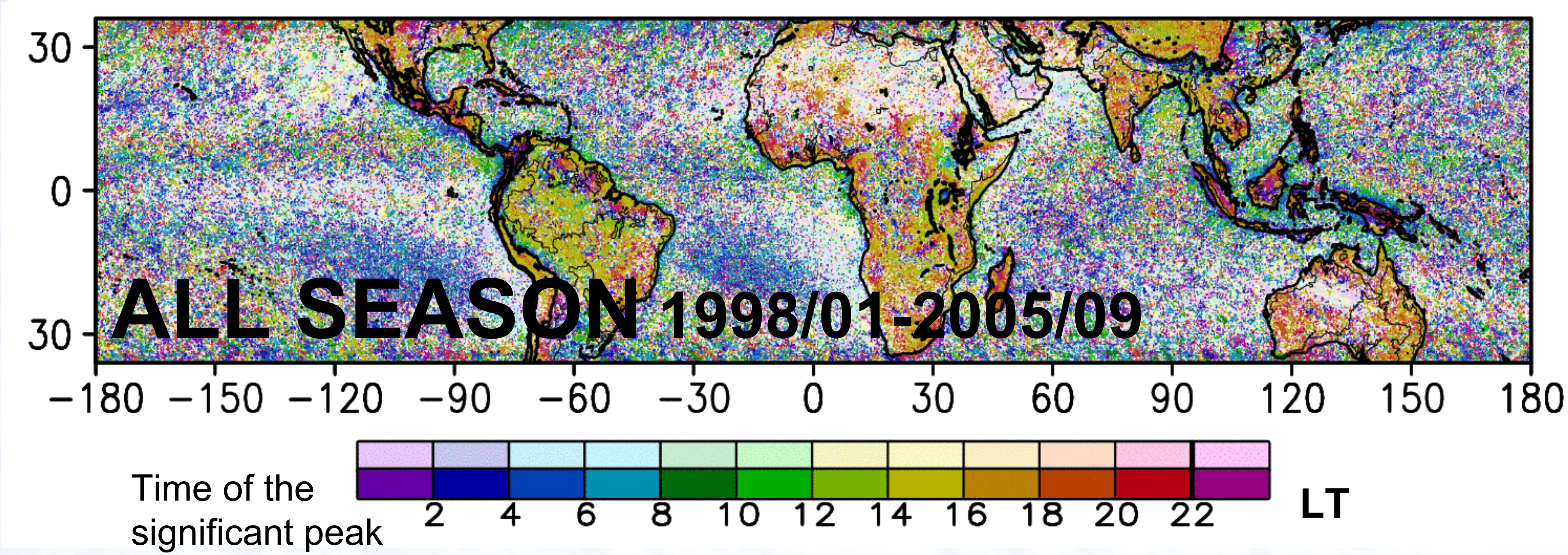

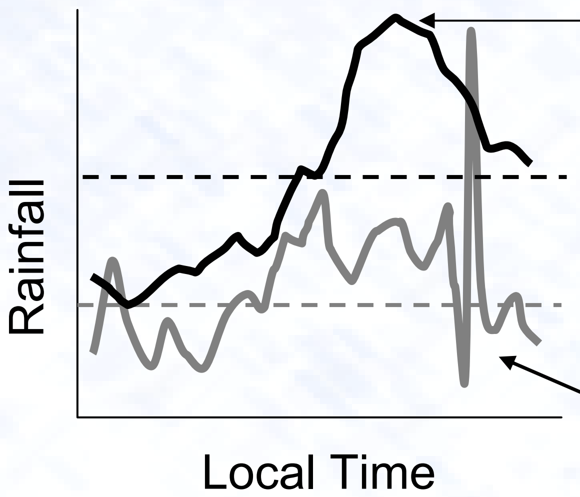

Time of maximum rainfall with consecutive positive anomalies for more than three hours is assumed to be **reliable** as the significant diurnal features. <Dark color>

Poor diurnal signature due to few precipitation samples. <Light color>

The percentage of significant features of time of maximum rainfall

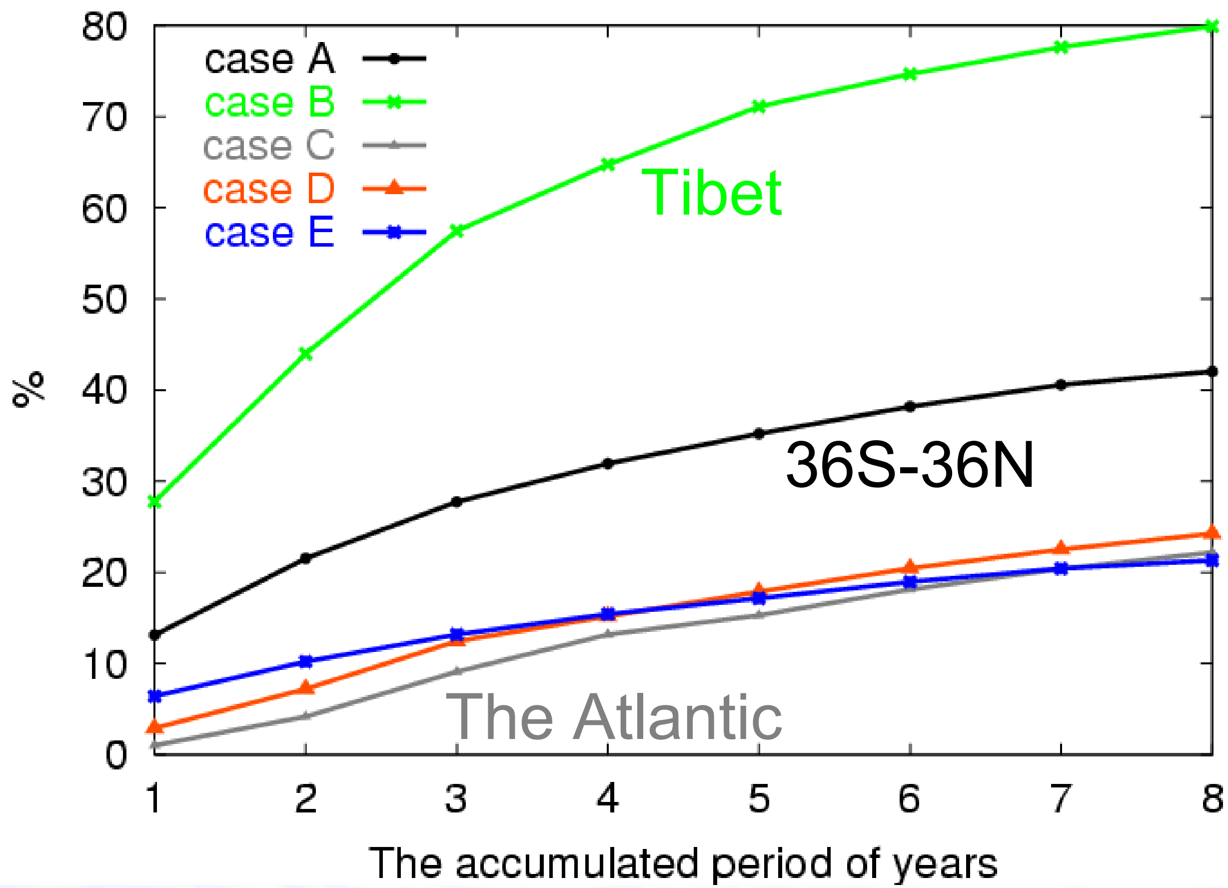

Definition of the meaningful signal of the diurnal cycle:

A: temporal continuity
B: same as A but over Tibet
C: same as A but over the southeastern Atlantic
D: same as A but for JJA
E: spatial and temporal continuity

The occurrence frequency of “the significant diurnal signal” over the global tropics is still increasing year by year according to the increase of the sampling. TRMM will be on orbit at least until 2009. There should be further examined the increasing possibility and limitation in utilizing the dataset.

Time of maximum rainfall over Africa

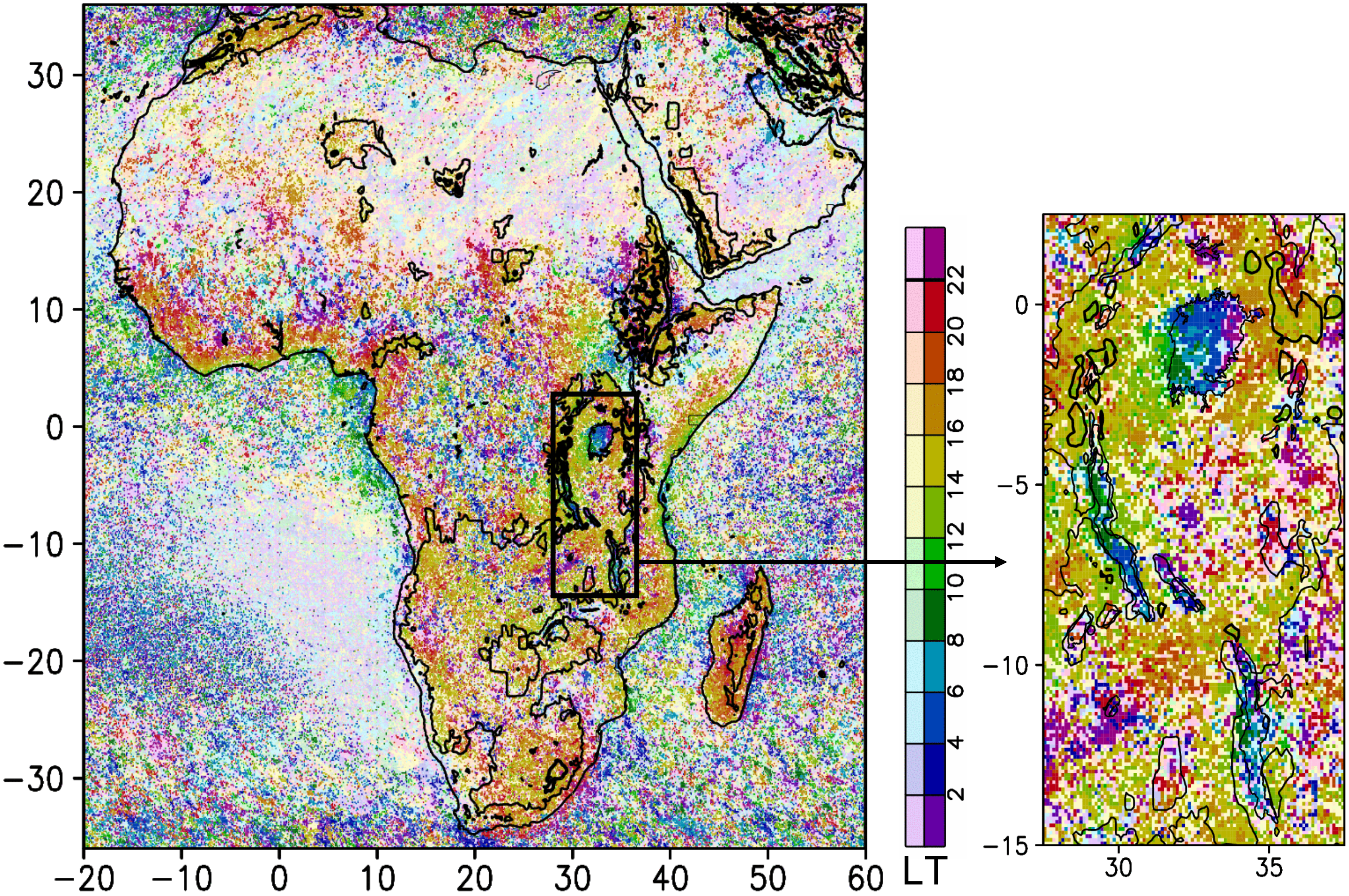

4. Rainfall map in view of "Precipitation system climatology"

The terminology is named by K. Nakamura

Seasonal variation of rainfall

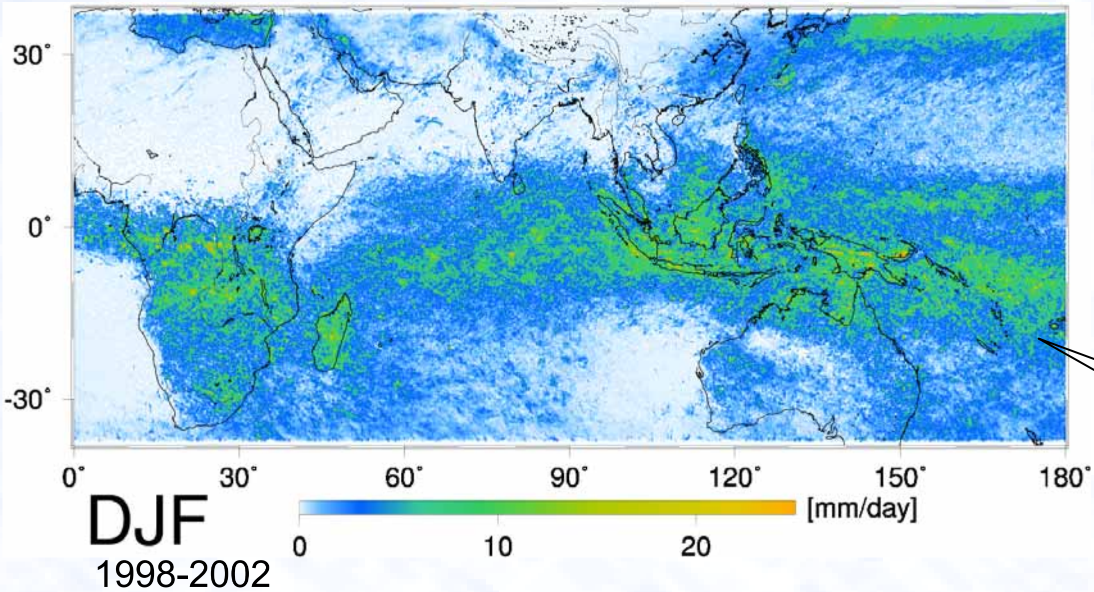

The total rainfall amount is the sum of the individual pixel rain intensities which are grouped into the precipitation system.

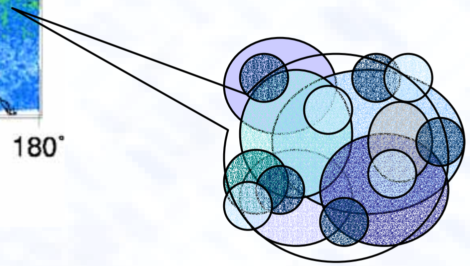

<u>Beyond more accurate estimates of rainfall, the climate variability will be further understood as conglomerates of precipitation systems.</u>

Spatial distribution of scale-based precipitation systems

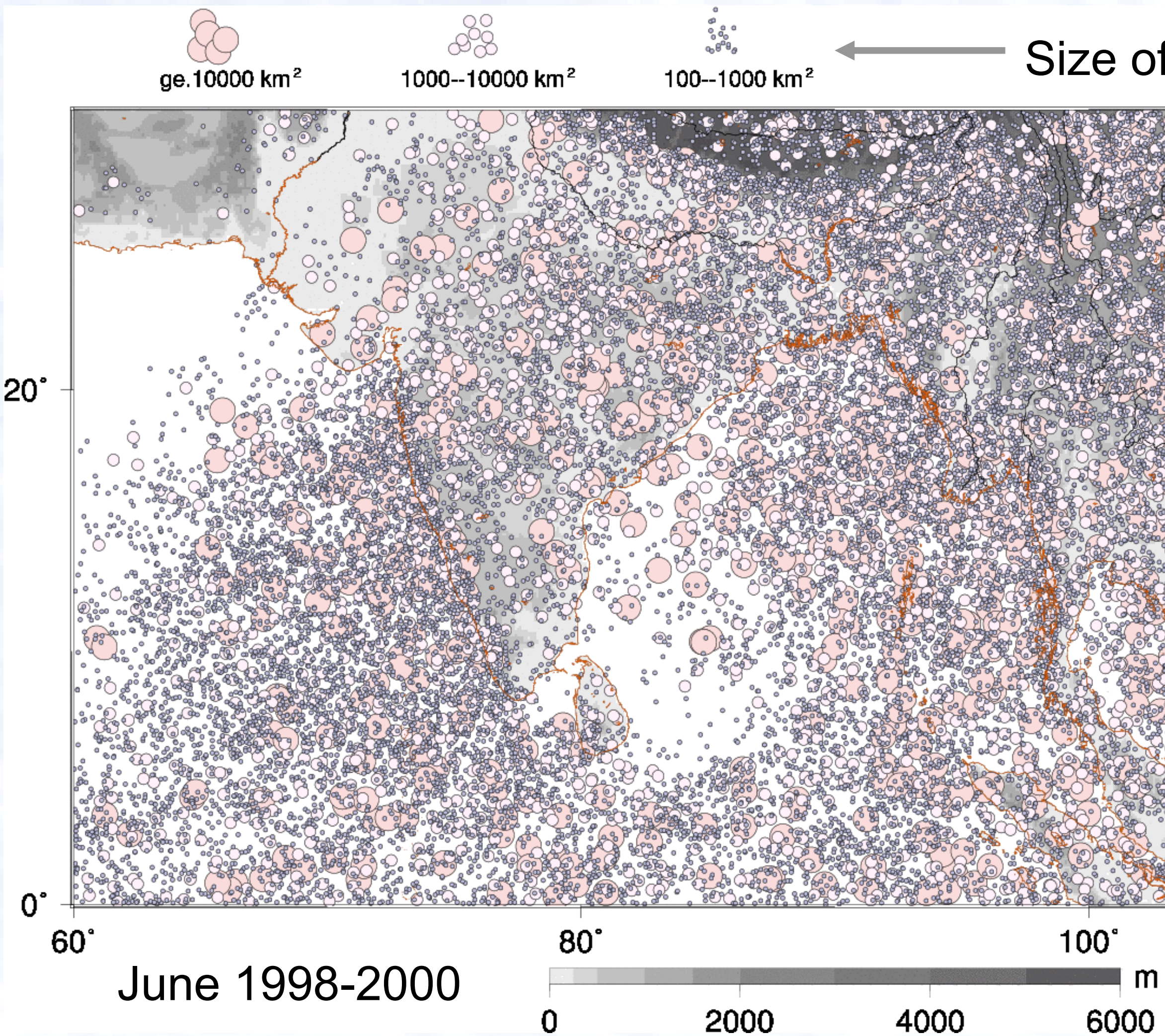

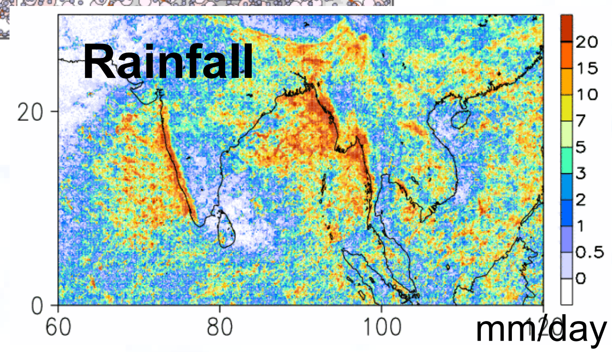

The eight-year observation captured millions of precipitation systems all over the globe.

Impact of the Scale-Based Systems in Rainfall

Diurnal variation of rainfall and the number of precipitation systems over inland India

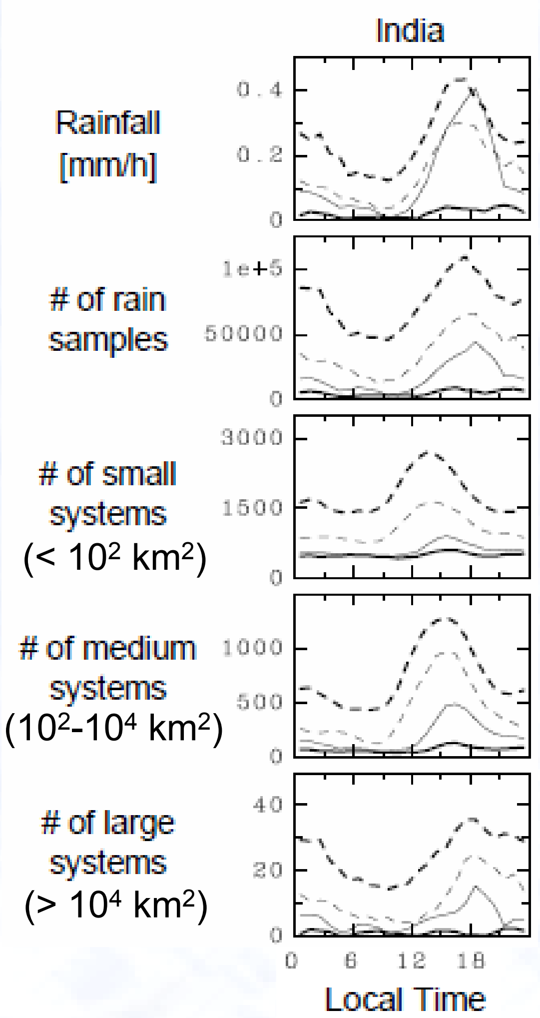

DJF: Thick solid lines
MAM: Thin solid lines
JJA: Thick dashed lines
SON: Thin dashed lines
1998-2003

Hirose and Nakamura (2005)

Clear contrast between early-afternoon rain over land and morning rain over ocean.

The peaks over land shift later.

Large systems show the geographical pattern more clearly.

Time of max R for JJA

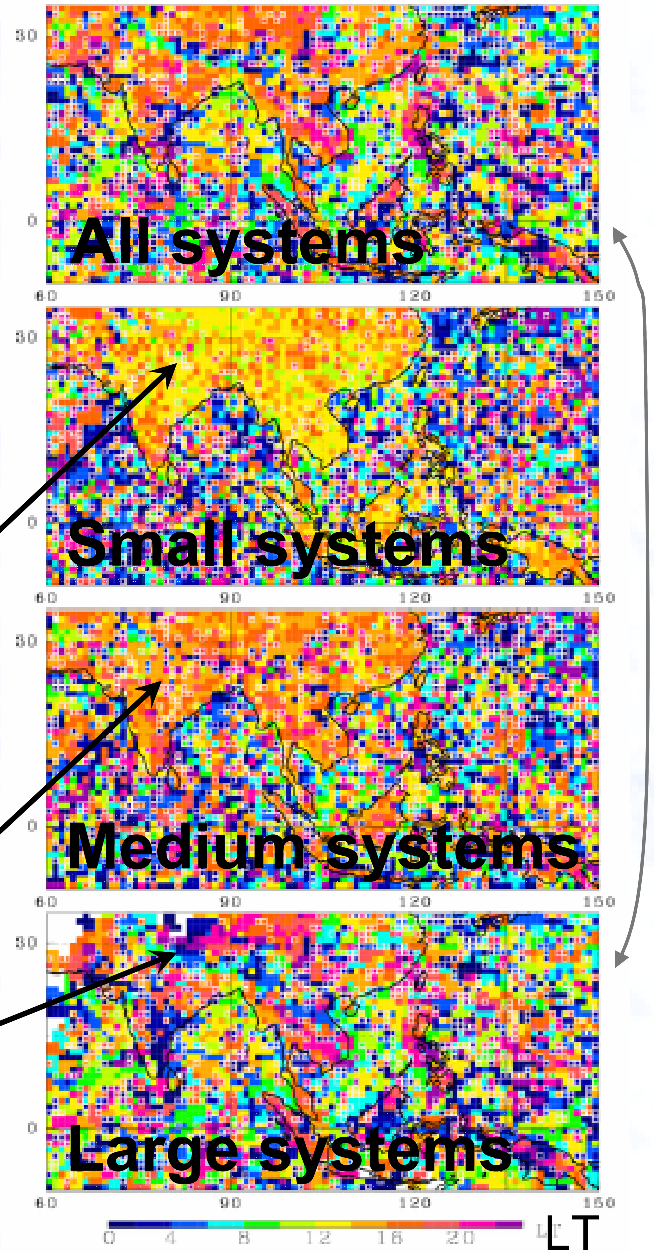

The global and regional understandings of precipitation properties will deepen from the further data accumulation and a diversity of researches.

Precipitation system climatology:

Diurnal variation in view of precipitation features: Nesbitt and Zipser (2003)
Statistics of precipitation features: Cecil et al. (2005)
Cluster analysis of precipitation profiles: Boccippio et al. (2005)
Precipitation type classification: Katayama and Takayabu (2004)
Prevailing precipitation systems: Hirose and Nakamura (2005)

5. Remaining issues on the precipitation retrieval

Adequate "truth" of global map of rainfall is in the absence. Reduction of differences, about 5 %, between TRMM PR and TMI has been discussed by evaluating each data characteristics.

Major possible error sources:

- Regional variation of the drop size distribution
- Radar calibration
- Uncertainty of path-integrated-attenuation
- Non-uniform-beam-filling effect
- Profiles in the surface clutter ranges
- Attenuation by cloud and water vapor
- Kind of solid precipitation particles
- Temporal variation of the freezing level

Uncertainty in the surface rainfall estimates

TRMM PR at nadir has vertical resolution of 250 m and the lowest level of meaningful data is about 500 m height. In the latest version, surface rainfall is estimated by assuming several constant slopes of dBZe.

Vertical cross section of rainfall rate

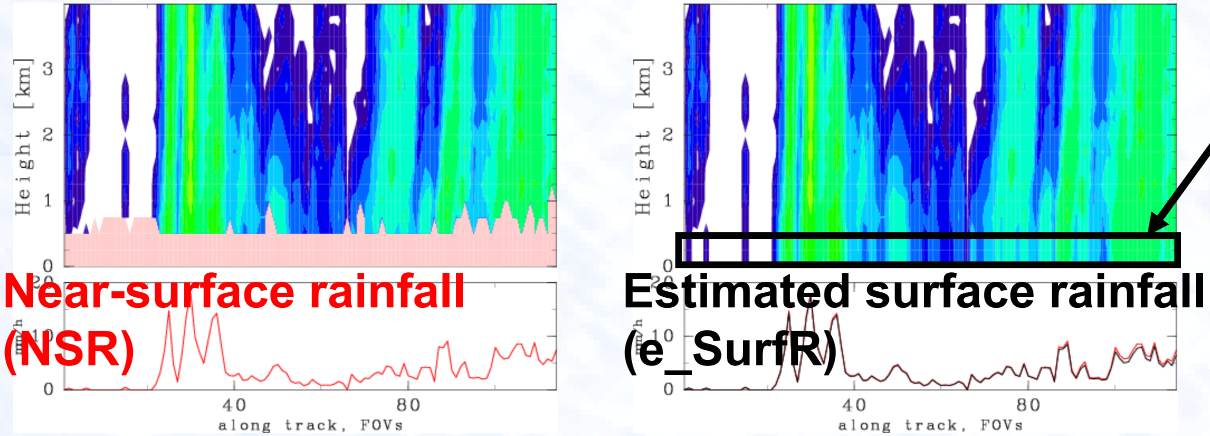

Slopes based on the WPR measurement:
0 dB/km except for stratiform rain over land (-0.5 dB/km)

Difference between e_SurfR and NSR

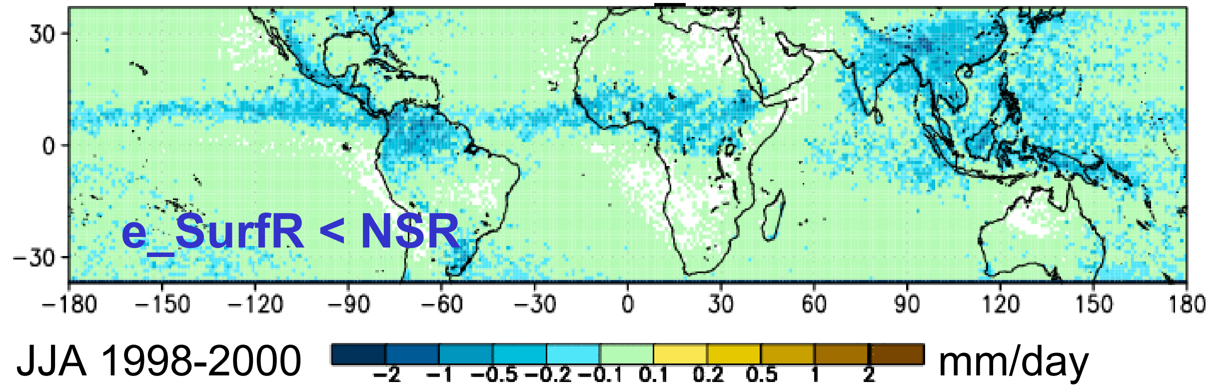

In average, e_SurfR is 2 % smaller than rain at 500 m level due to the slower terminal velocity near the surface.

The adequacy of the assumption is in controversy.

Another estimate of surface rainfall was done by utilizing the profiling capability of TRMM PR. The "SR2" was extrapolated by a linear regression of rainfall rates around 1 km above the surface.

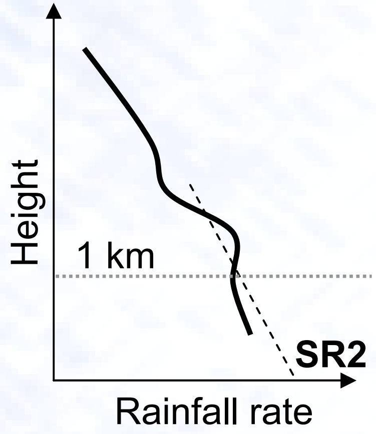

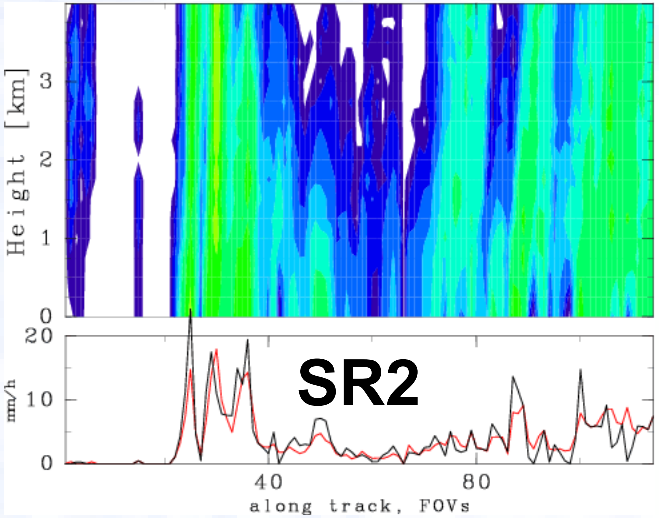

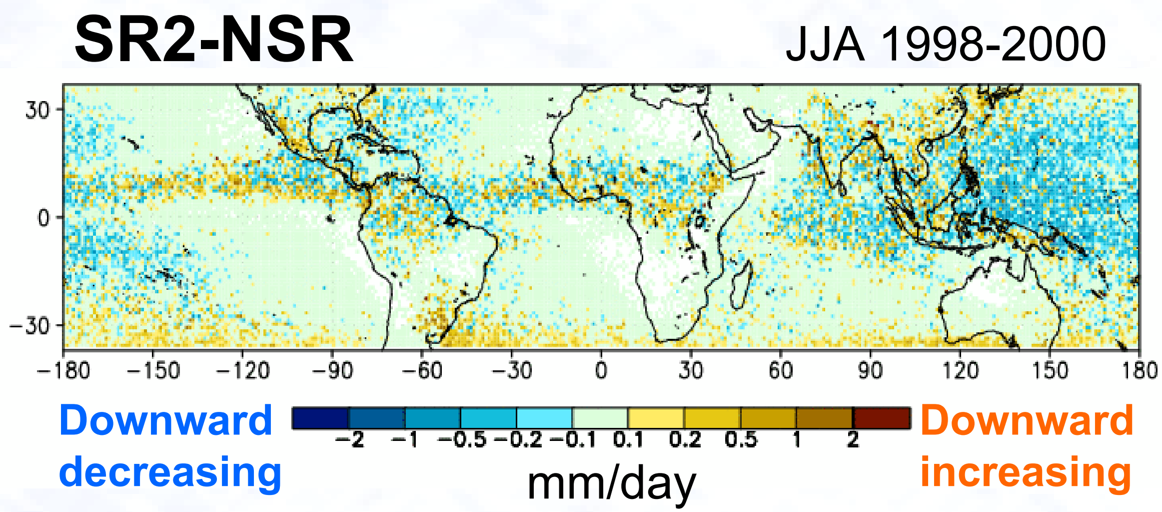

Slope around 1 km height does not always exhibit the negative gradient unlike the assumption in V.6.

Altitudinal differences of averaged rainfall

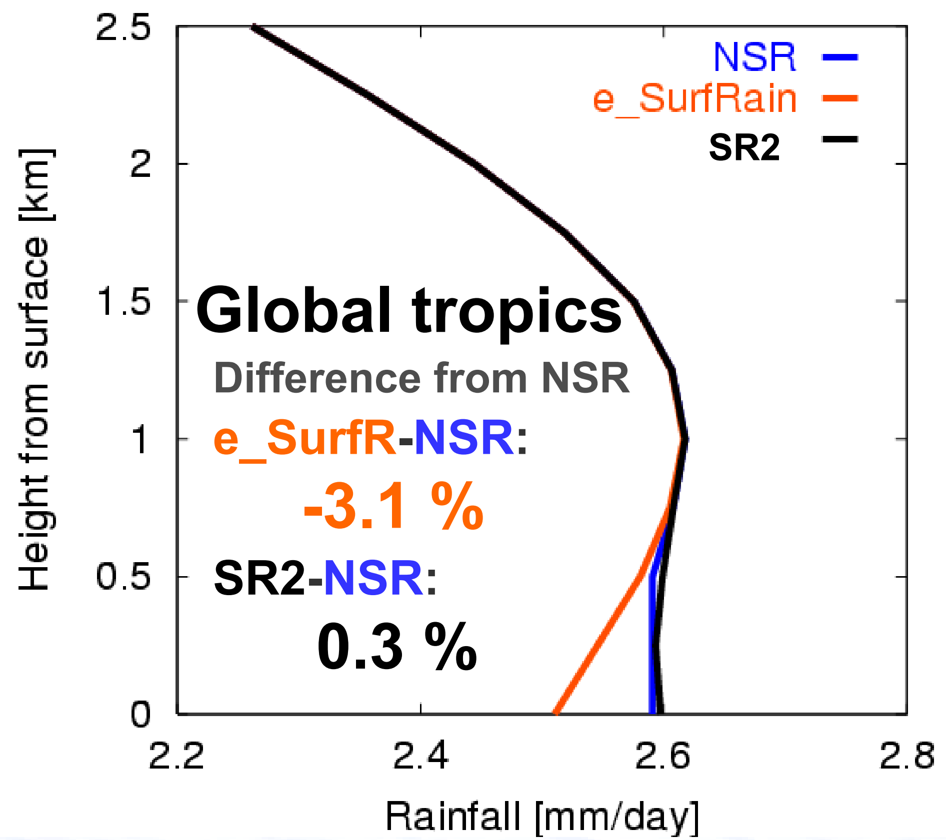

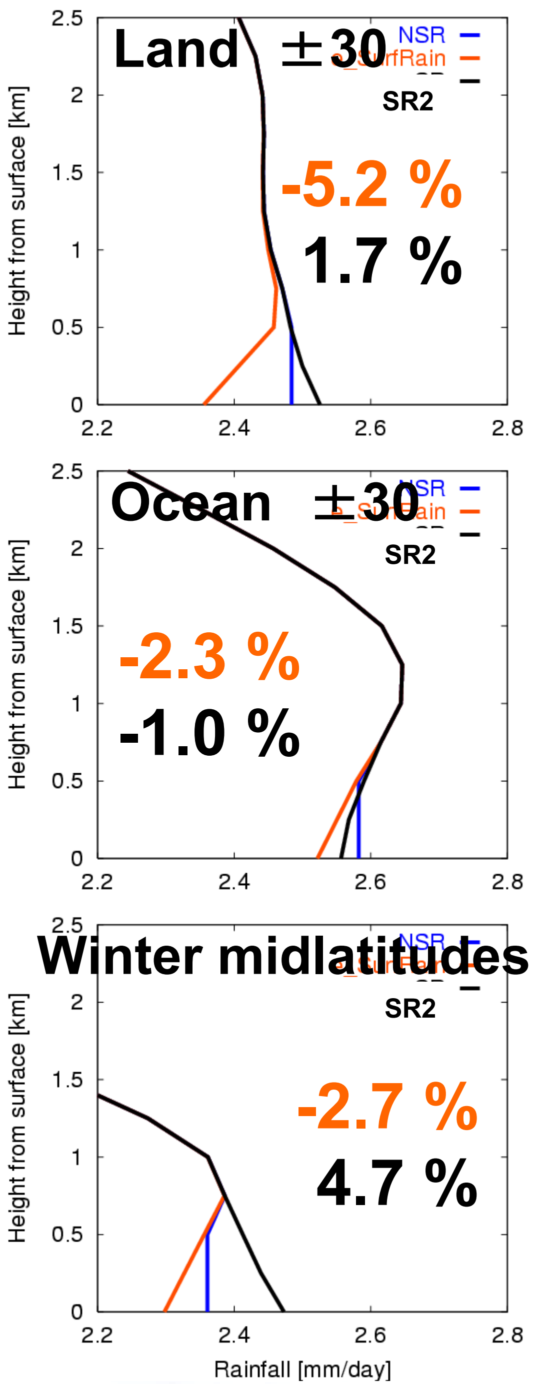

There is few statistics of the vertical gradients below the level of 1 km. With the collaboration of other ground-based observations, <u>some kind of model</u> is needed, considering the regional variation of the precipitation type.

Conclusions

The long-term data accumulation enabled us to examine more accurate rainfall at various temporal and spatial scales and the constituents of a particular climatic regime as being congregations of various precipitation systems.

Furthermore, the comprehensive and interdisciplinary discussions are needed for further scientific and algorithm benefits.

Extra slides follow

Importance of the sampling in hourly scale

In August over Tibet, the maximum number of samples and rainfall are in phase in the afternoon, hence 10 % overestimates were exhibited. By using long-term data, accurate monthly rainfall based on the hourly rainfall can be obtained.

The bias due to the diurnal variations of samples and rainfall

August 1998-2005
1 deg. grid

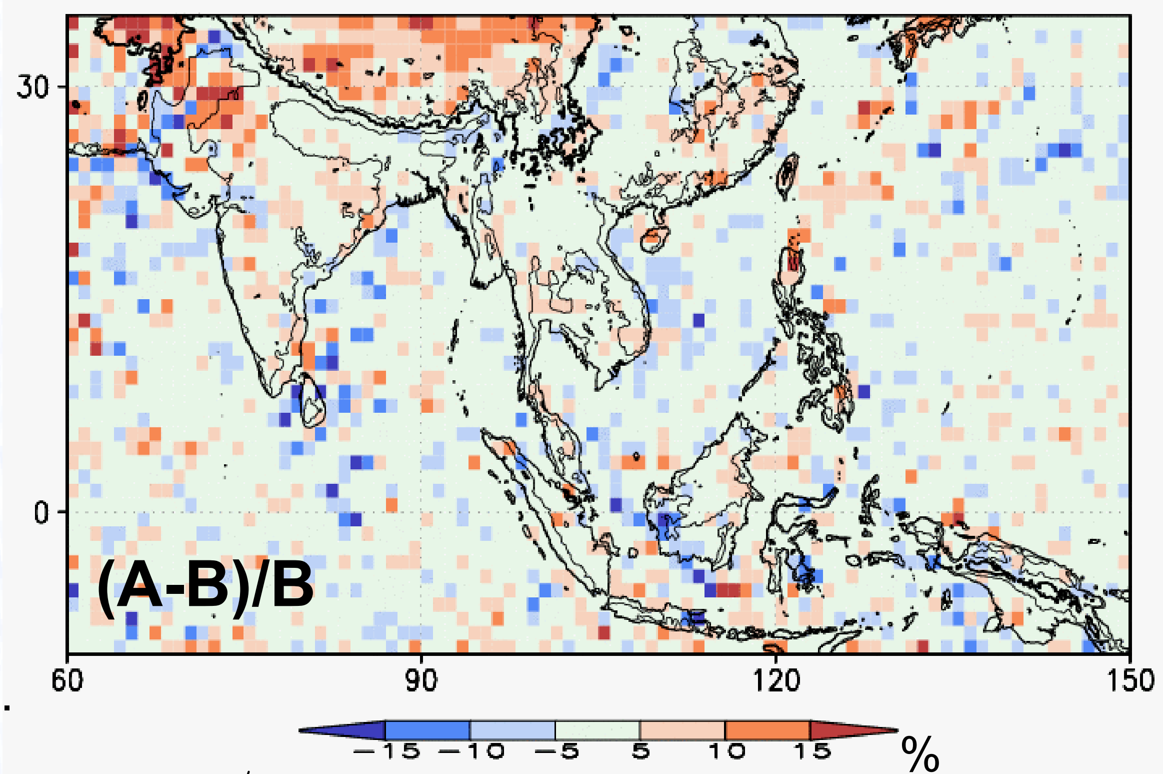

Rainfall A and B are calculated without and with considering on the diurnal effects, respectively.

Rainfall A [mm/day] $24\sum \mathrm{Rainfall} \Big/ \sum N$

Rainfall B [mm/day] $\sum_{t=1}^{8} \left(3\sum_{T=3t-2}^{3t} \mathrm{Rainfall}(T) \Big/ \sum_{t=3t-2}^{3t} N(T)\right)$

DJF

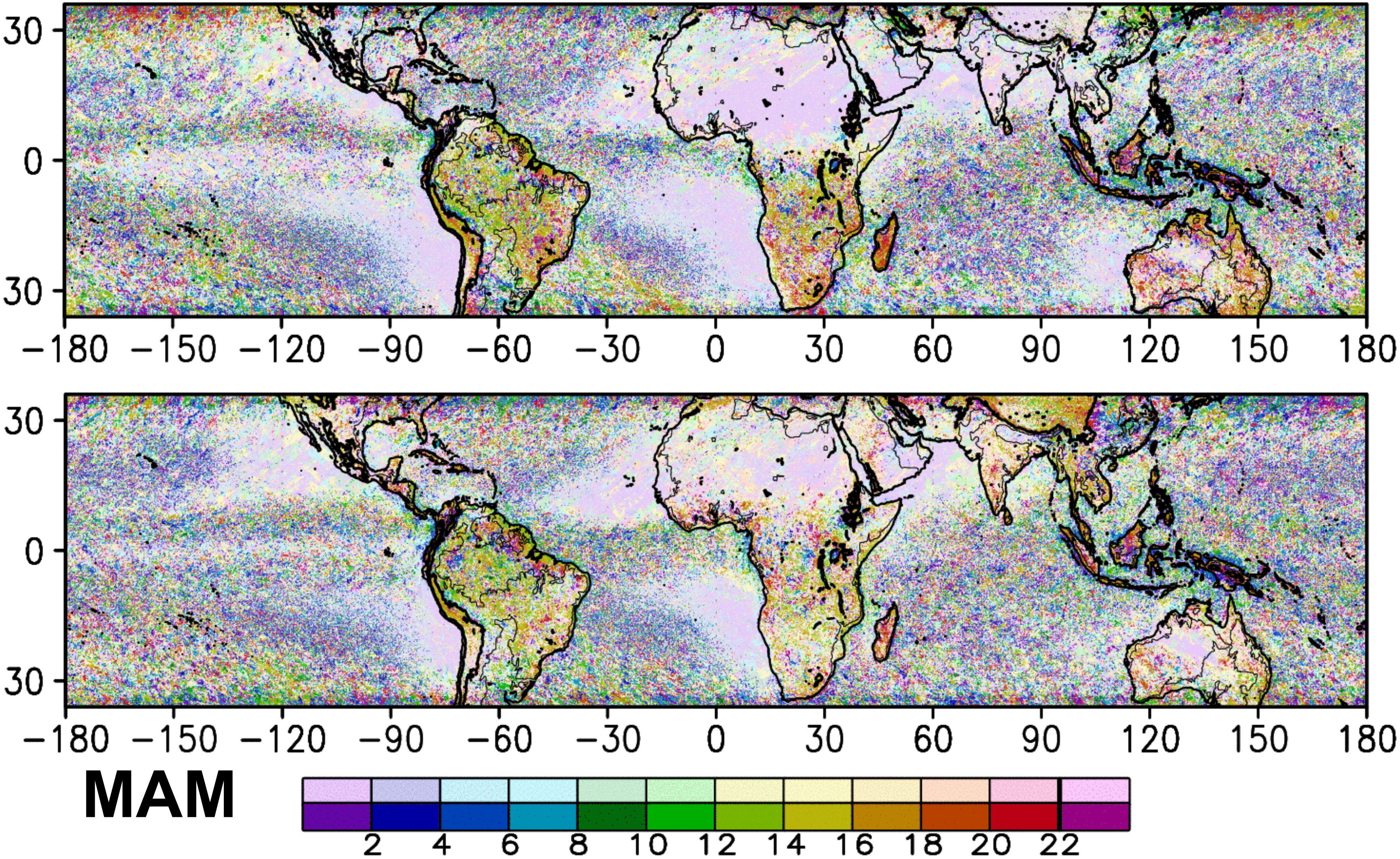

30
0
30
−180 −150 −120 −90 −60 −30 0 30 60 90 120 150 180
30
0
30
−180 −150 −120 −90 −60 −30 0 30 60 90 120 150 180
2 4 6 8 10 12 14 16 18 20 22

MAM

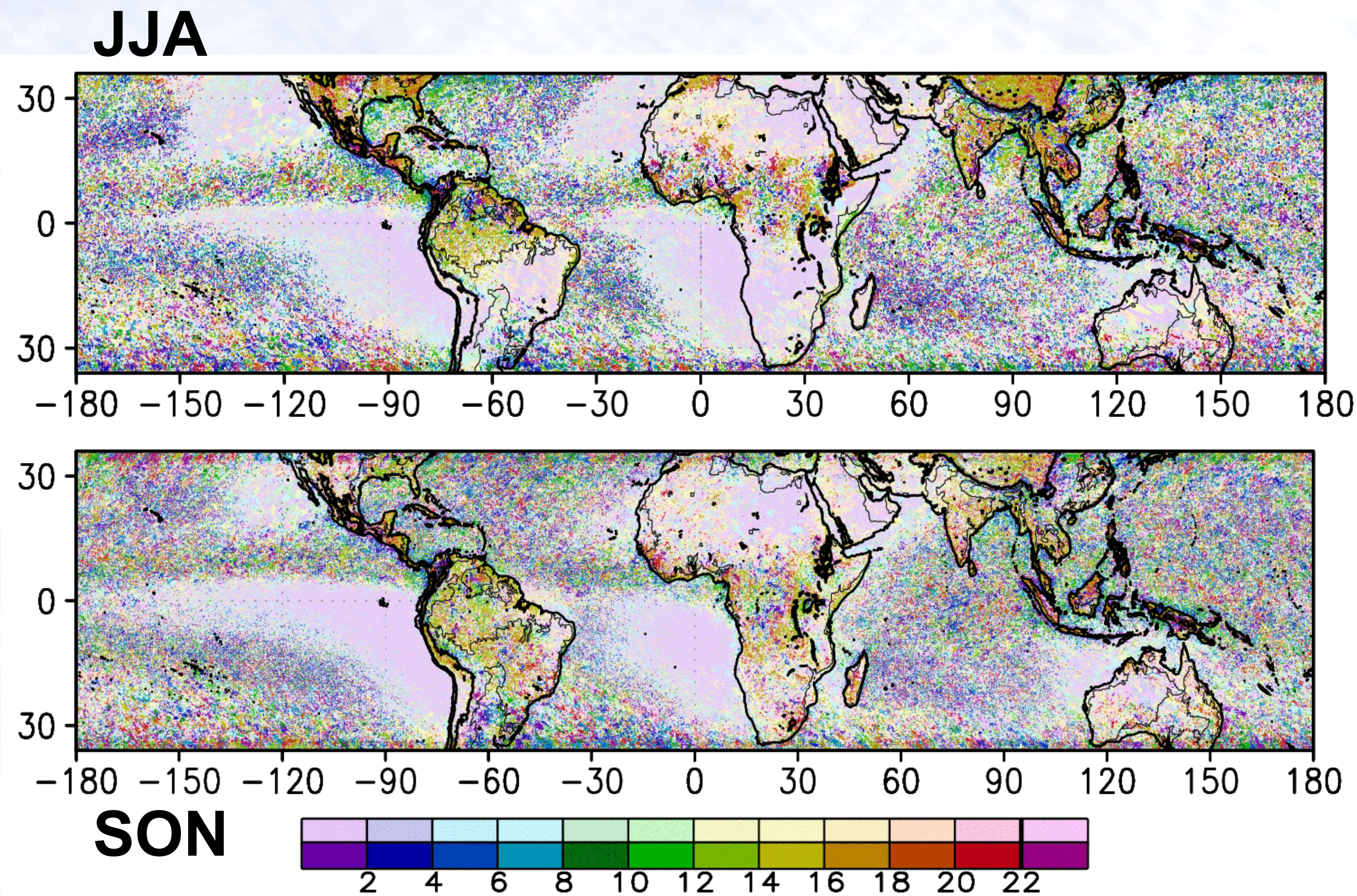
JJA
30
0
30
−180 −150 −120 −90 −60 −30 0 30 60 90 120 150 180
30
0
30
−180 −150 −120 −90 −60 −30 0 30 60 90 120 150 180
SON
2 4 6 8 10 12 14 16 18 20 22

Time of maximum rainfall

1998/01-2005/09

0.2 degree box

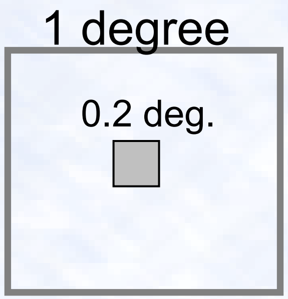

Spatial homogeneous feature:

Def. More than 50 % of the surrounding grids preserve time of maximum rainfall within 2 hours.

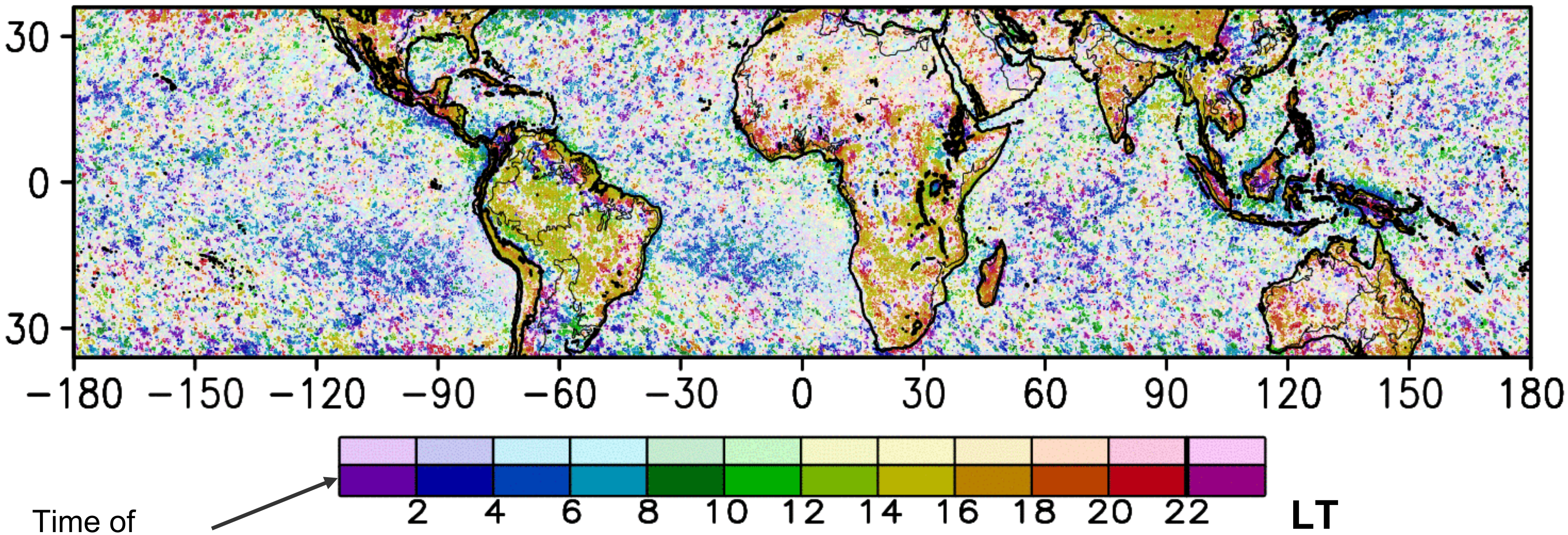

Time of
the significant peak in the spatial and temporal scale

Eight-year data accumulation gives opportunities to investigate spatiotemporal variation of rainfall in less time in fine scale.

Spatial distribution of medium (10^2-10^4 km^2) and large (>10^4 km^2) precipitation systems

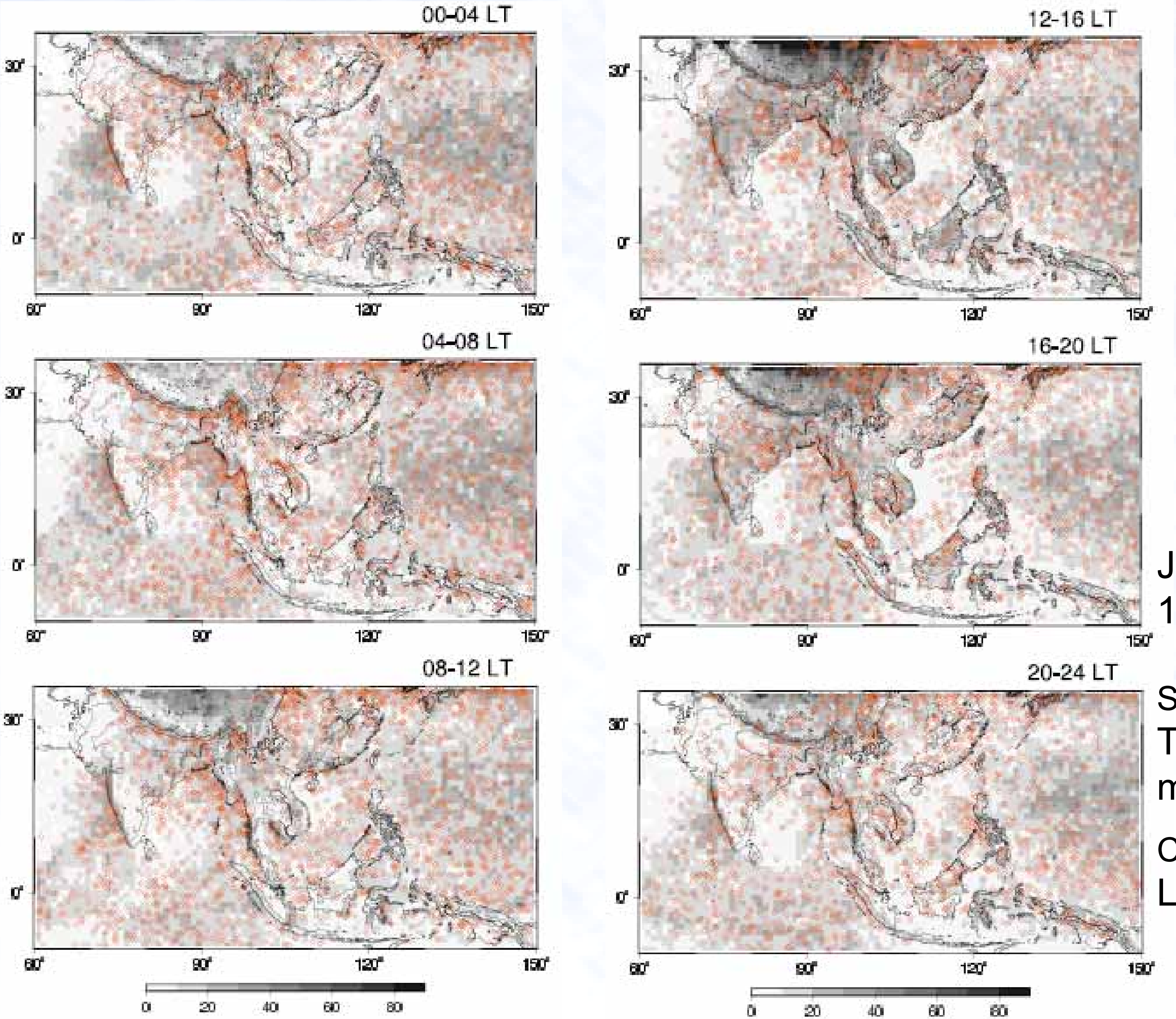

JJA
1998-2003

Shadings:
The number of medium systems

Circles:
Large systems

Some new insights and enhanced issues

The simple validation of global rainfall map could not be simply assessed since various volumetric microphysics therein have the uncertainty in surface-rainfall estimates from the ground and space.

The retrieval method has been sophisticated by the own quality database not only for the spaceborne radar but also for other instruments such as the microwave radiometers and ground-based radar.

Long-term data accumulation allows for a better climate-oriented dataset, requiring further understanding of precipitation properties at various spatial and temporal scales

Beyond more accurate rainfall estimates, understandings of precipitation systems make possible interpretation of the precipitation climatology and the mechanisms therein more specifically.

Constraints on the Global Measurement of Vegetation Structure Using L-band InSAR

- Fundamental Sensitivity
- Error Sources
- Design Tradeoffs

Microwave Remote Sensing Laboratory (MIRSL)
University of Massachusetts, Amherst

What MIRSL Does

Design and build microwave instruments for studying the environment

Why Microwaves??

- coherent control
- unique perspective
- day/night operation, robust in various weather conditions

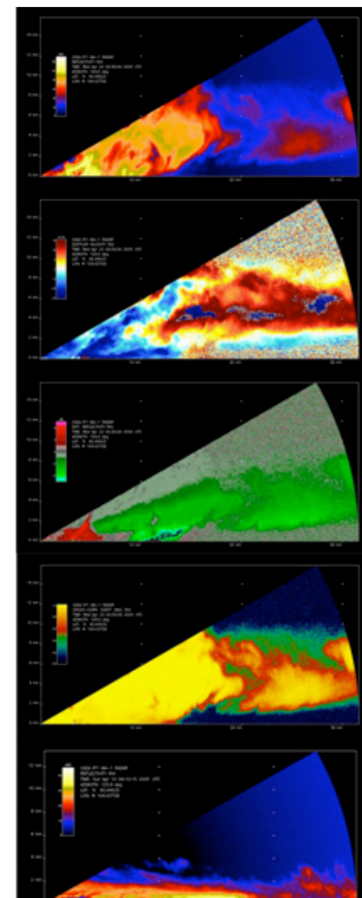

Interferometry & Ocean Currents

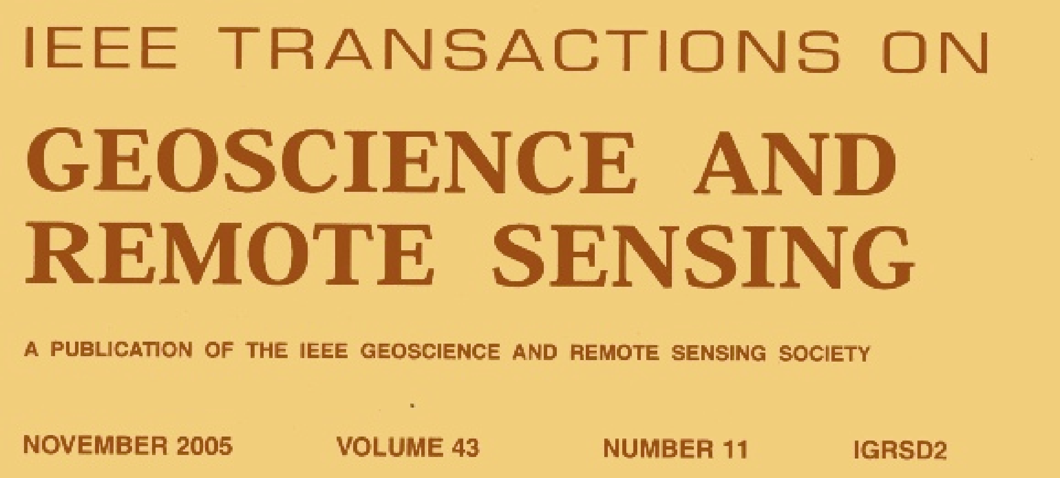

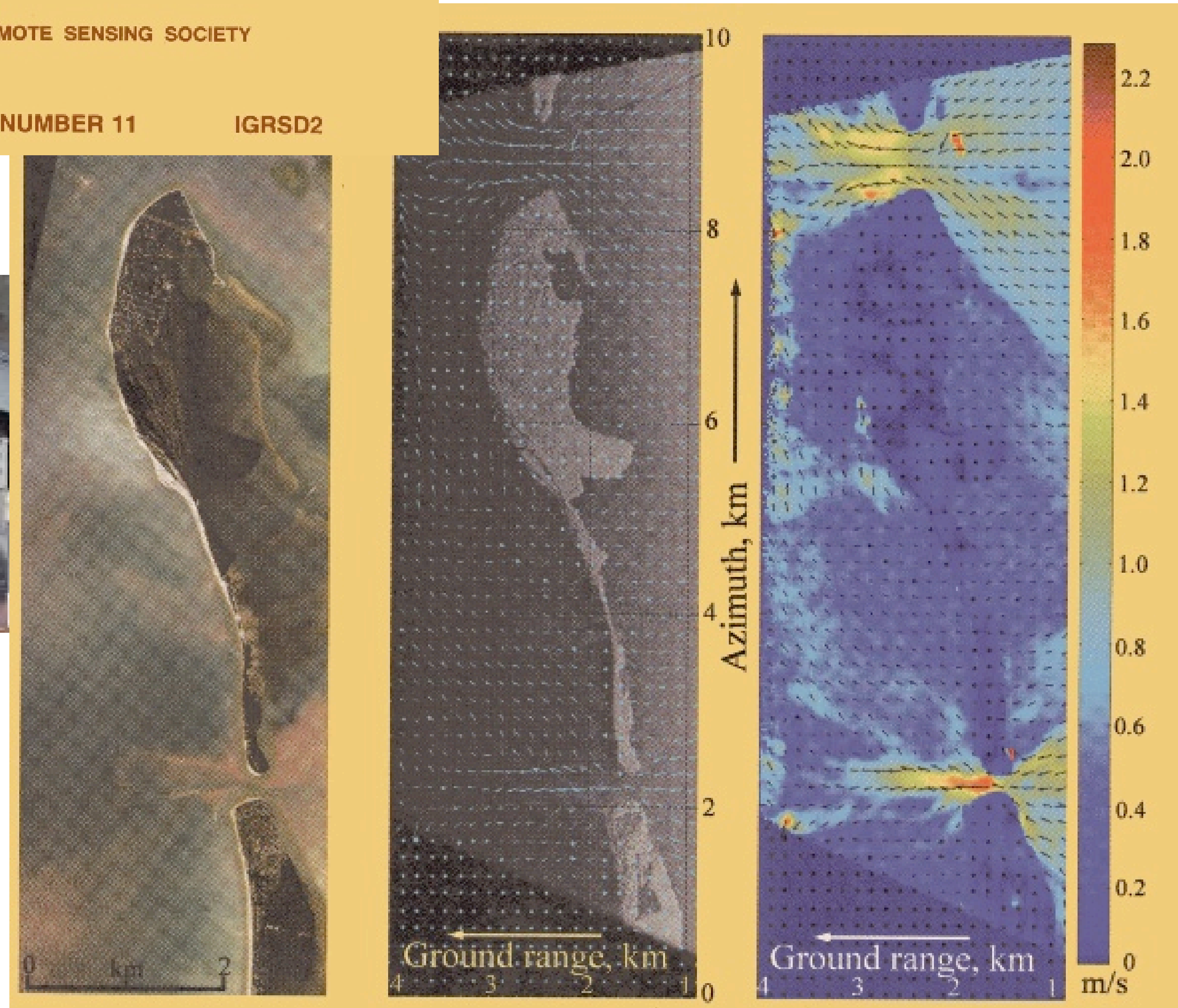

Scatterometry & Hurricanes

Millimeterwave Hardware Development

Advanced Performance Ku- and Ka-band Dual-Downconverter

Objective

• To build Ku- and Ka-band Dual-Downconverters (DDCs) suitable for use in spaceborne interferometric radar applications.

Description

- 20 MHz BW • ~70 dB gain • 4.5dB NF
- < 0.3 dB amplitude variation about best linear fit
- < 50 mdeg RMS relative phase accuracy over BW
- symmetric design aids in thermal stability
- parts layout and PWB construction designed to aid in testing of subunits.

Two-channel DDC

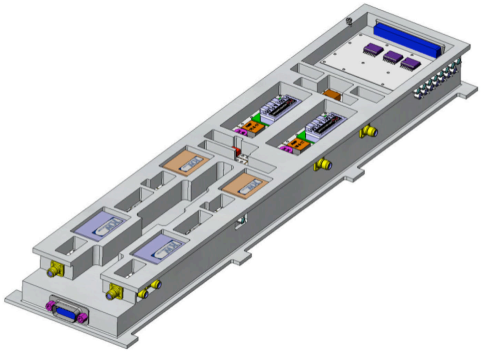

Ku-band Interferometer

Two-channel, dual-downcoverter and a Ku-band intefermetric radar conceptualization

Approach

- Test Ku-band breadboard model to guide construction of Ku-band DDC
- Use Ku-band DDC to guide development of Ka-band DDC
- Low thermal expansion materials used to maintain thermal stability
- characterized amplitude and phase stability between -10 and 50 deg C using a thermal chamber
- Stringent demands on testing accuracy will be met by recently developed measurement techniques

Entry TRL = 3, Exit TRL = 5

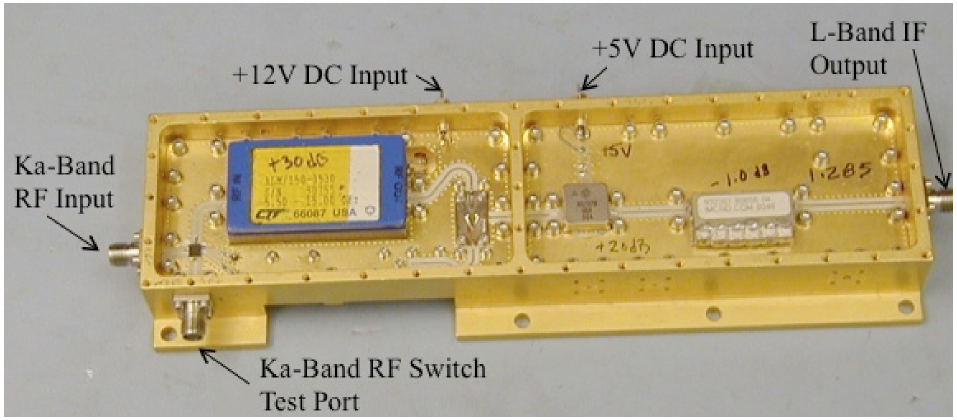

ALOS
Advanced Land Observing Satellite

JAXA/ALOS

Launch Date: January 19, 2006!!


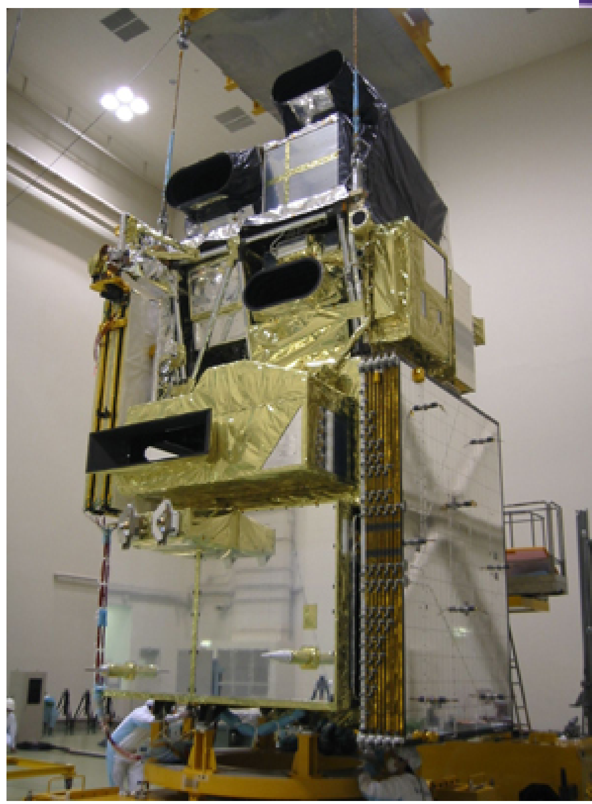

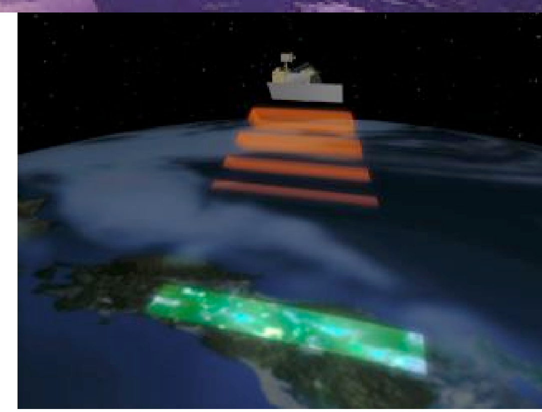

Three instruments: AVNIR-2, PRISM, & PALSAR

JERS-1 Mapping of Global Forests

- Geographic Locations

  Siberia, Africa (Congo), Asia, Brazil (Amazon)

- International Colaborations

  ESA, NASA, NASDA

  GRFM: Global Rain Forest Mapping

  GBFM: Global Boreal Forest Mapping

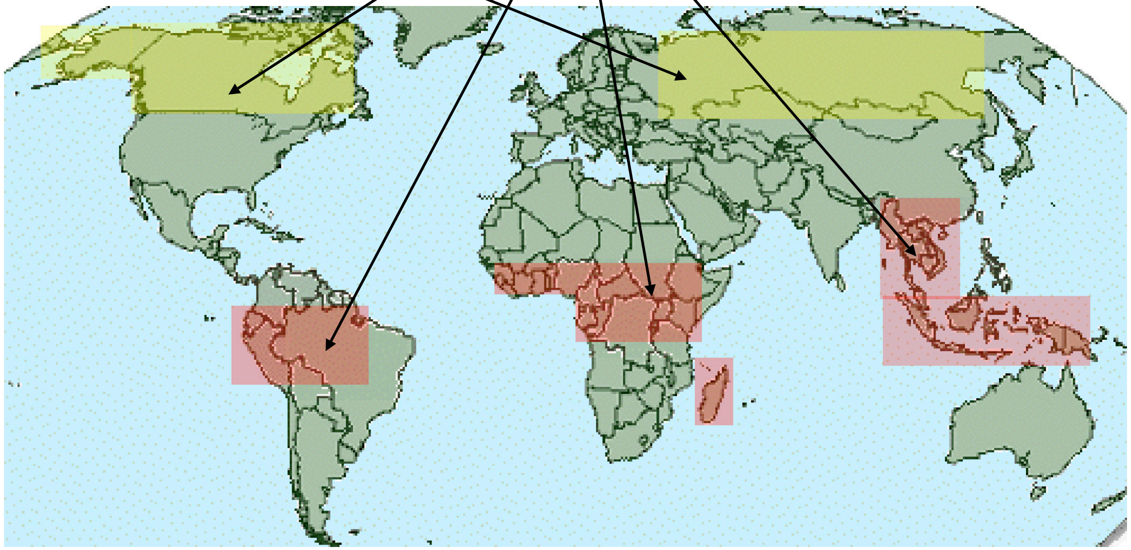

ALOS Kyoto & Carbon Initiative

Forest & Landcover Theme: Systematic Observations on a Global Scale at High Resolution of the World's Vegetated Regions

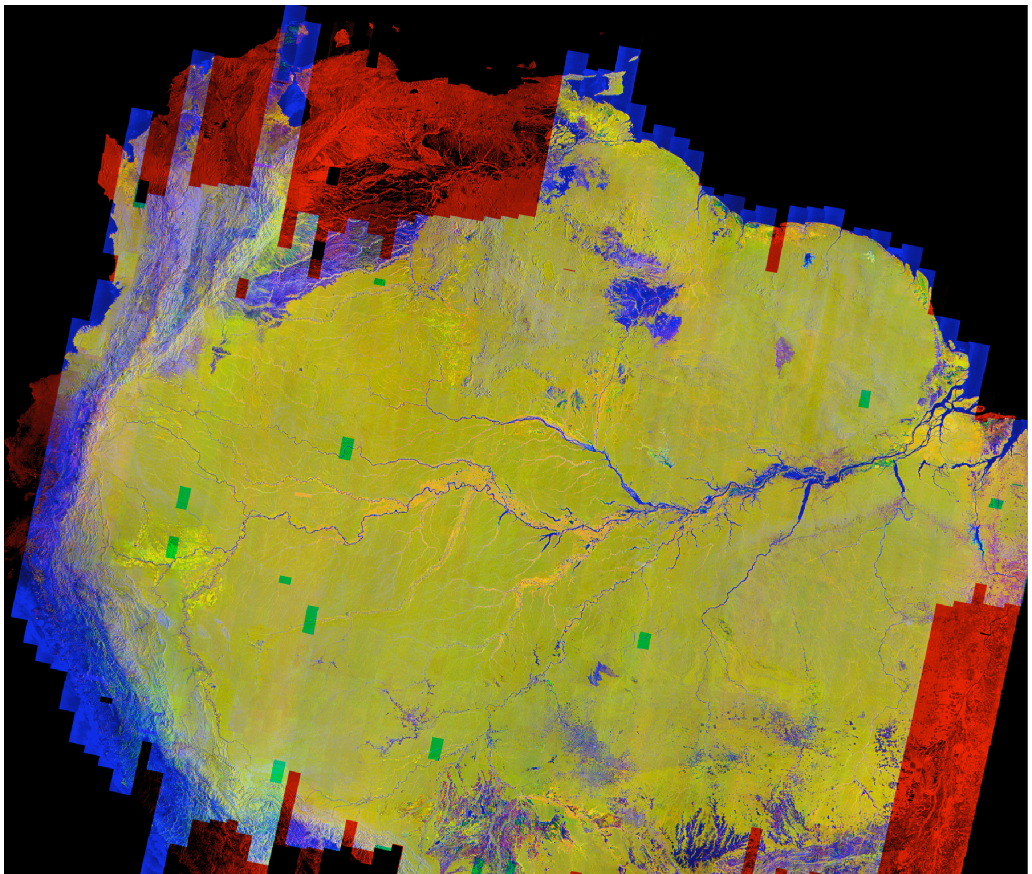

Building Blocks

- Measurement planning, data collection
- Processing, mosaicking, data fusion
- Quantitative estimation of target characteristics

In any given year, tens of billions of tons of carbon move between the atmosphere, hydrosphere, and geosphere. Human activities add about 5.5 billion tons per year of carbon dioxide to the atmosphere. The illustration above shows total amounts of stored carbon in black, and annual carbon fluxes in purple. (Illustration courtesy NASA Earth Science Enterprise)

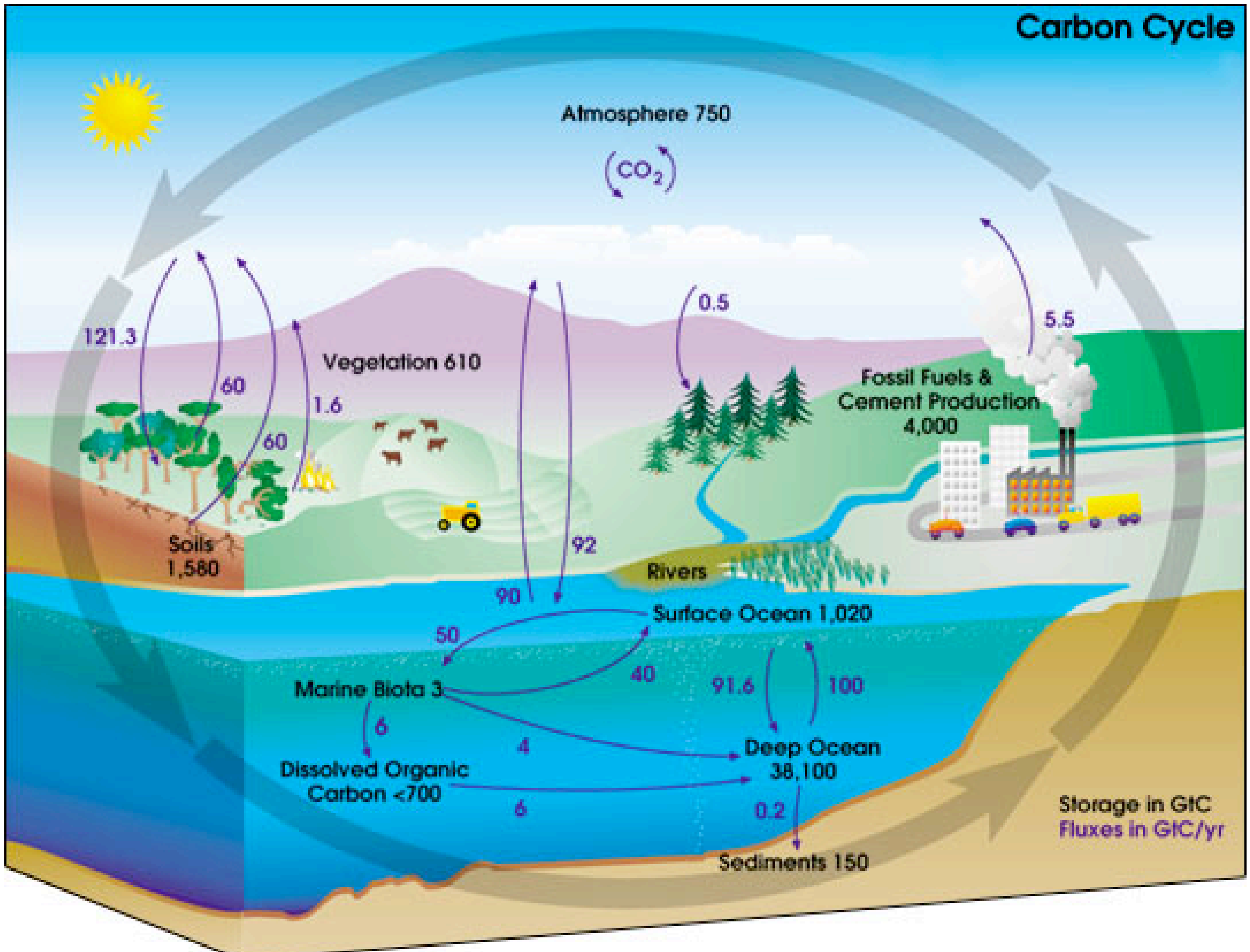

Techniques for Measuring Carbon Stored in Vegetation

Measurement Technique	Calibrated Target Measurement	Physical Interpretation	Physical Interpretation	Relation to Spatial Carbon Distribution
Lidar Profile	Lidar Height Profile	Lidar "Height", height of median energy, etc.	"Height" to Biomass conversion	Biomass to Carbon
Interferometric Correlation	Volumetric Correlation	InSAR "Height", density…	"Height" to Biomass conversion	Biomass to Carbon
Backscatter measurement	Vegetation Backscatter	Diameter at Breast Height, density, etc.	Backscatter to Biomass conversion	Biomass to Carbon
Destructive Sampling	Dry/Wet Weight	Biomass	---	Biomass to Carbon

Measurable → Modeling; Intermediate Results → Science Goal

ALOS/PALSAR Kyoto and Carbon Cycle Initiative

System Parameter	Value
Frequency	L-Band
Wavelength	24 cm
Bandwidth	14 & 28 MHz
Noise Equivalent σ^o	$\geq$ -23 dB
Signal to Ambiguity Ratio	$\leq$ 16 dB
Thermal SNR Over Vegetation	18 dB
Platform Height	700 km
Swath Width	40 - 70 km
Resolution	7 - 44 m
Effective Number of Looks Used	64
Look Angle Range	8 - 60 degrees
Repeat Track Time	46 days

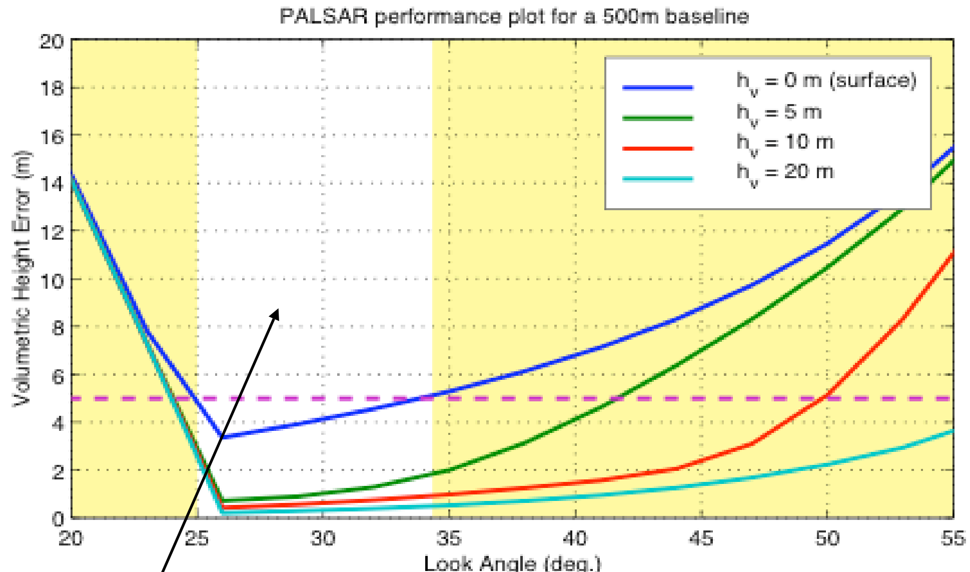

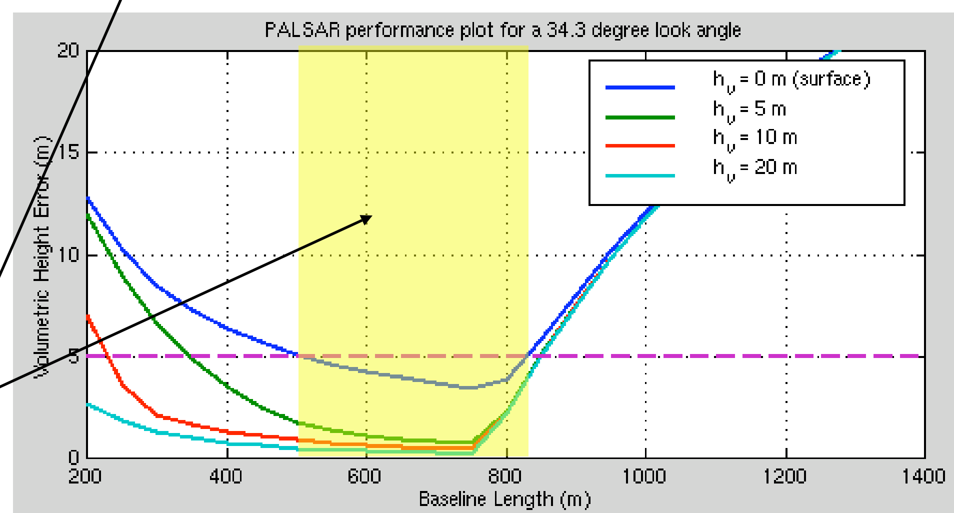

operating region

Radar and Optical Signatures of Forests

Using Microwaves to Measure Forest Biomass and Carbon Stocks

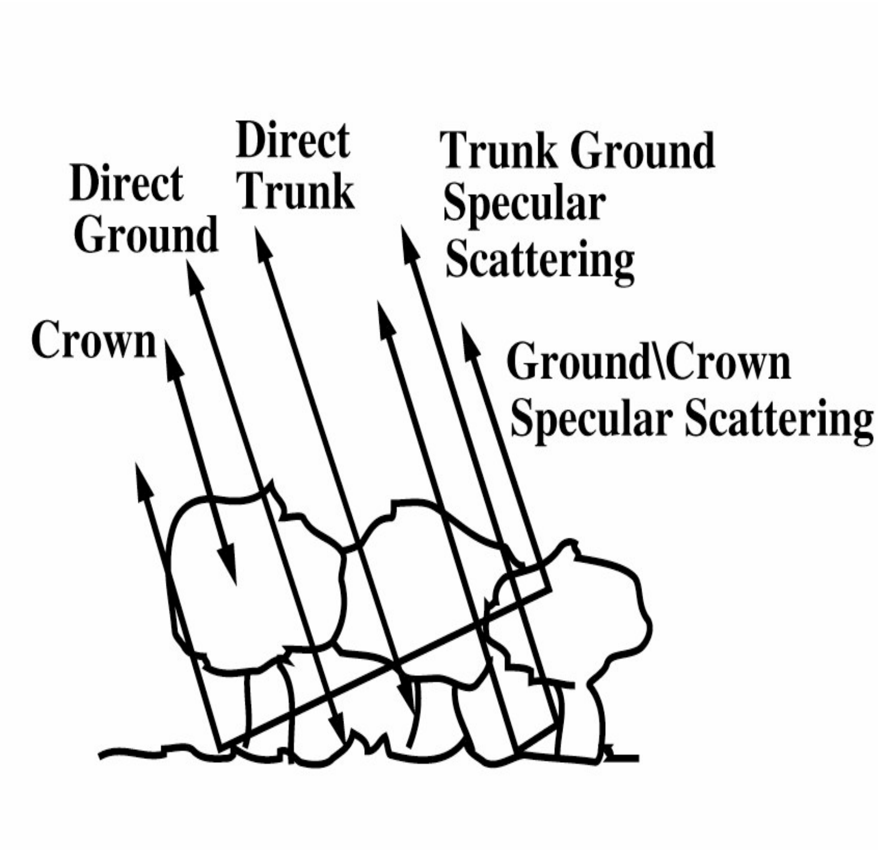

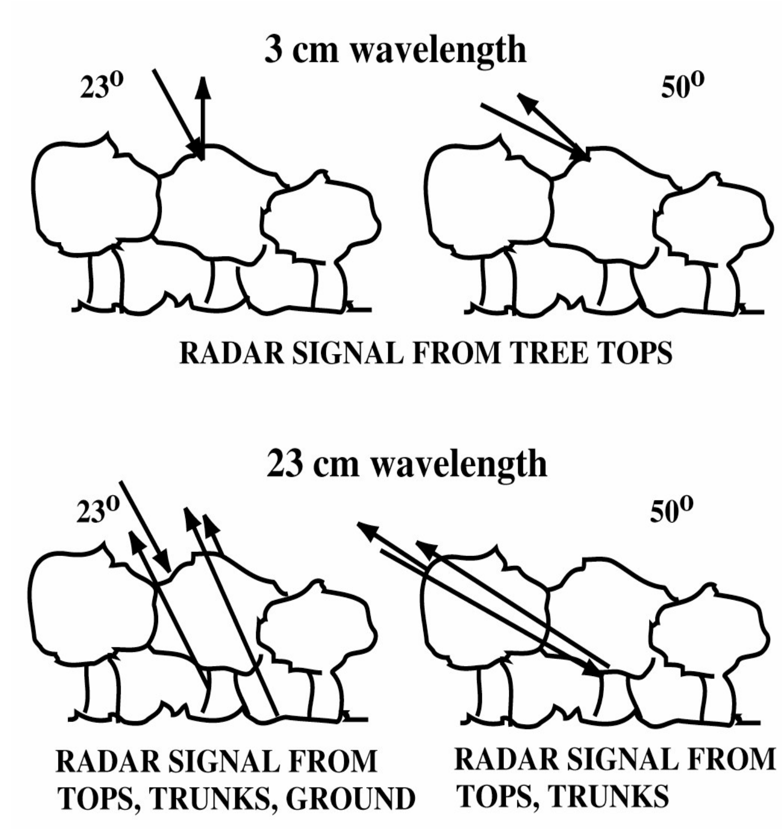

Backscatter Signature of Volume Scattering

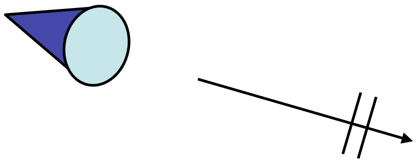

observed electric field

range and azimuth weighting functions

backscatter power

$$|E_1|^2 = A^4 \sum_i W_r^2 W_\eta^2 e^{-\kappa z/\cos\theta} f_{bi}^2$$

antenna gains and free space losses

attenuation losses

<u>Average over looks</u>

$$\left\langle |E_1|^2 \right\rangle = A^4 \int_{vol} W_r^2 W_\eta^2 e^{-\kappa z/\cos\theta} \rho(z) \left\langle f_b^2 \right\rangle d^3 r$$

density

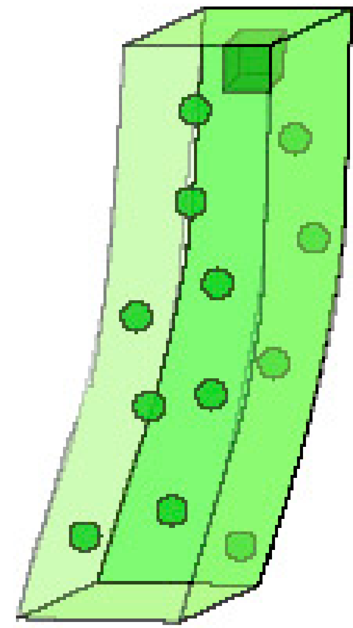

Backscatter vs. Biomass Curves

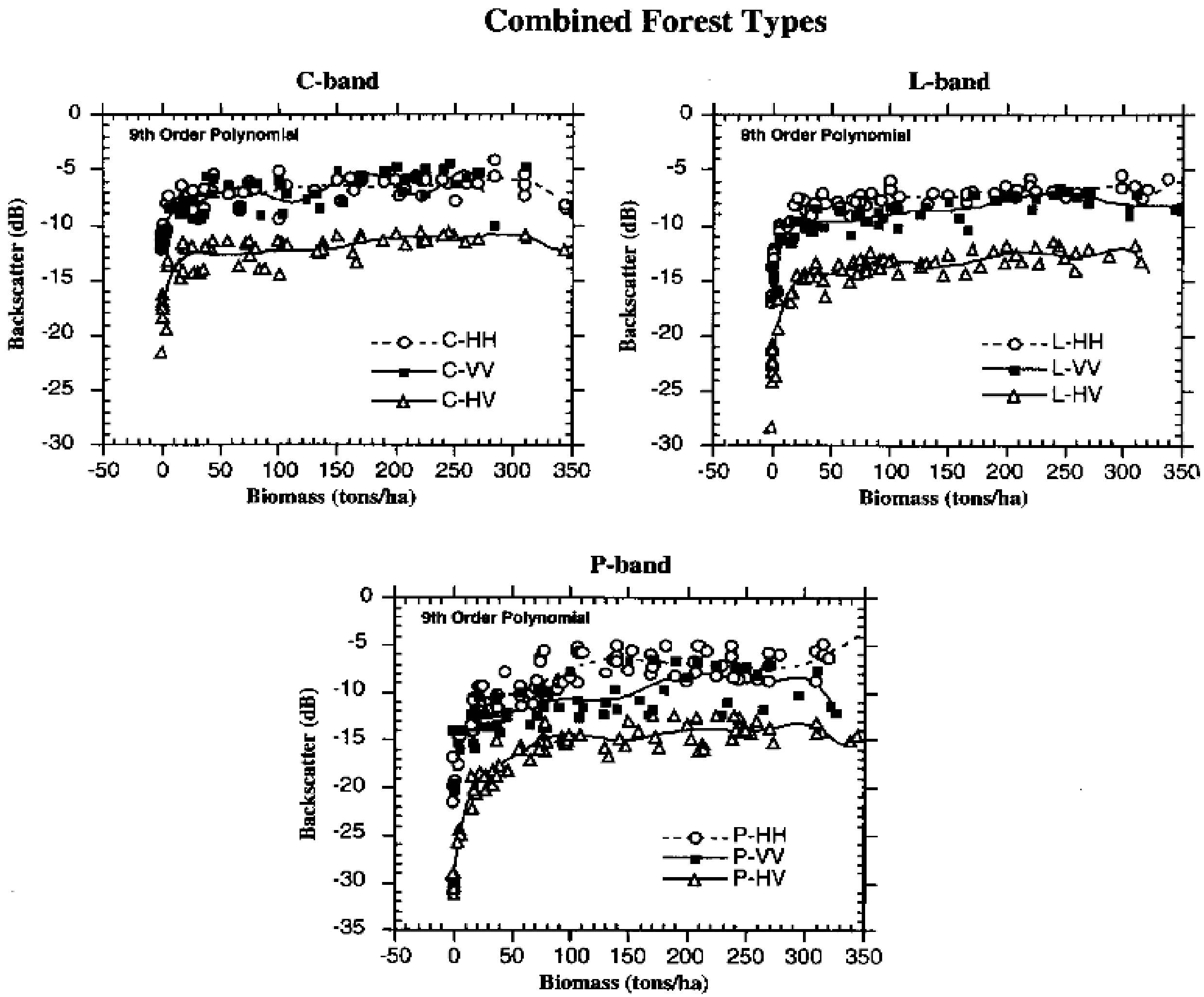

Fig. 3. SAR backscatter plotted against biomass for combined broadleaf evergreen and *Pinus* forest stands. Ninth order polynomial regression curves are shown for each polarization and band. Note locations of first maxima. Regression coefficients and the precise locations (in biomass) of the first maxima are shown in Table VI.

Data from Imhoff, M.L., "Radar Backscatter and BiomassSaturation: Ramifications for Global Biomass Inventory," *IEEE Trans. Geosci. Rem. Sens.*, 33(2):511-518, 1995.

SCANNING LIDAR IMAGER OF CANOPIES BY ECHO RECOVERY

(SLICER)

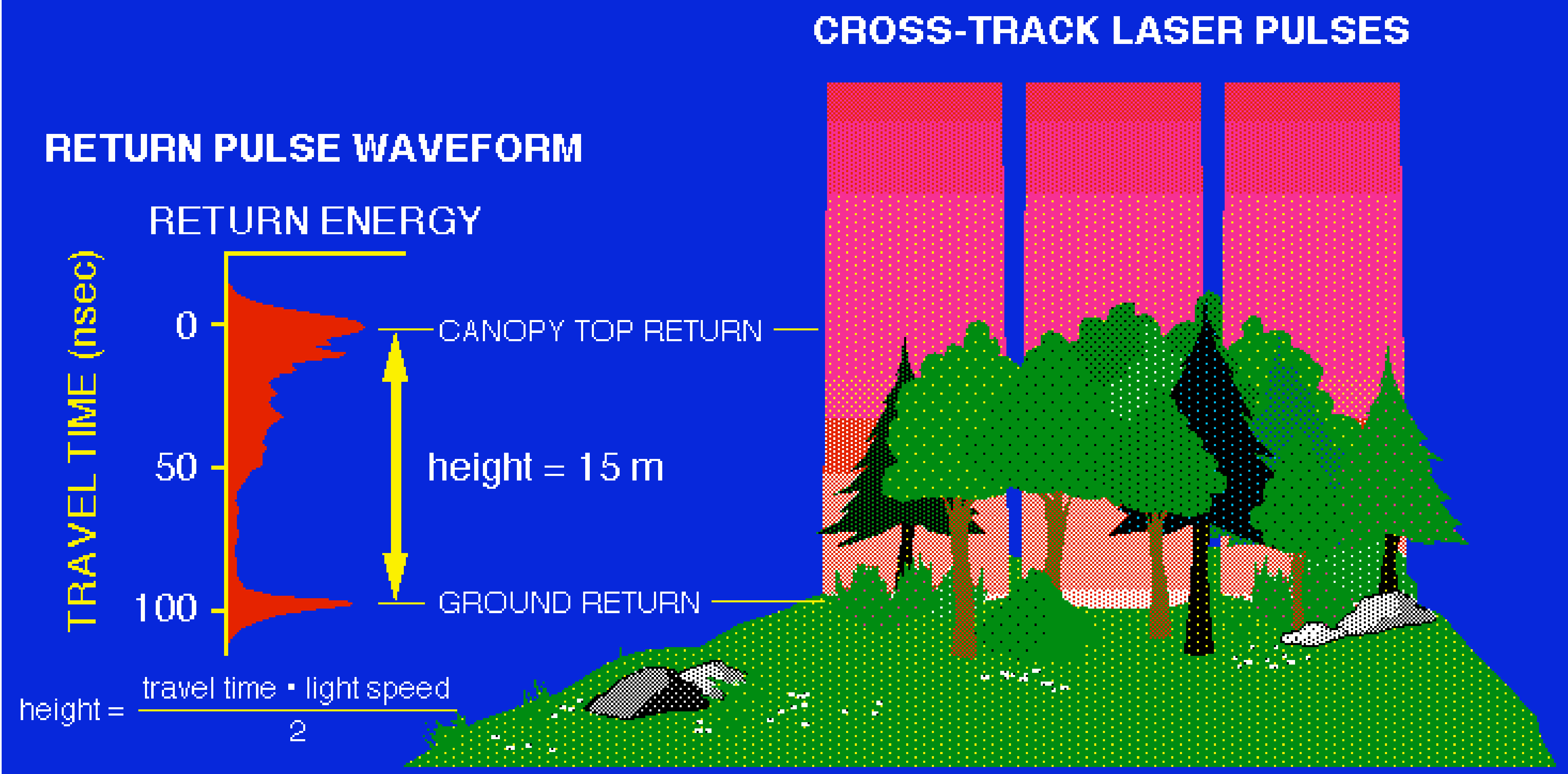

NASA/GSFC

Interferometric Signatures of Forests

Interferometry to resolve look angle ambiguities

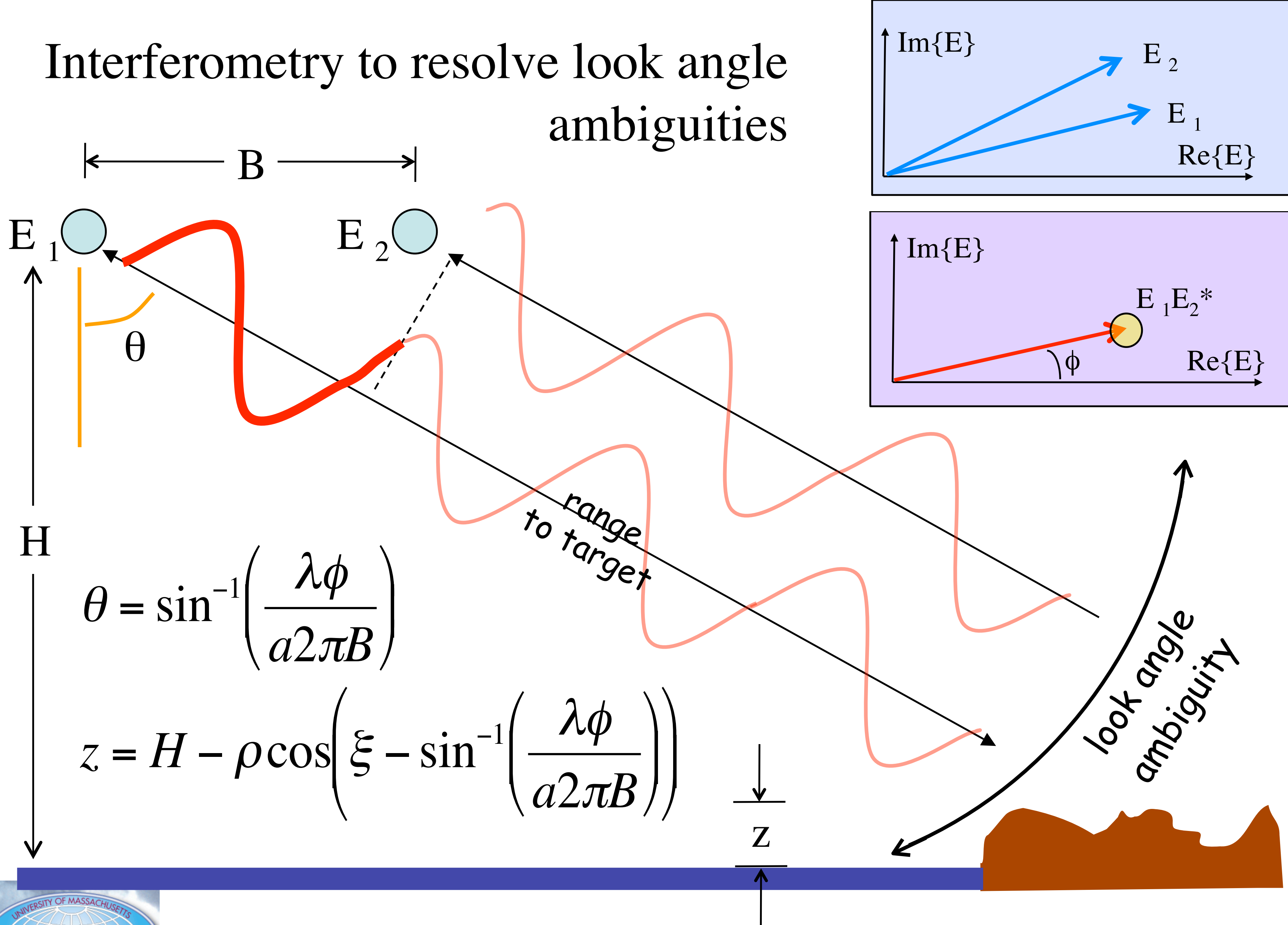

$$\theta = \sin^{-1}\left(\frac{\lambda\phi}{a2\pi B}\right)$$

$$z = H - \rho\cos\left(\xi - \sin^{-1}\left(\frac{\lambda\phi}{a2\pi B}\right)\right)$$

Tree Height Estimation from Radar Interferometry

Path length difference can be used to resolve positional ambiguity and determine the height of the terrain. Accuracy is on the order of meters, with a 25m resolution

$$h = H - \rho \cos\left(\sin^{-1}\left(\frac{\lambda\phi}{4\pi B} \right) \right)$$

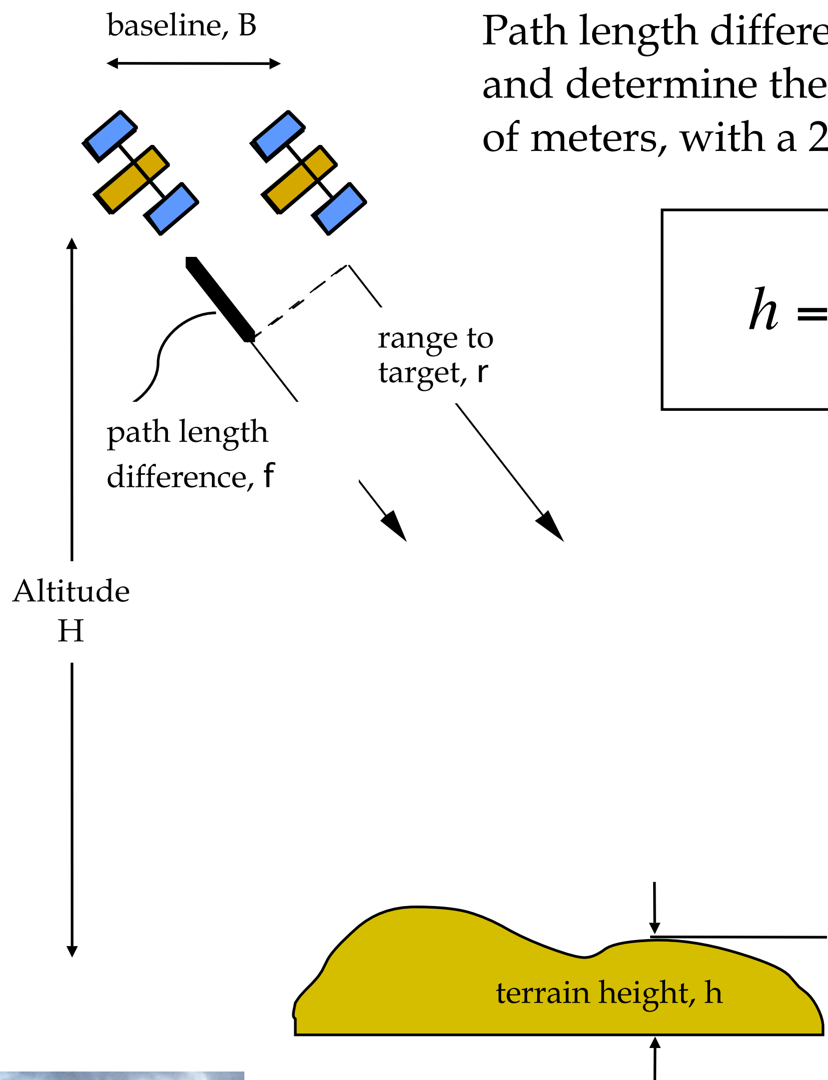

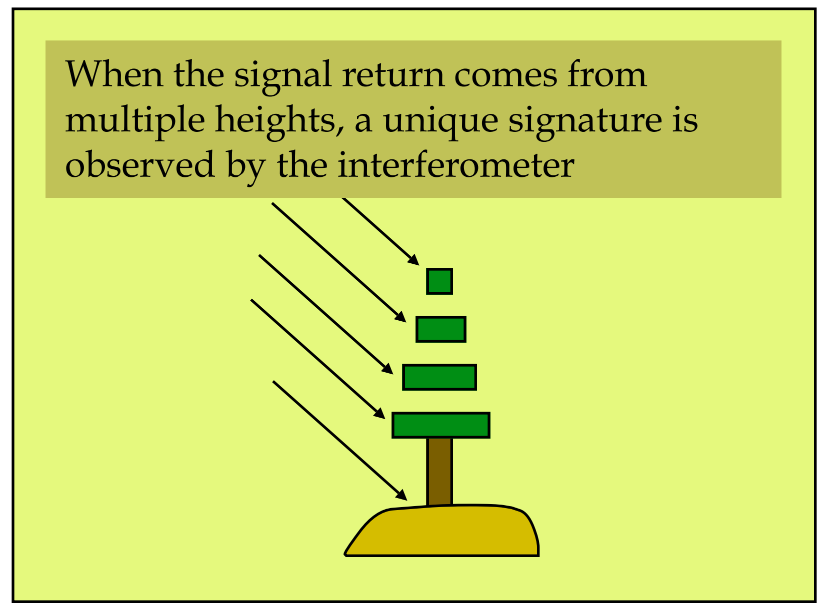

Interferometric Modeling

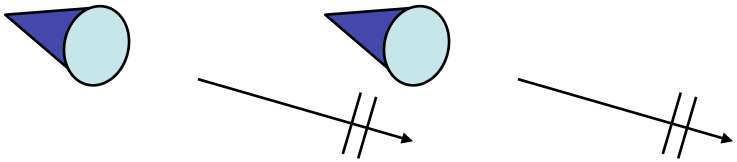

Single Antenna Backscatter

$$\left\langle \left|E_1\right|^2 \right\rangle = A^4 \int_{vol} W_r^{\,2} W_\eta^{\,2} e^{-\kappa z/\cos\theta} \rho(z) \left\langle f_b^{\,2} \right\rangle d^3 r$$

Two Antenna Interferometry

$$\gamma = \left\langle E_1 E_2^* \right\rangle = A^4 \int_{vol} e^{-ik_z z} W_r^{\,2} W_\eta^{\,2} e^{-\kappa z/\cos\theta} \left\langle f_b^{\,2} \right\rangle d^3 r$$

height dependent
phase term

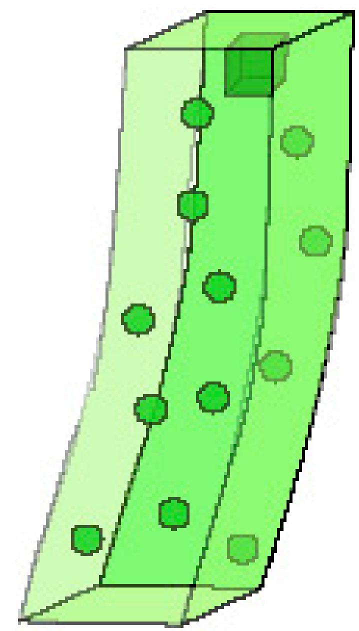

Interferometric Data Products

DEM from Interferometry

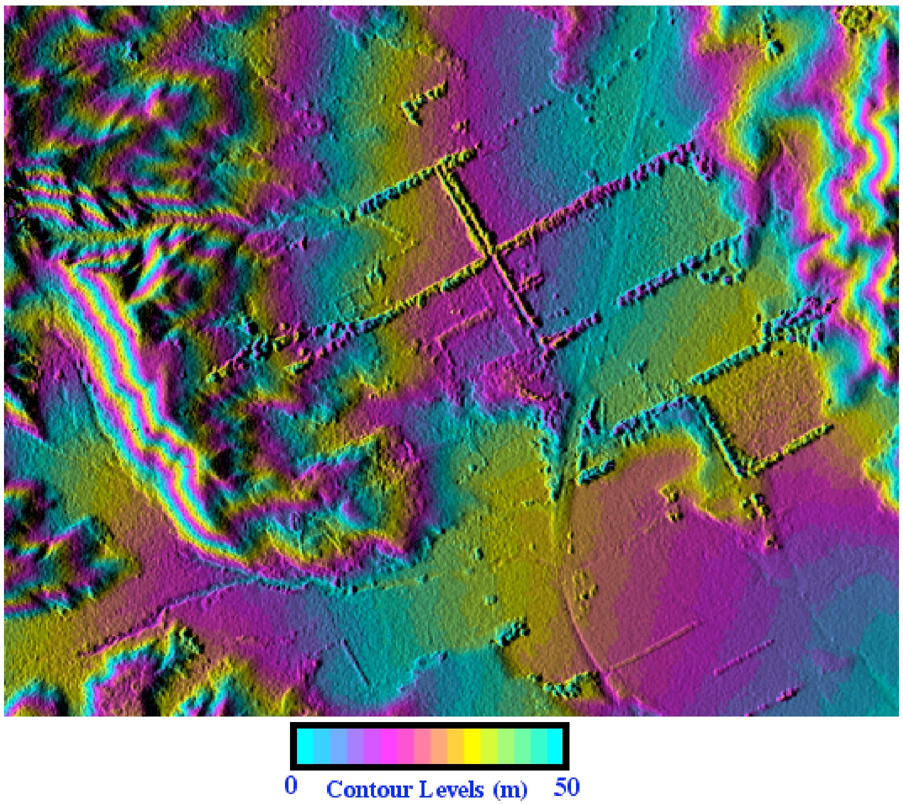

Correlation Map

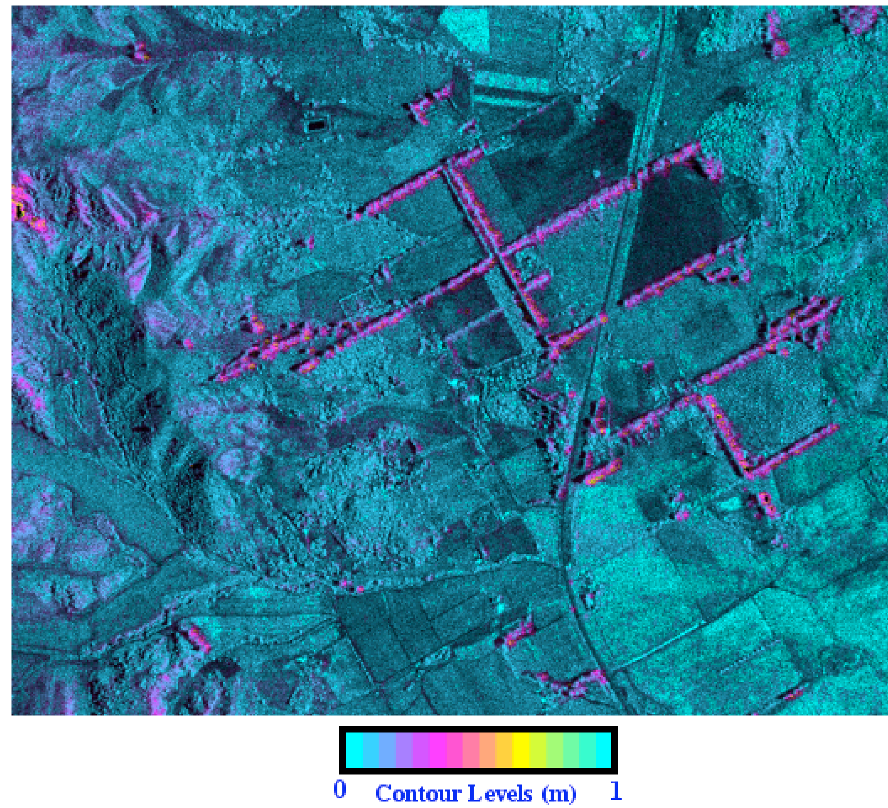

$$\gamma_{obs} = |\gamma_{obs}| e^{i\phi_{obs}} = \gamma_{vol}\gamma_{temp}\gamma_{SNR}\gamma_{geom}$$

Derivation of a first order approximation or metric

$$\gamma_{vol} = |\gamma_{vol}| e^{i\phi_{vol}} = \frac{\int \sigma(z) e^{ik_z z} dz}{\int \sigma(z) dz}$$

$$f(z) = \frac{\sigma(z)}{\int \sigma(z) dz}$$

$$\gamma_{vol} = \int f(z) e^{ik_z z} dz$$

$$\ln \gamma_{vol} = \sum_{n=0}^{\infty} \kappa_n \frac{(ik_z)^n}{n!}$$

$$\ln \gamma_{vol} \approx \mu i k_z - \mu_2 k_z^2 / 2! - \mu_3 i k_z^3 / 3! + \kappa_4 k_z^4 / 4! + \ldots$$

$$\mu_n = \int (z - \mu)^n f(z) dz$$

$$\ln \gamma_{vol} = \ln|\gamma_{vol}| + i\phi_{vol}$$

$$\phi_{vol} = \mu k_z \qquad \ln|\gamma_{vol}| = -\mu_2 k_z^2 / 2$$

$$\sqrt{\mu_2} \approx \sqrt{\frac{-2}{k_z^2} \ln|\gamma_{vol}|}$$

assume uniform vertical scattering profile

$$\mu_2 = \sigma^2 = h_v^2 / 12$$

assume uniform vertical scattering profile

$$\gamma_{vol} = e^{ik_z h_v / 2} \text{sinc } k_z h_v / 2$$

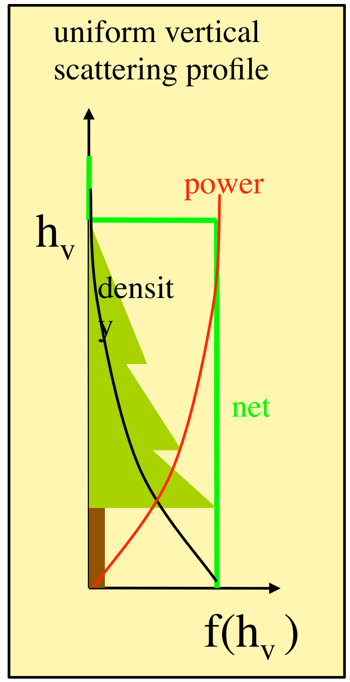

$$h_v \approx \sqrt{\frac{24}{k_z^2} \left(1 - |\gamma_{vol}|\right)}$$

Slicer Tree Height vs. GeoSAR Tree Heights based on X-band Correlation Magnitude

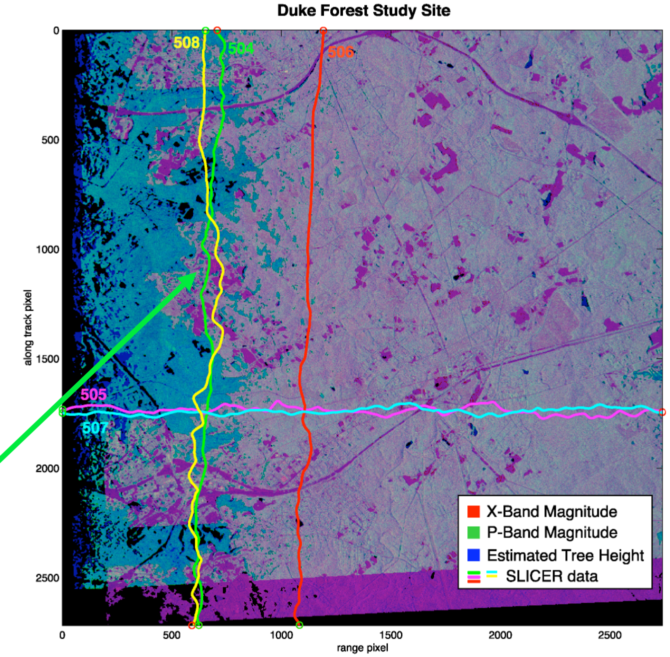

Slicer Line #504

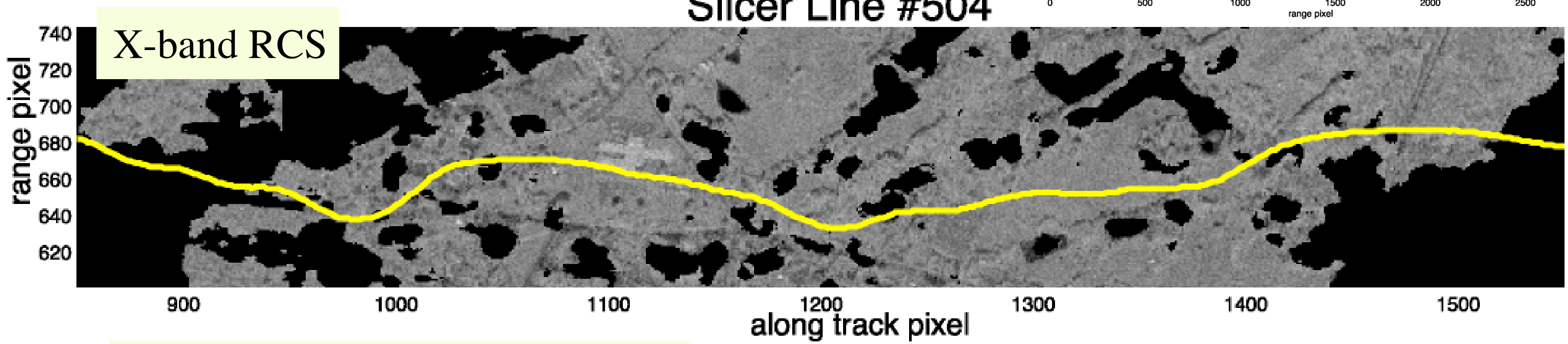

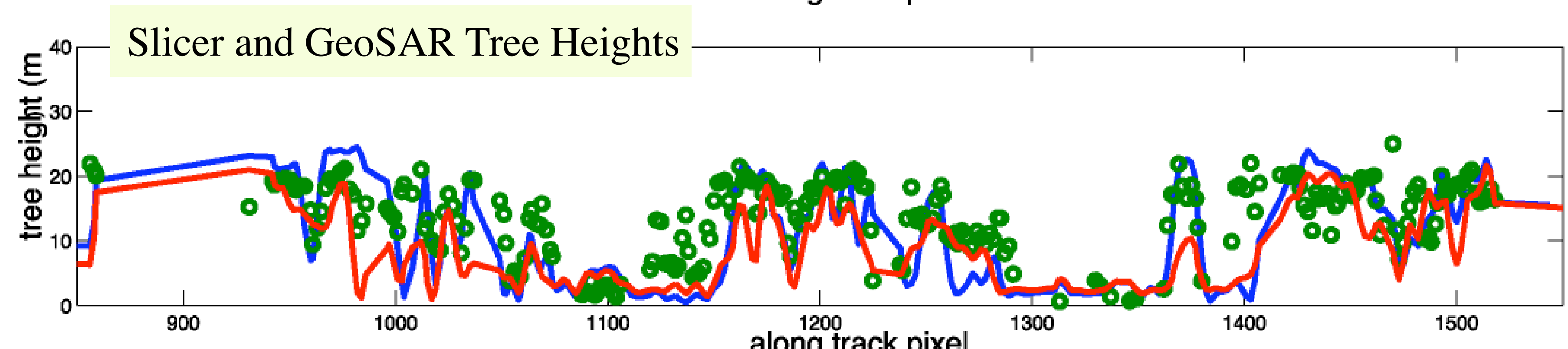

Calibration

- Need for a well calibrated signal
  - understand error sources
  - provide ability to unwrap desired signature from other observational artifacts.

- Observed correlation is modeled as the combination of a variety of sources

$$\gamma_{obs} = \gamma_{vol}\gamma_{SNR}\gamma_{geom}\gamma_{temp}$$

$$\Rightarrow \quad \gamma_{vol} = \frac{\gamma_{obs}}{\gamma_{SNR}\gamma_{geom}\gamma_{temp}} = f(h_v)$$

$$h_v = f^{-1}(\gamma_{vol})$$

InSAR Error Sources

- Total observed correlation arises from a combination of several sources.

$$\gamma_{obs} = \gamma_{vol}\gamma_{SNR}\gamma_{geom}\gamma_{temp}$$

- Geometric Decorrelation

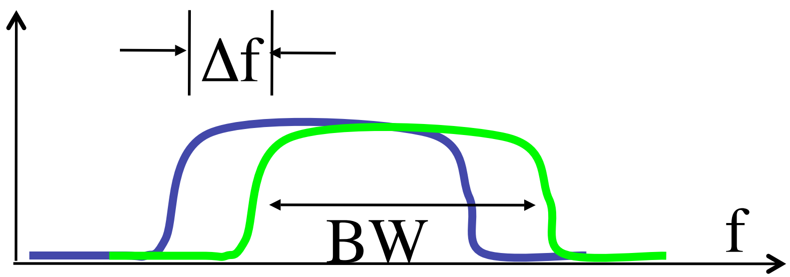

$$\Delta f = \frac{c\,B\cos(\theta-\alpha)}{2\;r_0\;\lambda\tan(\theta-\tau_y)}$$

$$\gamma_{geom} \approx 1 - \frac{c\,B\cos(\theta-\alpha)}{2\;BW\;r_0\;\lambda\tan(\theta-\tau_y)}$$

- Thermal Noise

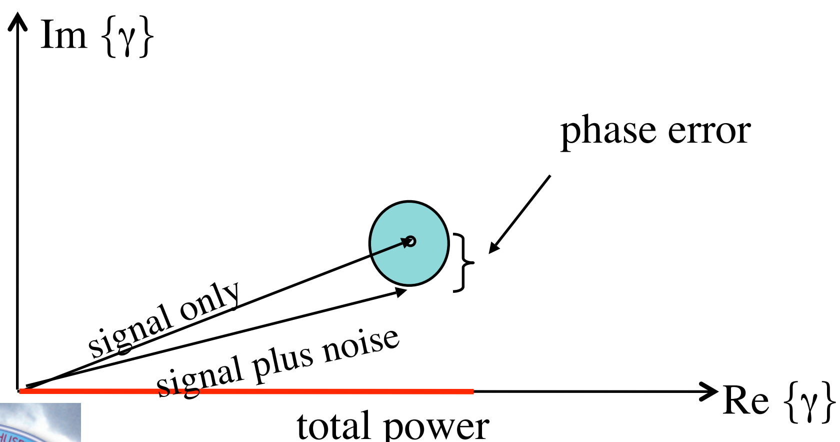

$$\gamma_{SNR} = \frac{S}{S(1+\alpha)+N_{th}}$$

Temporal Decorrelation

- Caused by scatterer motion between repeat-pass observations

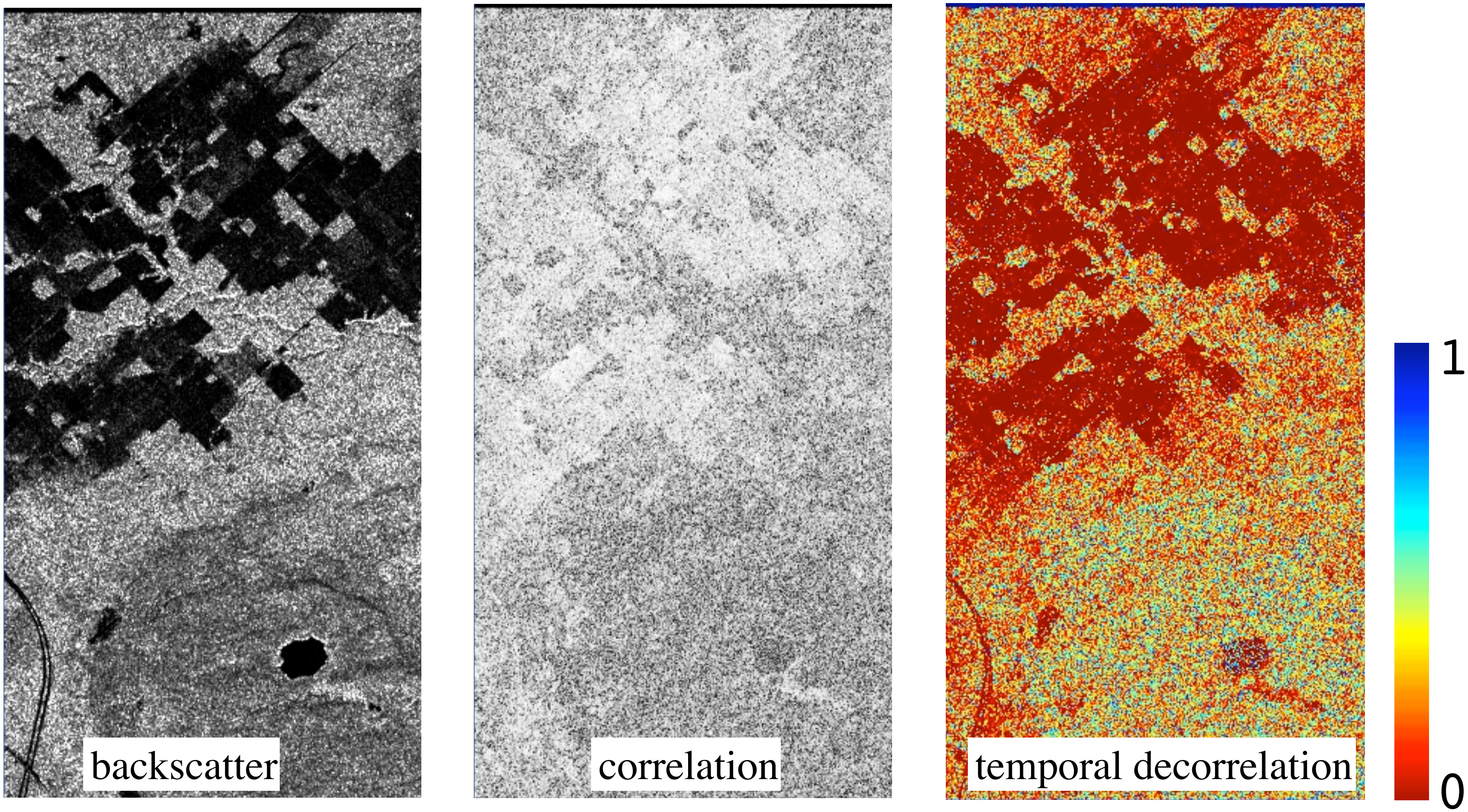

SIR-C, one-day repeat L-band over Raco, Michigan

Decorrelation likely due to a weather event occuring between observations

Temporal Decorrelation

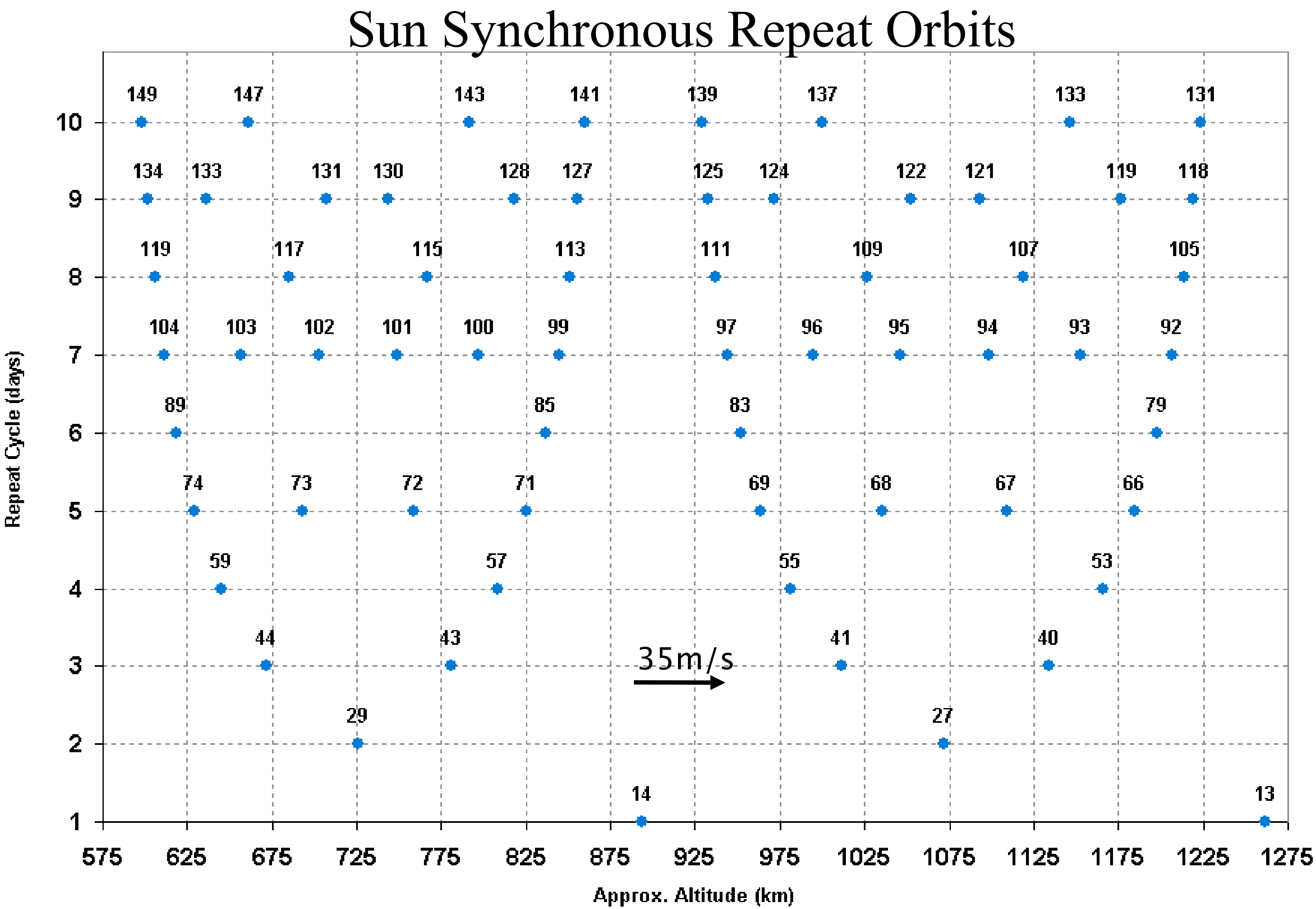

Slide courtesy of Tomas Martin/JPL

System/Measurement Design

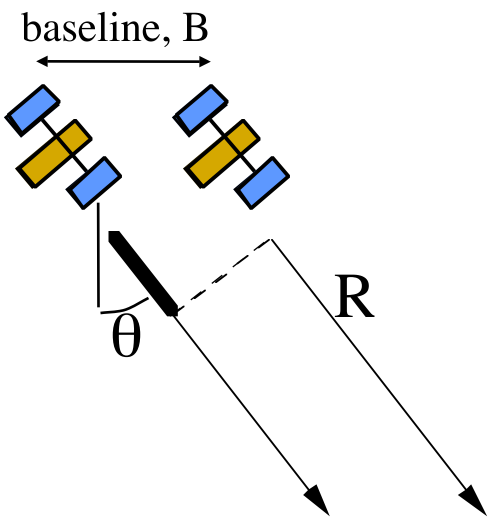

- Look Angle
- Baseline Length
- Altitude or Range
- Frequency (wavelength)
- Management of Measurement Errors
- Observing Strategy

$$\boxed{k_z = \frac{akB\cos(\theta - \alpha)}{R\sin\theta}}$$

Build an Error Model to take into account statistical uncertainty

$$\begin{tikzcd}
 & \sigma^2_{\text{model}}, p(\text{model}) \arrow[dl] & \sigma^2_{\gamma_{obs}}, p(\gamma_{obs}) \arrow[ddl] & \sigma^2_{S_1}, p(S_1) \arrow[dl] \\
 & & \sigma^2_{\gamma_{snr}}, p(\gamma_{snr}) \arrow[dl] & \sigma^2_{N_{Th}}, p(N_{Th}) \arrow[l] \\
\sigma^2_{h_v}, p(h_v) & \sigma^2_{\gamma_{vol}}, p(\gamma_{vol}) \arrow[l] & & \sigma^2_{\alpha}, p(\alpha) \arrow[ul] \\
 & & \sigma^2_{\gamma_{geom}}, p(\gamma_{geom}) \arrow[ul] & \\
 & & \sigma^2_{\gamma_{temp}}, p(\gamma_{temp}) \arrow[uul] &
\end{tikzcd}$$

Approach to System/Measurement Design

- Explore the effects of changing baseline, B, and look angle, θ, on the estimate error.

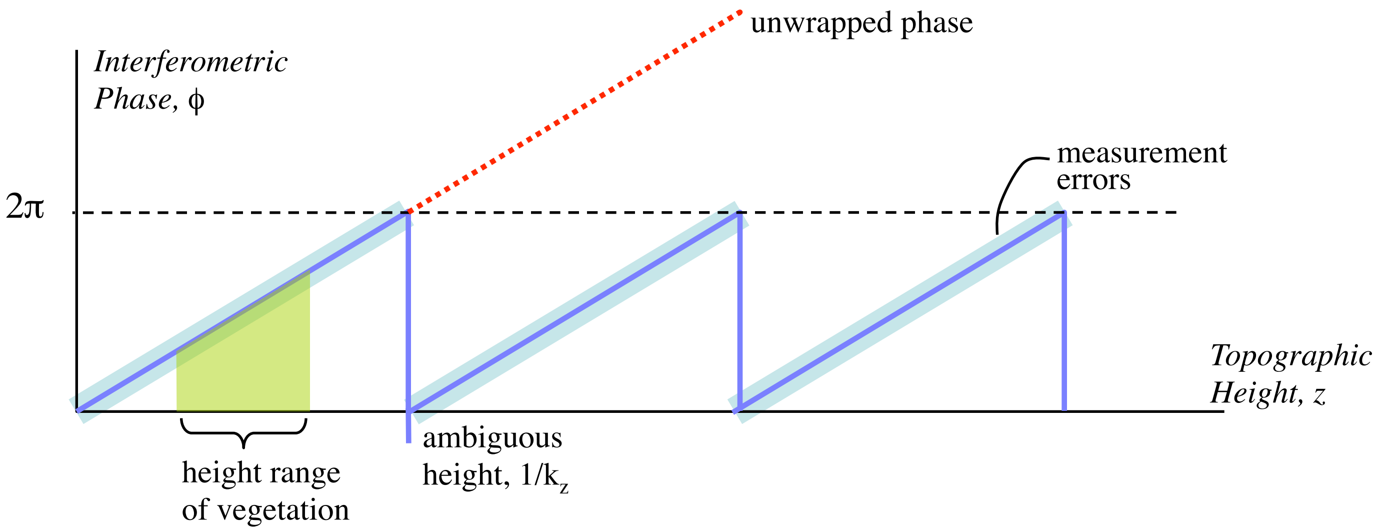

slope of line is set by the sensitivity of interferometric phase to height

$$k_z = \frac{akB\cos(\theta - \alpha)}{R\sin\theta}$$

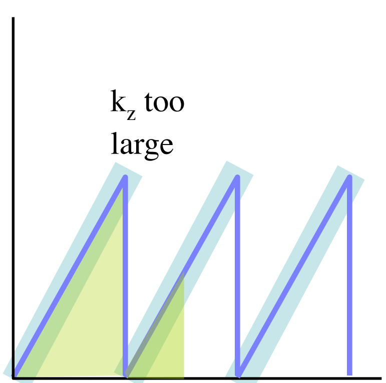

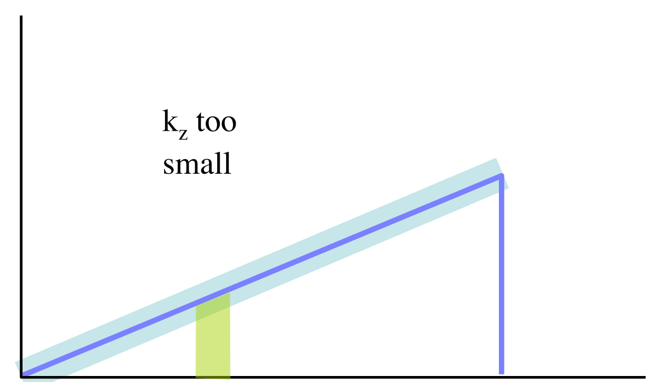

Choose kz to maximize signal and minimize errors

max baseline for 28 MHz BW L-band signal (ALOS/PALSAR) set by upper limit to decorrelation

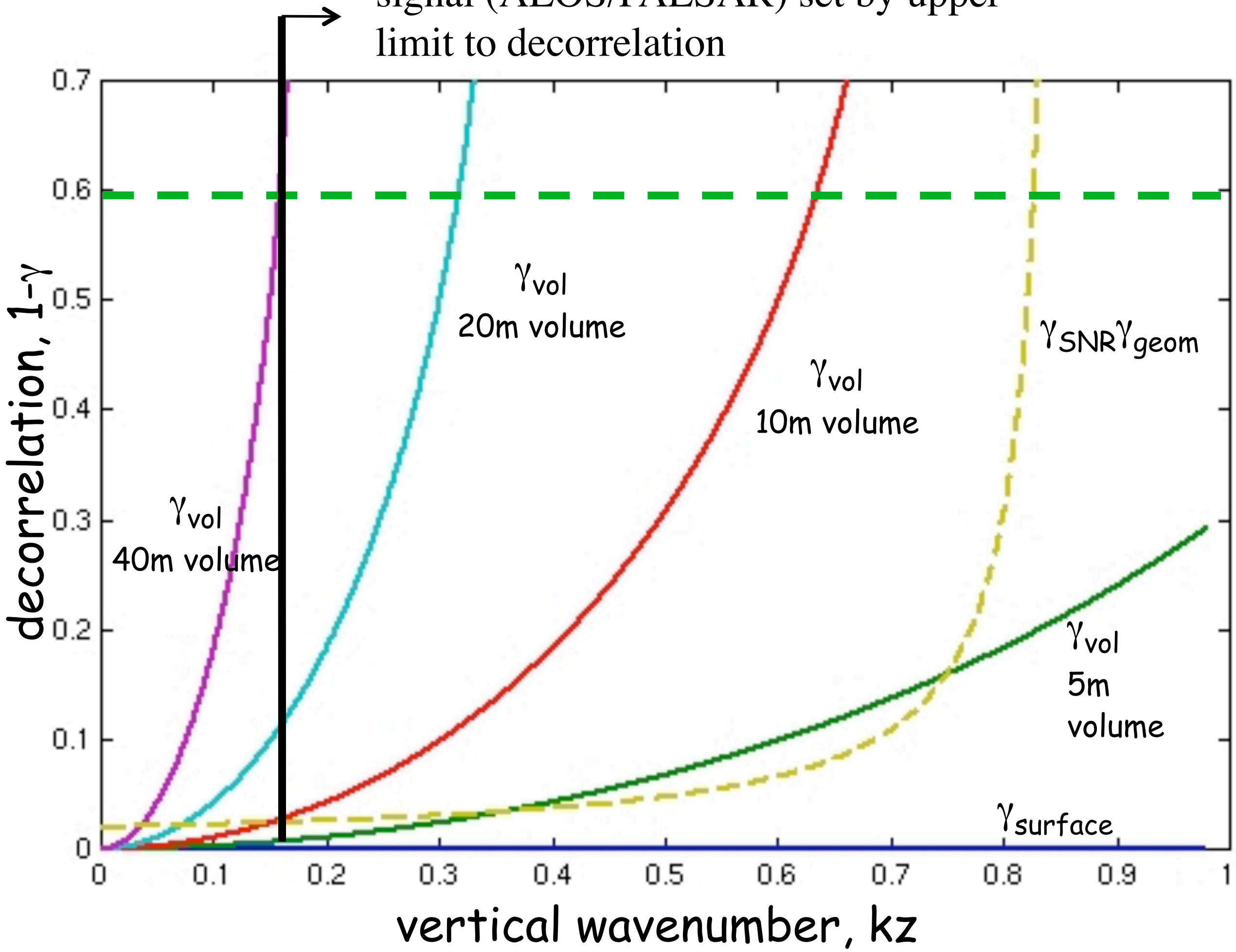

- large baseline desired to maximize sensitivity to volumetric decorrelation

  (short volumes have small decorrelation signatures)
- maximum baseline is limited by
  - loss of signal due to the wavenumber shift (Prati filtering)
  - maximum decorrelation allowable for phase unwrapping (γ=0.4)
- simple volumetric model used to demonstrate this tradoff in figure at left.

JPL

Some Comparisons

- Observational characteristics for various interferometers can be compared with a proposed InSAR observation that would be sensitive to vegetation

Sensor	Altitude (km)	θ, α (deg)	B, λ (m)	k_z (rad/m)	h_{ambig} (m)	BW, B_{crit} (MHz, m)
GeoSAR X	10,000	45, 0	2(2.6), 0.03	0.08	160	160, 230
GeoSAR P	10,000	45, 0	2(20), 0.87	0.02	310	160, 6500
AIRSAR C	10,000	45, 65	2(2.5), 0.056	0.05	120	40, 85
SRTM	230,000	40, 45	60, 0.056	0.03	240	10, 600
DLR - L	3,000	39, 0	2(15), 0.24	0.24	27	100, 260
ALOS/PALSAR	700,000	35, 0	2(800), 0.24	0.07	90	28, 13400

ALOS/PALSAR Kyoto and Carbon Cycle Initiative

System Parameter	Value
Frequency	L-Band
Wavelength	24 cm
Bandwidth	14 & 28 MHz
Noise Equivalent σ^o	$\geq$ -23 dB
Signal to Ambiguity Ratio	$\leq$ 16 dB
Thermal SNR Over Vegetation	18 dB
Platform Height	700 km
Swath Width	40 - 70 km
Resolution	7 - 44 m
Effective Number of Looks Used	64
Look Angle Range	8 - 60 degrees
Repeat Track Time	46 days

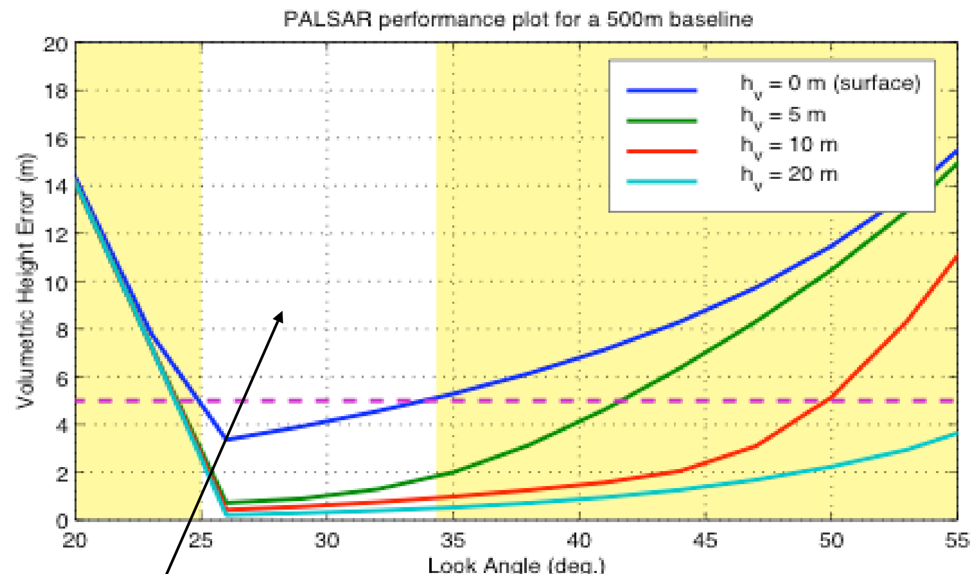

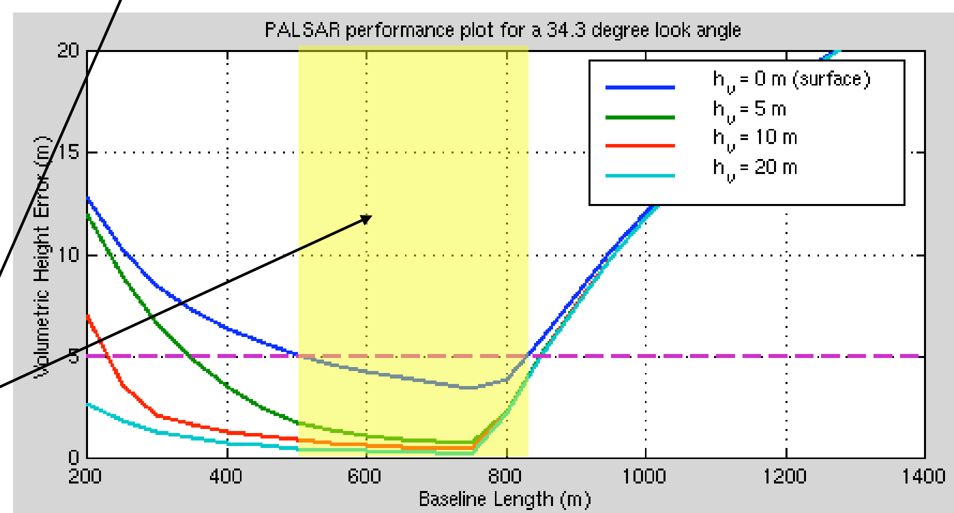

operating
region

Repeat Pass Cross-Track Baseline

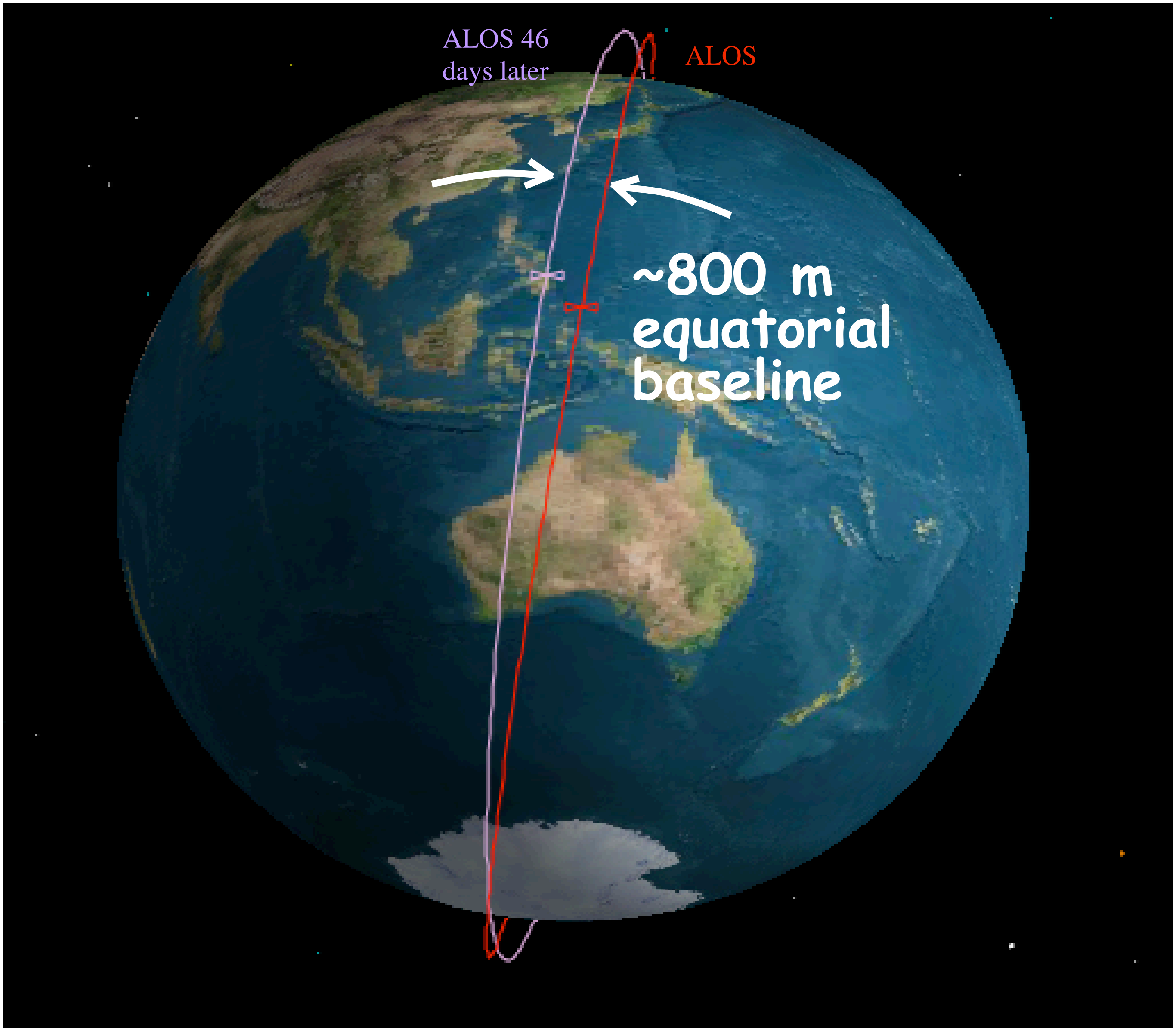

Implementation Issues

- Baseline changes as a function of latitude

- Very small amount of lateral thrust (<0.001 m/s) applied to spacecraft at equator crossing to achieve "time of day" shift in crossing.

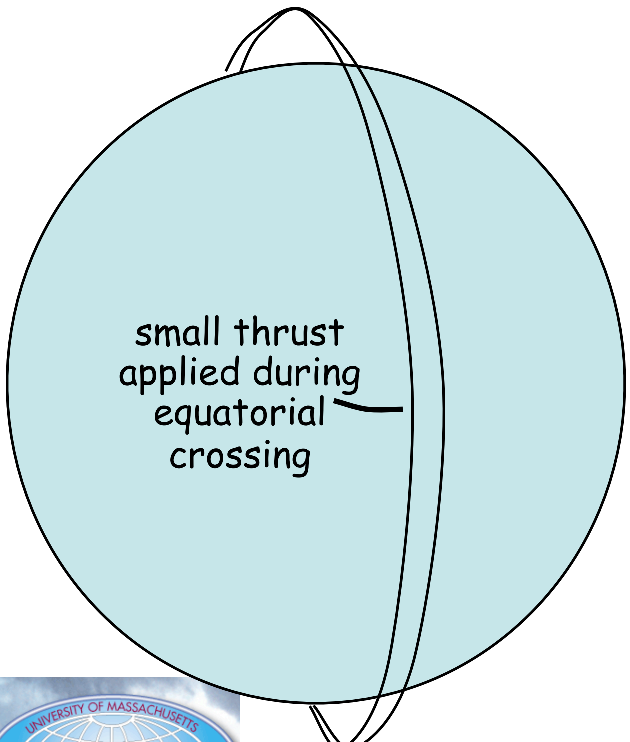

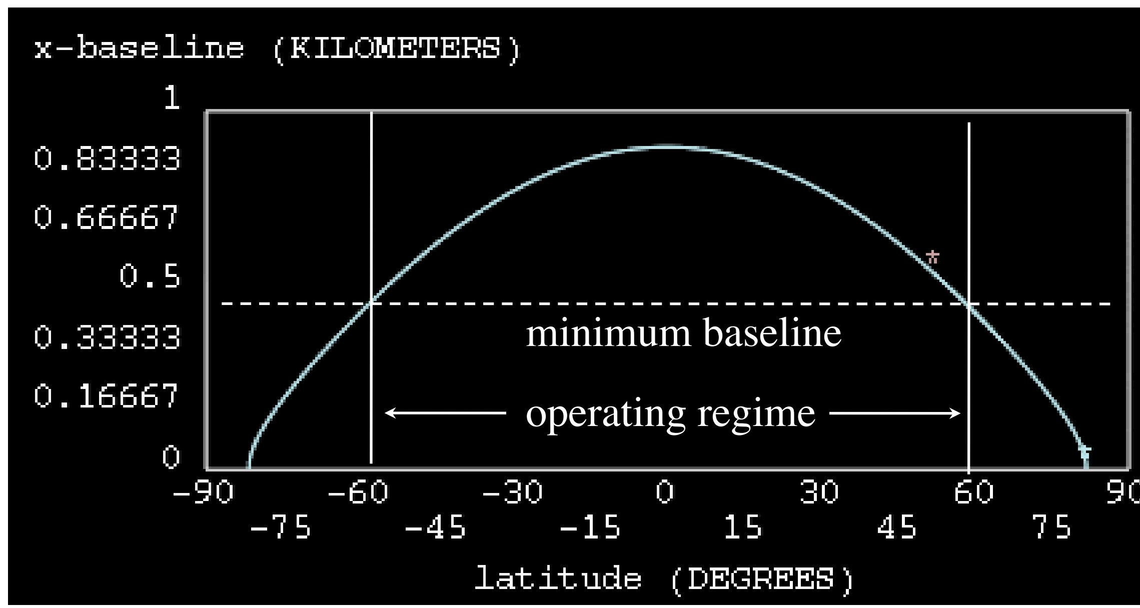

Fully Polarimetric or only Co-pol/Cross-pol??

- Fully Polarimetric: Increases data rate, increases range ambiguities, decreases swath

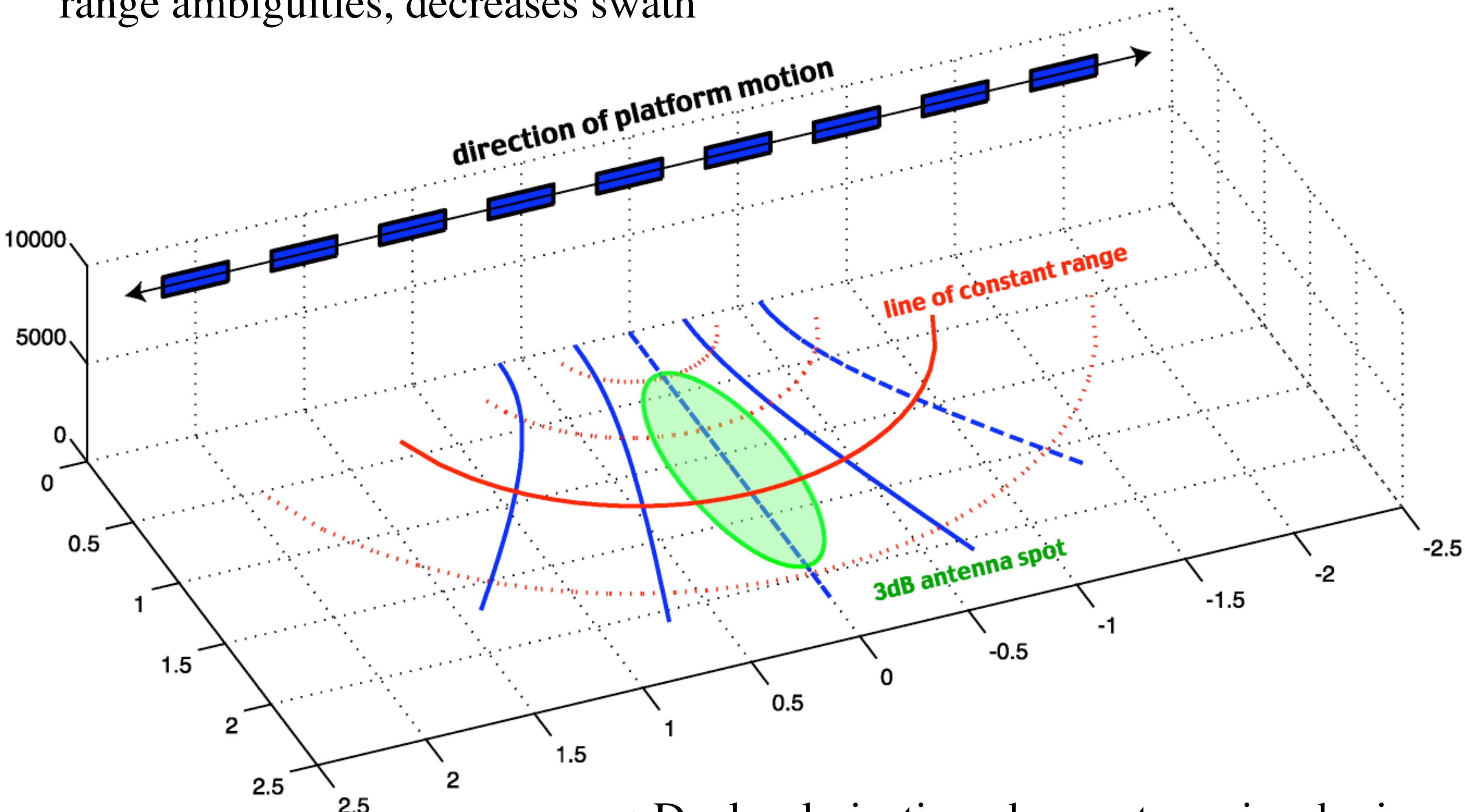

- Dual-polarization: does not require sharing of aperture, may have similar utility

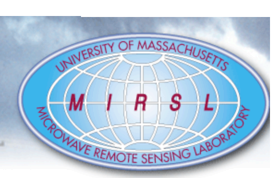

Research Tasks in Remote Sensing

Science Question

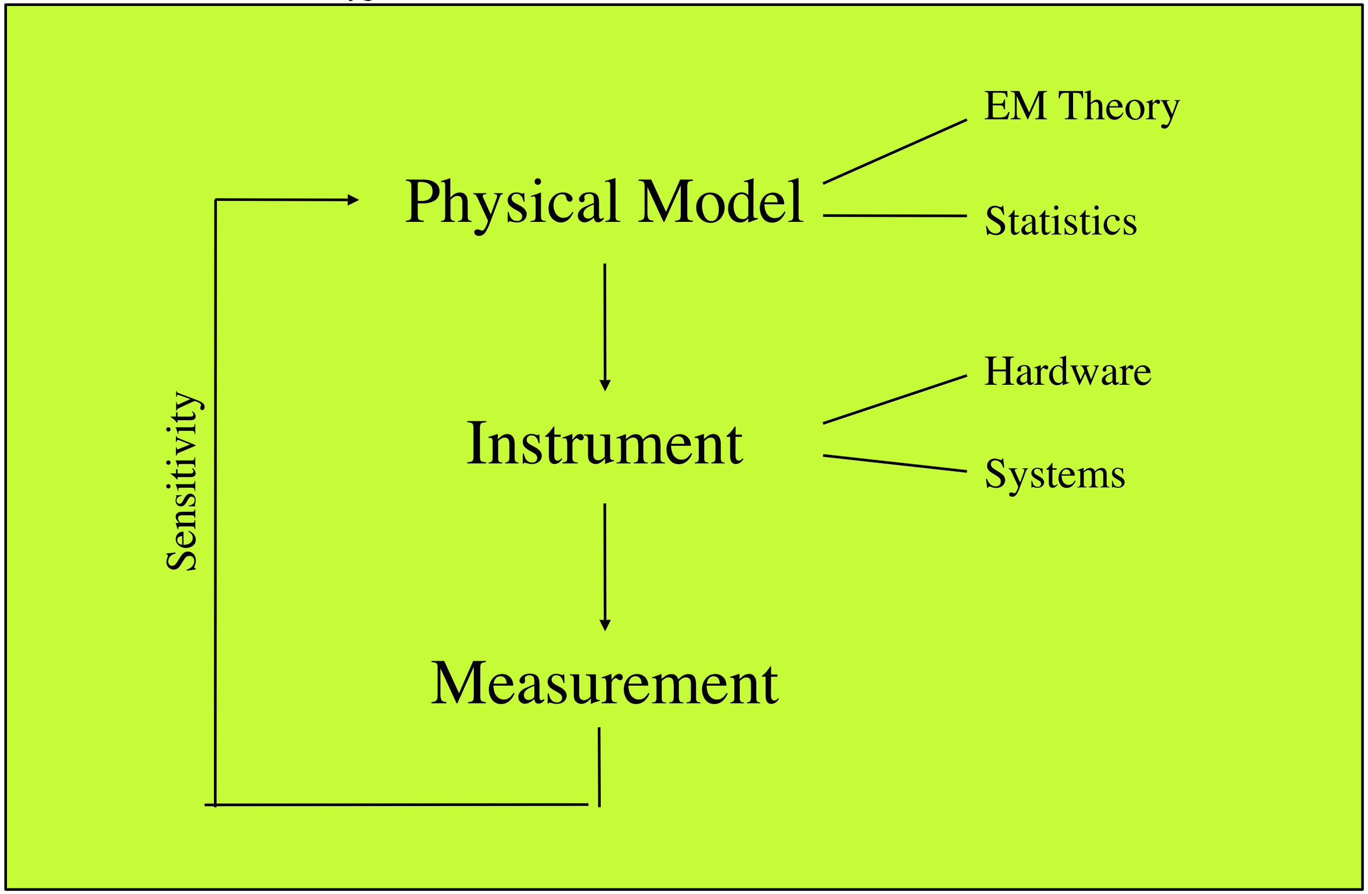

Conclusions

- Demonstrated InSAR Sensitivity to Vegetation
- Discussed Error Sources Involved in Observations
- Determined “Best” Baseline & Look Angle for ALOS/ PALSAR for measuring vegetation characteristics
  - best baseline is between 500 - 800 m
  - best look angle is between 25 and 35 degrees.
- Greatest Risk is Due to Temporal Decorrelation
- Looking Forward to the Launch of ALOS/PALSAR

Global Coverage of ASTER Data And Its Accuracy and Availability

December 13, 2005

The 11th International Symposium on Remote Sensing

Chiba University, Japan

Hiroshi Watanabe, ERSDAC

ASTER VNIR Image with GIS Information
Chiba September, 2005

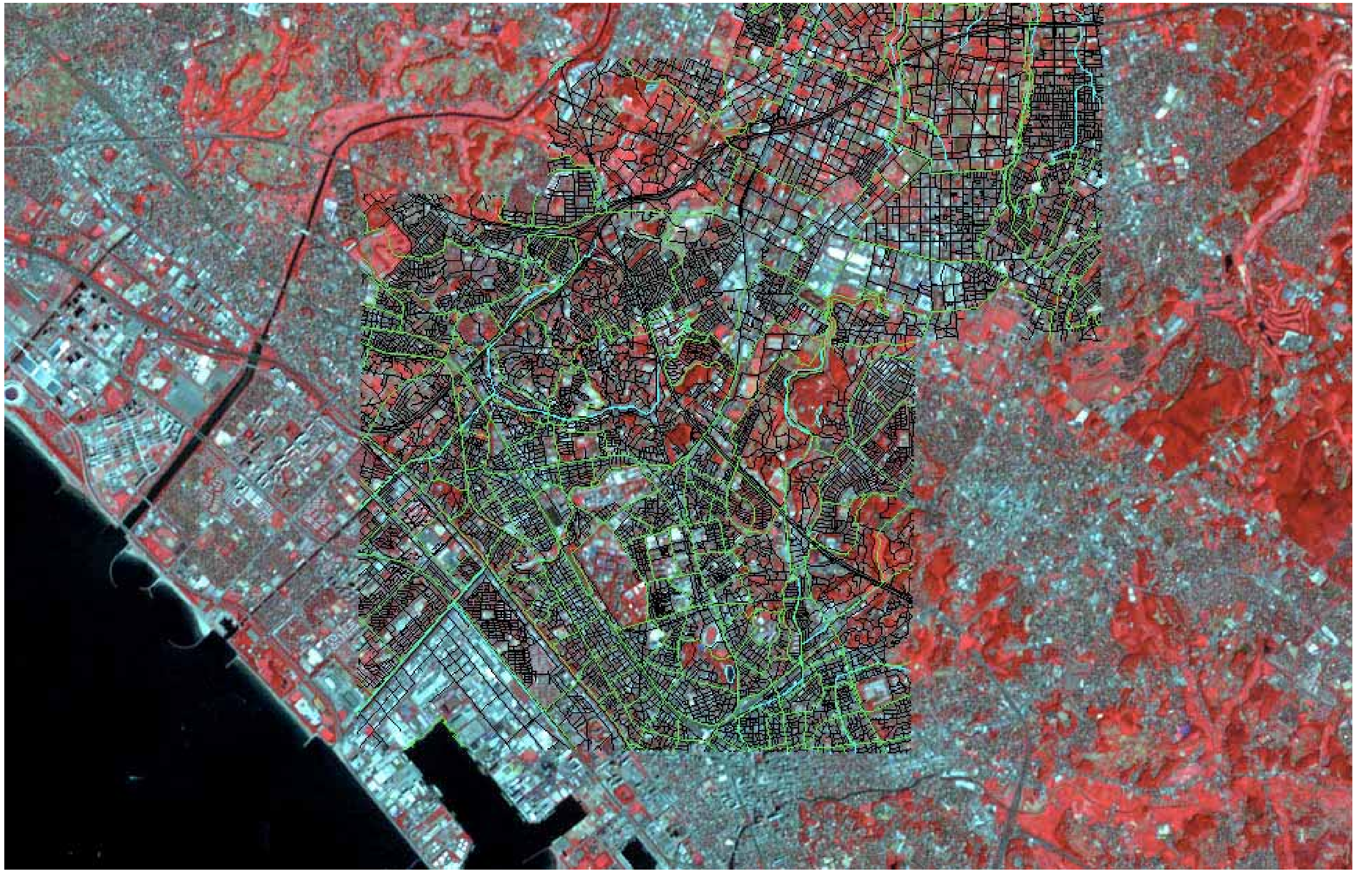

Brief Introduction to ASTER

METI's Earth Observation Satellite Lineups

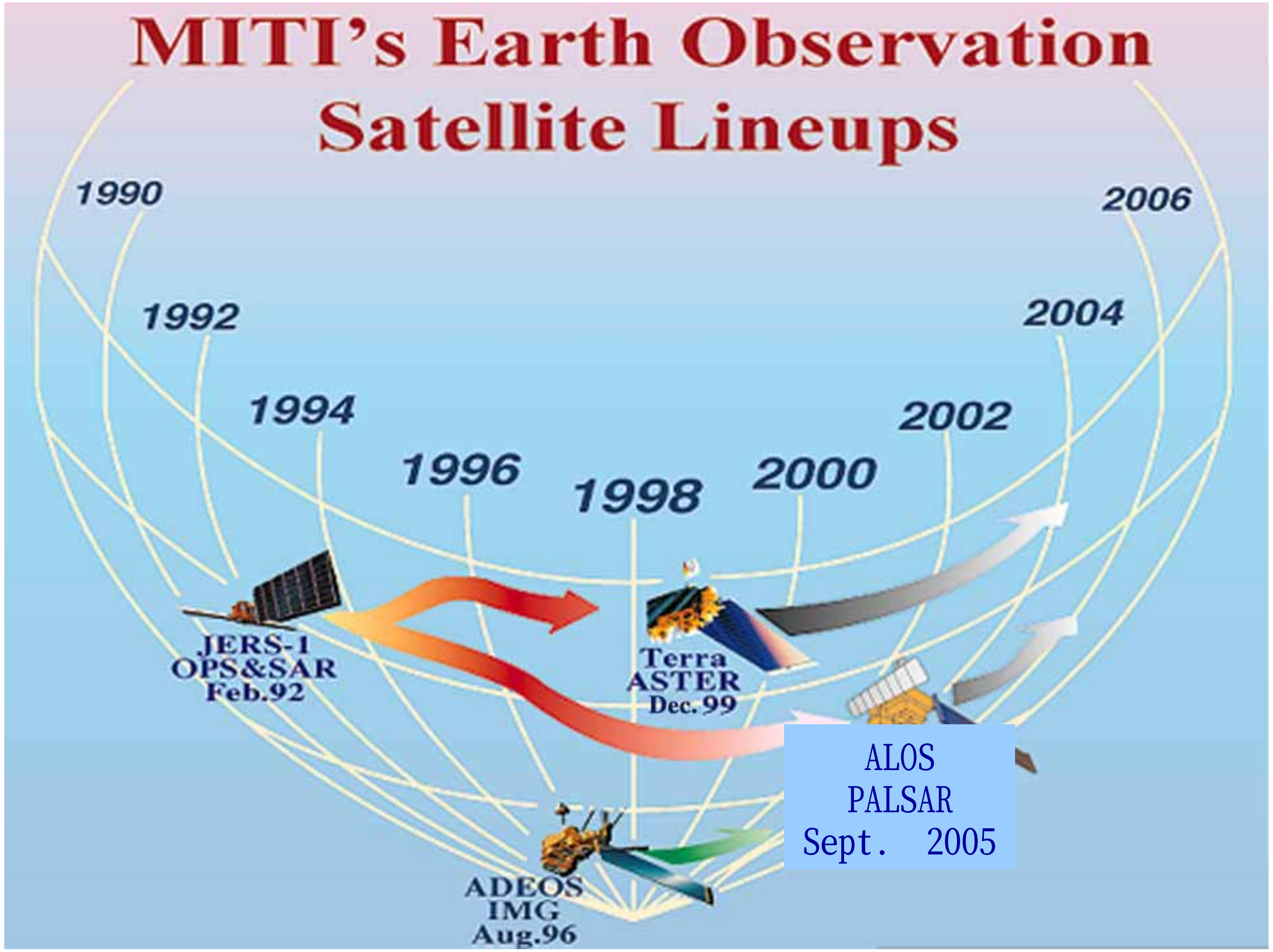

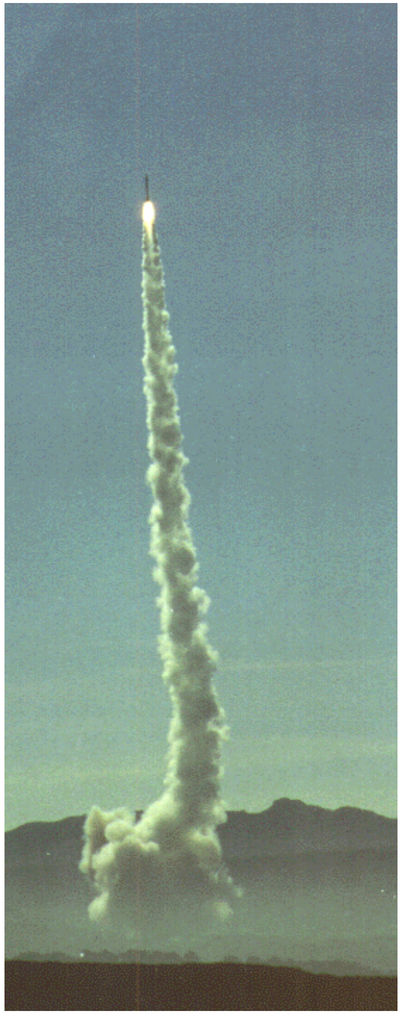

EOS-AM1(TERRA)

Launched

on December 18th, 1999

at 18:57:40GMT

What is Terra ?

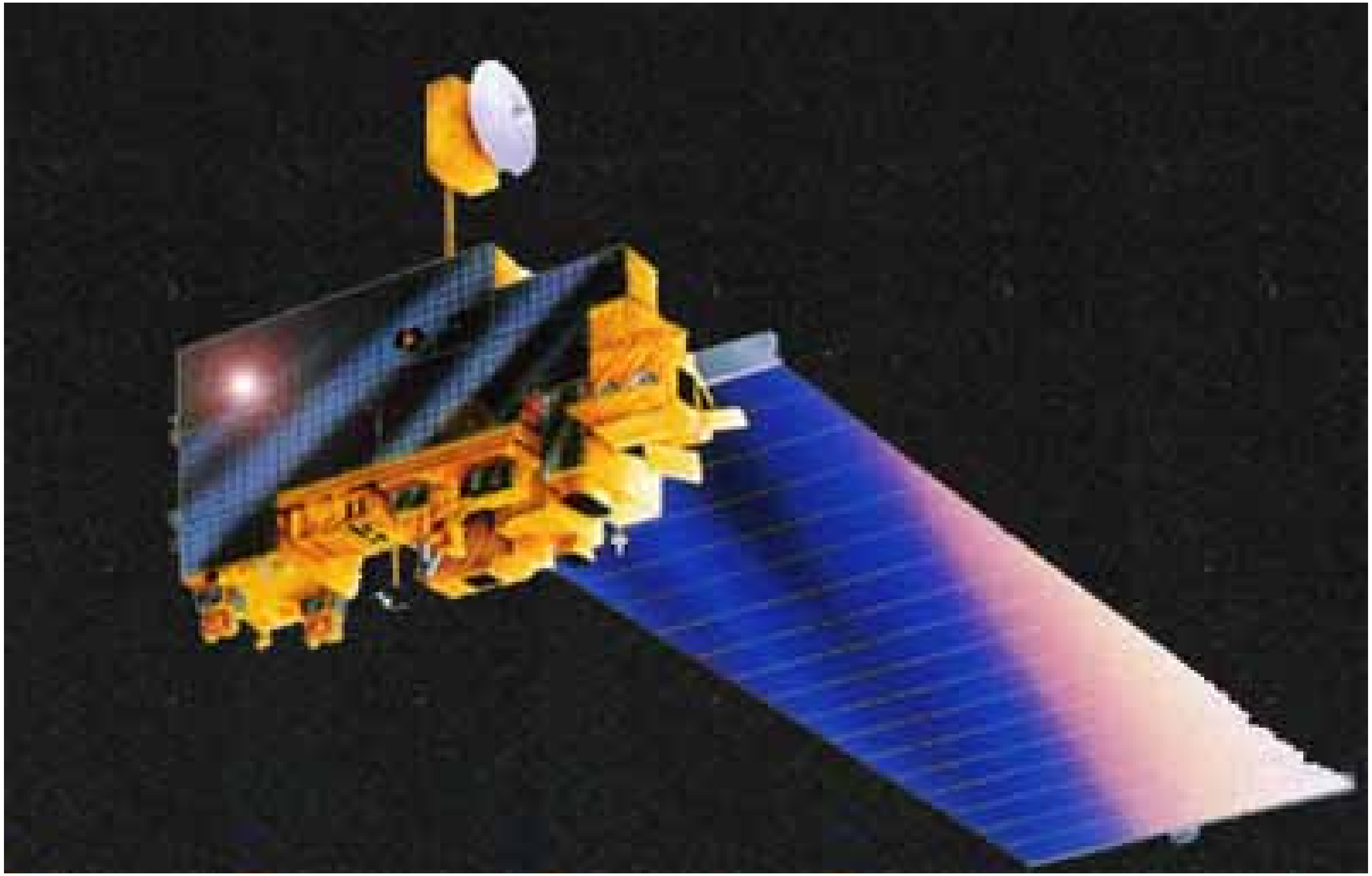

Orbit of Terra

Orbit	**Sun Synchronous**
Local time at equator	**10:30 a.m. ±15min.**
Altitude range	**700-737 km (705 km at equator)**
Inclination	**98.2° ±0.15°**
	16 days (233 revolutions/16 days)
Distance between adjacent orbits	**172 km at equator**
Repetition accuracy	**±20 km,3σ**

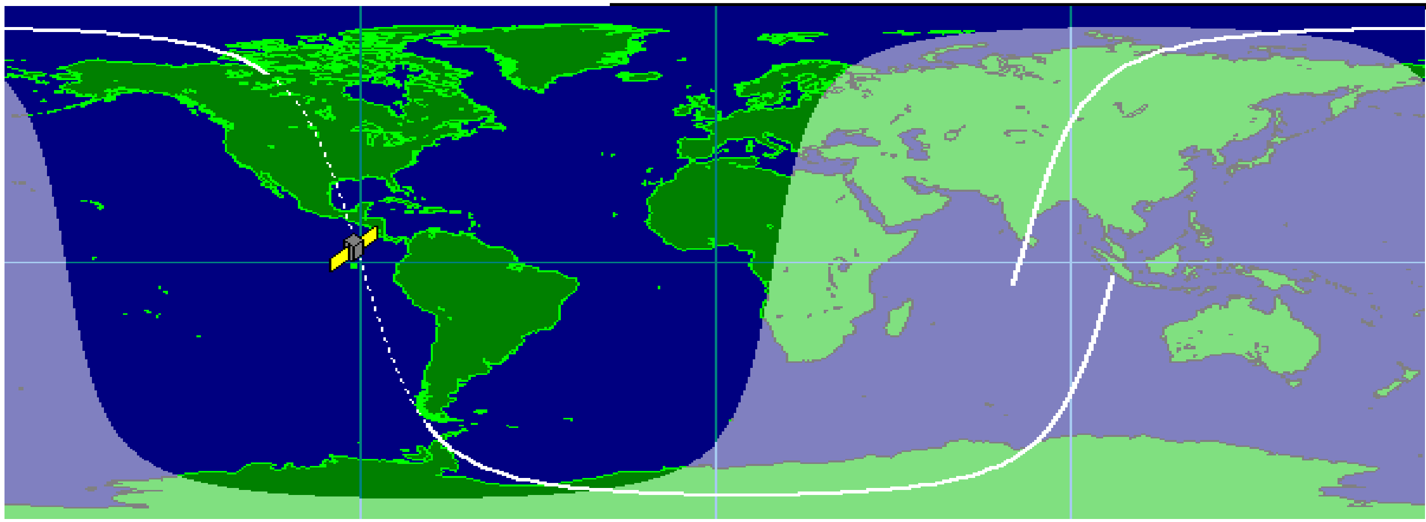

Terra / NASA

CORE SENSORS:

- ASTER

Advanced Spaceborne Thermal Emission & Reflection Radiometer

- CERES

Clouds and the Earth's Radiant Energy System

- MISR

Multi-angle Imaging Spectro-Radiometer

- MODIS

Moderate-resolution Imaging Spectroradiometer

- MOPITT

Measurements of Pollution in the Troposphere

PURPOSES:

(1) To promote research into geological phenomena of tectonic surfaces and geological history through detailed mapping of the Earth's topography and geological formations. (This goal includes contributions to applied research in remote sensing.)

(2) To understand distribution and changes of vegetation.

(3) To further understand interactions between the Earth's surface and atmosphere by surface temperature mapping.

(4) To evaluate impact of volcanic gas emission to the atmosphere through monitoring of volcanic activities.

(5) To contribute to understanding of aerosol characteristics in the atmosphere and of cloud classification.

(6) To contribute to understanding of the role coral reefs play in the carbon cycle through coral classification and global distribution mapping of corals.

What is ASTER ?

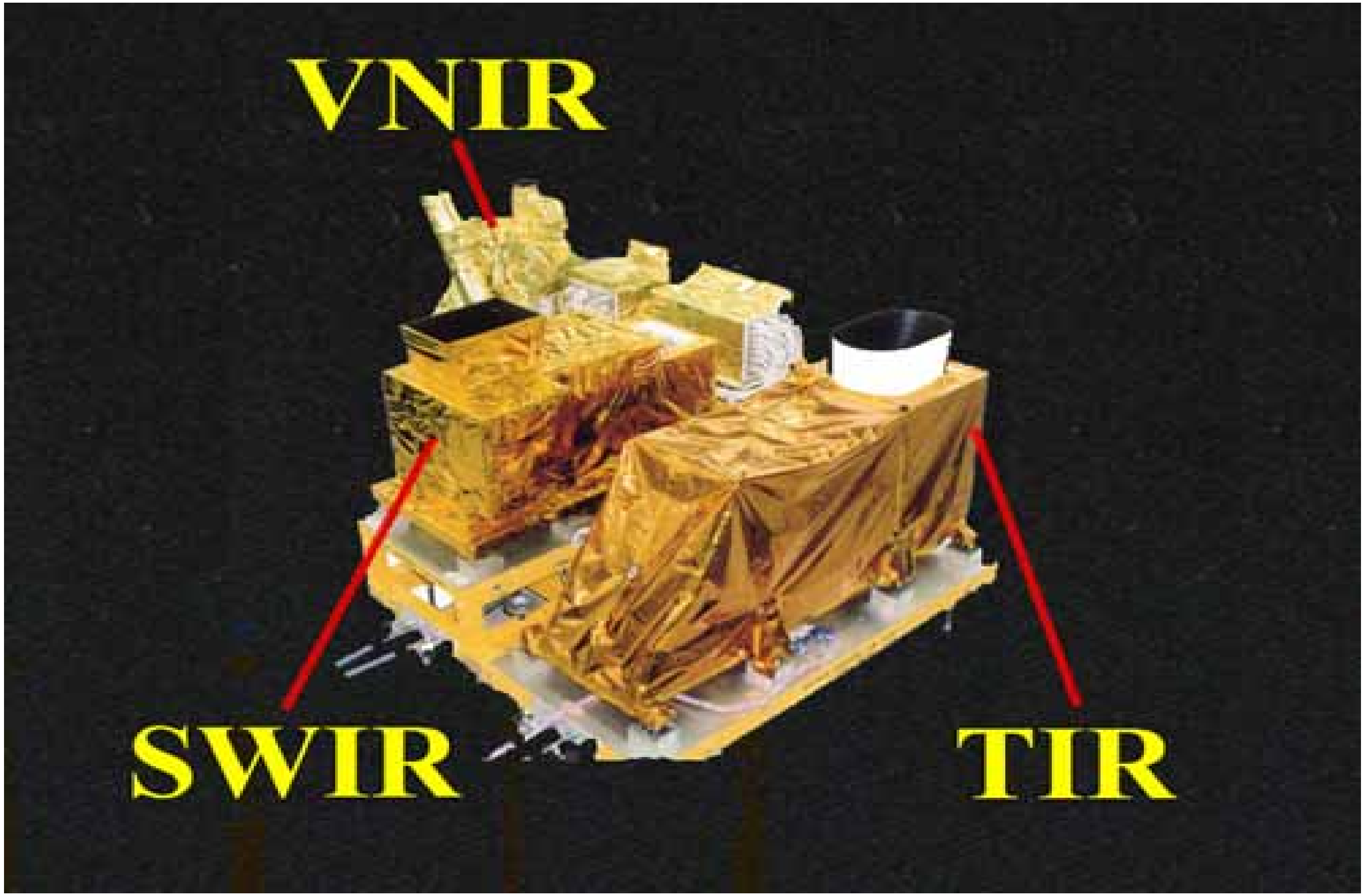

ASTER sensors

Terra

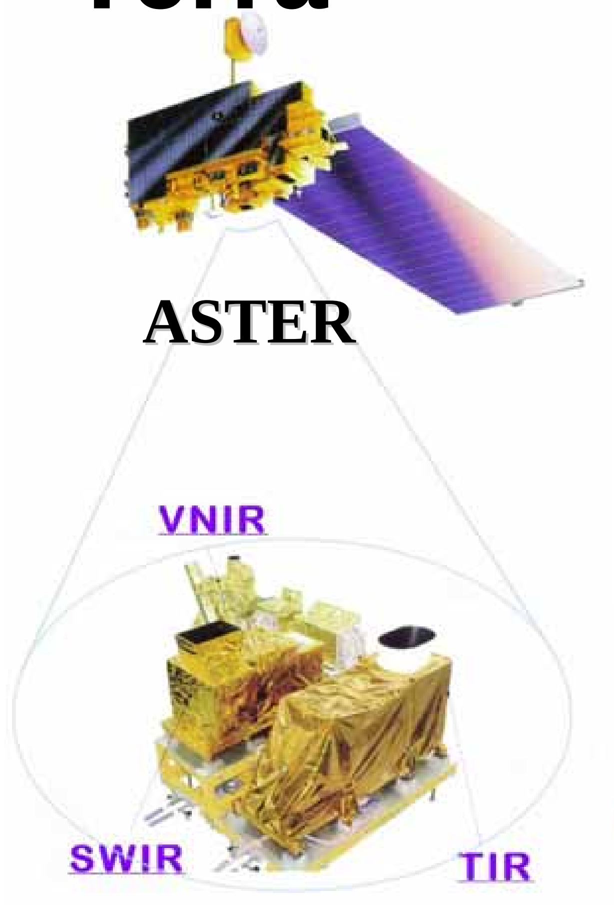

VNIR

Visible Near Infrared Radiometer

Wave Length： **3 Bands+Backward**

0.52 - 0.86 μm

Spatial Resolution: **15 m**

Pointing Angle: **±24 °**

(Cross-track Direction)

SWIR

Short Wave Infrared Radiometer

Wave Length： **6** Bands

1.60 - 2.43 μm

Spatial Resolution： **30 m**

Pointing Angle： **±8.55 °**

(Cross-track Direction)

TIR

Thermal Infrared Radiometer

Wave Length： **5** Bands

8.125 -11.65 μm

Spatial Resolution： **90 m**

Pointing Angle： **±8.55 °**

(Cross-track Direction)

Data Flow and Relationship between JAPAN and USA

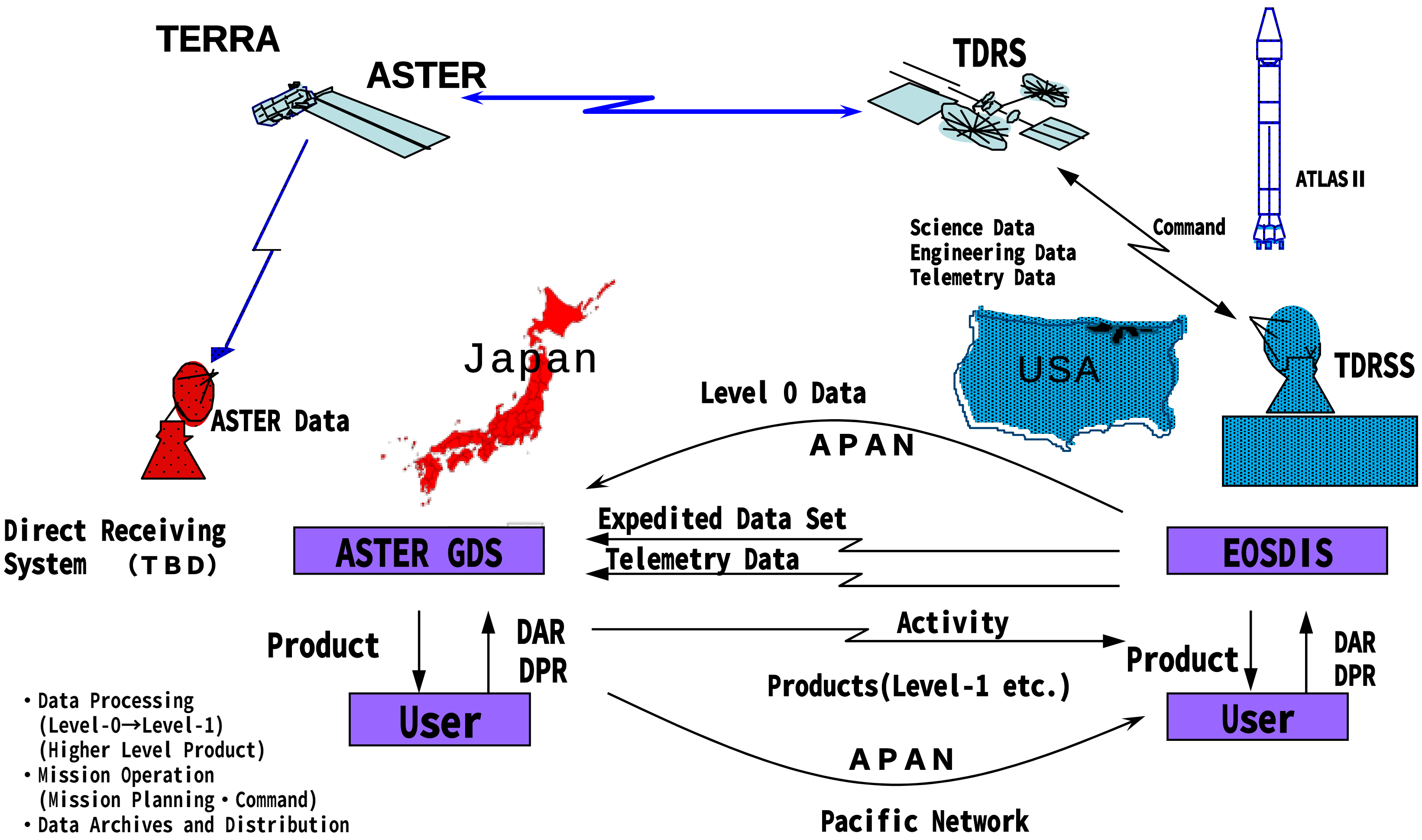

Comparison ASTER:Landsat:SPOT

		Spatial Resolution	Swath	# of Bands	Stereo Function
		(m*m)	(km)		
ASTER	Multi/VNIR	15*15	60	3	○(along track)
	MultiSWIR	30*30	60	6	
	Multi/TIR	90*90	60	5	
Landsat7/ETM+	Multi	30*30#	185	7	
	Pan	15*15	185	1	
SPOT5/HRG	Multi/VNIR	10*10	60	3	○(cross track)
	Multi/SWIR	20*20	60	1	○(cross track)
	Pan	5*5	60	1	
SPOT5/HRS	Pan	10*5	120	1	○(along track)

TIR:60*60

Landsat 5 has a problem in Solar Panels, and Landsat 7 has a problem in Scan Line Corrector

Resolution of ASTER, JERS-1 and LANDSAT VNIR data

ETM+(B,G,R : 2,3,4)

30m

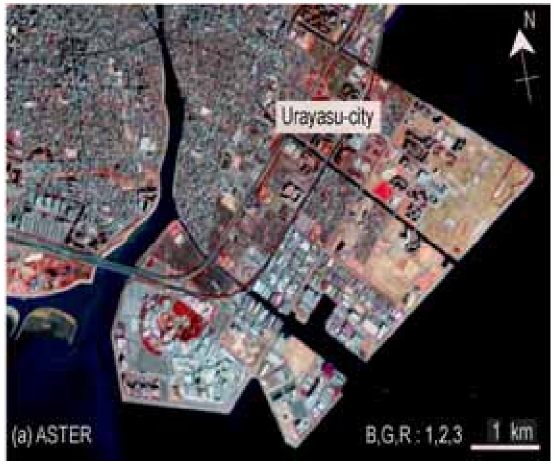

ASTER(B,G,R : 1,2,3)

15m

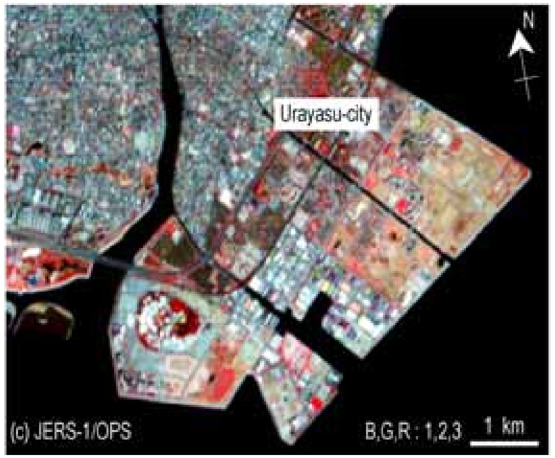

JERS-1 OPS(B,G,R : 1,2,3)

18m

ASTER

JERS-1

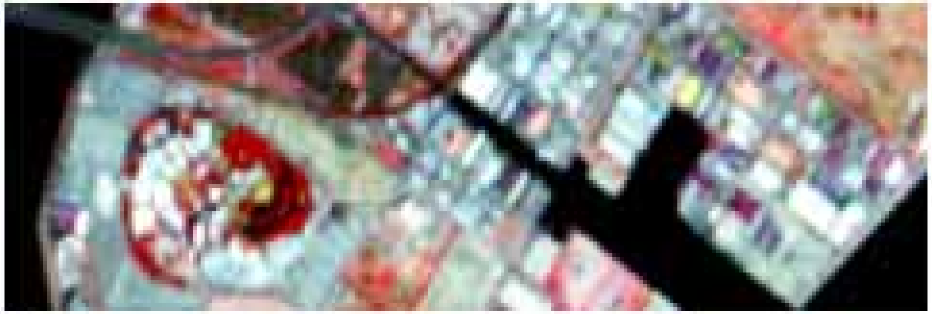

LANDSAT

Availability of ASTER Data

- Time between Data Acquisition and Data Distribution
- Total Number of Scenes and Degree of Repeated Observation

Number of the ASTER data acquisition per day

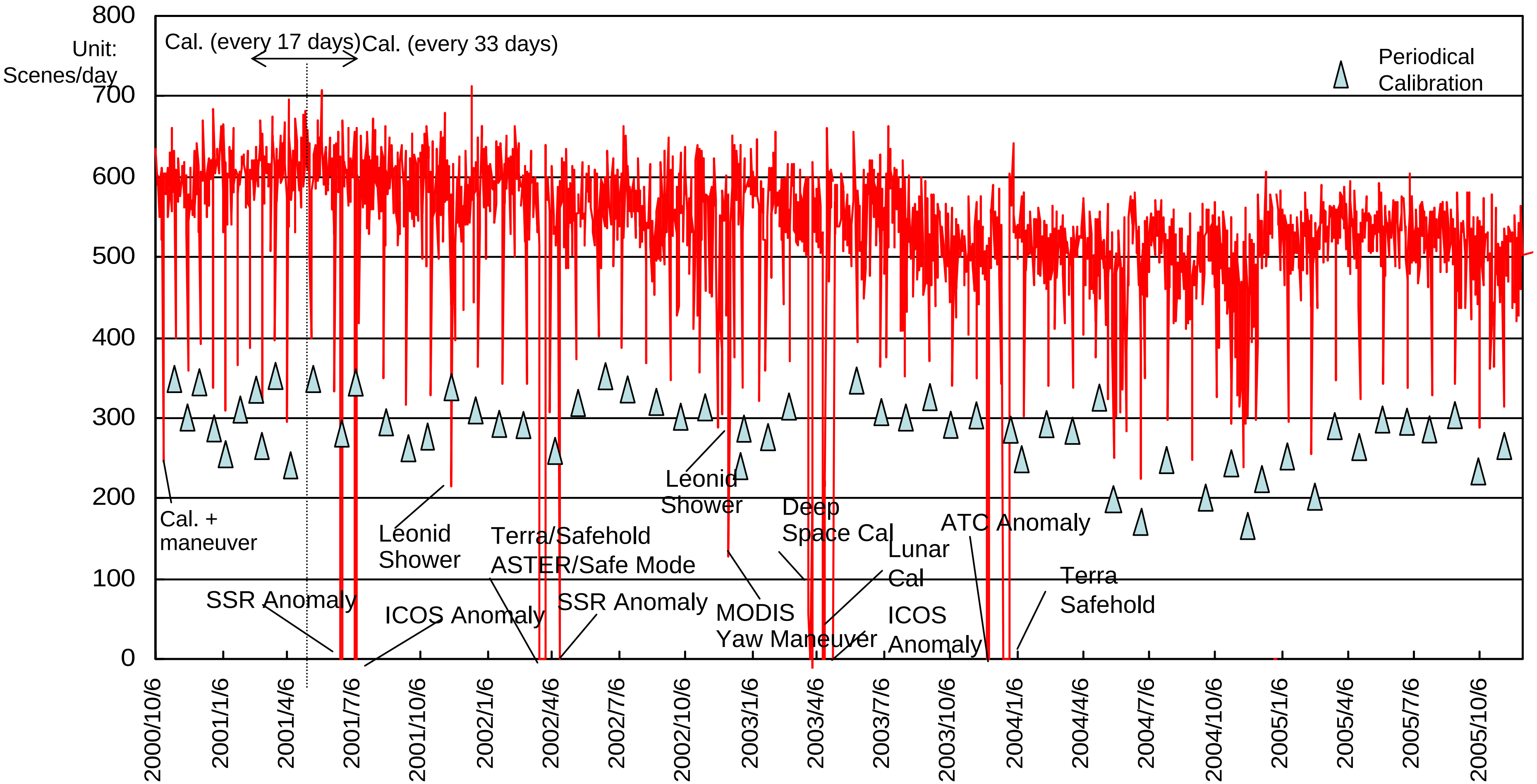

The total no. of acquired scenes from Feb. 28th, 2000 to Dec.1, 2005 is ***1,073,626***

LC Operation (1)
Timeline for Observation Schedule

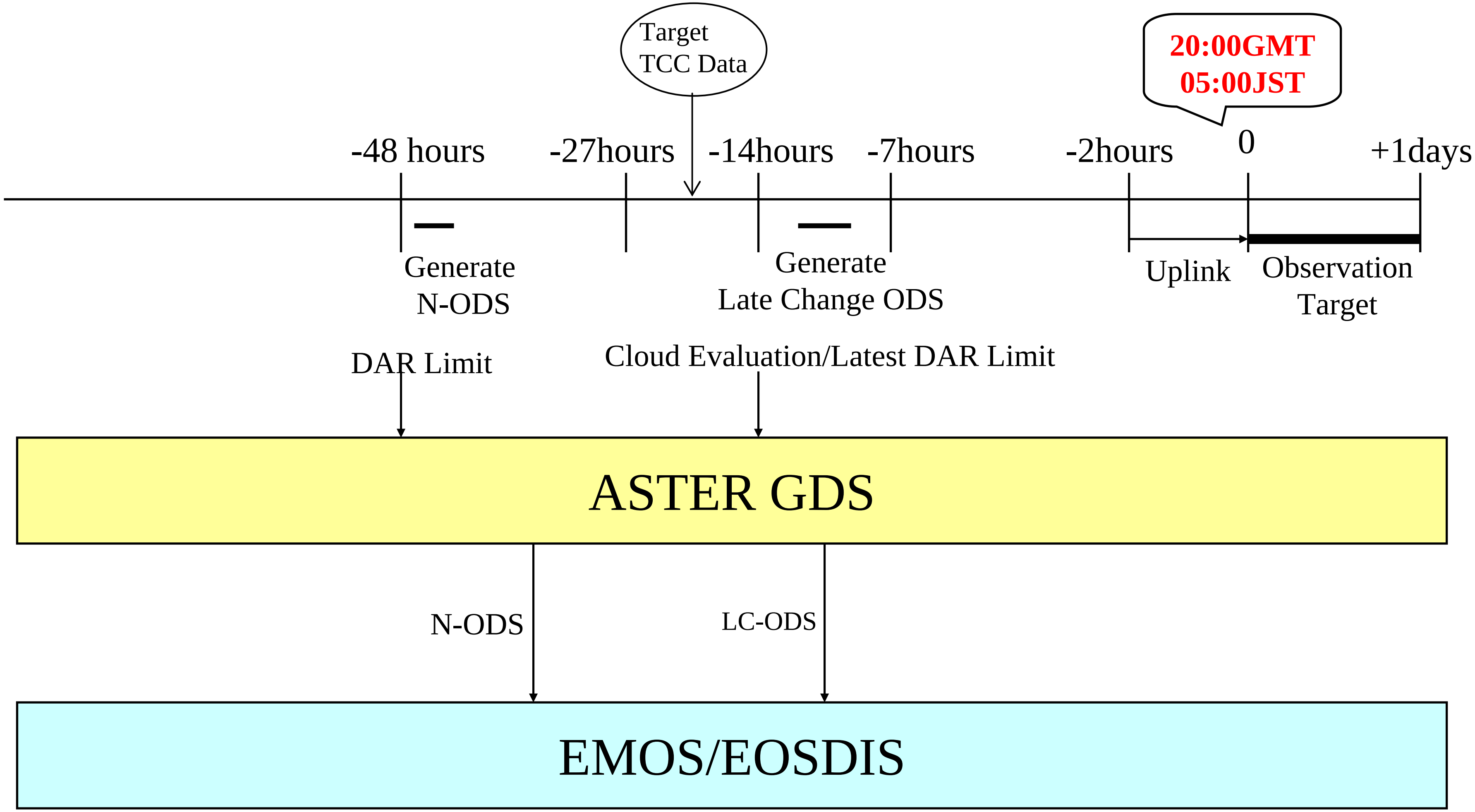

Effectiveness of Late Change-ODS Operation

	No L/C		L/C		Checking Method
	Cloud Coverage	No. of Scenes	Cloud Coverage	No. of Scenes	
00/11-12	**45.4 %**	2756	**36.5 %**	3120	Visual Check
01/5-7	**40.6 %**	5103	**36.7 %**	5192	L1 Auto.
02/2-7	**40.4 %**	19,288	**35.0 %**	52,445	L1 Auto.

World Coverage Map (Day time)

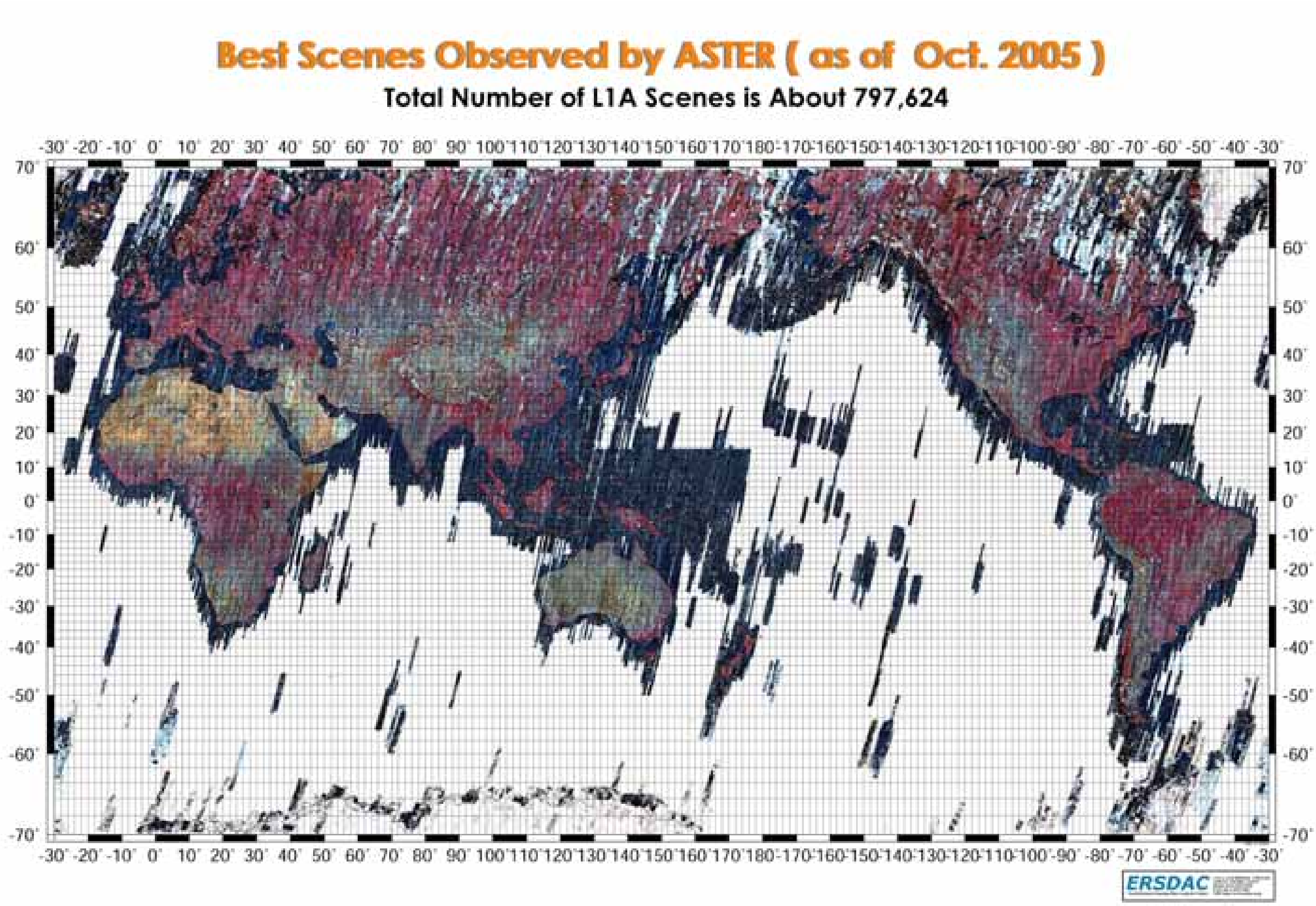

World Coverage Map(Night Time)

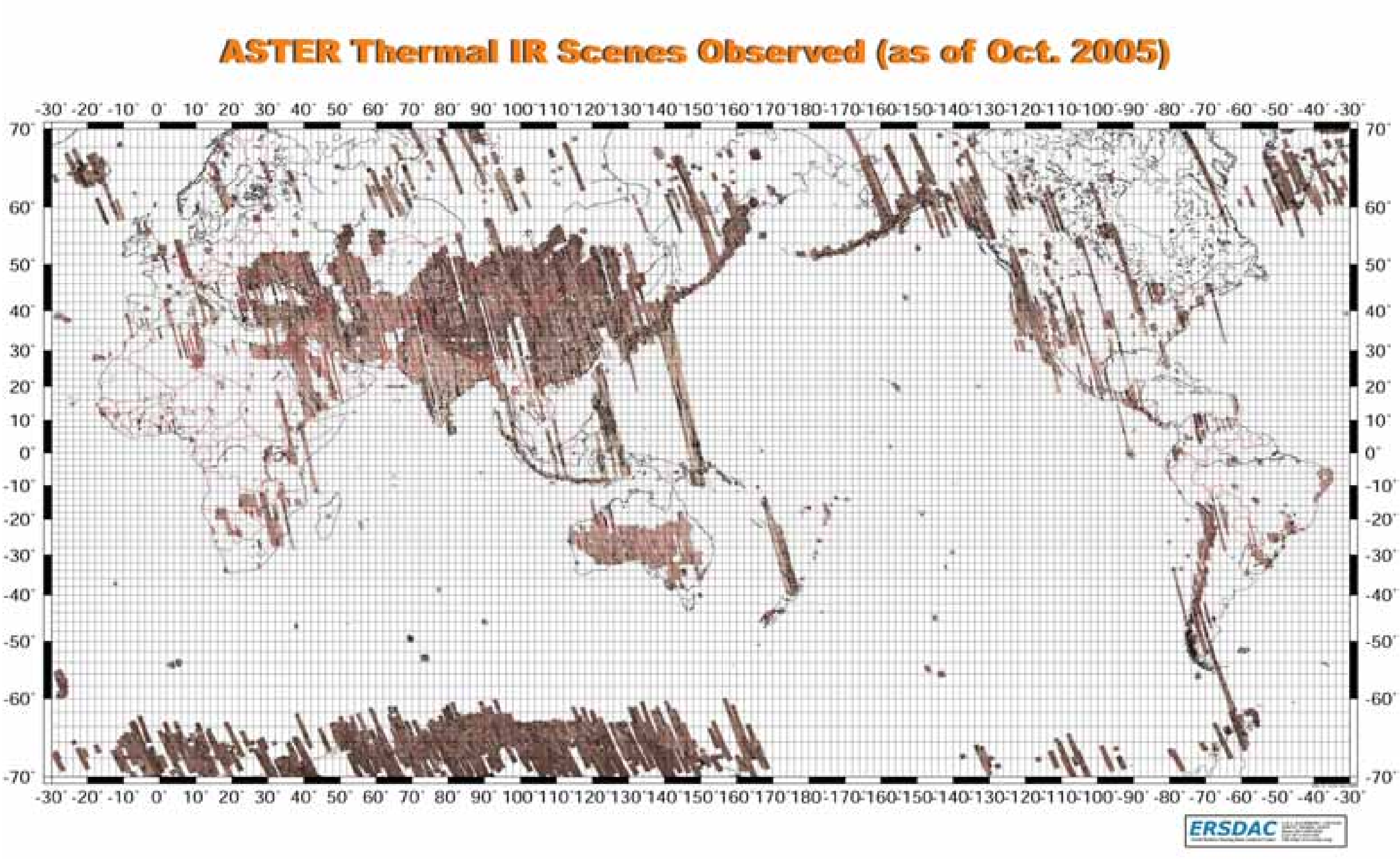

Time between Data Acquisition and L1A Generation

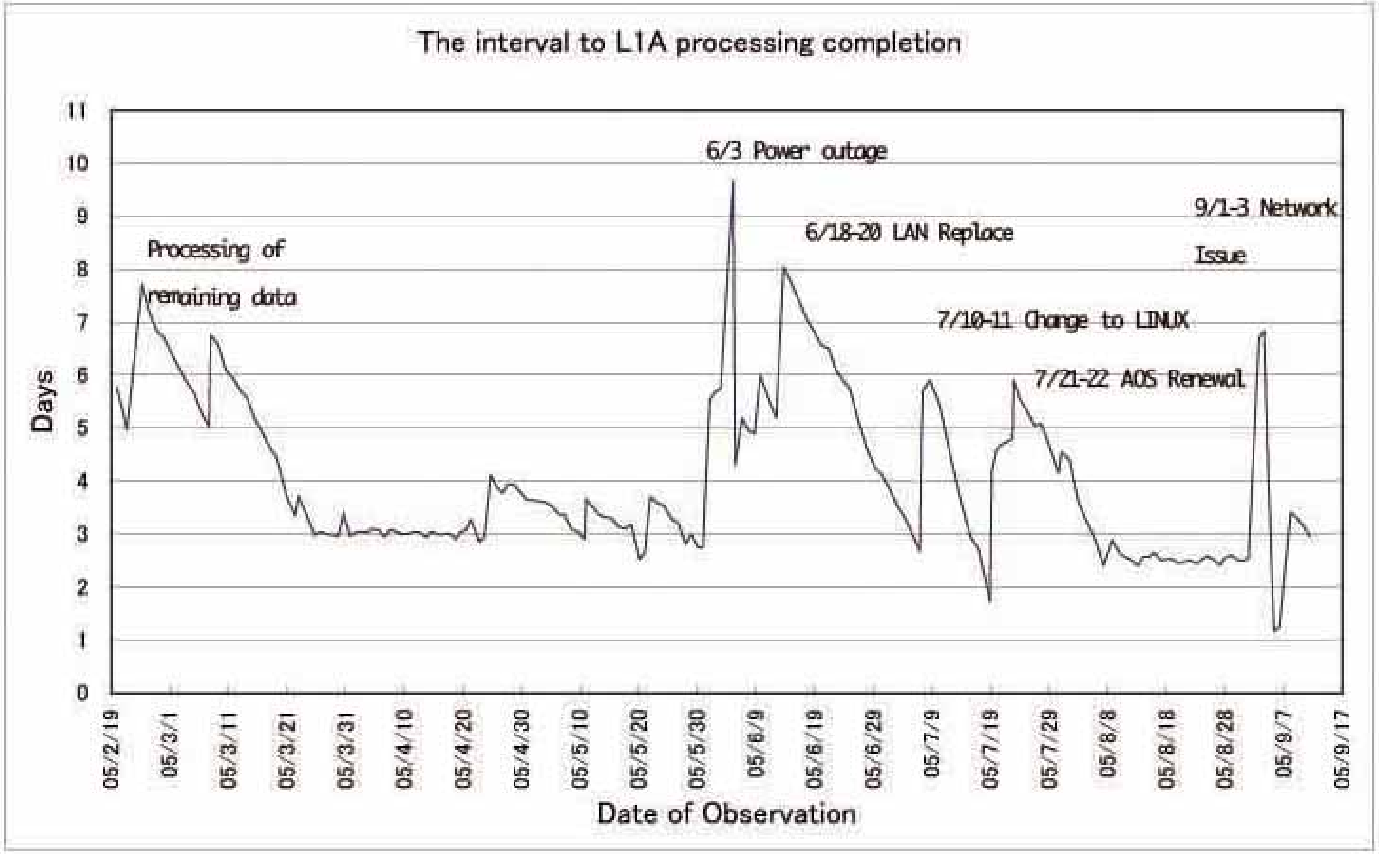

Flow of ASTER Urgent Observation

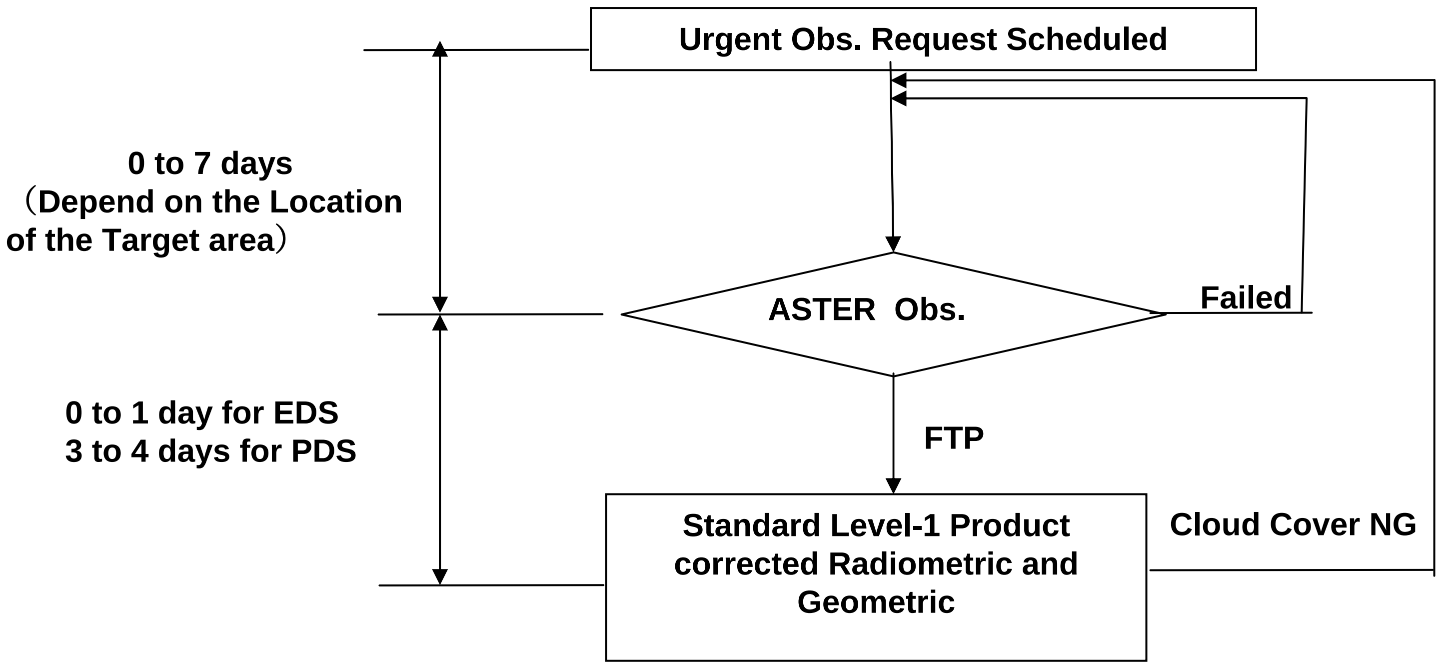

ASTER Data Production

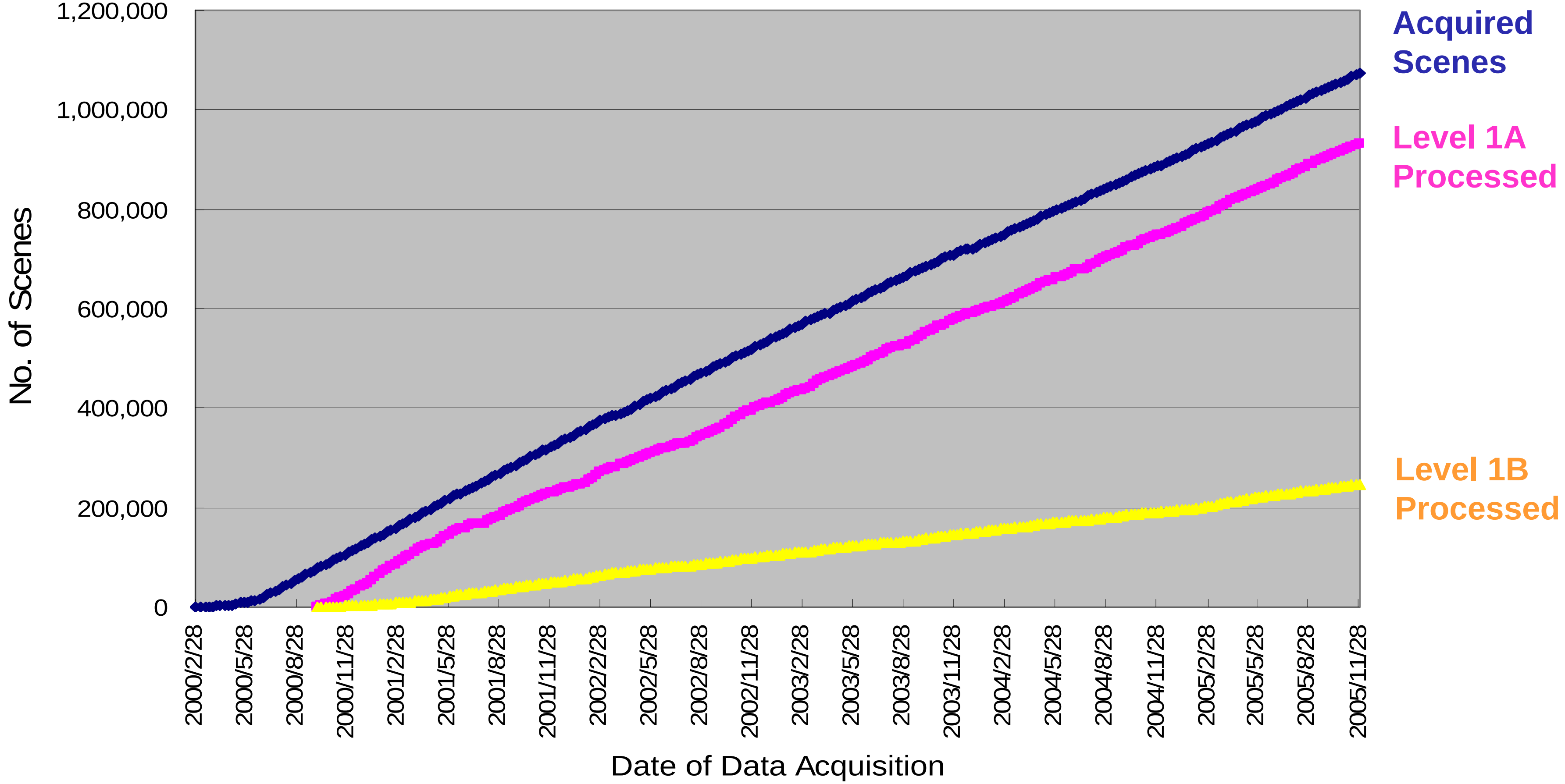

Higher Level Products

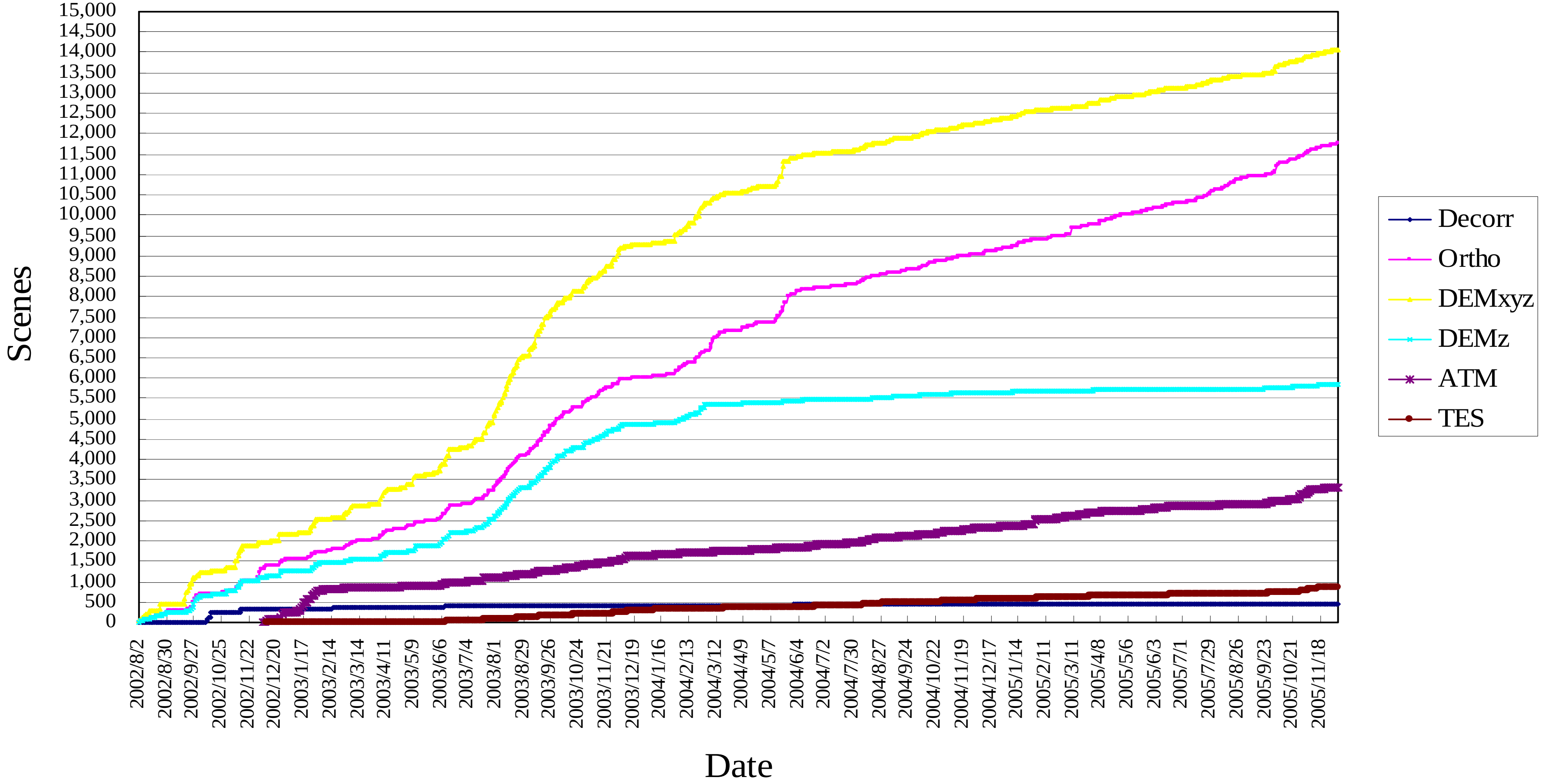

Data Distribution

Statistics

No. of Registered Users (General Users)

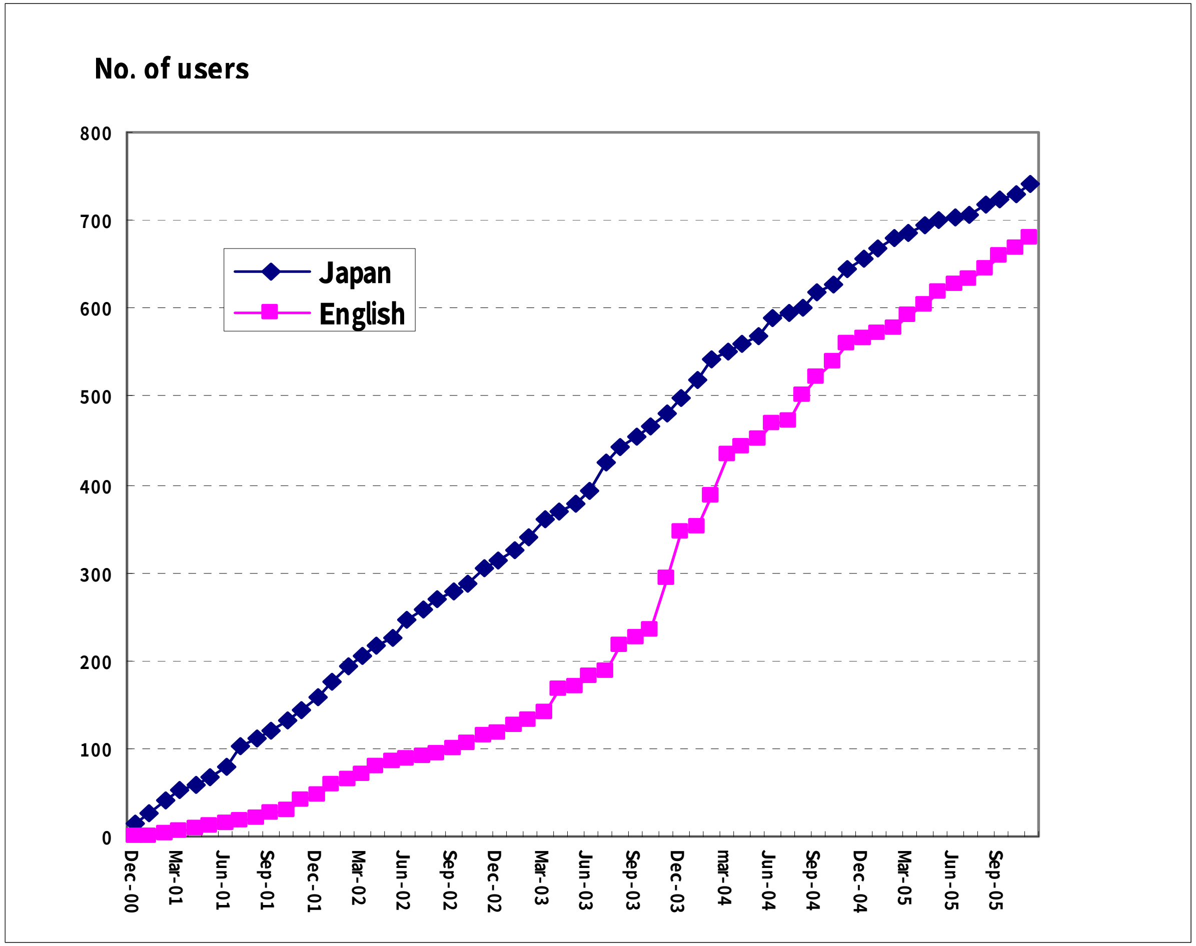

Japan Cum	**740**
Eng Cum	**679**
TOTAL	**1419**
FY2000	58
FY2001	219
FY2002	224
FY2003	482
FY2004	297
FY2005	139

No. of Scenes Ordered (General Users)

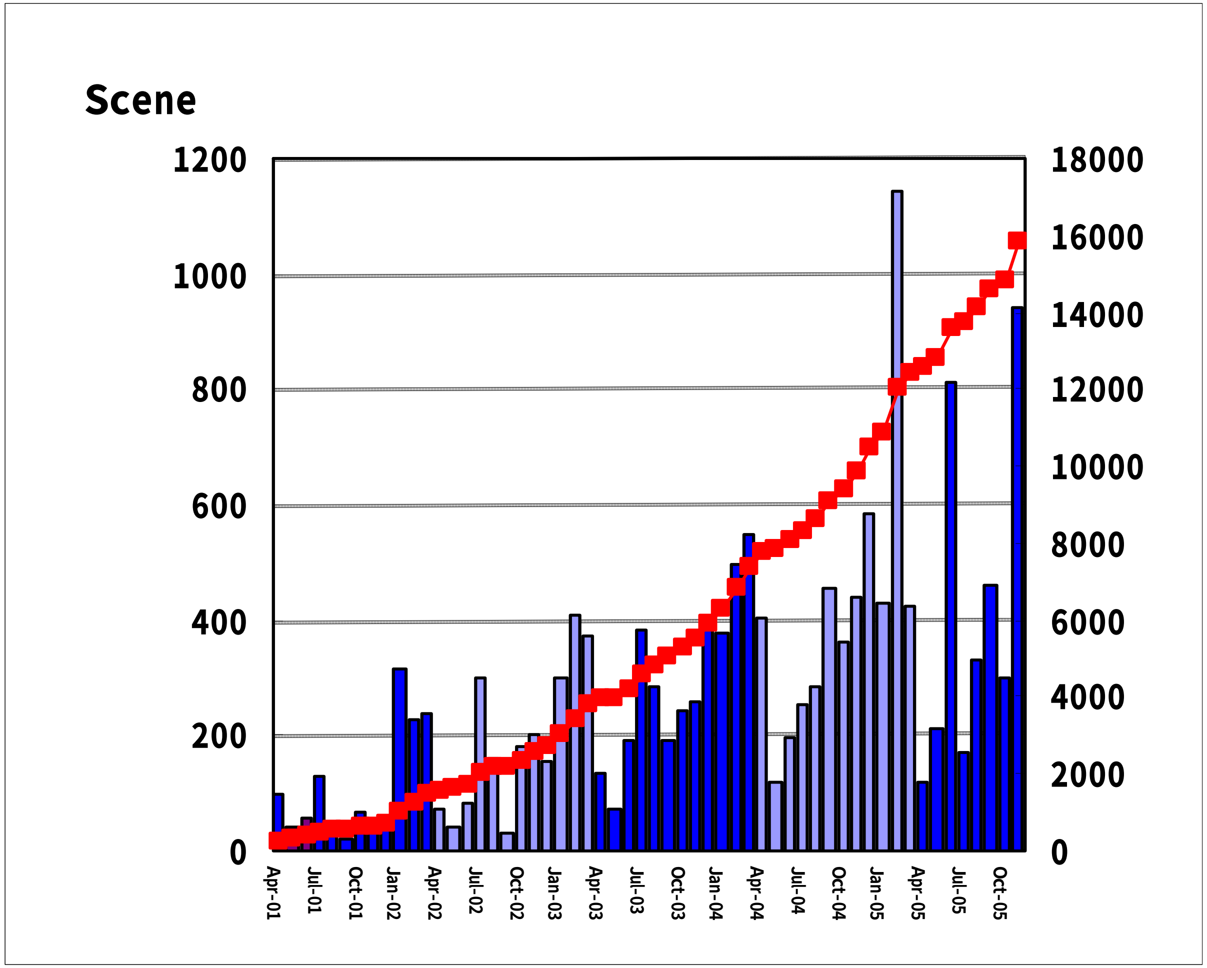

FY2000	171
FY2001	1,317
FY2002	2,301
FY2003	3,562
FY2004	5,092
FY2005	3,348
TOTAL	15,791

No. of Total Scenes Distributed (Free Users)

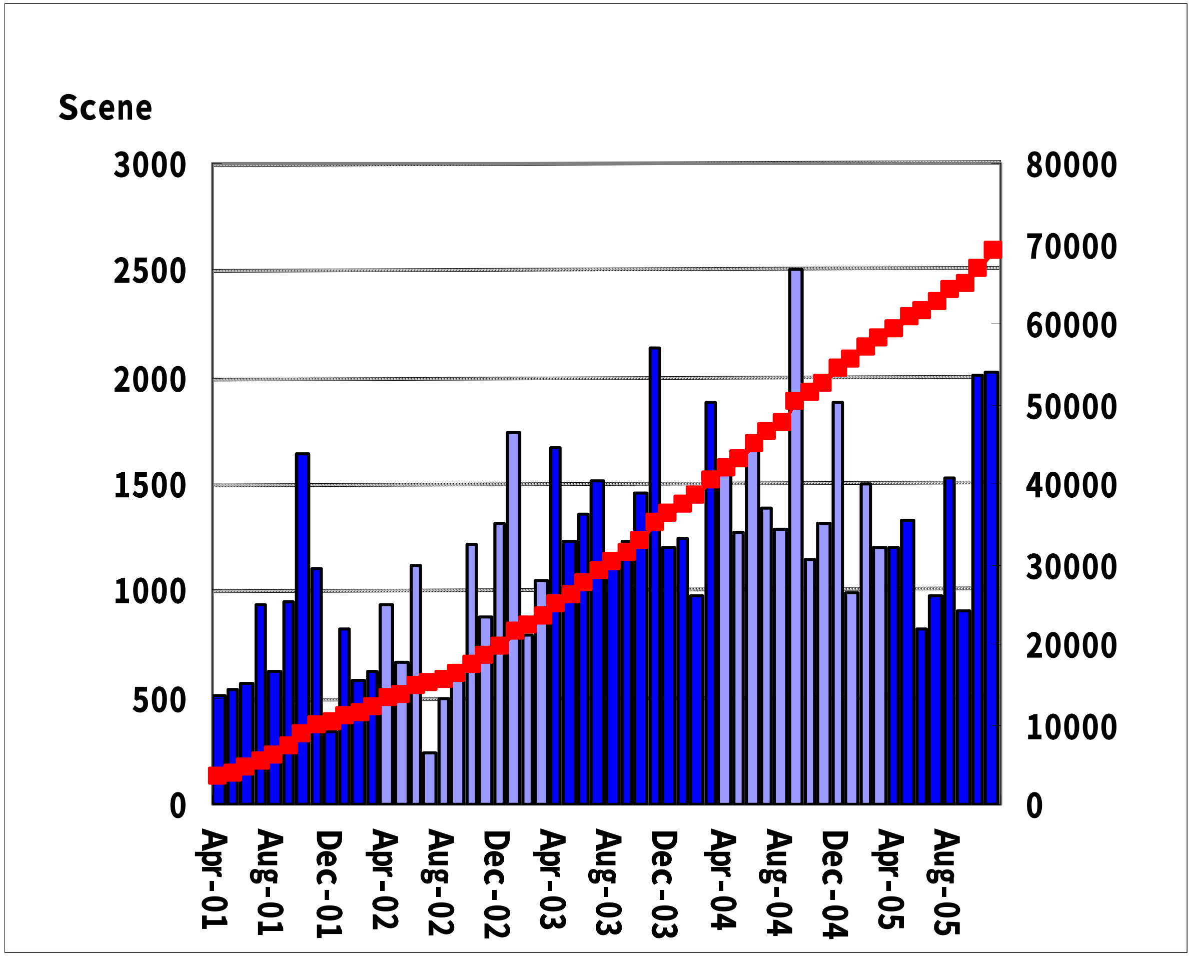

FY2000	2,886
FY2001	9,233
FY2002	11,120
FY2003	17,063
FY2004	17,833
FY2005	11,135
TOTAL	69,270

Categorization of General Users

Category	Domestic	Abroad
Geology, Resources	76	56
Education	257	277
Software	53	6
Civil Engineering	77	5
National,Local Government, NPO	117	131
Remote Sensing & Its Application	29	78
Miscellaneous	30	92
Photogrammetry	38	7
Private	17	9
Environment	23	18
Agriculture	4	
Mass Media	19	
Total	740	679

Data Distribution by General User Category

Category	Domestic		Abroad	
	FY2004 or earlier	FY2005	FY2004 or earlier	FY2005
Geology, Resources	**2642**	**759**	**687**	**78**
Education, Academia	**1597**	**250**	**673**	**232**
Software	**1009**	**55**	**1**	
Civil Engineering	**837**	**107**	**0**	**13**
State, Local Government, NPO	**2145**	**173**	**734**	**207**
R/S and Its Application	**506**	**136**	**733**	**883**
Miscellaneous	**166**	**17**	**277**	**271**
Photogrammetry	**203**	**77**	**0**	**4**
Private	**13**	**3**	**7**	**1**
Environment	**155**	**66**	**5**	**9**
Agriculture	**15**	**3**	**0**	
Mass Media	**38**	**4**	**0**	
Total	9326	1650	3117	1698

General User Distribution by Region

Area	# of Registration	FY2004 or earlier	FY2005
Europe	120	321	**207**
Asia	296	1316	**944**
South America	21	586	**14**
North and Central America	77	87	**28**
Oceania	26	340	**156**
Africa	18	106	**14**
Middle East	88	361	**335**
Total	646	3117	1698

Geometric and Radiometric Accuracy

- Geometric Accuracy
  - Geolocation
  - DEM
- Radiometric Accuracy

Simplified Explanation of DEM Extraction from ASTER Data

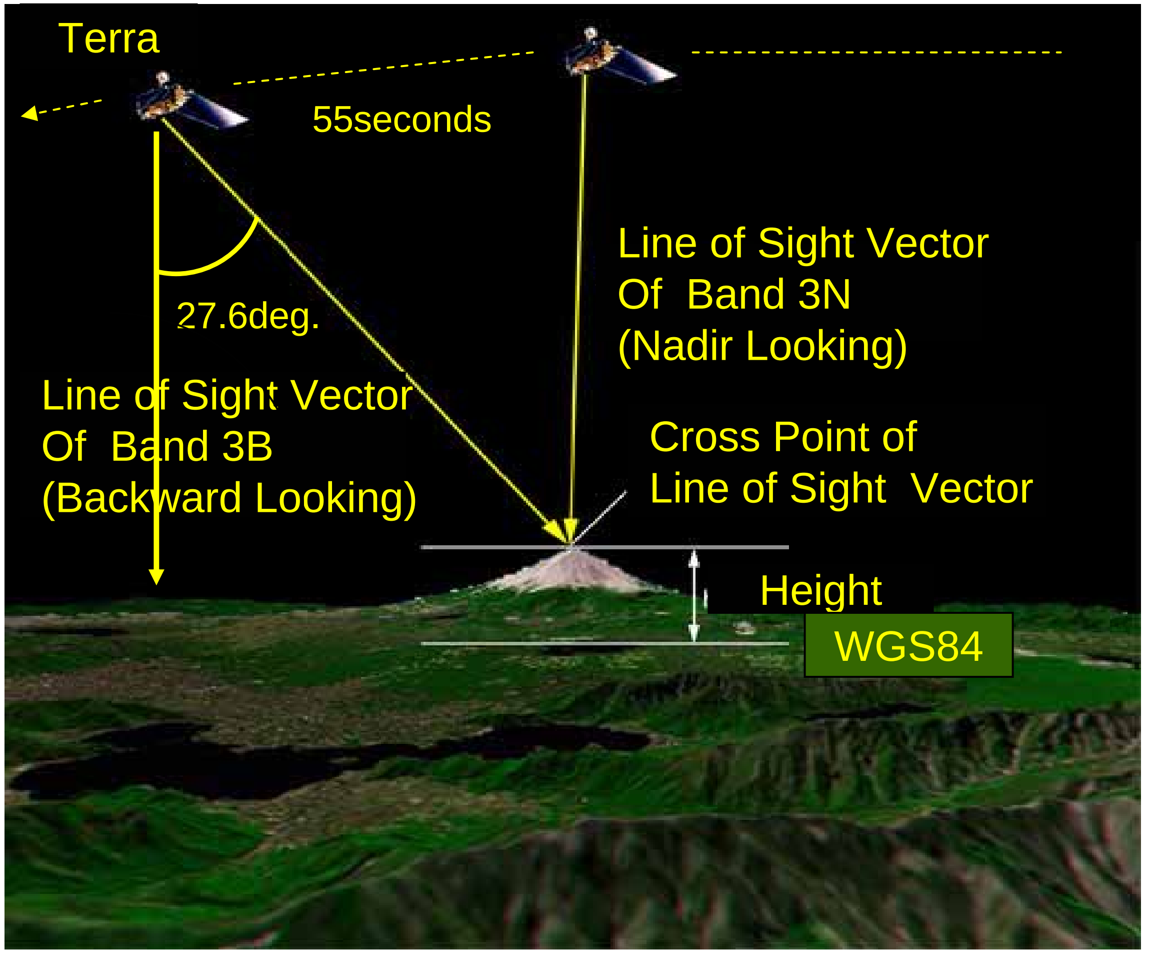

Hardware Setting

- The band 3B data is not only rotated backward direction by 27.6 degrees around the pitch axis but also 1.33 degrees by roll axis to compensate the Earth Rotation. This configuration is kept when there is a cross track pointing.
- In the Band 3B sensor, there are 5,000 CCDs, and when the data is downloaded from the Terra, 4,100 pixel data are selected in function of the latitude to compensate the Earth Rotation.
- To keep the pixel size of the Band 3B the same as that of the band 3N, the instantaneous field of view is designed slightly smaller than that of band 3N. (respectively, 21.3 and 18.6 micro radian)

Note on B/H

- The band 3B looks at the same location of the Earth approximately 55 seconds after the data take by the band 3N. A set of the bands 3N and 3B constitutes a stereo pair, from which user can see ASTER data stereoscopically, even in Level 1B data set, with the Base to Height Ratio (B/H)= 0.6 calculating as follows (Fujisada et.al., 1998):
  - tan(arcsin((R_E +H)/ R_E *sin(27.6))

  where R_E and H denote the radius of the Earth and the Altitude of the Spacecraft(6378 km and 705 km at the Equator, respectively).

- Note this value of B/H is not necessarily equal to 0.6, but slightly changing depending on the relative location of the pair pixel.

- Note the overlap of the Bands 3N and 3B does not cover the completely the same location, the coverage of the stereo pair is usually slightly less than the coverage of nadir looking data, 60 km.

Error Evaluation by GCPs for the data of 2003

	delta lon	delta lat	delta h
	(m)	(m)	(m)
Results for all the 90 data			
mean	40.75	-11.82	-19.81
std	44.67	11.43	7.65
Results for each scenes			
mean	42.86	-10.56	-19.19
std	6.86	5.48	4.12

Estimated Errors in Longitude Direction(m) (2003)

Date of Data Acquisition	Longitude	Estimated Errors in Longitude Direction (m)
2003.9.15	N35	58.2
2003.10.15	N35	38.4
2003.11.15	N35	46.8
2003.12.15	N35	76.3

Summary of Results of DEM Accuracy Measurement by Comparing with GCP conducted in FY 2004

Site	Observation Date	Pointing (deg)	GCT Ver.	Gain	Mean Error [m]			Standard Deviation [m]			No. of GCP
					lon	lat	h	lon	lat	h	
Tsukuba 14	2004.9.9	-8.583	3.00	NOR	138.69	-12.88	-3.25	5.89	3.47	3.53	7
Saga 10	2004.10.12	2.873	3.00	NOR	129.42	-26.52	-18.28	4.61	3.73	2.86	15
Unzen 4	2004.10.12	2.873	3.00	NOR	130.60	-22.16	-15.96	5.79	6.77	5.61	1
Fujisan 3	2004.10.18	-5.727	3.00	NOR	121.96	-27.21	-8.73	2.60	3.65	4.52	5
Aso 11・12	2004.11.22	-5.729	3.00	NOR	156.77	-20.62	-14.81	5.74	3.61	5.24	15
Kisokoma 7	2004.12.28	-2.826	3.00	NOR	183.62	-12.97	-6.36	7.82	3.20	7.05	10
Mean Value					143.51	-20.39	-11.23	5.41	4.07	4.80	

Estimated Errors in Longitude Direction (2004)

Site	Observation Date	Latitude	Errors by GCP	Estimated Errors in longitude direction (m)
Tsukuba 14	2004.9.9	N34/10	138.69	168.1
Saga 10	2004.10.12	N33/20	129.42	144.1
Unzen 4	2004.10.12	N32/50	130.60	145.4
Fujisan 3	2004.10.18	N34/10	121.96	134.5
Aso 11・12	2004.11.22	N33/10	156.77	153.5
Kisokoma 7	2004.12.28	N35/50	183.62	153.5

Change in errors due to earth nutation (Fujisada)

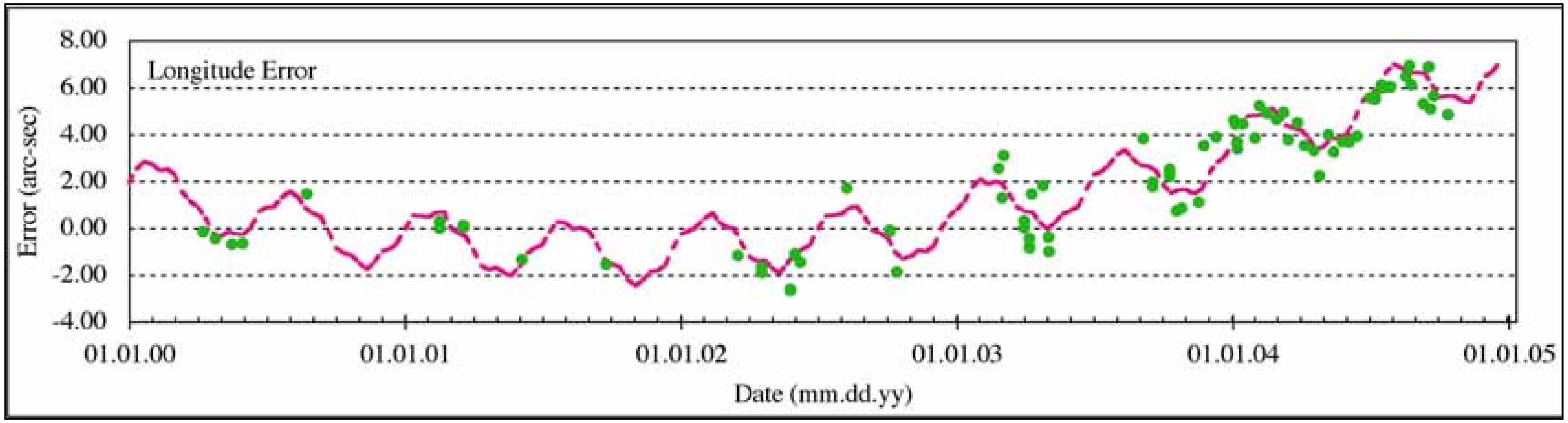

Validation of ASTER DEM

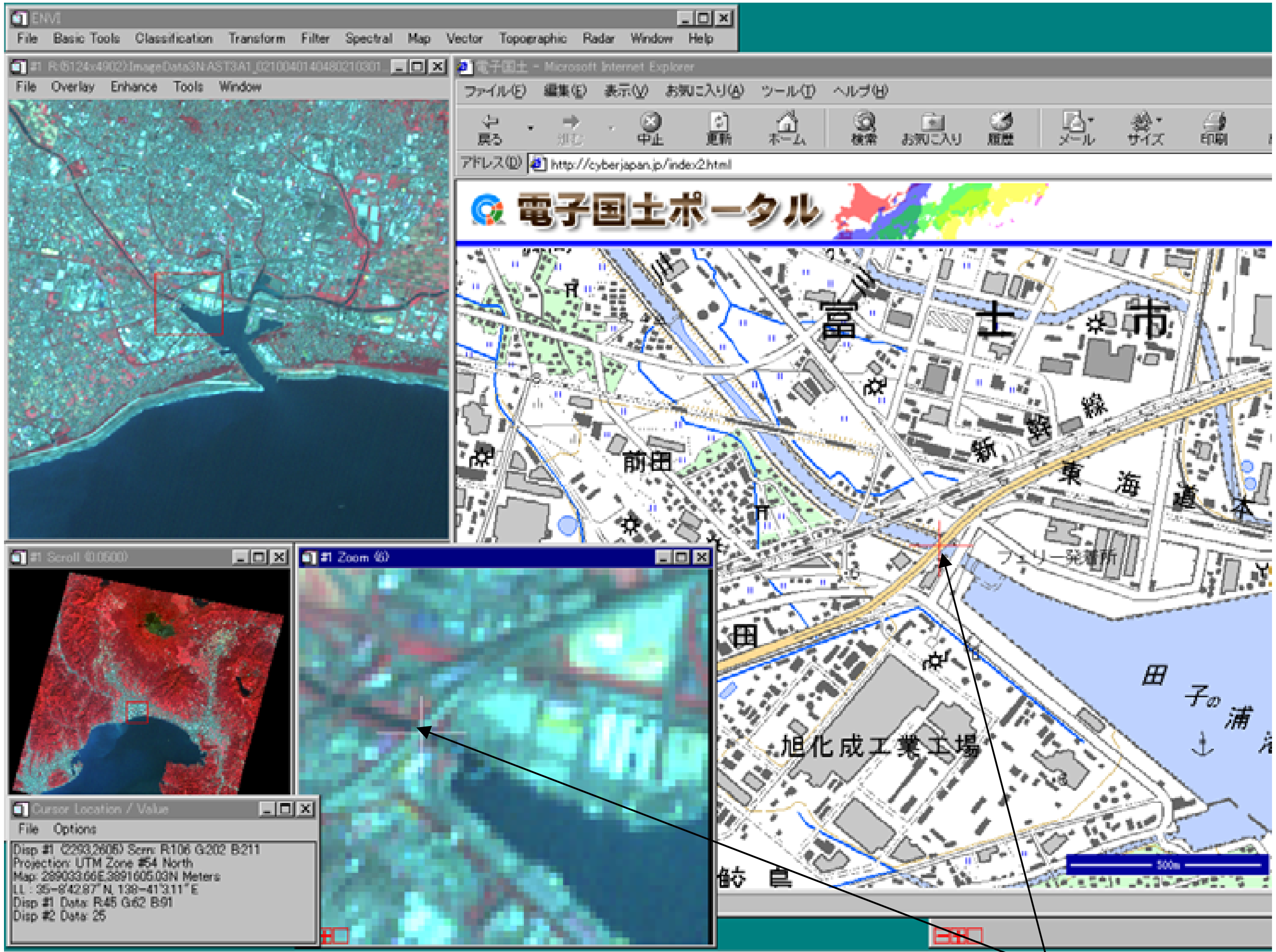

N35d8m43s、E138d41m3s

Geo-location accuracy in horizontal direction

Level 1A: no gemetric correction

L1B: System correction applied

L3A: Ortho-rectified

	Level 1B		Level 3A		Inst.of Geography	
	latitude	Longitude	latitude	Longitude	latitude	Longitude
Tagonoura	N35/08/42	E138/41/04	N35/08/43	E138/41/03	N35/08/43	E138/41/03
difference	00/00/01	00/00/01	00/00/00	00/00/00		
Top of Mt. Fuji	N35/21/37	E138/43/45	N35/21/37	E138/43/38	N35/21/37	E138/43/38
difference	00/00/00	00/00/07	00/00/00	00/00/00		

Date of Data Acquisition: 2002/10/04)

In L1B product, only system correction is applied.

In L3A product, geometric distortion caused by the elevation is corrected.

Major Parameters of the three scenes used for the geolocation error evaluation

Obs.Date	Proc. Level	Proc.Date of L1A	Pointing Ang.	Est, Error by Elev	Est.Error by Nutation
030521	L1B	030609	-5.721	155m to W	35m to E
040320	L3A	040406	-5.727	0m	128m to E
040320	L3A	050725	-5.727	0m	0m

Geolocation of Target Point: N37/45/09, W112/52/30

Elevation of Target Point: 1550 m in L3A

Path of the Orbit =38

Error caused by the nutation

L3A Data(Latest Version)   L3A (Older Version)

Geometric Configuration

to explain error caused by Elevation and Pointing

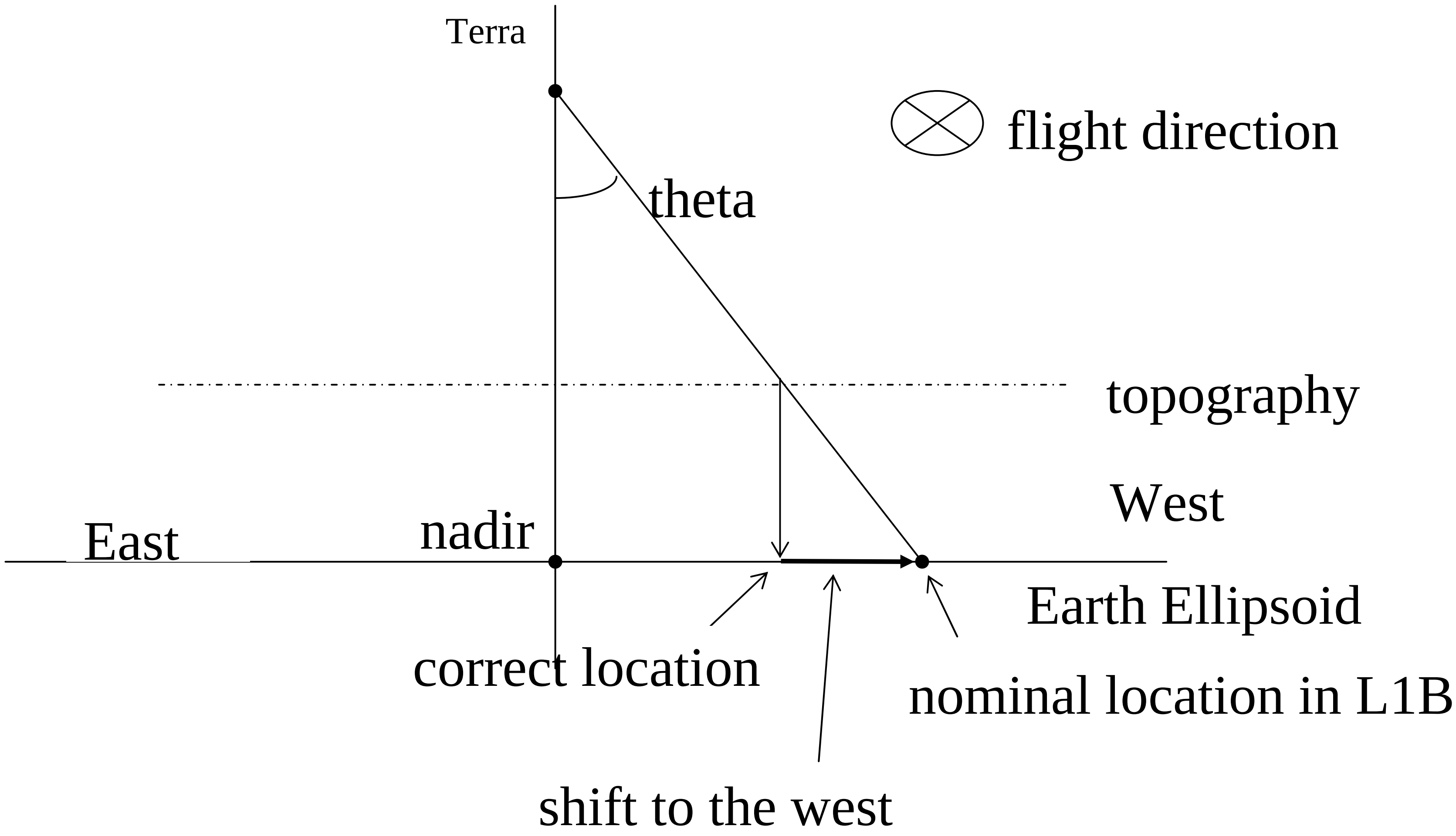

Error caused by Elevation

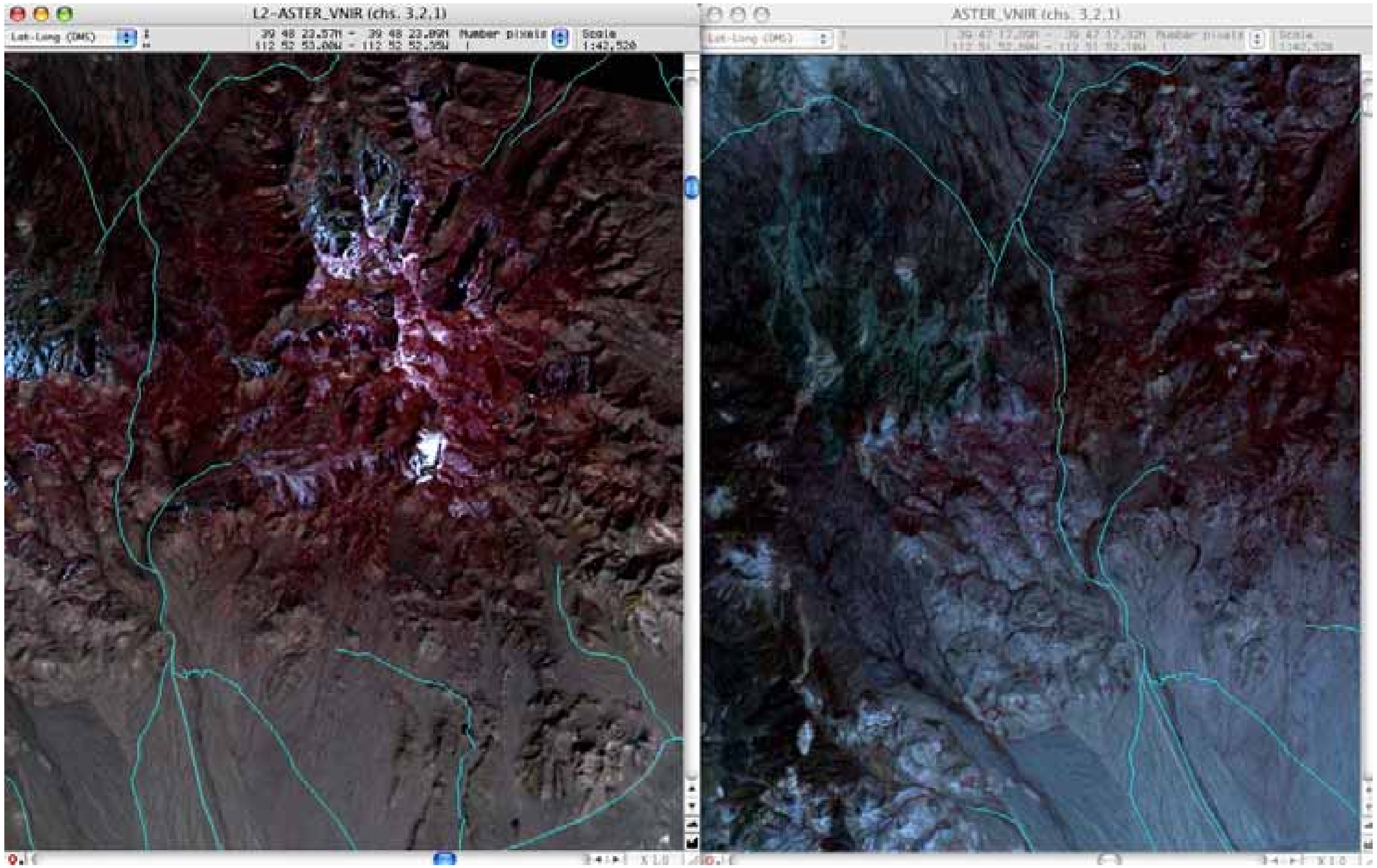

L3A Data(Latest Version)

L1B data

Study Site Selection and Characteristics by B.G.Bailey of USGS

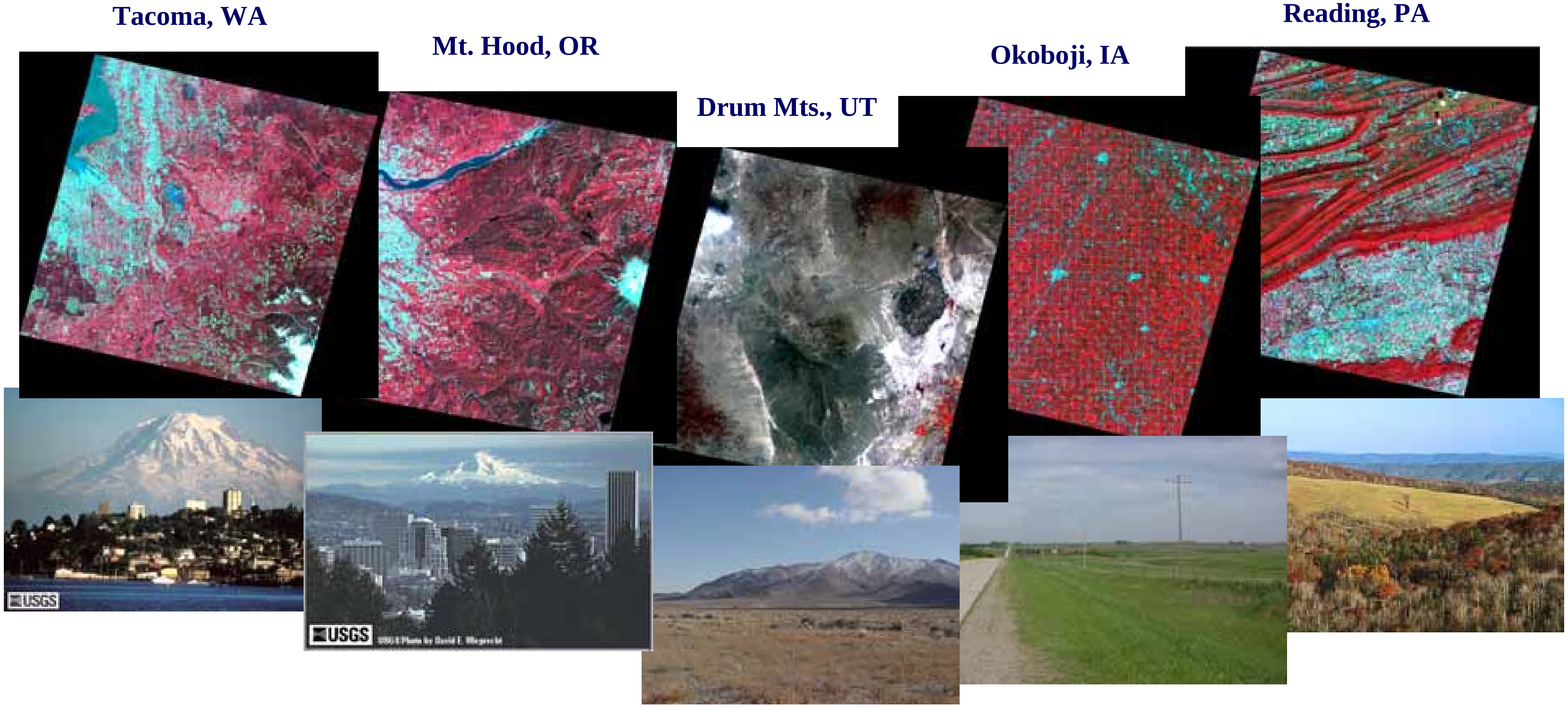

- Five sites selected
- Variable terrain
- Two ASTER scenes per site
- Early & recent dates
- Multiple pointing angles

Horizontal Accuracies by DEM Generation System- Phase 2 Results -

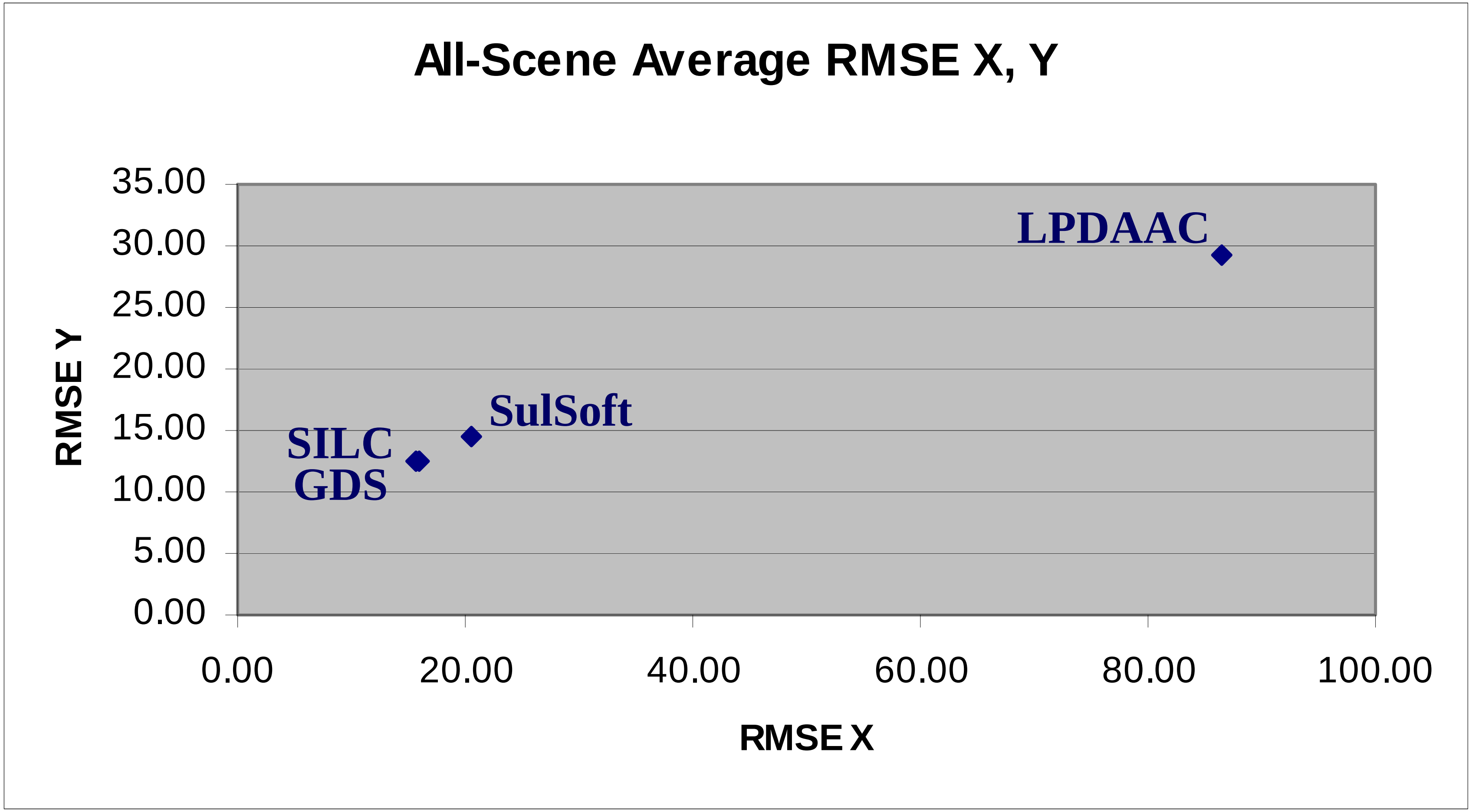

Vertical Accuracies by DEM Generation System

- Phase 2 Results -

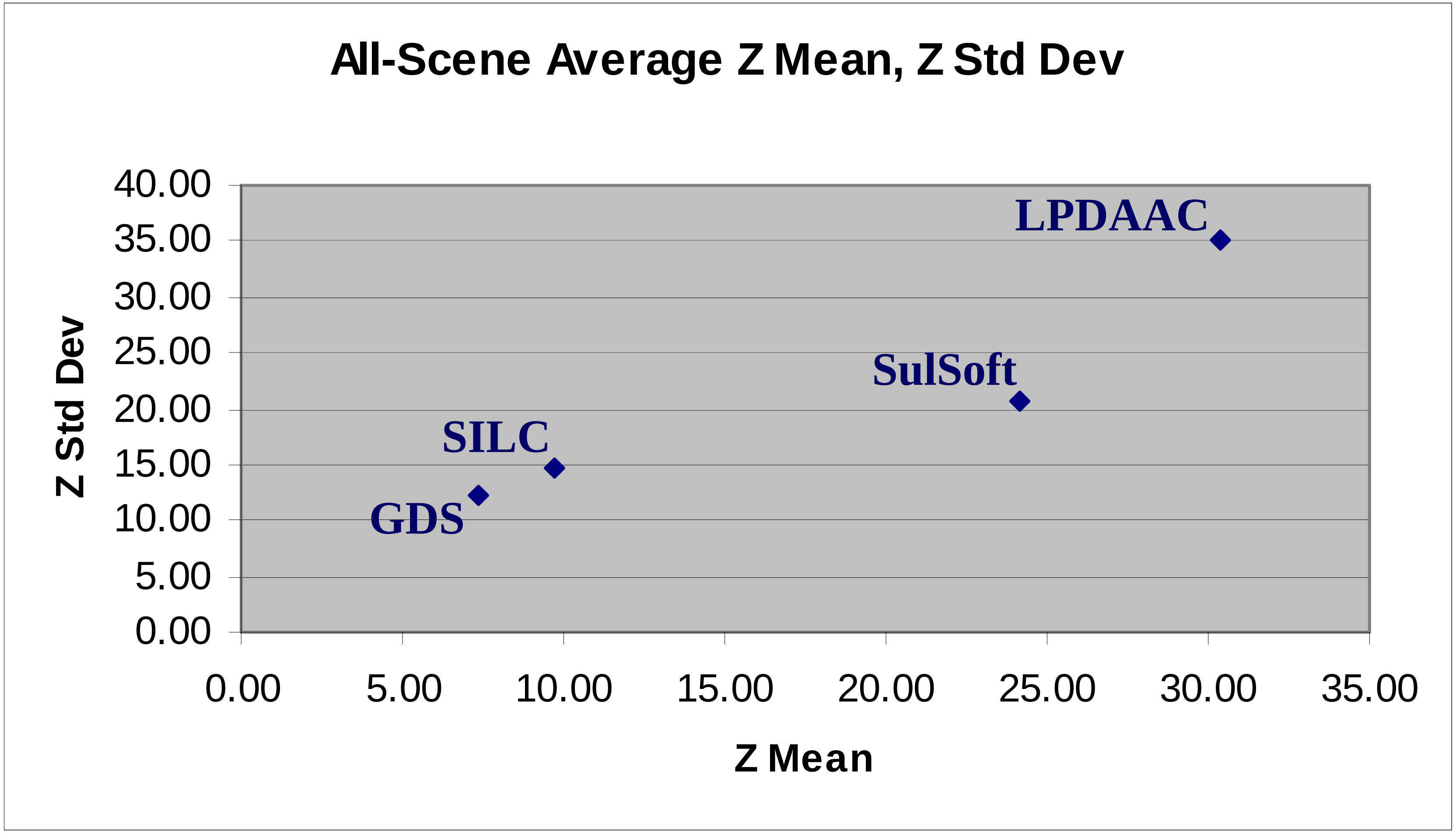

General Processing Efficiency Table

Software System	Average Production Time	Manual Intervention Required
Silcast (SILC)	15-20 min.	Virtually None
AsterDTM (SulSoft)	35-40 min.	Minimal
LP DAAC (PCI)	2-3 hours	Considerable

Summary & Conclusions

- **Horizontal and vertical accuracies of four ASTER DEM generation systems were thoroughly assessed.**
- **Processing efficiency also was evaluated for three of the four systems.**
- **In terms of overall accuracy, ASTER DEM's produced by** GDS and SILC **systems were virtually the same, and they were significantly more accurate than DEM's produced by the SulSoft and LP DAAC systems.**
- **Of the systems evaluated, the Silcast software system of SILC was the most efficient. The GDS system was not assessed.**
- **Based on these results, the LP DAAC should replace its production ASTER DEM generation software system with the same system used by GDS or with a production version of the SILC system.**

Radiometric Performance
--Sensitivity Trend Data--

VNIR

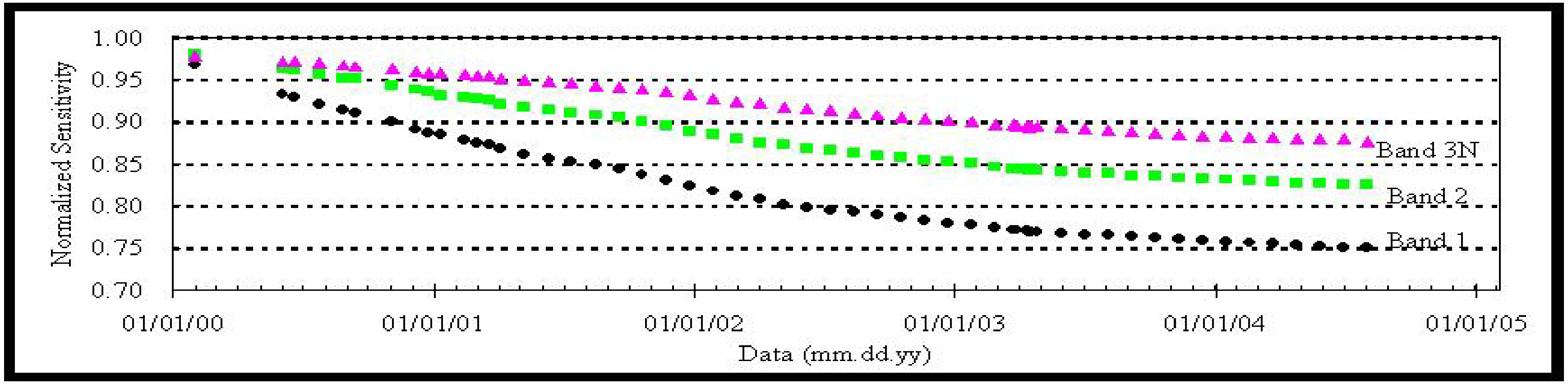

SWIR

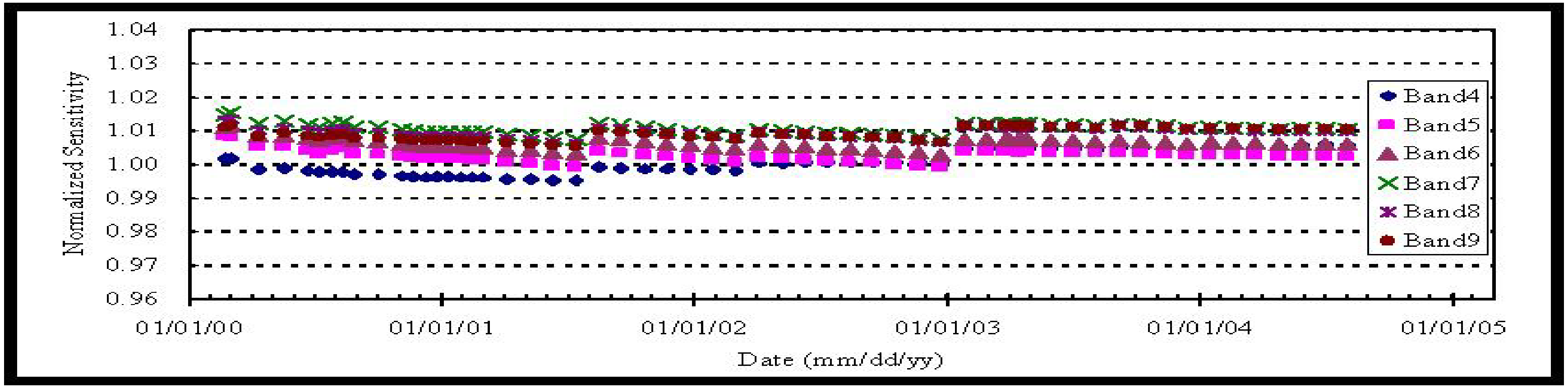

Radiometric Performance
--Sensitivity Trend Data--

TIR

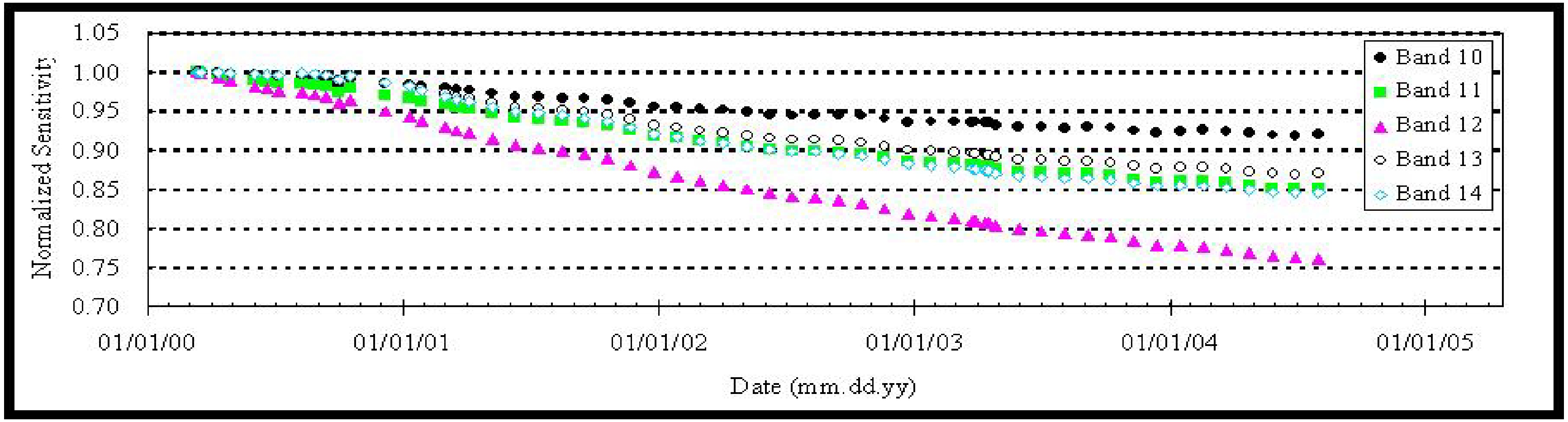

• The radiometric performance will be kept within the required accuracy by the database update.

Radiometric Performance

Radio DB	Application Time Period (mm/dd/yyyy)	Corresponding Telescope
Ver.2.01	02/02/2000-06/03/2000	VNIR
Ver.2.02	06/04/2000-09/13/2000	VNIR
Ver.2.03	09/14/2000-11/03/2000/	TIR
Ver.2.04	11/04/2000-02/13/2001	VNIR
Ver.2.05	02/14/2001-11/30/2001	VNIR, TIR
Ver.2.06	12/01/2001-10/11/2002	TIR
Ver.2.09	10/12/2002-12/15/2002	VNIR, SWIR, TIR
Ver.2.11	12/16/2002-01/29/2003	TIR
Ver.2.12	01/30/2003-05/14/2003	VNIR
Ver.2.13	05/15/2003-08/25/2003	TIR
Ver.2.14	08/26/2003-12/05/2003	TIR
Ver.2.15	12/06/2003/-01/04/2004	TIR
Ver.2.16	01/05/2004/-03/09/2004	VNIR
Ver.2.17	03/10/2004-08/09/2004	TIR
Ver.2.18	08/10/2004/-??/??/????	TIR

Application using high availability of ASTER data

- Global coverage
- High repetition cycle
- Synergism with other sensor

Forest Fire in the neighborhood of San Bernadino, CA, USA, by MODIS

2003/10/29

Forest Fire in the neighborhood of San Bernadino, CA, USA, by ASTER

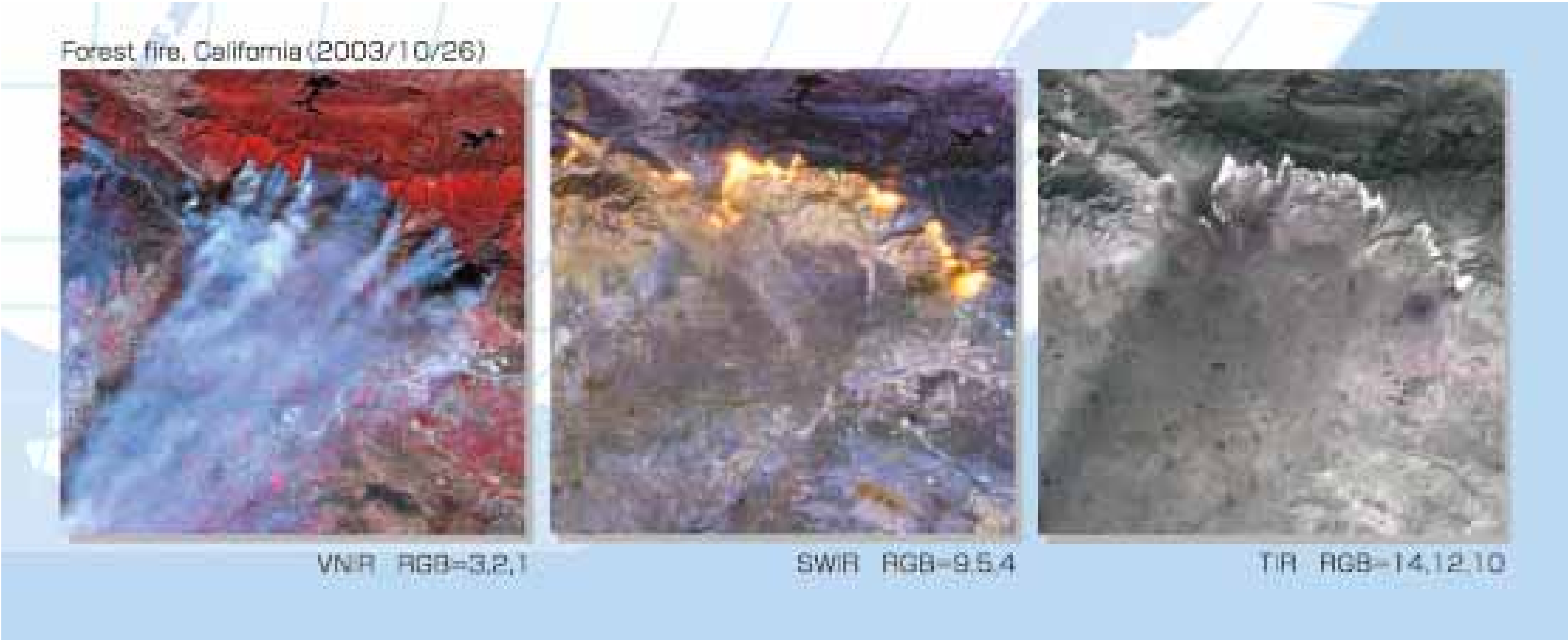

2003/10/29

Blue Tide occurred in Tokyo Bay-1

Right 2000/03/29

Below: 2000/10/07

Lower Right: 2000/11/8

Blue Tide occurred in Tokyo Bay-2

- ASTER VNIR Image of Tokyo Bay, 2000/10/07

ASTER DEM MOSAIC IMAGE Afghanistan

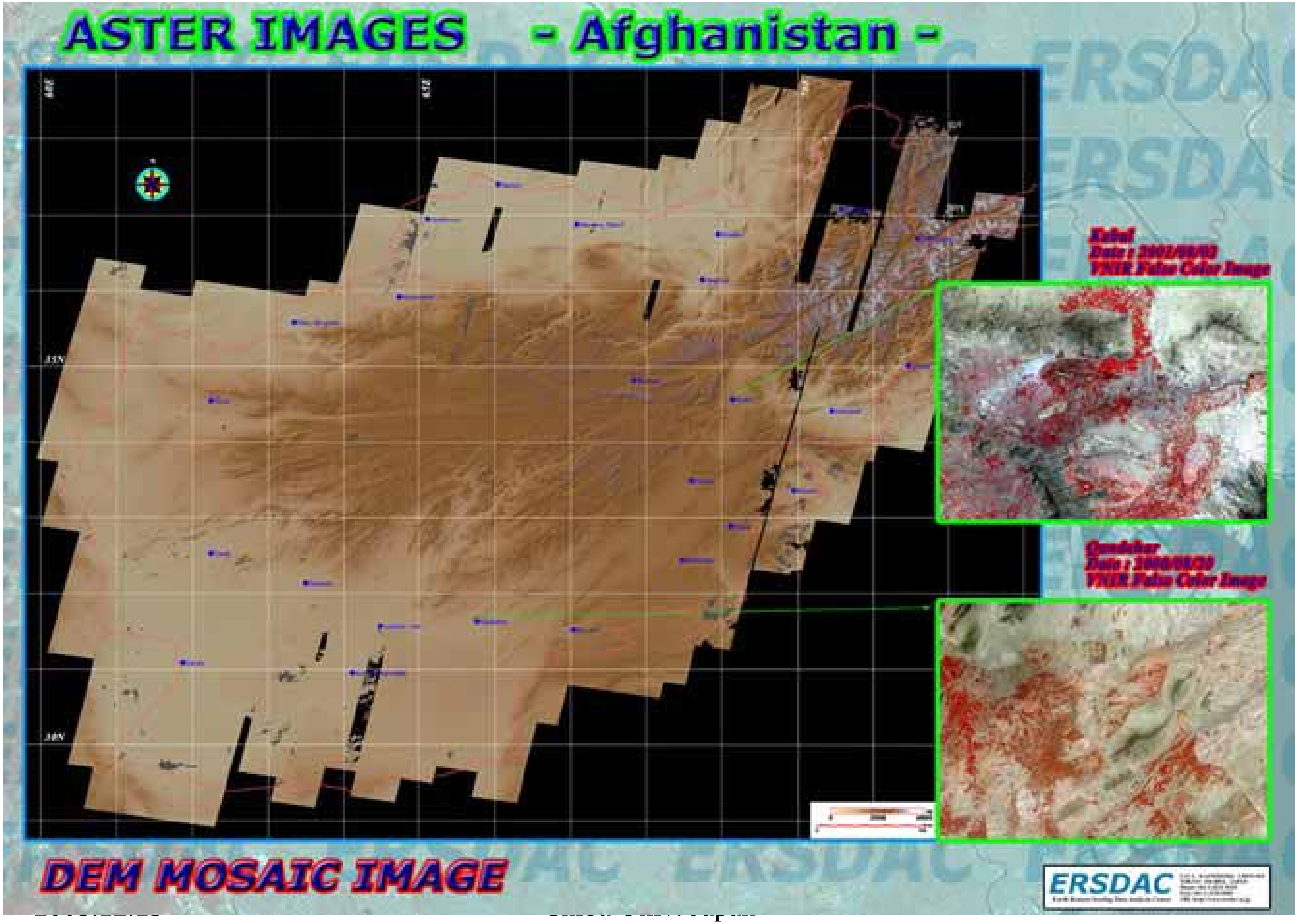

Conclusion

- ASTER achieves the high performance of data coverage, high speed data distribution, high geometric and radiometric accuracy.
- Such performance enables not only the application based on the high geometric, radiometric and spectral characteristics, but also environmental, agricultural and disaster monitoring based on the efficient operation.

Overview

- The Global Land Cover Validation Report
- Global Land Cover from Space
- Challenges to Validation
- Recommendations
- Example: GLC2000 Validation
- Example: MODIS Land Cover Validation

The GLCV Report

GLOBAL LAND COVER VALIDATION:

RECOMMENDATIONS FOR EVALUATION AND ACCURACY

ASSESSMENT OF GLOBAL LAND COVER MAPS

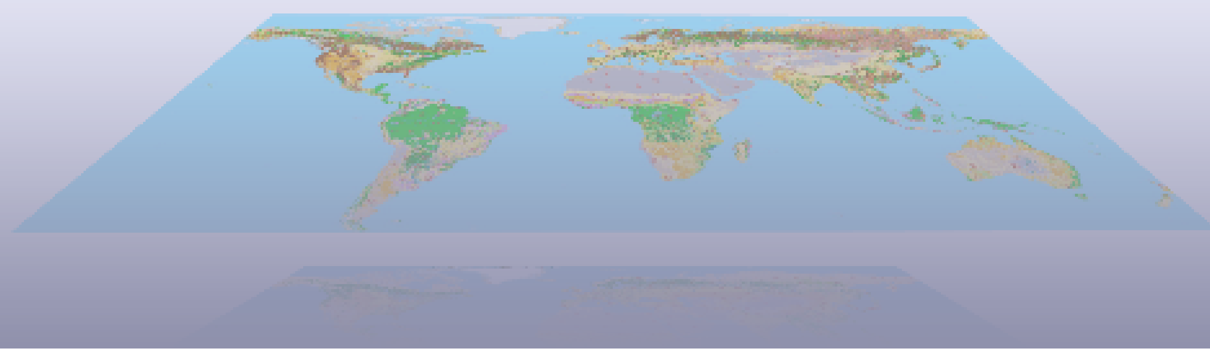

Report Provenance

CEOS
Committee On Earth Observation Satellites

WGCV
Working Group on Calibration and Validation

LPV
Land Product Validation Subgroup

GLCV
Global Land Cover Validation Sub-subgroup

Activity of Global Observation of Forest Cover-Global Observation of Land-Cover Change (GOFC-GOLD)

History

- **Outcome of Two Two-Day Workshops**
  - JRC Institute of Environmental Sustainability, Ispra, March, 2003
  - Boston University Center for Remote Sensing, February, 2004
- **Report Preparation and Iteration, 2004, early 2005**
- **Report Publication as JRC-IES Technical Report, January 2006**

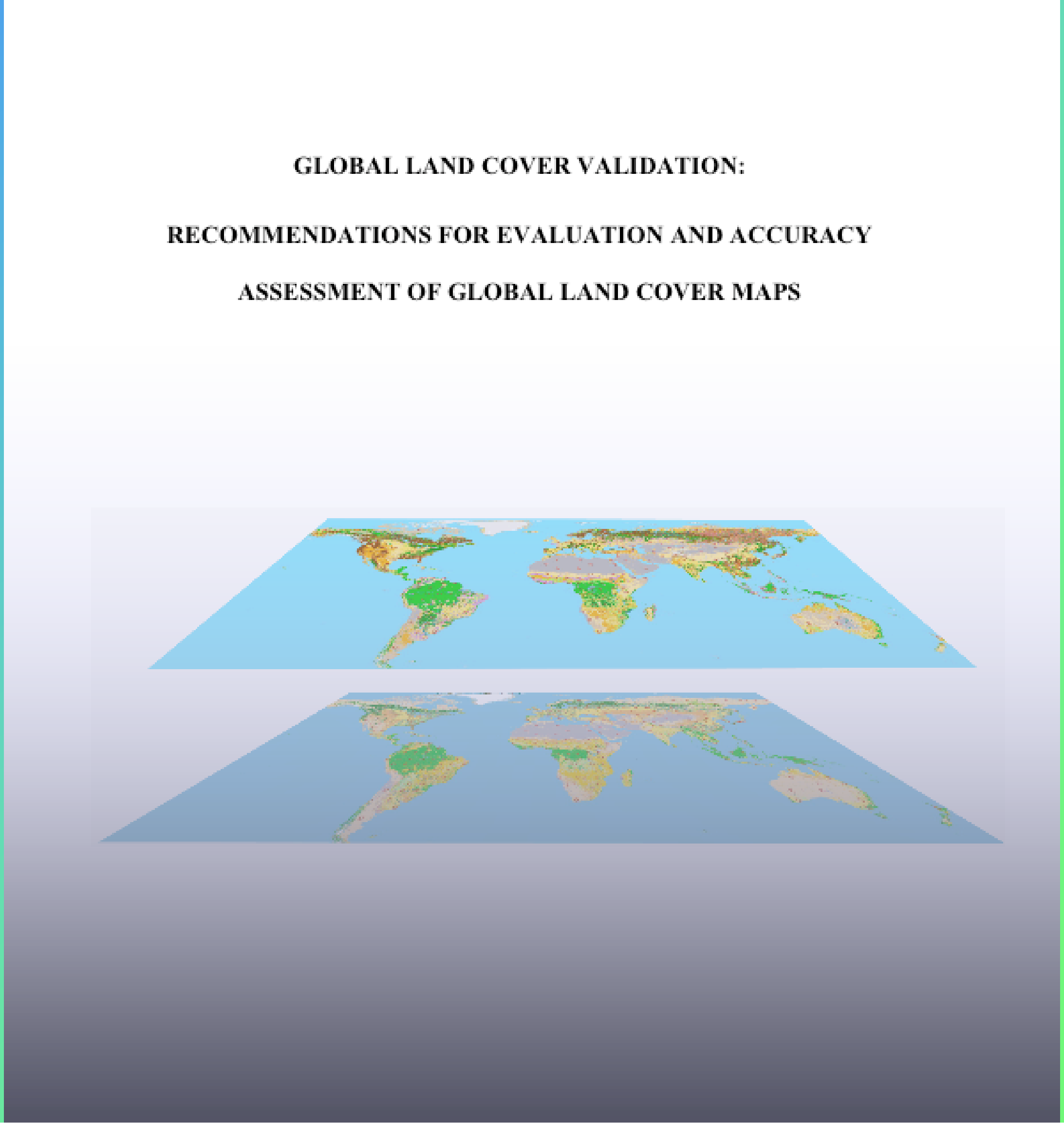

Report Contents

- Introduction
  (Alan Strahler)
- Issues in Accuracy Assessment
  (Giles Foody)
- Probability Sampling in Global Validation
  (Steve Stehman)
- Qualitative/Descriptive Analyses
  (Philippe Mayaux)
- Validation of Land Cover Change
  (Matt Hansen)
- Recommendations and Conclusions

Global Land Cover Validation:

Recommendations for Evaluation and Accuracy Assessment

Of Global Land Cover Maps

Contents

AVHRR NDVI

- **AHVRR—Advanced Very High Resolution Radiometer 1982–present**

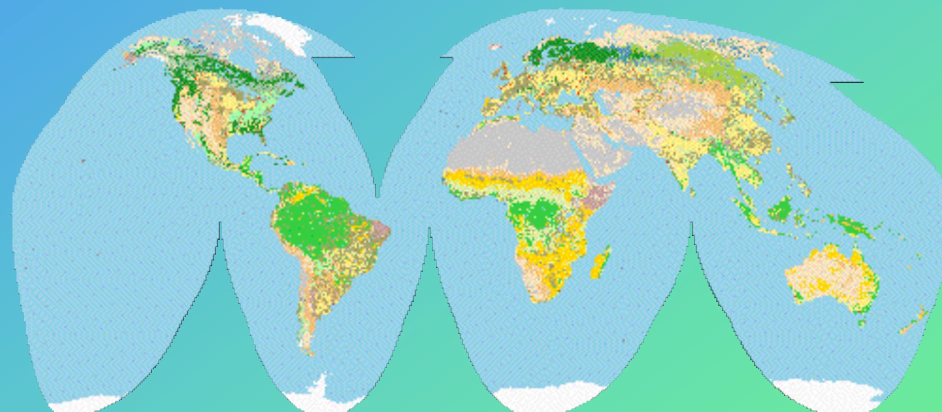

EDC DISCover Land Cover Product

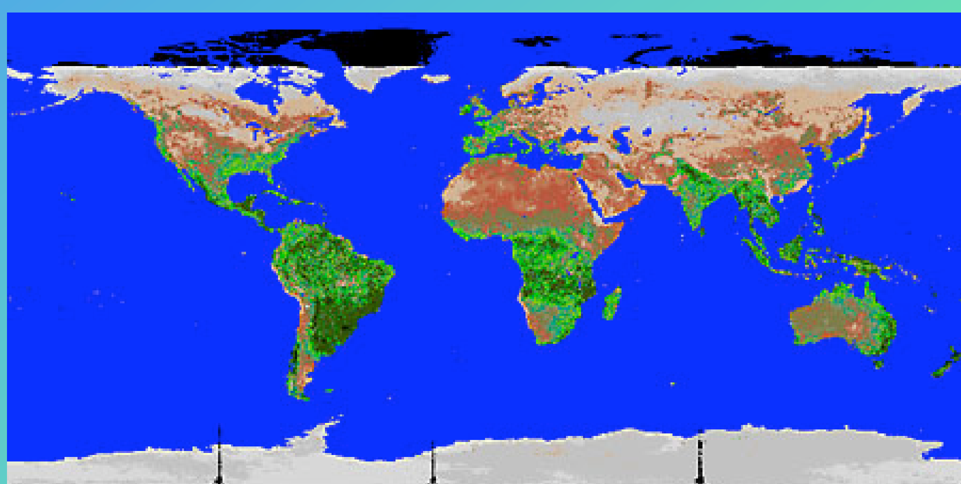

Composited NDVI February 1992

SPOT-Vegetation

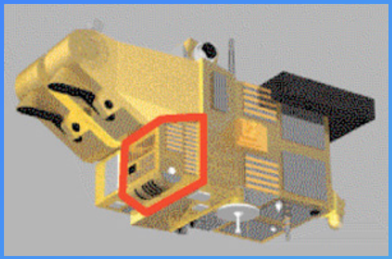

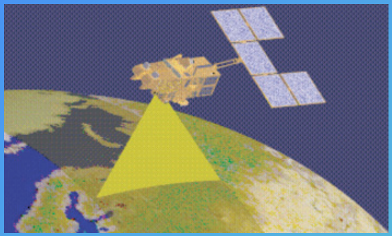

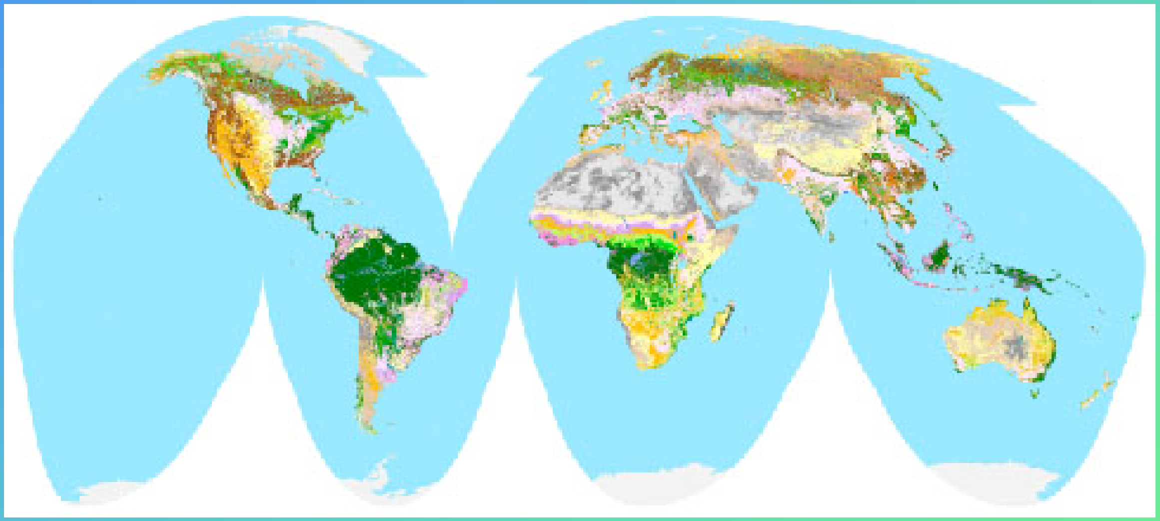

GLC2000 Land Cover Product

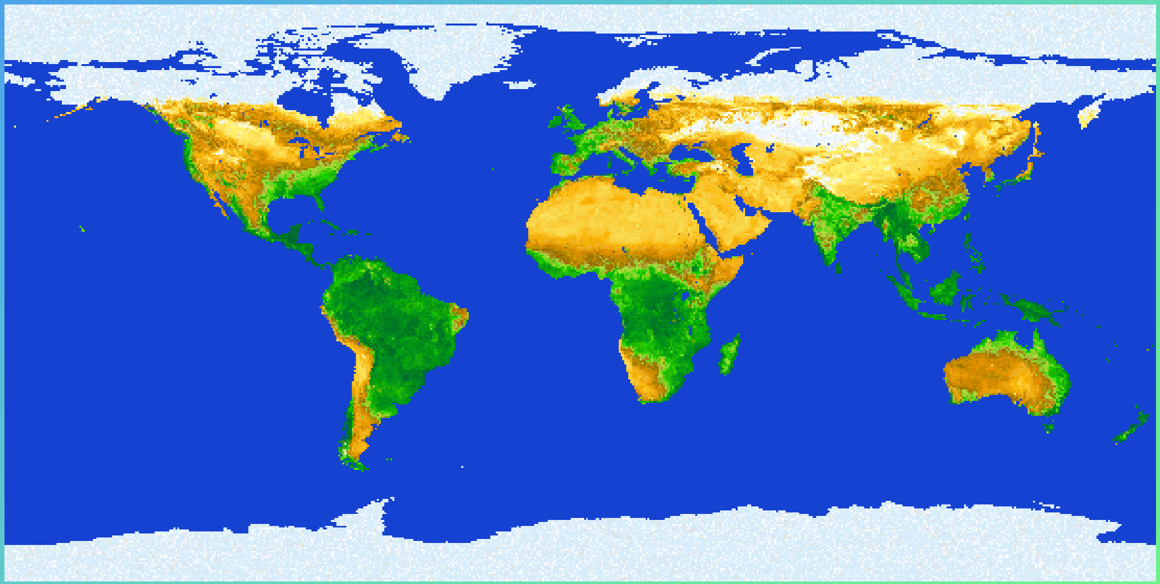

SPOT-Vegetation NDVI

MODIS

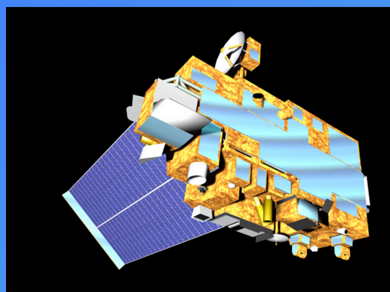

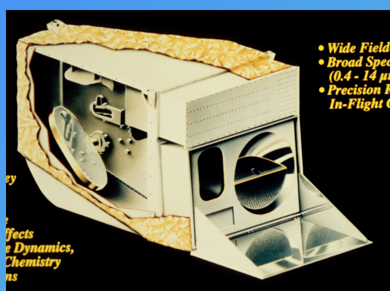

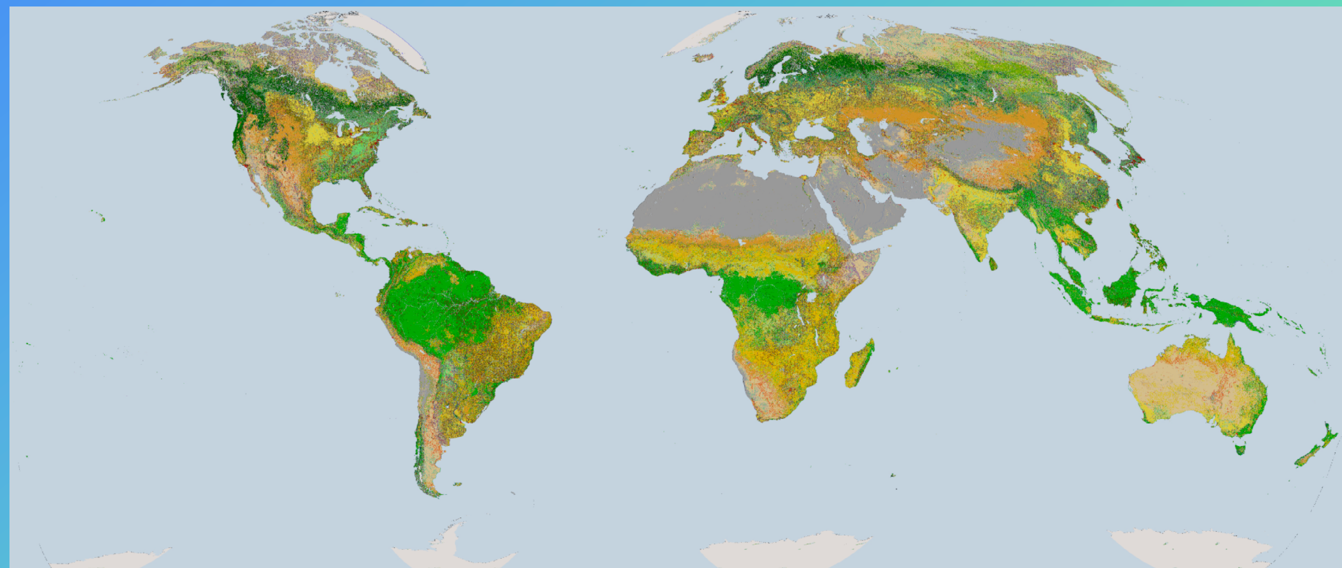

MODIS Land Cover Product 2001

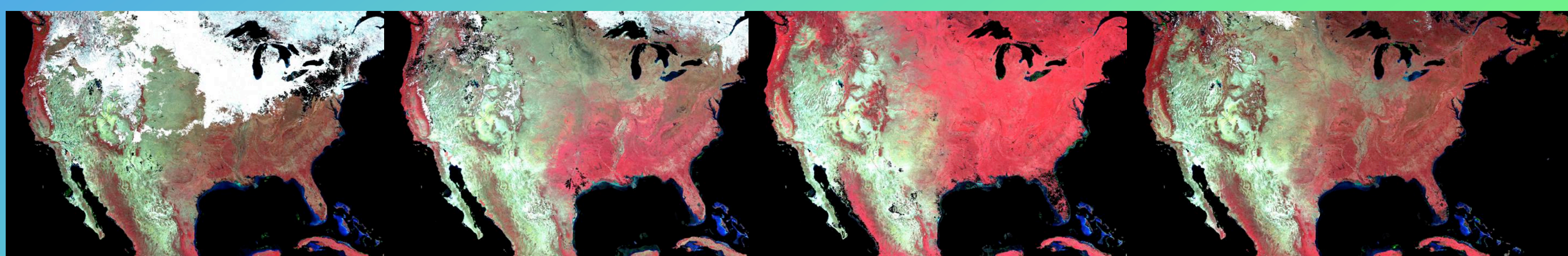

January 1–16 April 7–22 July 12–27 October 16–31

MODIS Nadir BRDF-Adjusted Reflectance 2001

Future Maps

- **MERIS**
  - Planned GLOBCover 2005, JRC, Ispra, 500 m
- **NPOESS**
  - Will have a quarterly land cover product
  - Launch in >2010
- **MODIS**
  - Prof. Tateishi’s Global Land Cover Product

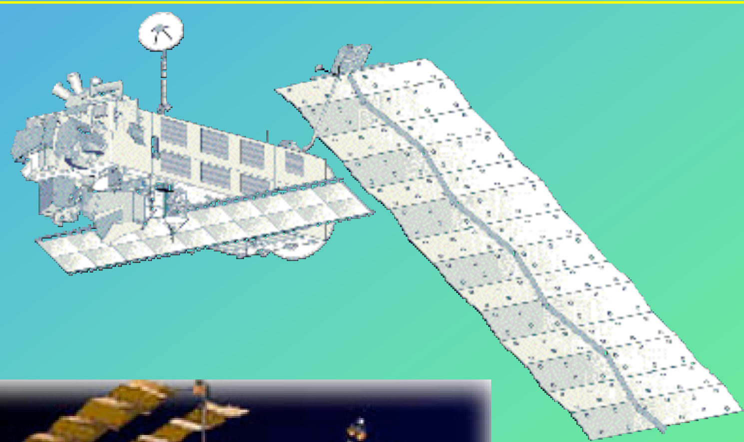

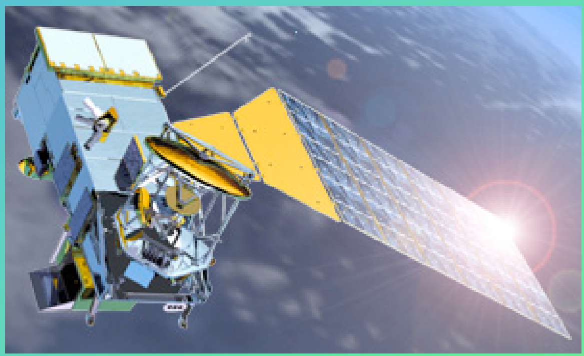

NBAR Time Trajectories

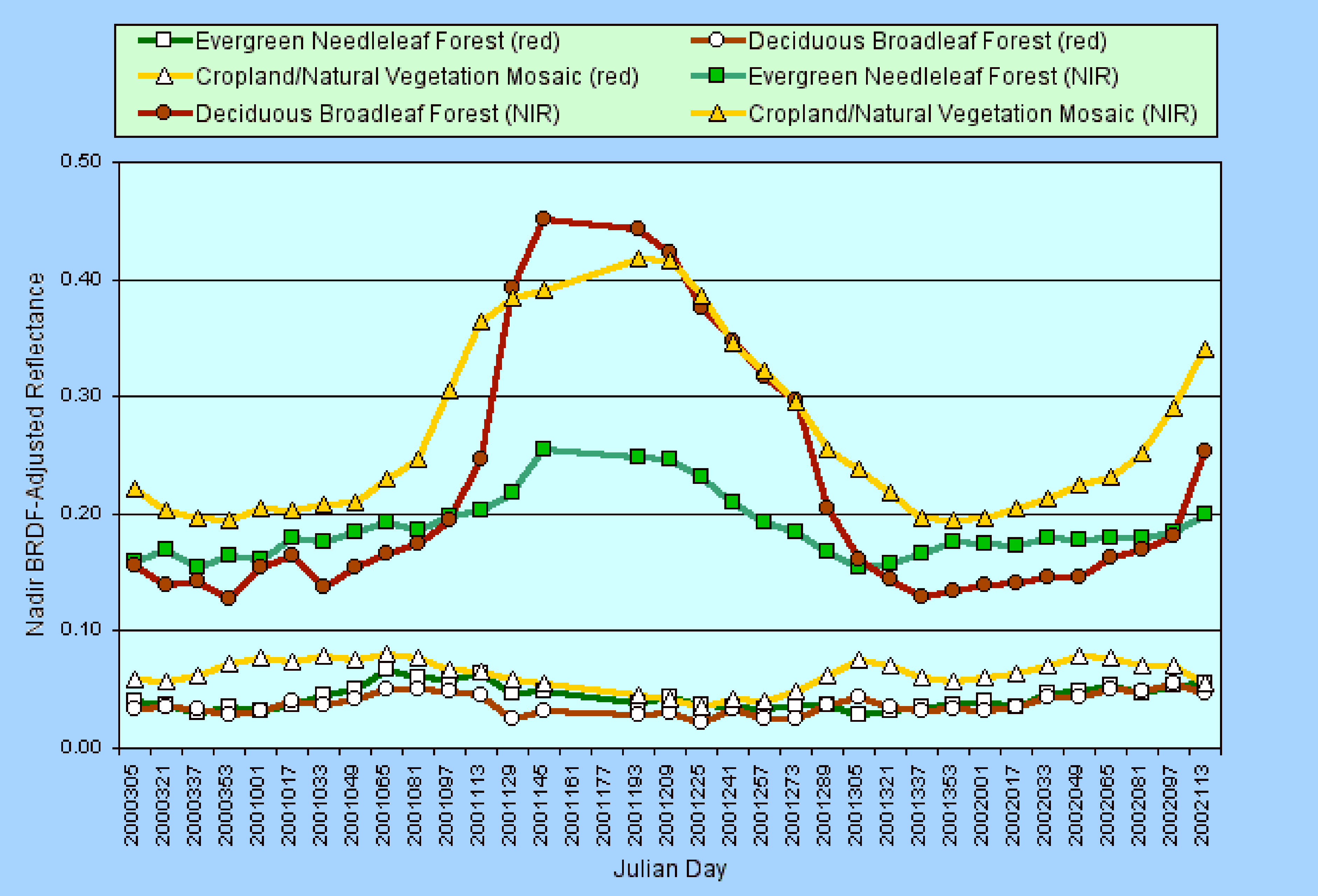

Challenges to
Global Land Cover Mapping and Validation

- **Satellite Sensor Limitations**
  - Spectral Data Quality
  - Geolocation
- **Land Cover Type Model**
  - Legend Definitions
  - Mixed Pixels
- **Challenges to Classification**
  - Variability of Cover Types
  - Obtaining Global Training Data
  - Registration
  - Temporal Change
- **Challenges to Accuracy Assessment**
  - Accuracy Parameters and Definitions
  - Sample Design
  - Global Sampling

Calibration

- Instrument calibration is essential to accurate imaging
- Example: Striping in Band 3 (Blue) in early MODIS data

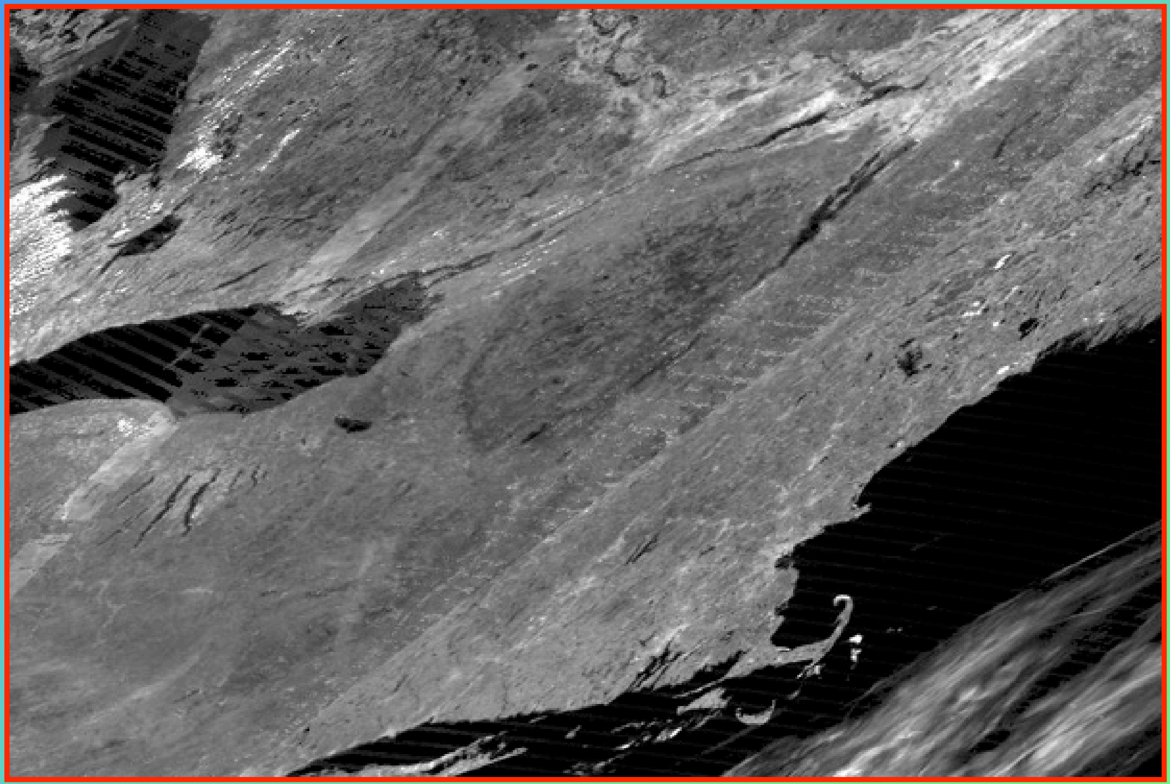

Atmospheric Effects

- Atmospheric correction is also essential for high-quality data
- Example: Atmospheric correction of MODIS swath from central Africa

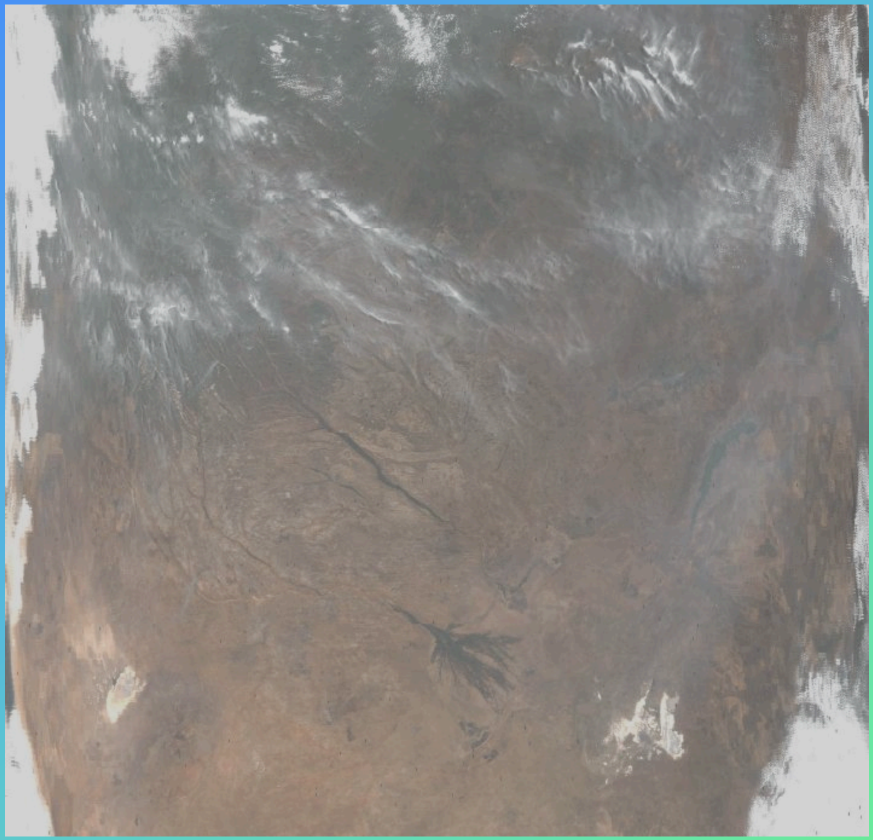

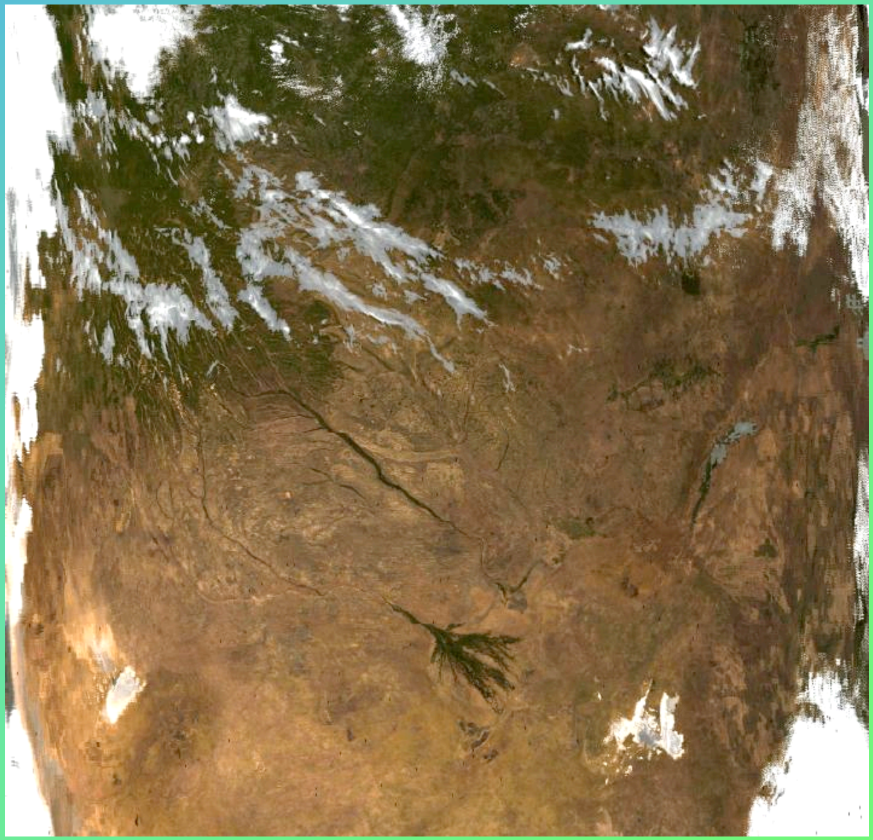

Angular Effects

- **View angle effects can affect wide-scan imagery**
- **Example: Adjacent MODIS scans and BRDF correction**

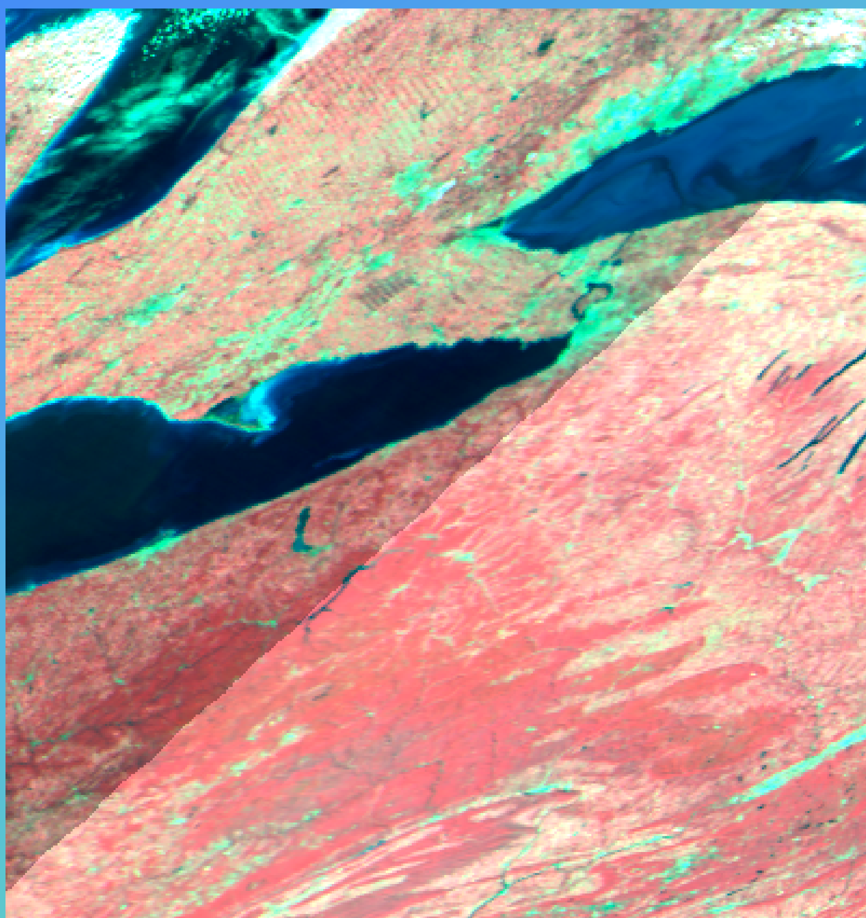

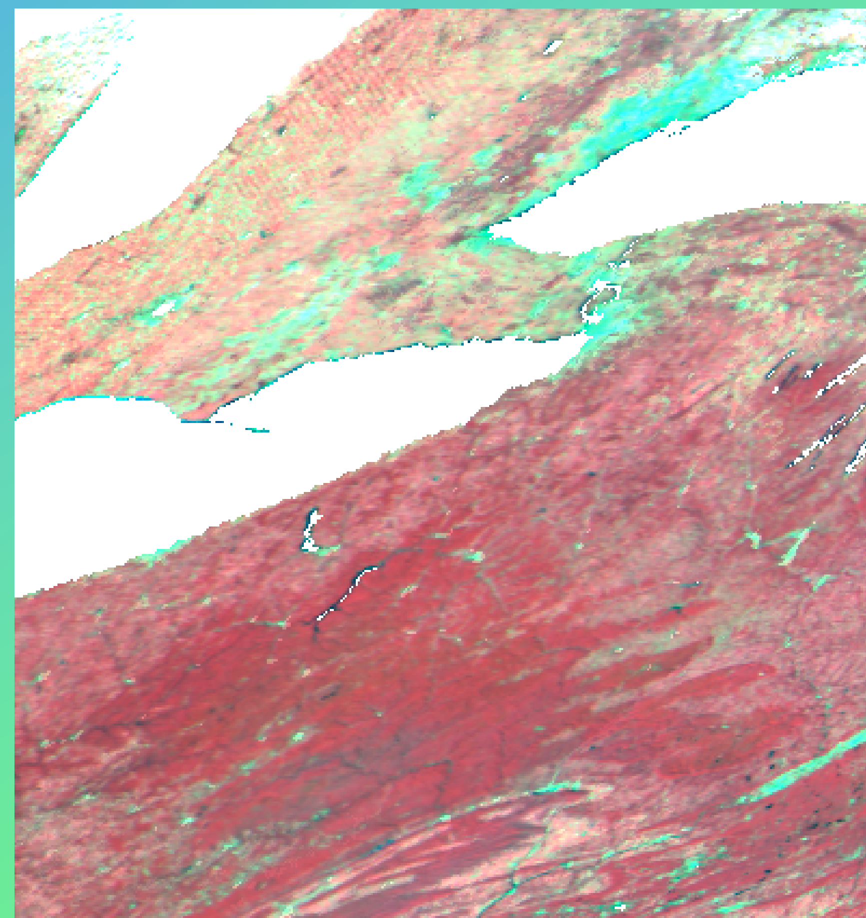

Geolocation

- Spacecraft Position and Velocity
- Instrument Imaging Parameters
- Topographic Height of Terrain

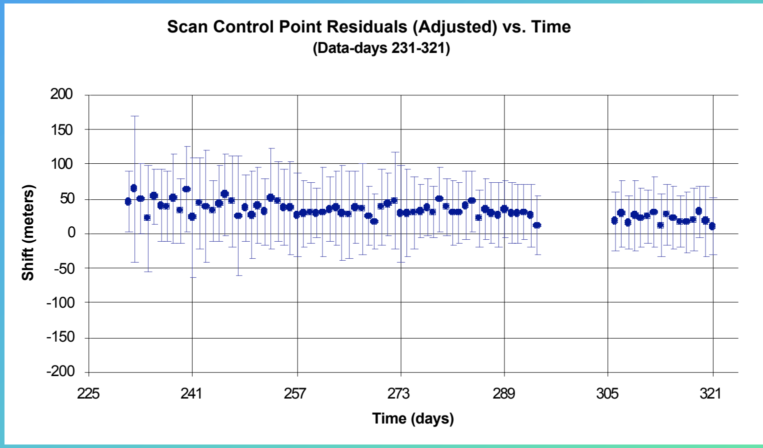

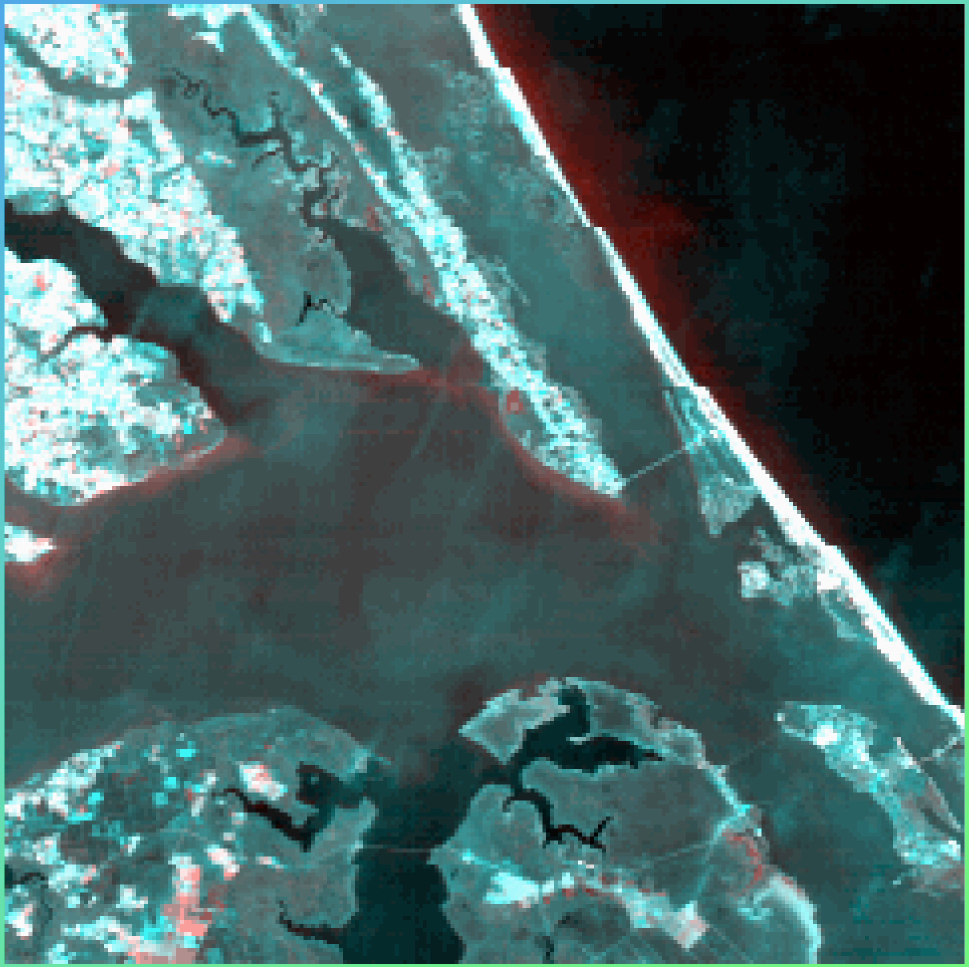

MODIS (blue); Landsat-simulated MODIS (red)

Land Cover Type Model

- **Legend Definitions**

MODIS—IGBP

International Geosphere-Biosphere Programme
Land Cover Class Names

1 EVERGREEN NEEDLELEAF FOREST
2 EVERGREEN BROADLEAF FOREST
3 DECIDUOUS NEEDLELEAF FOREST
4 DECIDUOUS BROADLEAF FOREST
5 MIXED FORESTS
6 CLOSED SHRUBLANDS
7 OPEN SHRUBLANDS
8 WOODY SAVANNAS
9 SAVANNAS
10 GRASSLANDS
11 PERMANENT WETLANDS
12 CROPLANDS
13 URBAN AND BUILT-UP
14 CROPLAND/NATURAL VEGETATION MO

GLC2000—LCCS

Domain		**I. Aggregation Global Classes** (mandatory)		**II. Suggestion for regional a classes** (additional classes may be add achievable)
Forest types	1.	**Tree Cover, broadleaved, evergreen** *(LCCS >15% tree cover, tree height >3m)*	1.1	**-closed** *> 40% tree cover (LCCS >65% and >40-65%*
			1.2	**-. open** *15-40% tree cover*
	2.	**Tree Cover, broadleaved, deciduous**	2.1	**- closed**
			2.2	**- open**
	3.	**Tree Cover, needle-leaved, evergreen**	3.1	**- closed**
			3.2	**- open**
	4.	**Tree Cover, needle-leaved, deciduous**	4.1	**- closed**
			4.2	**- open**
	5.	**Tree Cover, mixed phenology or leaf type**	5.1	**- closed**
			5.2	**- open**
Flooded & inundated forest types	6.	**Tree Cover, regularly flooded: Mangrove**	6	**Tree Cover, regularly floo**
		>>>>-flooded forest types other than mangrove (swamp, peat swamp, ..) are not displayed at the global level but grouped under class (1)<<<<	1.3	**Tree Cover, other, regular**
			1.4	**Tree Cover, other, regular**
Shrubland type& Shrub-Tree Savannas types	7.	**Shrub Cover, closed-open, evergreen (with or without sparse tree layer)**	7.	- minimum same as global optional: > 7.1 without, 7.2 wit
	8.	**Shrub Cover, closed-open, deciduous (with or without sparse tree layer)**	8.	- minimum same as global optional: > 8.1 without, 8.2 wit
Grassland, Savannas ,Heath Pasture	9.	**Herbaceous Cover, closed-open**	9.1	**Herbaceous Cover, closed** 9.11 natural; 9.12 pasture[1]
Tree Savanna type			9.2	**Herbaceous Cover, closed sparse trees or shrubs (>**
Steppe types	10.	**Sparse Herbaceous or sparse shrub cover**	10	- minimum same as global -
Tundra types	11.	**Lichens & Mosses**	11	- minimum same as global -
Wetland types	12.	**Regularly flooded shrub and/or herbaceous cover**	12	- minimum same as global -
Bog type	13.	**Regularly flooded cover of mosses (and lichens)**	13	- minimum same as global -

Mixed Pixels

- Mississippi Delta—Land-water mixed pixels

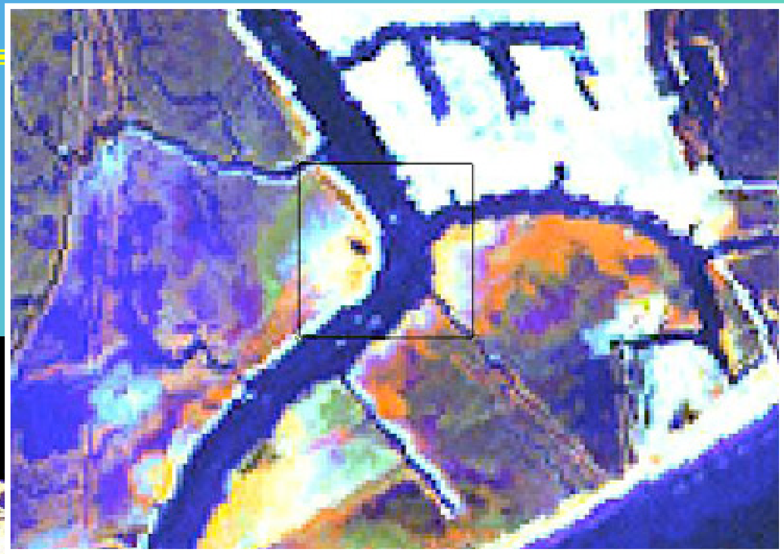

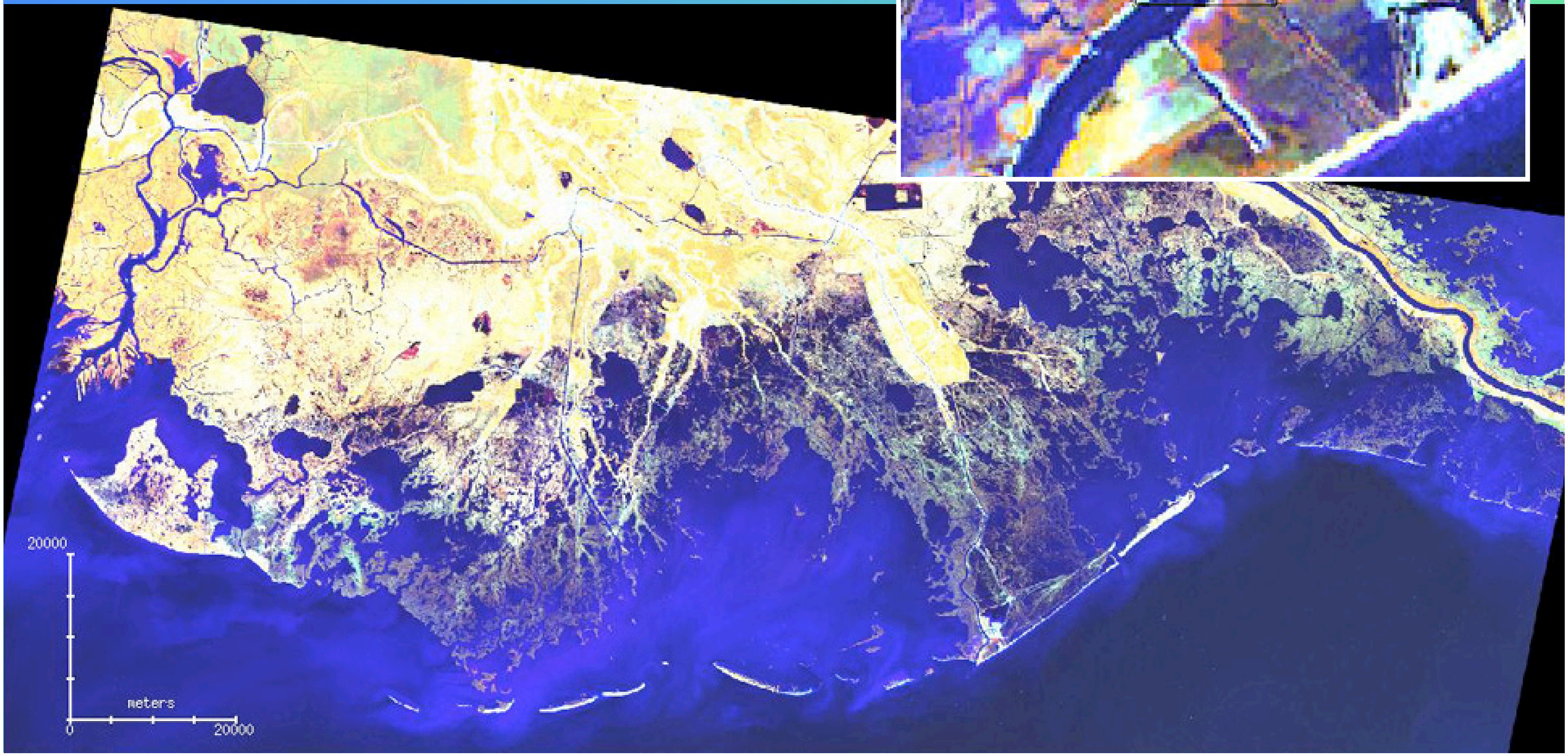

Variability of Cover Types

- Arid East Africa, gradations of barren–open shrubland–closed shrubland

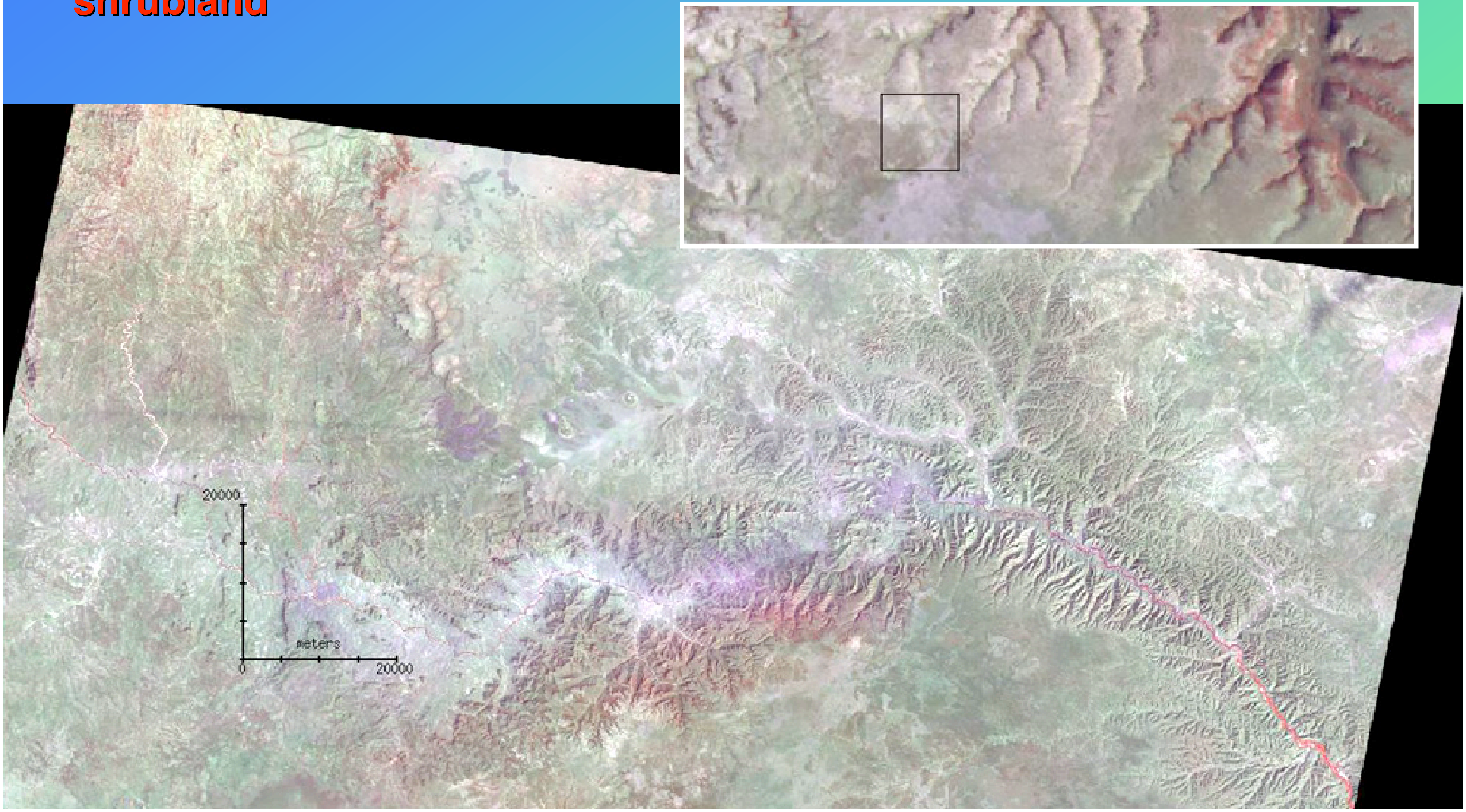

Obtaining Global Training Data

- Global Training Site Database—MODIS
- 2300 Sites—"Living" Database
- Map shows locations of Landsat scenes

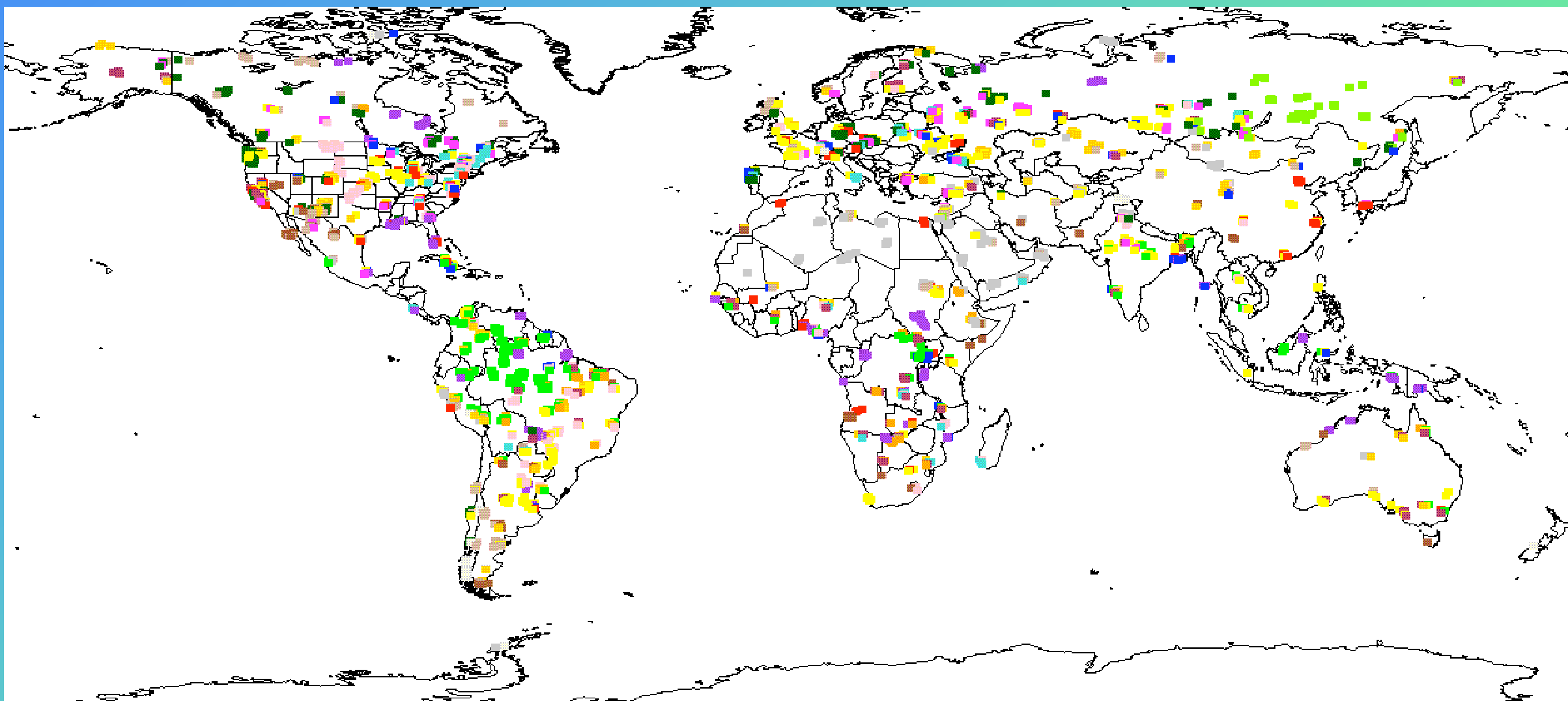

Missing Data

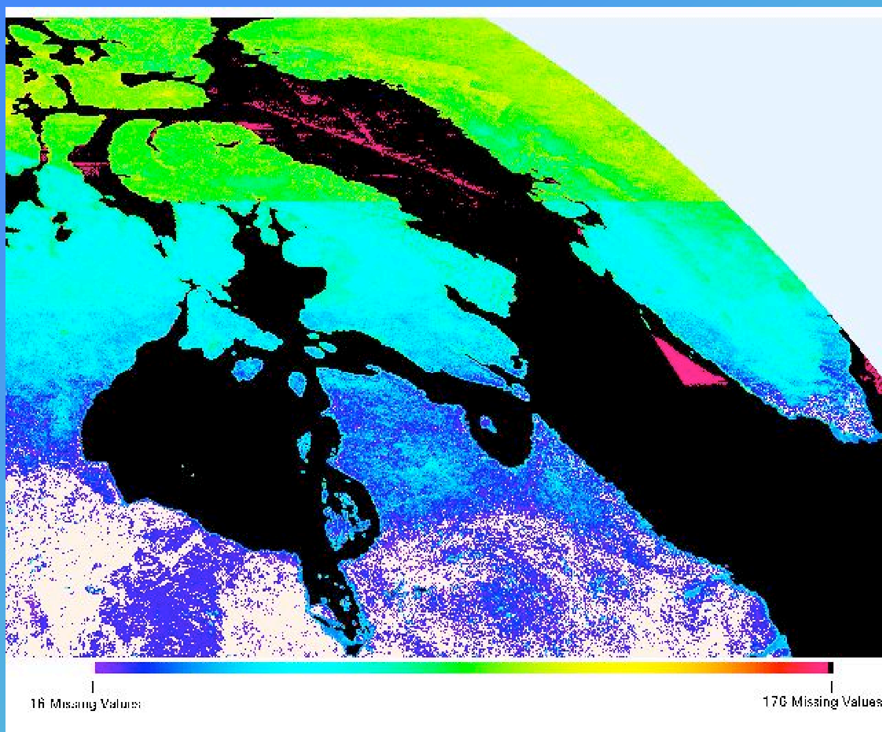

High Latitudes

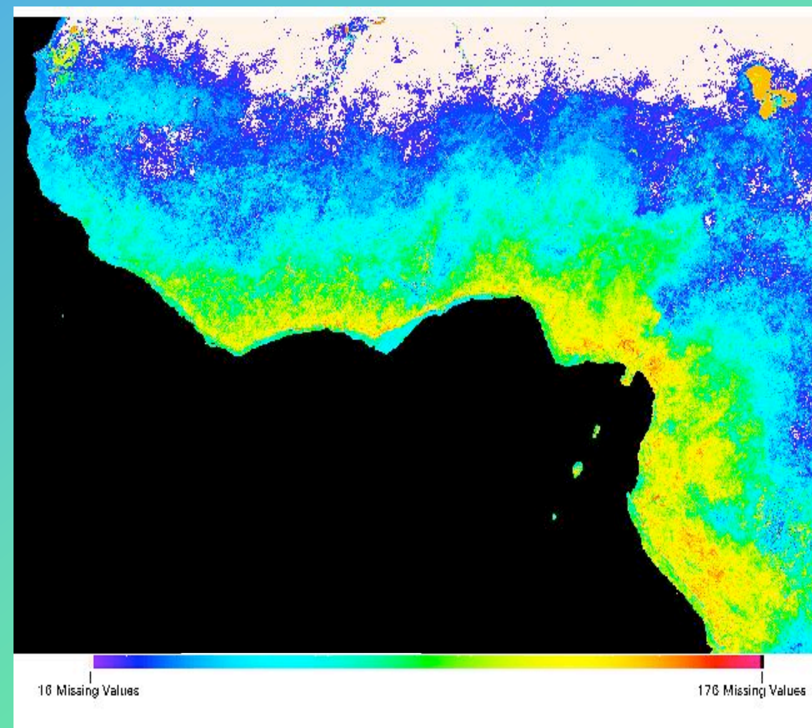

Cloud Cover in Tropics

Color scale indicates number of missing values, 16-day NBARs

16 **176**

Accuracy Assessment Issues

- **Accuracy Parameters and Definitions**
  - Overall accuracy
  - Per-class accuracies, users’ and producers’
  - Standard errors on accuracies
  - Fuzzy accuracy
    - Some types of errors are more important than others
- **Sample Design**
  - Stratification strategy, e.g., equal samples from each class
- **Global Sampling**
  - Obtaining samples randomly from anywhere on the globe
  - Use of high-resolution images and photointerpretation is the only practical way

Validation Approaches

- **Probability Sampling and Accuracy Assessment**
  – Examples: IGBP DISCover Validation, GLC2000 Validation
- **Use of Training Sites for Validation**
  – Example: MODIS Land Cover Product
- **Confidence Observations and Maps**
  – Example: MODIS Land Cover Product
- **Qualitative-Systematic Accuracy Assessment**
  – Example: GLC2000 Validation

Report Recommendations

- **All global land cover maps should have statistically valid estimates of map accuracy**
- **Core methods to be routinely applied include :**
  – Design-based inference
  – Probability sampling
  – Consistent estimators
- **Core methods may be extended to include:**
  – Validation both during and after map production
  – Use of confidence-based quality assessments
  – Addition of fuzzy accuracy methods
  – Use of qualitative and descriptive methods

EUROPEAN COMMISSION
DIRECTORATE-GENERAL
Joint Research Centre

Validation of the GLC2000 Land Cover Dataset

Philippe Mayaux

Institute of Environmental Sustainability

Joint Research Center, Ispra, Italy

Institute for Environment and Sustainability

Published by: EUROPEAN COMMISSION Joint Research Centre

In association with: UNEP

Global Land Cover for the Year 2000

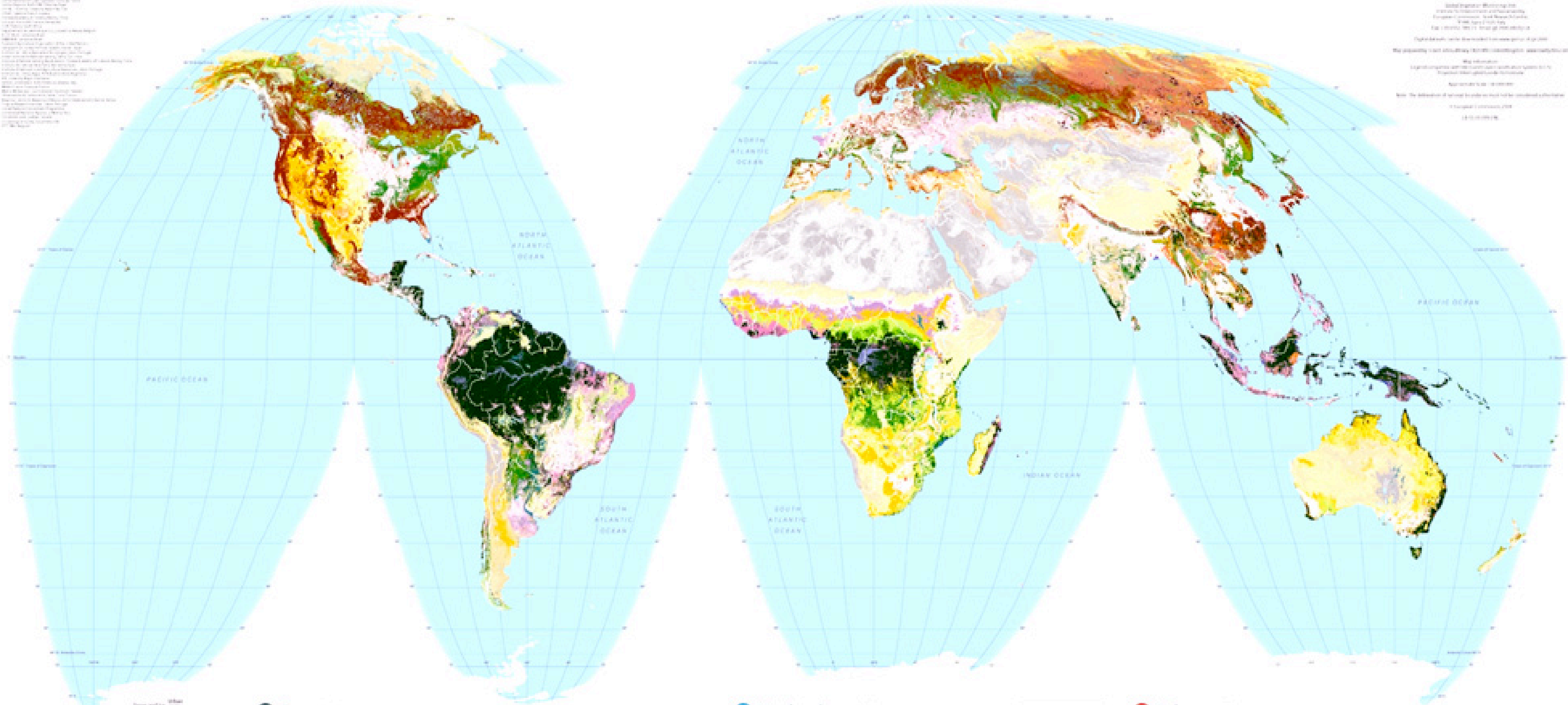

Land Cover Themes

GLC2000 Global Legend

Forest

Agriculture

Wetlands

Grassland/Shrubland

Bare Areas

Snow and Ice

Urban

Forest

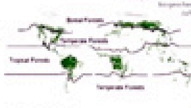

Wetlands

Urban

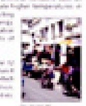

Grass/Shrubland

Agriculture

15.7%

Bare Areas

23%

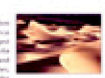

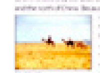

Snow & Ice

EUROPEAN COMMISSION
DIRECTORATE-GENERAL
Joint Research Centre

Qualitative-Systematic Accuracy Assessment

- **Objectives**
  - **elimination of macroscopic errors and**
  - **improvement of the global acceptance by the users.**
- **Systematic descriptive protocol**
  - **each cell of the map (200x200 km) is compared with reference material (quick-looks, local maps…)**
- **Overall accuracy**
  - **and qualification of errors per cell**

Institute for Environment and Sustainability

EUROPEAN COMMISSION
DIRECTORATE-GENERAL
Joint Research Centre

An Example in Russia

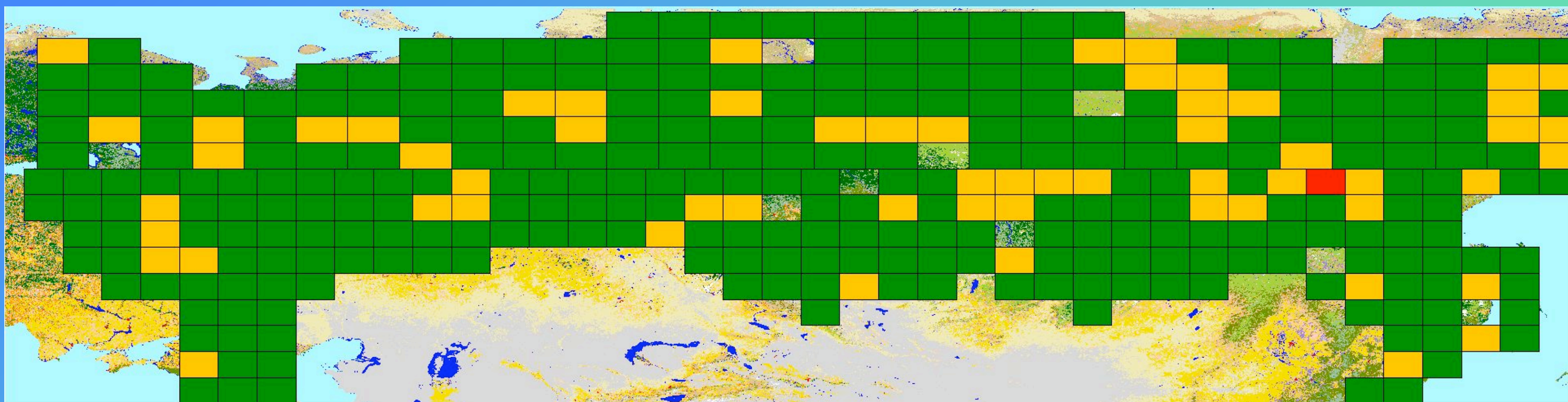

Institute for Environment and Sustainability

EUROPEAN COMMISSION
DIRECTORATE-GENERAL
Joint Research Centre

Design-Based Strategy

- Validation of the global product but sampling units should cover the different continents.
- Focus on priority classes (forests, wetlands, croplands) ⇒ stratification
- Landscape complexity taken into account for the sampling.
- Validation derived from one single sensor dataset, Landsat
- Deformation of the geographical grid in high latitudes.
- Use of regional experts for interpretation
- The interpretation key follows the classifiers used in the map production .
- Locational accuracy = 300m =>use of pixel-blocks

Institute for Environment and Sustainability

EUROPEAN COMMISSION
DIRECTORATE-GENERAL
Joint Research Centre

GLC 2000 Global Classes

Priority classes	Non-priority classes
FORESTS Tree Cover Broadleaved Evergreen Tree Cover Broadleaved Deciduous Open Tree Cover Broadleaved Deciduous Closed Tree Cover Needleleaved Evergreen Tree Cover Needleleaved Deciduous Tree Cover Mixed Tree Cover / Other Natural Vegetation	SHRUBLANDS & GRASSLANDS Shrubland Evergreen Shrubland Deciduous Open-Closed Grassland Sparse Grassland Lichen & Mosses
WETLANDS AND INLAND WATER Flooded Forest Mangrove Regularly Flooded Grass- & Shrublands Water	OTHER Bare Soil Cities Snow/Ice
CROPLANDS Cultivated & Managed Areas Cropland / Tree Cover Cropland / Other Natural Vegetation	

Institute for Environment and Sustainability

Computation of LC Proportion

- **Priority Classes**
  - **Proportion of priority classes in each polygon**

    >30% forest   >30% croplands   >10%wetlands

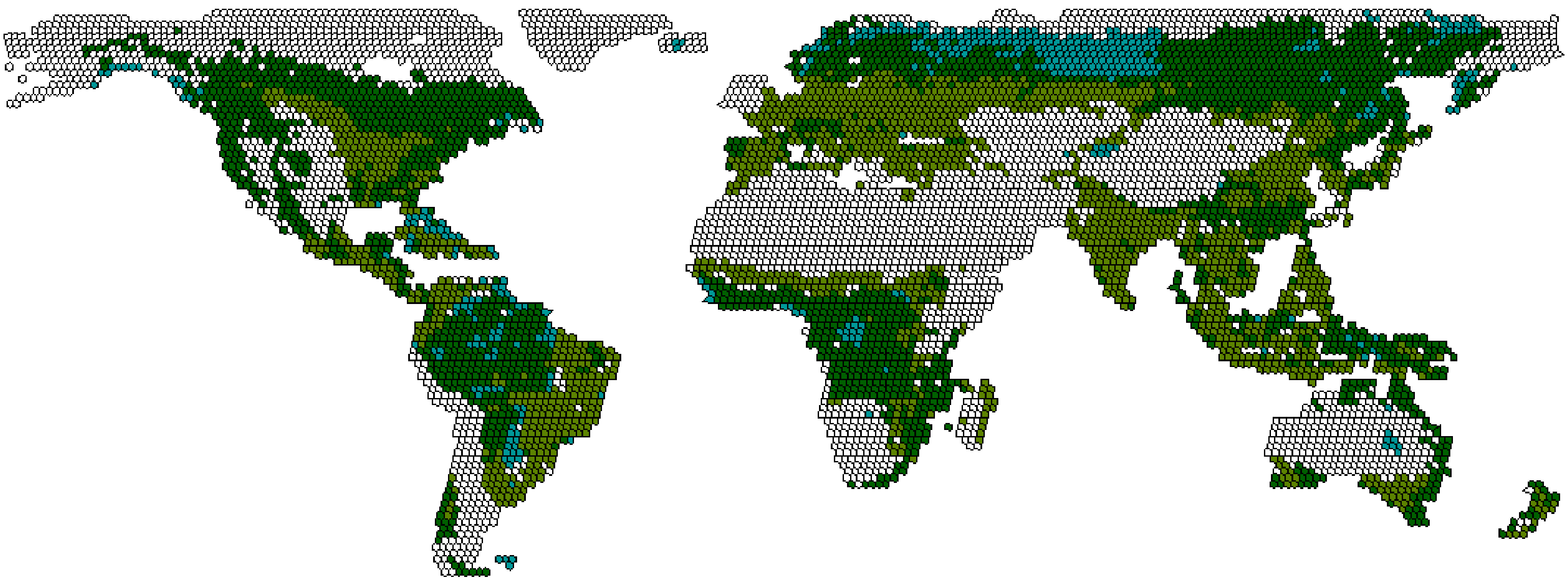

EUROPEAN COMMISSION
DIRECTORATE-GENERAL
Joint Research Centre

Computation of Fragmentation

- **Landscape Complexity**
  - Shannon index calculated on the total number of classes in the polygon

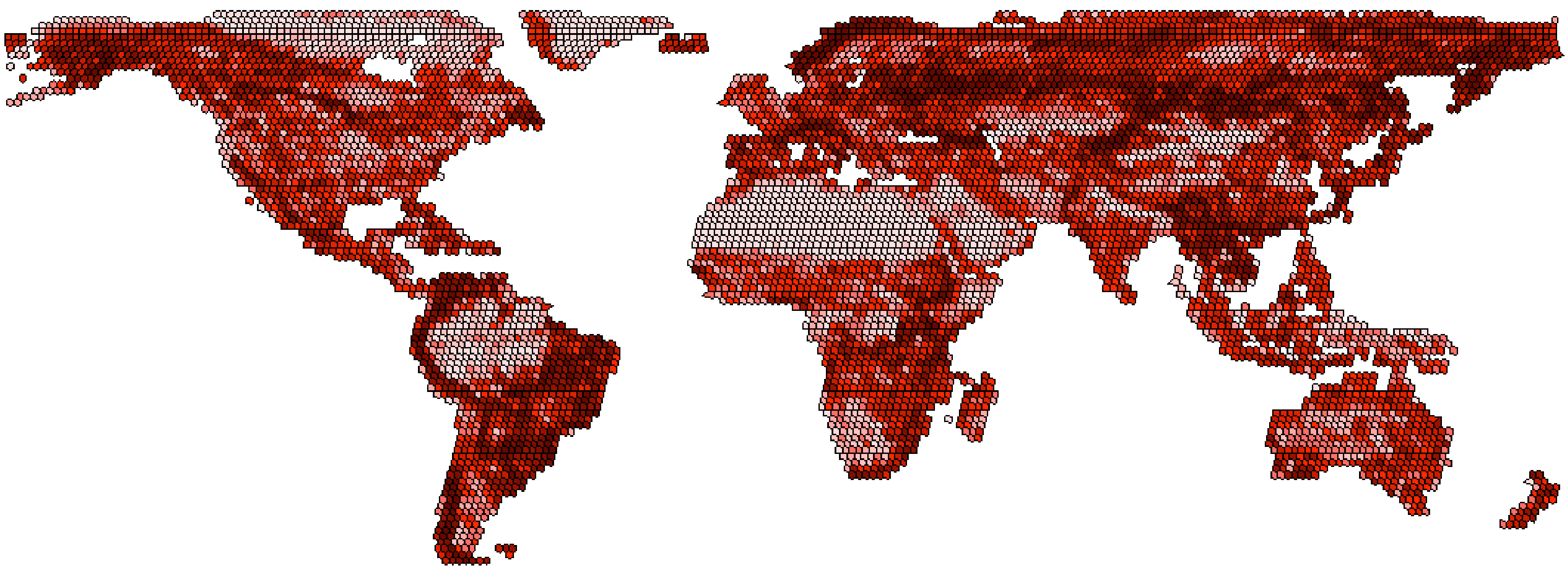

Institute for Environment and Sustainability

Stratification

4 strata

Stratum	Landsat	%	Landsat area (km²)	%
Priority classes Homogenous	2267	28.2%	15,769,715	31.2%
Priority classes Heterogeneous	2936	36.6%	19,115,193	37.9%
Non - Priority classes Homogenous	2174	27.1%	12,794,538	25.3%
Non - Priority classes Heterogeneous	649	8.1%	2,809,180	5.6%
	8026		50,488,626	

EUROPEAN COMMISSION
DIRECTORATE-GENERAL
Joint Research Centre

Stratified Sampling

4 strata

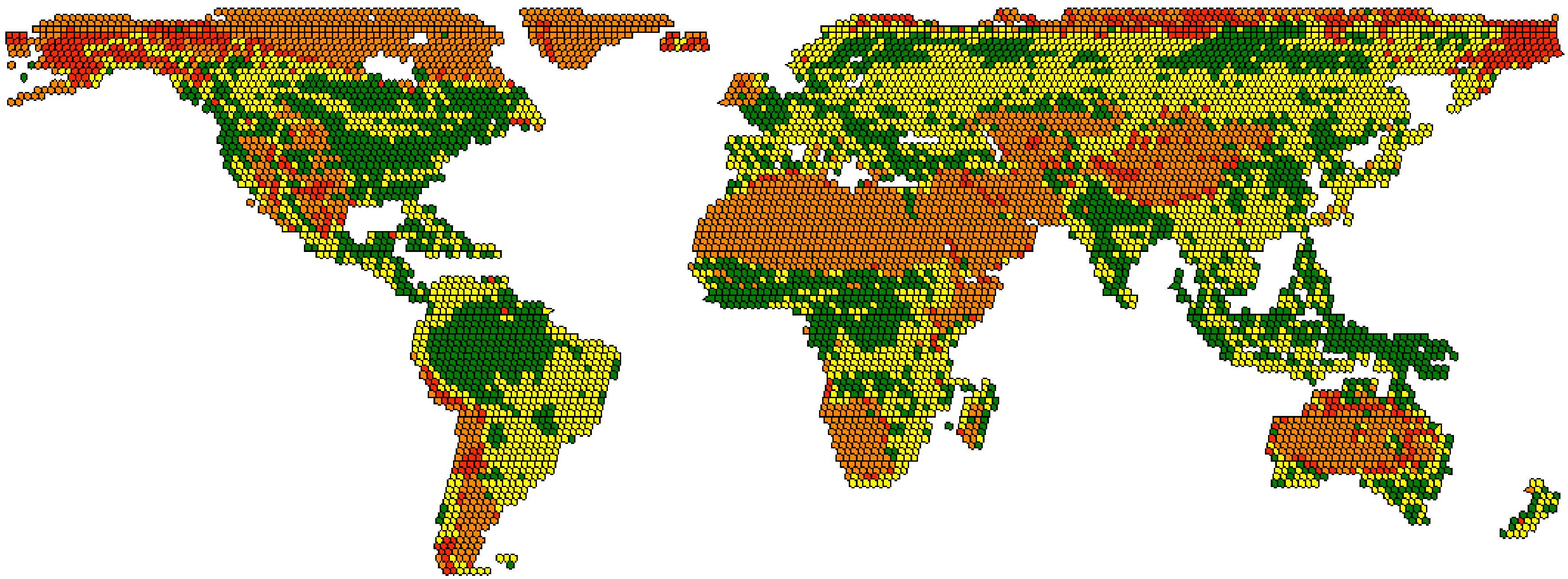

Institute for Environment and Sustainability

Primary Sampling Units

245 Landsat scenes

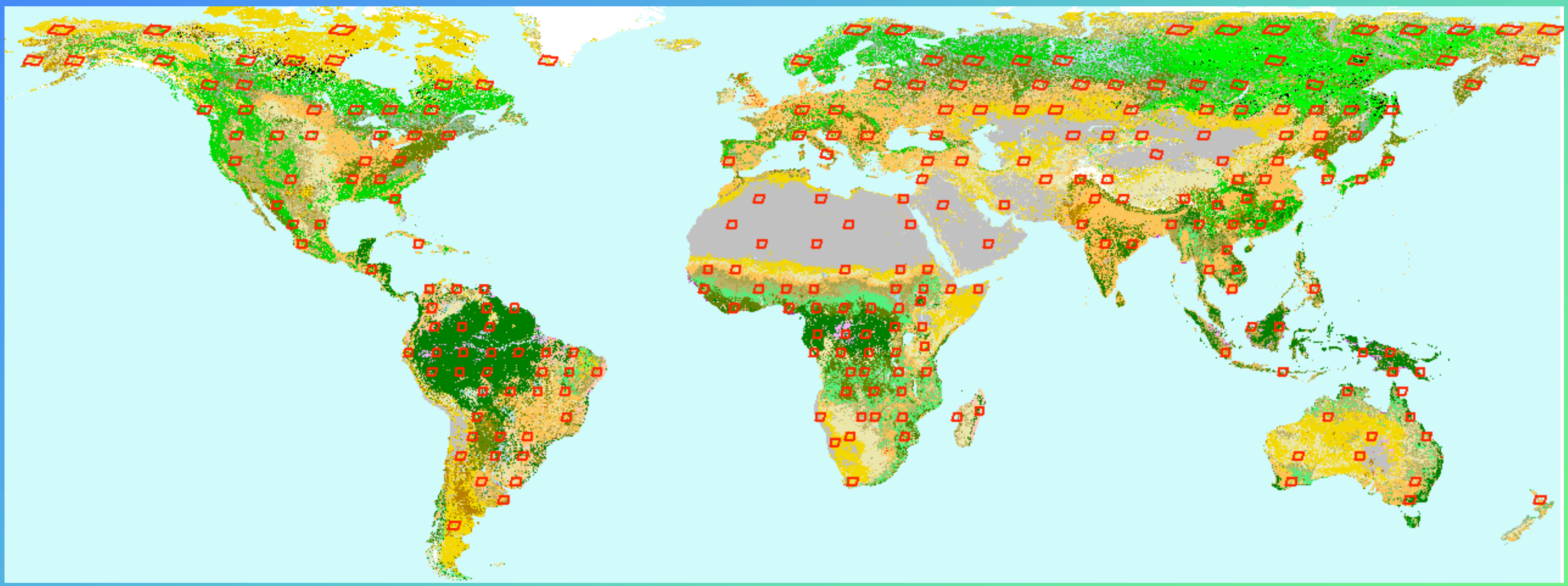

Secondary Sampling Units

- 5 blocks of 3 x 3 km per Landsat scene
- Centre ± 50km in X and Y (spatial autocorrelation)

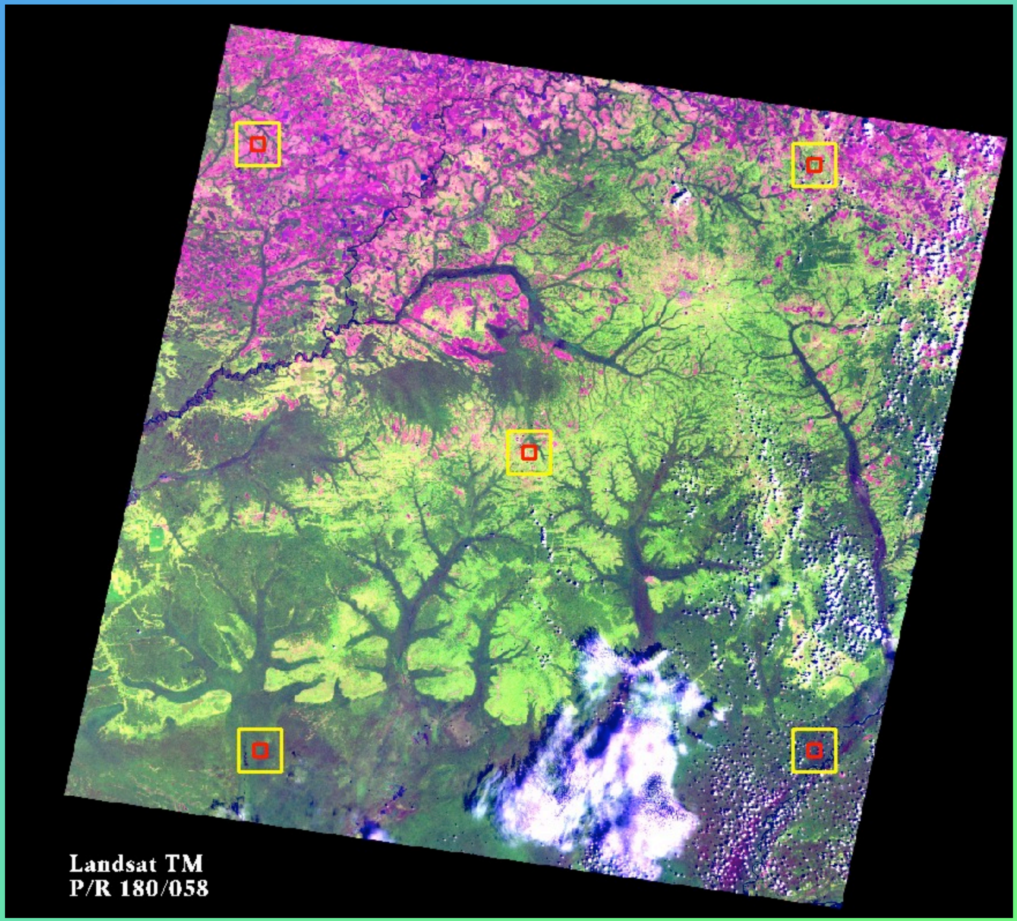

EUROPEAN COMMISSION
DIRECTORATE-GENERAL
Joint Research Centre

Example in South America (Homogeneous Agriculture)

GLC2000 Validation form

1. Landsat — ID: 2333 | Path_Row: P223R076 | Landsat Date: 20000512 | Box: Lower left box | Fraction(%): 100
2. Interpreter — Company: ECOFORCA | Interpreter: ECOFORCA | Interpretation Date: 20040608
3. Key parameters — Vegetated: Vegetated | Natural / managed: Artificial / managed | Dominant layer: Herbaceous
4. Water — Water regime: Terrestrial | Water seasonality: | Water quality:
5. Tree layer — Tree cover: <10% | Tree height: 05-15m | Leaf type Tree: Broadleaved | Phenology Tree: Deciduous
6. Shrub layer — Shrub cover: 05-10% | Shrub height: 1-3m | Leaf type Shrub: Broadleaved | Phenology shrub: Deciduous
7. Grass layer / Bare soil — Grass cover: 40-70% | Grass height: 0.3-1m | Grass phenology: Undetermined | Bare soil:
8. Agriculture — Agriculture cycle: Annual | Agriculture water: Rainfed | Agriculture intensity: Permanent high intensity | Spatial pattern: Continuous fields
9. Additionnal Information — Common name (english): agriculture | Local name (local language): agricultura | Additionnal information:

Registro: 193 de 380

ies Institute for Environment and Sustainability

EUROPEAN COMMISSION
DIRECTORATE-GENERAL
Joint Research Centre

Example in South America (Forest + Agriculture)

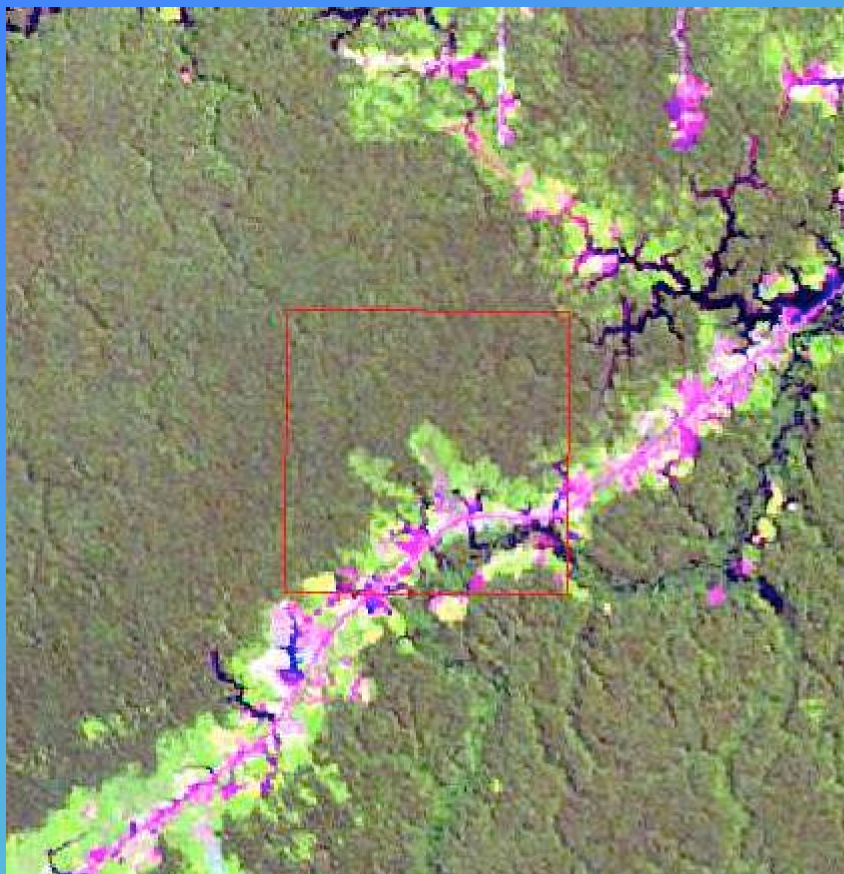

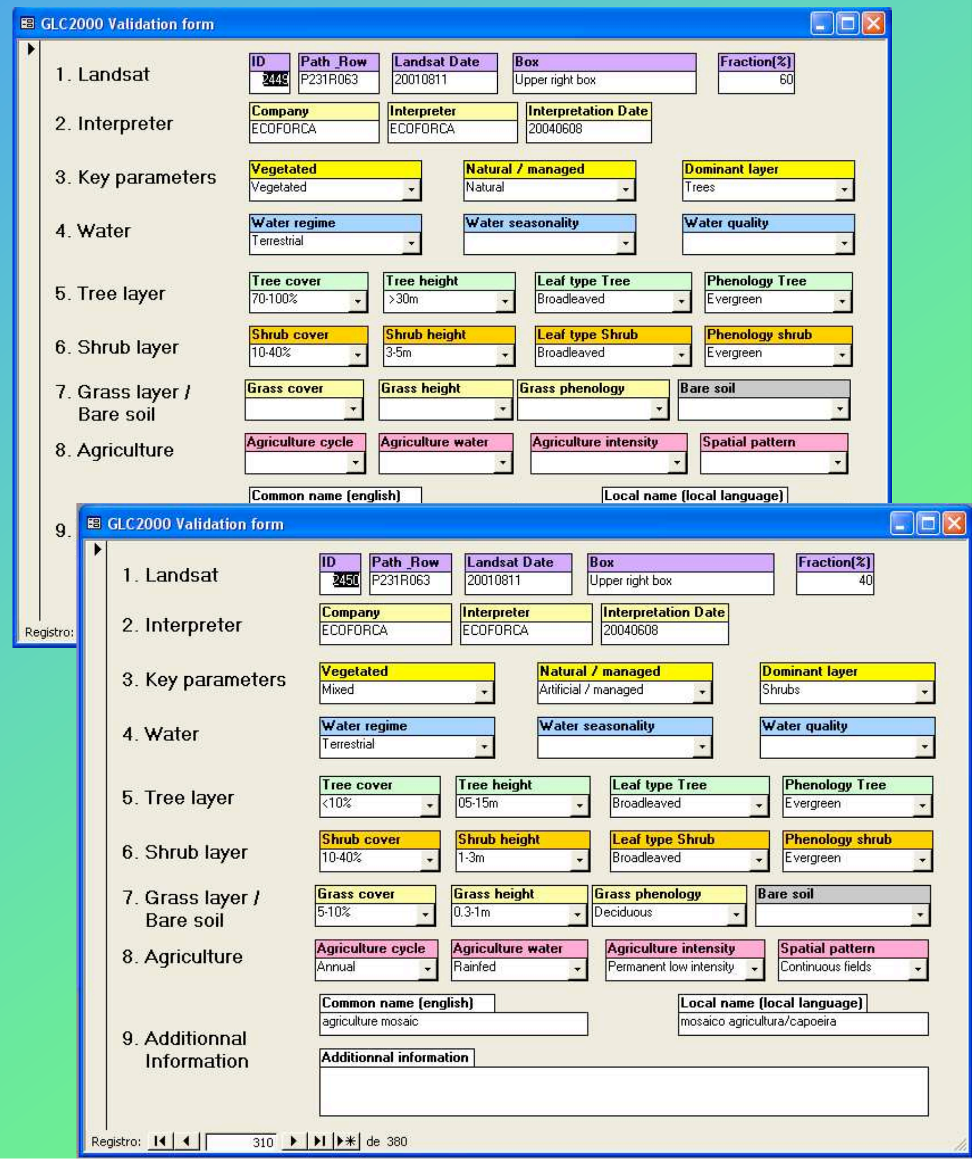
GLC2000 Validation form

1. Landsat	ID: 2449	Path_Row: P231R063	Landsat Date: 20010811	Box: Upper right box	Fraction(%): 60
2. Interpreter	Company: ECOFORCA	Interpreter: ECOFORCA	Interpretation Date: 20040608		
3. Key parameters	Vegetated: Vegetated	Natural / managed: Natural	Dominant layer: Trees		
4. Water	Water regime: Terrestrial	Water seasonality:	Water quality:		
5. Tree layer	Tree cover: 70-100%	Tree height: >30m	Leaf type Tree: Broadleaved	Phenology Tree: Evergreen	
6. Shrub layer	Shrub cover: 10-40%	Shrub height: 3-5m	Leaf type Shrub: Broadleaved	Phenology shrub: Evergreen	
7. Grass layer / Bare soil	Grass cover:	Grass height:	Grass phenology:	Bare soil:	
8. Agriculture	Agriculture cycle:	Agriculture water:	Agriculture intensity:	Spatial pattern:	
9.	Common name (english)	Local name (local language)			

Registro:

GLC2000 Validation form

1. Landsat	ID: 2450	Path_Row: P231R063	Landsat Date: 20010811	Box: Upper right box	Fraction(%): 40
2. Interpreter	Company: ECOFORCA	Interpreter: ECOFORCA	Interpretation Date: 20040608		
3. Key parameters	Vegetated: Mixed	Natural / managed: Artificial / managed	Dominant layer: Shrubs		
4. Water	Water regime: Terrestrial	Water seasonality:	Water quality:		
5. Tree layer	Tree cover: <10%	Tree height: 05-15m	Leaf type Tree: Broadleaved	Phenology Tree: Evergreen	
6. Shrub layer	Shrub cover: 10-40%	Shrub height: 1-3m	Leaf type Shrub: Broadleaved	Phenology shrub: Evergreen	
7. Grass layer / Bare soil	Grass cover: 5-10%	Grass height: 0.3-1m	Grass phenology: Deciduous	Bare soil:	
8. Agriculture	Agriculture cycle: Annual	Agriculture water: Rainfed	Agriculture intensity: Permanent low intensity	Spatial pattern: Continuous fields	
9. Additionnal Information	Common name (english): agriculture mosaic	Local name (local language): mosaico agricultura/capoeira	Additionnal information:		

Registro: 310 de 380

EUROPEAN COMMISSION
DIRECTORATE-GENERAL
Joint Research Centre

Contingency Matrix

	GLC 2000 (Map samples																						
	Tree Cover, broadleaved, evergreen	Tree Cover, broadleaved, deciduous, dense	Tree Cover, broadleaved, deciduous, open	Tree Cover, needle-leaved, evergreen	Tree Cover, needle-leaved, deciduous, open	Tree Cover, mixed leaf type	Tree Cover, regularly flooded, fresh	Tree Cover, regularly flooded, saline	Tree cover / Other natural vegetation	Shrub Cover, closed-open, evergreen	Shrub Cover, closed-open, deciduous	Herbaceous Cover, closed-open	Sparse Herbaceous or sparse shrub cover	Regularly flooded shrub and/or herbaceous cover	Cultivated and managed areas	Cropland / Tree Cover / Other natural vegetation	Cropland / Shrub and/or grass cover	Bare Areas	Water Bodies (natural & artificial)	Snow and Ice (natural & artificial)	Artificial surfaces and associated areas	Total	Producer's accuracy
Tree Cover, broadleaved, evergreen	**62.0**		0.8	1.1					1.1							1.1						66.0	**0.94**
Tree Cover, broadleaved, deciduous, dense		**11.6**										0.4										12.0	**0.96**
Tree Cover, broadleaved, deciduous, open	2.1	6.2	**2.1**						2.3		1.1											13.8	**0.15**
Tree Cover, needle-leaved, evergreen		1.5		**19.3**																		20.9	**0.93**
Tree Cover, needle-leaved, deciduous, open				1.1	**2.1**																	3.2	**0.67**
Tree Cover, mixed leaf type	0.8	5.5		12.3	1.1	**12.5**				0.4	1.1											33.7	**0.37**
Tree Cover, regularly flooded, fresh	3.0			0.8			**1.5**															5.3	**0.29**
Tree Cover, regularly flooded, saline	1.1							**1.1**														2.1	**0.50**
Tree cover / Other natural vegetation									**1.5**						1.1							2.6	**0.59**
Shrub Cover, closed-open, evergreen	1.1								1.1		3.9	1.5	5.0		1.8							14.4	**-**
Shrub Cover, closed-open, deciduous		2.6	5.8	0.8					3.0		**12.1**	9.1	10.6	1.1	2.1			0.4				47.5	**0.26**
Herbaceous Cover, closed-open		1.1	0.8						2.3		4.9	**12.4**			2.1		3.4					26.9	**0.46**
Sparse Herbaceous or sparse shrub cover											1.5	6.9	**20.1**		1.5			2.4				32.4	**0.62**
Regularly flooded shrub and/or herbaceous cover	1.1	2.1		1.1								0.4		**3.7**	0.8		1.1					10.2	**0.36**
Cultivated and managed areas				1.2								5.6	0.8		**49.1**	1.1	2.3	3.0	1.1			64.0	**0.77**
Cropland / Tree Cover / Other vegetation	2.1	1.1	1.1	2.6		0.8									4.3	**9.7**	1.8	1.5				25.0	**0.39**
Cropland / Shrub and/or grass cover		1.1									1.1				3.4							5.5	**-**
Bare Areas												0.8	3.3		1.1		0.4	**111.0**				116.6	**0.95**
Water Bodies (natural & artificial)																			**39.2**			39.2	**1.00**
Snow and Ice (natural & artificial)																				**2.0**		2.0	**-**
Artificial surfaces and associated areas				0.8																		0.8	**-**
Total	73.3	32.8	10.5	41.0	3.2	13.3	1.5	1.1	11.2	0.4	25.6	37.1	39.7	4.7	67.2	11.9	9.0	118.4	40.3	2.0	0.0	544.0	
User's accuracy	**0.85**	**0.35**	**0.20**	**0.47**	**0.67**	**0.94**	**1.00**	**1.00**	**0.14**	**-**	**0.47**	**0.33**	**0.51**	**0.77**	**0.73**	**0.82**	**-**	**0.94**	**0.97**	**1.00**	**-**	372.96	**68.6%**

Overall accuracy = 68.6 %
(Blocks with >80% in one land cover type)

Institute for Environment and Sustainability

Distance Calculated from LCCS

EUROPEAN COMMISSION
DIRECTORATE-GENERAL
Joint Research Centre

Distance in %

LANDSAT_LC1LC2	Tree Cover, broadleaved, evergreen	Tree Cover, broadleaved, deciduous, dense	Tree Cover, broadleaved, deciduous, open	Tree Cover, needle-leaved, evergreen	Tree Cover, needle-leaved, deciduous, open	Tree Cover, mixed leaf type	Tree Cover, regularly flooded, fresh	Tree Cover, regularly flooded, saline	Mosaic: Tree cover / Other natural vegetation	Shrub Cover, closed-open, evergreen	Shrub Cover, closed-open, deciduous	Herbaceous Cover, closed-open	Sparse Herbaceous or sparse shrub cover	Regularly flooded shrub and/or herbaceous cover	Cultivated and managed areas	Mosaic: Cropland / Tree Cover / Other natural vegetation	Mosaic: Cropland / Shrub and/or grass cover	Bare Areas	Water Bodies (natural & artificial)	Snow and Ice (natural & artificial)
Tree Cover, broadleaved, evergreen	**0.00**	0.25	0.25	0.25	0.50	0.25	0.38	0.25	0.31	0.19	0.44	0.41	0.49	0.56	0.49	0.19	0.44	0.75	1.00	1.00
Tree Cover, broadleaved, deciduous, closed	0.25	**0.00**	0.00	0.50	0.25	0.25	0.50	0.50	0.31	0.44	0.19	0.29	0.24	0.69	0.49	0.31	0.31	0.75	1.00	1.00
Tree Cover, broadleaved, deciduous, open	0.25	0.00	**0.00**	0.50	0.25	0.25	0.50	0.50	0.31	0.44	0.19	0.29	0.24	0.69	0.49	0.31	0.31	0.75	1.00	1.00
Tree Cover, needle-leaved, evergreen	0.25	0.50	0.50	**0.00**	0.25	0.25	0.50	0.50	0.31	0.31	0.56	0.66	0.74	0.69	0.69	0.31	0.56	0.75	1.00	1.00
Tree Cover, needle-leaved, deciduous	0.50	0.25	0.25	0.25	**0.00**	0.25	0.63	0.75	0.31	0.56	0.31	0.54	0.49	0.81	0.69	0.44	0.44	0.75	1.00	1.00
Tree Cover, mixed leaf type	0.25	0.25	0.25	0.25	0.25	**0.00**	0.38	0.50	0.06	0.31	0.31	0.41	0.49	0.56	0.46	0.19	0.31	0.75	1.00	1.00
Tree Cover, regularly flooded, fresh	0.38	0.50	0.50	0.50	0.63	0.38	**0.00**	0.13	0.44	0.44	0.56	0.66	0.74	0.19	0.48	0.31	0.56	1.00	0.75	1.00
Tree Cover, regularly flooded, saline	0.25	0.50	0.50	0.50	0.75	0.50	0.13	**0.00**	0.56	0.44	0.69	0.66	0.74	0.31	0.46	0.44	0.69	1.00	0.75	1.00
Mosaic: Tree cover / Other natural vegetation	0.31	0.31	0.31	0.31	0.31	0.06	0.44	0.56	**0.00**	0.31	0.31	0.35	0.43	0.50	0.40	0.38	0.50	0.75	1.00	1.00
Shrub Cover, closed-open, evergreen	0.19	0.44	0.44	0.31	0.56	0.31	0.44	0.44	0.31	**0.00**	0.25	0.35	0.43	0.38	0.41	0.38	0.50	0.75	1.00	1.00
Shrub Cover, closed-open, deciduous	0.44	0.19	0.19	0.56	0.31	0.31	0.56	0.69	0.31	0.25	**0.00**	0.23	0.18	0.50	0.41	0.50	0.38	0.63	1.00	1.00
Herbaceous Cover, closed-open	0.41	0.29	0.29	0.66	0.54	0.41	0.66	0.66	0.35	0.35	0.23	**0.00**	0.08	0.48	0.25	0.60	0.35	0.56	1.00	1.00
Sparse Herbaceous or sparse shrub cover	0.49	0.24	0.24	0.74	0.49	0.49	0.74	0.74	0.43	0.43	0.18	0.08	**0.00**	0.55	0.33	0.68	0.43	0.50	1.00	1.00
Regularly flooded shrub and/or herbaceous cover	0.56	0.69	0.69	0.69	0.81	0.56	0.19	0.31	0.50	0.38	0.50	0.48	0.55	**0.00**	0.28	0.38	0.38	0.83	0.75	1.00
Cultivated and managed areas	0.49	0.49	0.49	0.69	0.69	0.46	0.48	0.46	0.40	0.41	0.41	0.25	0.33	0.28	**0.00**	0.38	0.25	0.83	0.88	0.88
Mosaic: Cropland / Tree Cover / Other natural vegetation	0.19	0.31	0.31	0.31	0.44	0.19	0.31	0.44	0.38	0.38	0.50	0.60	0.68	0.38	0.38	**0.00**	0.25	0.74	1.00	1.00
Mosaic: Cropland / Shrub and/or grass cover	0.44	0.31	0.31	0.56	0.44	0.31	0.56	0.69	0.50	0.50	0.38	0.35	0.43	0.38	0.25	0.25	**0.00**	0.70	1.00	1.00
Bare Areas	0.75	0.75	0.75	0.75	0.75	0.75	1.00	1.00	0.75	0.75	0.63	0.56	0.50	0.83	0.83	0.74	0.70	**0.00**	0.50	0.50
Water Bodies (natural & artificial)	1.00	1.00	1.00	1.00	1.00	1.00	0.75	0.75	1.00	1.00	1.00	1.00	1.00	0.75	0.88	1.00	1.00	0.50	**0.00**	0.25
Snow and Ice (natural & artificial)	1.00	1.00	1.00	1.00	1.00	1.00	1.00	1.00	1.00	1.00	1.00	1.00	1.00	1.00	0.88	1.00	1.00	0.50	0.25	**0.00**
Artificial surfaces and associated areas	1.00	1.00	1.00	1.00	1.00	1.00	1.00	1.00	1.00	1.00	1.00	1.00	0.98	1.00	1.00	0.99	1.00	0.25	0.50	0.50

Based on 4 attributes: aquatic/terrestrial; life form; phenology; leaf type

Institute for Environment and Sustainability

Adjusted Accuracies

- From the producer's perspective
  - Accuracy based on the 4 most efficient classifiers: 90.3%
  - 22% of the errors can be explained by a confusion in the legend (overlap, absence of explicit criteria…)
- From the user's perspective
  - Based on carbon in the plants : 76.3 %
  - Carbon in plants and soil : 76.6 %
  - Net Primary Productivity : 74.4 %

Validation of the
MODIS 2001 V4 Land Cover Product

Mark Friedl and Alan Strahler
Boston University

Dual Approach to Validation

- ***Use of Confidence Values from Classifier***
  - **Values are probabilities a pixel belongs to a class given the training data provided**
  - **Allows mapping of spatial pattern of confidence**
- ***Use of Unseen Training Sites***
  - **Hold back 10 percent of sites, train with remainder, repeat 10 times for all sites**

Relation Between Confidence and Class Accuracy

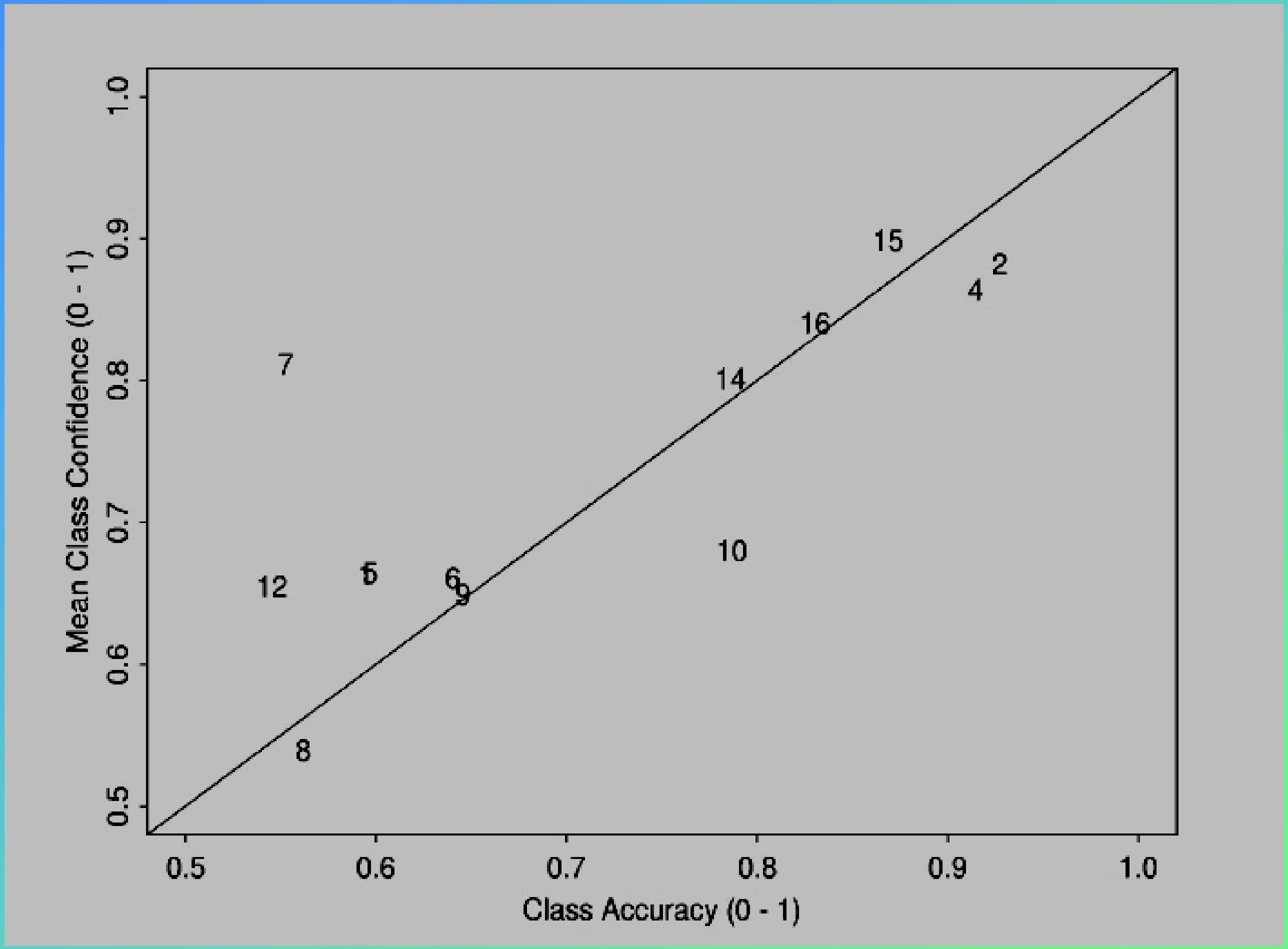

(from AVHRR prototype of North America)

Consistent Year Land Cover Product, Nov 00–Oct 01

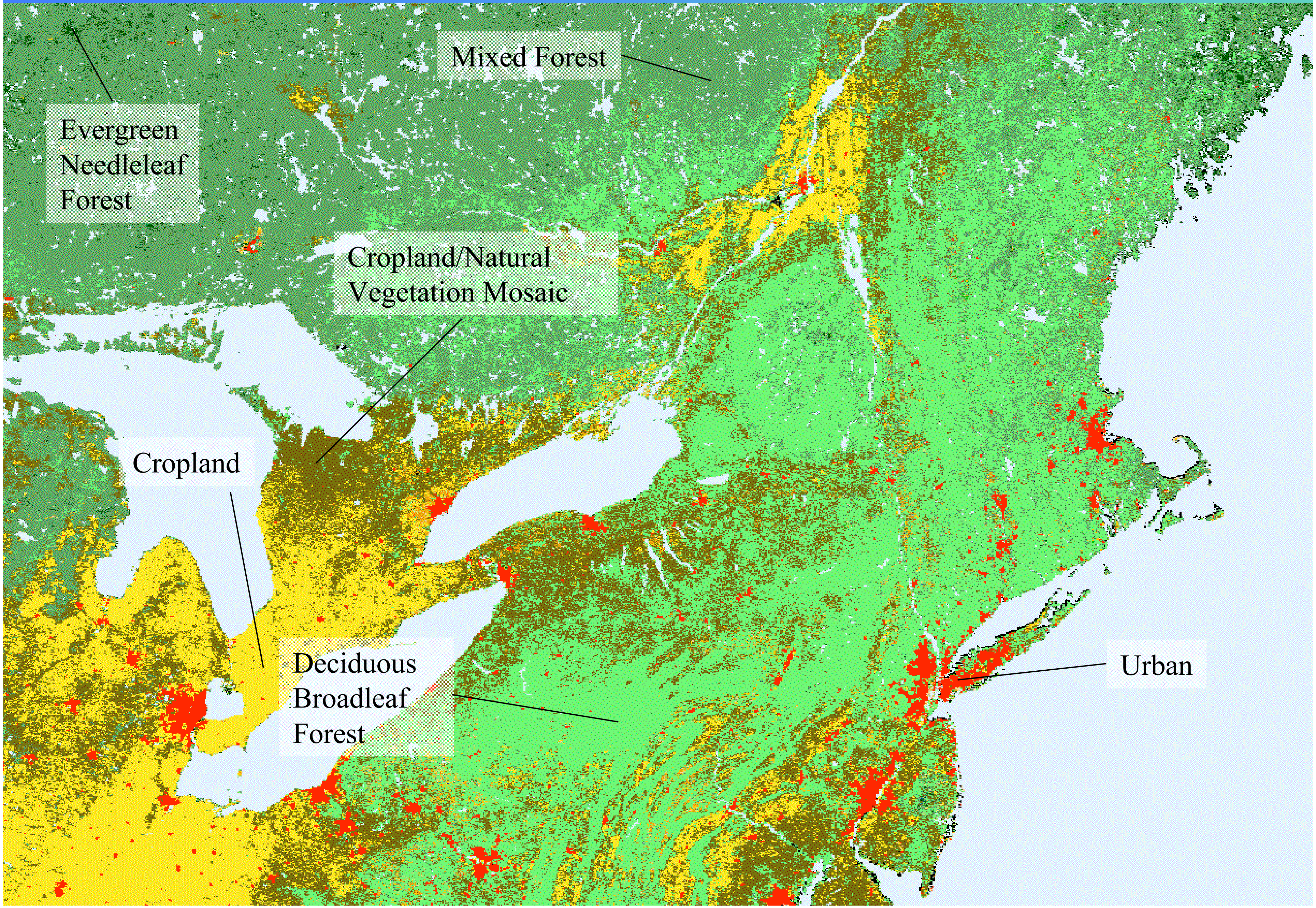

Classification Confidence Map

Second Most-Likely Class

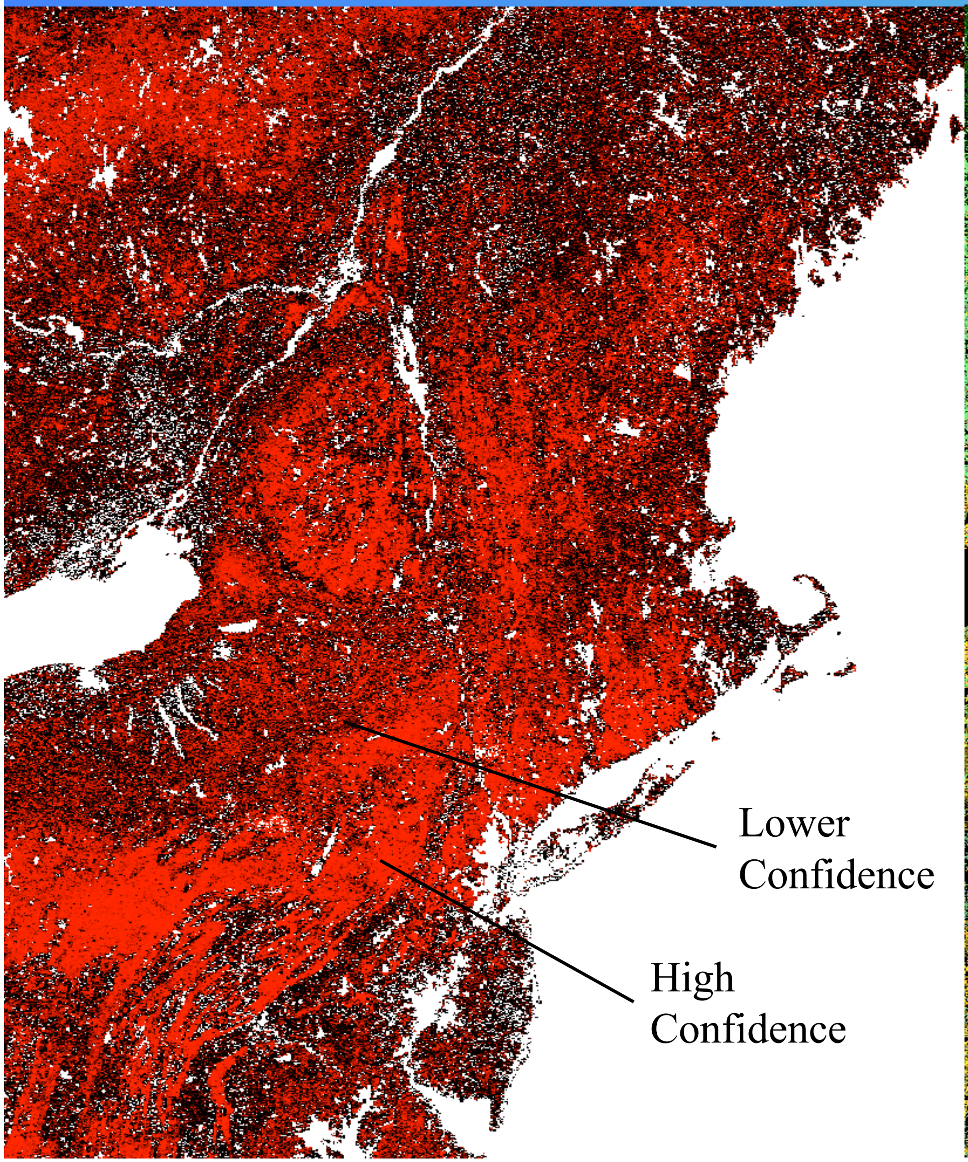

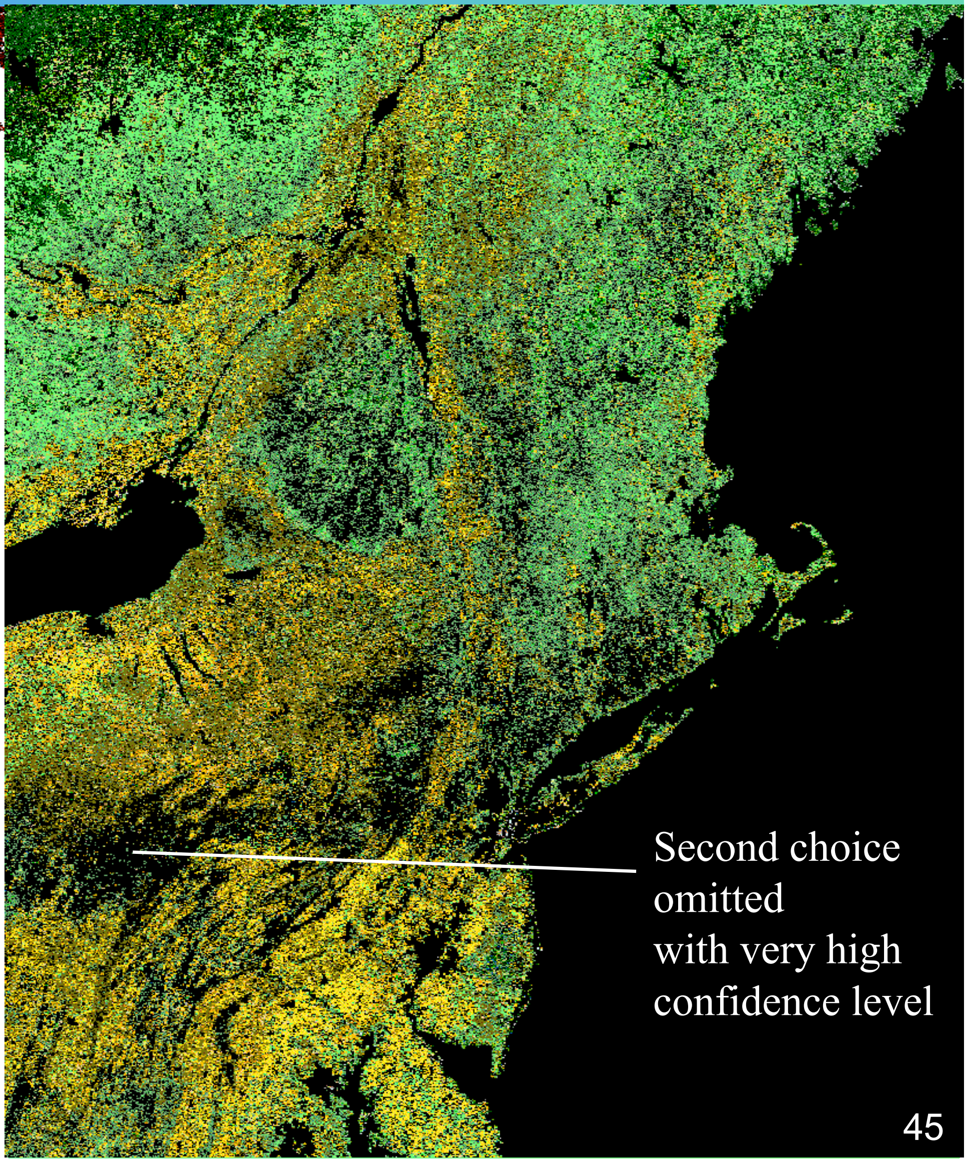

Cross Validation with Training Sites

- *Cross-Validation Procedure*
  - Hide 10 percent of training sites, classify with remaining 90 percent; repeat ten times for ten unique sets of all sites
  - Provides "confusion matrix" based on unseen pixels where whole training site is unseen
  - NOT a stratified random sample, but a useful indication of global and within-class accuracies

Confusion Matrix

Site Class	Class Name	Classification Outcome																
		1	2	3	4	5	6	7	8	9	10	11	12	14	15	16	17	Total
1	Evergreen Needleleaf	1446	10	19	3	180	27	8	86	0	4	517	5	31	6	0	0	2342
2	Evergreen Broadleaf	38	4852	0	15	6	11	4	80	17	22	1629	150	163	38	1	1	7027
3	Deciduous Needleleaf	81	0	439	0	14	0	0	2	1	0	24	0	2	0	0	0	563
4	Deciduous Broadleaf	9	6	2	614	149	2	40	14	4	9	66	36	136	0	15	0	1102
5	Mixed Forest	507	10	169	215	1171	6	7	78	3	6	226	15	76	17	8	0	2514
6	Closed Shrubland	10	2	0	5	1	277	44	18	2	7	63	23	5	0	11	0	468
7	Open Shrubland	22	23	7	3	2	246	1946	108	52	446	59	276	32	52	420	50	3744
8	Woody Savanna	108	174	9	100	70	78	72	867	352	34	362	239	174	2	9	9	2659
9	Savanna	4	21	0	98	2	50	44	322	742	247	211	608	296	13	5	0	2663
10	Grasslands	9	29	0	32	8	92	214	43	107	1196	72	412	130	19	92	1	2456
11	Pmnt Wtlnd	0	3	0	0	2	0	0	0	0	1	1138	46	4	17	18	11	1240
12	Cropland	2	16	1	10	31	37	27	34	30	71	19	5872	306	2	7	0	6465
14	Cropland/Natural Vegn	1	2	0	4	2	1	0	10	23	11	35	352	453	0	5	0	899
15	Snow+ice	0	0	0	0	0	0	0	0	0	0	0	0	0	1250	0	0	1250
16	Barren	2	0	0	0	0	17	201	13	4	27	5	20	2	129	4097	1	4518
17	Water	0	0	0	0	0	0	1	0	0	0	32	0	0	112	0	7756	7901
	Total	2239	5148	646	1099	1638	844	2608	1675	1337	2081	4458	8054	1810	1657	4688	7829	47811

Overall Accuracy: 70.3 ± 2.4% (65.6%, 75.0%)

Per-Class Accuracies

Table 5. Global per-class accuracies, 2001 V4 land cover product (percent)								
IGBP Land Cover Class	Producer's Accuracy				User's Accuracy			
	Est.	Std. Err.	CI -	CI +	Est.	Std. Err.	CI -	CI +
1. Evergreen Needleleaf	64.6	3.9	56.9	72.3	60.2	5.2	52.6	67.9
2. Evergreen Broadleaf	94.3	1.4	91.4	97.1	69.0	34.1	66.2	71.9
3. Deciduous Needleleaf	68.0	7.5	53.3	82.7	77.8	0.5	63.1	92.5
4. Deciduous Broadleaf	55.9	5.7	44.6	67.1	54.2	2.1	43.0	65.4
5. Mixed Forest	71.5	3.6	64.4	78.5	45.8	6.1	38.8	52.9
6. Closed Shrubland	32.8	6.2	20.7	44.9	53.9	0.4	41.8	66.0
7. Open Shrubland	74.6	4.5	65.9	83.4	50.0	17.1	41.2	58.7
8. Woody Savanna	51.8	5.3	41.3	62.2	32.2	6.8	21.8	42.6
9. Savanna	55.5	4.2	47.2	63.8	27.5	6.0	19.3	35.8
10. Grasslands	57.5	5.2	47.2	67.7	47.1	5.9	36.8	57.4
11. Permanent Wetlands	25.5	2.7	20.2	30.8	91.8	0.9	86.5	97.1
12. Cropland	72.9	2.7	67.6	78.2	88.8	14.7	83.5	94.2
14. Cropland/Nat Veg Mosaic	25.0	3.3	18.6	31.5	49.8	0.9	43.4	56.3
15. Snow and Ice	75.4	10.9	54.1	96.7	100.0	0.0	78.7	121.3
16. Barren/Sparse	87.4	2.3	82.8	92.0	88.7	10.1	84.2	93.3
17. Water	99.1	0.8	97.6	100.6	98.1	12.4	96.6	99.6

Confidence Values by Land Cover Type

Table 6. Global confidence values by land cover class (percent)	
IGBP Land Cover Class	Average Confidence Value
1. Evergreen Needleleaf	68.3
2. Evergreen Broadleaf	89.3
3. Deciduous Needleleaf	66.7
4. Deciduous Broadleaf	65.9
5. Mixed Forest	65.4
6. Closed Shrubland	60.0
7. Open Shrubland	75.3
8. Woody Savanna	64.0
9. Savanna	67.8
10. Grasslands	70.6
11. Permanent Wetlands	52.3
12. Cropland	76.4
14. Cropland/Natural Veg	60.7
15. Snow and Ice	87.2
16. Barren	90.0
17. Water	(Not Available)
Average Value, All Classes	70.7
Area-Weighted Average (Table 5)	78.3

(Example based on Version 3 data)

Overall Accuracies

- *Proper accuracy statements require proper statistical sampling*
- *AVHRR state of the art has been around 60 percent, depending on class and region*
- *SPOT-Vegetation has been around 65 percent (GLC2000)*
- *MODIS accuracies are around 70 percent*
- *Most “mistakes” are between similar classes*

Conclusions

- Training sites are NOT a random sample
  - Many (perhaps most) training sites are placed in equivocal areas where the classifier needs new and better examples
  - Thus, the training sites do not represent well the broad regions of core areas for land cover classes
  - This leads to the conclusion that actual accuracies are probably better than observed from the training sites
  - So we estimate that:

GLOBAL ACCURACY IS 75–80 PERCENT

PER-CLASS ACCURACIES RANGE 60–90 PERCENT

CONTINENTAL REGION ACCURACIES RANGE 70–85 PERCENT

Report Recommendations

- **All global land cover maps should have statistically valid estimates of map accuracy**
- **Core methods to be routinely applied include :**
  - Design-based inference
  - Probability sampling
  - Consistent estimators
- **Core methods may be extended to include:**
  - Validation both during and after map production
  - Use of confidence-based quality assessments
  - Addition of fuzzy accuracy methods
  - Use of qualitative and descriptive methods

Areas of Future Research

- Standardization of legends and mapping units
- Methods for validation of more continuous measures of land cover
- Effect of spatial aggregation on accuracy estimates
- Reuse of existing validation samples
- Linkages between spatially-distributed confidence metrics and design-based sampling methods
- Effects of misregistration, mixed pixels, and sensor point spread function
- Integrating error in reference data
- Error magnitude effects
- Better understanding of users’ needs
- Defining priorities for future research

12th CEReS International Symposium on Remote Sensing

13-14 December 2005 - Chiba University.

Necessary paths for developing harmonized global land use classification systems

Christophe Duhamel

One guiding idea

Land use has a cumbersome neighbour: land cover…

but systematic and pragmatic ways for improving the availability of land use data sets should be applied

Introduction 1

Land use information is of significant value but:

- paucity of global data sets that contain land use information
- Variable quality of available information
- confused mixture of land use and land cover categories.
- often inadequate for studies that focus on the collection of aspects of land use and on context related socio-economic data.

Introduction 2

Development of information systems on land use has increased but:

- although many initiatives launched in order to improve the availability and the quality of land use information the result is extremely scarce and discouraging

This is resulting from

- a lack of consciousness on the importance to build a sound theoretical framework together with a careful analysis of user's requirements
- may be also from evidence: land use data is difficult to collect into global data sets

Introduction 3

In terms of harmonization of data sets, one element is fundamental :

the question of classification.

- not built in order to create an aesthetic effect
- close links between the development of scientific concepts and classifications
- classification systems as mirrors of the conceptualization of the domain to be investigated.

Specific objectives of the presentation

Discussing the necessary prerequisites for classifications for land use which would:

- answer user's requirements
- take into account capabilities of available data collection tools
- through an appropriate theoretical framework

Guiding principle for structuring land use information : following the general concepts of classification systems

- the demarcation of a universe of discourse (what is land use)
- the establishment of a classification of all land use objects in this universe
- a system for naming the groups linked to the structure
- the procedures for allocating any land use object to one established group.

What is land use (1)

The demarcation of the domain of investigation

Any given portion of Earth's surface can be observed and described in various ways

When observing a portion of Earth's surface, several questions may arise:

- **what is this**
- **what is it for**
- why and how is it like this
- was it like this before
- will it stay like this in the future etc…?

What is land use (2)

The demarcation of the domain of investigation

Starting with land cover: a physical description of land

- with a definition: *the observed physical cover of the earth's surface*

    - biophysical categories: areas of vegetation
    - bare soil and hard surfaces (rocks, buildings)
    - wet areas/bodies of water

In most cases, land cover is directly detectable by human observation or less directly from remote sensing.

What is land use (2)

The demarcation of the domain of investigation

For land use

Two main approaches:

functional approach (the one referred as land use here)

- corresponds to *the description of land in terms of its* ***socio-economic purpose*** (agricultural, residential, forestry etc...)
- easy to handle since it has direct correspondences into widely utilized statistical nomenclatures.

sequential approach developed for agricultural purposes: *a series of operations on land, carried out by humans, with the intention to obtain products and/or benefits through using land resources.*

,

What is land use (3)

The demarcation of the domain of investigation

Distinguishing between land cover and land use is easy but….

– **not often reflected into the existing systems.**

– **two major issues to be dealt with is that land cover and land use are often intertwined and that objects may be mixed**

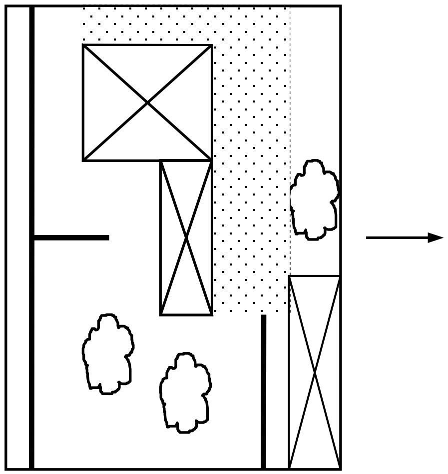

Land Cover :
Tile roofs, Lawns, Trees, Tarmac roads, Bare soil

Land Use:
Residential

What is land use (4)

The demarcation of the domain of investigation

Some additional prerequisites before classifying

Specific constraints due to the intrinsic nature of geographic data:

- **spatial consistency** (classification systems should be designed in a way to allow compatibility of results between various geographical locations),

- **temporal consistency** (observation at time of observation , no classes on previous or future land uses).

- ensure the **independence of the system from the data collection tools** (a lot of systems have been built on the basis of the technical capacities of the tools, e.g. remote sensing)

Classifying the land use objects (1)

Classification:

the organisation of sub-classes of a domain through a (hierarchical) series of nested categories that have been arranged to show relationships to one another.

Groups of land use objects have therefore to be described through:

- the selection of shared characteristics that make the members of each group similar to one another and unlike members of other groups

Any proposed land use classification system is conceptual

- describing selected aspects of the real world
- the same reality described according to several classifications
- it simply depends of the purpose of the classification.

Classifying the land use objects (2)

The purpose for which the classification is designed necessarily shapes its structure and content

- this is why each user, in general, builds an individual classification adapted to specific needs

- spontaneous development of classifications therefore leads inevitably to incompatibility: this is frequent for land use classifications.

Classifying the land use objects (3)

Two approaches for building land use classifications

A classical theory where land use objects are allocated according to a set of individually necessary and jointly sufficient properties.

- Top-down approach:
  - many nomenclatures are built following this a-priori approach
  - the domain of study is divided into categories and sub-categories
  - Strong disadvantage: the rigid structure

- Classifiers approaches
  - a tool consisting of a combinatory system applied on a common basis.
  - the basis is just a set of necessary characteristics to describe the objects.
  - the characteristics allow, through combinations, the definition of the objects and the grouping of the objects for all possible systems.

The prototype theory: prototypes brought from pre-existing classifications and setting-up the beginning of main categories

A system for naming the groups (1)

Six main basic components:

- principle of completeness
- absence of overlap
- general rules of interpretation
  - cases of overlap, ontological or logical relations between objects, problems of mixtures)
- rules concerning the elaboration of headings and labels
  - kernel method of description, definitions by extension and intension, boundaries problems, cross-references of exclusions and inclusions)
- elaboration of index of objects
- principles of coding

.

A system for naming the groups (2)
An example: LUCAS system

D01 Shrubland with sparse tree cover

Areas dominated (more than 20% of the surface) by shrubs and low woody plants generally below 5 meters of height, including sparsely occurring trees within a limit of a tree-crown area density between 5 and 10 %

this class includes:

- Scrub land (pines, rhododendrons, maquis, matorral and deciduous thickets)
- Heathland with gorse, heather or broom

this class excludes:

- Shrubland where tree cover is more than 10% (C)
- Shrub like crops: orchards, vineyards in production (B7- B8))

Principles of observation

Extended window of observation

Links with Land Use (U)

D01 ➢ U11 Agricultural use: grazing
D01 ➢ U12 Forestry (Wood production)
D01 ➢ U36x Leisure areas
D01 ➢ U40 Wooded areas not utilized
D01 ➢ U50 Wetland.

Procedures of allocation of objects

Approaches directly linked with the types of classification system

Classifier approaches,

- classes through a predefined set of inherent traits utilizing for example a decision tree. objects are systematically matched with candidate

Top-down trees or prototypes

- the process is theoretically more empirical since the link between the object and the class is not direct
- this is why it is fundamental to have made available a textual part of the classification (in particular the definitions by intension and extension).
- And sometimes to have an index of objects (a good example of index may be found into the UK Land use database).

A first set of conclusions

Developing a land use classification system needs therefore to be **systematic**:

– the strict utilization of **appropriate framework**- ensures that dta sets will have a sufficient quality.

However two **pragmatic** issues remain to be dealt with:

- **the purpose of the classification**

user's needs have to be strongly reflected and existing classification and information systems should be taken into account.

- **the scarce opportunities to collect exhaustive data on land use on large areas**

Collecting global land use data (1)
A challenge…

Collecting with mapping approaches:

- The coverage of the territory is exhaustive.
- Main source of information is generally photo-interpretation or processing of aerial photographs and earth observation data together with ground truth.
- Choice of observation units is driven by technical constraints: the scale of observation and the scale of restitution of information
- No doubt that remote sensing data represent a data source which contributes to a deeper understanding of processes on the earth's surface and enables map production up to scales of 1:5.000.
- **But remote sensing images capture only land cover**, i.e. the physical features. Although one can interfere from some land cover categories to land use, remote sensing images are not really suitable for this aim.

Collecting global land use data (2)
A challenge…

Suitable alternative approaches to acquire land use data: area frame surveys.

- Statistical surveys provide information on samples from a population.
- Sampling theory is applied so that inference about the whole area can be made.
- The sample is made of a set of area units: the statistical units may be of different size (points, areas) or different shape (squares, circles).
- Possibility of being independent of the difficult problem of observation units: the population may be divided up into a grid on a systematic basis; each area unit thus obtained being a statistical unit (observation unit) of the same size and same shape.
- These approaches are commonly used in agricultural statistics and also widely applied in ecological monitoring surveys

A paradox as conclusion

- Increasing availability of land cover data sets but with low concrete impact on land use data availability
- Accurate and precise information on land use comes from statistical approaches where limited portions of earth can be observed

- How to do “reconciliation” or to have a mutual benefit from the two approaches?

- Is it worth to develop specific land use classifications for global data sets utilizing mapping approaches?

Harmonisation of land-use class sets to facilitate compatibility and comparability of data across space and time

12th CEReS International Symposium on Remote Sensing,
13-14 December 2005, Chiba, Japan

Louisa J.M. Jansen (E-mail: Louisa.Jansen@tin.it)

Introduction

- Introduction
- Definition of domain of interest
- Previous attempts
- Major parameters for harmonisation of class sets
- Basic unit of measurement
- Data quality
- Example of land-use harmonisation in Albania
- Conclusions and discussion

Introduction

- Both space and time dimensions are essential for making land-use data compatible and hence comparable.
- Harmonisation of land-use classifications includes harmonisation of land-use change.
- The data quality need to be analysed.

Harmonisation of class sets as presented here will address the semantic aspect of harmonisation, i.e. the class definitions because these imply the parameters used in the formation of classes.

Domain of interest

- Land use: "the type of human activity taking place at or near the surface" (Cihlar and Jansen, 2001).
- Classification: "the ordering or arrangement of objects into groups or sets on the basis of relationships. These relationships can be based upon observable or inferred properties" (Sokal, 1974).
- The key principles of classification are:
  - Completeness and absence of overlap of classes;
  - Existence of definitions and explanatory notes;
  - Existence of an index of objects;
  - Spatial and temporal consistency; and
  - Independence from scale and data collection tools.

- Data standardisation: "the use of a single standard basis for classification of a specific subject".

  Data standardisation will allow direct comparison of class sets but would disregard the financial and intellectual investments made in established methods and data sets.

- Data harmonisation: "the intercomparison of data collected or organised using different classifications dealing with the same subject matter" (McConnell and Moran, 2001).

  Data harmonisation will allow the continued use of existing data systems and classifications. However, if many class sets are involved the number of pair-wise class combinations becomes excessive because comparison of n data sets requires $n(n-1)/2$ comparisons to be made.

Previous attempts

- The United Nations Statistical Division - International Standard Classification of all Economic Activities (ISIC) published in 1948 with tmajor revisions in 1958, 1968 and 1989.
- The International Geographic Union - Commission on World Land-Use Survey in 1949 led to the creation of the Commission on Agricultural Typology (e.g., Types of Agriculture Map of Europe in 1983).
- The American Society of Planning Officials identified different land-use dimensions (1959).
- The Commission on Geographic Applications of Remote Sensing of the Association of American Geographers – the Anderson classification (1976).
- The Economic Commission for Europe of the United Nations - Standard International Classification of Land Use (1989).
- The Land-Based Classification Standards (LBCS) project, co-ordinated by the Research Department of the American Planning Association in corporation with several U.S. departments and agencies (1999).
- The improvement of the FAO Land Utilization Type (LUT) led to several studies analysed by Duhamel (1998).

Major parameters used

Main sector	Land-use characteristics			
	Function	Activity	Biophysical	Legal
Agriculture	x	x	x	
Fisheries	x	x	x	
Forestry	x	x	x	x
Economics	x	x		
Sociology	x	x		
Statistics	x	x	x	
Industry		x		x
Housing	x	x	x	x
Services		x		x

Based upon: World Land-Use Survey (IGU, 1976), Anderson (Anderson *et al*., 1976), ISIC 3rd revision (UN, 1989), Standard International Classification of Land Use (ECE-UN, 1989), NACE 1st revision (CEC, 1993), Central Product Classification (UN, 1998), FAOSTAT (FAO, 1998), Land-Based Classification Standard (APA, 1999) and http://home/att.net/~gklund/DEFpaper.htm.

- Just two parameters suffice: “function” and “activity”.
  - The function approach describes land uses in an economic context and is able to group land uses together that do not possess the same set of observable characteristics but serve the same purpose.
  - The activity approach describes what actually takes place on the land in physical or observable terms. Activity is defined as “*the combinations of actions that result in a certain type of product*” (UN, 1989).
- It is important to note that the function approach is independent of the activity approach: a variety of activities may serve a single function (e.g., both farm housing and farming activities serve agriculture).

Basic unit of measurement

- The cadastral parcel unit
  - The lowest-level unit of a cadastre that has a legal status.
  - Can be regrouped according to ownership, cadastral zone, administrative units, similar type of uses and socio-economic properties.
  - Level corresponds with decision making by landowner/landholder.
- The land-cover polygon
  - Remote sensing can be used as a tool for observation.
  - Too much emphasis on land cover embodies the risk not to capture socio-economic, institutional, cultural and legal aspects of land use.
  - Establishment of land-cover/land-use relationships that however may change with time.
- The statistical sample unit
  - Areas selected as being representative for a much larger area.
  - Example is the LUCAS methodology as applied in the EU.

Data quality

- Semantic harmonisation of class sets should consider the data quality aspect in a comprehensive manner and would need to address also the following two aspects that are still at the level of research:
  - A quantitative measure should be provided of the harmonisation result of a class. In existing examples, the impression is often given that class correspondence is 100%, whereas more often than not the result will be much lower.
  - A quantitative measure should be provided for the overall correspondence between two class sets similar to the overall accuracy calculated from the confusion matrix.

Example: Albania

- One of the aims of the EU Phare Land-Use Policy II project was to provide the Albanian government with an analysis of land-use change dynamics to better understand the past, monitor the current situation and to predict future trajectories in order to plan land uses and develop and implement appropriate policies.
- A standard hierarchical methodology for description of land use has been developed for Albania, the Land-Use Information System of Albania (LUISA):
  - Adopts the function and activity parameters for description;
  - Uses the cadastral parcel as basic unit of measurement;
  - The use of the cadastre as basis implies high data accuracy.
  - Has been developed in complete synergy by the subject-matter specialist and information technology specialist.

LUISA class set

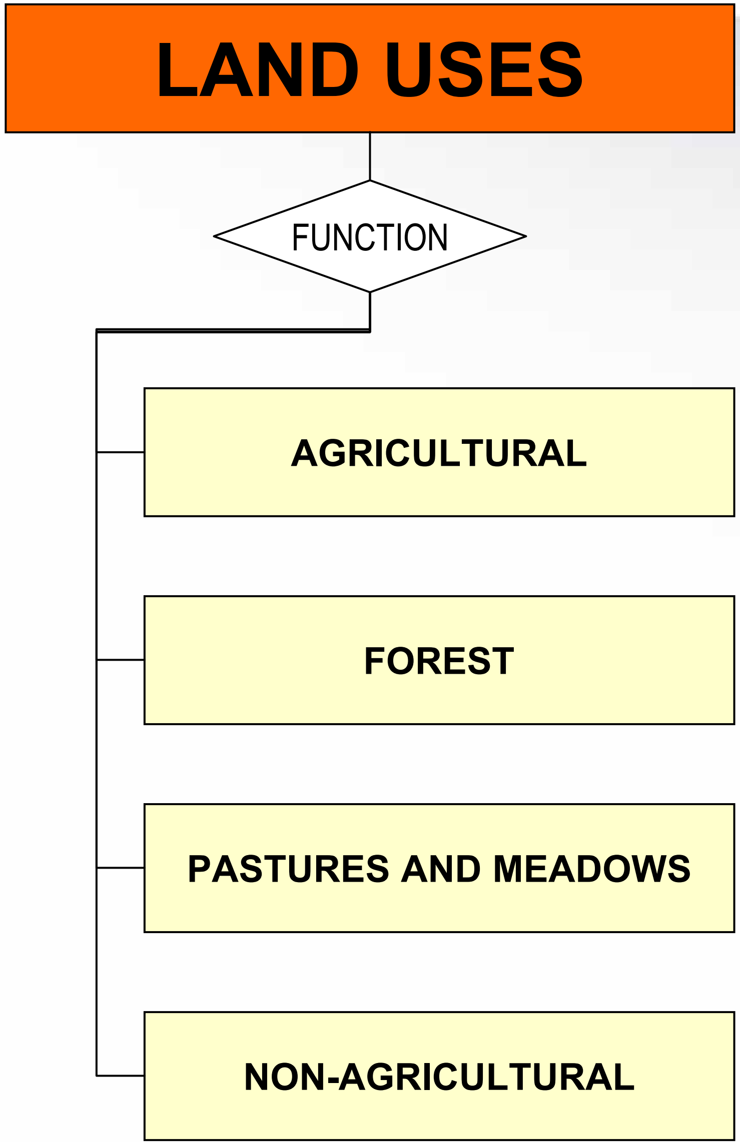

Land-use modifications occur within a land-use category and the degree of modification depends on the level of the class (see next slide). Land-use conversion occurs between land-use categories.
With the exceptions of the Non-agricultural land-use classes, where modifications occur within one group and conversions between groups.

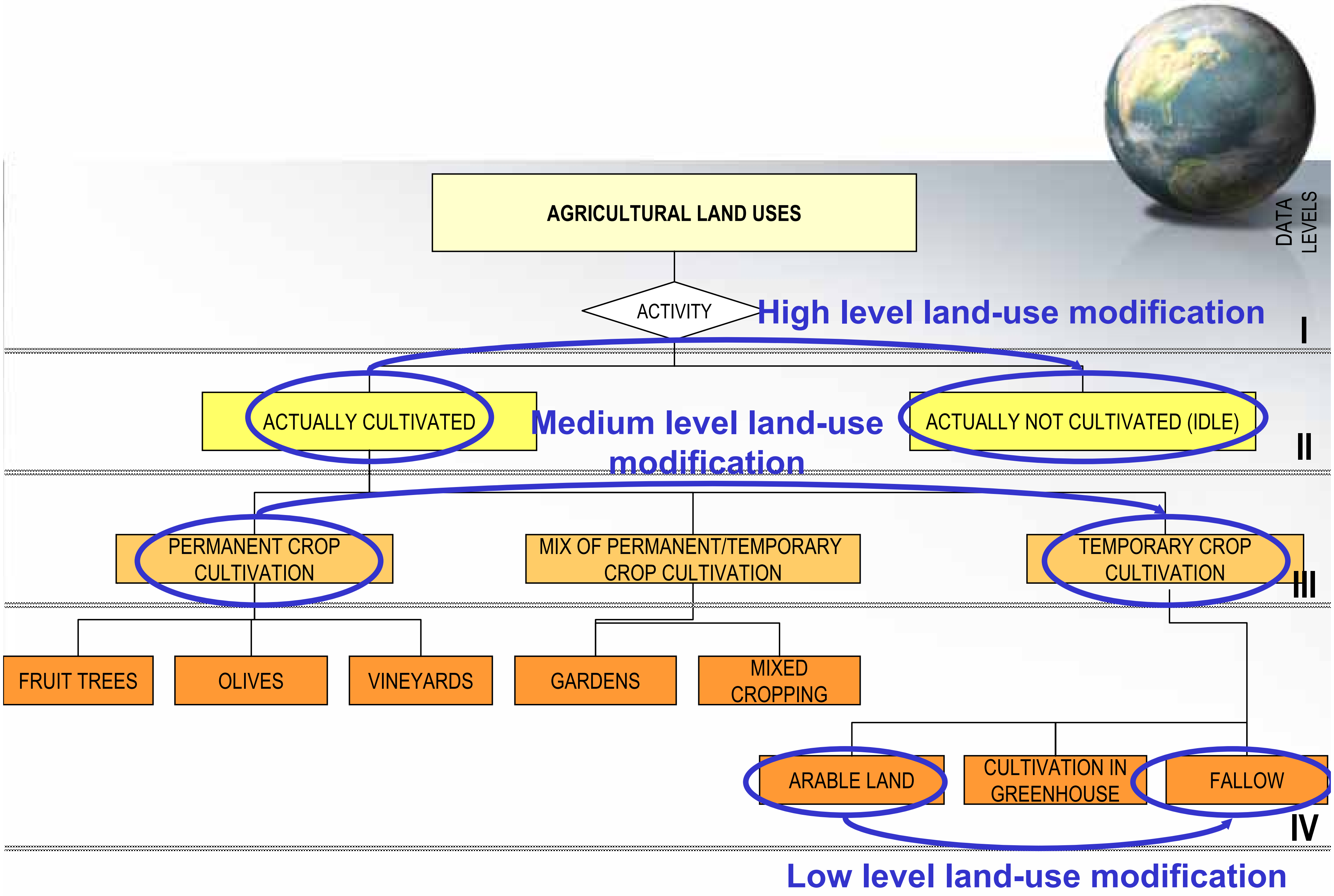
DATA LEVELS
AGRICULTURAL LAND USES
ACTIVITY
High level land-use modification
I
ACTUALLY CULTIVATED
Medium level land-use modification
ACTUALLY NOT CULTIVATED (IDLE)
II
PERMANENT CROP CULTIVATION
MIX OF PERMANENT/TEMPORARY CROP CULTIVATION
TEMPORARY CROP CULTIVATION
III
FRUIT TREES
OLIVES
VINEYARDS
GARDENS
MIXED CROPPING
ARABLE LAND
CULTIVATION IN GREENHOUSE
FALLOW
IV
Low level land-use modification

Available class sets

- In the context of the LUP II project, four data sets covering the period 1991-2003 (e.g., under socialist government, before and after privatisation) are important:

    1. Statistical data from the Institute of Statistics (INSTAT) comprising seven classes;
    2. Cadastral data from the Immovable Property Registration System (IPRS Kartela) comprising 41 classes (spatially explicit data);
    3. The commune data comprising 14 classes (spatially explicit data);
    4. The LUISA data comprising 48 classes where the most detailed levels of the hierarchy were used for land-use data collection (spatially explicit data).

Harmonisation at generic level

Legal categories	Land use classes	Class sets			
		INSTAT	IPRS Kartela	Commune	LUISA
Agricultural land uses	Used agricultural area	b	-	1	1, 2, 3, 4, 5, 6, 7
	Area with arable land crops	c, d	101, 102	1a	6, 7
	Area with permanent crops	f	116, 125, 128, 131, 148	1b, 1c, 1d	1, 2, 3, 4, 5
	Non utilised agricultural area	e	-	-	8, 9
Pastures & meadows	Grassland and pastures	g	108, 110, 153	2, 3a	51, 52, 53, 54, 55
Forests	Forests	h	118	3	31, 32, 33, 34, 35, 36, 37
Non agricultural land uses	Water bodies	-	107, 109, 111, 120, 138, 153	4a	131, 132, 133, 134, 135, 136, 137, 138
	Wetlands	-	336	-	81, 82
	Built up areas	-	100, 103, 106, 114, 121, 129, 130, 136, 144, 152, 213, 261, 332, 337, 338, 339, 340, 341, 342	4b, 4c, 4d, 4e	91, 92, 93, 94, 95,
	Barren	-	119, 135	4f	111, 112, 113, 114, 121, 122, 123, 124
	Mining/extraction	-	117, 343	-	61

Harmonisation process

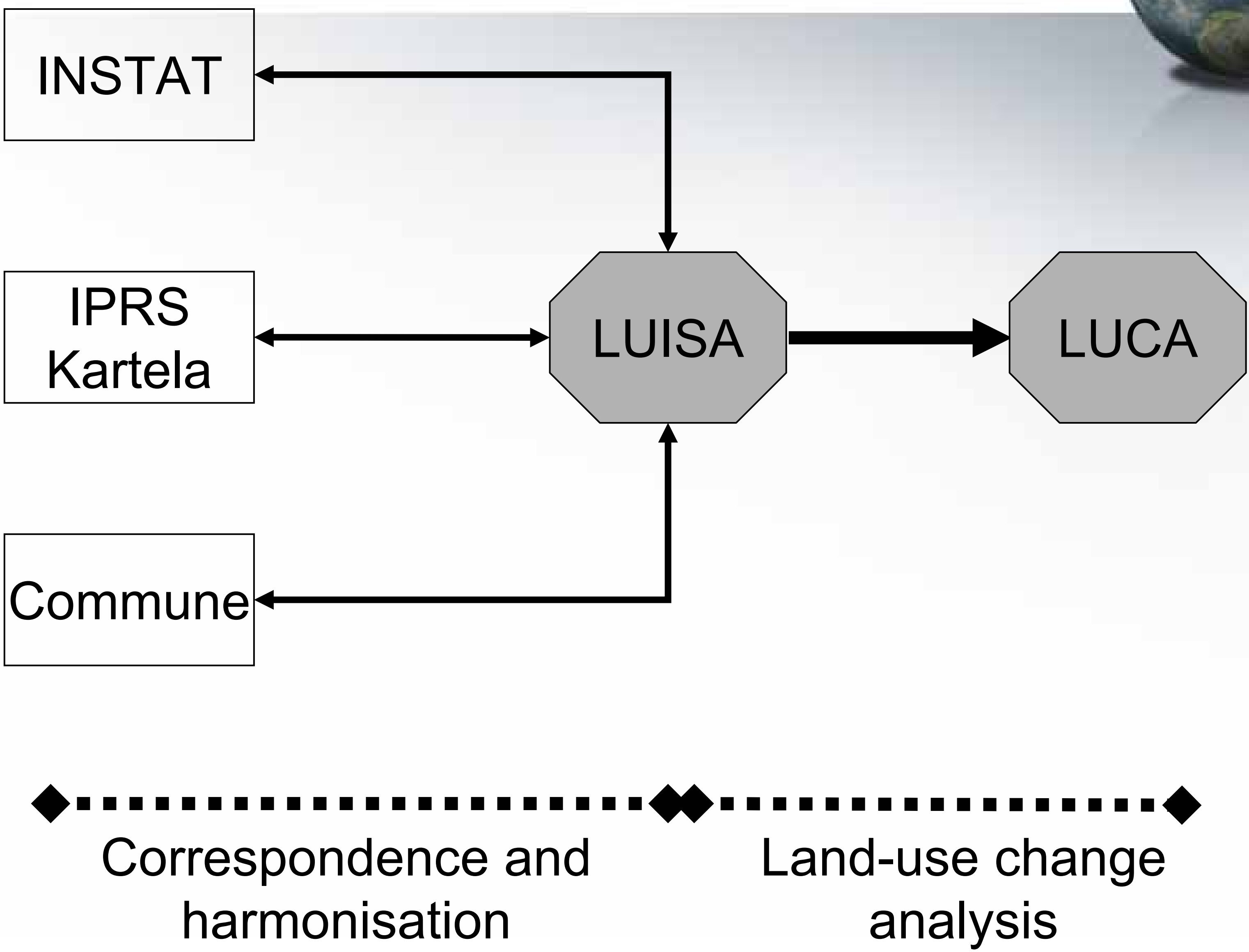

Land-use change analysis (LUCA) types

No change		No change	1
Modifications	Low level	Low level modification in Agriculture	201
		Low level modification in Forests	202
		Low level modification in Pastures	203
		Low level modification in Non-Agriculture	204
	Medium level	Medium level modification in Agriculture	301
		Medium level modification in Forests	302
		Medium level modification in Pastures	303
		Medium level modification in Non-Agriculture	304
	High level	High level modification in Agriculture	401
		High level modification in Forests	402
		High level modification in Pastures	403
		High level modification in Non-Agriculture	404
Conversions		Agriculture to Forest	5
		Agriculture to Pasture	6
		Agriculture to NonAgriculture	7
		Forest to Pasture	8
		Forest to Agriculture	9
		Forest to NonAgriculture	10
		Pasture to Agriculture	11
		Pasture to Forest	12
		Pasture to NonAgriculture	13
		NonAgriculture to Agriculture	14
		NonAgriculture to Forest	15
		NonAgriculture to Pasture	16
No correspondence			99

LUCA results at commune level

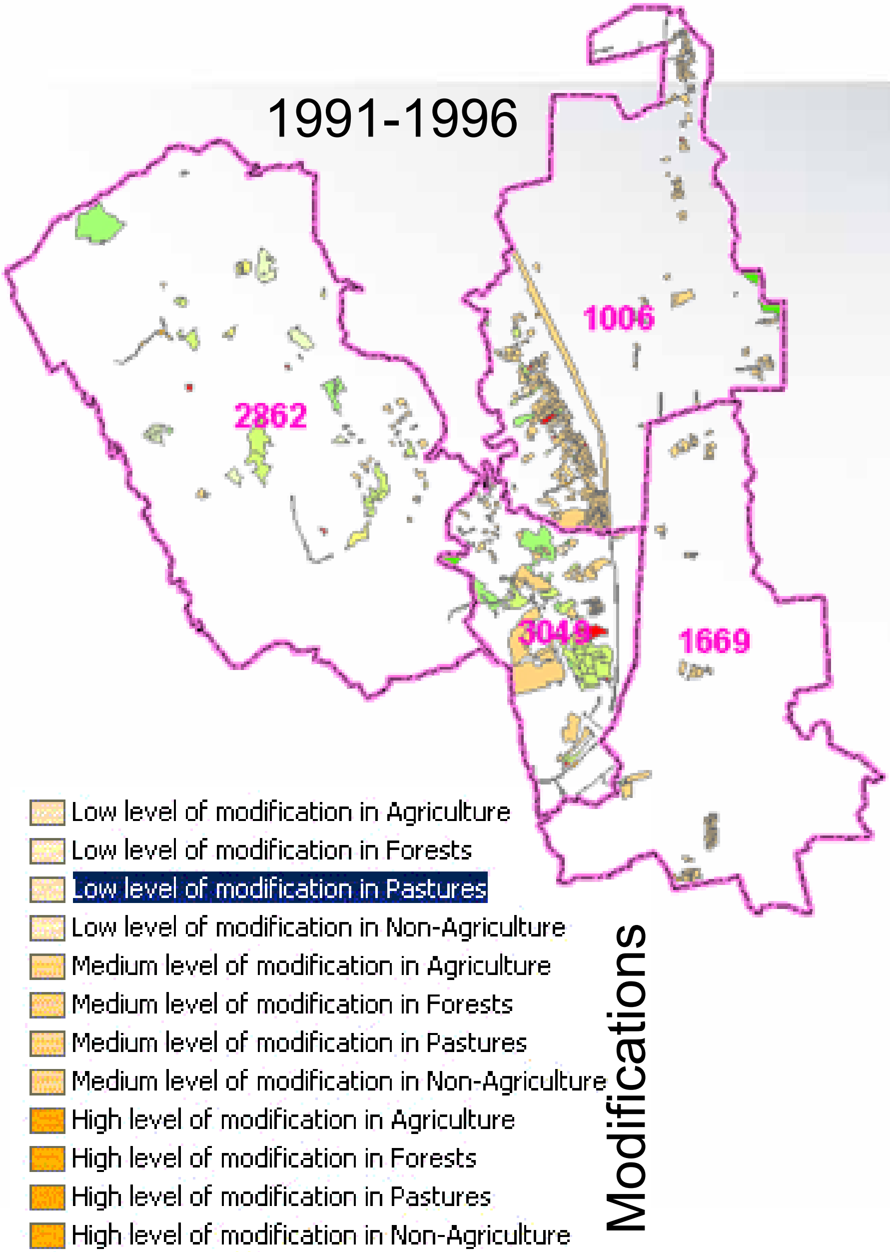

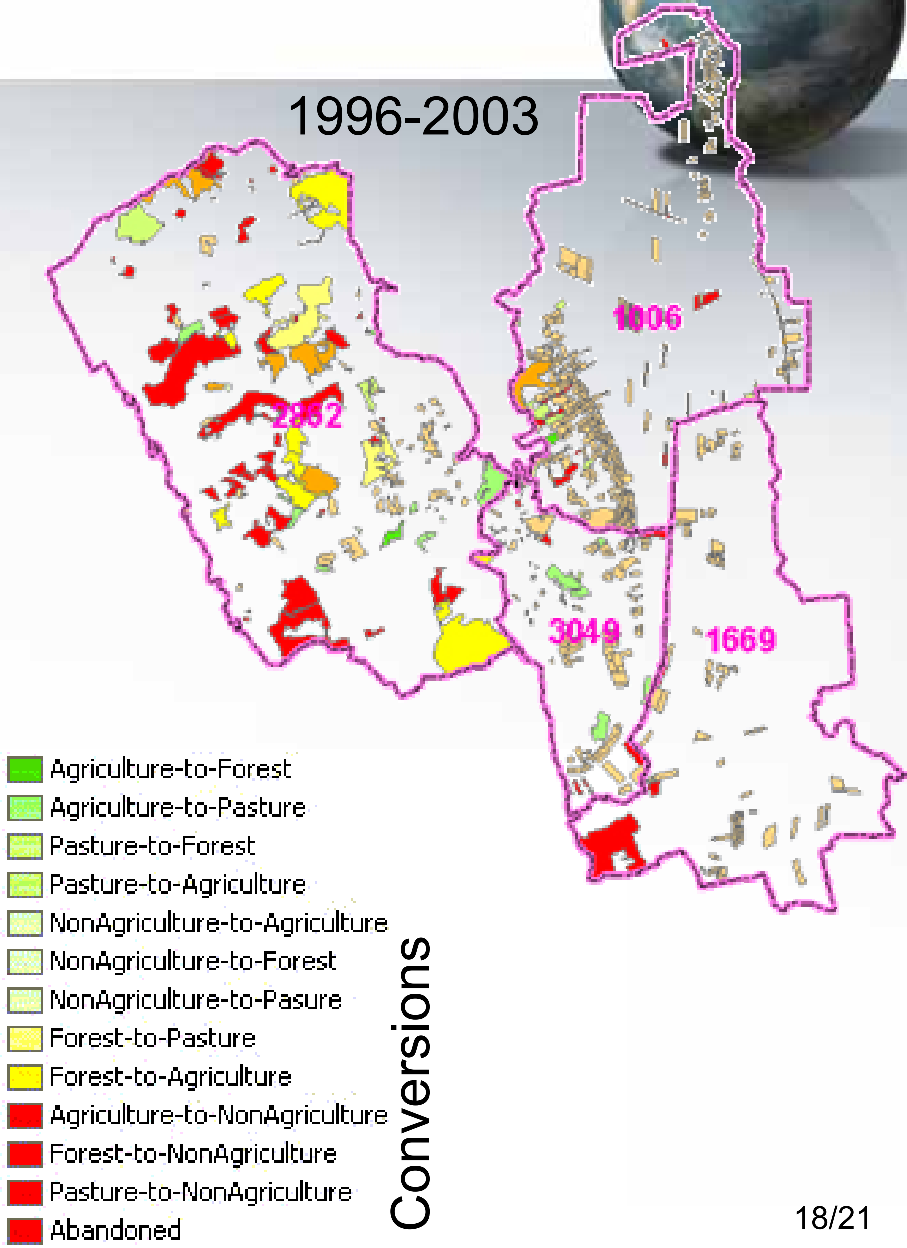

Comparison with RS data

- The detailed LUISA land-use data can be compared to the coarser ANFI data (scale 1:2,500 vs 1:100,000), as far as space and time considerations both data sets represent more or less the same period (1991-2003 vs 1991-2001):
  - ANFI provides a national overview of the major change processes (e.g., deforestation, urbanisation and increased pasture) but cannot provide conclusive evidence on the use of agricultural land.
  - LUISA provides an insight into the non-use of low productivity areas in hilly terrain and the extensive forms of agriculture practised on prime agricultural land due to the lack of fertilizer use and breakdown of irrigation systems.
- Remote sensing can provide a quick overview of the type and location of land-cover types. However, land use contains socio-economic, institutional, cultural and legal aspects. Even with the use of the most detailed RS images, these aspects will not be covered.

Conclusions and discussion

- The combination of just two parameters may suffice to describe any land use: function together with activity.
- The example in Albania shows how harmonisation of class sets can include harmonisation of land-use change using a reference system.
- Remote sensing is a useful tool for gaining a quick overview of land-cover related land uses but the potential for a detailed and in-depth knowledge of land use is limited as other aspects, such as socio-economics, institutional, cultural and legal factors, are not captured by remotely sensed based land cover.

- The way forward for harmonisation of land-use class sets is to promote and fully develop a parametric approach to classification.
- Commonalities in existing approaches should be emphasized and a set of commonly used parameters should be identified.
- Lessons can be learnt from harmonisation attempts at local, regional and national levels that are equally valid for a globally applicable land-use classification.
- Furthermore, a quantitative measure should be defined to express the harmonisation result of a class and between class sets.

Land cover/tree cover mapping of the Global Mapping project

Ryutaro Tateishi
Center for Environmental Remote Sensing (CEReS)
Chiba University
e-mail: tateishi@faculty.chiba-u.jp
URL: http://www.cr.chiba-u.jp/tateishi/home.htm

Ideal concept for the future

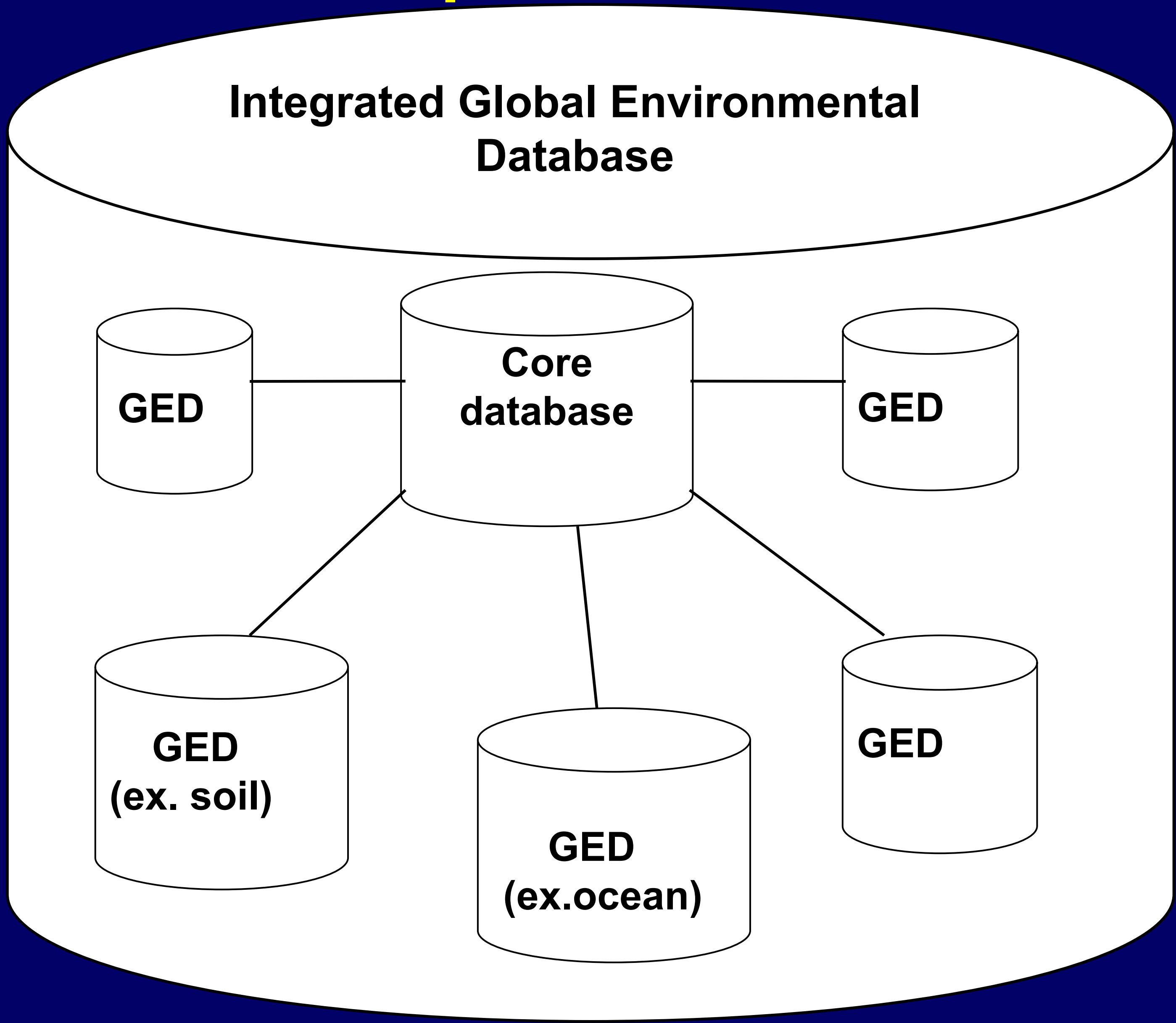

GED:
Global Environmental Database

Global Mapping Project – Birth -

- **1992** UNCED
  - Adoption of "Agenda 21"
  - Global Mapping Concept proposed by Japanese Government

Concept -> Project

- **1996** Establishment of International Steering Committee for Global Map (ISCGM) http://www.iscgm.org/
- **1998** Preparation of the specifications

Invite National Mapping Organizations (NMO) to the Project in cooperation with UN Statistics Division

Global Map Specifications

- Spatial resolution: 1km

  (equivalent to 1:1,000,000 scale)

- 8 layers
  - Vector data (point, line, area)

    Boundaries (Administrative/Coast),

    Drainage (Rivers/Lakes),

    Transportation (Roads/Railways/Airport),

    Population centers
  - Raster data (grid)

    Elevation, Land Cover, Land Use, Vegetation

Global Map Data（Vector Data）

Boundaries

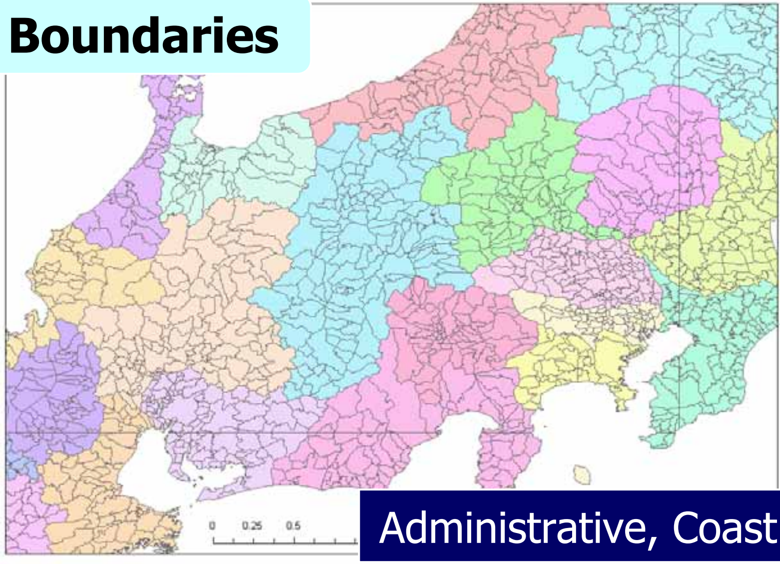

Administrative, Coast

Drainage

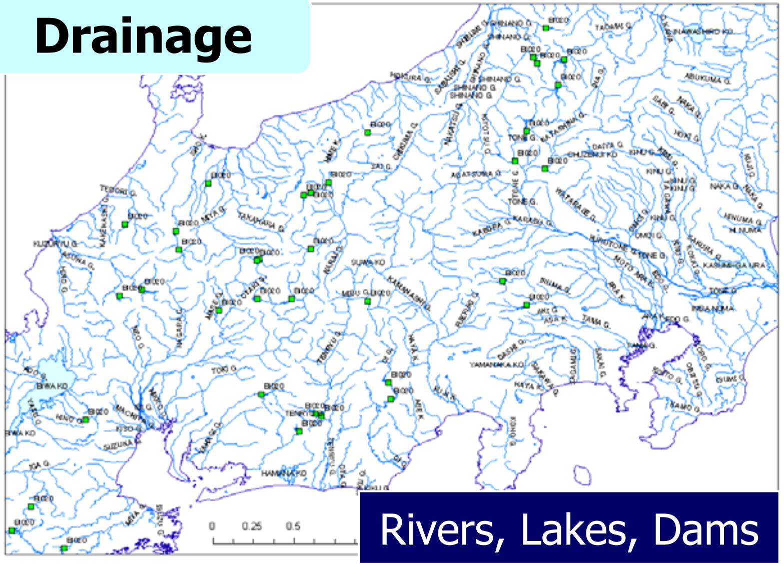

Rivers, Lakes, Dams

Transportation

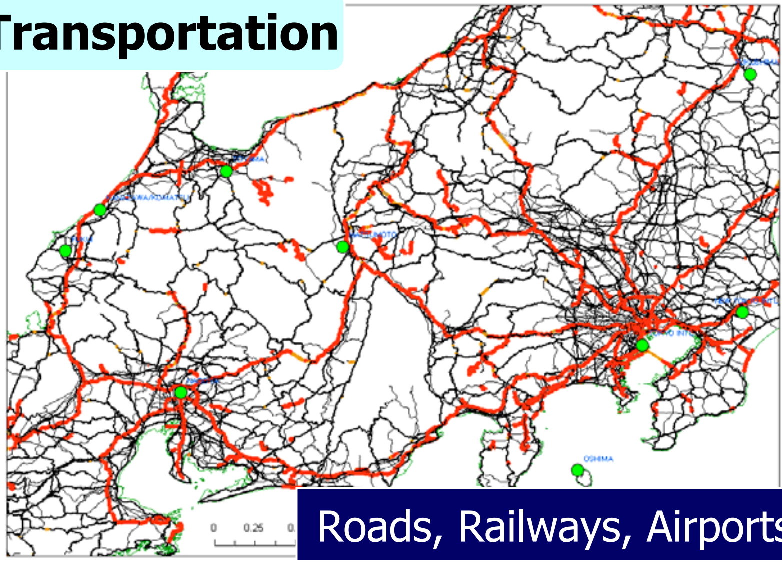

Roads, Railways, Airports

Population Centers

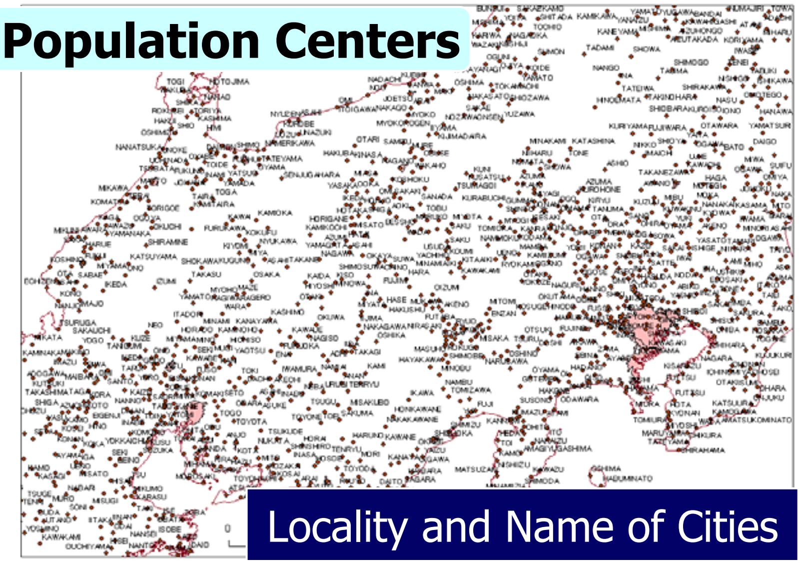

Locality and Name of Cities

Global Map Data（Raster Data）

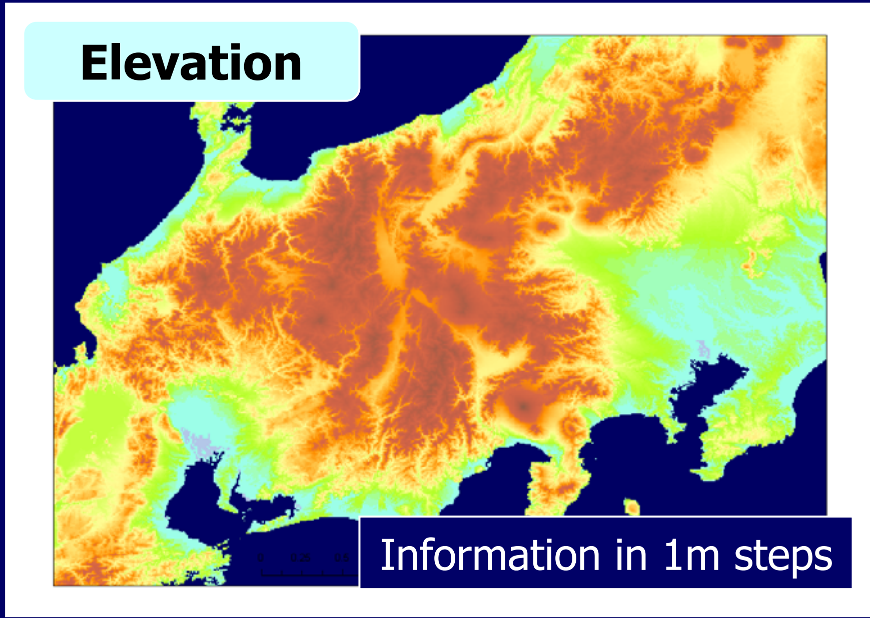

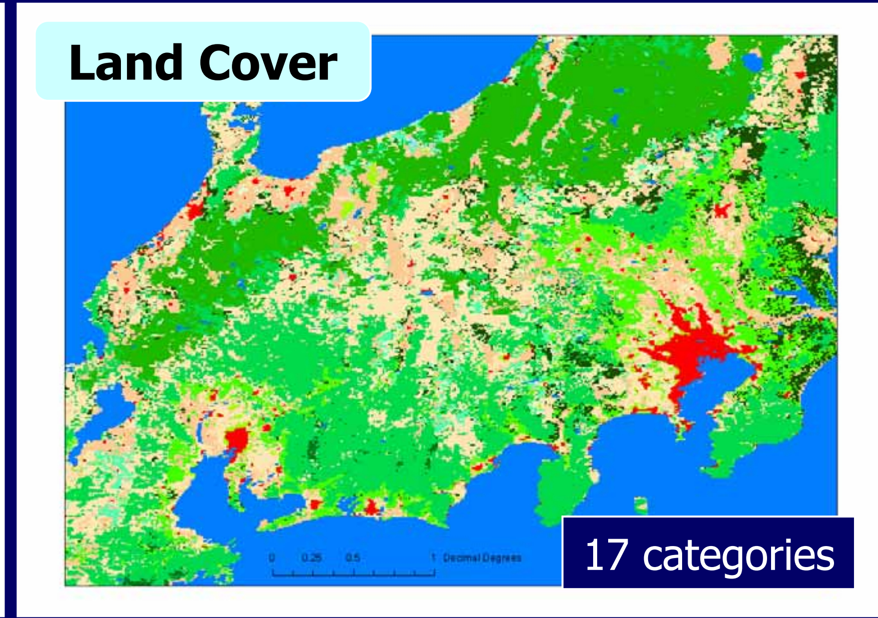

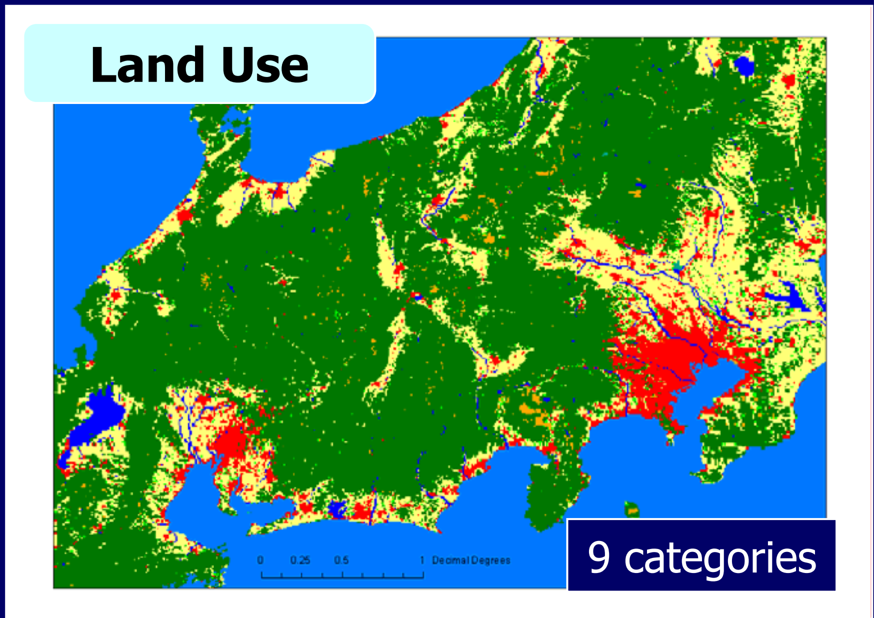

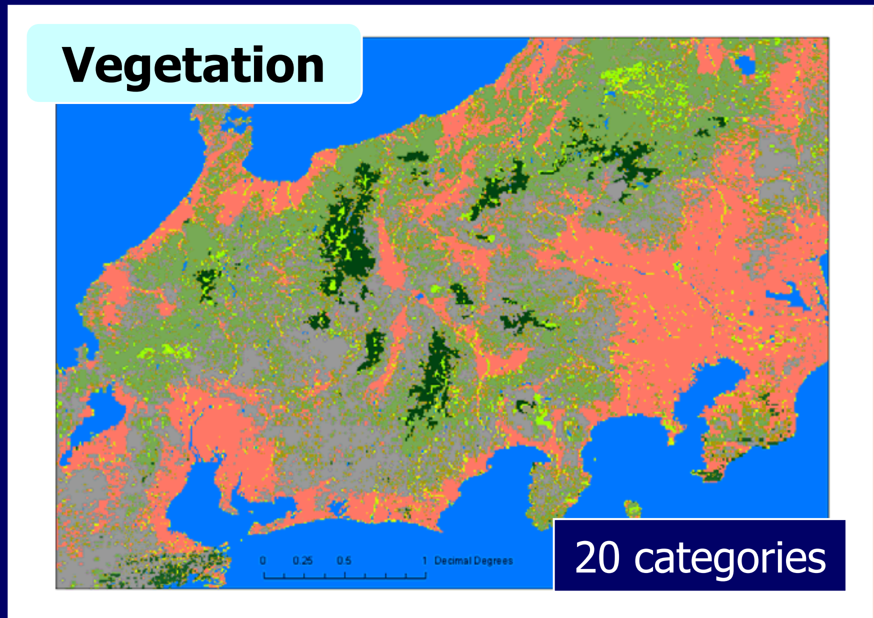

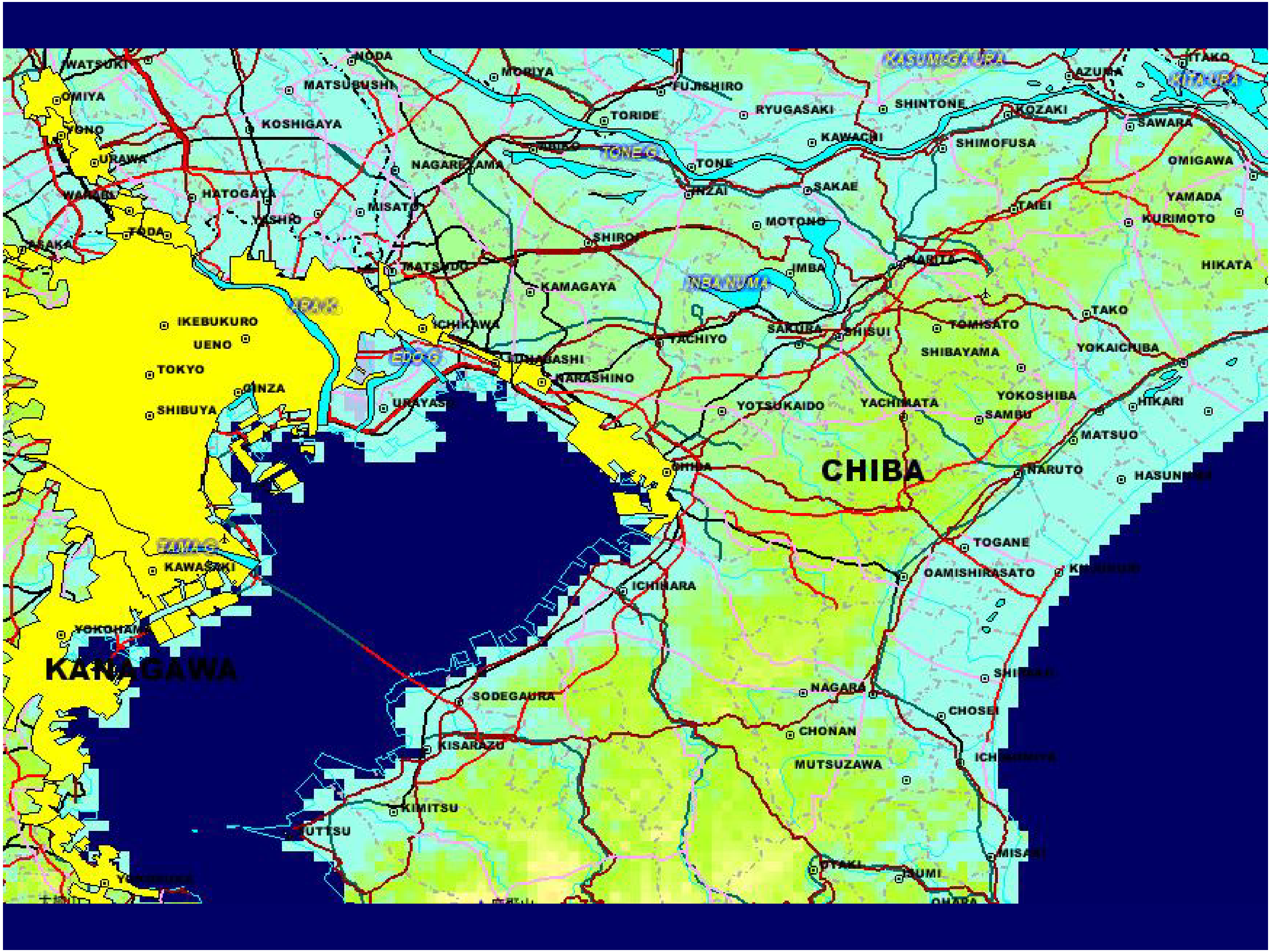
IWATSUKI
OMIYA
YONO
URAWA
WARABI
TODA
HATOGAYA
YASHIO
KOSHIGAYA
MATSUBUSHI
NODA
MORIYA
FUJISHIRO
TORIDE
RYUGASAKI
SHINTONE
AZUMA
ITAKO
KITA-URA
KOZAKI
SAWARA
KAWACHI
SHIMOFUSA
TONE-G
TONE
INZAI
SAKAE
OMIGAWA
YAMADA
KURIMOTO
TAIEI
MOTONO
NAGAREYAMA
MISATO
MATSUDO
SHIROI
KAMAGAYA
IMBA
INBA-NUMA
NARITA
HIKATA
IKEBUKURO
UENO
TOKYO
GINZA
SHIBUYA
ICHIKAWA
EDO-G
FUNABASHI
NARASHINO
URAYASU
YACHIYO
SAKURA
SHISUI
TOMISATO
TAKO
SHIBAYAMA
YOKAICHIBA
YOTSUKAIDO
YACHIMATA
YOKOSHIBA
SAMBU
HIKARI
MATSUO
CHIBA
NARUTO
CHIBA
TOGANE
OAMISHIRASATO
KAWASAKI
ICHIHARA
YOKOHAMA
KANAGAWA
SODEGAURA
NAGARA
CHOSEI
CHONAN
KISARAZU
MUTSUZAWA
KIMITSU
MISAKI
OTAKI
ISUMI
OHARA

Progress of Global Mapping Project

As of 2005-06-10
Secretariat of
International Steering Committee for Global Mapping

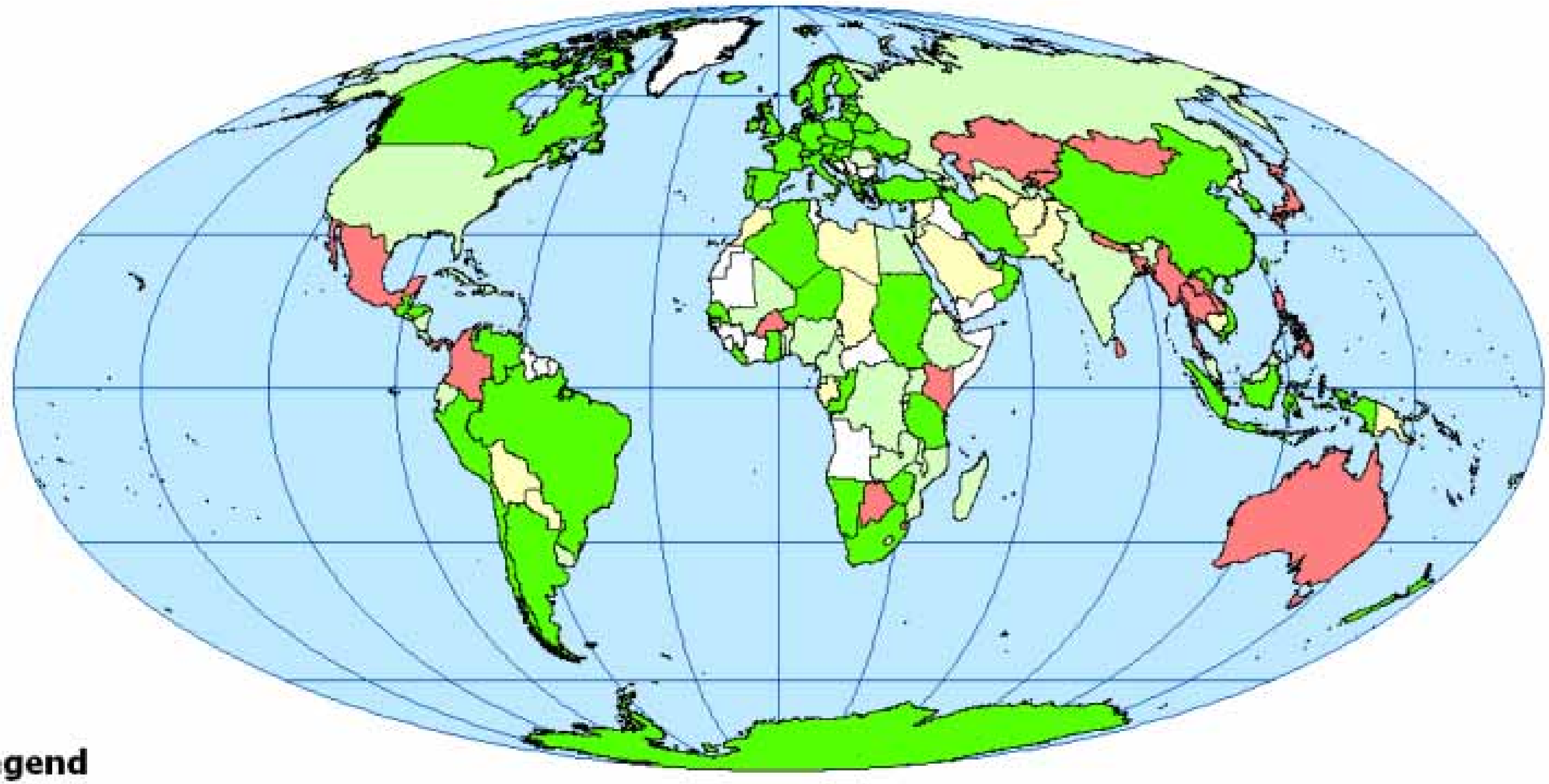

Legend

- data available
- data for verification
- developing data
- considering joining the project
- not participating in the project

Most raster data of current Global Map are compiled from GTOPO30 and GLCC, contribution of United States of America.

This map is for the purpose of reference and the boundaries in this map are not authorized by any organizations.

- Implementation of the Project -

- Data development

  by National Mapping Organizations
- Management by ISCGM

	version 2 (complete by 2007)
Land cover	new production (GLCNMO)
Vegetation	new production (percent tree cover)
Land use	no

Global Land Cover by National Mapping Organizations

(GLCNMO)

Development of Global Land Cover Dataset in Global Mapping project

- Legend will be defined by LCCS of FAO
- MODIS 1km data 2003
- Ground truth collection by the cooperation with <u>National Mapping Organizations</u>
- Decision tree method
- Validation by the cooperation with <u>National Mapping Organizations</u>
- Complete by 2007

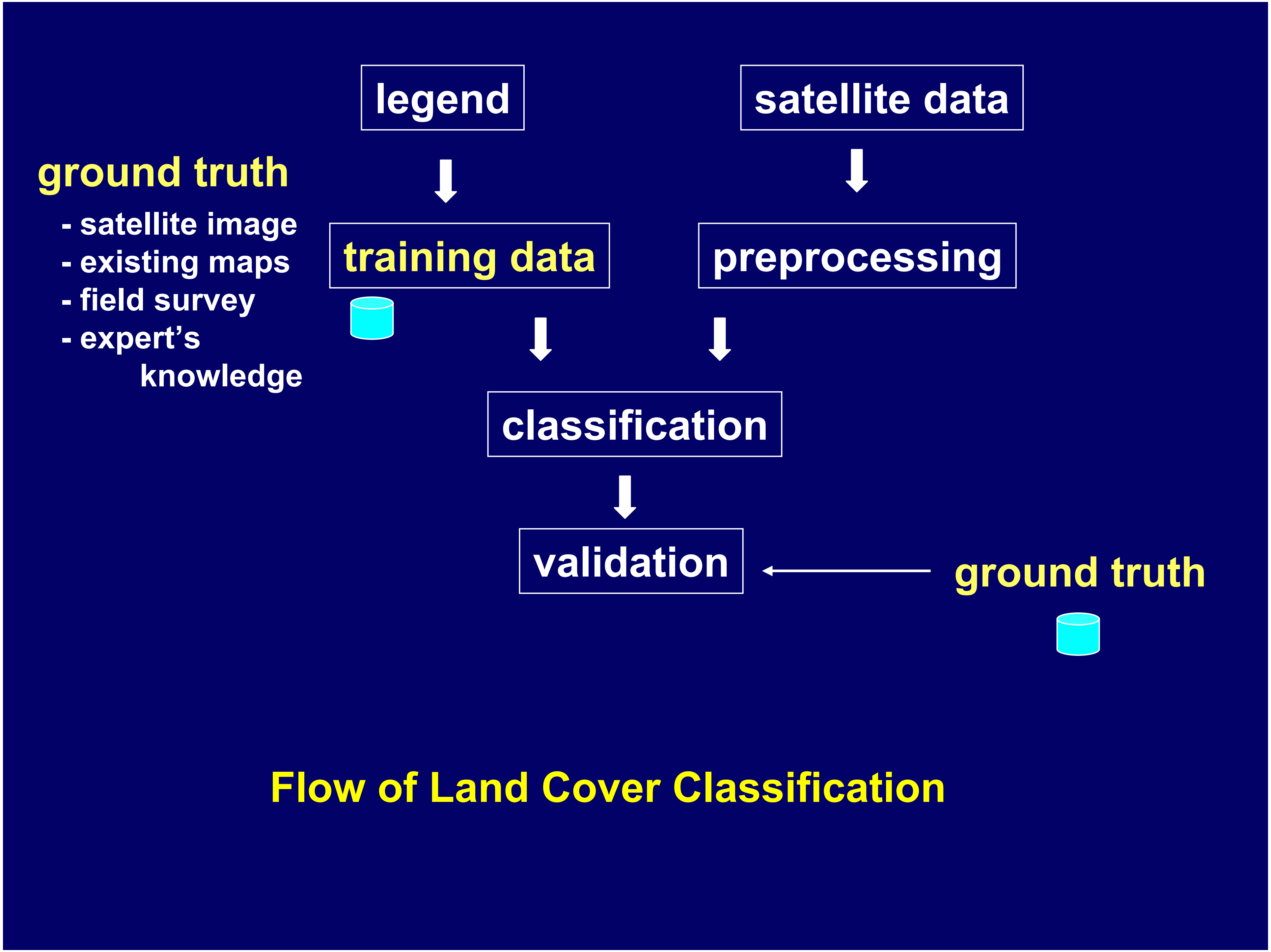
legend
satellite data
ground truth
- satellite image
- existing maps
- field survey
- expert's knowledge
training data
preprocessing
classification
validation
ground truth
Flow of Land Cover Classification

Tentative global land cover legend for Global Map version 2

1. Broadleaf Evergreen Forest
2. Broadleaf Deciduous Forest
3. Needleleaf Evergreen Forest
4. Needleleaf Deciduous Forest
5. Mixed Forest
6. Tree Open
7. Shrub
8. Herbaceous, single layer
9. Herbaceous with Sparse Tree/Shrub
10. Sparse Herbaceous / Shrub
11. Cropland (herbaceous crops except rice)
12. Rice, paddy
13. Cropland / Natural Vegetation Mosaic
14. Tree-Water (Brackish to Saline)
15. Wetland
16. Bare area, consolidated (gravel, rock)
17. Bare area, unconsolidated (sand)
18. Urban
19. Snow / Ice
20. Water bodies

Land Cover Classification System (LCCS) by FAO

- eight basic classes based on vegetation, water, and artificial

- hierarchical

- comprehensive

- defined in detail

Land Cover Classification System (LCCS) by FAO

Dichotomous Classification Phase at the top of the hierarchical system

vegetated	terrestral	managed/artificial
		natural
	aquatic	managed/artificial
		natural
non-Vegetated	terrestrial	managed/artificial
		natural
	aquatic	managed/artificial
		natural

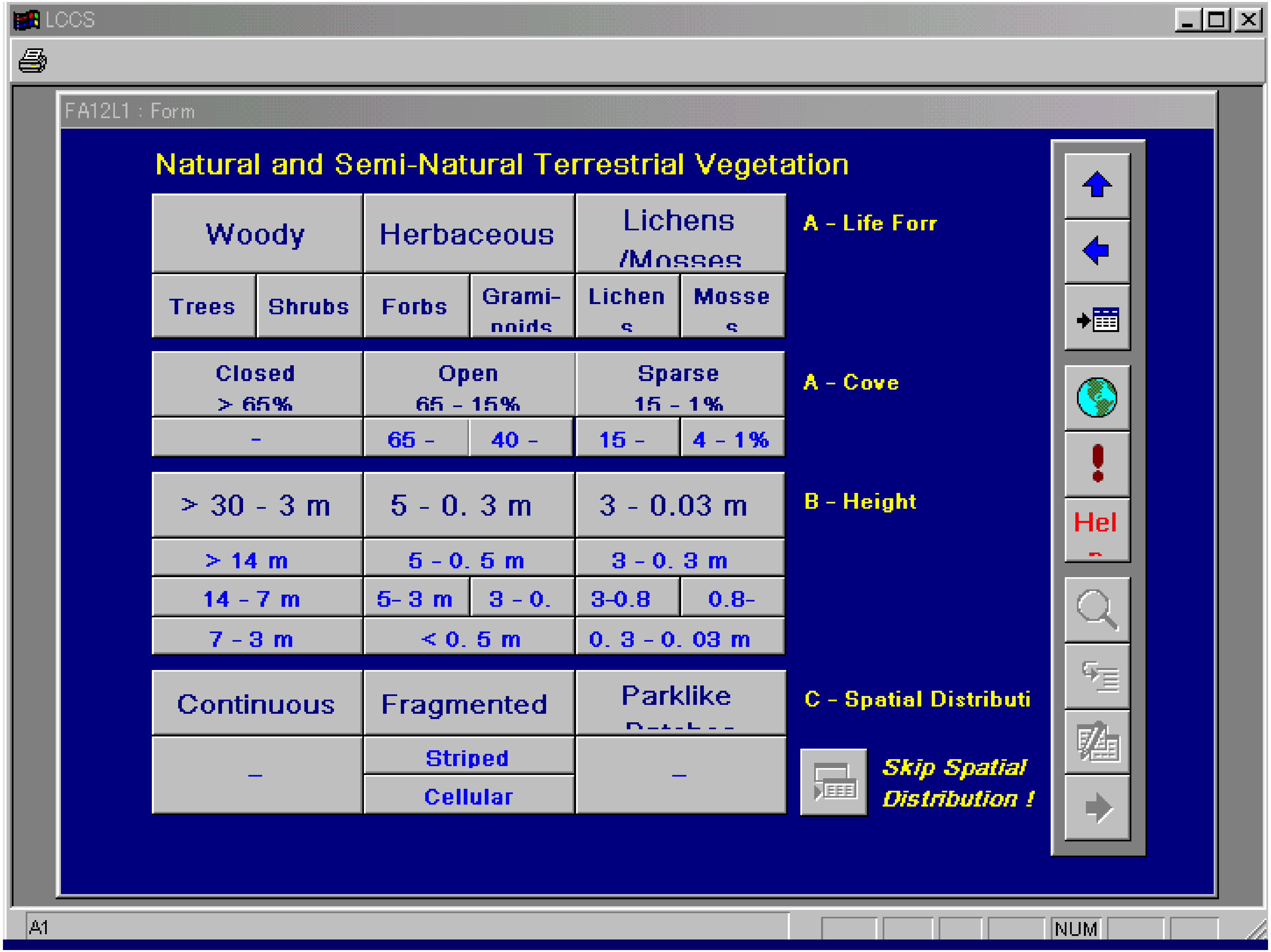

LCCS
FA12L1 : Form
Natural and Semi-Natural Terrestrial Vegetation
Woody
Herbaceous
Lichens /Mosses
Trees
Shrubs
Forbs
Grami-noids
Lichens
Mosses
A - Life Forr
Closed > 65%
Open 65 - 15%
Sparse 15 - 1%
-
65 -
40 -
15 -
4 - 1%
A - Cove
> 30 - 3 m
5 - 0. 3 m
3 - 0.03 m
> 14 m
5 - 0. 5 m
3 - 0. 3 m
14 - 7 m
5- 3 m
3 - 0.
3-0.8
0.8-
7 - 3 m
< 0. 5 m
0. 3 - 0. 03 m
B - Height
Continuous
Fragmented
Parklike
C - Spatial Distributi
Striped
Cellular
Skip Spatial Distribution !
Hel
A1
NUM

USGS MOD43B4 NBAR Product

Characteristics :

No. of Bands: 7 Bands

Area = ~ 10 x10 lat/long

Size = 1200 x1200 rows/columns

Volume = ~31MB

Resolution = 1 kilometer

Projection = Sinusoidal

Data Type Reflectance = 16-bit Signed Integer

Data Format = HDF-EOS

16-day composite

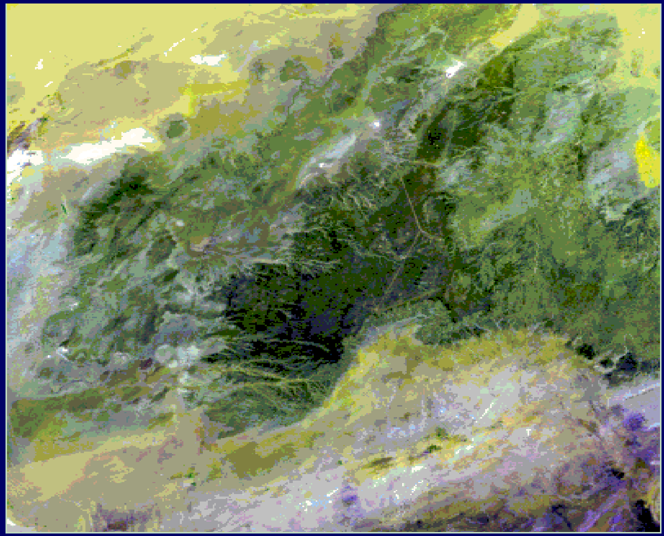

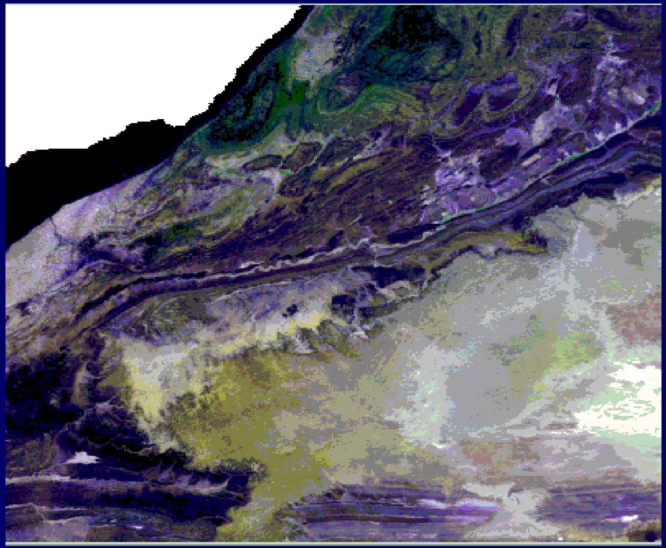

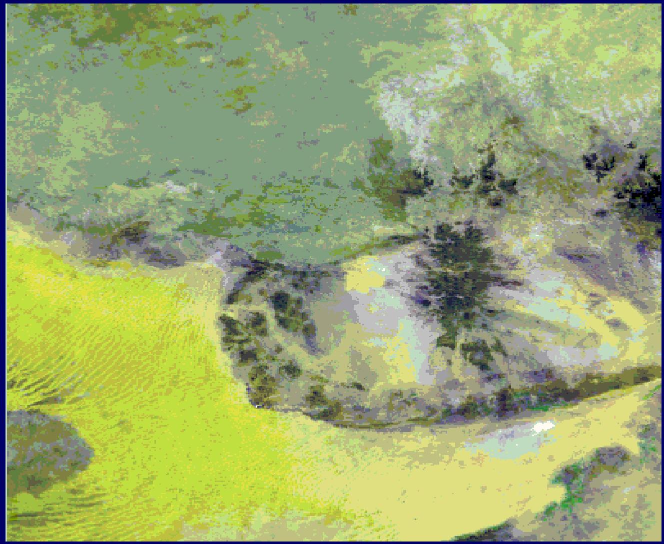

Preprocessing of MODIS

- Mosaicing from 10x10 deg. tiles to continent

- Add snow flag using MODIS snow product

- Cloud removal using 2002 & 2004 MODIS data and temporal interpolation

16-Day Composite of MODIS 1km of 2003

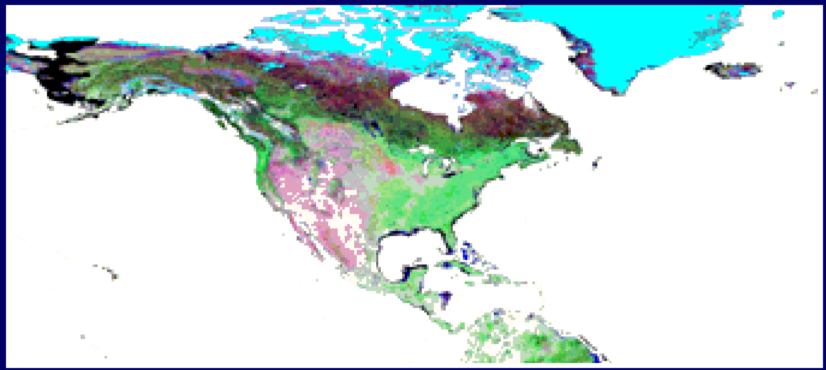

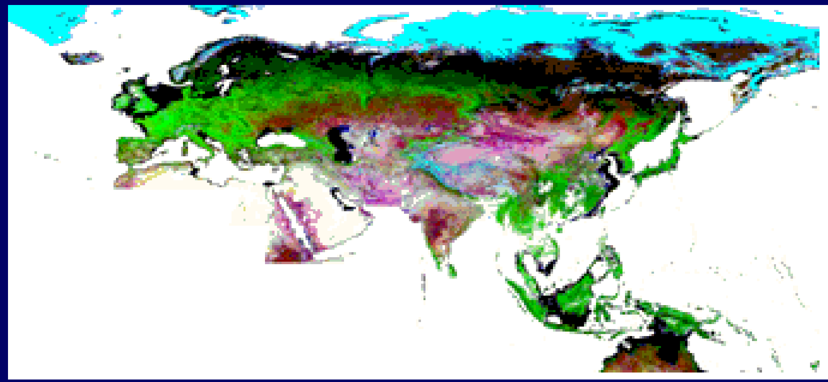

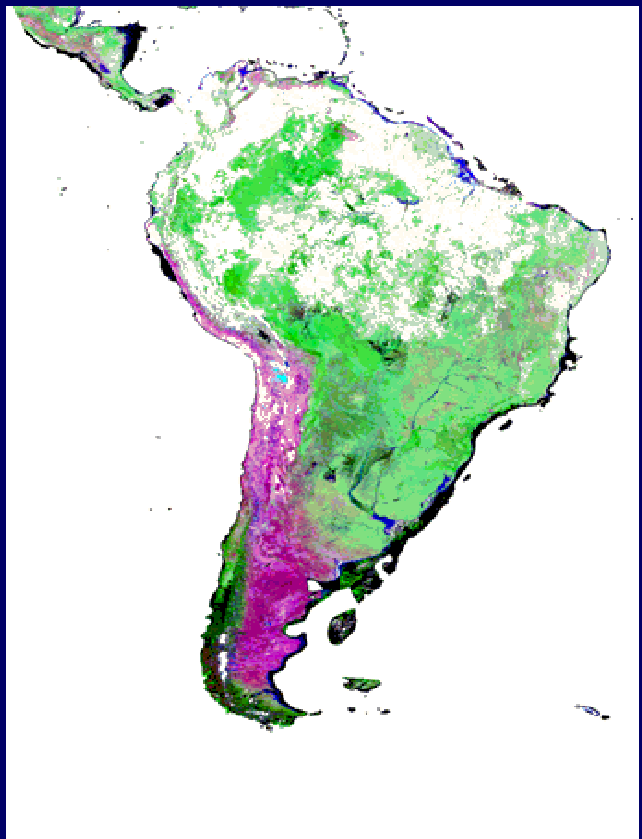

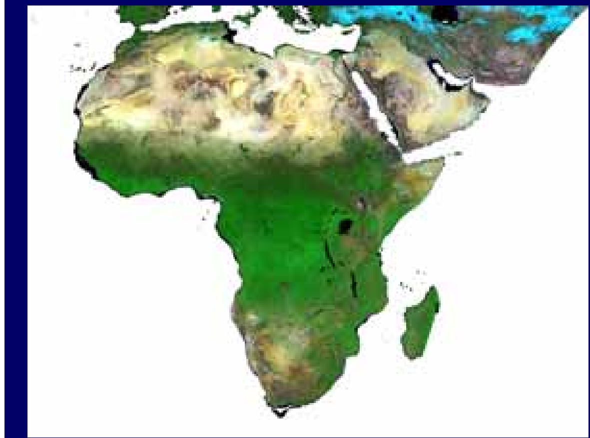

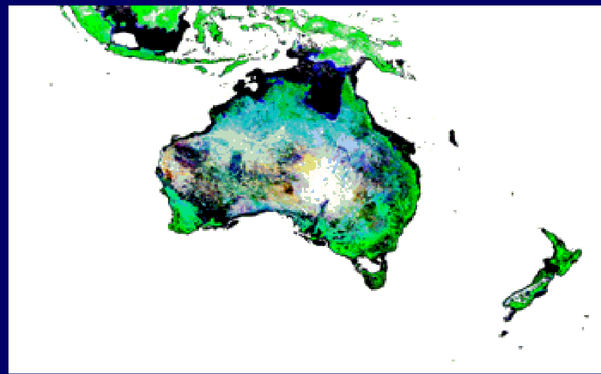

Cloud Removal

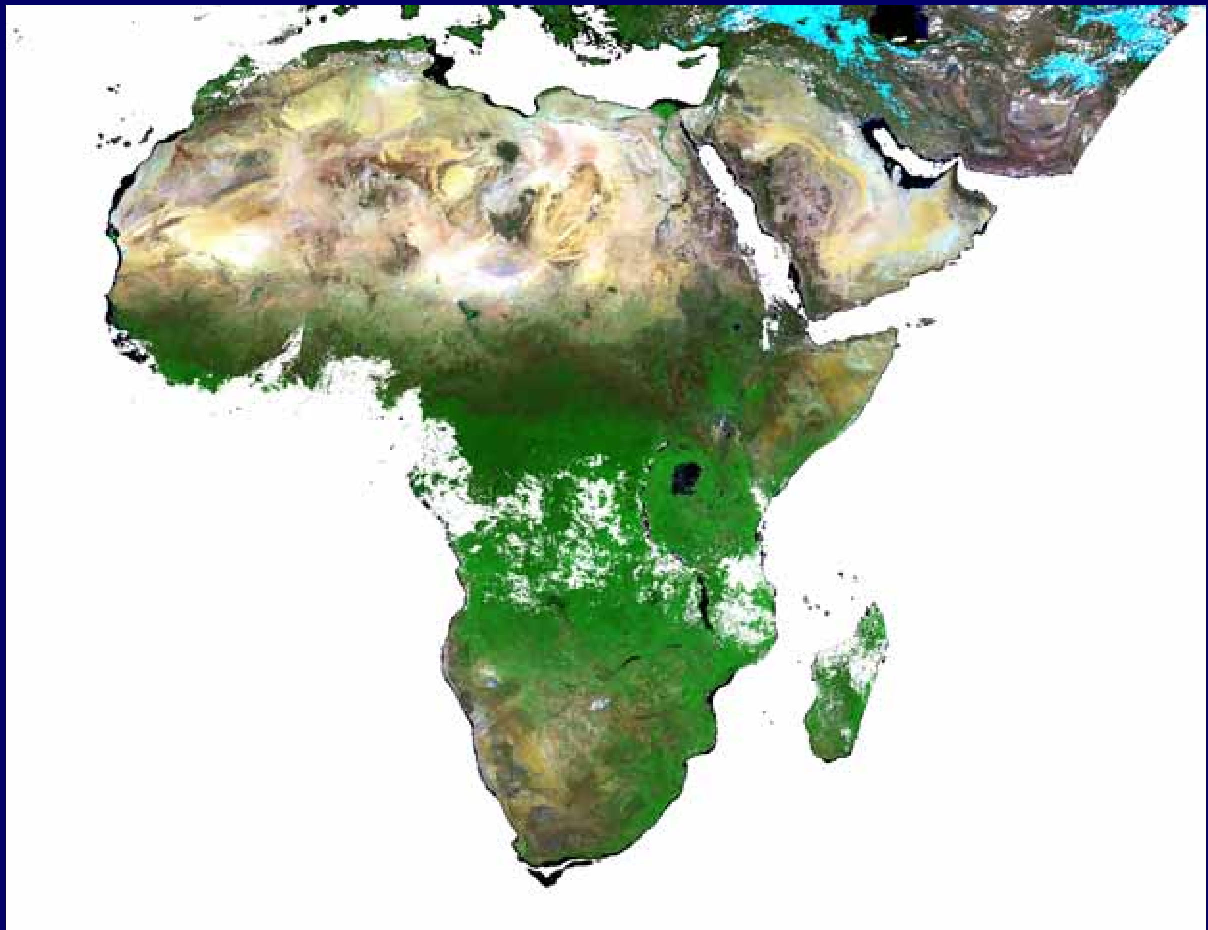

MODIS DATA 2003/1/1 Before processing

Cloud Removal (intermediate)

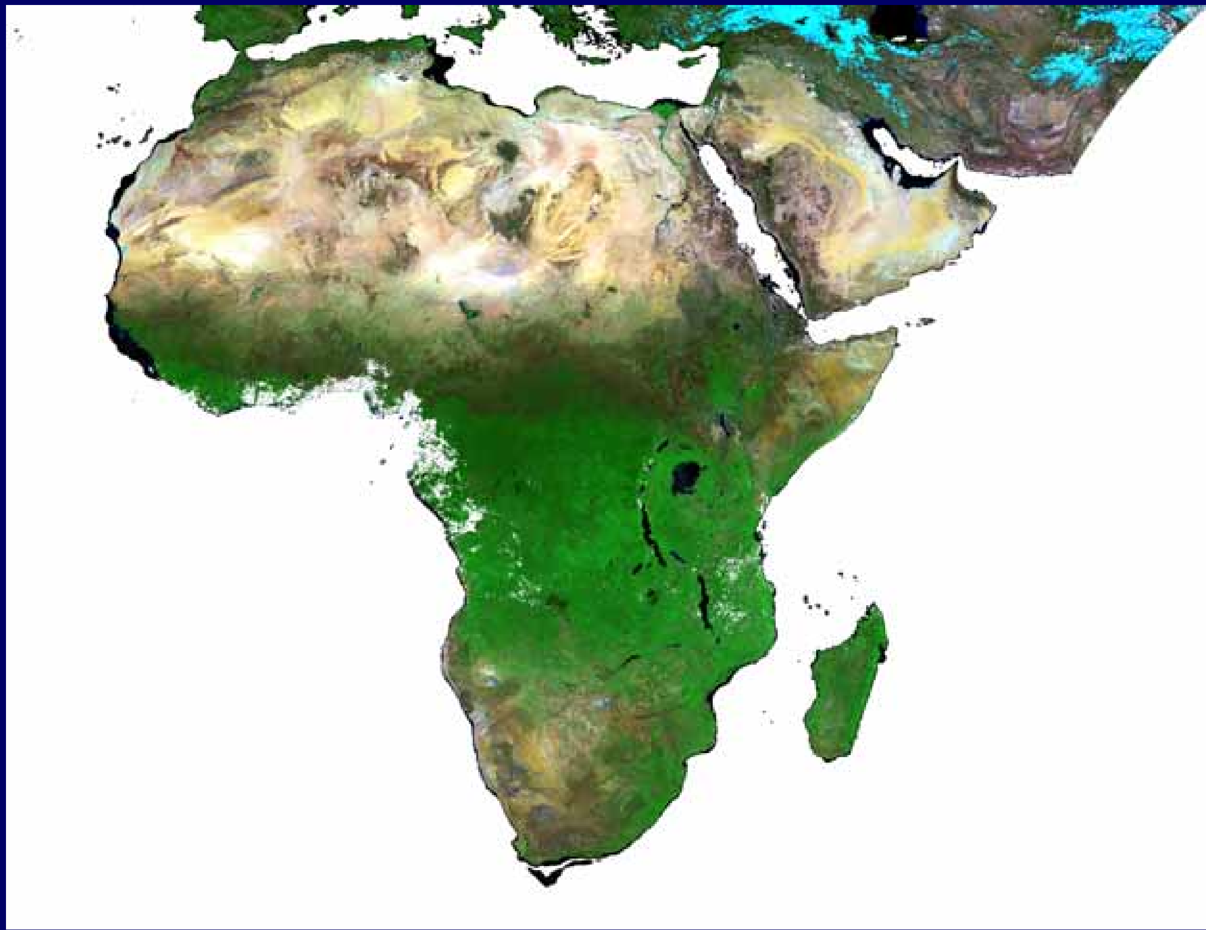

MODIS DATA 2003/1/1 After overlay by MODIS 2002 and MODIS 2004

Cloud Removal (final)

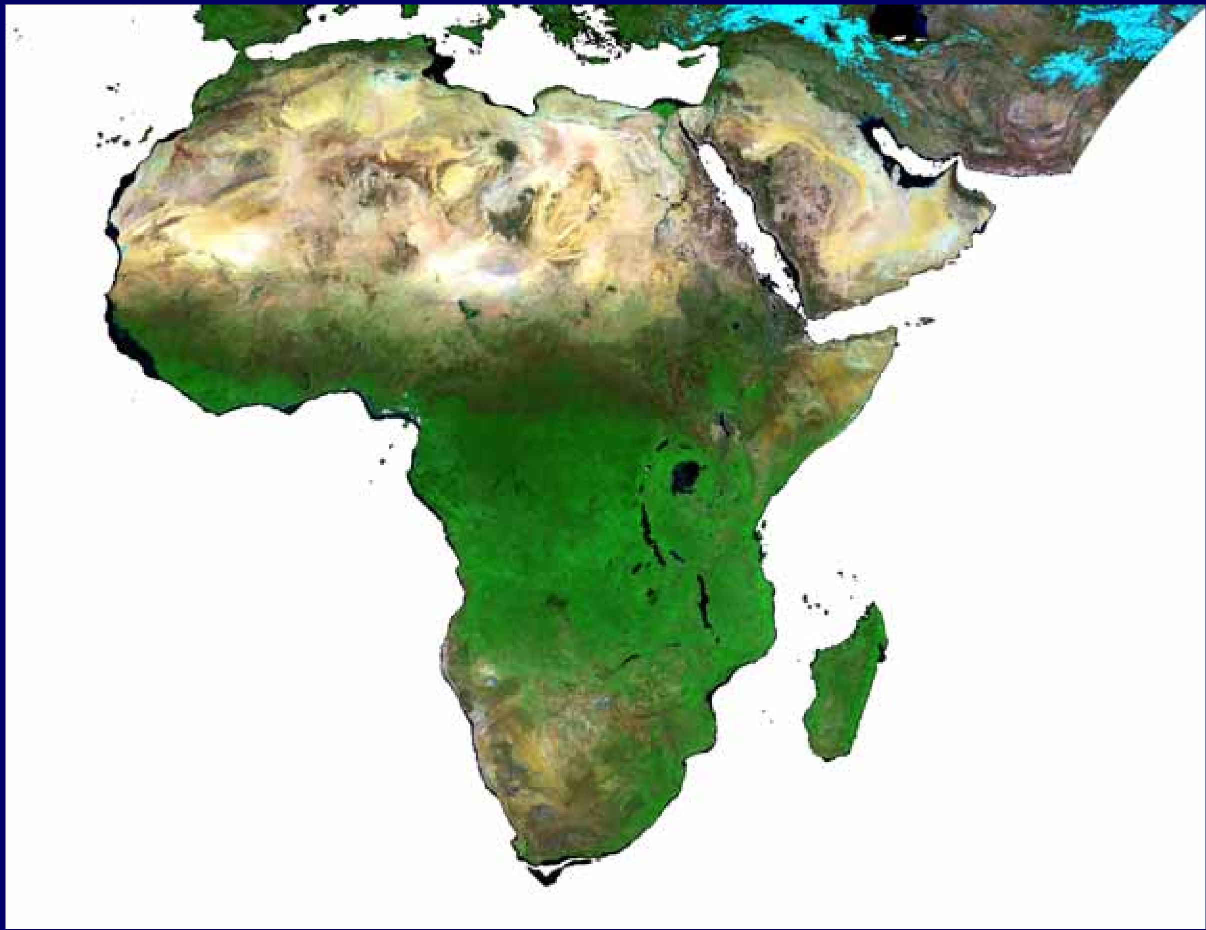

MODIS DATA 2003/1/1 After temporal interpolation

Selection of training sites

from (1) common areas of three land cover products, GLC2000, IGBP-Discover, and Boston Univ.

(2) GLC2000 regional products

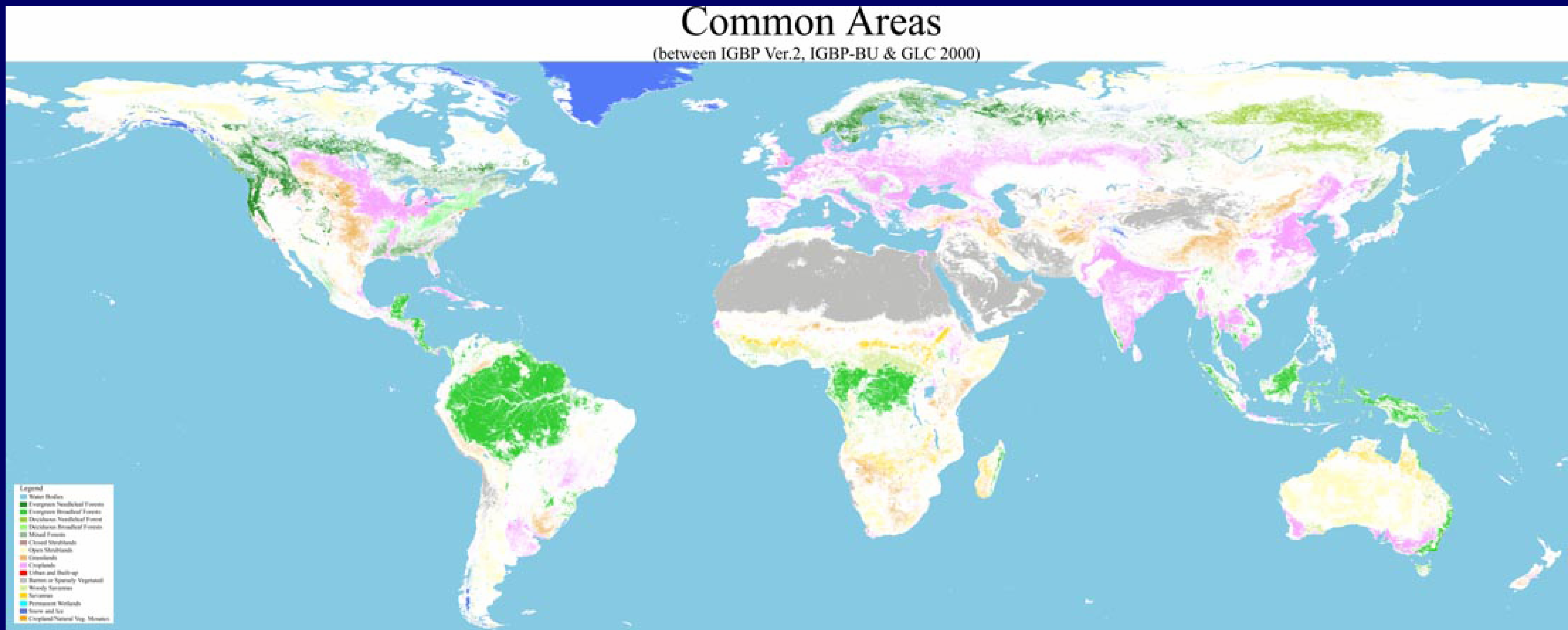

Candidate of ground truth sites

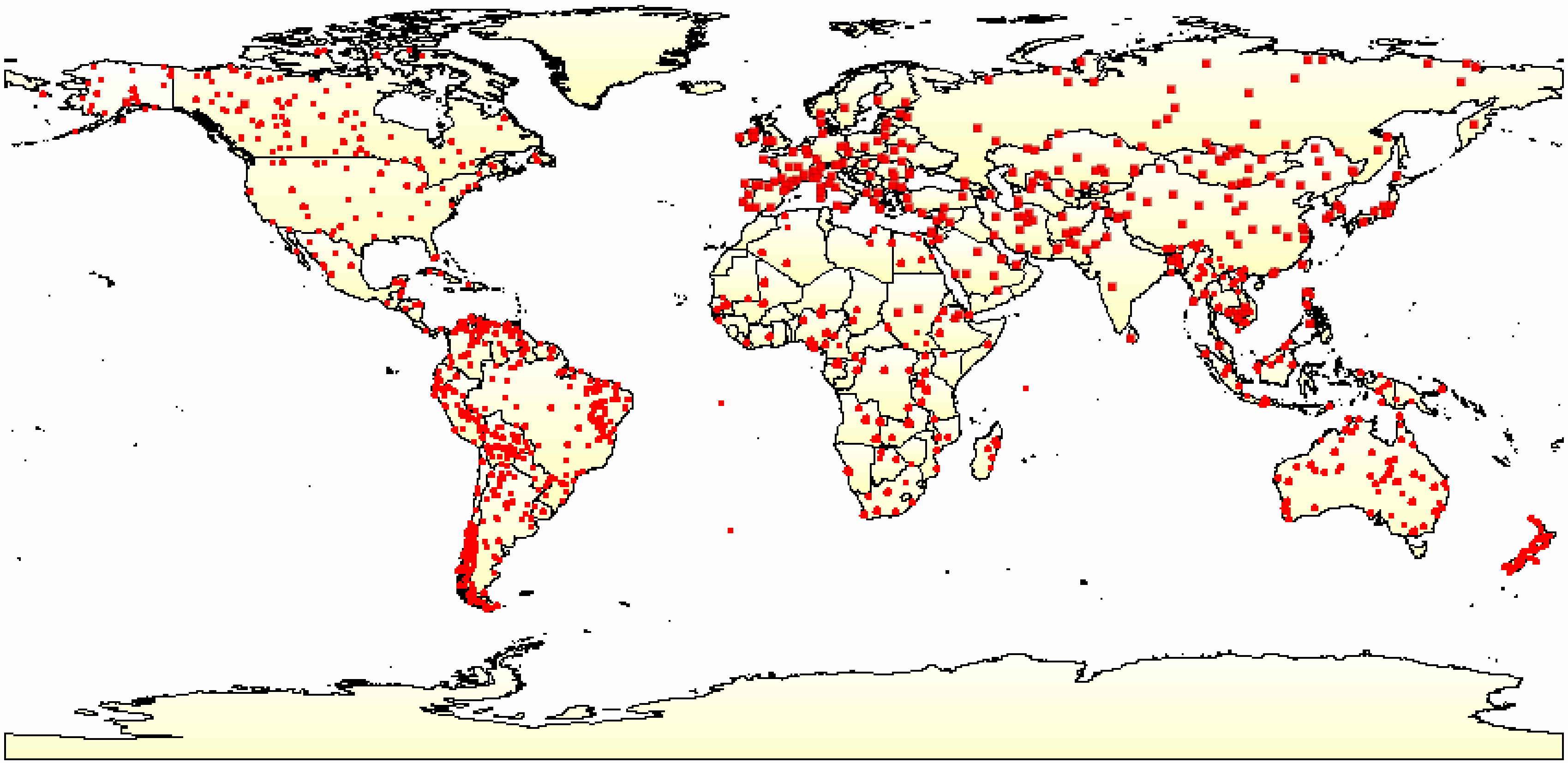

Sample of satellite images of ground truth site

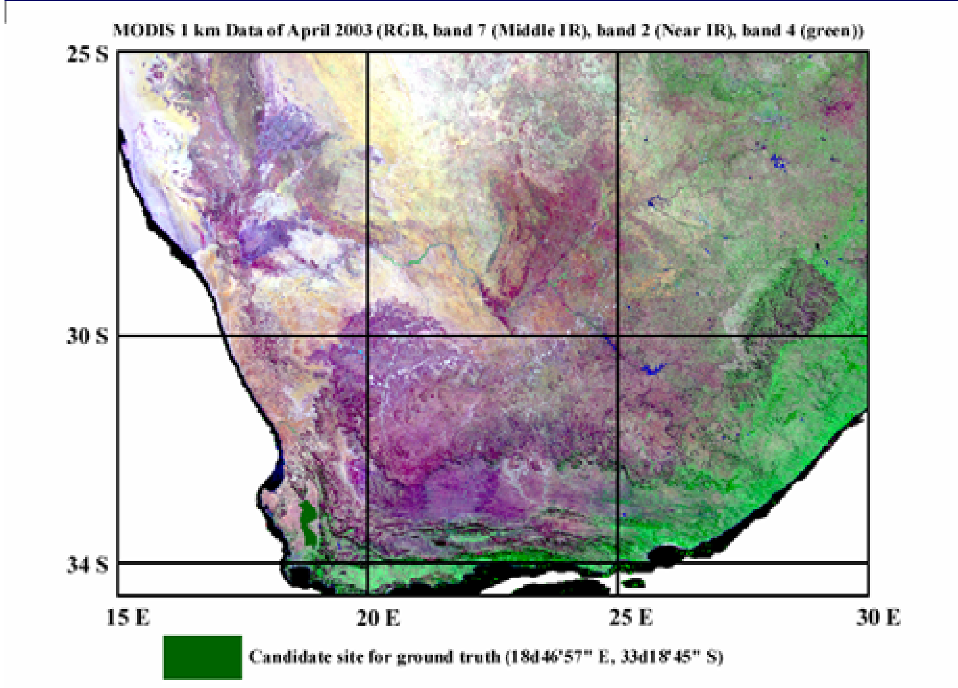

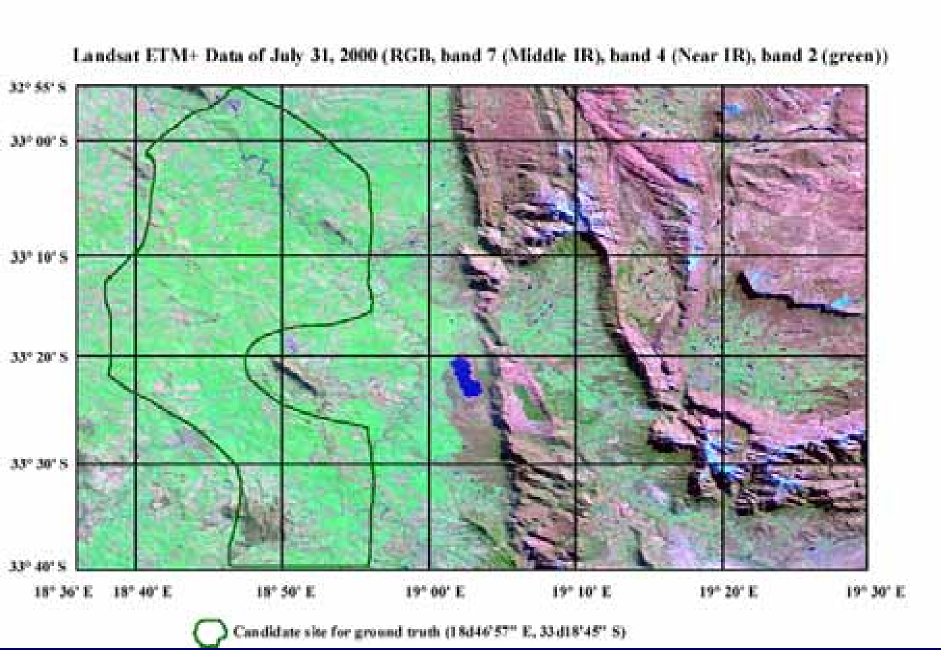

MODIS

Landsat

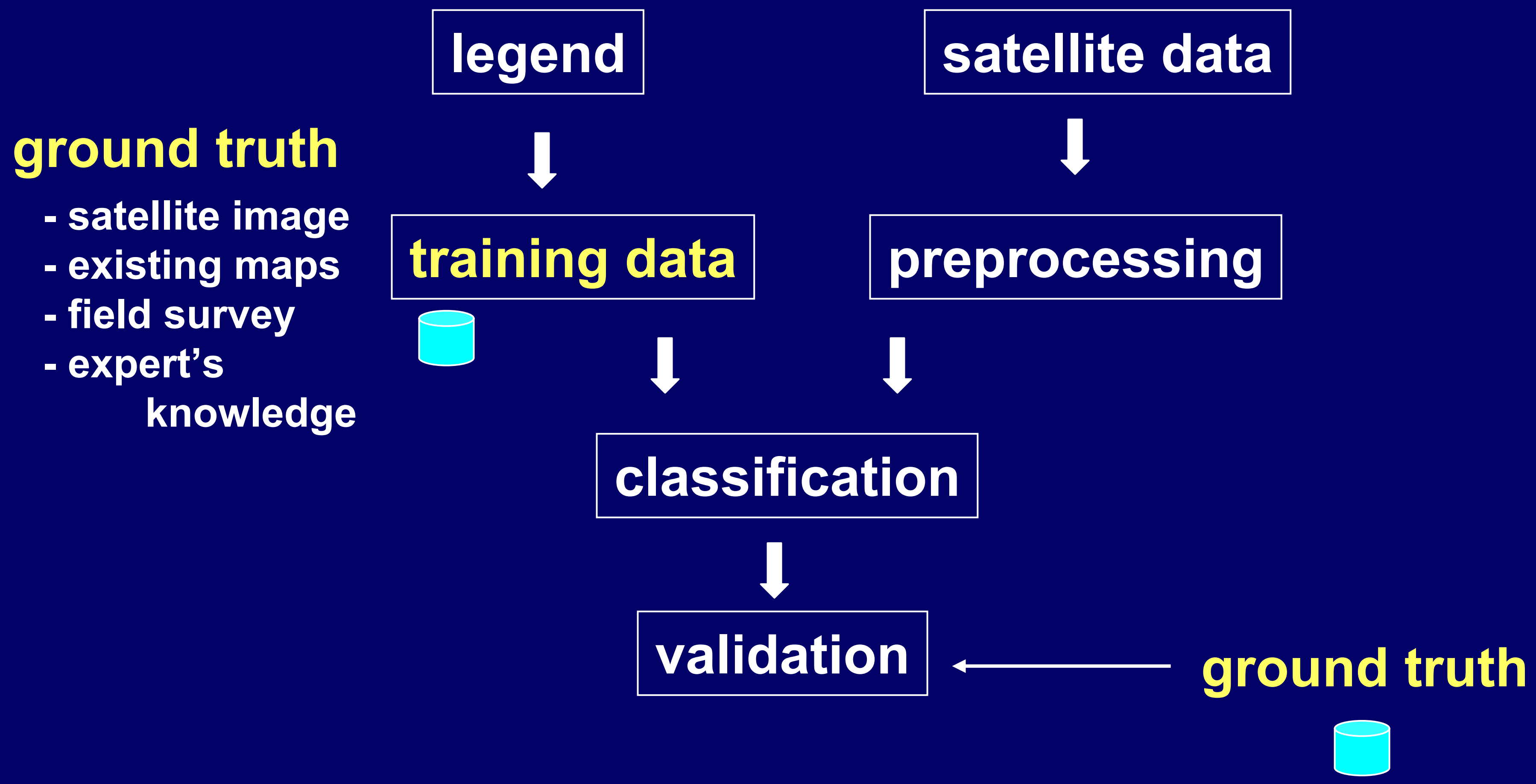

Flow of Land Cover Classification

Percent tree cover

Percent tree cover

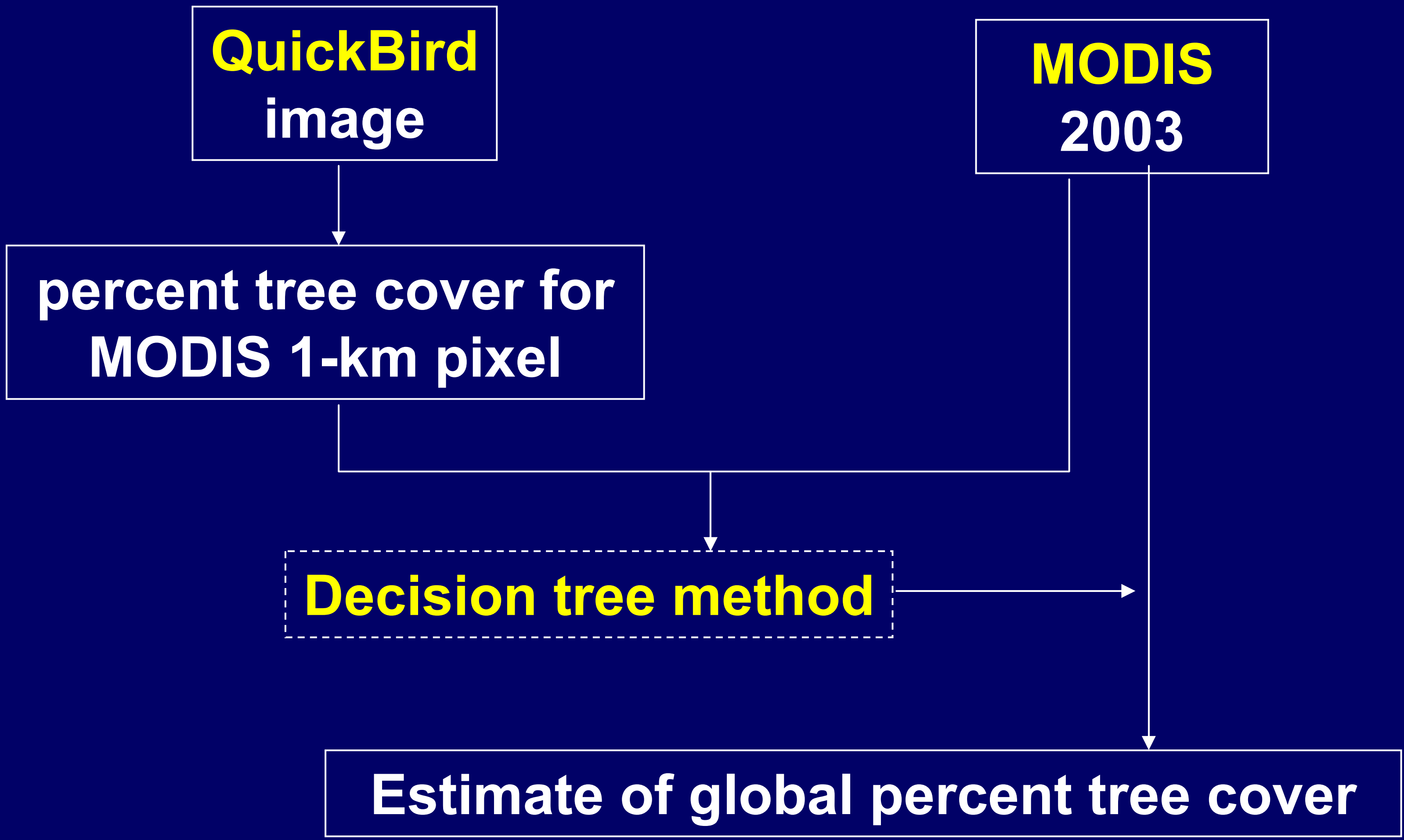

Methodology

Regression Tree

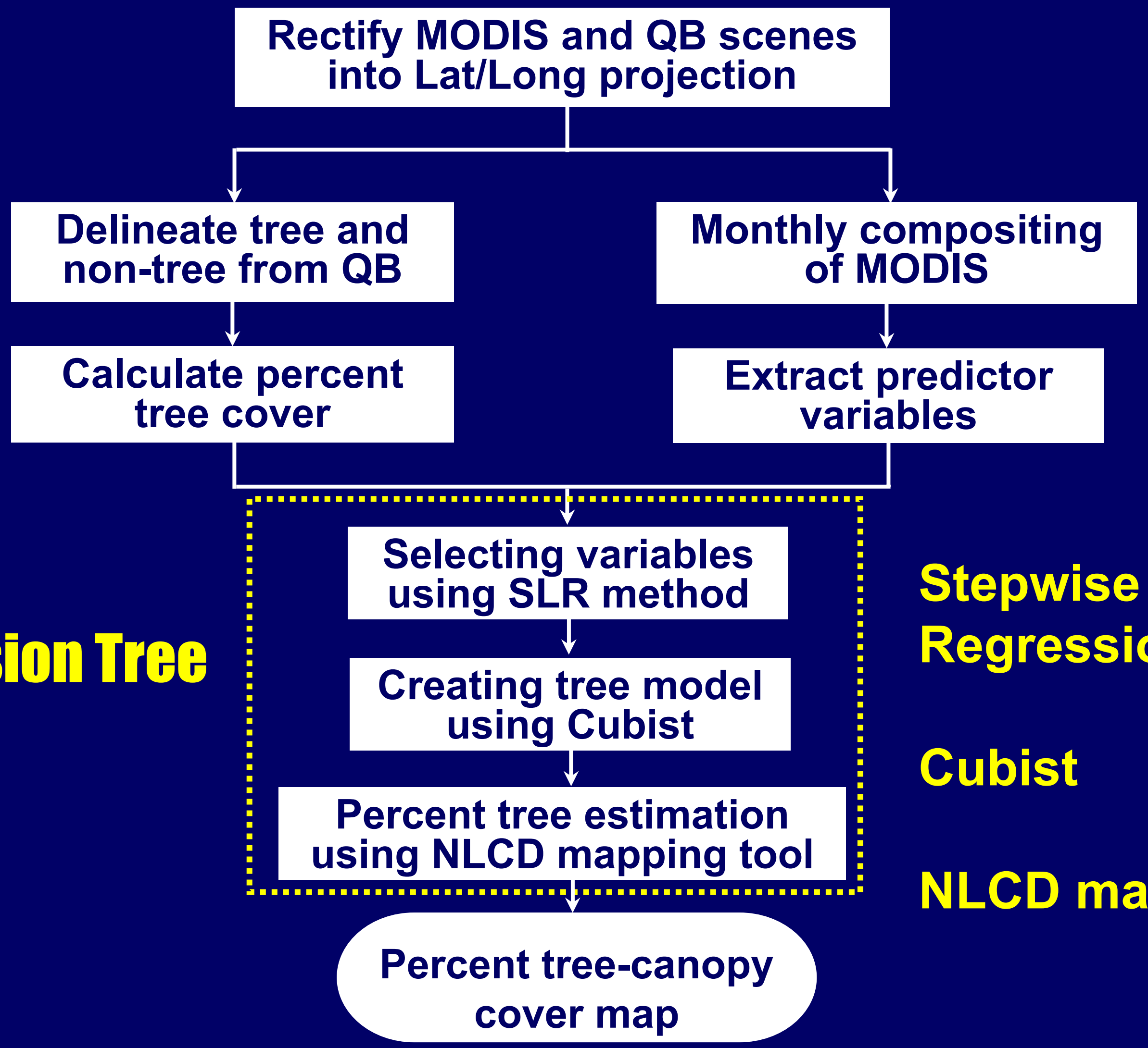

Stepwise Linear Regression (SLR)

Cubist

NLCD mapping tool

59 QuickBird images (5 by 5 km)

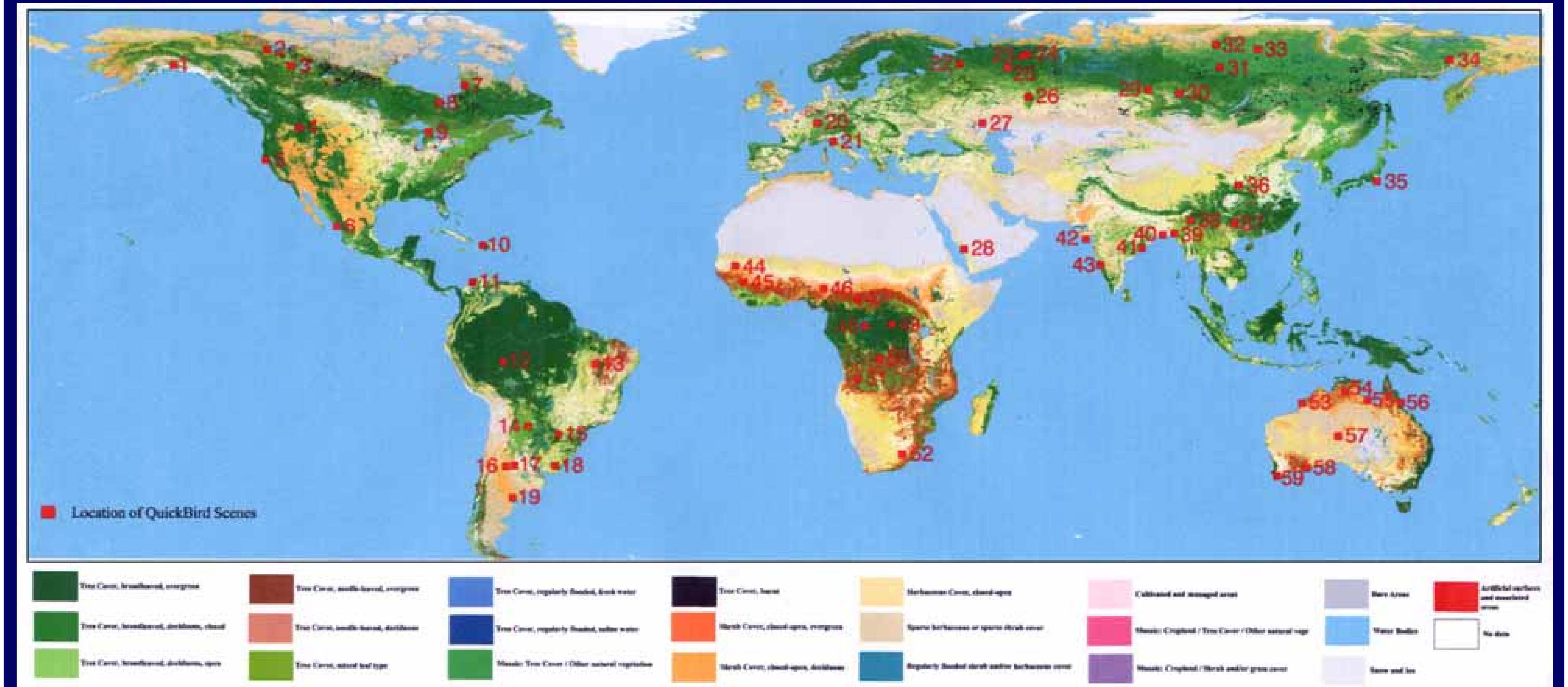

Some QB scenes for TD

no.1-Japan(Kisarazu)

no.2-Japan(Makuhari)

no.6-Bangladesh

no.12-Kazakhstan

no.13-Russia

no.21-Russia

Characteristic of QB scenes for TD

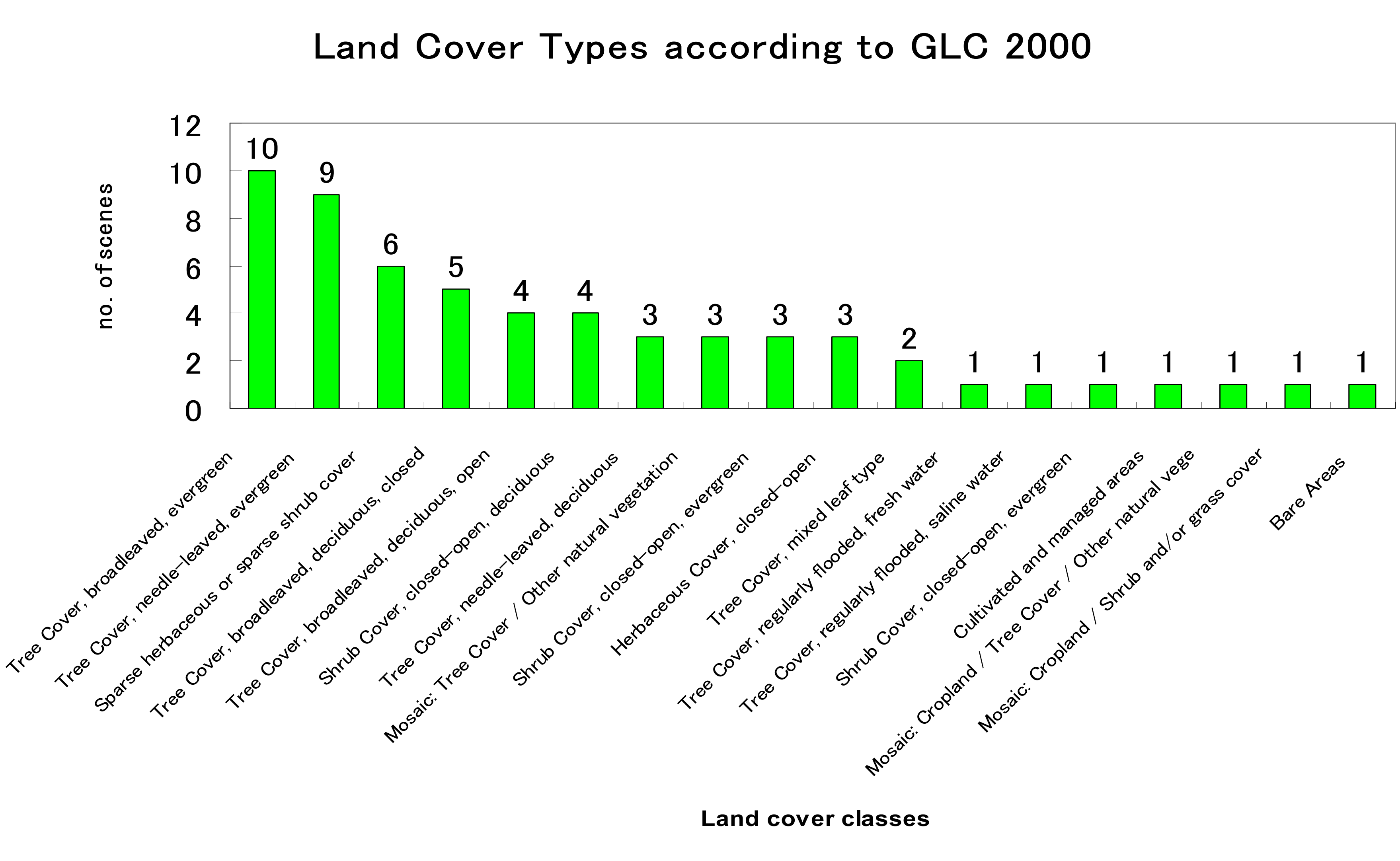

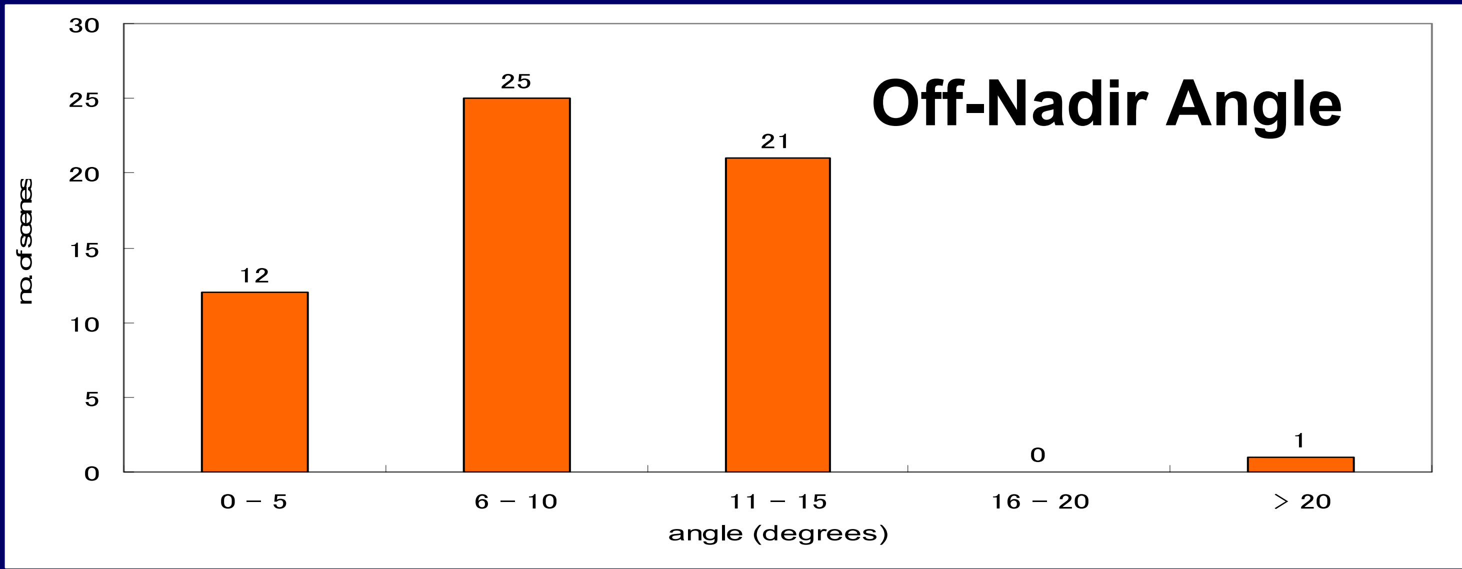
Off-Nadir Angle
no. of scenes
angle (degrees)
0 – 5
6 – 10
11 – 15
16 – 20
> 20
12
25
21
0
1
0
5
10
15
20
25
30

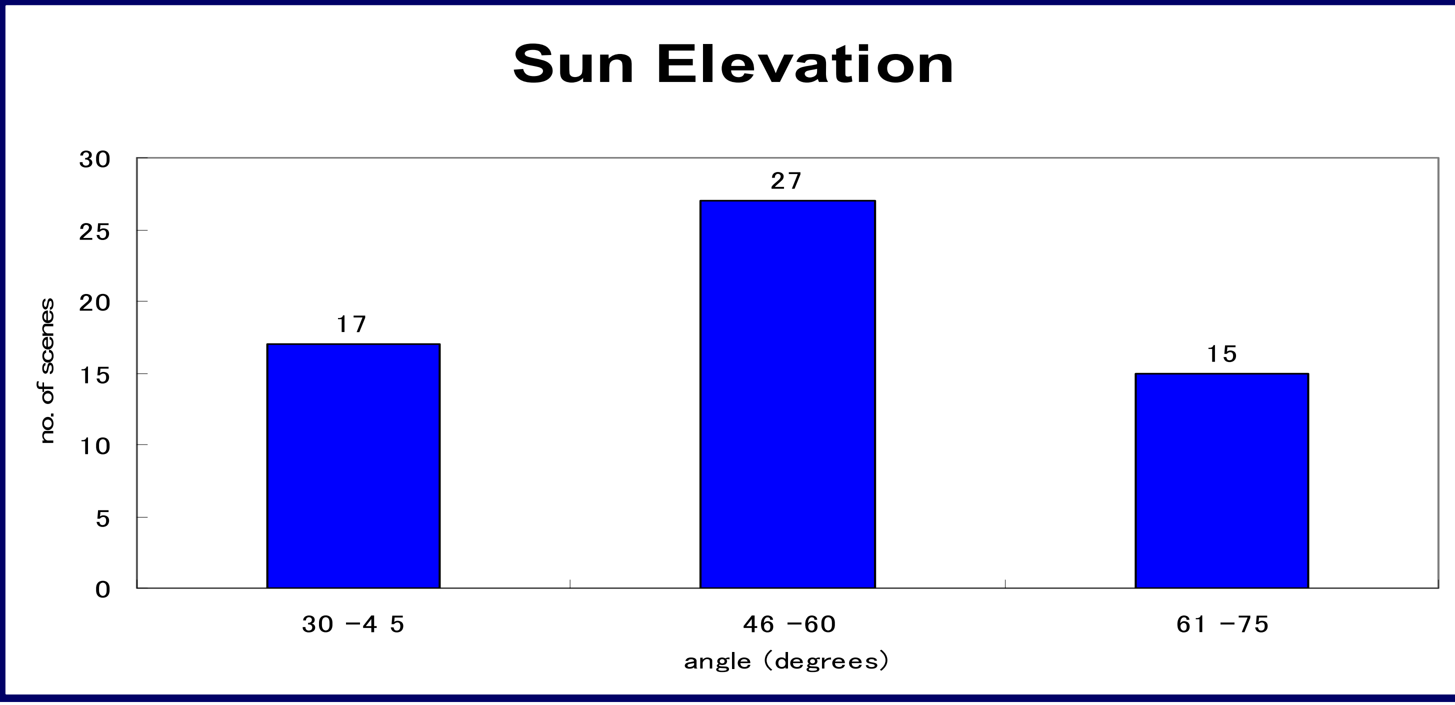
Sun Elevation
no. of scenes
angle (degrees)
30 -4 5
46 -60
61 -75
17
27
15
0
5
10
15
20
25
30

QuickBird image with the grid of MODIS 1km pixel size

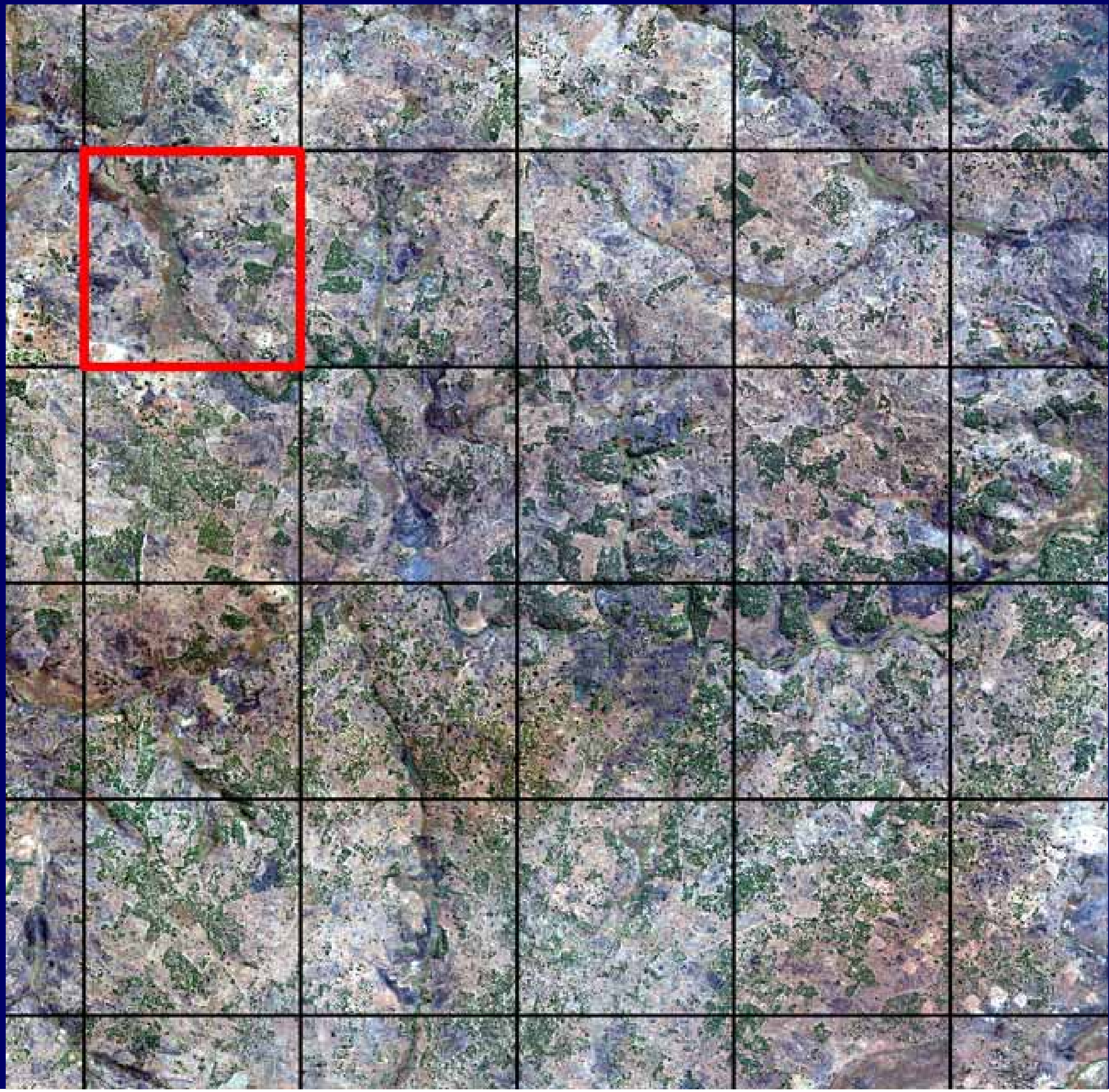

QuickBird image with percent tree cover for MODIS 1km pixel area

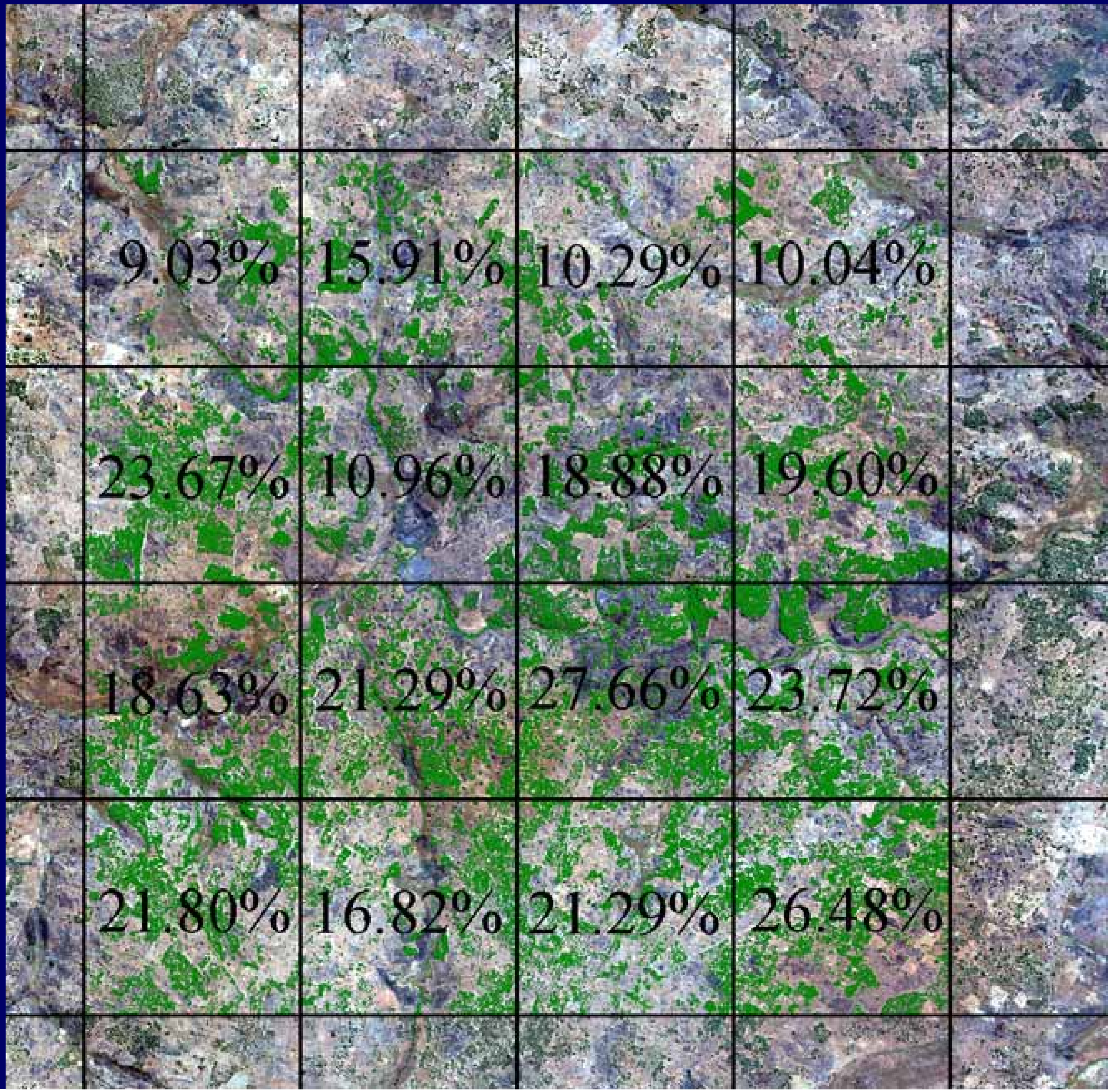

MODIS 2003

Predictor Variables
(Extracted from MODIS)

- Surface Reflectance: band 1 - 7,
- NDVI: band1 and band 2,
- EVI (Enhanc. Veg. Index): band 1, band 2 and band 3,
- NDSI (Norm. Diff. Soil Index): band 2 and band 6,
- LST (Land Surf. Temp.)-LST Day & Night: band 20, 22, 23, 29, 31 and 32.

Selecting Predictor Variables

Based on *Cp* statistics, *the higher Cp means the more relevance variables*:

$$Cp = p + \frac{(n-p)(s_p^{\,2} - \boldsymbol{\sigma}^2)}{\boldsymbol{\sigma}^2}$$

n: number of observations,

p : number of coefficients (number of explanatory variables plus 1),

$s_p^{\,2}$: mean square error of this *p* coefficient model,

$\boldsymbol{\sigma}^2$: the best estimate of the true error

Tree model by Cubist

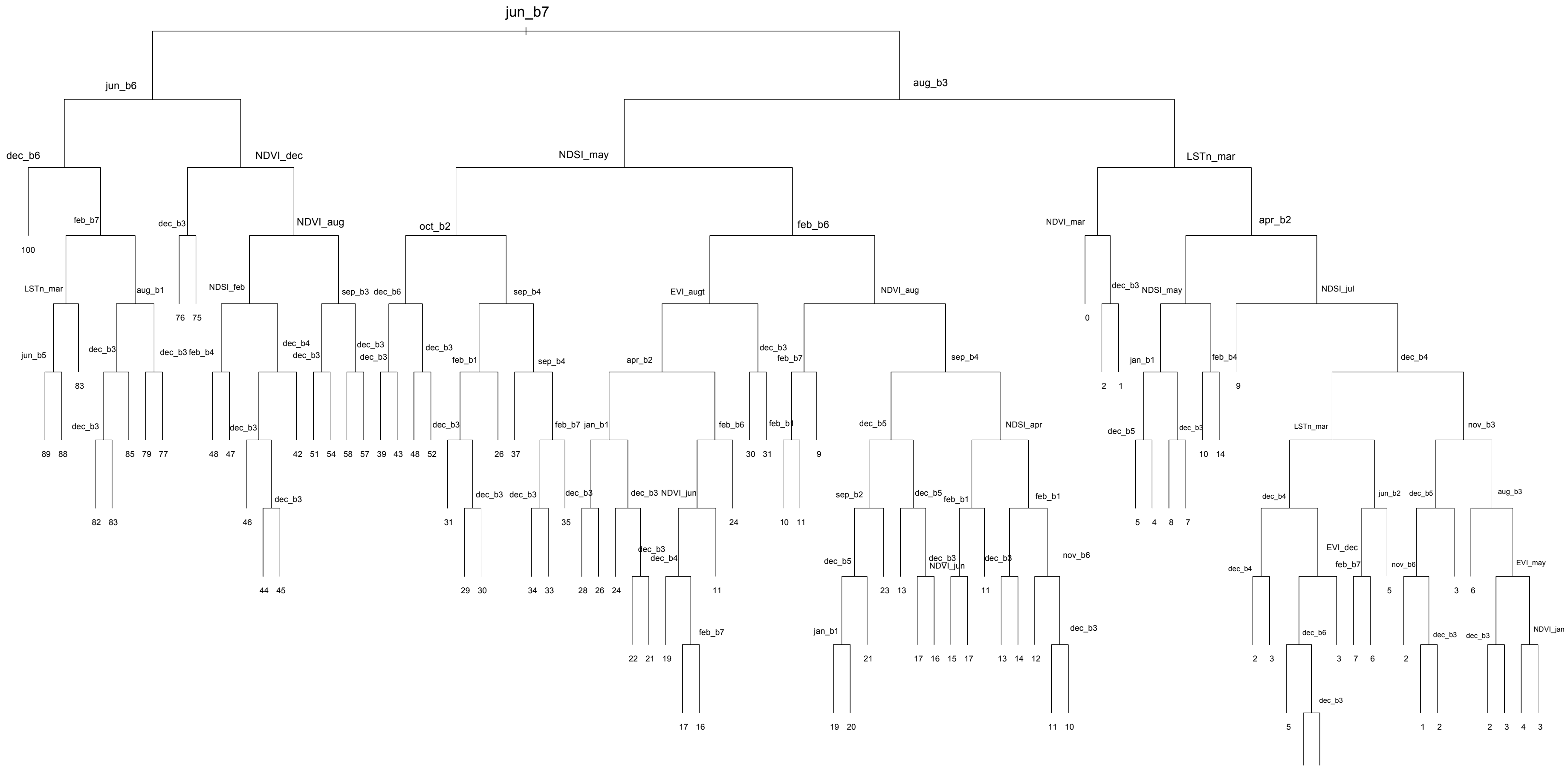

Estimated percent tree cover by MODIS and QuickBird

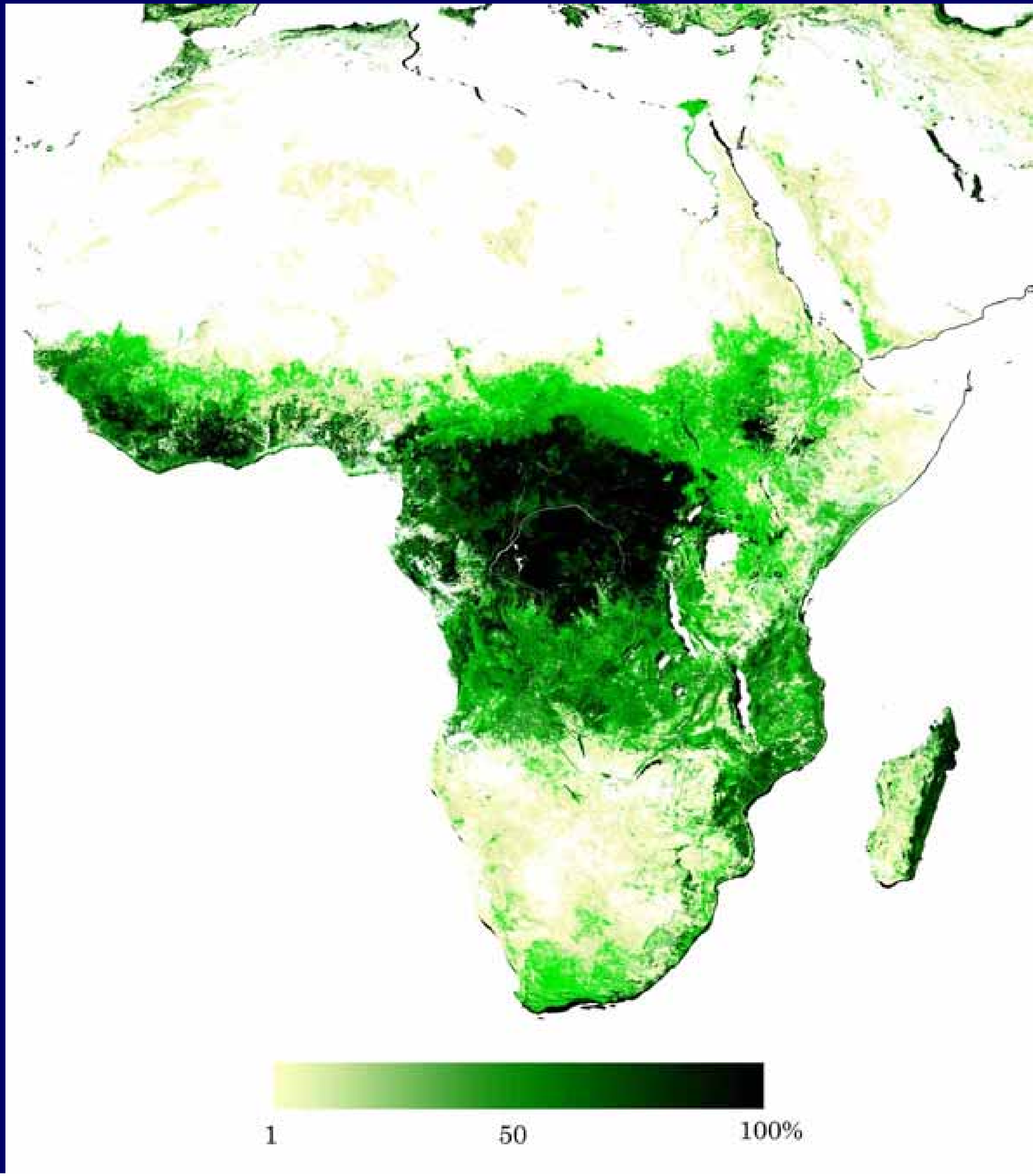

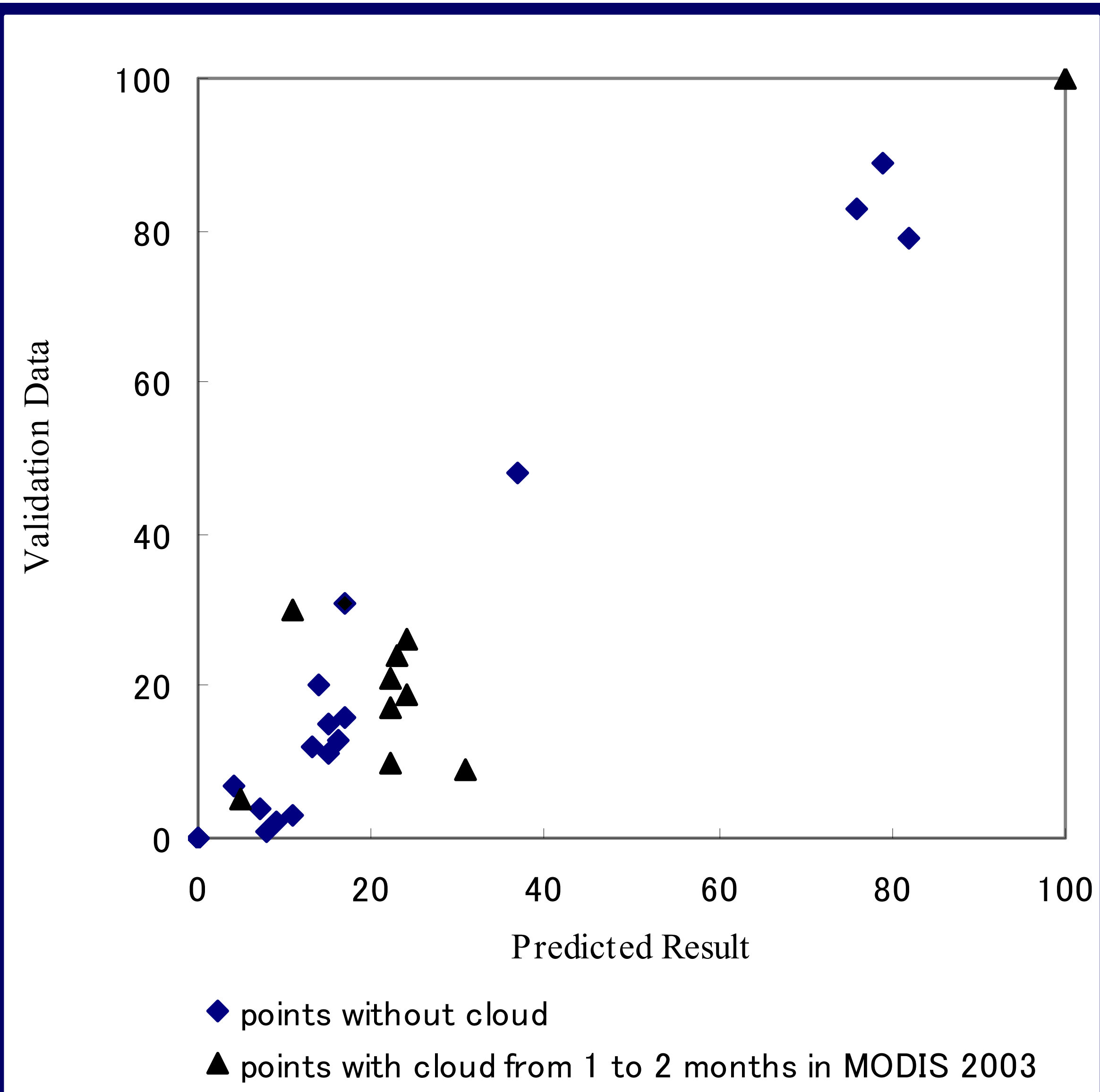

Scatter plot depicts comparison between predicted result and validation data derived from QuicBird

Accuracy assessment

Case	Predictor Variables	Prediction Errors (%)	Correlation Coefficients (R^2)
1	All variables	3.44	0.956
2	Surface reflectance variables	7.50	0.731
3	SLR-selected variables	1.60	0.959

Validation points: 25 % of all ground truth points (126 points)

Land use

Land use

purpose	area
model of land use change	local/regional
environmental analysis	local/regional/global

global land use mapping

- need harmonization
  "land use" version of "LCCS"
- challenge
  global mapping of agricultural land

Conclusion

- Global Mapping is on going to complete global land area coverage by 2007 with the participation of 153 NMOs in the world.
- New scheme to develop land cover data “GLCNMO” has started as part of GM by the cooperation with NMOs.
- Percent tree cover will be produced as GM version 2 by 2007.
- Needs more investigation for global land use mapping.

Ryutaro Tateishi

Thank you

11th CEReS Symposium Session 3
Land Cover and Climate Change

Atmospheric Change, Radiation Change, and the Terrestrial Carbon Cycle

Dennis G. DYE　デニス　ダイ
Hideki KOBAYASHI　小林　秀樹

地球環境フロンティア研究センター
Frontier Research Center for Global Change
Ecosystem Change Research Program
Yokohama, Japan

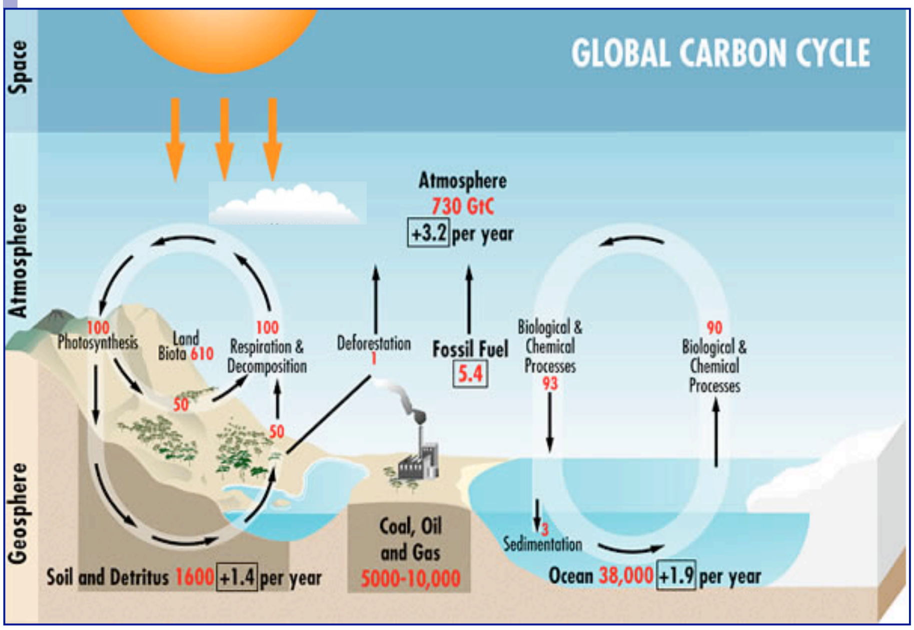

"Greenhouse Effect and Climate Change", BOM, Australia

Photosynthetically Active Radiation (PAR)

- 400-700 nm wavelength
- Delivers energy used in photosynthesis
- Key variable in carbon cycle models

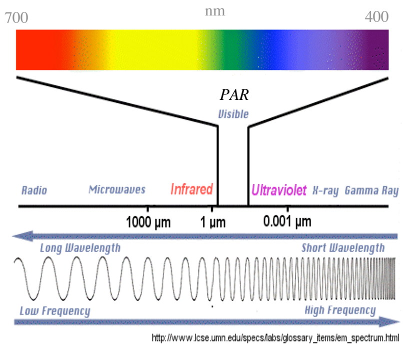

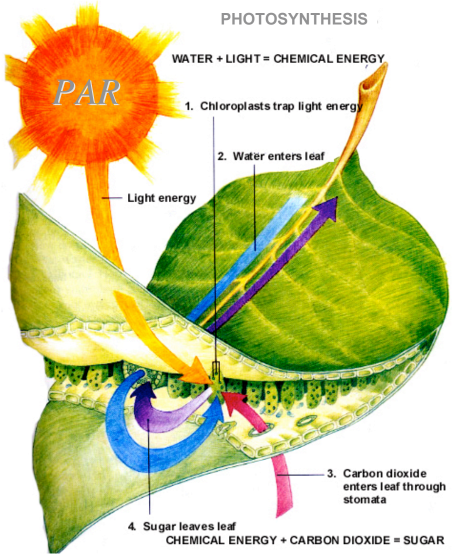

Current Challenges

- Empirical & model-based process studies
- Proposed Global Observation System for PAR

- ***Insufficient understanding***
  - **How does a changing radiation regime influence vegetation photosynthesis, productivity, and terrestrial carbon source/sink dynamics?**
- ***Insufficient Data Availability***
  - ***In situ* PAR data are rare**
  - **No operational, observation-based, global-coverage PAR data source for land**
    - Important for accurate modeling of terrestrial C cycle

Sources of Change in Solar Radiation & PAR at the Earth's Surface

- Aerosols
- Clouds

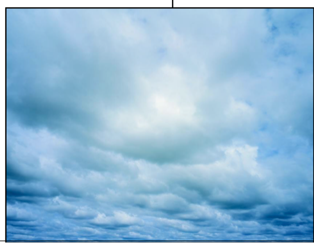

Evidence of Change

Satellite-observed Trend in Global Average Solar Irradiance at Surface

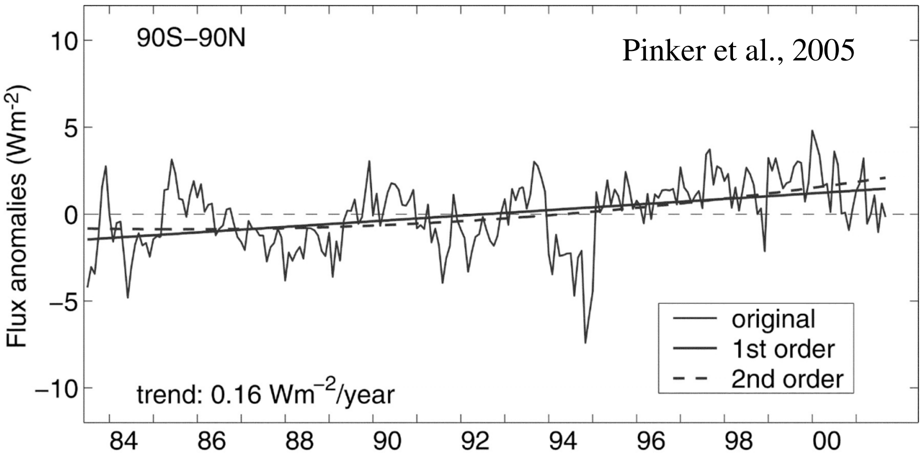

Evidence of Change

Annual Mean Solar Irradiance in Japan from Surface Measurements, 1960-2003

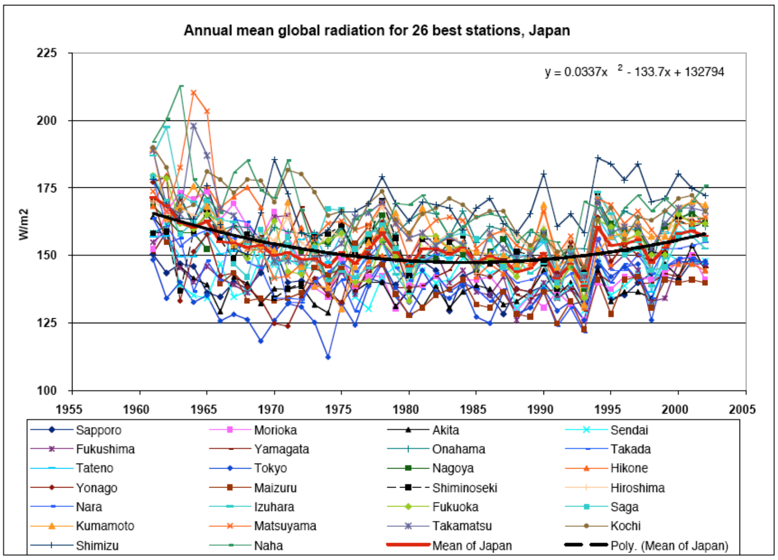

Wild et al., 2005

Evidence of Change

From Global Dimming to Global Brightening: Changes in Solar Irradiance after 1990

Measurements from Baseline Surface Radiation Network (BSRN)

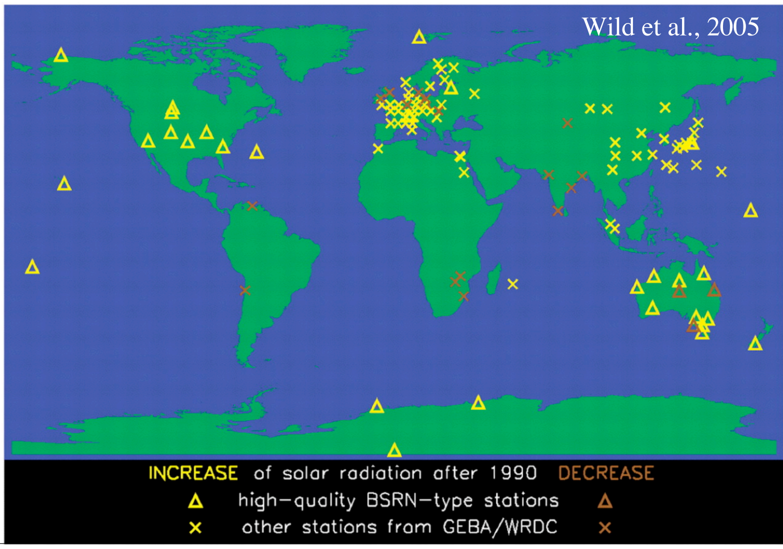

Underlying Factors for Observed Trends

- Pre-1990 "Dimming"
  - **Increased aerosol loads (air pollution)**
  - **Increased cloudiness**
- Post-1990 "Brightening"
  - **Reduced cloudiness**
  - **Reduced aerosol loads (Wild, 2005)**
    - Enhanced air pollution control
    - Curtailed economic/industrial activity with breakup of Soviet Union

Effects of Changing Atmospheric Conditions Surface Irradiance

- Solar radiation and PAR may be altered with respect to:
  - **Amount and intensity**
  - **Source geometry (sky radiance distribution & diffuse:beam ratio)**
  - **Spectral composition**
- Such changes have implications for
  - **Vegetation photosynthesis & carbon cycle**
  - **Surface energy budget, global warming & water cycle**
    - Global dimming correlated in decline in pan evaporation (Roderick, 2005)

Significance of Change

CO_2 uptake by forest is enhanced under cloudy skies (diffuse PAR)

Results from eddy covariance for boreal forest
Goulden et al., 1997

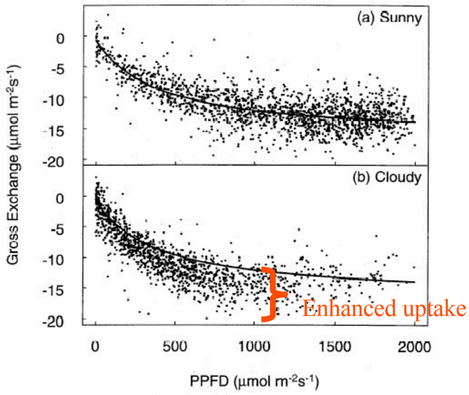

Figure 8. Gross CO_2 exchange as a function of incident photon flux density (PPFD) for (a) sunny periods (below-canopy PPFD/above-canopy PPFD < 0.12) and (b) cloudy periods (below/above > 0.12). Points are half-hour intervals from June 9 to September 17 of all 3 years when the air temperature was greater than 14°C, $u^* > 0.20$ m s^{-1}, and wind from a suitable direction. The best fit for the sunny periods is replicated on each panel to allow comparison (GEE (μmol m^{-2} s^{-1}) = $-0.8 + (-15.7$ PPFD)/(389.9 + PPFD); n = 1650, quantum yield as PPFD approaches 0 is 0.040 mol CO_2 mol^{-1} photons). The best fit line (not shown on plots) for cloudy periods was GEE (μmol m^{-2} s^{-1}) = $-0.4 + (-16.9$ PPFD)/(258.0 + PPFD); n = 1250.

Response of Daily Canopy Photosynthesis to Diffuse PAR

- For LAI=6, daily net photosynthesis increases by ~11% as diffuse fraction increases from 0.2 to ~0.6
- Results from:
  - **Sun-shade model of canopy photosynthesis (de Pury & Farquhar, 1997)**
  - ***in situ* PAR data for Sri Samrong, Thailand**

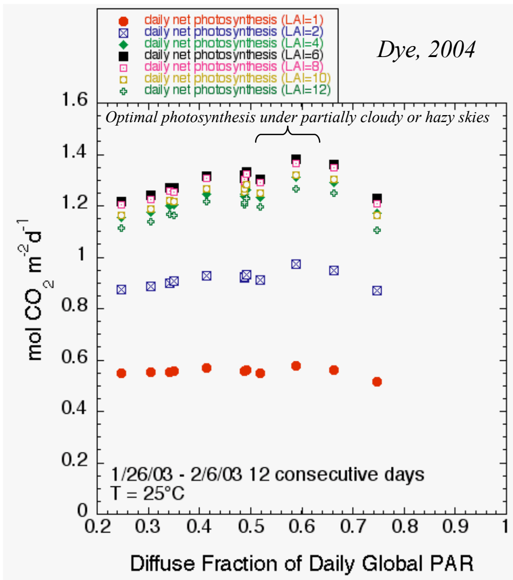

Significance of Change

No consensus on role of diffuse PAR in terrestrial C source/sink dynamics

Significant

- Goulden et al., 1997
- Healey et al., 1998
- Roderick, 2001
- Gu et al., 2003
- Farquhar & Roderick, 2003
- Robock, 2005
- *et al.*

Insignificant

- Nemani et al., 2003
- Krakauer & Randerson, 2003
- Angert et al., 2004
- *et al.*

• **Many results are highly MODEL DEPENDENT**

Improving Fundamental Understanding

Atmospheric Effects on PAR

- PAR may be altered with respect to:
  - **amount and intensity**
  - **source geometry (diffuse fraction)**
  - **spectral composition**

How does diffuse PAR enhance LUE and photosynthesis?

Diffuse PAR under cloudy/hazy sky is efficiently distributed throughout canopy

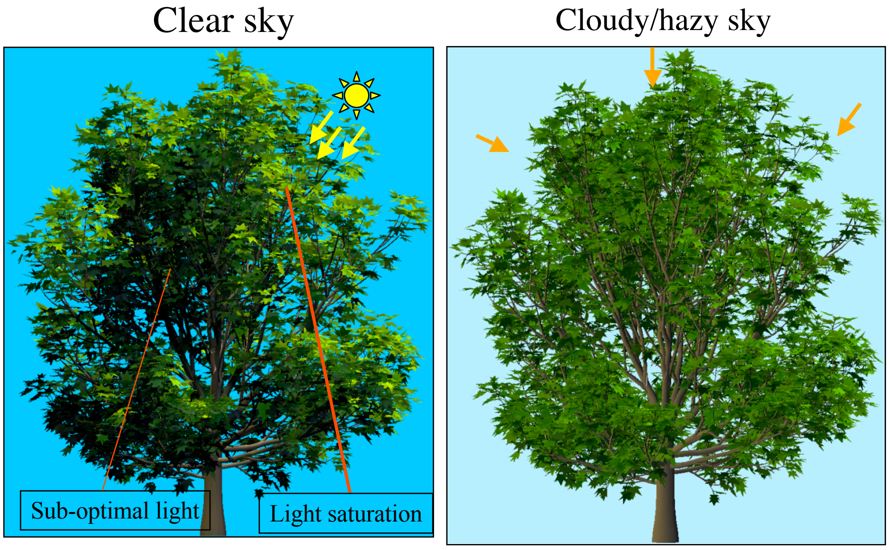

D. Dye, FRCGC

How does diffuse PAR enhance LUE and photosynthesis?

3-D Radiative Transfer Model of Forest Light Environment by Monte Carlo method (Canopy, Understory, Surface)

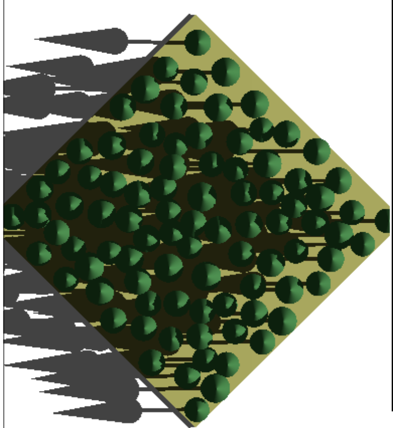

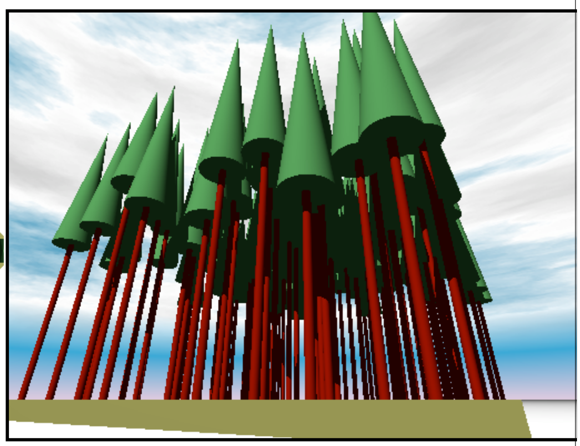

Forest Light Environment Simulator (FLiES)
H. Kobayashi, JAMSTEC-FRCGC

How does diffuse PAR enhance LUE and photosynthesis?

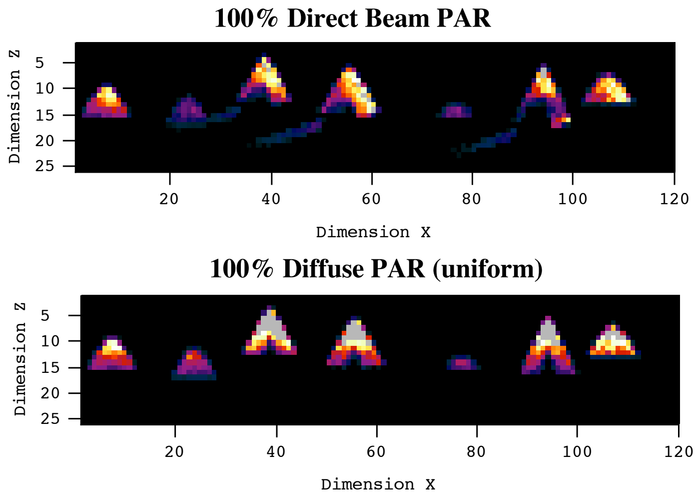

Diffuse PAR is efficiently distributed throughout canopy

H. Kobayashi JAMSTEC-FRCGC

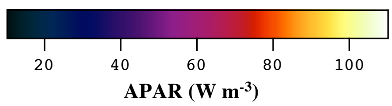

SZA = 40 deg.
Total PAR flux = 352 W m^{-2}
LAD (crown) = 0.56
Horiz. Resolution = 0.25 m
Vert. resolution = 1 m

Atmospheric Effects on PAR

- PAR may be altered with respect to:
  - **amount and intensity**
  - **source geometry (diffuse fraction)**
  - **spectral composition**

How Does Diffuse PAR Enhance Canopy Photosynthetic Rates?

- Existing knowledge:
  - **efficient distribution within canopy (less light saturation)**
- Our findings:
  - **Diffuse PAR has favorable spectral composition**
    - Scattering causes diffuse PAR spectrum to shift towards red [see figure -->]
    - Therefore **MORE PHOTONS RECEIVED PER UNIT ENERGY**

Dye, 2004, *J. Geophys. Res. -Atmospheres*

f = diffuse fraction of PAR

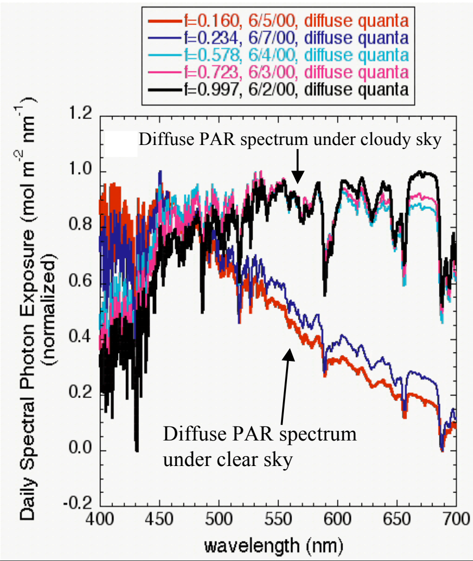

Scattering Increases Photon Content of Diffuse PAR Energy

Quanta-to-energy ratio (µmol/J)

Dye, 2004
JGR-Atmospheres

103 days, March-July, 2000

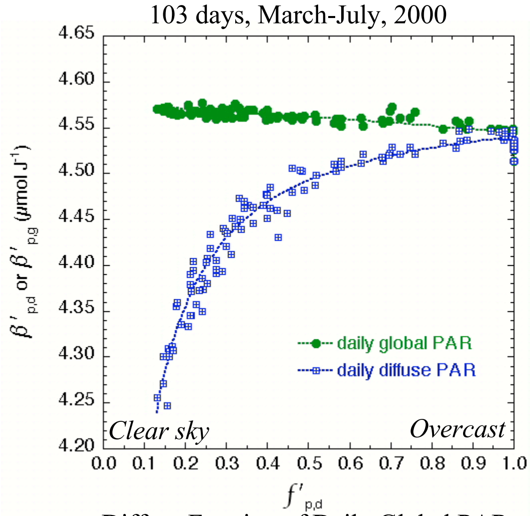

Diffuse Fraction of Daily Global PAR

Reliable Simulation and Interpretation of Terrestrial Carbon Source/Sink Dynamics Requires Adequate and Appropriate Treatment of Radiation-related Effects

- Example: Satellite-based modeling of Net Primary Production (NPP) in Amazonia

Investigating the Effects of Decreased Cloudiness on Photosynthesis in the Amazon Region

- Question
  - **Does accounting for diffuse radiation effects alter the conclusions of Nemani et al. (2003)?**
- Approach
  - **Sun-shade model of canopy photosynthesis (de Pury & Farquhar, 1997)**
  - **Diffuse & beam PAR data from NCEP/NCAR reanalysis (1982-2002)**

Results

- Decline in diffuse PAR associated with:
  - **lower canopy light use efficiency**
  - **lower rates of canopy photosynthesis**
- Simulated regional CO_2 uptake slightly *decreased* during 1981-2000
- Consistent with theory

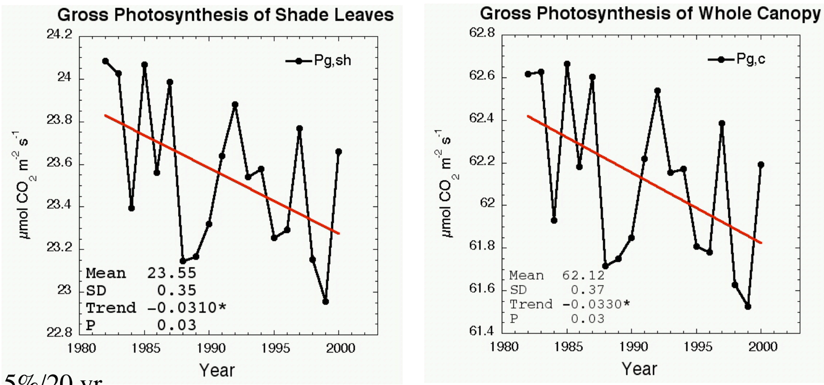

-2.5%/20 yr

Simulated with dePury & Farquhar's [1997] sun-shade model and PAR data from NCEP-NCAR Reanalysis.

Results

Average Diffuse Fraction of Global PAR Flux ($f_{p,d}$) during 1200-1800 GMT

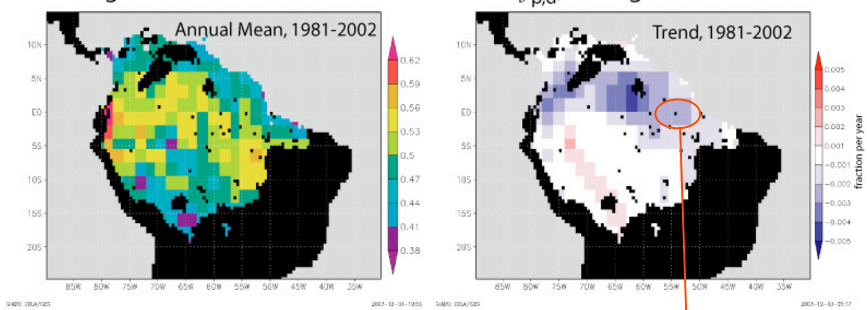

Region of declining diffuse PAR corresponds to sites with negative trends in annual biomass production from field observations

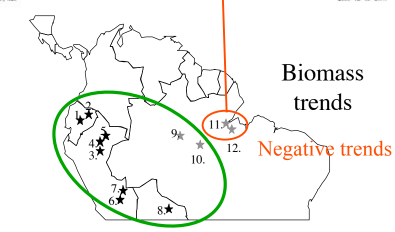

(Baker et al., 2004, *Phil. Trans. Roy. Soc. Lon.)*

Dye, 2004

Problem:
Insufficient PAR data

- Accurate modeling and monitoring of terrestrial carbon cycle requires accurate PAR data
- Current sources of PAR data are inadequate
  - PAR estimated from total shortwave irradiance (common approach) have large errors
  - Diffuse and direct-beam PAR are rarely available
  - Ground-based PAR datasets are also rare

Potential Solution:
Establishment of a Global Observing System for PAR (GOSPAR)

- Comprehensive strategy for improving availability and quality of satellite- and ground-based PAR data
- Potential contribution to GEOSS (Global Earth Observing System of Systems)

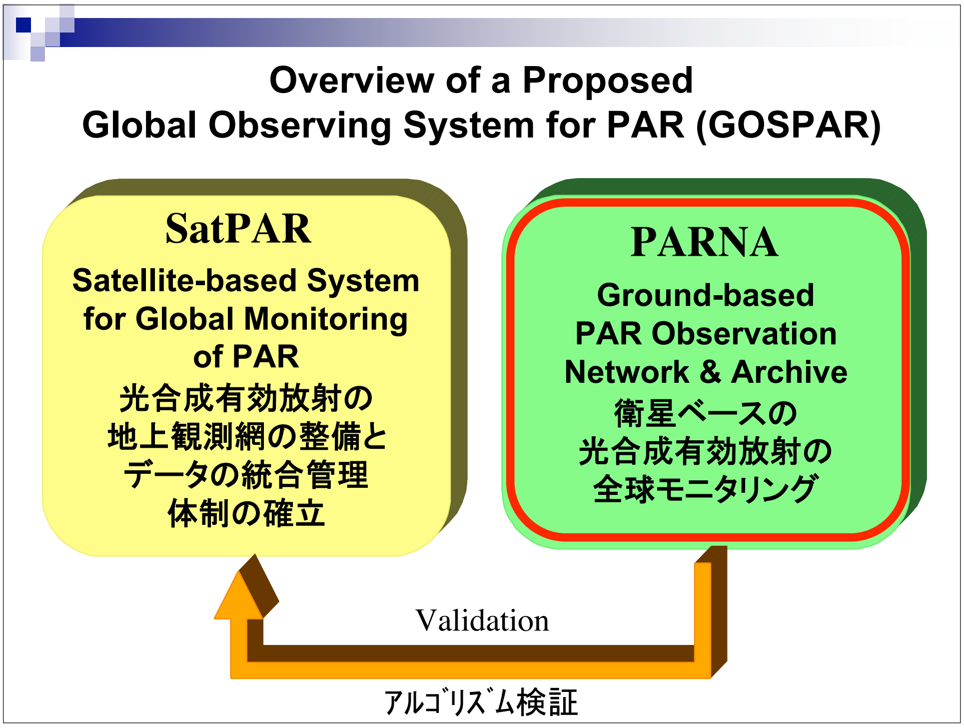
Overview of a Proposed
Global Observing System for PAR (GOSPAR)
SatPAR
Satellite-based System for Global Monitoring of PAR
光合成有効放射の
地上観測網の整備と
データの統合管理
体制の確立
PARNA
Ground-based PAR Observation Network & Archive
衛星ベースの
光合成有効放射の
全球モニタリング
Validation
ｱﾙｺﾞﾘｽﾞﾑ検証

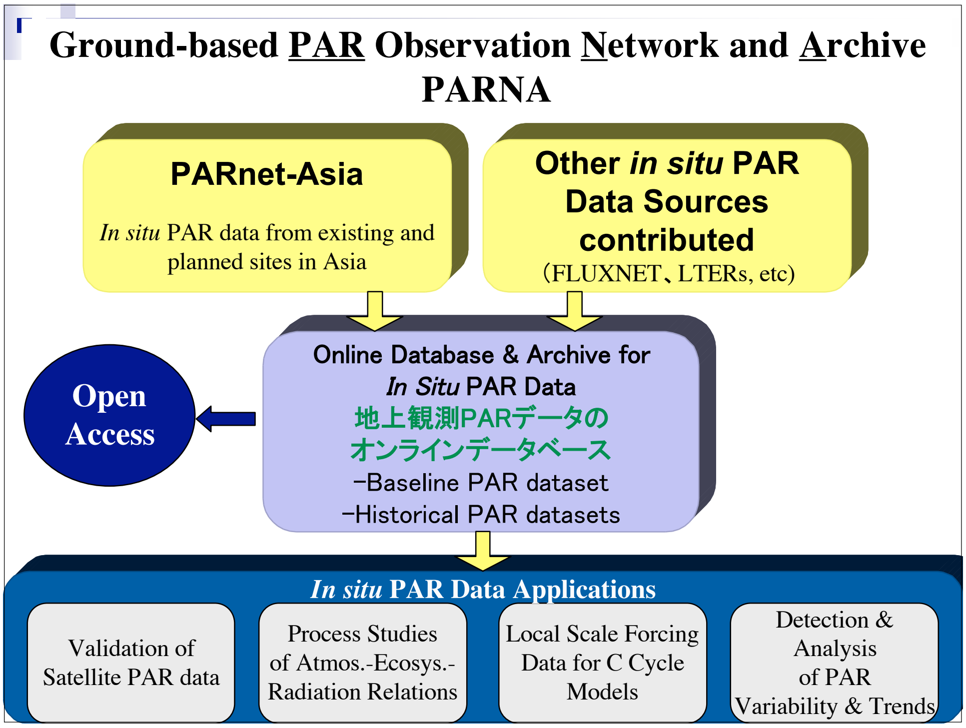
Ground-based PAR Observation Network and Archive
PARNA
PARnet-Asia
In situ PAR data from existing and planned sites in Asia
Other in situ PAR Data Sources contributed
(FLUXNET、LTERs, etc)
Online Database & Archive for In Situ PAR Data
地上観測PARデータの
オンラインデータベース
−Baseline PAR dataset
−Historical PAR datasets
Open Access
In situ PAR Data Applications
Validation of Satellite PAR data
Process Studies of Atmos.-Ecosys.-Radiation Relations
Local Scale Forcing Data for C Cycle Models
Detection & Analysis of PAR Variability & Trends

PAR観測ネットワーク (PARnet-Asia)

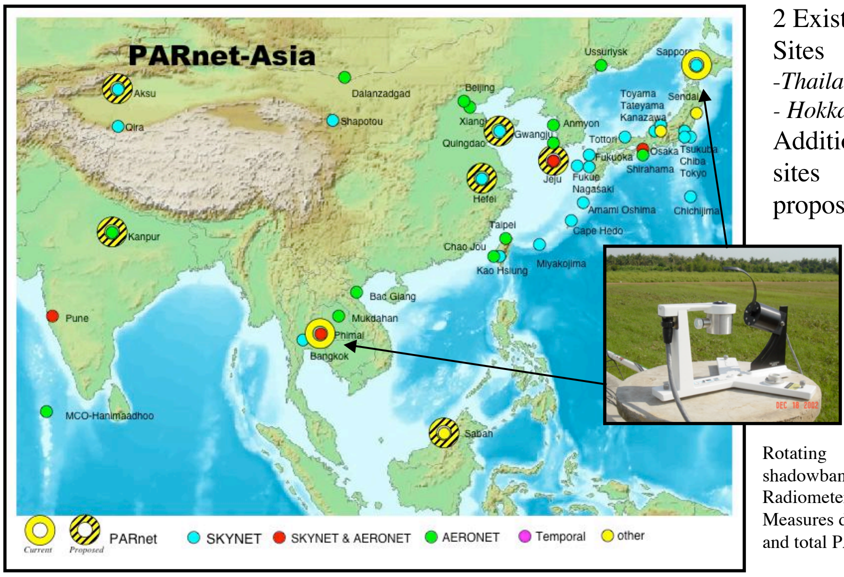

2 Existing Sites
-Thailand
- Hokkaido
Additional sites proposed

Rotating shadowband Radiometer (RSS) Measures diffuse and total PAR

Measured Diurnal Variation in Total & Diffuse PAR at Sri Samrong, Thailand, June 2-7, 2003

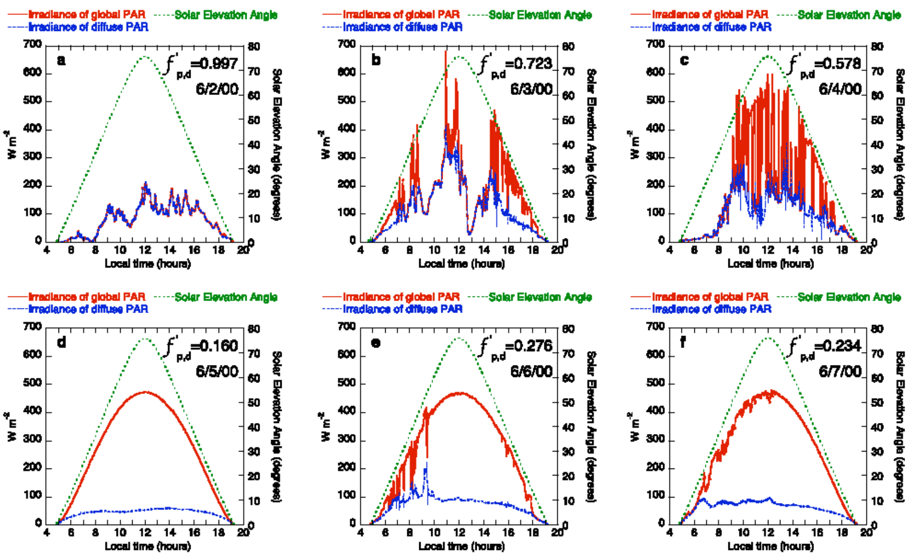

Overview of Proposed Global Observing System for PAR (GOSPAR)

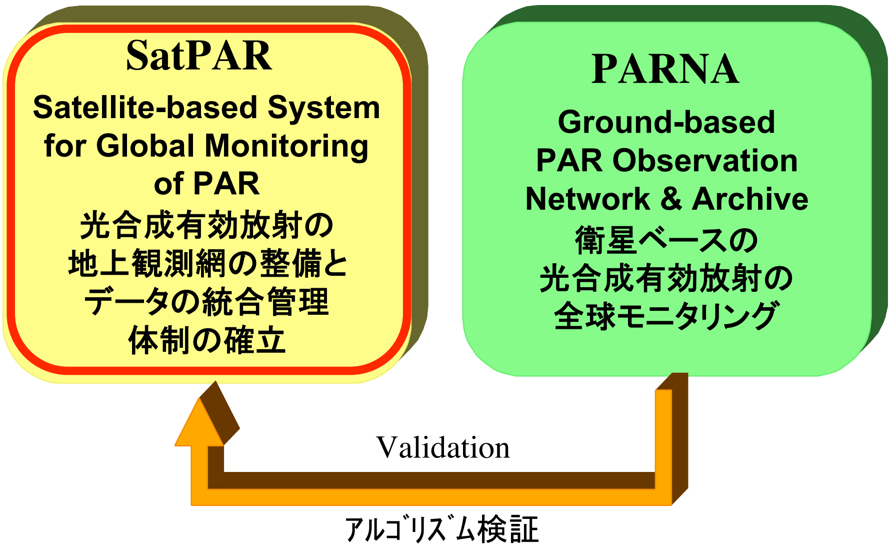

Desired Features of Satellite-based PAR data for Improved Carbon Cycle Modeling

- **Separate data for direct beam and diffuse fluxes**
- Quantum units (μmol m^{-2} s^{-1})
- High spatial resolution (1-10 km)
- High temporal resolution (3 hrly - daily)
- Global coverage of land areas
- Routine data product
- Continuous, multi-year time-series

Application of Satellite PAR to Carbon Cycle Monitoring

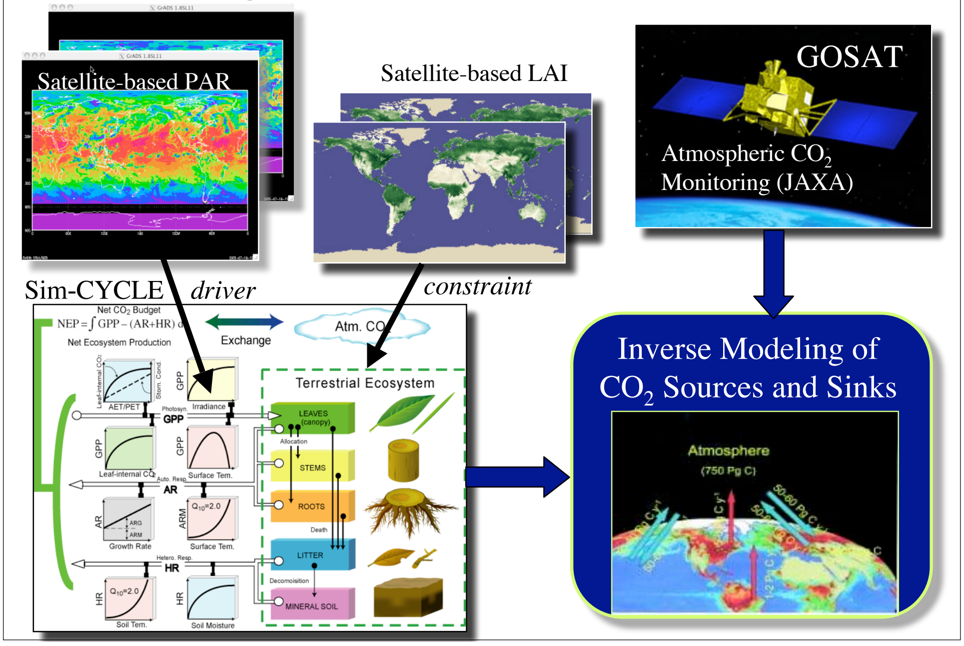

Early results combining Sim-CYCLE with 3-hrly PAR data (diffuse & beam) from GEWEX-SRB

A. Ito
D. Dye
JAMSTEC-FRCGC

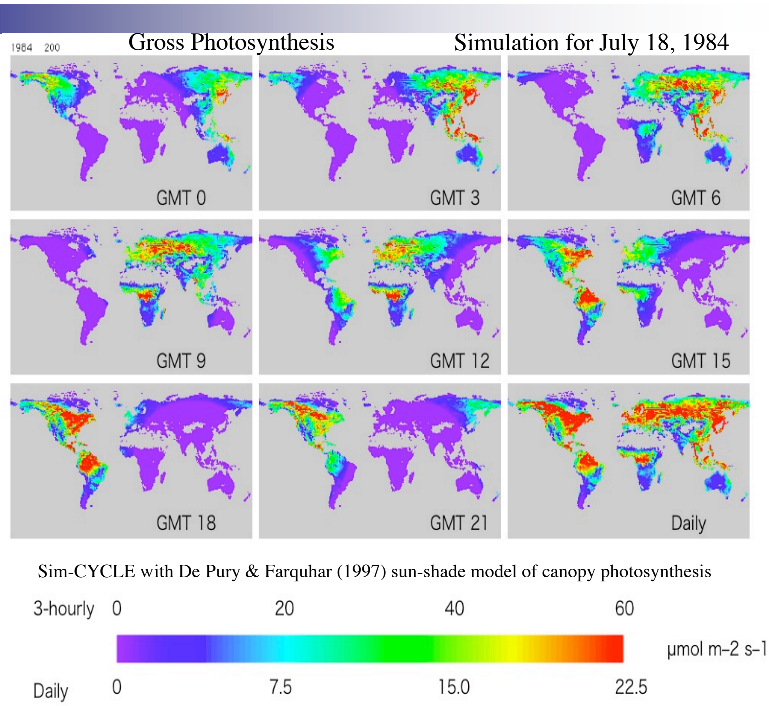

Conclusions

- Improved certainty in terrestrial carbon cycle modeling requires accounting for effects of changing atmospheric conditions on quality & quantity of PAR

- Improved availability of satellite-based and *in situ* PAR data sources are needed
  - **Trend detection**
  - **Simulation and validation**
- Proposed Global Observing System for PAR (GOSPAR) will address these needs

The 11th CEReS International Symposium on Remote Sensing

Satellite active and passive microwave sensing of sea ice in the Okhotsk Sea

Leonid M. Mitnik, Vyacheslav Dubina, and Maia Mitnik

V.I. Il'ichev Pacific Oceanological Institute
Far Eastern Branch, Russian Academy of Sciences

43 Baltiyskaya St., 690041, Vladivostok, Russia
Phone: 07.4232.312854, fax: 07.4232.312573 E-mail: mitnik@poi.dvo.ru

14 December 2005

Outlines

1. Introduction
2. Passive microwave sensing. Simulation of brightness temperatures over sea ice
3. Active microwave sensing
4. Sensors (SAR, ASAR, SeaWinds, AMSR, AMSR-E), supplementary satellite and *in situ* data
5. Sea ice on ERS-2 SAR and Envisat ASAR images
   - 5.1. Aniva Bay
   - 5.2. Northern and Western Okhotsk Sea
   - 5.3. Eastern Okhotsk Sea
6. Conclusions

Introduction

The importance of studying the sea ice, as well as atmospheric and oceanic parameters and processes in the open ocean and in the Marginal Ice Zone (MIZ) is due to scientific and practical requirements.

The large heat and salt fluxes associated with polynyas and thin ice area play an important role in air/sea interaction. Air-sea interaction is particularly intense in the MIZ, resulting in abrupt horizontal and vertical gradients of hydrometeorological parameters which promote formation of various mesoscale structures both in the atmosphere (convective rolls and cells) and in the ocean (ice edge waves, ice streets, bands and eddies).

Accurate estimation of their area and ice thickness will allow to improve the large-scale ice mass balance and the oceanic salt production.

Passive microwave sensing

Satellite passive microwave measurements of brightness temperatures $T_B(\nu)$ have been used for sea ice, wind speed, SST, atmospheric water vapour content V and total cloud liquid water content Q and precipitation studies. The changes of the sea surface emissivity caused by variations of water temperature and salinity and wind action can be estimated reasonably well.

Over the compact ice cover **and** ***over marginal ice zone,*** **variations of $T_B(\nu)$ are due to the change of sea ice concentration C (from 0.0 to 1.0), types of sea ice, the evolution of snow/sea-ice thermophysical properties including** ***liquid water presence*** **in the system, snow pack density and snow grain metamorphism, air temperature and wind. V and Q retrieval presents a difficult problem due to the larger values and higher variability of the underlying surface emissivity compare to the water surface.**

Simulation of the AMSR brightness temperatures

Modeling of microwave measurements over the open ocean, the MIZ and compacted ice was carried out with a microwave radiative transfer program. The program allows to compute the brightness temperatures of the underlying surface-atmosphere system $T_B^{V,H}(\nu)$ at frequency ν with the vertical (V) and horizontal (H) polarizations. The radiosonde (r/s) database was built up to model atmospheric conditions observable near and over the MIZ. Total 478 r/s with SST $t_S \leq 1°C$ were selected: 69 sets from research vessels and 409 sets from 6 polar coastal and island stations. Every set consists of radiosonde, meteorological data (wind speed W and direction, forms and amount of clouds) and t_S values. In the database, the water vapor content V = (0.63-18.5) kg/m^2, cloud water content $Q \leq 0.25$ kg/m^2 and wind speed $W \leq 18.0$ m/s. R/s atmospheric profiles were complimented by the cloud liquid water content profiles. For each r/s, the T_Bs(ν) were computed for unifrmly distributed values of sea ice concentration C = 0.0 - 1.0.

$$T_B^{V,H}(\nu,\theta) = T_{Bocean}^{V,H}(\nu,\theta)e^{-\tau(\nu,\theta)} + T_{Batm}^{\uparrow}(\nu,\theta) + T_{Batm}^{\downarrow}(\nu,\theta)[1-\kappa^{V,H}(\nu,\theta)]e^{-\tau(\nu,\theta)} + T_C[1-\kappa^{V,H}(\nu,\theta)]e^{-2\tau(\nu,\theta)}$$

- brightness temperature of the atmosphere-underlying surface system with vertical (*V*) and horizontal (*H*) polarization as a function of frequency ν and incidence angle θ.

$T_{Bocean}^{V,H}(\nu,\theta) = \kappa^{V,H}(\nu,\theta)T_S$ is the brightness temperature of the underlying surface, *T*s is surface temperature .

$\kappa^{V,H}(\nu,\theta,t_S,W)$ is emissivity of the surface

$\tau(\nu,\theta)$ is integral absorption of the atmosphere

$T_{Batm}^{\uparrow}(\nu,\theta)$ is the upwelling brightness temperature of the atmosphere

$T_{Batm}^{\downarrow}(\nu,\theta)$ is the downwelling brightness temperature of the atmosphere

T_c is brightness temperature of cosmic radiation

Emissivity

For each radiosonde, the brightness temperatures T_Bs(ν) were computed for 10 values of sea ice concentration C = 0.0 - 1.0. The emissivity of the underlying surface $\kappa^{V,H}$ was determined by Eq. 1

$$\kappa^{V,H}(\nu,\theta,t_S,W) = \kappa_W{}^{V,H}(\nu,\theta,t_S,W)(1 - C) + \kappa_I{}^{V,H}(\nu,\theta, t_I)\, C\,, \quad (1)$$

where κ_W and κ_I are sea surface and sea ice emissivity, correspondingly, t_S is sea surface temperature, W is wind speed, t_I is temperature of ice surface .

Emissivity of the calm sea surface at frequencies ν = 18.7, 23.8 and 36.5 GHz was computed from the Fresnel formulas [*Ellison et al., Radio Sci., 1998***] . Increments of emissivity associated with the wind action were found on the basis of experimental data [***Rosenkranz, 1992; Sasaki et al., 1987; Wentz, 1992***].**

Emissivity of calm water and sea ice at $\theta = 55°$

Frequency, GHz (polarization)	18.7 (V/H)	23.8 (V/H)	36.5 (V/H)
Water (t_S = -0.6°C) [1]	0.6358/0.2825	0.6685/0.3045	0.7332/0.3524
Dark nilas [2]	0.76/0.67	0.76/0.67	0.80/0.77
Gray nilas [2]	0.84/0.80	0.85/0.82	0.88/0.84
Light nilas [2]	0.95/0.89	0.96/0.91	0.97/0.94
First-year ice (*no melting*) [2] Thick first-year ice [4]	0.95/0.91 0.97/0.90	0.945/0.91	0.94/0.90 0.97/0.90

1. *Ellison et al., 1998*; 2. *Eppler et al., 1992*; 3. *Svendson et al., 1987*;
4. *Harouche, I.P-F. and D.G. Barber (2001)*

Emissivity of new ice, nilas and water

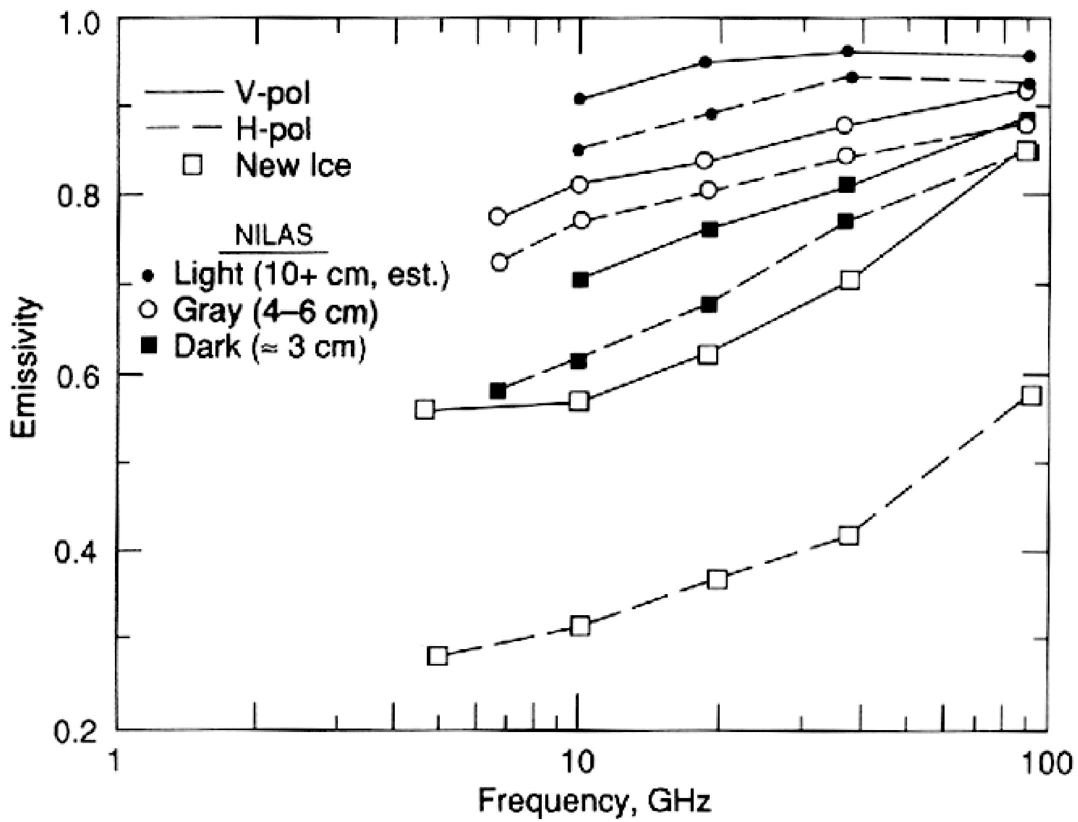

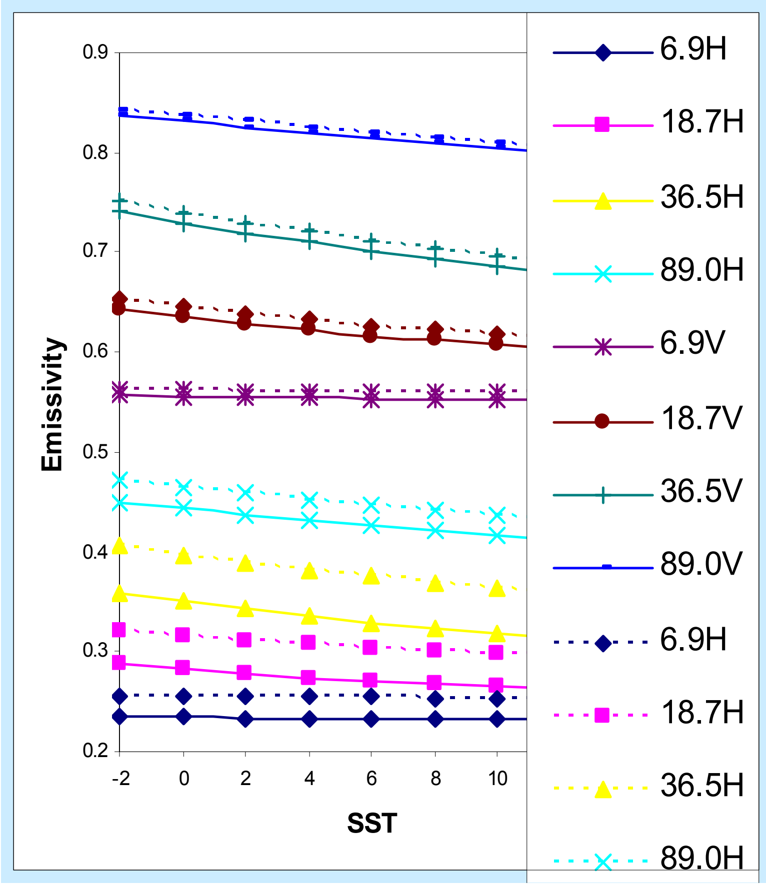

Emissivity as a function of *frequency* for grease ice and nilas of three different thickness ($\theta = 50^o$) (*left, Eppler et al., 1992*) and *water as a function of temperature* at AMSR-E frequencies at V- and H-pol (*right*)

Emissivity of sea ice

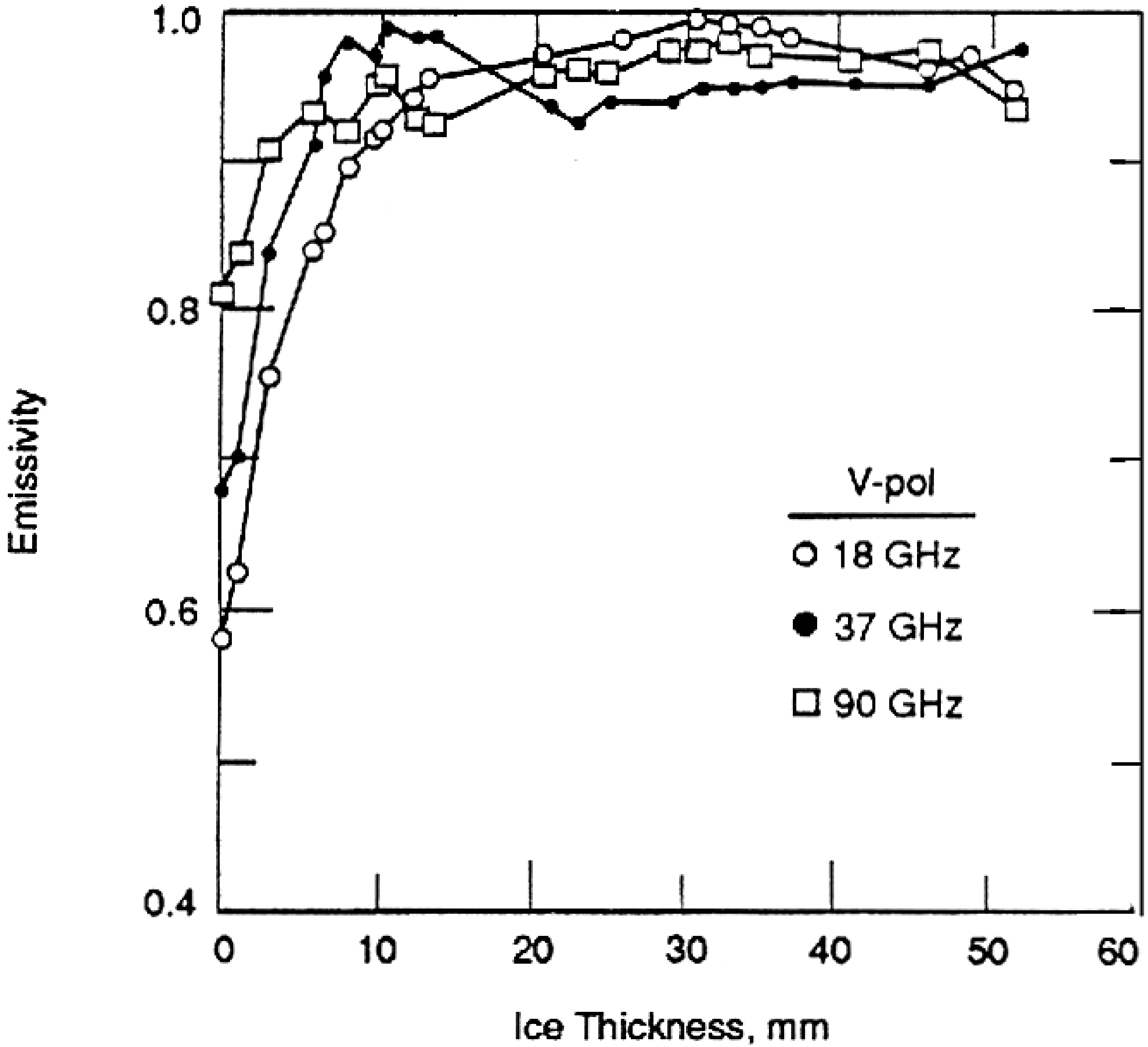

Emissivity *as a function of* ***ice thickness*** **at 18, 37 and 90 GHz (V-pol) for saline ice** [*Grenfell et al., 1988*].

Brightness temperature of calm sea surface

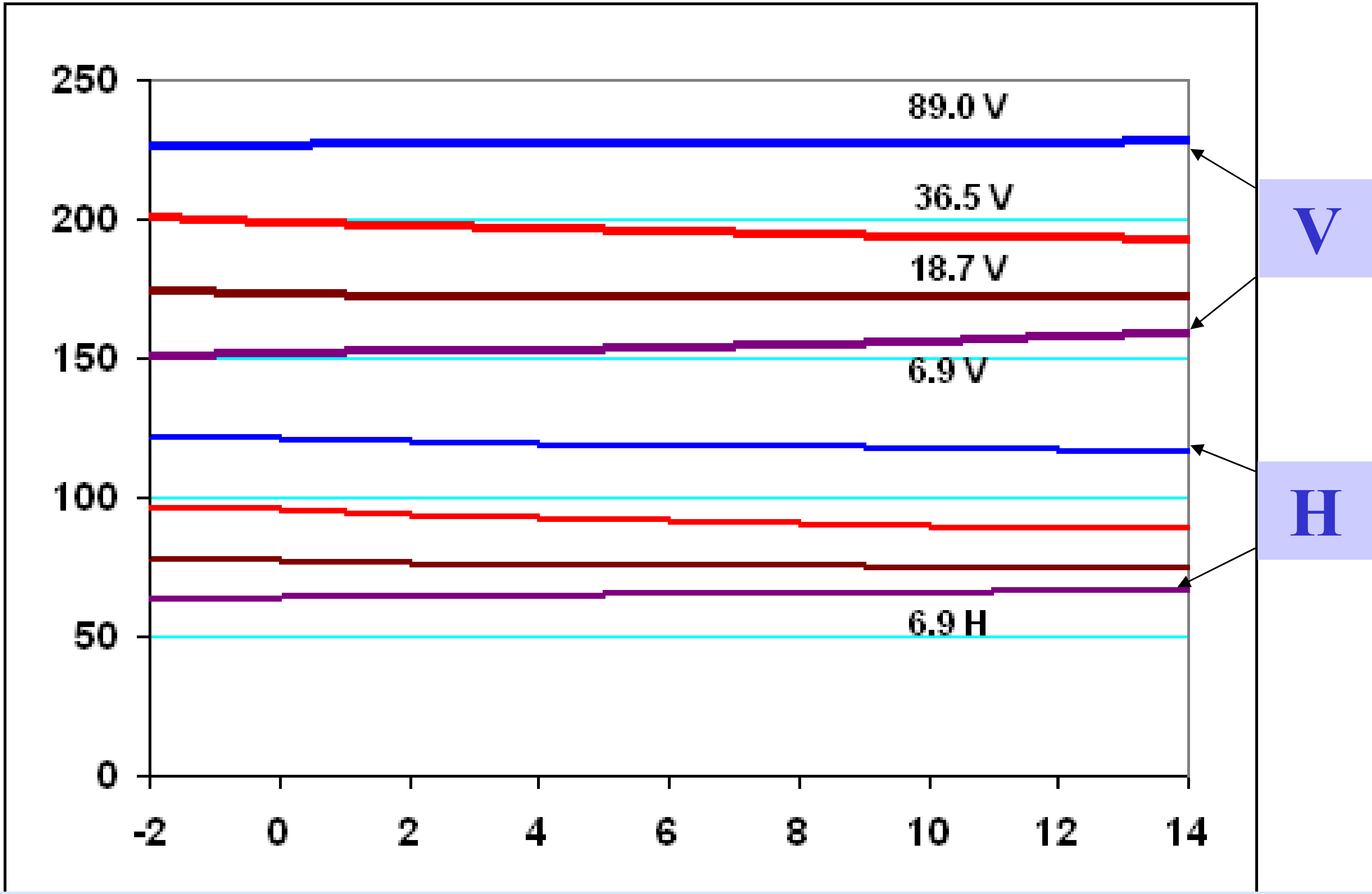

Brightness temperature of the calm sea surface **as a function of** *water temperature* **(V- and H-pol) at** AMSR-E **frequencies.**

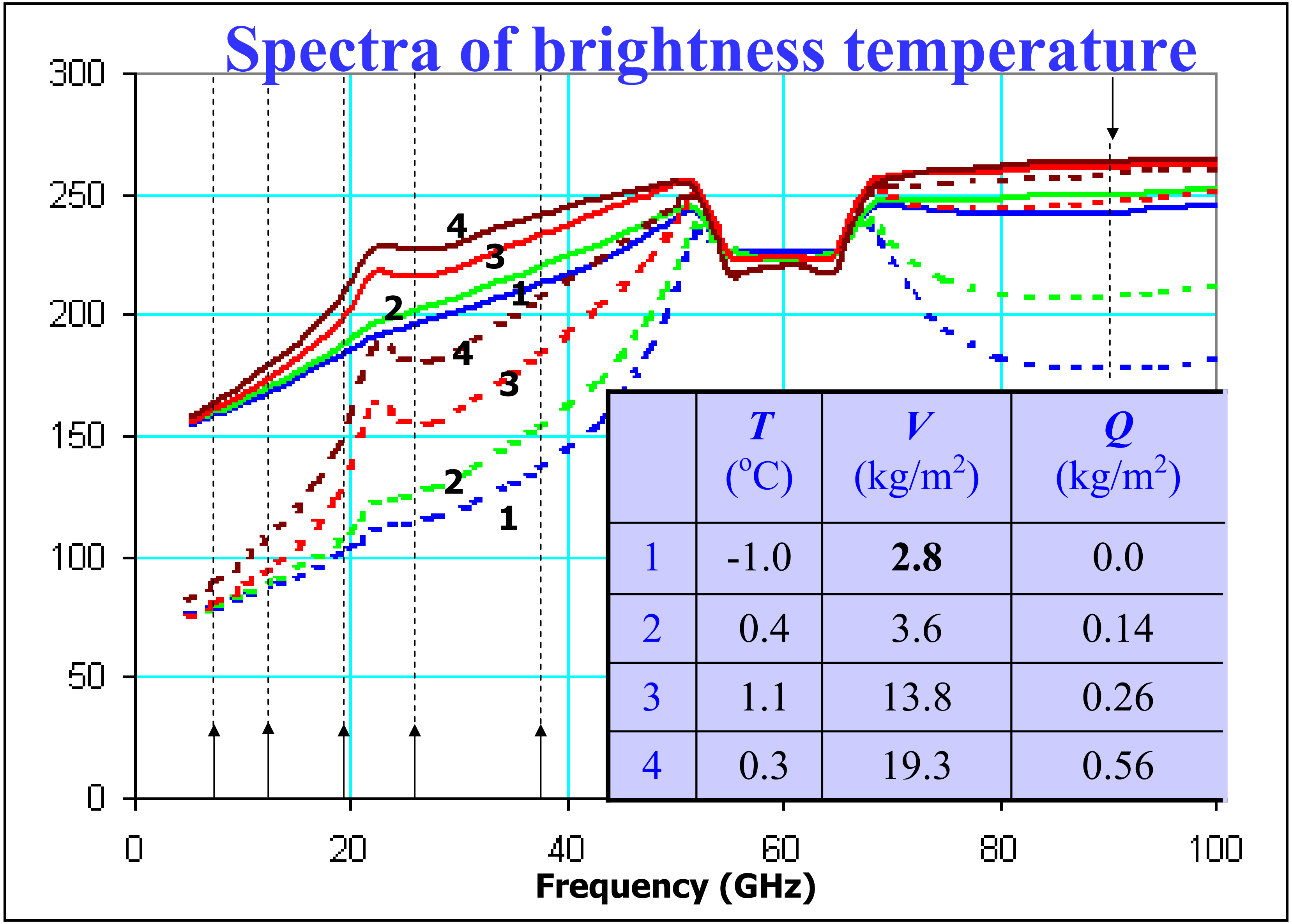

	T (°C)	*V* (kg/m^2)	*Q* (kg/m^2)
1	-1.0	**2.8**	0.0
2	0.4	3.6	0.14
3	1.1	13.8	0.26
4	0.3	19.3	0.56

Computed spectra of brightness temperature of the ocean-atmosphere system with V-pol (solid curves) and H-pol (dashed curves). Arrows mark AMSR-E frequencies.

Spectra of brightness temperature over the Marginal Ice Zone

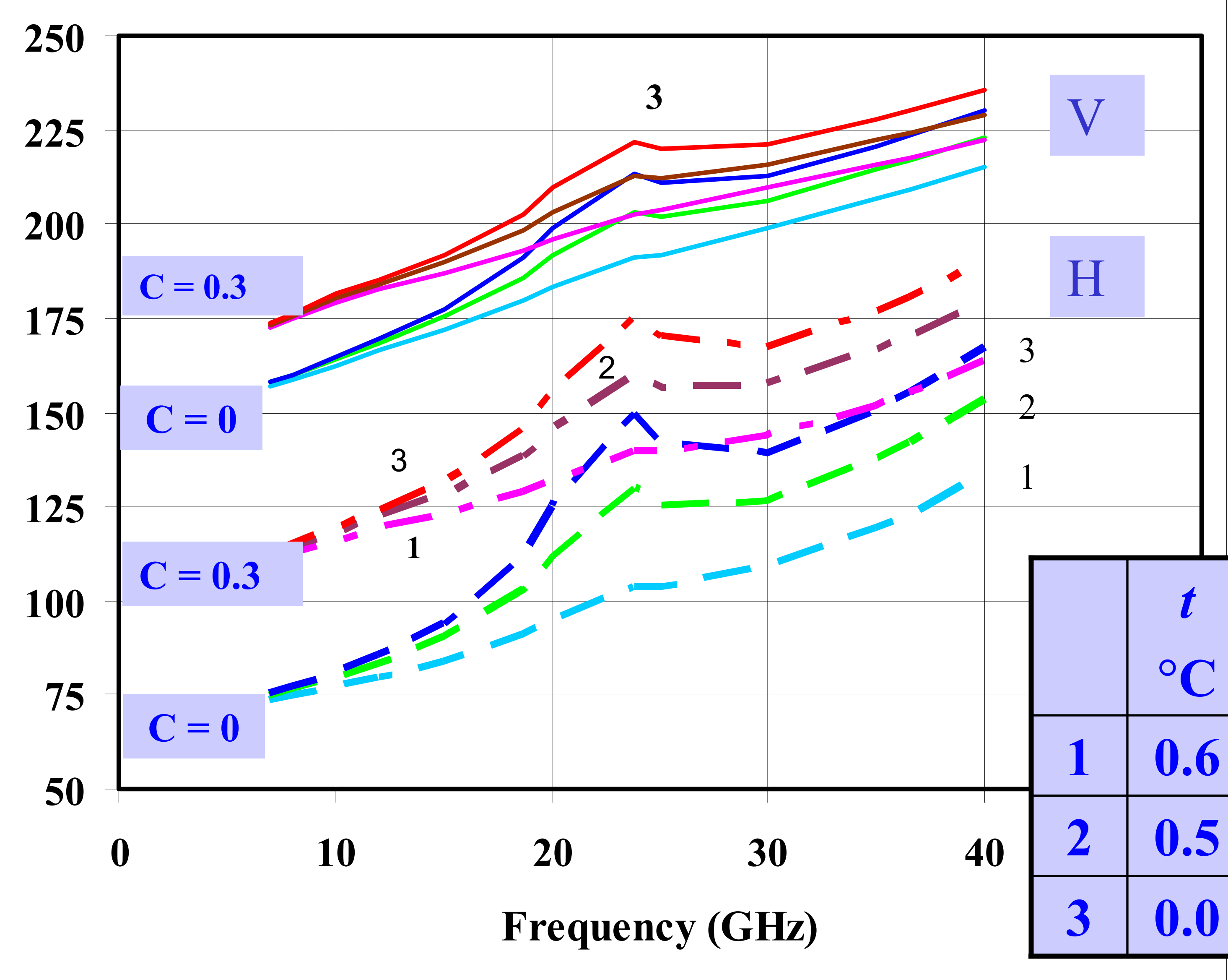

	t °C	V kg/m²	Q kg/m²
1	0.6	2.8	0.0
2	0.5	9.1	0.09
3	0.0	15.6	0.17

Active microwave sensing

Brightness of radar image is determined mainly by small-scale roughness and permittivity of the underlying snow-ice surface. These characteristics, in turn, are function of types of sea ice, the evolution of snow/sea-ice thermophysical properties including *liquid water presence* in the system, snow pack density and snow grain metamorphism, air temperature and wind.

The grease ice damps the small gravity and capillary waves due to increased viscosity and the corresponding areas look dark on SAR images. The areas with weak winds also look dark that hinders detection of the grease ice on the images.

Winds and waves are also favor to the formation of the pancake ice. It is characterized by the presence of plentiful cm-scale nonuniformities resulting in the increased backscatter. These features make possible their reliable identification.

Surface scattering

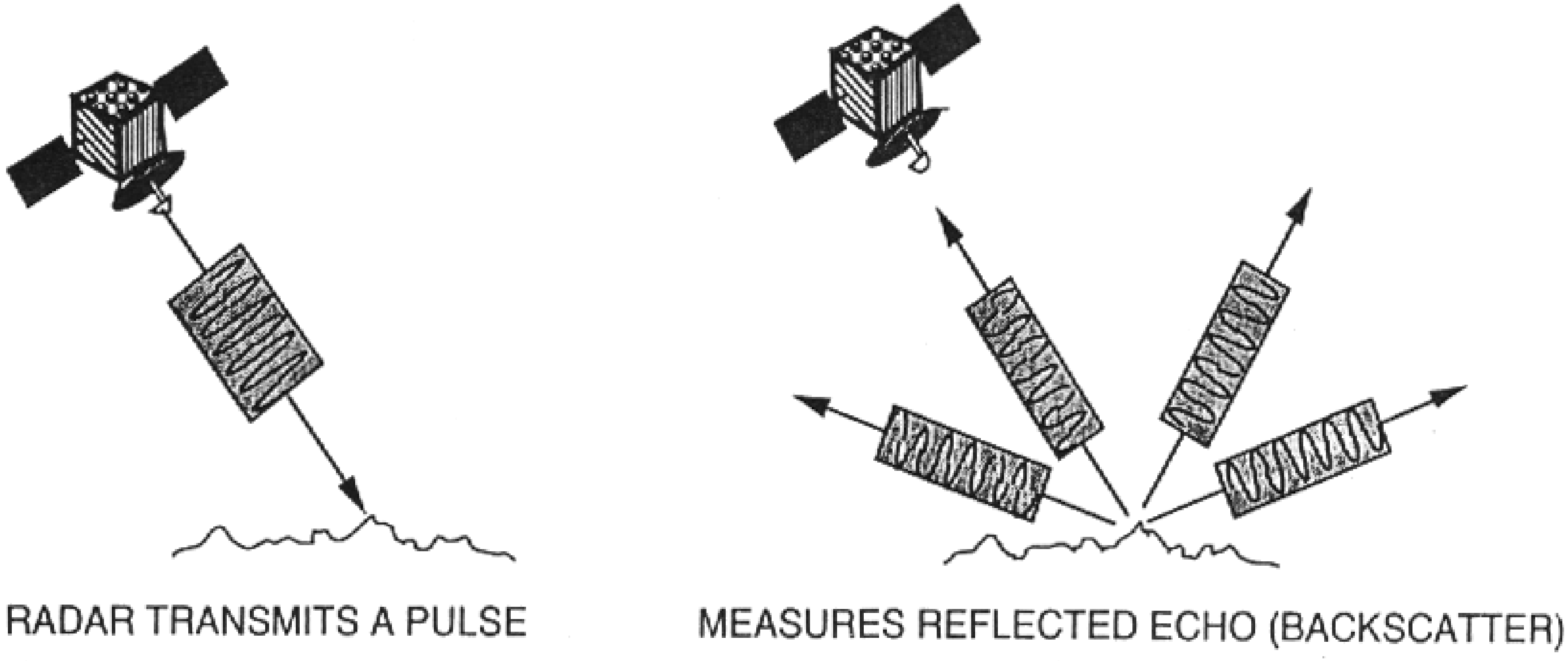

- Backscatter is measured in units of area (radar cross section or RCS)
- Scientists use normalized RCS, or $\sigma°$, which is dimensionless (decibels - dB)
- $\sigma°$ is usually between -45 dB (very dark) and +5 dB (very bright)

Sensors: AMSR, AMSR-E, SAR, ASAR, SeaWinds and supplementary satellite and *in situ* data

Microwave radiometers

The Advanced Microwave Scanning Radiometer for EOS (AMSR-E) is a Japanese sensor that was launched on the NASA Aqua satellite in May 2002.

The AMSR, a similar instrument was launched on the Japan ADEOS-II satellite in December 2002. AMSR has about twice the spatial resolution of SSM/I with resolution as low as 5 km at frequency of 89.0 GHz. This is a substantial improvement over SSM/I and yields improved benefits from passive microwave imagery both over the ice-free sea and ice areas.

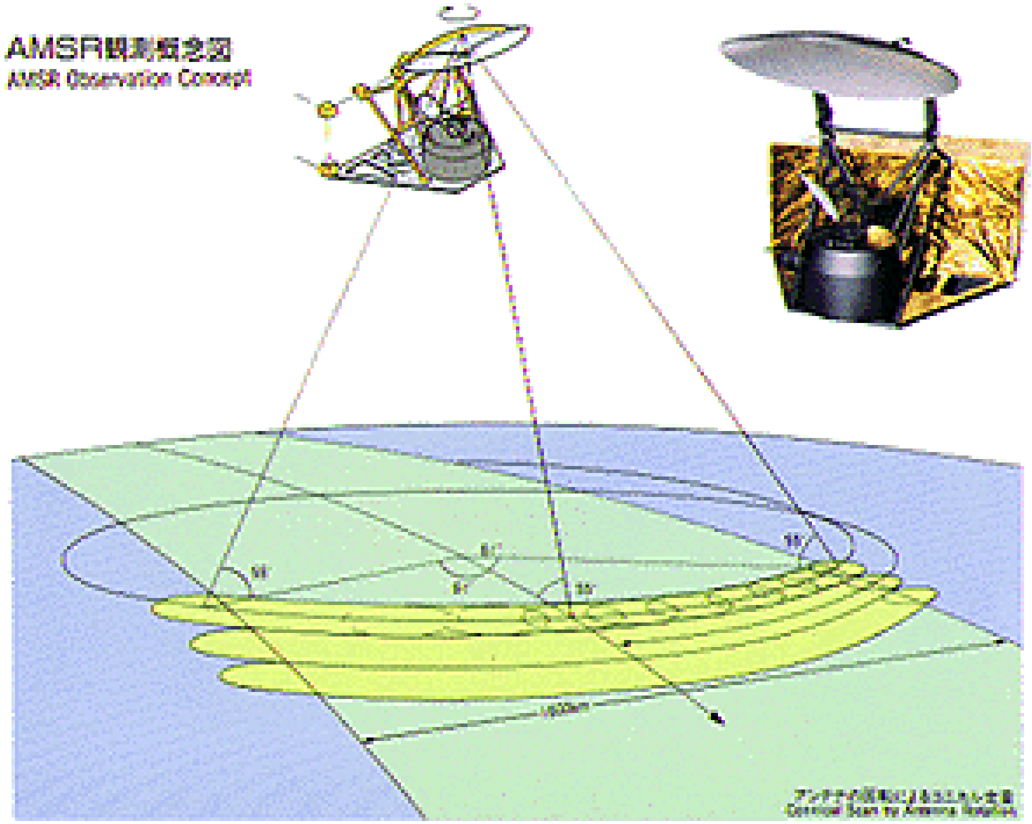

AMSR observation concept

Advanced Microwave Scanning Radiometer AMSR is an 8-frequency total-power microwave radiometer with dual polarization (except two vertical channels in the 50-GHz band). AMSR has a conical scanning geometry. Incidence angle is 55 deg.

Center frequency (GHz)	6.925	10.65	18.7	23.8	36.5	50.3	52.8	89.0 A	89.0 B
Band width (MHz)	350	100	200	400	1000	200	400	300	
Polarization	Vertical and Horizontal					Vertical		V, H	
IFOV (km x km)	40x70	27x46	14x25	17x29	8x14	6x10	6x10	3x6	
Sampling interval (kmxkm)	10x10							5x5	
Swath width (km)	Approximately 1600								

SAR characteristics

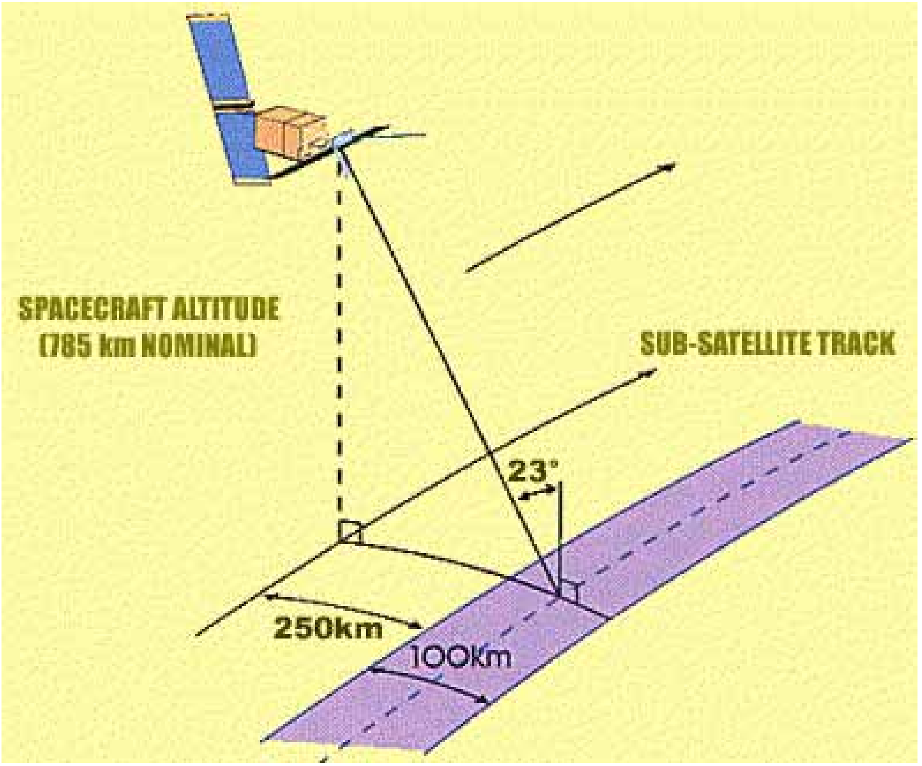

Satellite	ERS-1/2	ENVISAT
SENSOR	SAR	ASAR
Frequency, GHz	5.3	5.3
Wavelength, cm	5.6	5.6
Polarization	VV	VV, HH
Incidence angle, deg	20-26	15-45 (variable)
Swath width, km	100	100-405
Ground resolution , m	25 x 25	25 x 25 150x150

European Remote Sensing Satellite ERS-1 was launched on 17 July 1991, ERS-2 was launched on 21 April 1995 and ENVISAT was launched on 1 March 2002.

Envisat ASAR

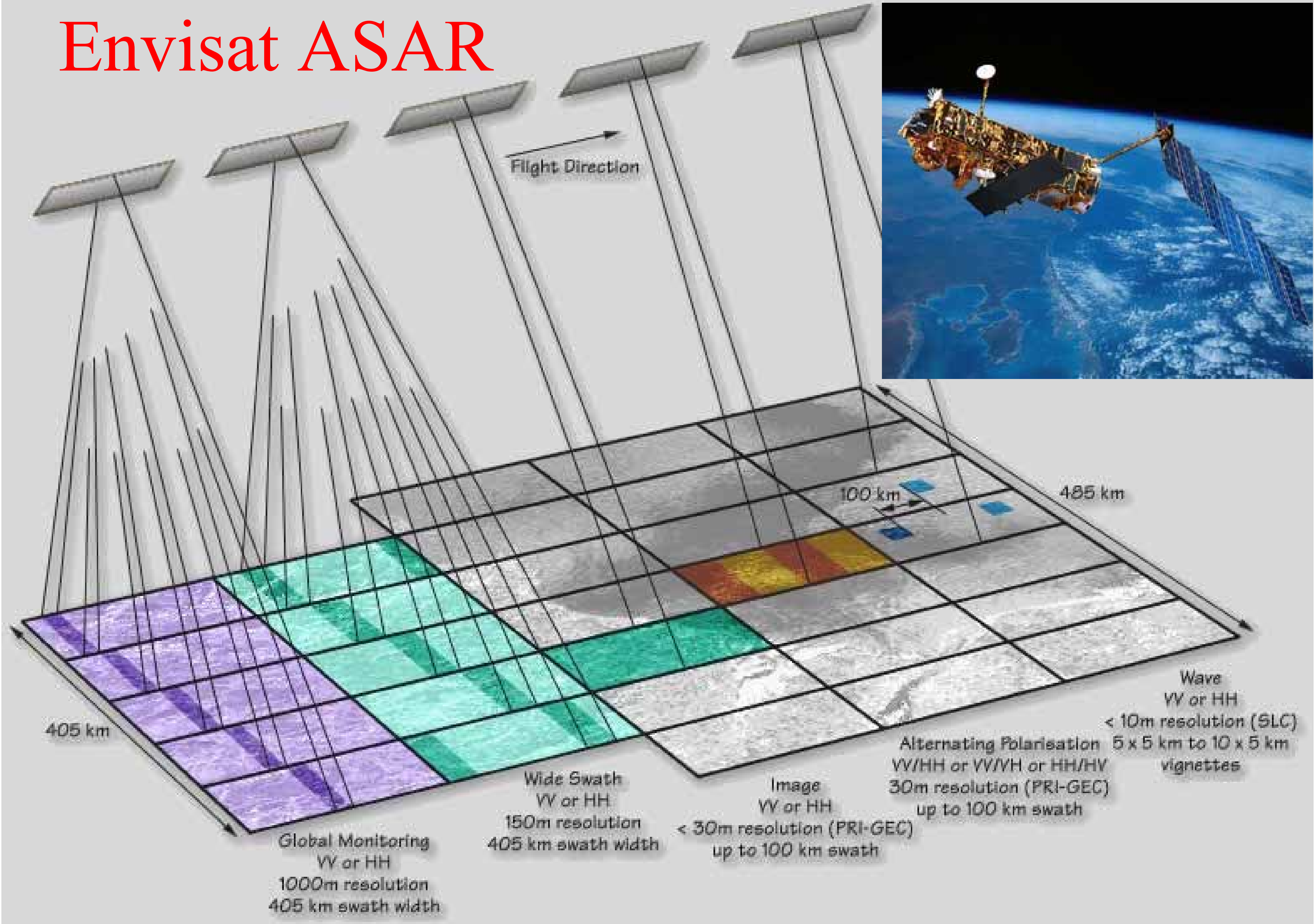

Scatterometer SeaWinds

Radar:	13.4 GHz
Pulse repetition:	189 Hz
Antenna:	1 m
Swath width:	1,800-km
Wind vector resolution	25 km.
Wind-speed:	3-20 m/s,
accuracy:	2 m/s.
Wind direction accuracy:	20 deg.

Rotating dish produces two spot beams, sweeping in a circular pattern.
90% coverage of Earth's oceans every day.

Satellite SAR

Precision (PRI) and quick look (QL) ERS-2 SAR and Envisat ASAR images taken in 2002-2005 are used for the sea ice study in the Okhotsk and Japan Seas. High spatial resolution of a SAR permits to determine the areas of grease ice, pancake ice and transition zone between them. The growth rate of the ice-covered areas can be estimated by comparison of the overlapping SAR images acquired on ascending and descending orbits.

ADEOS-II AMSR and Aqua AMSR-E data, NOAA AVHRR and MODIS images, QuikSCAT-derived wind fields as well as weather maps were used to confirm interpretation of SAR signatures. Several case studies cover the Aniva Bay and the northern, western and eastern Okhotsk Sea are considered.

SAR image location

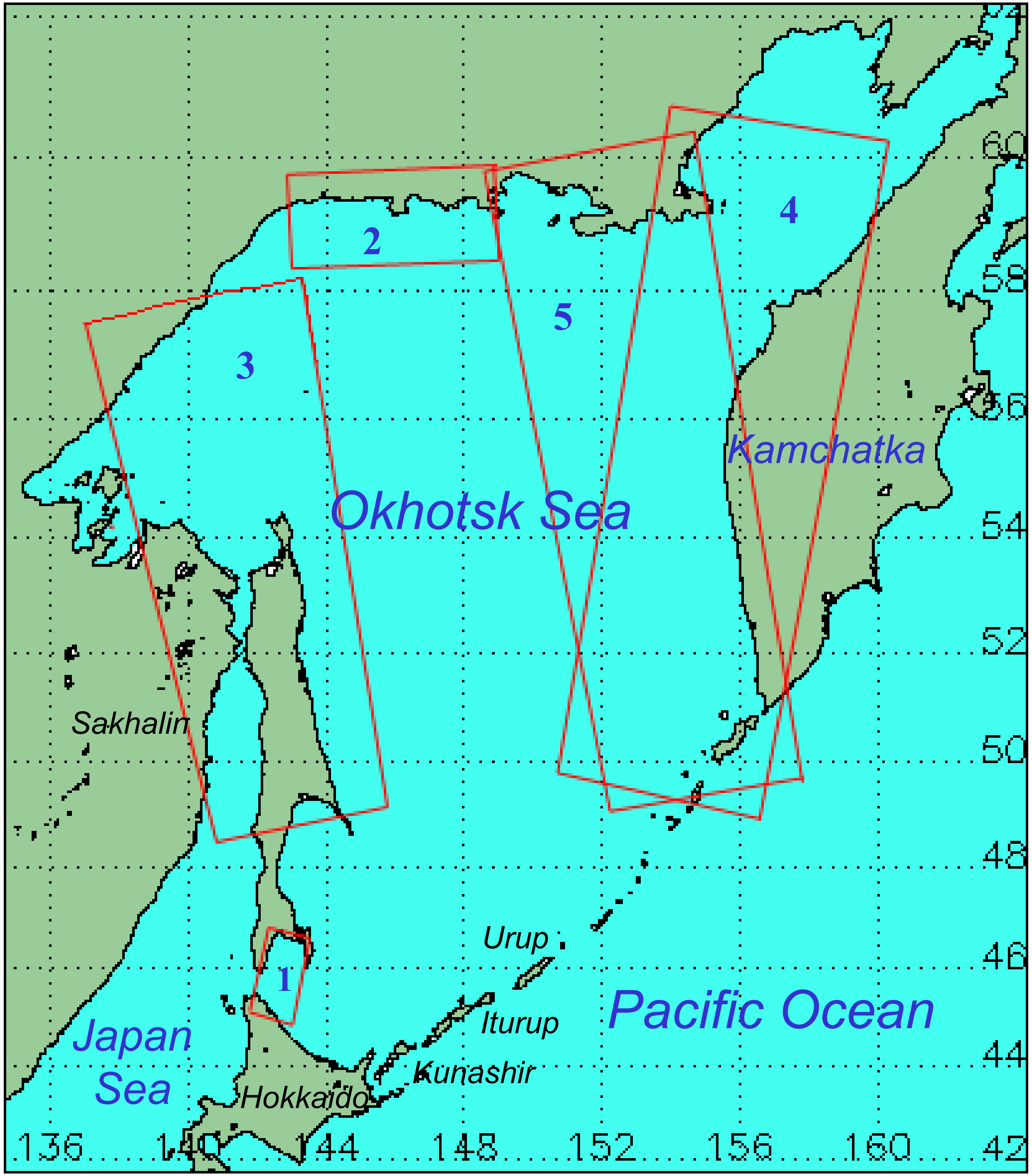

Map of the Okhotsk Sea

(1) **ERS-2 SAR** for 24 Jan 2000 at 01:17 UTC

(2) **Envisat ASAR** for 1 Dec 2004 at 11:46 UTC

(3) **Envisat ASAR** for 9 Dec 2002 at 12:11 UTC

(4) **Envisat ASAR** for 28 Feb 2003 at 00:02 UTC

(5) **Envisat ASAR** for 28 Feb 2003 at 11:25 UTC

Aniva Bay. ERS-2 SAR frames

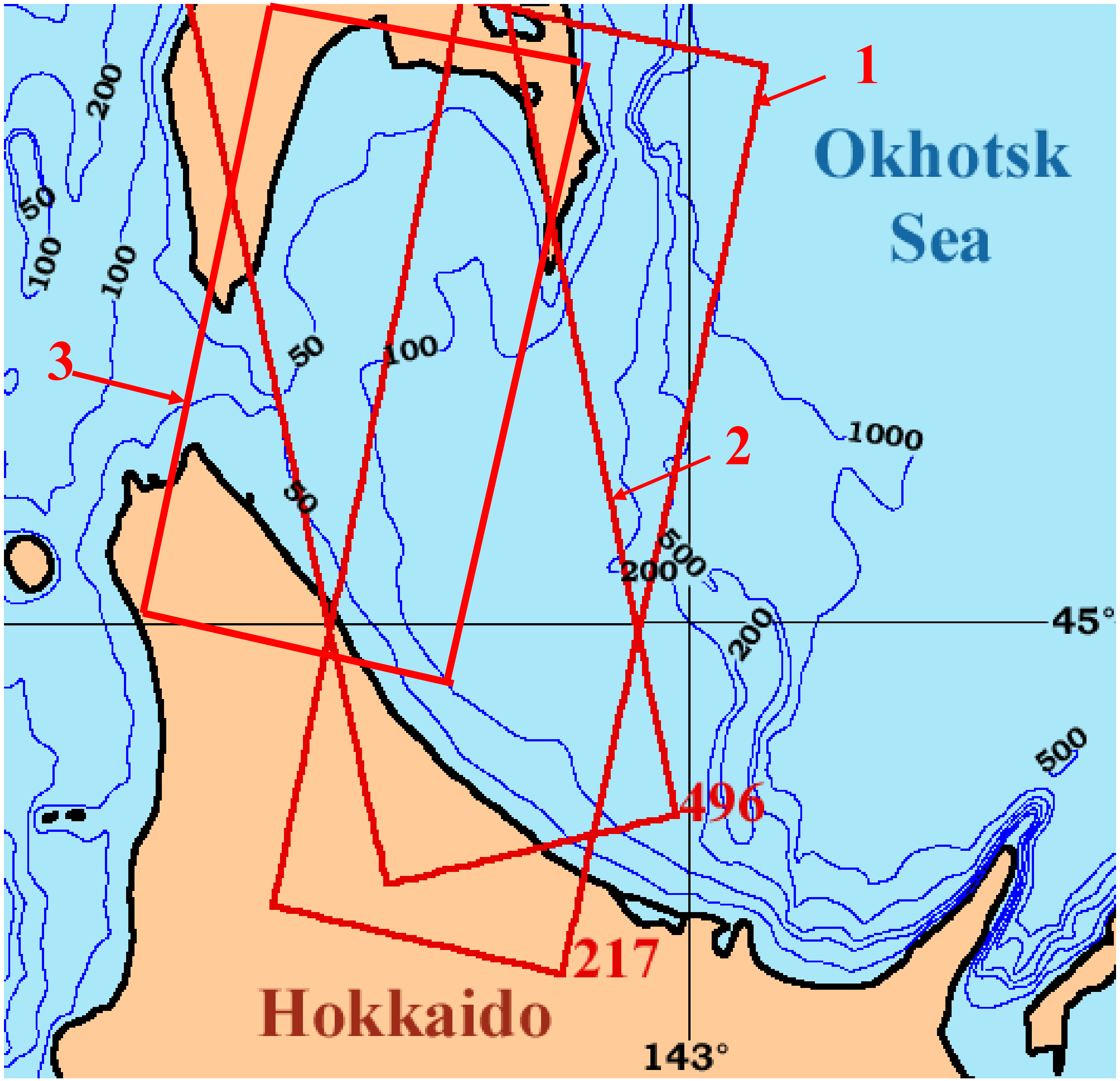

Bathymetric map off the Hokkaido coast

Red rectangles mark the location of the ERS-2 SAR images acquired on 18 February 1996 at 01:19 UTC (1) and at 12:39 UTC (2) ; 24 January 2000 and 15 March 1999 at 01:17 UTC (3).

ERS-2 SAR images for 18 February 1996

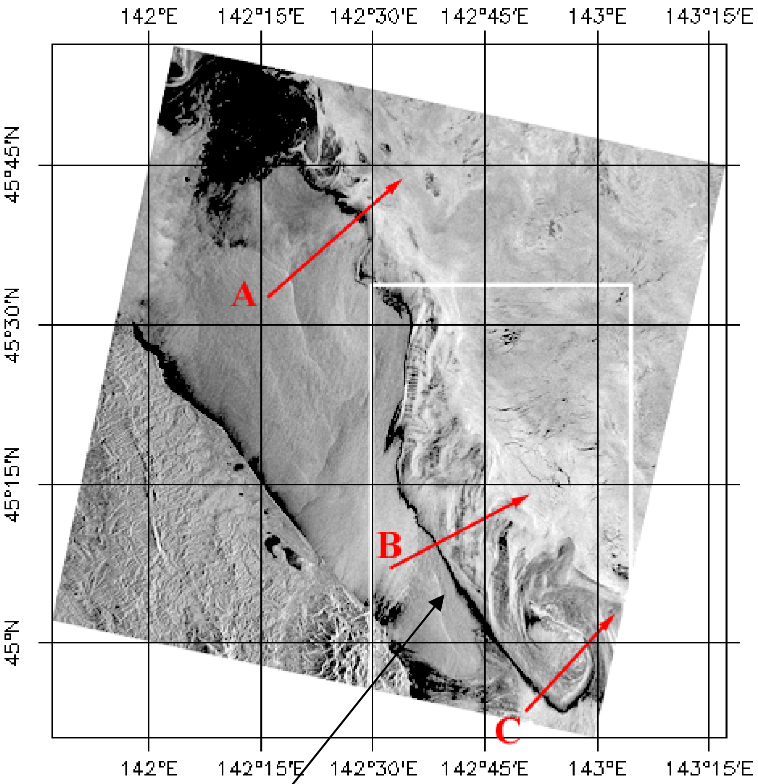

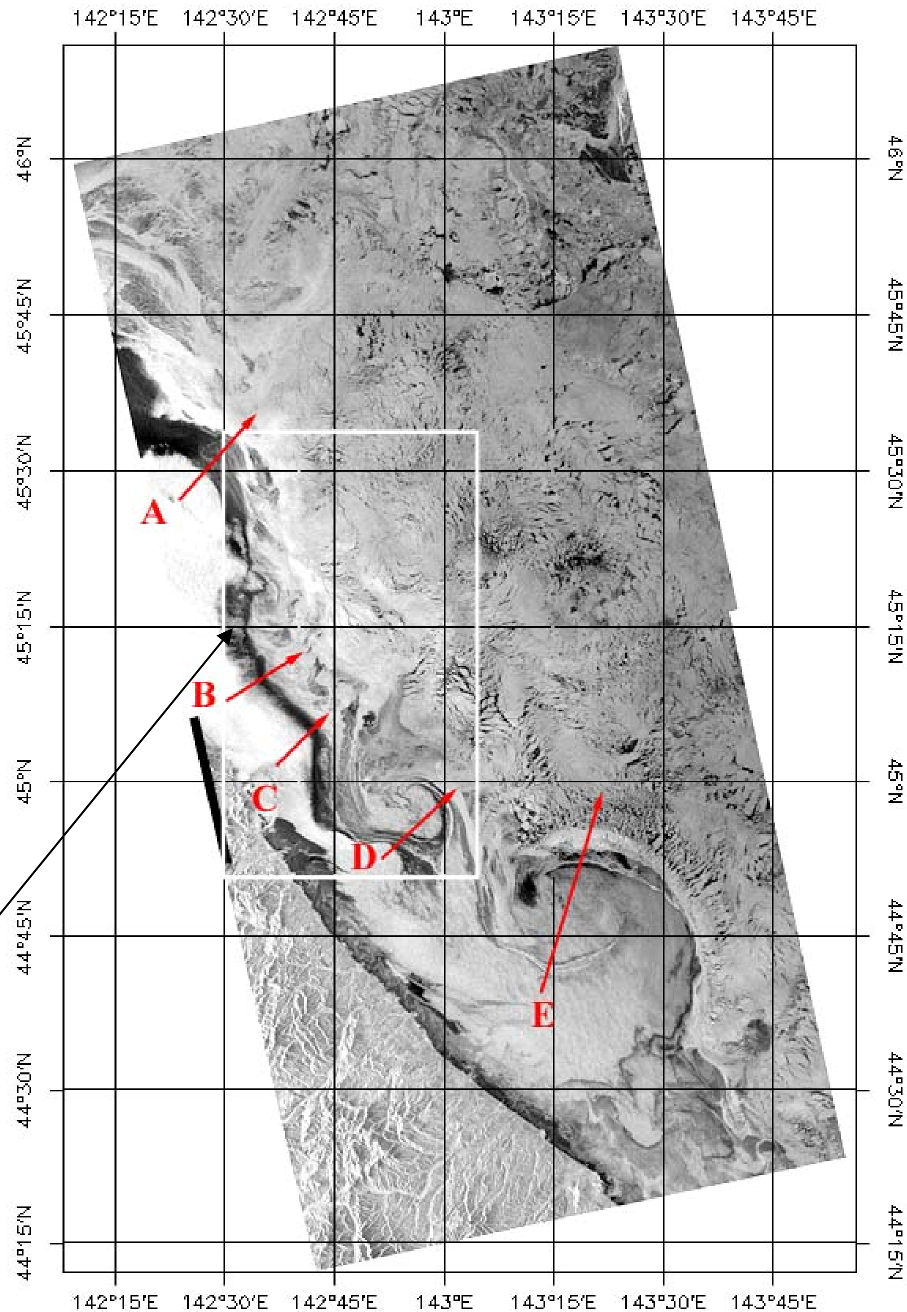

85 km^2 480 km^2

grease ice

18 Feb 1996, 01:19 UTC
Track 217

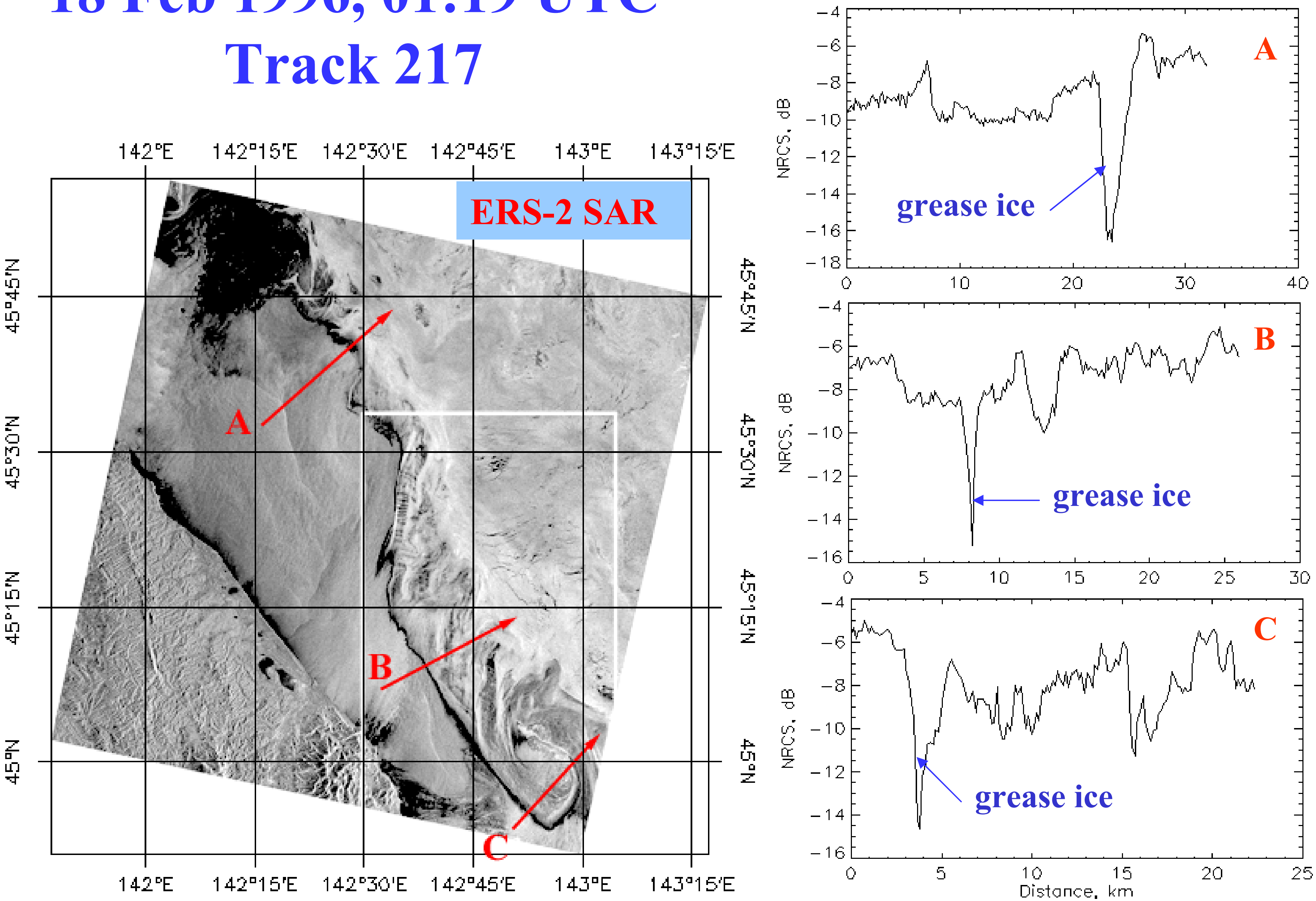

18 Feb 1996, 12:39 UTC Track 496

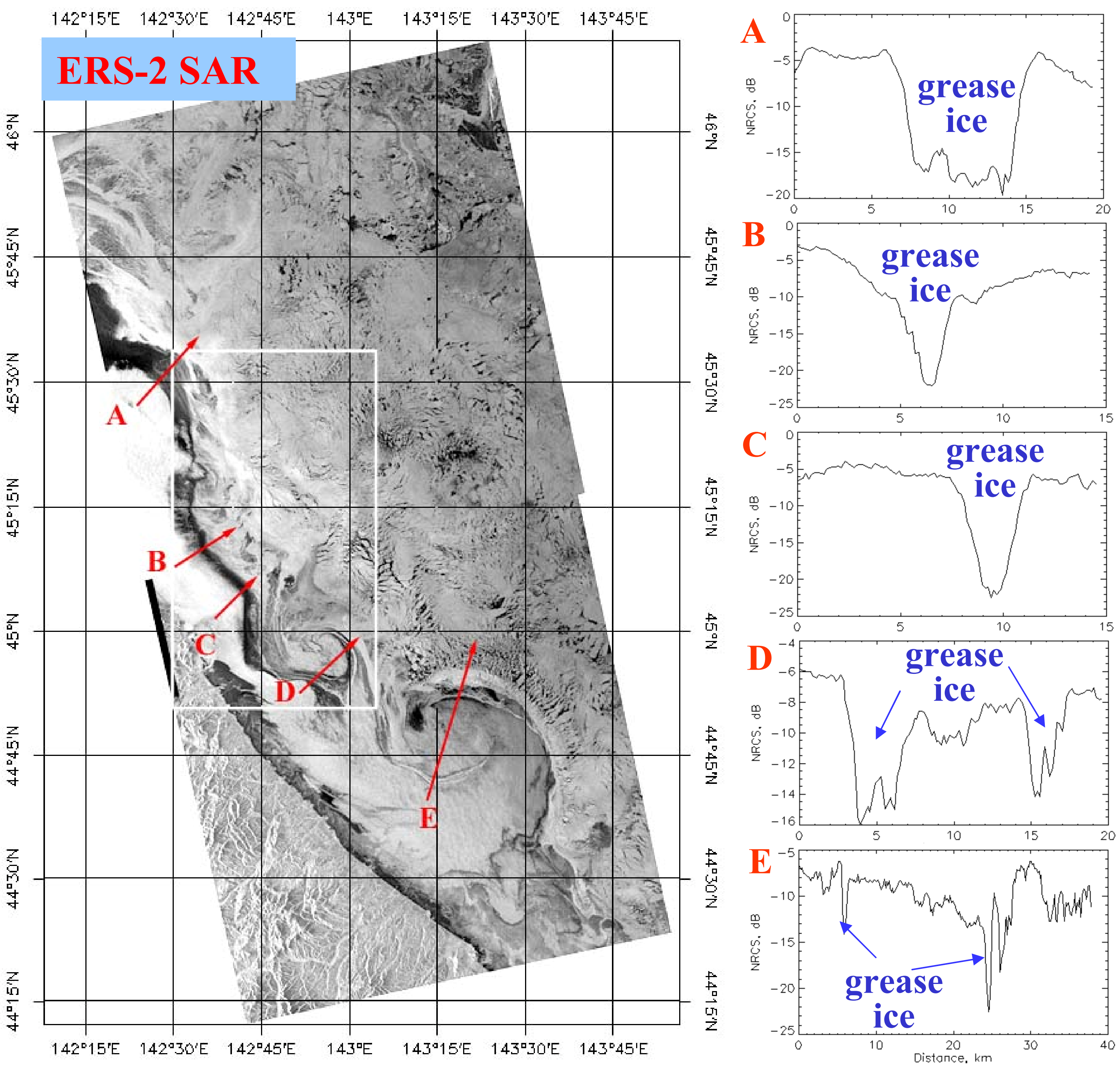

Ice drift and ice eddies

01:19 UTC

ERS-2 SAR

12:39 UTC

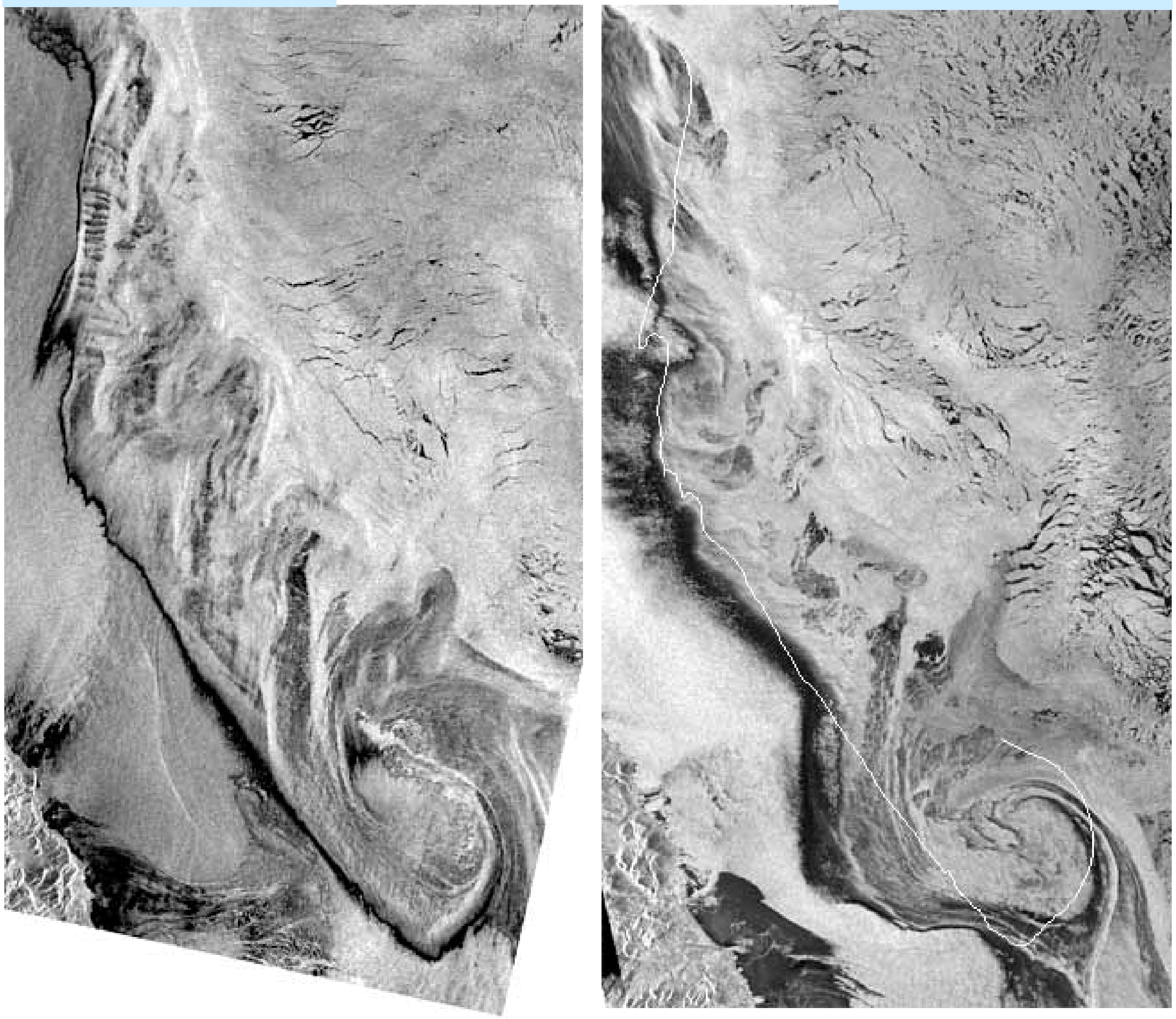

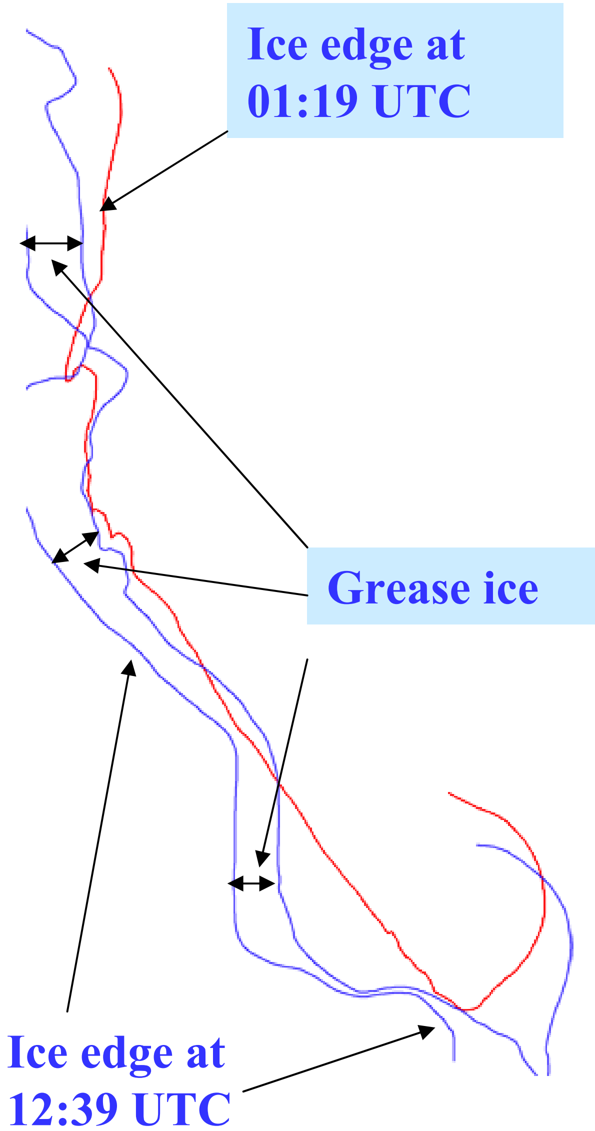

The change of ice cover off Hokkaido for 11 h 20 min

Envisat ASAR

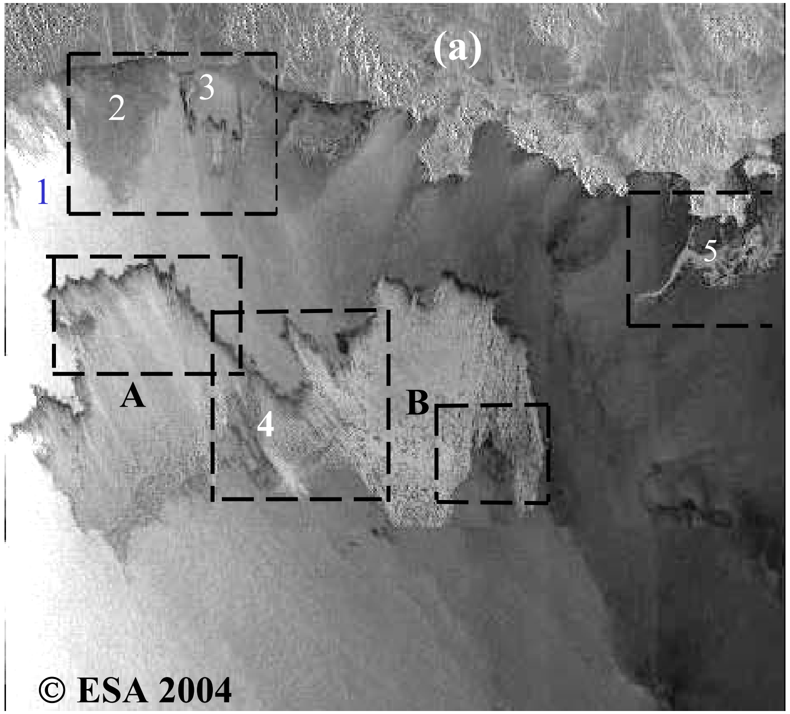

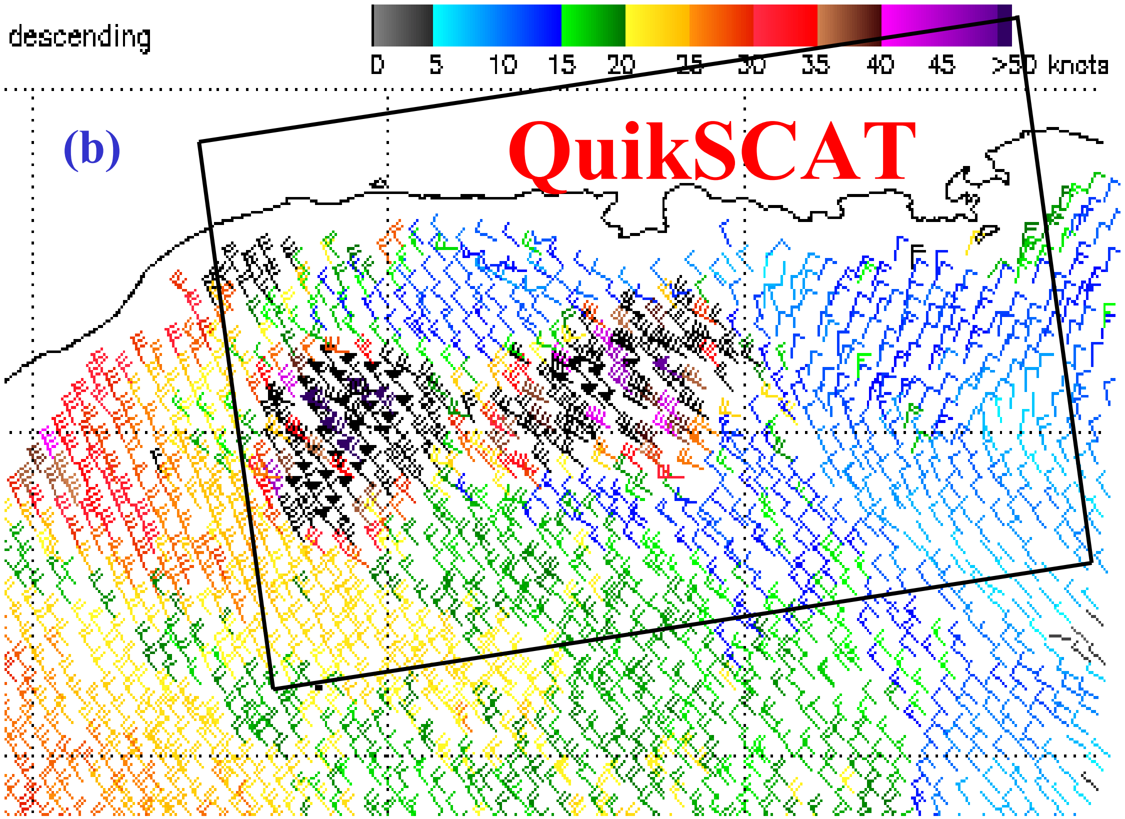

Fragment of ASAR quick look image with HH-pol at 11:46 UTC (a) and SeaWinds-derived wind field at 10:02 UTC on 1 December 2004 (b).

The ice bands 1 and ice field 2 have negative contrast against the open sea likely due to the presence of the grease ice. Ice fields 3 is in the area where wind speed lower than to the west of it. Their brightness is higher compare to 1 and 2 likely due to the presence of the pancake ice. The narrow dark bands adjacent to the fields 3 are very likely grease ice. The grease ice is clearly seen on the upwind side of ice massive 4. Its area is ≈16300 km^2 and the grease ice area is ≈1600 km^2.

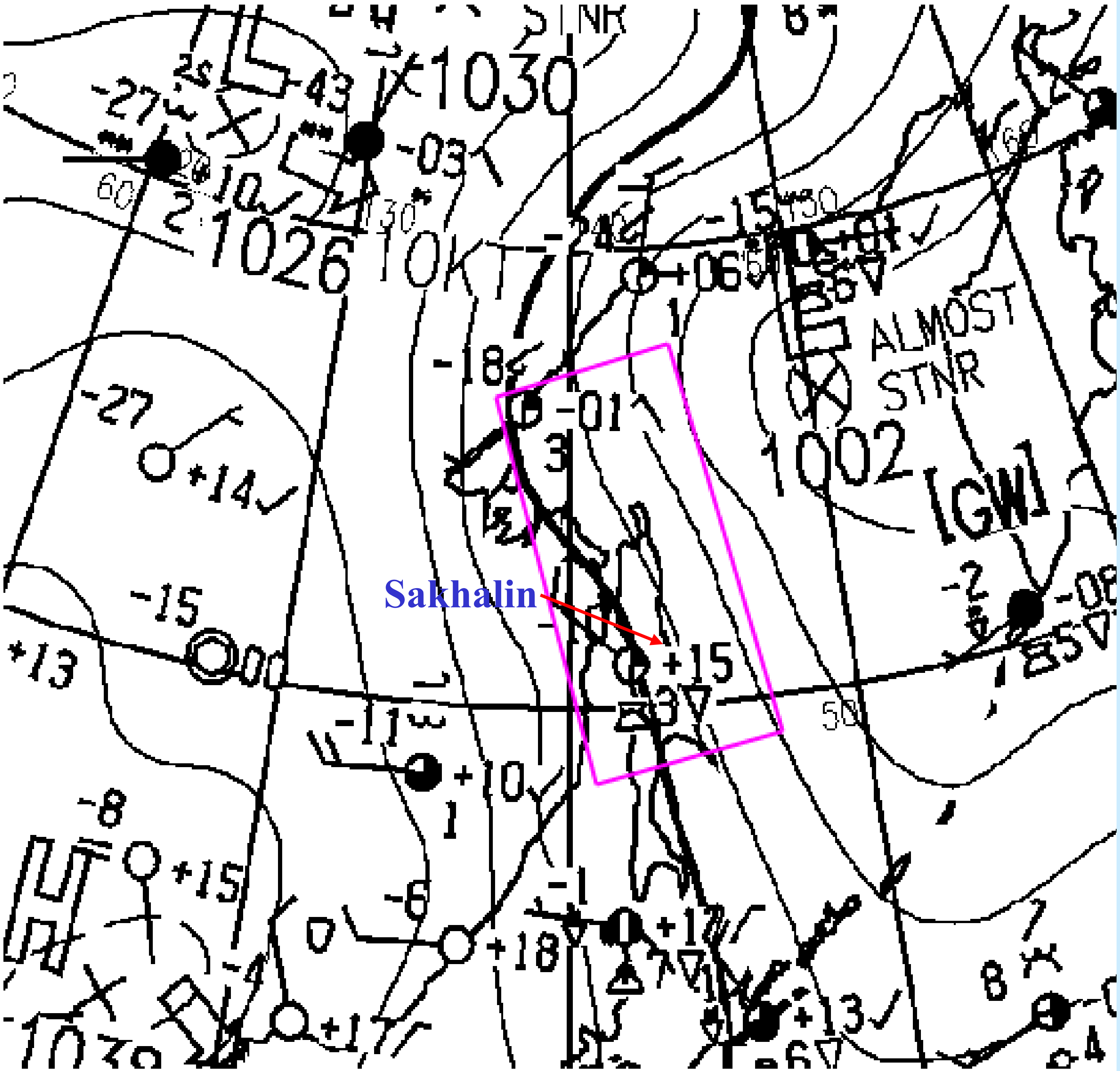

Surface analysis map of the JMH for 1 Dec 2004 at 12:00 UTC.

Pink rectangle marks the boundaries of Envisat ASAR image taken on 1 Dec 2004 at 11:46 UTC.

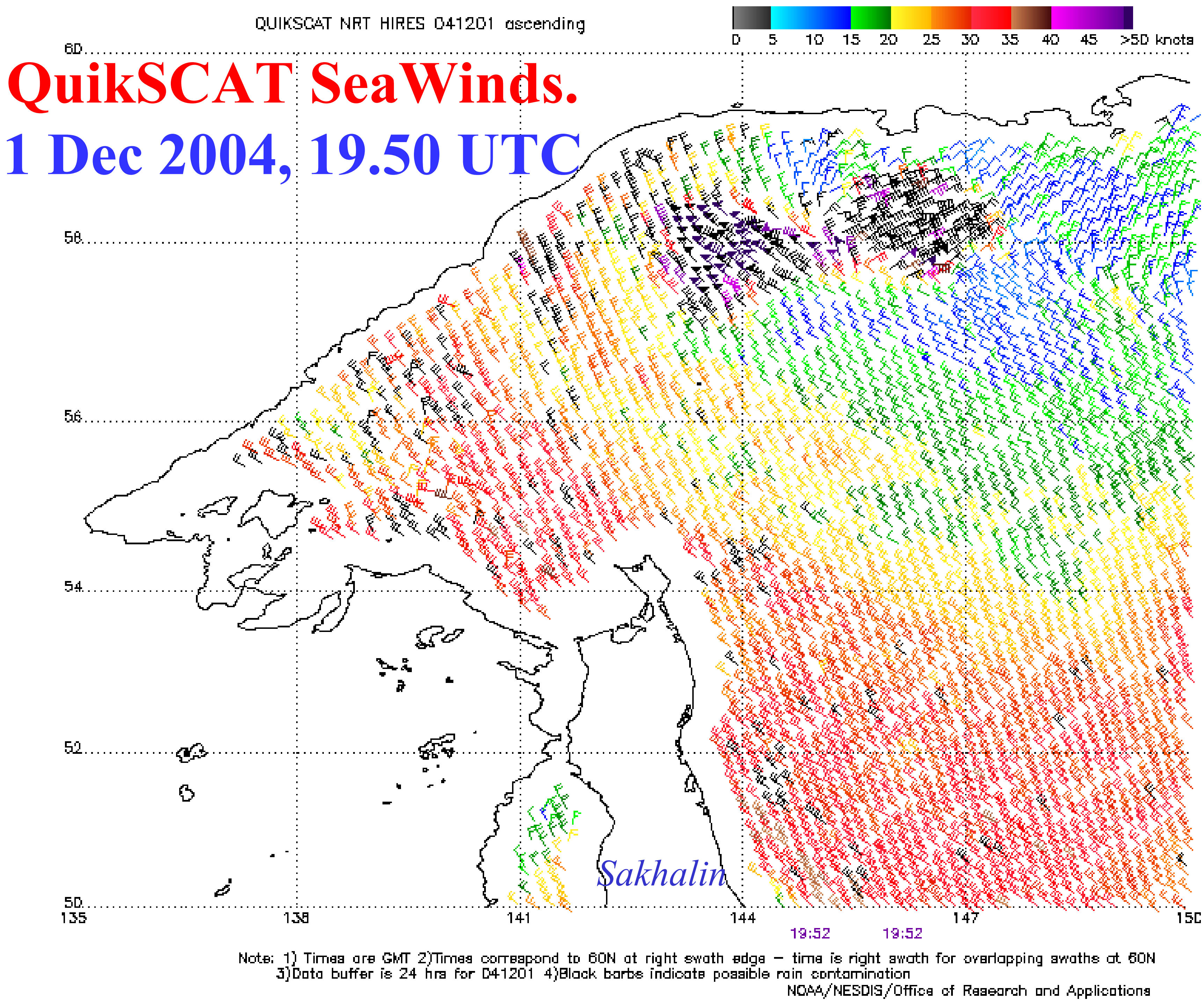
QuikSCAT SeaWinds.
1 Dec 2004, 19.50 UTC
QUIKSCAT NRT HIRES 041201 ascending
0 5 10 15 20 25 30 35 40 45 >50 knots
60
58
56
54
52
50
135
138
141
144
147
150
19:52 19:52
Sakhalin
Note: 1) Times are GMT 2)Times correspond to 60N at right swath edge – time is right swath for overlapping swaths at 60N
3)Data buffer is 24 hrs for 041201 4)Black barbs indicate possible rain contamination
NOAA/NESDIS/Office of Research and Applications

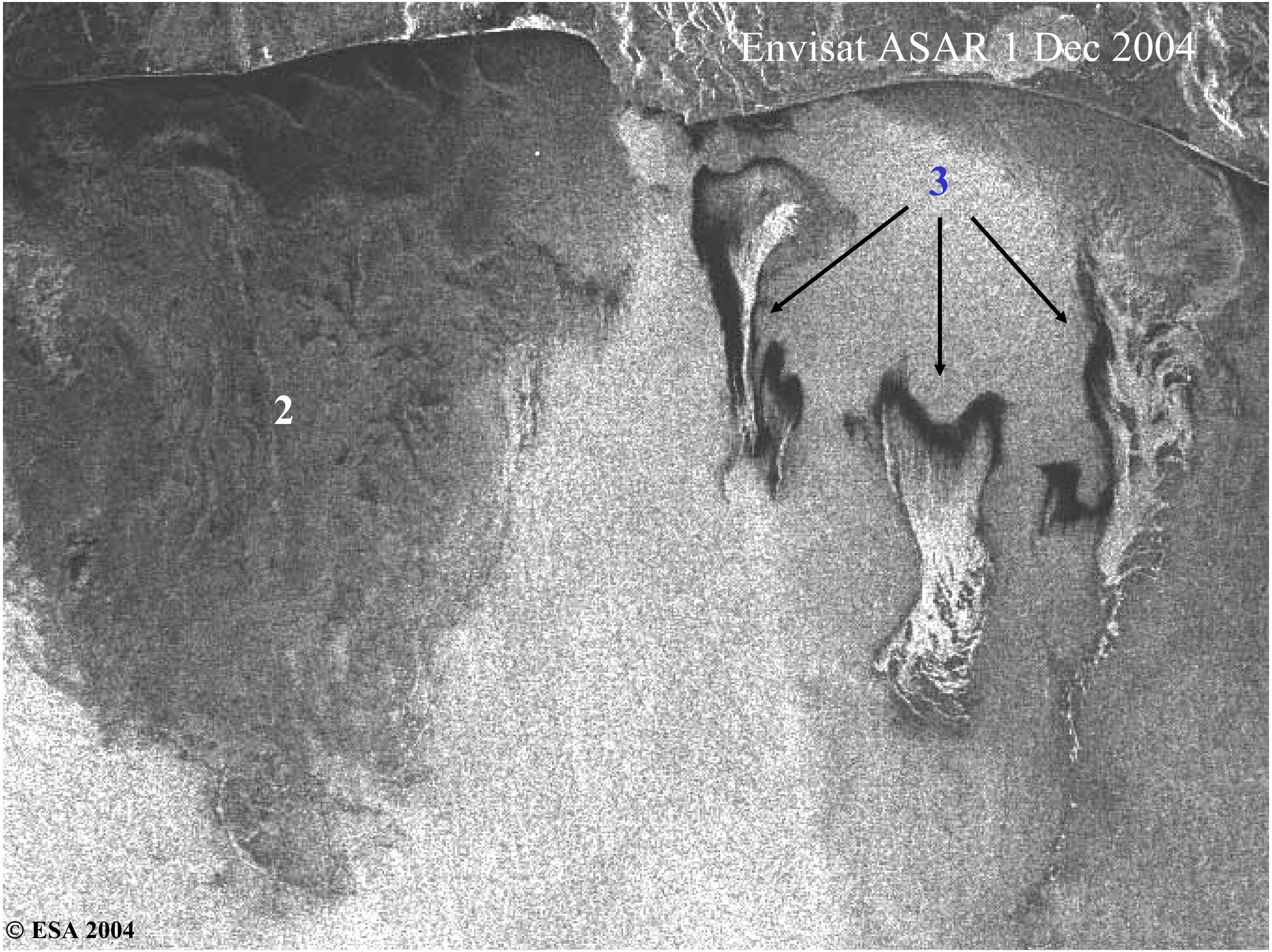
Envisat ASAR 1 Dec 2004
3
2
© ESA 2004

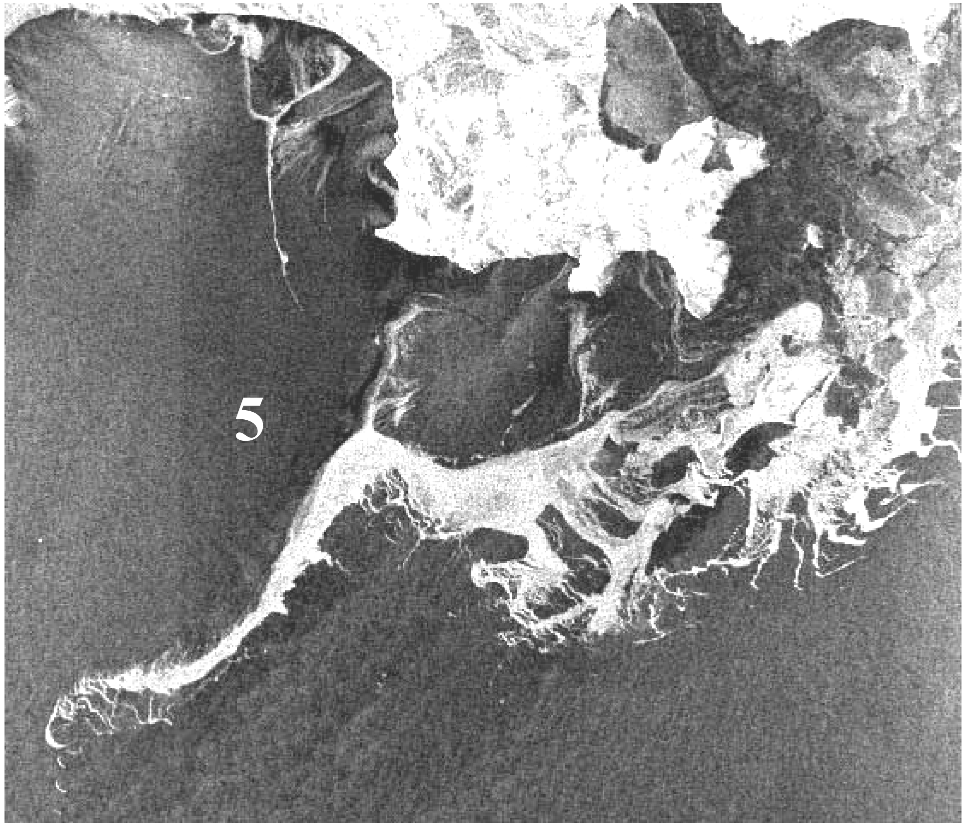

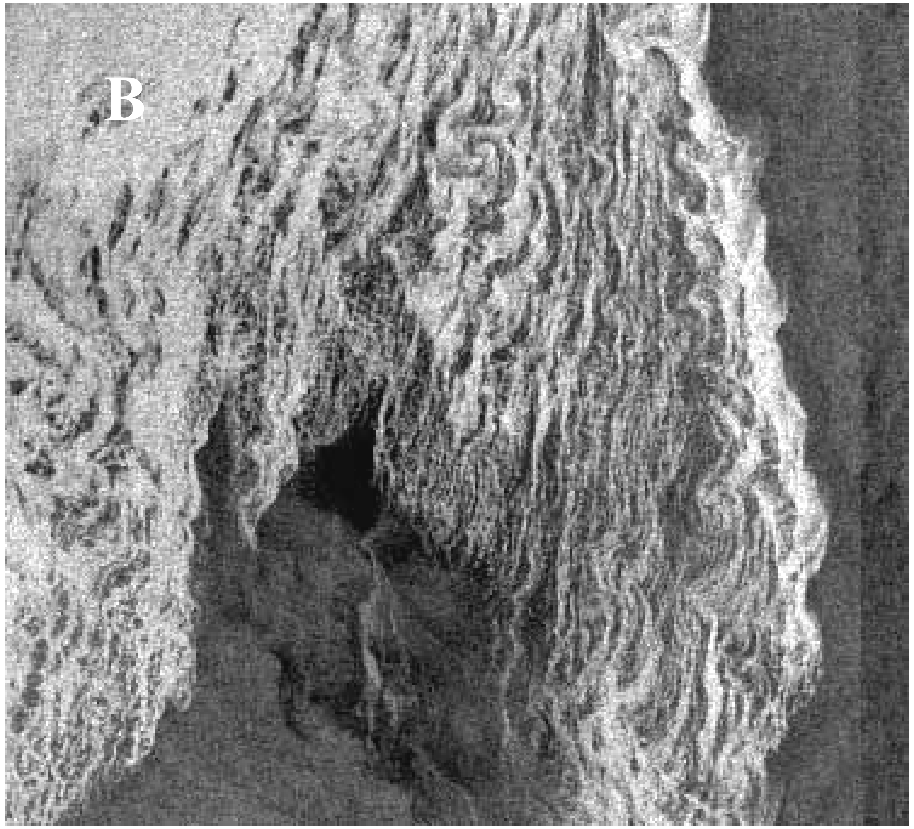

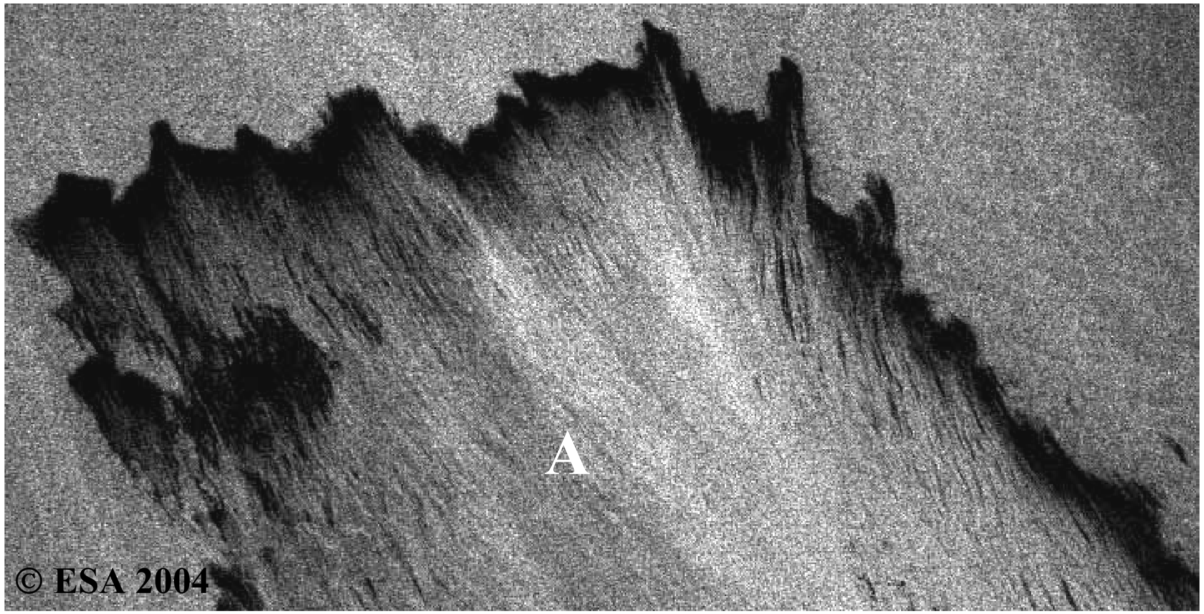

Envisat ASAR

1 December 2004

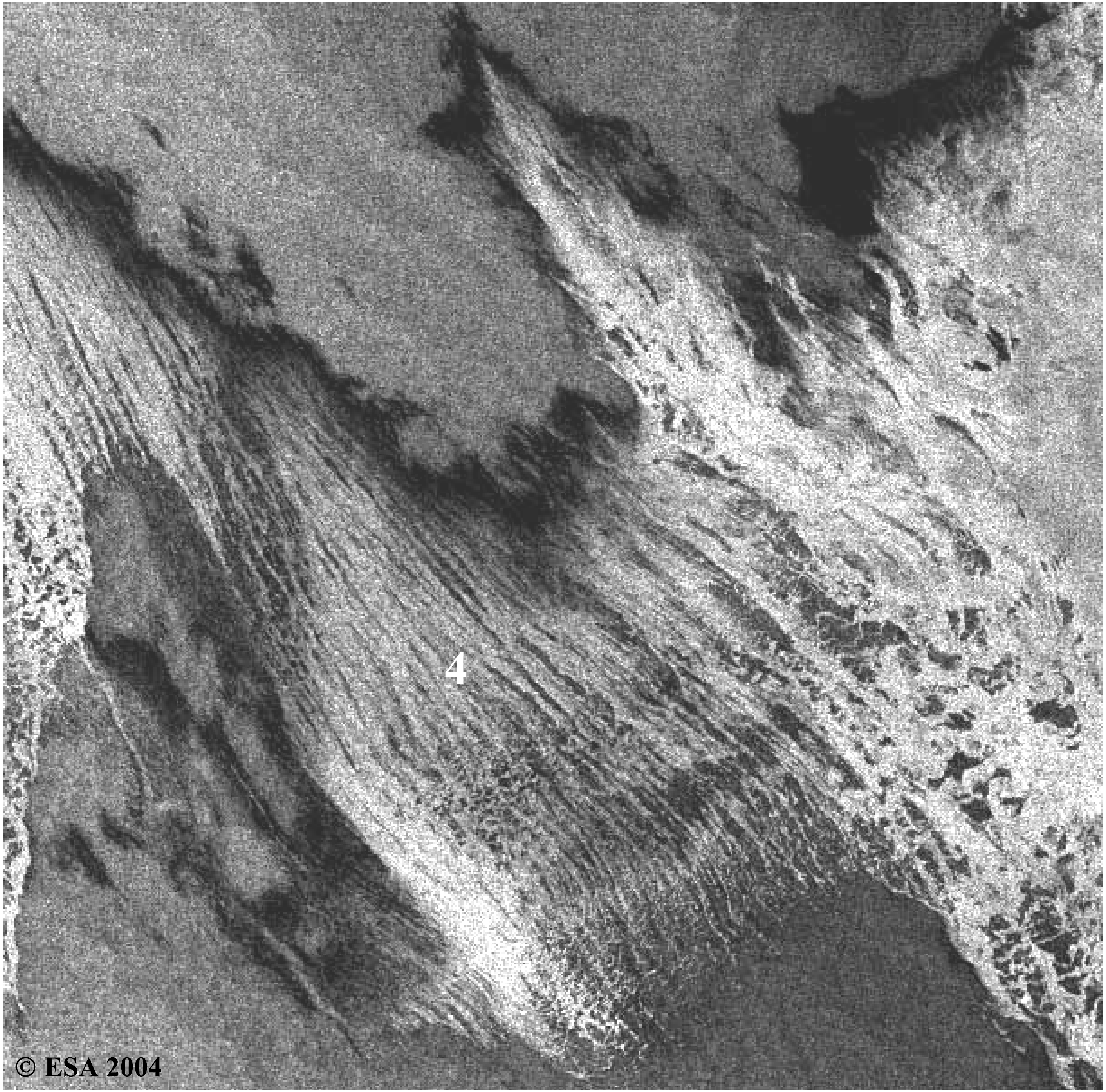

Envisat ASAR

1 December 2004 at 11:46 UTC

Western Okhotsk sea

9 December 2002

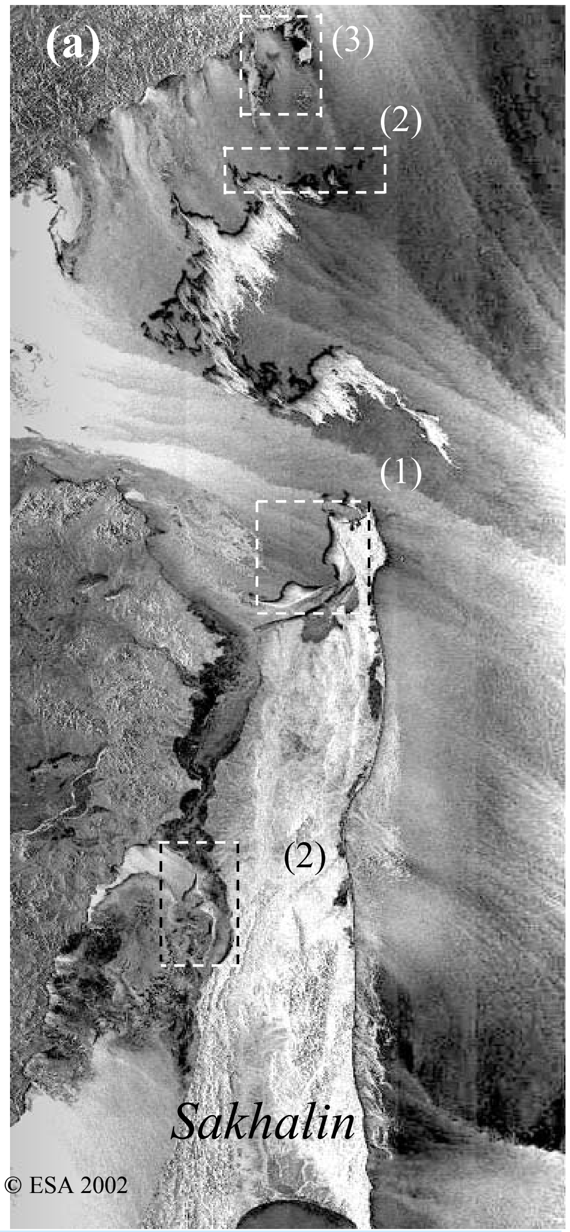

Envisat ASAR, HH, 12:11 UTC

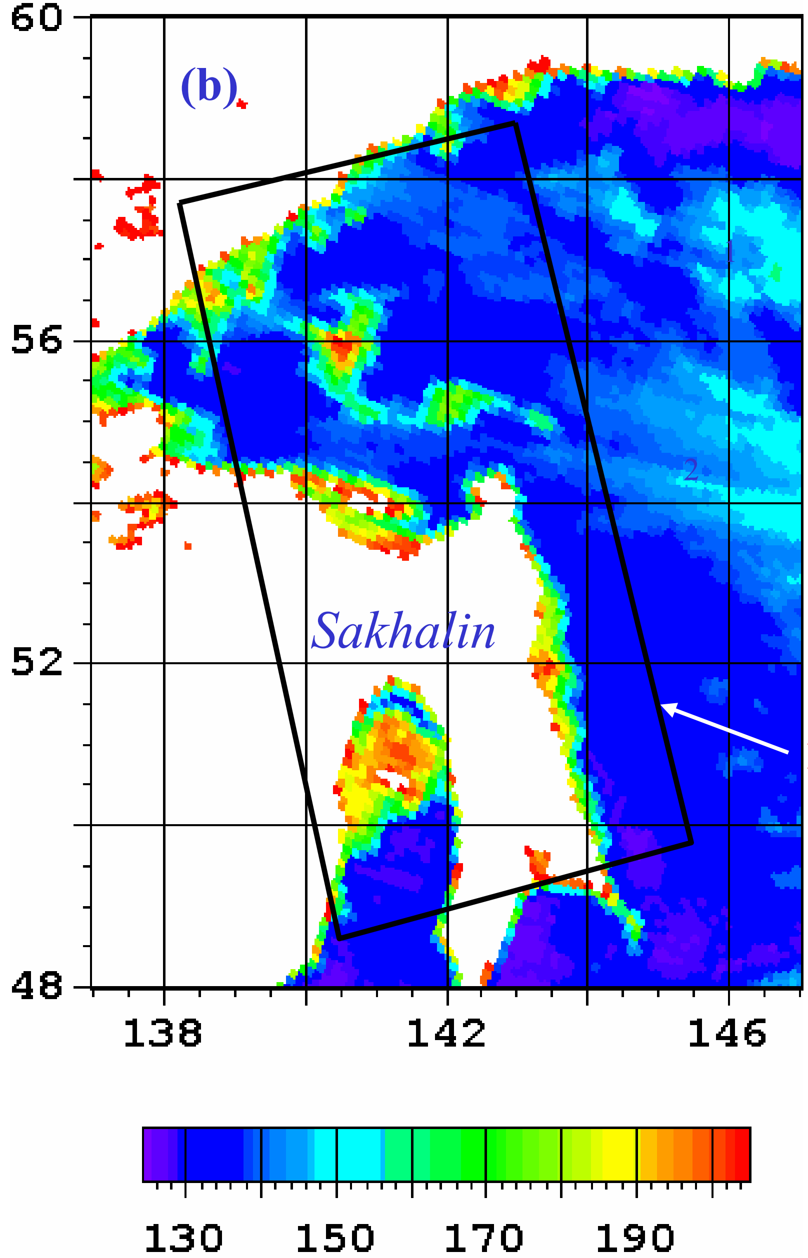

Aqua AMSR-E at 15:23 UTC, 36.5 GHz, H-polarization

Grease ice 3260 km^2.

Pancake ice 6470 km^2.

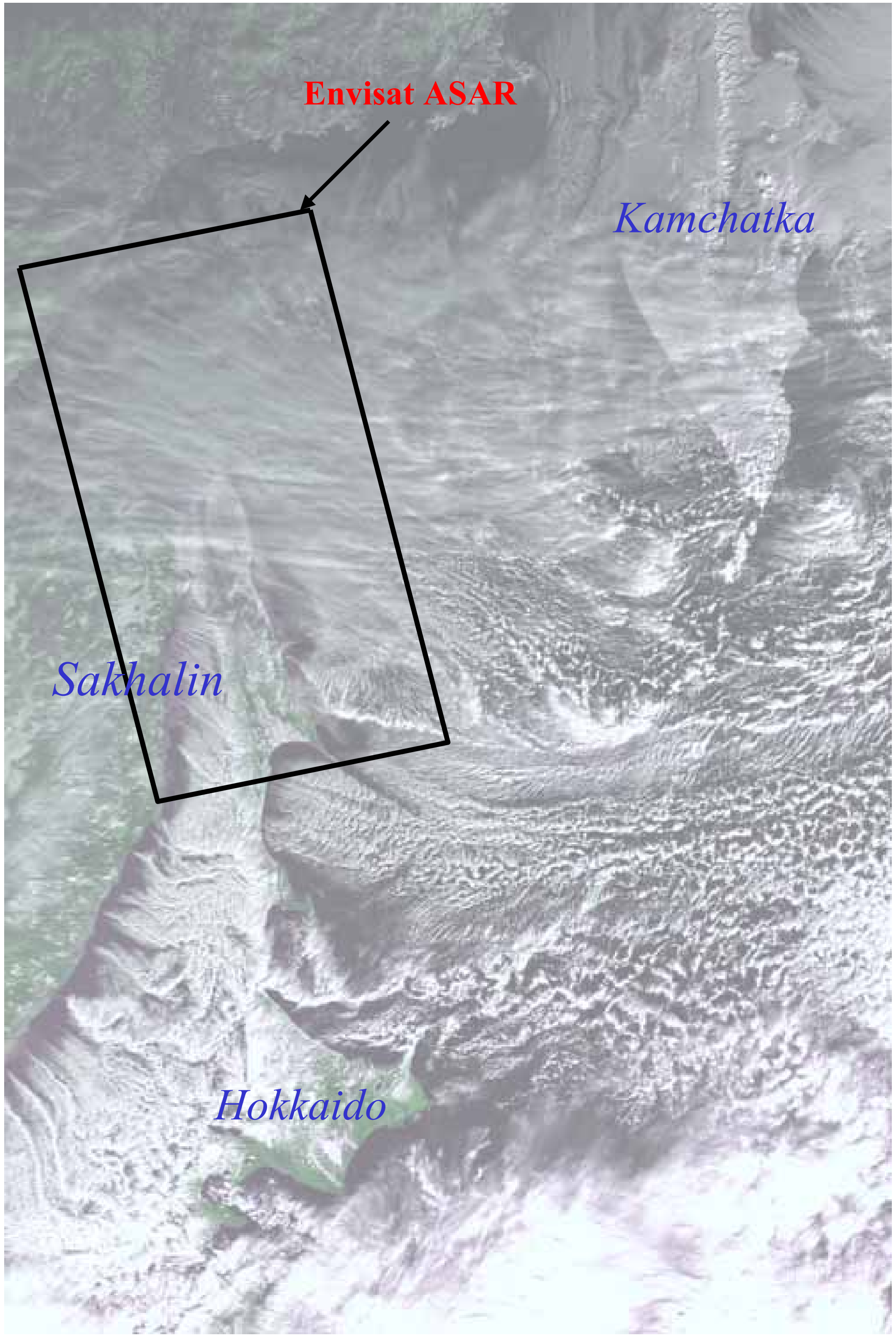

NOAA AVHRR
9 December 2002

9 December 2002, at 15:23 UTC

Western Okhotsk Sea

Aqua AMSR-E

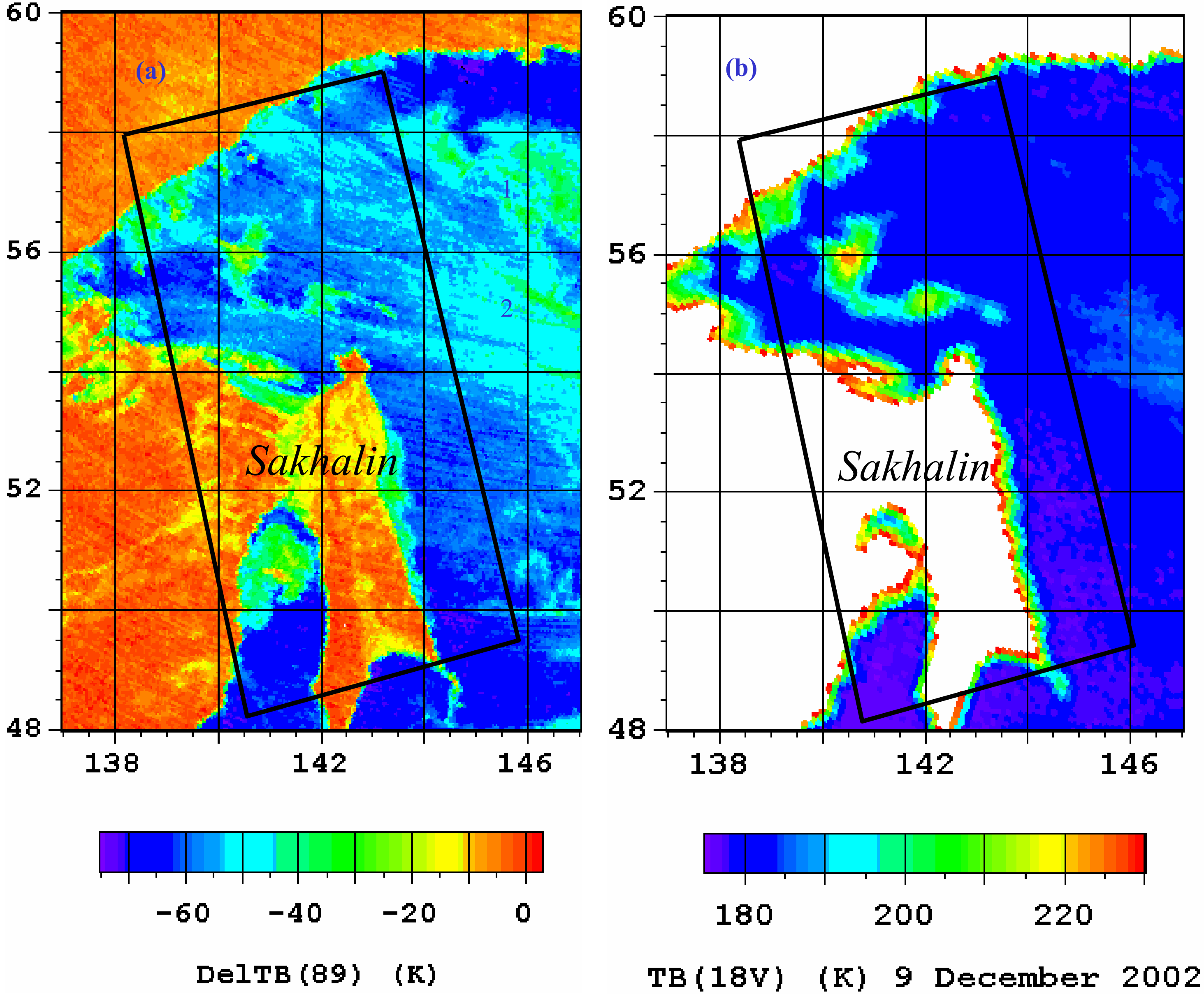

Polarization difference at 89 GHz

18.7 GHz, H-polarization

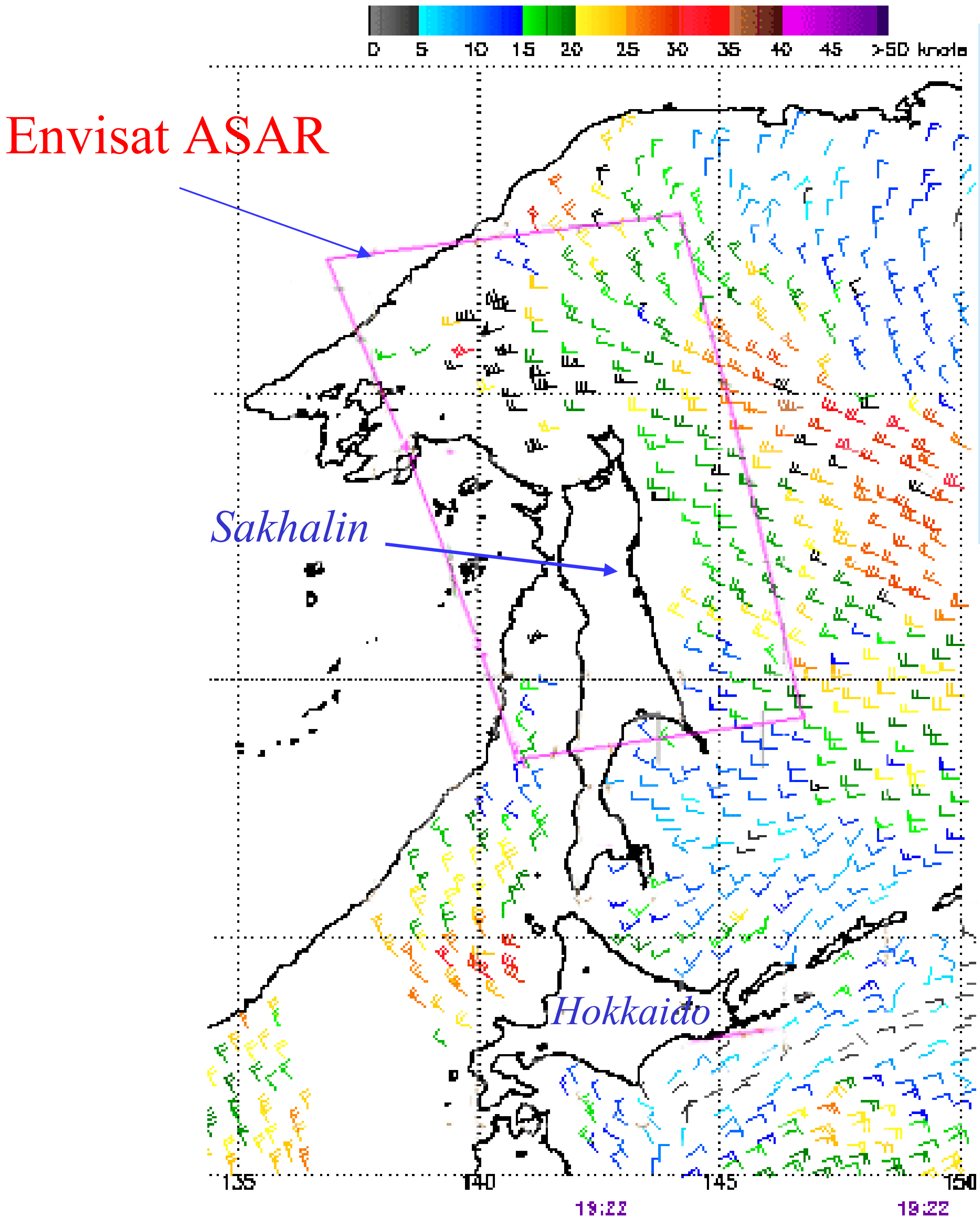

QuikSCAT SeaWnds.

9 December 2002, 19:20 UTC

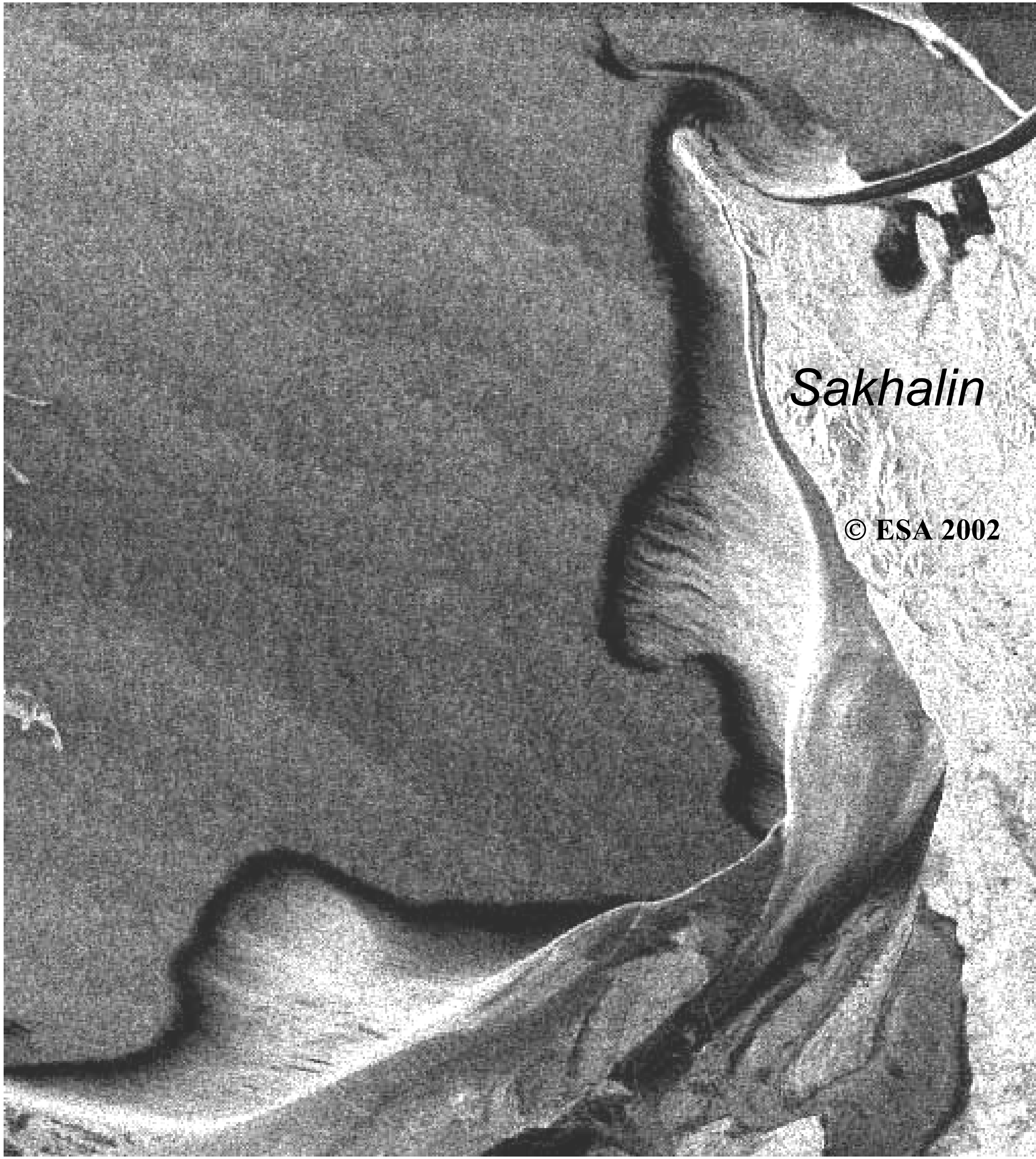

Envisat ASAR, HH, 9 December 2002, 12:11 UTC

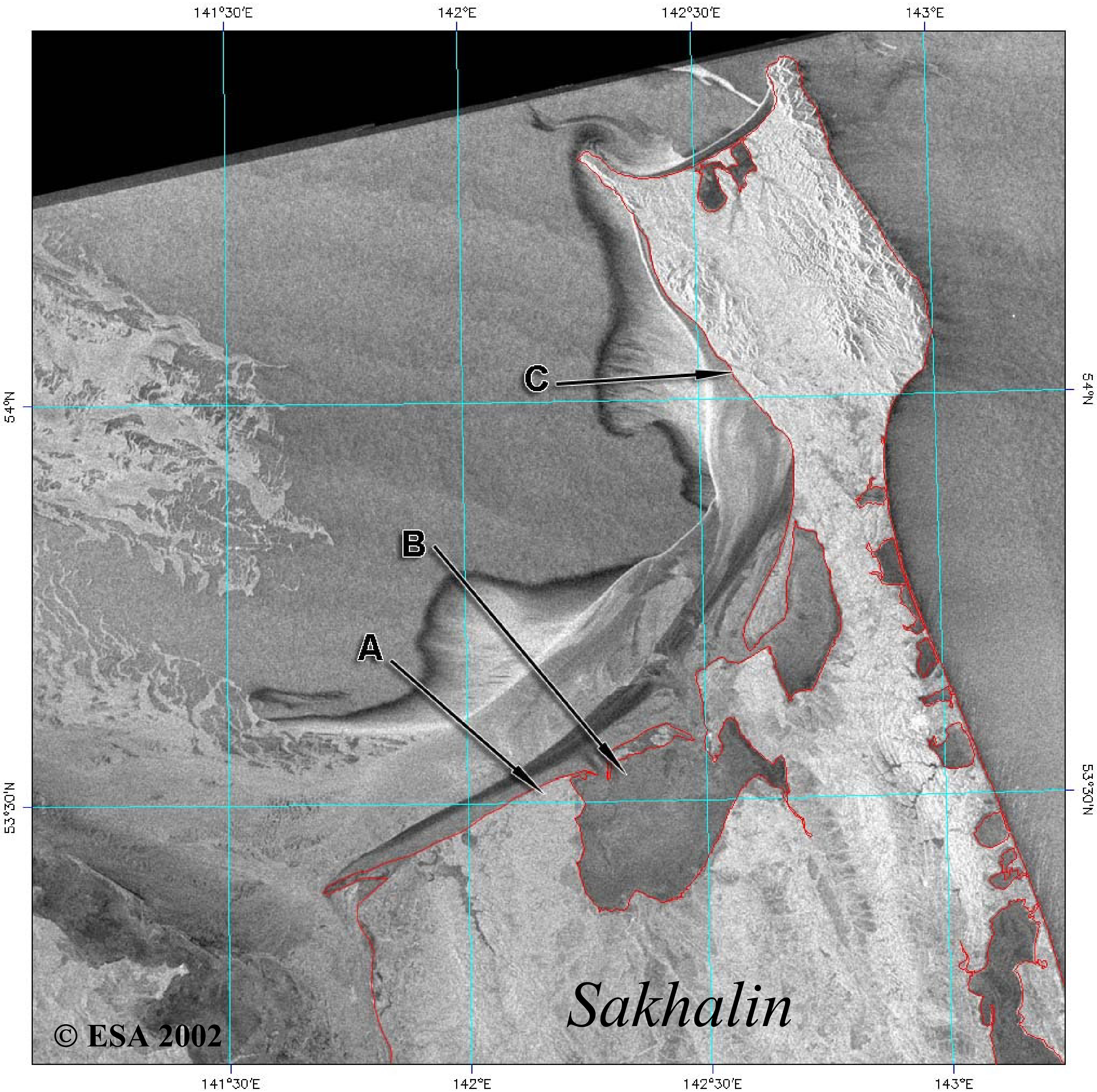

Envisat ASAR HH

9 Dec 2002
12:11 UTC

NRCS profiles

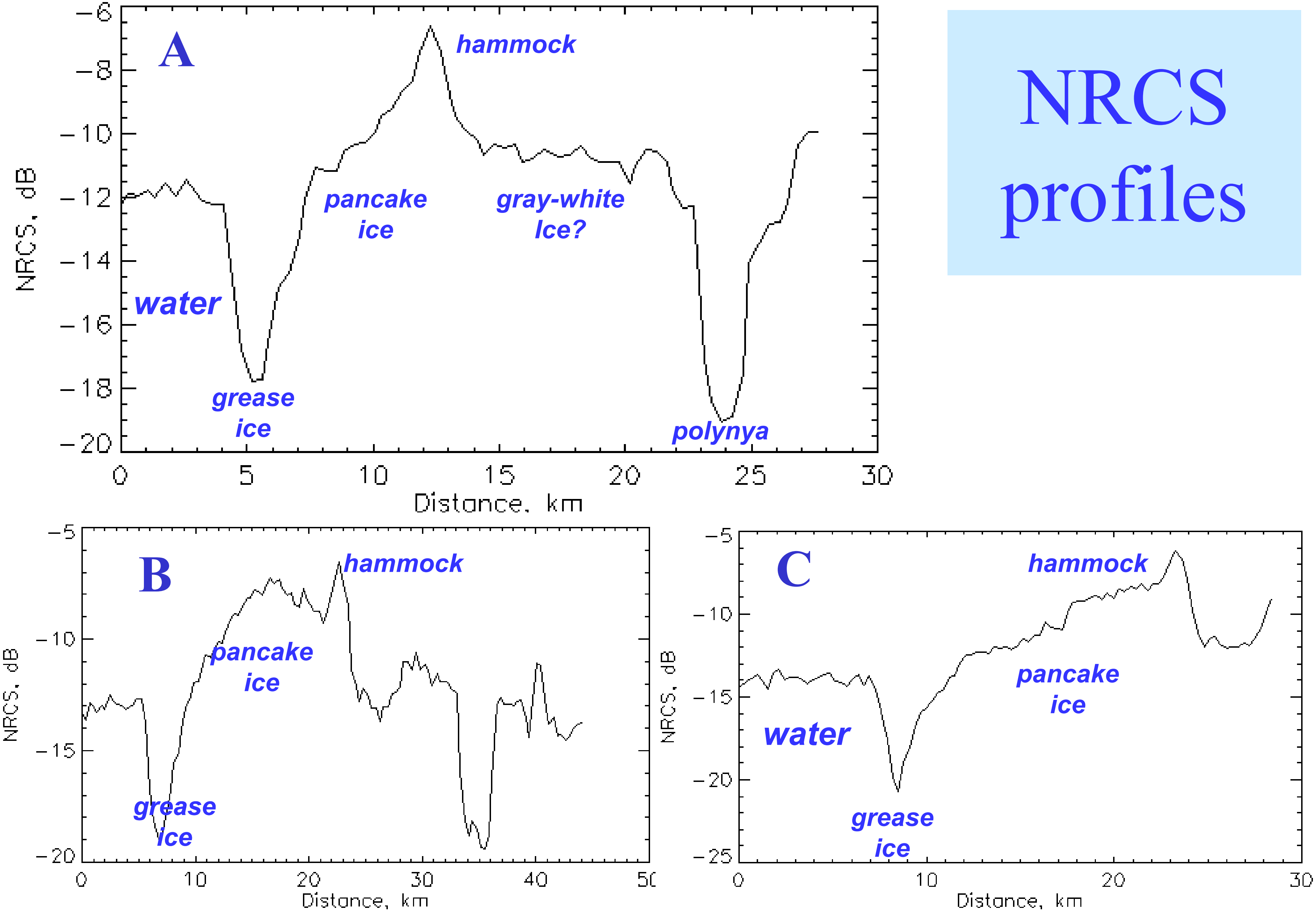

Envisat ASAR, 9 Dec 2002, 12: 11 UTC

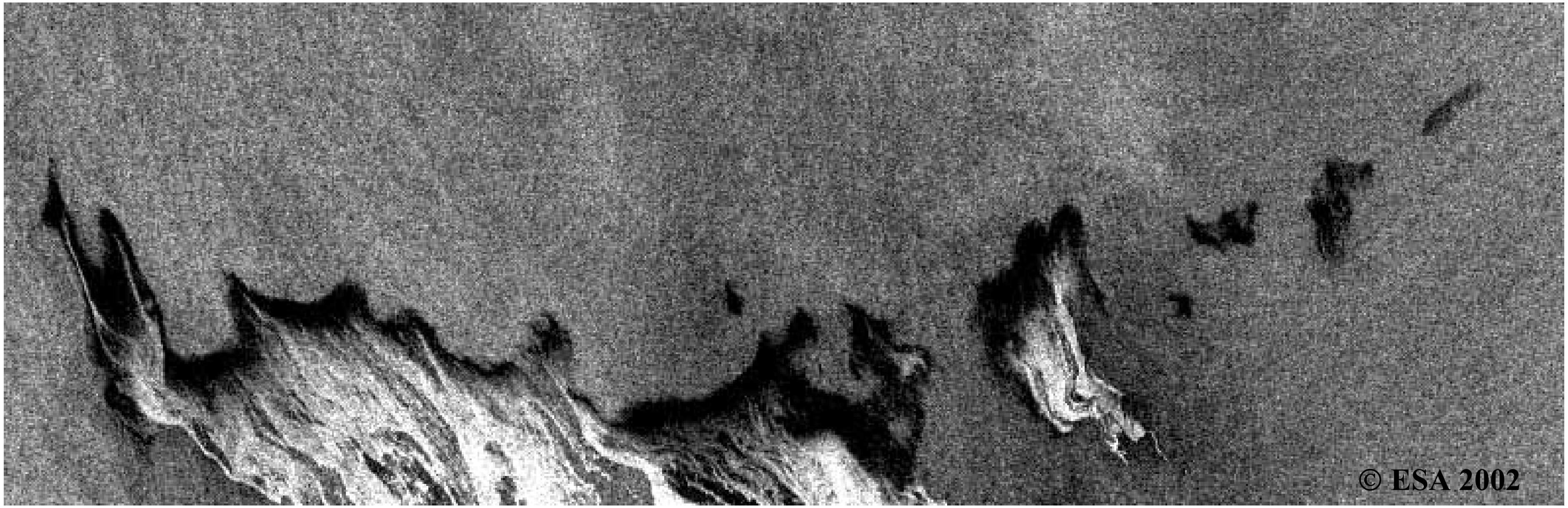

Patches of sea ice in the open sea

Envisat ASAR

31 January 2005

30 January 2005

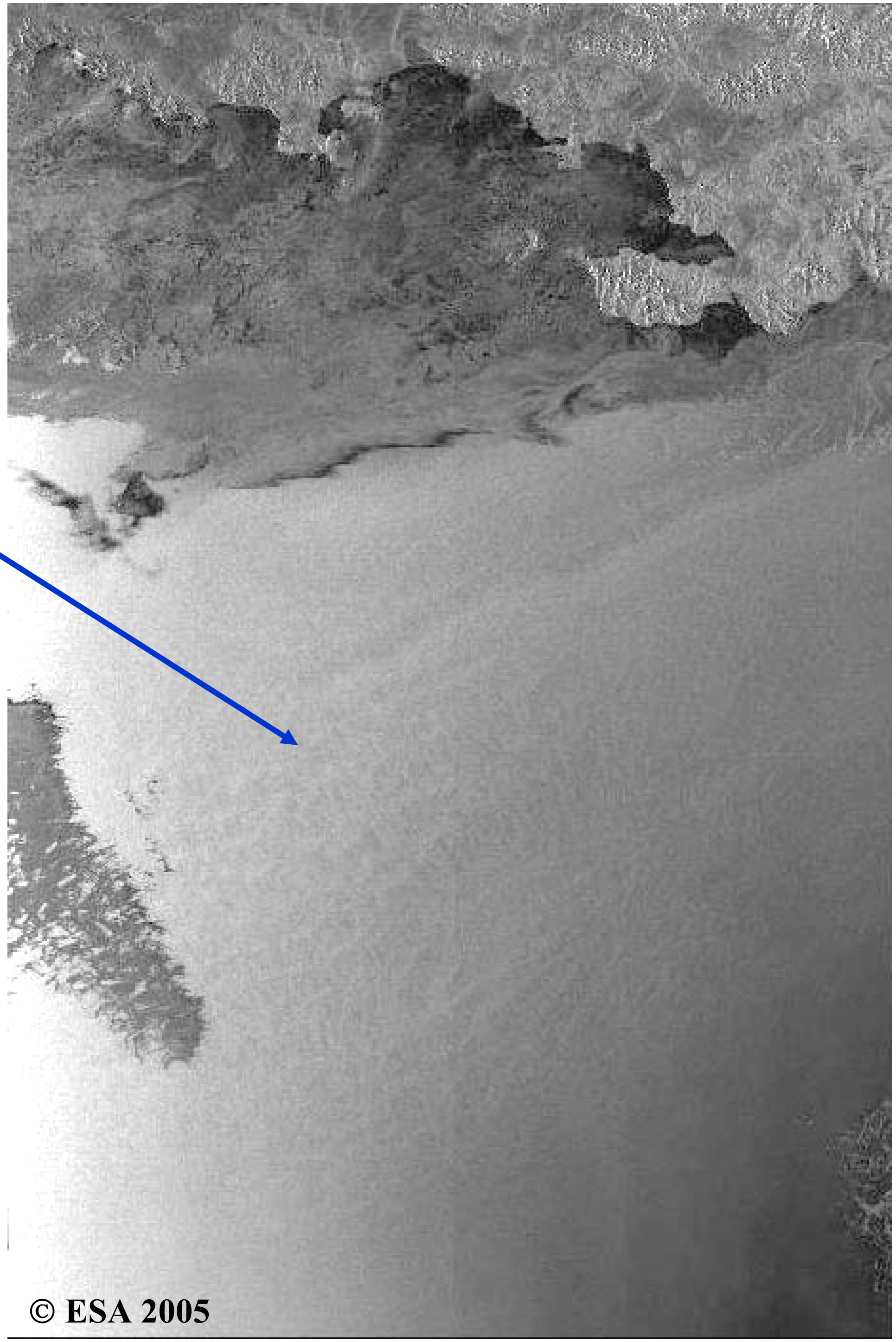

31 January 2005

Envisat ASAR, 11:31 UTC

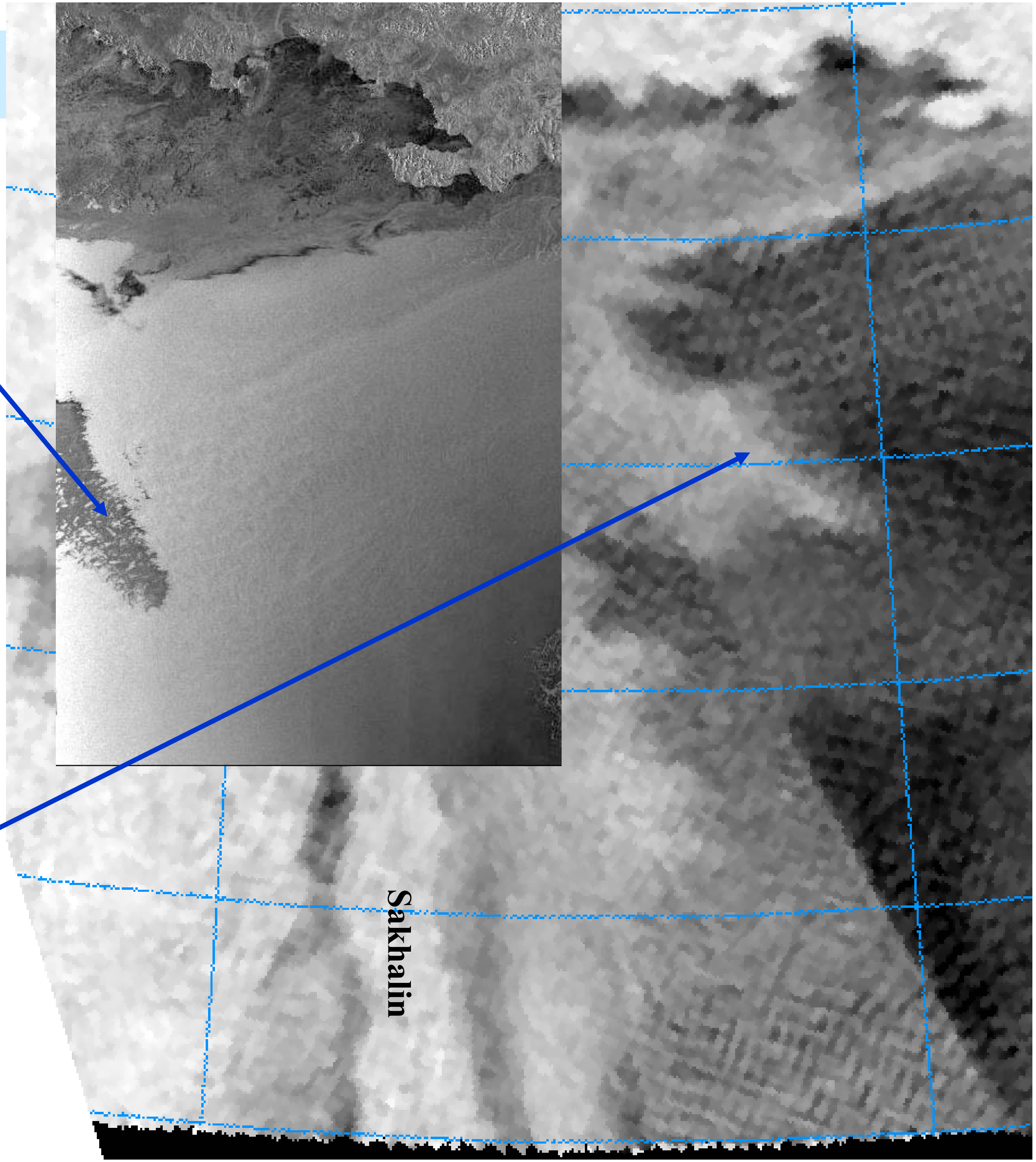

QuikSCAT SeaWinds 8:48 UTC

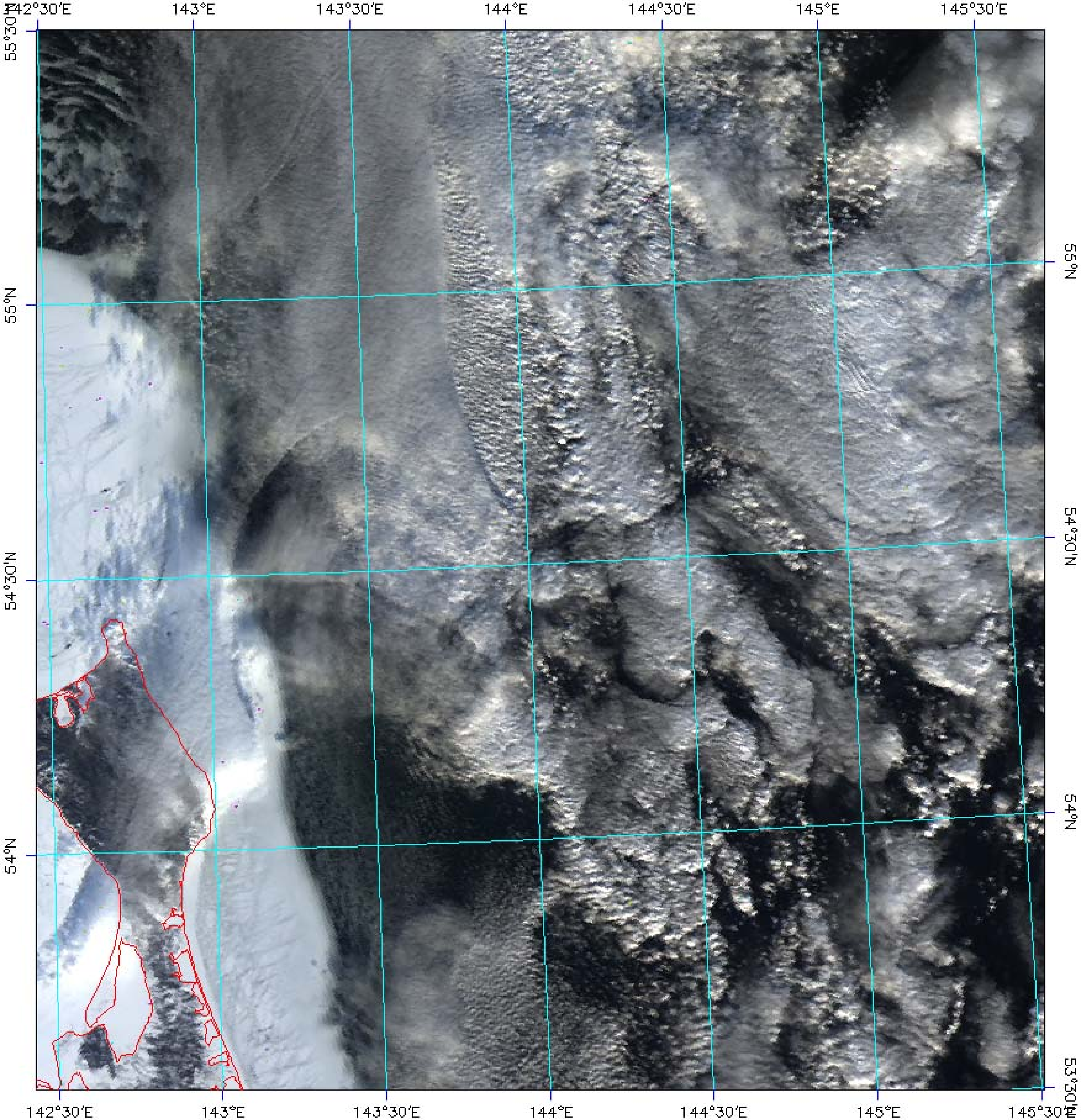

MODIS
14 January 2005

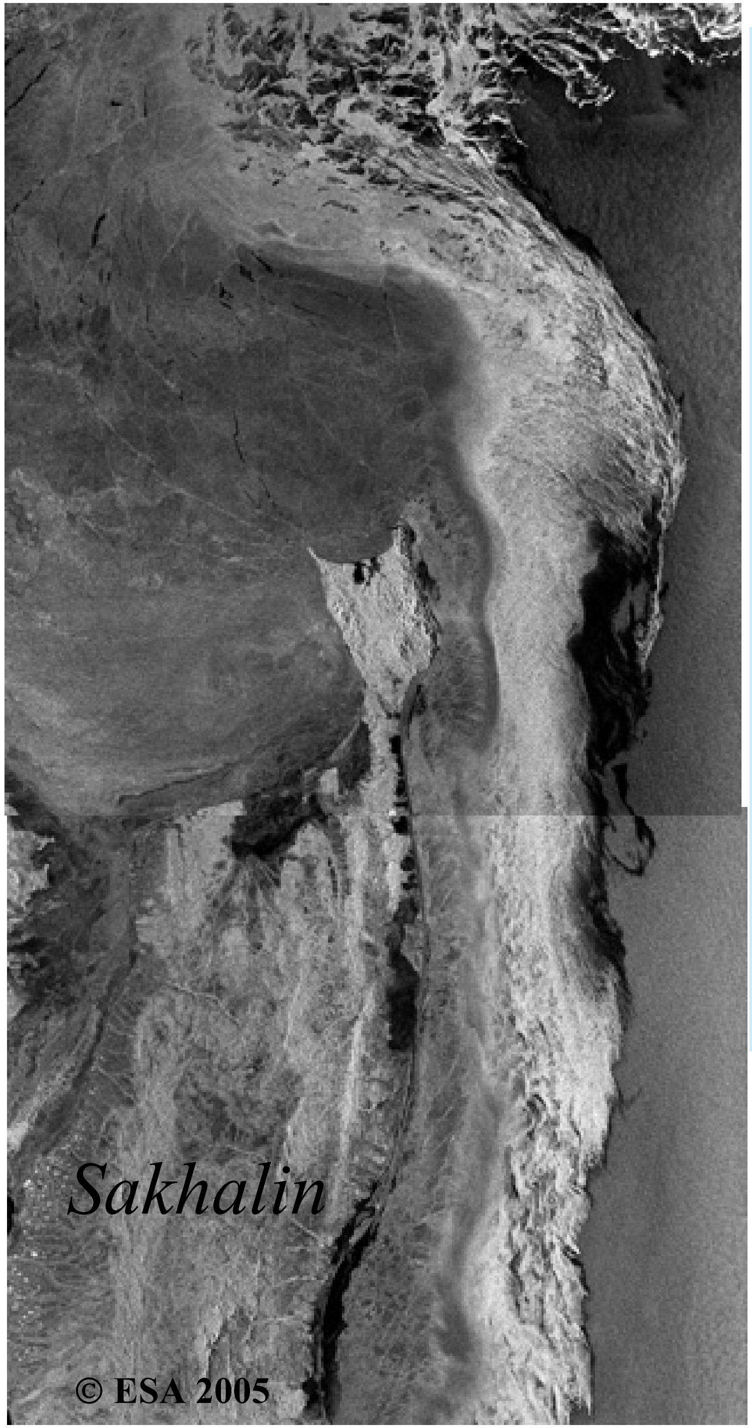

Envisat ASAR images taken on 14 January 2005 at 00:41 and at 12:04 UTC

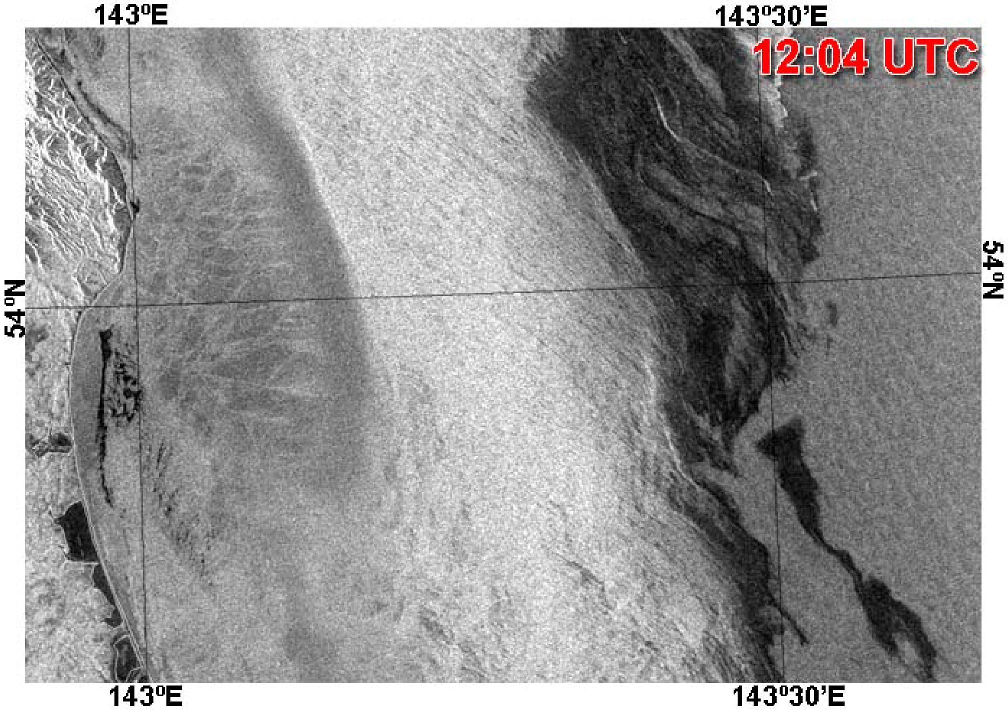

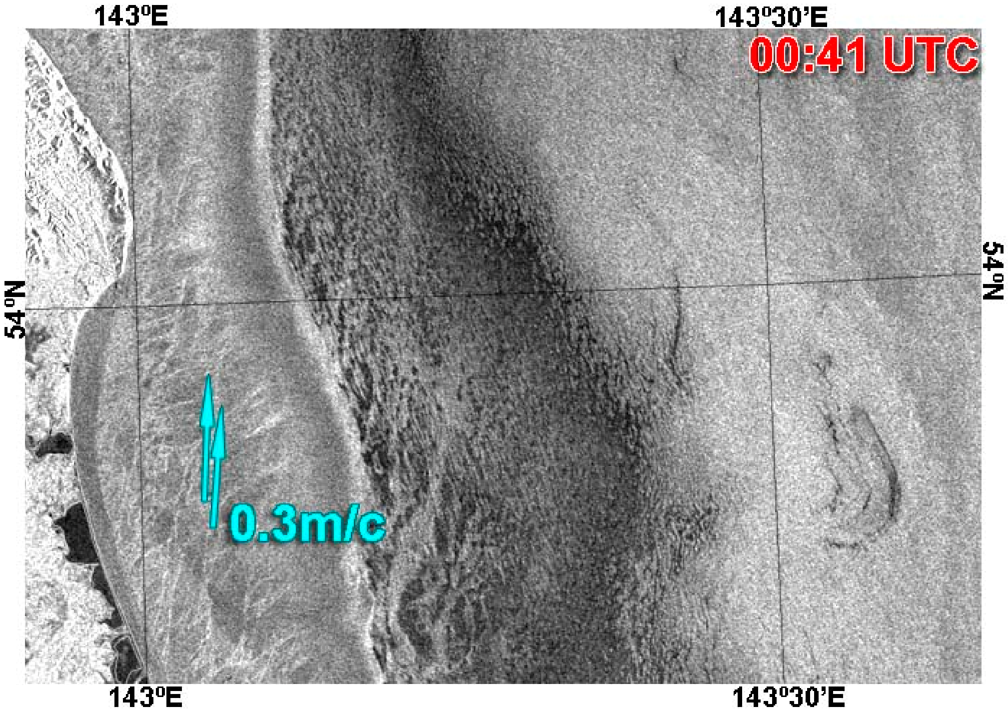

Envisat ASAR
images taken at 00:41 UTC and at 12:04 UTC on 14 January 2005

Eastern Okhotsk Sea

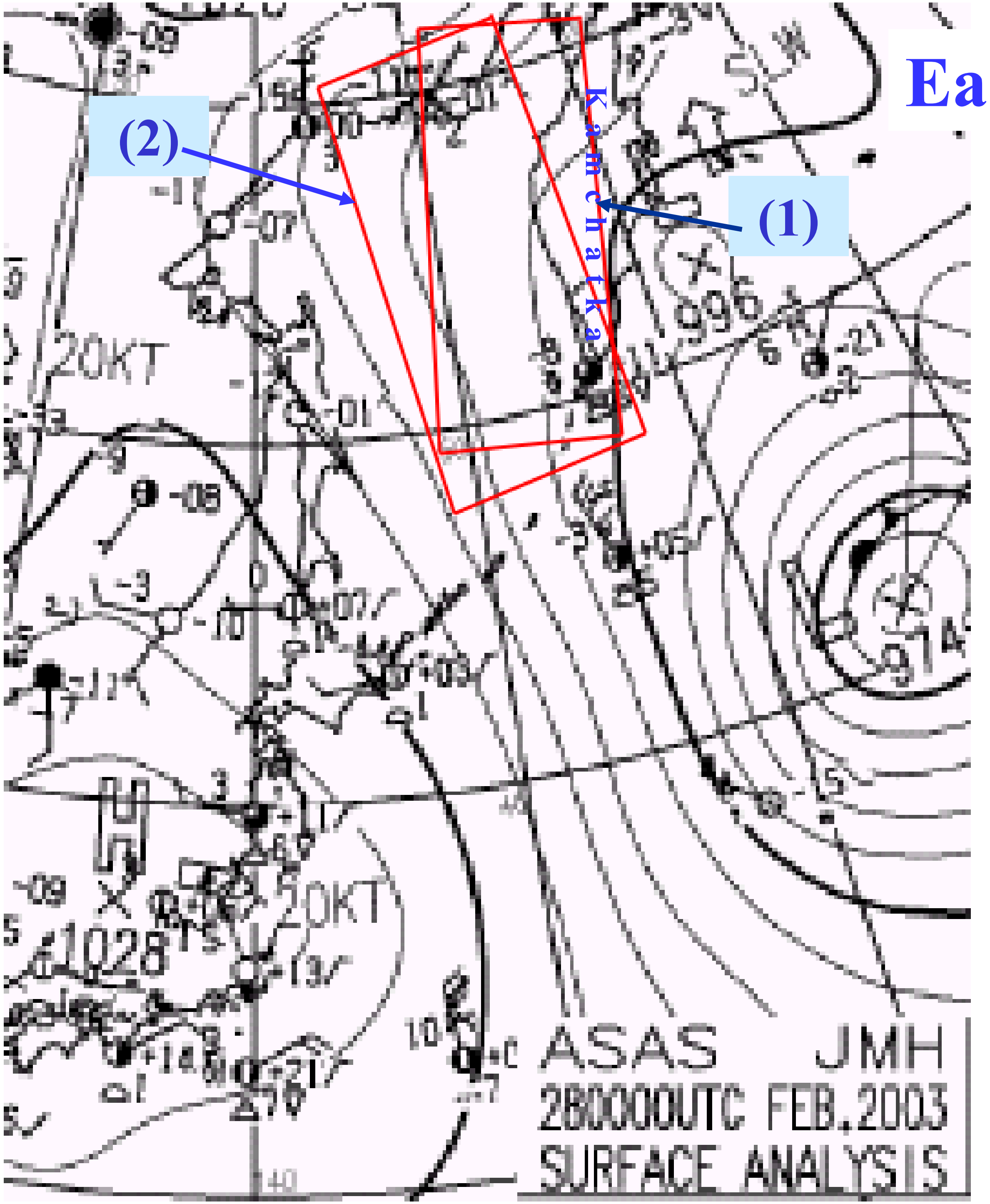

Surface analysis map of the JMH for 28 February 2003, 00:00 UTC

Red rectangles mark the boundaries of Envisat ASAR images taken on 28 Feb 2003

at 00:00 UTC (1) and at 11:25 UTC (2)

28 February 2003

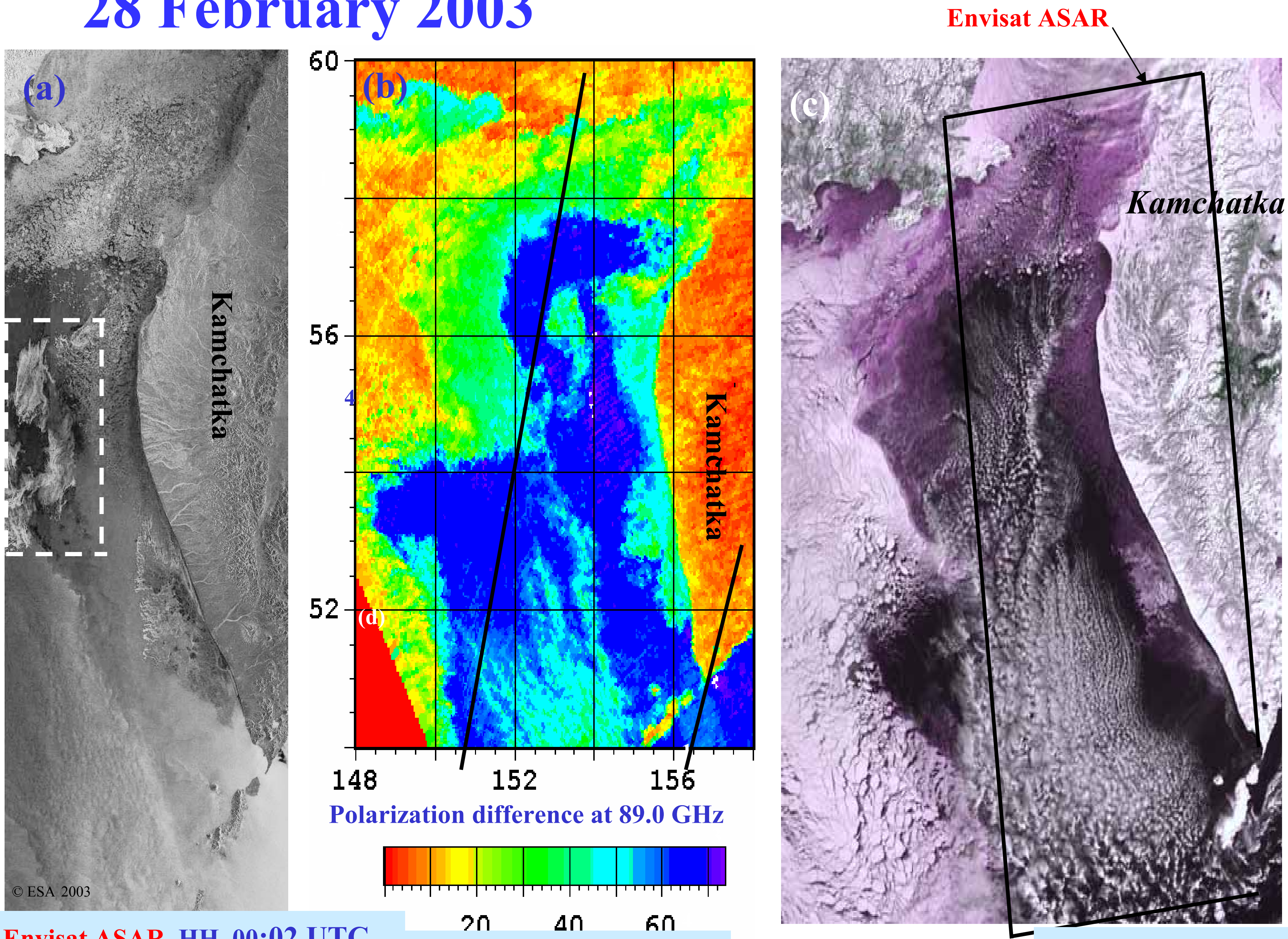

Envisat ASAR, HH, 00:02 UTC

Aqua AMSR-E at 01:29 UTC

NOAA AVHRR

28 February 2003

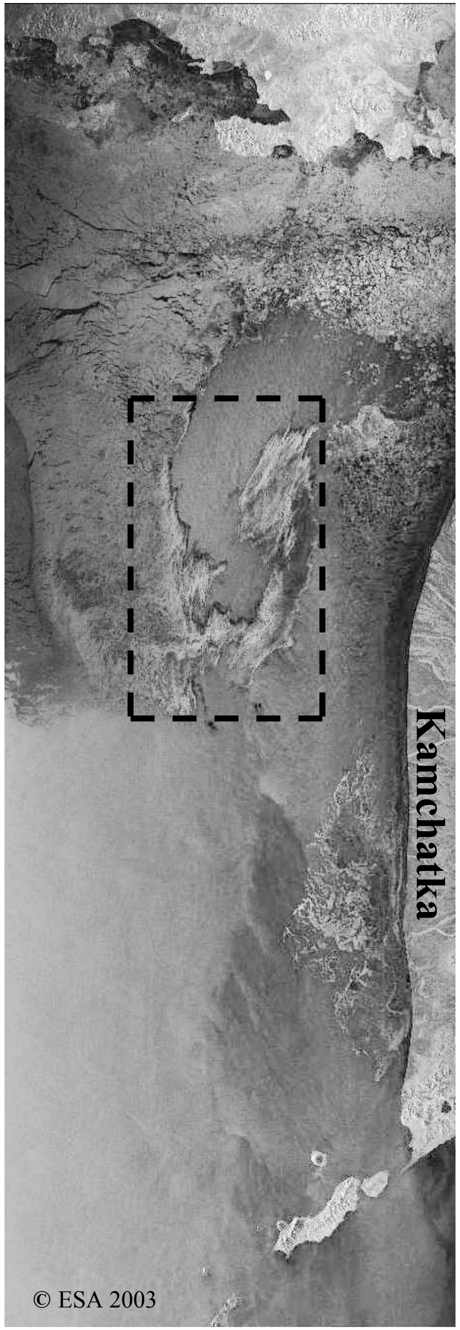

Envisat ASAR, HH, 11:25 UTC

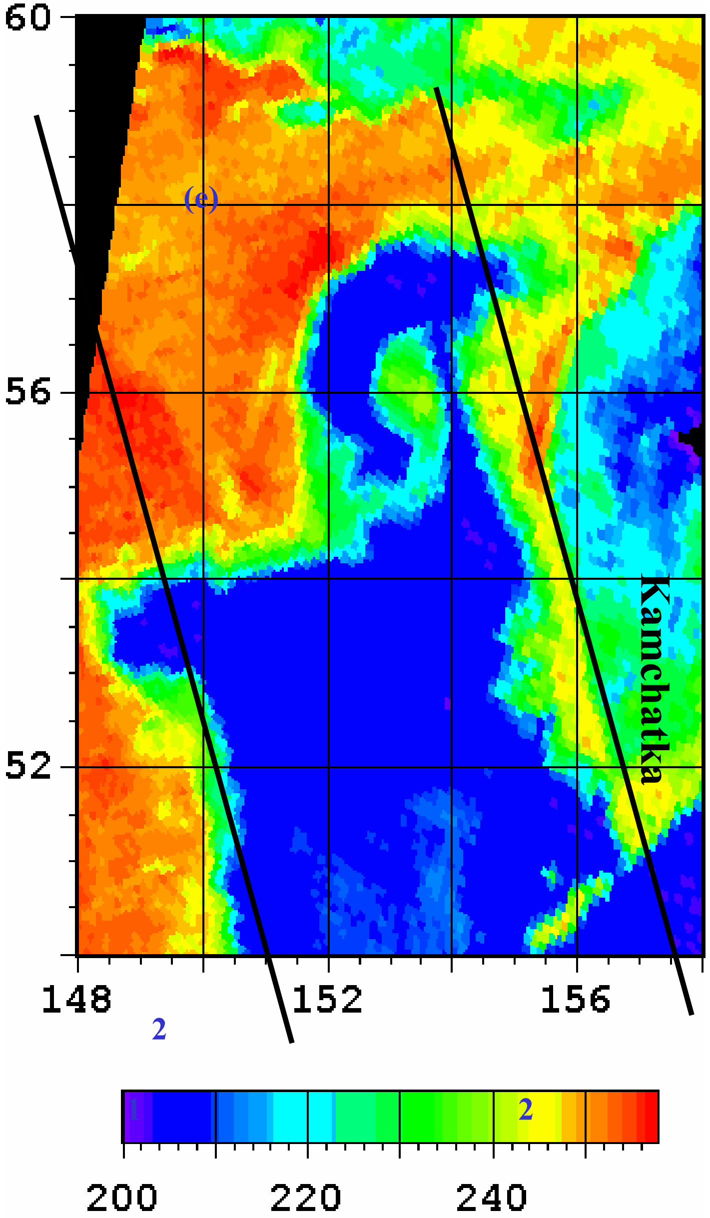

Aqua AMSR-E. 15:29 UTC
T_B(36V)

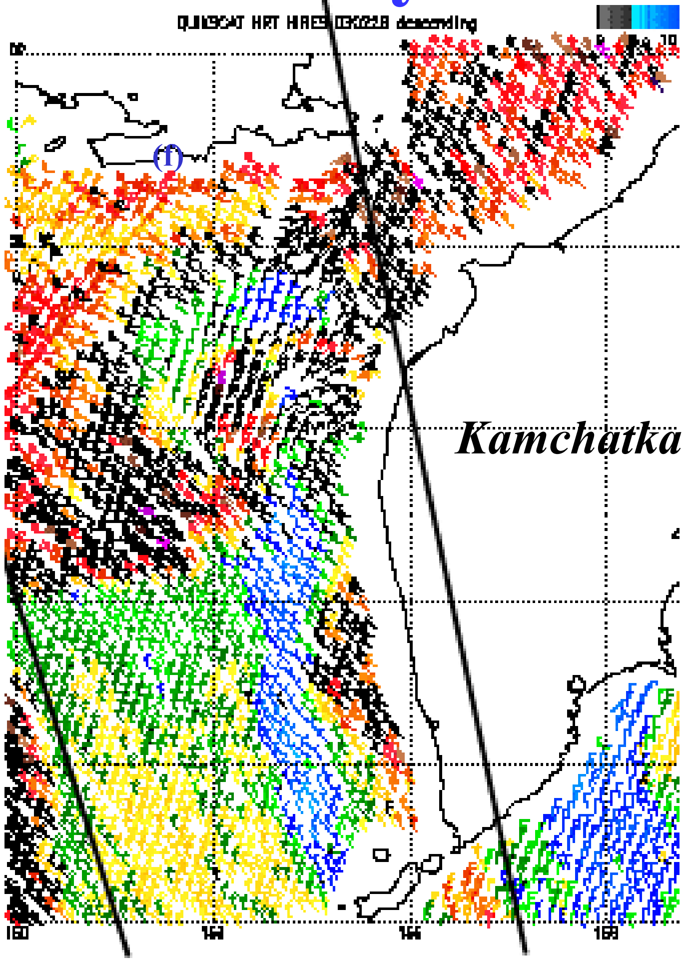

QuikSCAT SeaWinds-derived wind field at 08:08 UTC

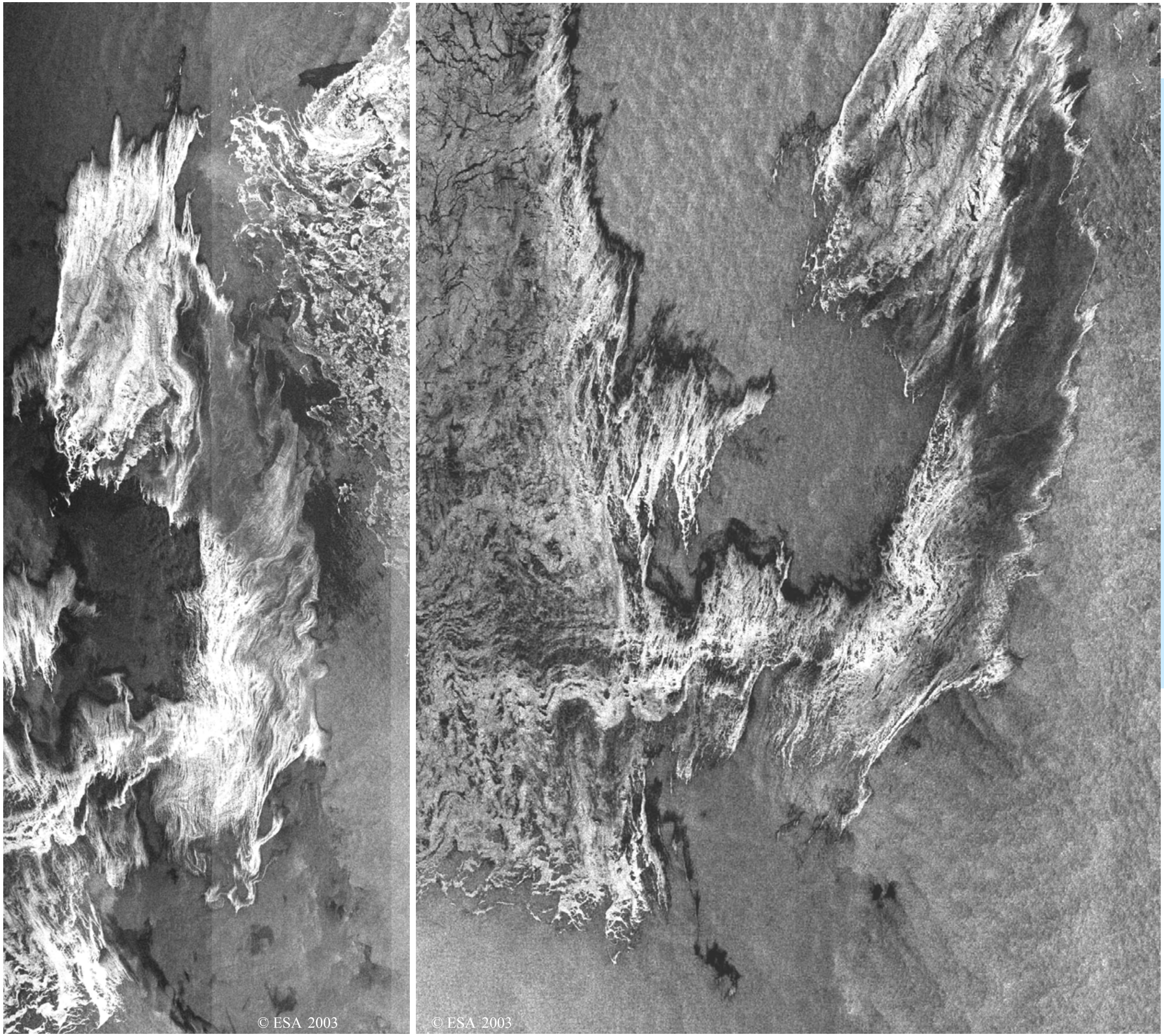

Envisat ASAR 28 Feb 2003 at 00:02 and at 11:25 UTC

Conclusions

This study has demonstrated the utility of a multiscale multisensor approach for the sea ice study in the Okhotsk Sea. Data from satellite SAR, microwave scanning radiometer, scatterometer, AVHRR and MODIS were used for several case studies in different regions of the Sea. The sensors were chosen for their temporal simultaneity of measurement collection.

The primary attention was given to the satellite SAR due to the high spatial resolution capability of the instruments. SAR can provide precise data on the location and type of ice boundary, concentration and the presence or absence of polynyas and leads. Interpretation of SAR images is not straightforward due to the ambiguities associated with SAR backscatter from sea ice features that vary by season and geographic region.

Application of AMSR, AMSR-E, SeaWinds scatterometer and MODIS visible/ infrared observations decreases the ambiguities in the interpretation of SAR data.

Acknowledgments

This study was carried out within

•the cooperation between
National Space Development Agency JAXA **(Japan) and** ***V.I. Il'ichev Pacific Oceanological Institute, Far Eastern Branch of the Russian Academy of Sciences*** **(Russia) in the ADEOS-II Research Activity**

(PROJECTS A2ARF006 and AD2M-3RA-UF002)

as well as within

•ESA ERS project AO3-401: "Mesoscale oceanic and atmospheric phenomena in the coastal area of the Japan and Okhotsk seas: Study with ERS SAR and research vessels" and

•ESA Envisat project AO-ID-391: "Study of the interaction of oceanic and atmospheric processes in the Japan Sea and the Southern Okhotsk Sea".

This work is partially sponsored by a grant for a project: "Investigation of ocean-atmosphere system with passive and active microwave sensing from new generation satellites" from Far Eastern Branch of the Russian Academy of Sciences.

Evaluation of sea ice thickness estimations by satellite passive microwave and thermal infrared radiometers

*T. TANIKAWA (Kitami Inst. Of Tech.),
K. TATEYAMA, H. ENOMOTO (Kitami Inst. Of Tech.),
and K. SHIRASAWA (SIRL, ILTS, Hokkaido Univ.)

Background

Sea ice thickness estimation by the satellite remote sensing

Qualitatively → ***Quantitatively***

- **AVHRR ice thickness**: AVHRR + Heat flux
  - -Groves and Stringer [1991]: AVHRR + Kuhn's model
  - -Drucker et al. [2003]: AVHRR + Yu and Rothrock [1996]
- **Active microwave ice thickness**: ERS, RADARSAT
  - - Kwok and Cunningham [2002] : RGPS
  - - Peacock and Laxon [2004] : altimeter
- **Passive microwave ice thickness**: SSM/I
  - - Tateyama et al., [2002]: $R_{37V/85V}$, $R_{19H/85V}$, PR_{19}
  - - Martin et al., [2004]: R_{37}

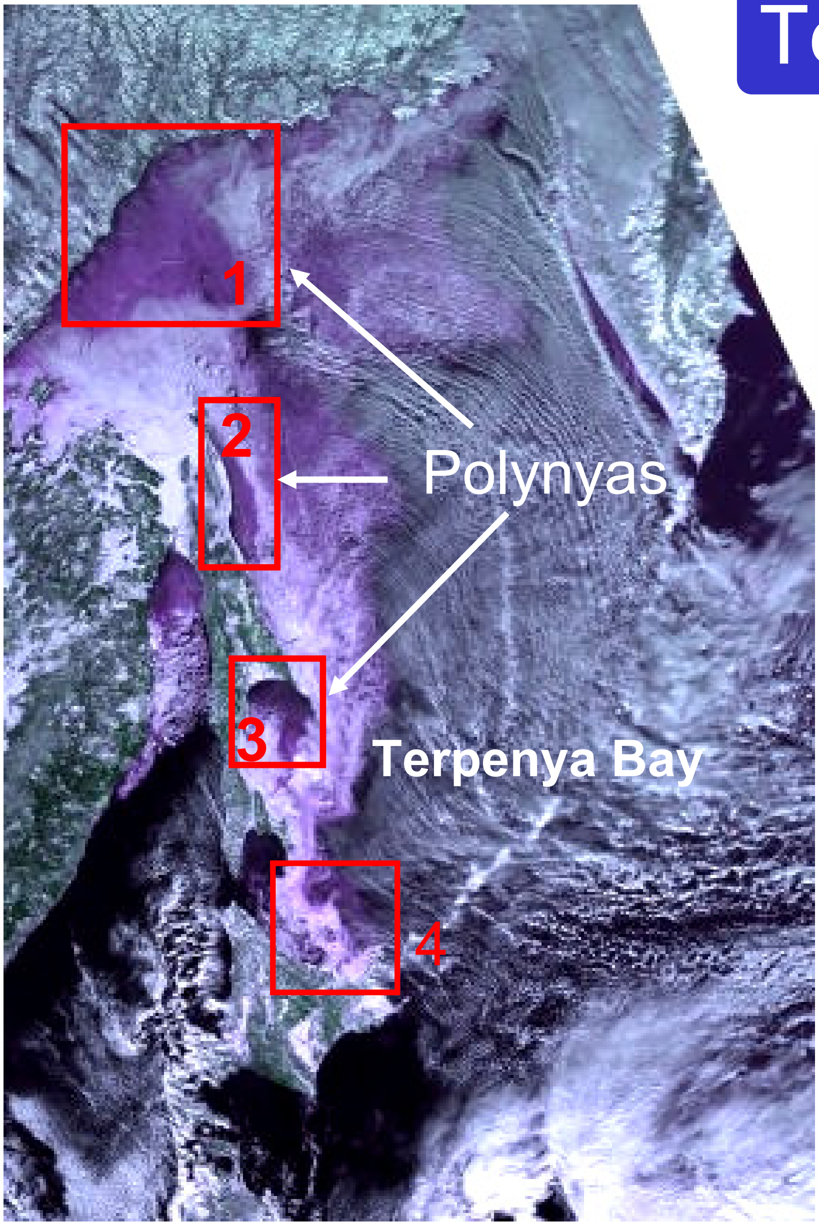

Test site

Terpenya Polynya

'Terpenya Bay' polynya in 1997 winter.

- no ice movement
- no snow cover

Thick ice

Data and Spatial Resolution

- **DMSP SSM/I**
  - ✓**Tateyama algorithm [2002]**
  - ✓**Martin algorithm [2004]**
    - Daily brightness temperature (BT) from DMSP SSM/I

For validation

- **NORR AVHRR**
  - ✓**Yu and Rothrock algorithm [1996]**
    - Daily surface temp. data from NOAA AVHRR
    - Daily meteorological data from NCEP/NCAR reanalysis
- **Ship-borne video data (for thick ice)**

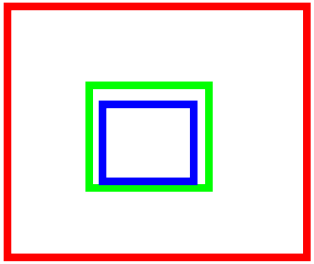

NCEP/NCAR : 2.5° mesh → 280km×280km
AVHRR : 1.1km x 80pixel → 88km×88km
SSM/I : 12.5km x 6pixel → 75km×75km

Method 1 — Tateyama algorithm (2002)

- Tateyama algorithm is developed based on the SSM/I data and *in-situ* ice thickness data taken by ship-borne video camera.

The ice thickness H_T (m) is estimated using empirical equation;

$$H_T = -5.37 \cdot PR_{19} + 0.84 \cdot R_{37V/85V} - 0.07, \quad (1)$$

where

$$PR_{19} = \frac{TB_{19V} - TB_{19H}}{TB_{19V} + TB_{19H}}, \qquad R_{37V/85V} = \frac{TB_{37V}}{TB_{85V}}, \quad (2)$$

➢ Sea-ice surface roughness ➢ Temperature gradient

When a new ice signal is detected ($R_{37V/85V}$ <0.97), $^*R_{37V/85V}$ is converted to $R_{37V/85V}$ by following equation,

$$R_{37V/85V} = 0.3 \cdot \left({}^*R_{37V/85V} - R_{19H/85V} \right) + 0.6 \cdot R_{19H/85V} - 0.29_5 \quad (3)$$

Method 2

Martin algorithm (2004)

- Martine algorithm is useful for ice production in polynyas.

  - This algorithm is developed based on the ratio of H- and V-polarized 37GHz channels.

The ice thickness H_M (m) is calculated using the following equation

$$H_M = \exp^{1/(\alpha R_{37} + \beta)} - \gamma, \tag{4}$$

where $\alpha = 230.47$, $\beta = -243.60$, $\gamma = 1.0080$, and,

$$R_{37} = \frac{TB_{37V}}{TB_{37H}}. \tag{5}$$

Method 3 Yu and Rothrock algorithm (1996)

- Yu & Rothrock algorithm is based on surface-heat balance model using AVHRR thermal data.
  - In absence of melting and a snow cover, heat energy balance at the ice surface can be assumed that conductive heat loss at ice-surface through the ice is equal to the total heat flux F_{TL}.

The ice thickness H_A (m) is calculated using the following equation,

$$H_A = \frac{K_i (T_F - T_i)}{F_{TL}}, \tag{6}$$

where $K_\mathrm{i} = 2.034$ (W/m/K), $T_\mathrm{F} = -1.8$ (ºC). T_i can be calculated from the AVHRR data given by [Key and Haefliger, 1992],

$$T_i = a + b \cdot TB_{ch4} + c \cdot (TB_{ch4} - TB_{ch5}) + d \cdot (TB_{ch4} - TB_{ch5})(\sec\theta - 1), \tag{7}$$

$$F_{TL} = F_{SH}(T_i) + F_{LH}(T_i) + F_{LW}(T_i) + F_{SW} + F_{DL}(T_a). \tag{8}$$

Results 1

Meteorological data from NCEP/NCAR
- Air temp. at 1000 hPa
- Sea level pressure

Ice concentration from the SSM/I

Estimated ice thickness from SSM/I and AVHRR data

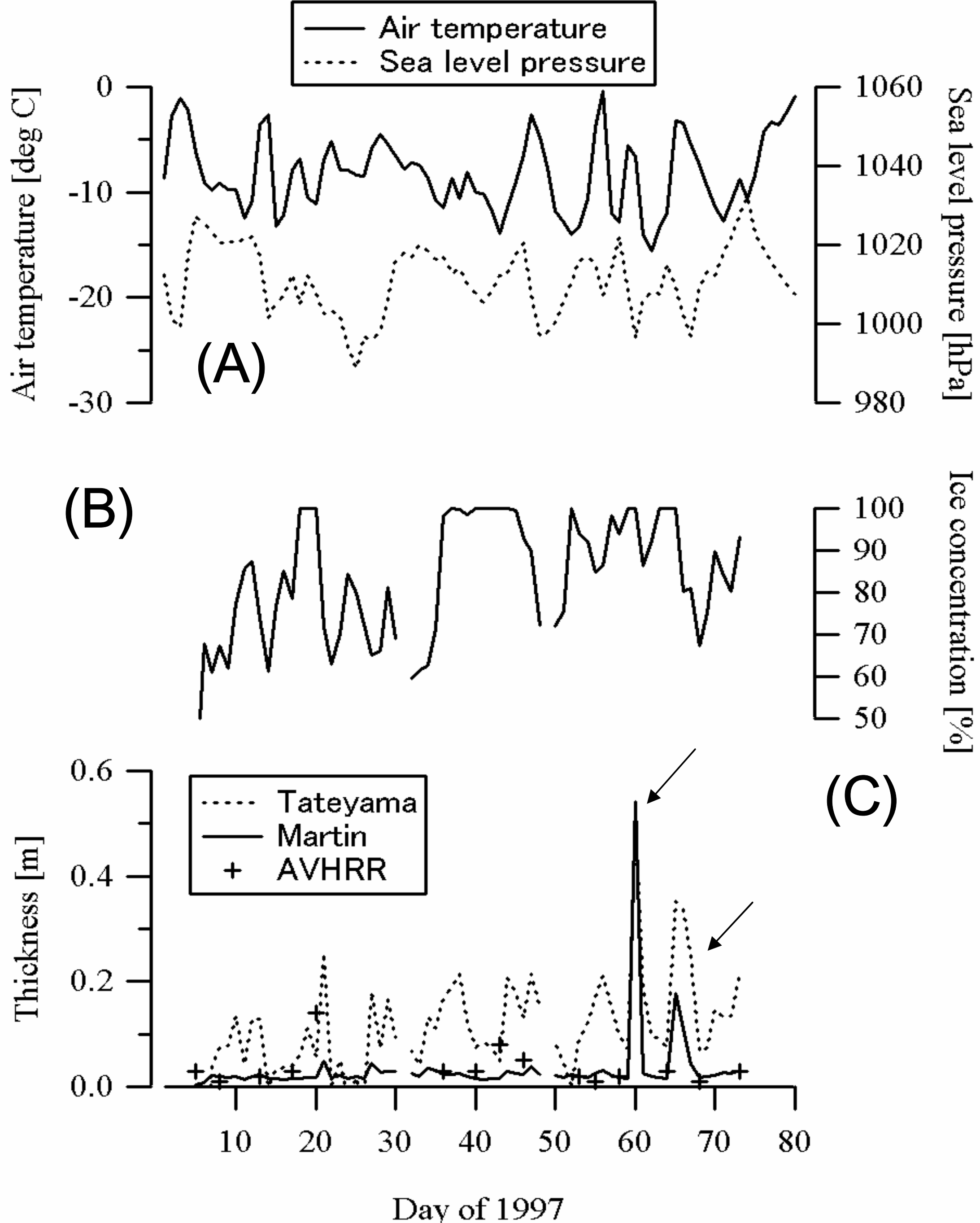

Comparison 1 | *Thin* Sea Ice

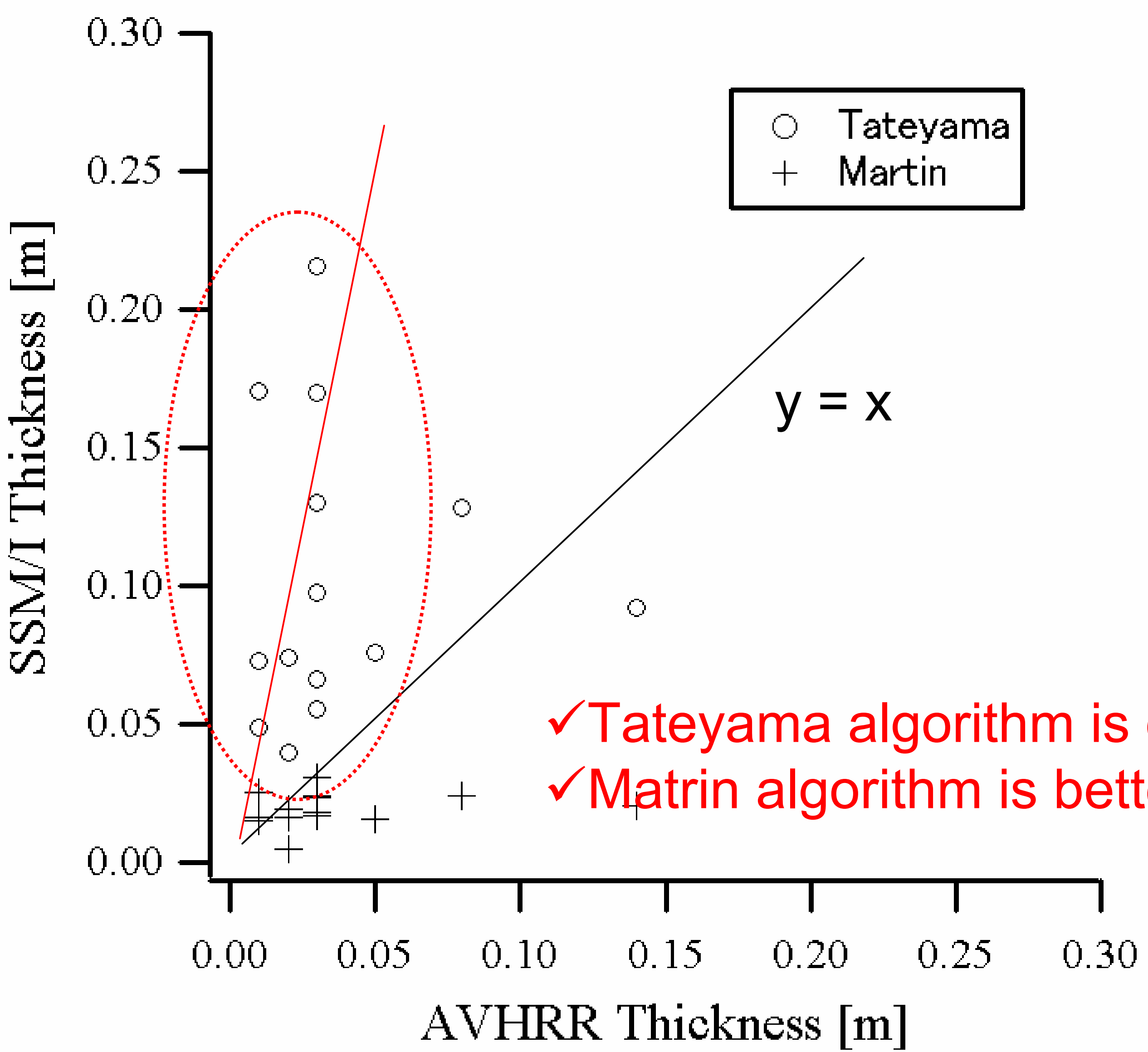

✓Tateyama algorithm is overestimated.
✓Matrin algorithm is better for thin sea ice.

Comparison 2 | *Thick* Sea Ice

✓Matrin algorithm is underestimated.
✓Tateyama algorithm is better for thick sea ice.

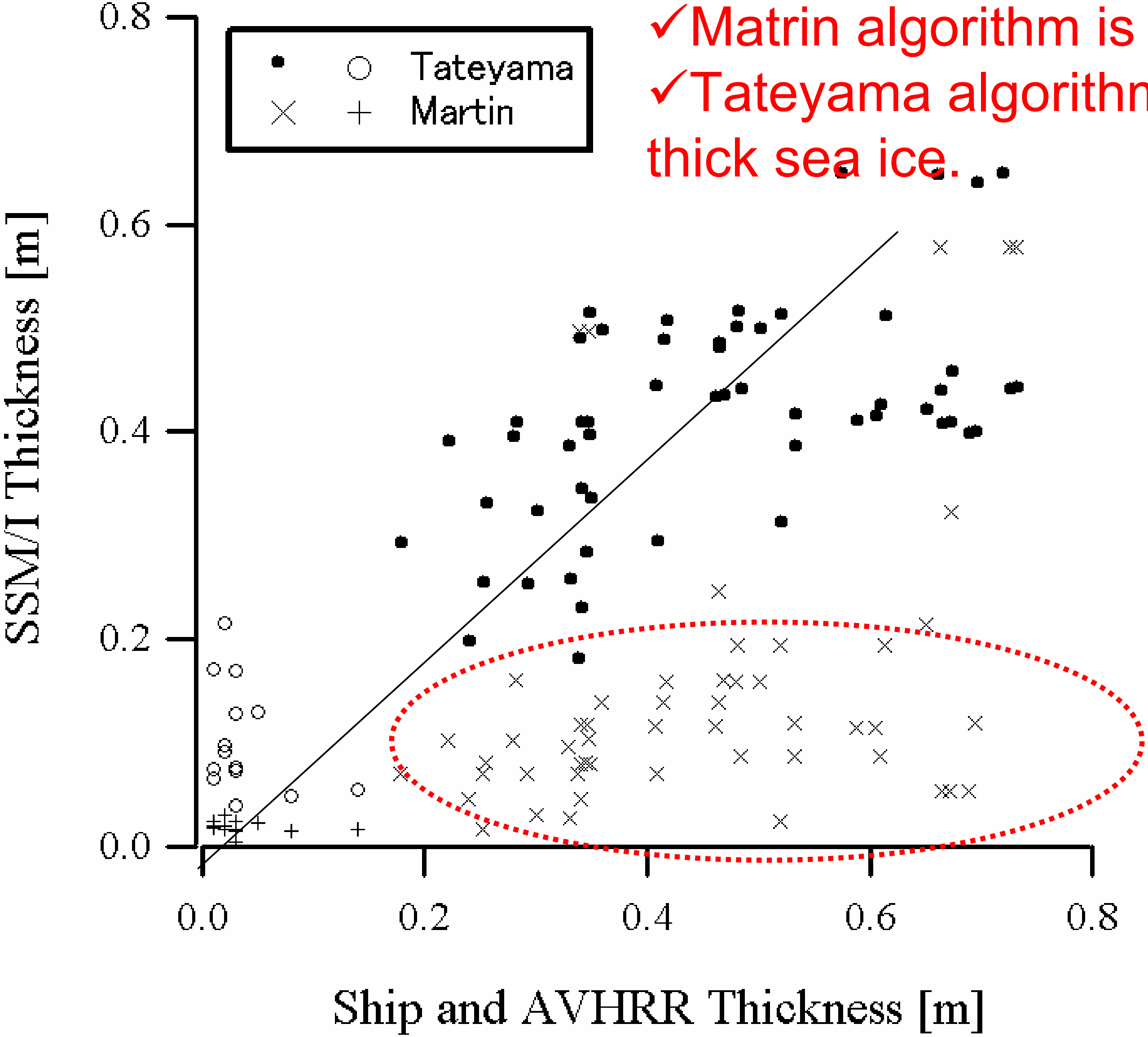

Discussion

- Uncertainties in the ice-thickness from AVHRR data.

  ✓ Ice thickness derived from AVHRR agrees with that from upward looking sonar within 10%.
  ✓ A coarse spatial resolution of AVHRR (1.1 km).
  ✓ The largest uncertainty is in NCEP data.
    - a course spatial resolutions of (2.5^{o}x 2.5^{o} ; 280 km x 280km)
    - covers the bay and surrounding land.
  ✓ High thin cold clouds and low warm fogs over polynya.

Summary

Ice thickness estimation algorithms for thin sea ice in the Terpeniya Bay and for thick ice in Sea of Okhotsk were validated.

- Tateyama algorithm:
  - ✓A very poor relationship with AVHRR of RMSE 0.17 m for $<$ 0.2 m thick ice.
  - ✓A high correlation with the thick ice of RSME 0.14m.

- Martin algorithm:
  - ✓Efficient result for thin ice with RMSE 0.04 m.
  - ✓A coarse accuracy for thick ice with RMSE 0.47 m.

✓Tateyama algorithm and Martin algorithm are suitable for thick ice and thin ice estimation, respectively.

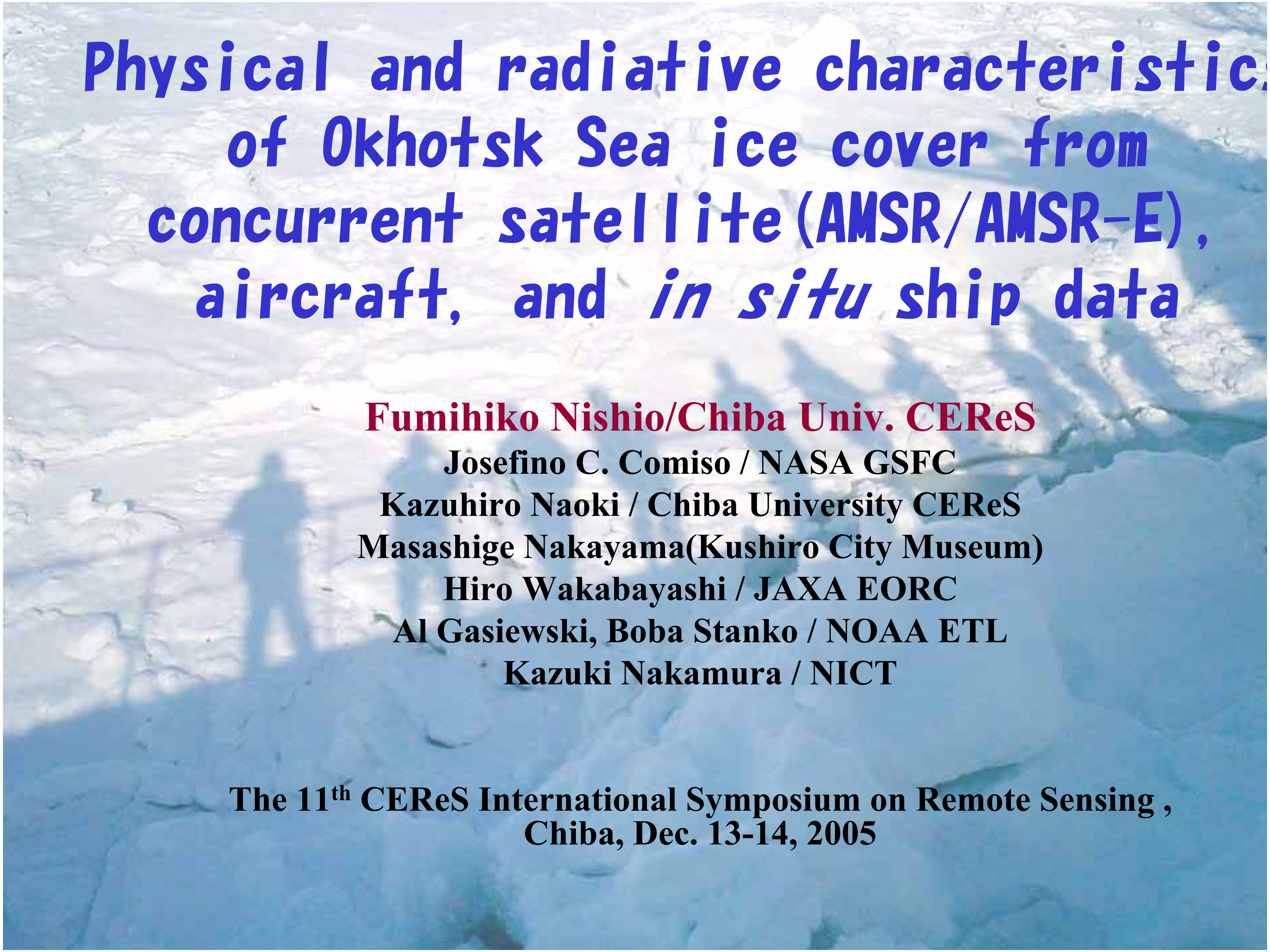

Physical and radiative characteristics of Okhotsk Sea ice cover from concurrent satellite(AMSR/AMSR-E), aircraft, and *in situ* ship data

Fumihiko Nishio/Chiba Univ. CEReS

Josefino C. Comiso / NASA GSFC

Kazuhiro Naoki / Chiba University CEReS

Masashige Nakayama(Kushiro City Museum)

Hiro Wakabayashi / JAXA EORC

Al Gasiewski, Boba Stanko / NOAA ETL

Kazuki Nakamura / NICT

The 11th CEReS International Symposium on Remote Sensing , Chiba, Dec. 13-14, 2005

March	June	September	December

Arctic Ocean & NH Seas

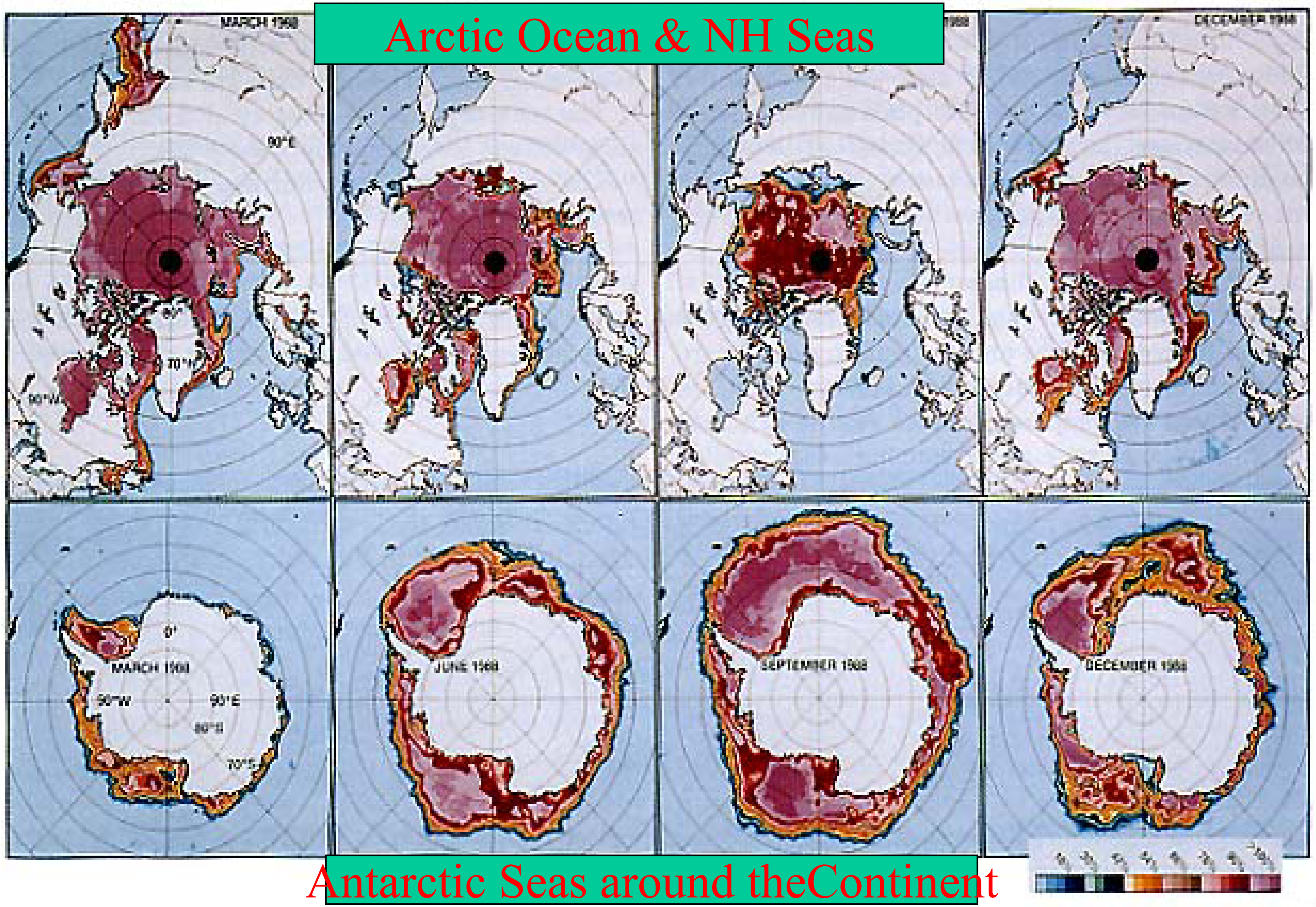

Antarctic Seas around theContinent

Sea Ice Cover in the Arctic & Antarctic, Okhotsk Sea

Arctic Sea Ice

retreating

1979

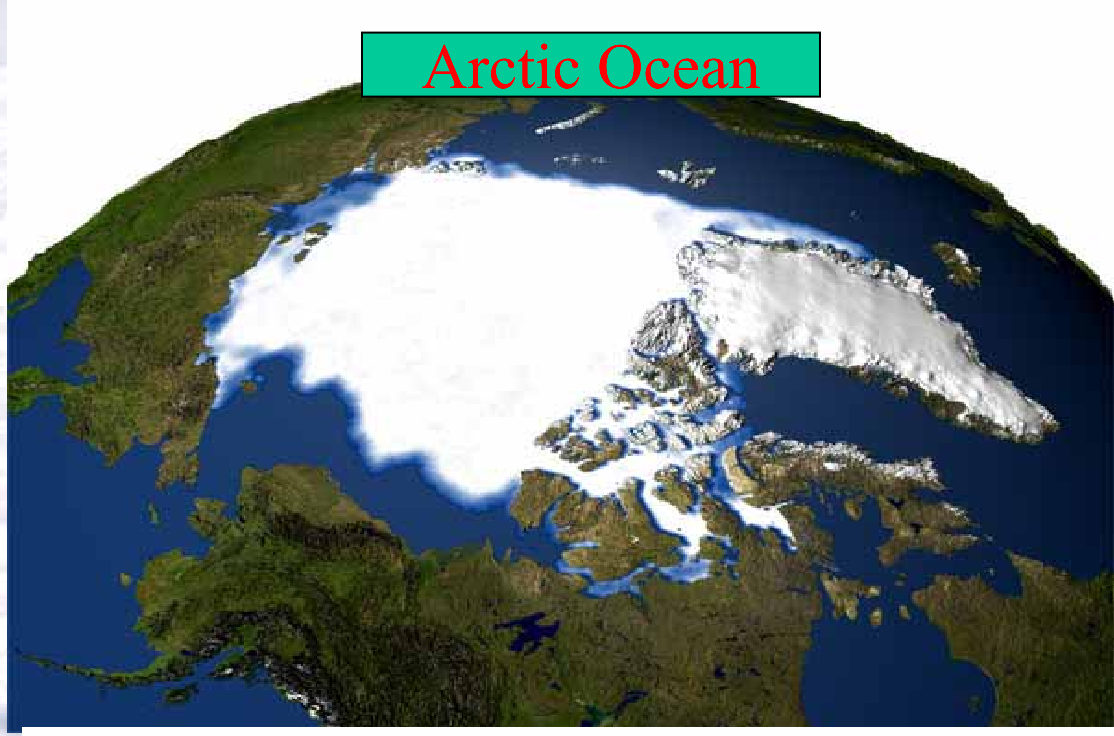

2003

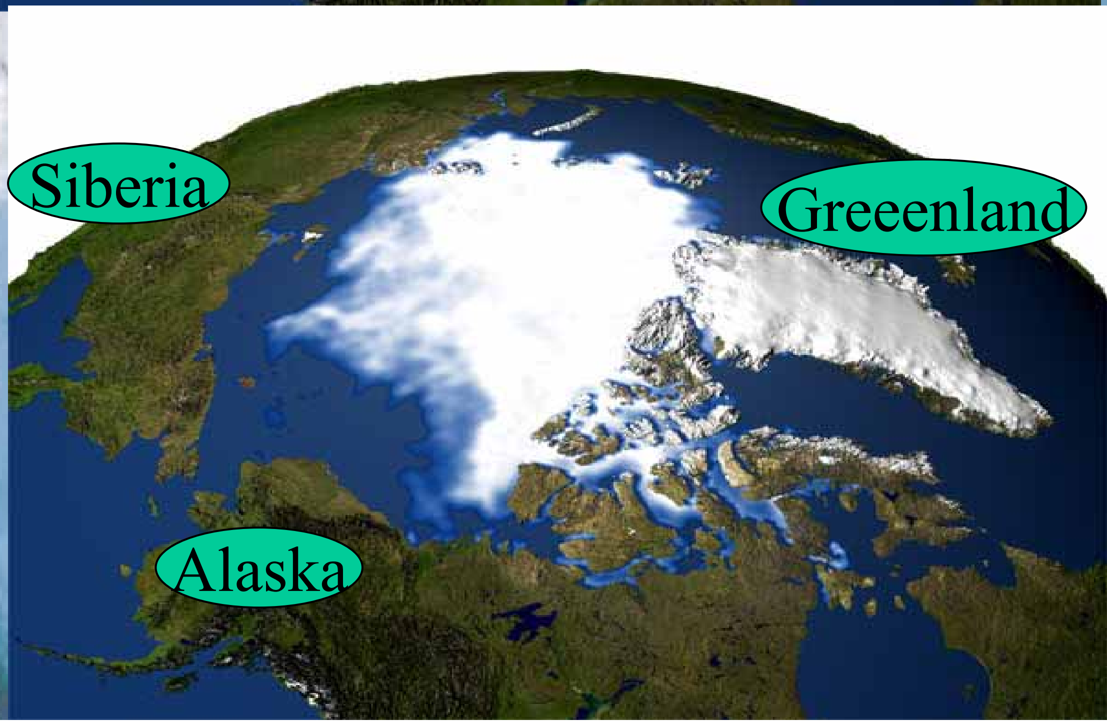

Scientific Motivations:

1) Evaluate the true benefit of having an AMSR for sea ice stud

2) Do comparative studies of AMSR and SSMI data, Landsat ar
   other high resolution sensors and assess improvements

3) Evaluate the role of AMSR in long term/trend studies

4) The polar regions may provide the earliest signal of a climate
   change because of feedbacks between ice, ocean &
   atmosphere

5) The Okhotsk sea (SH) is the southern-most ocean covered wi
   sea ice in the winter and may also provide the earliest signal
   a climate change.

6) *Sea ice concentration* & *ice thickness is most inportant*

7) The entire Antarctic sea ice cover has been observed to be
   increasing at less than 1%/decade while the B/A Seas regior
   has been declining at about 6%/decade.

Validation Schedule (ADEOS2/AMSR＆Aqua/AMSR･E: Sea Ice)
-Post lauching-

	Okhotsk Sea	Antarctic Ocean & Continent
2002	**ADEOS2 launching（Dec.14）, Aqua/AMSR-E(May 5)** **Okhotsk Sea** **Field experiments(February~March)** Aircraft(AMR, VTR, etc.),**Icebreaker,** field campaign	**ADEOS2 launching** **New Glaciological Program(JARE)** 5-year term **Wintering at Showa St. (GLI Receiving)**
2003	**Okhotsk Sea** **Field experiments(February~March)** Aircraft(AMR, VTR, etc.), **NASA/P3** **Icebreaker, field campaign**	**ntarctic Campaign-AASI** **(August~September, NASA) Punta Arenas**
2004	**Okhotsk Sea** **Field experiments(February~March)** **Aircraft-PiSAR** **Icebreaker, field campaign**	**Weddell Sea & Belingshausen** **ntarctic Campaign-AASI** **(P3, Icebreaker)** **(October, NASA) –P3 Ushuaia** **Australian icebreaker(Oct.-Nov.)** Ross Sea (P3, Icebreaker)
2005	**Okhotsk Sea** **Field experiments (February~March)** **Aircraft-PiSAR** **Icebreaker, Field campaign**	**Antarctic Campaign** tudy on sea ice & snow cover on ice sheet(AMSR & GLI) by JARE(Wintering) **(JARE)** winter(August~October,) near Syowa St. & Ice sheet to inland
2006	**Okhotsk Sea** **Field experiments(February~March)**	**Antarctic Campaign** **(NASDA & JARE)** winter(August~October, DC8) near Syowa St. & Ice sheet to inland
2007	**Okhotsk Sea** **Field experiments(February~March)**	**IGY/IPY memorial year**

AMSR-E(ice concentration)

09/Feb/2003

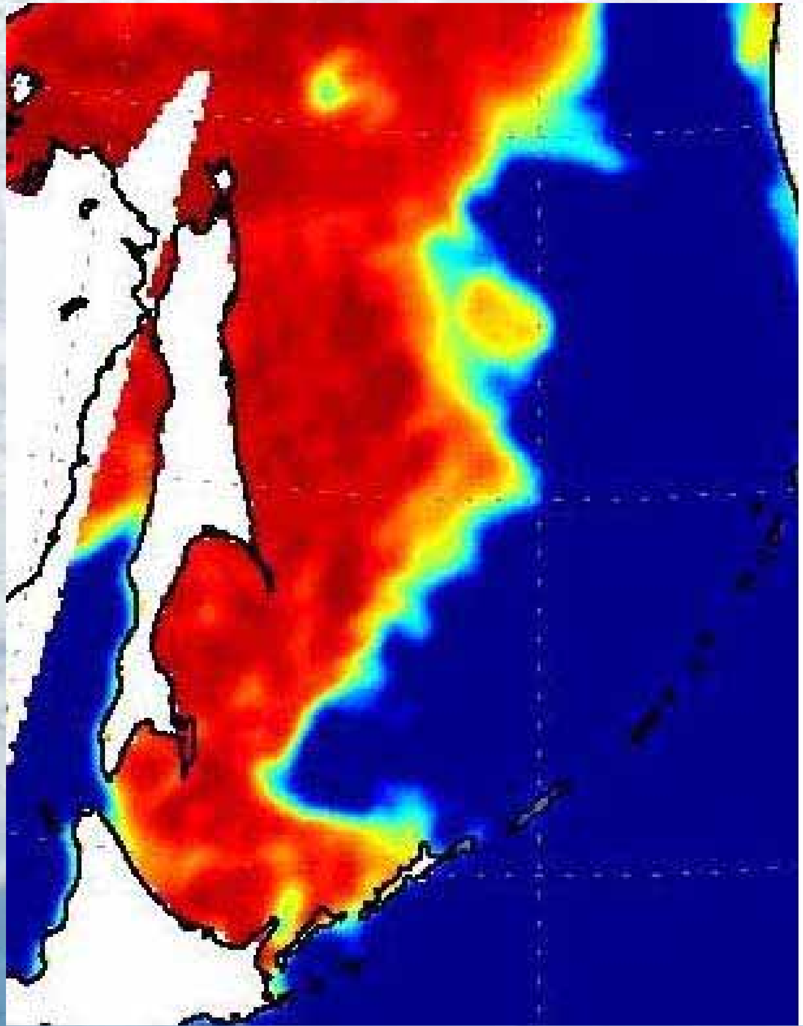

09/Feb/2004

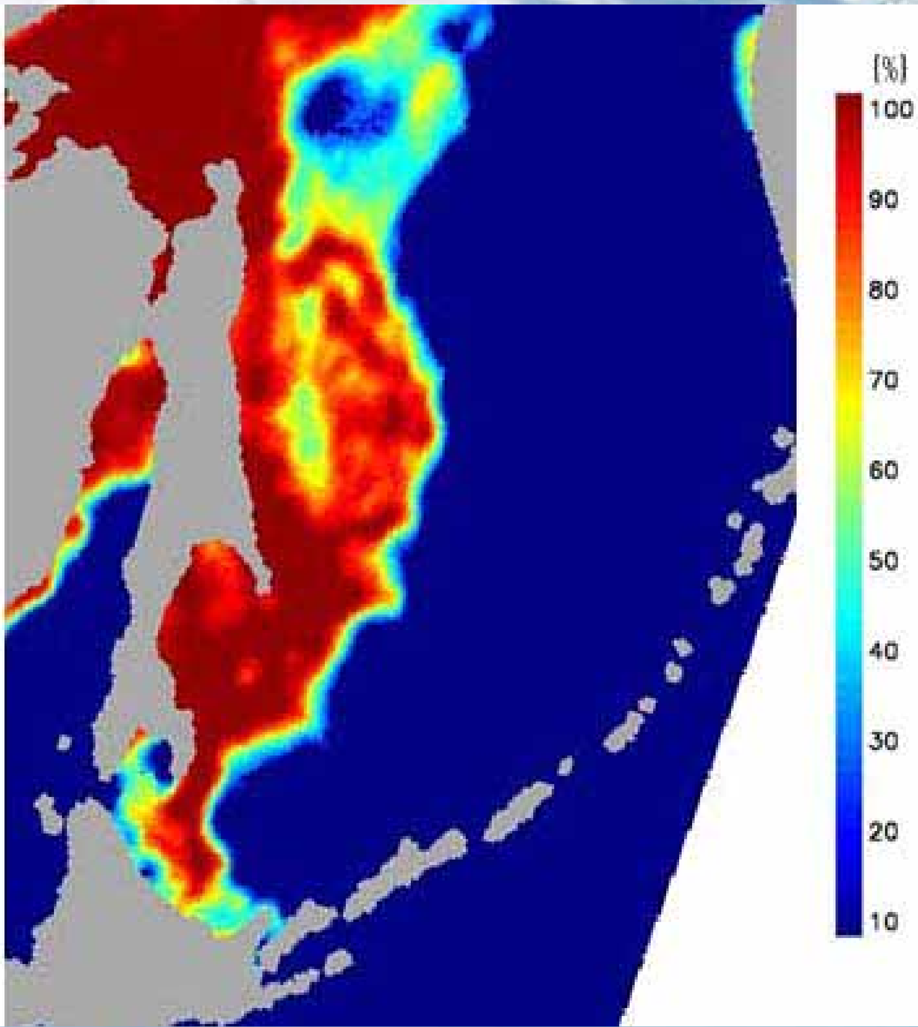

•These are images of sea ice concentration. From AMSR/E data. This is a 09/feb/2003 this is a 09/feb/2004

•At first This year was estimated to be difficult for observation because of low sea ice cover but sea ice existed on observation day.

•However, especially, Hokkaido coast find the low extent of the sea ice compared to last year.

Sea ice concentration (Bootstrap) by AMSR

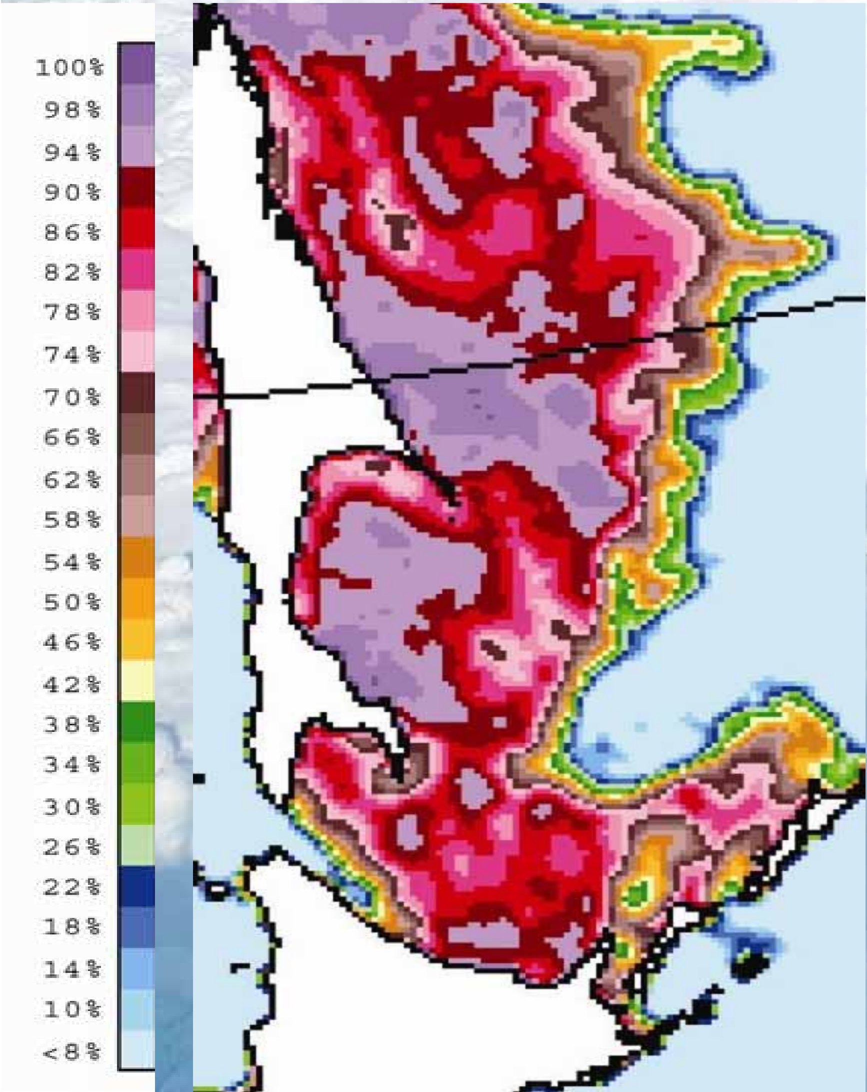

2003 February 7 AMSR-E
36.5H, 36.5V

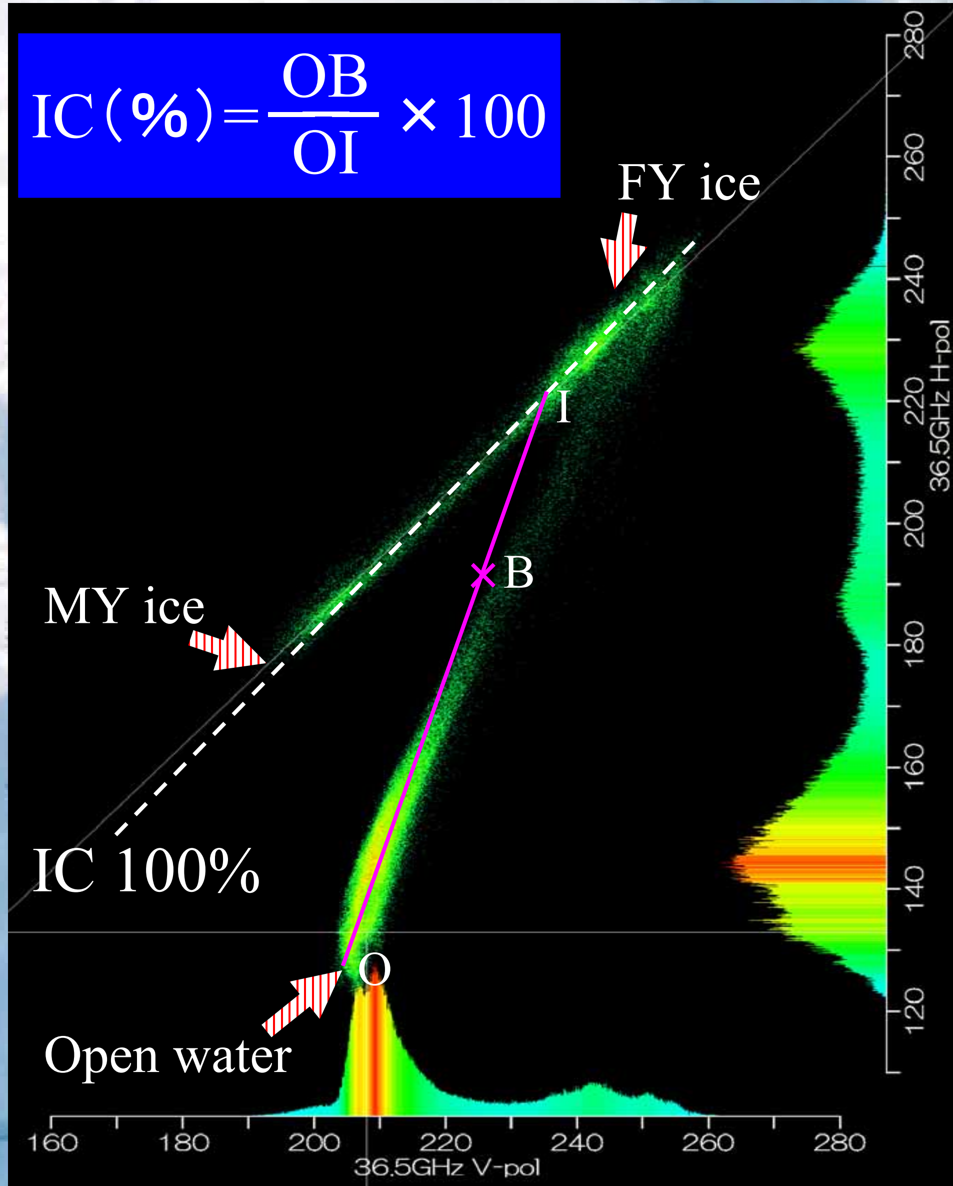

オホーツク海の海氷をAMSRで見ると

Concurrent observatio

February 7, 2003 Sea of Okhot

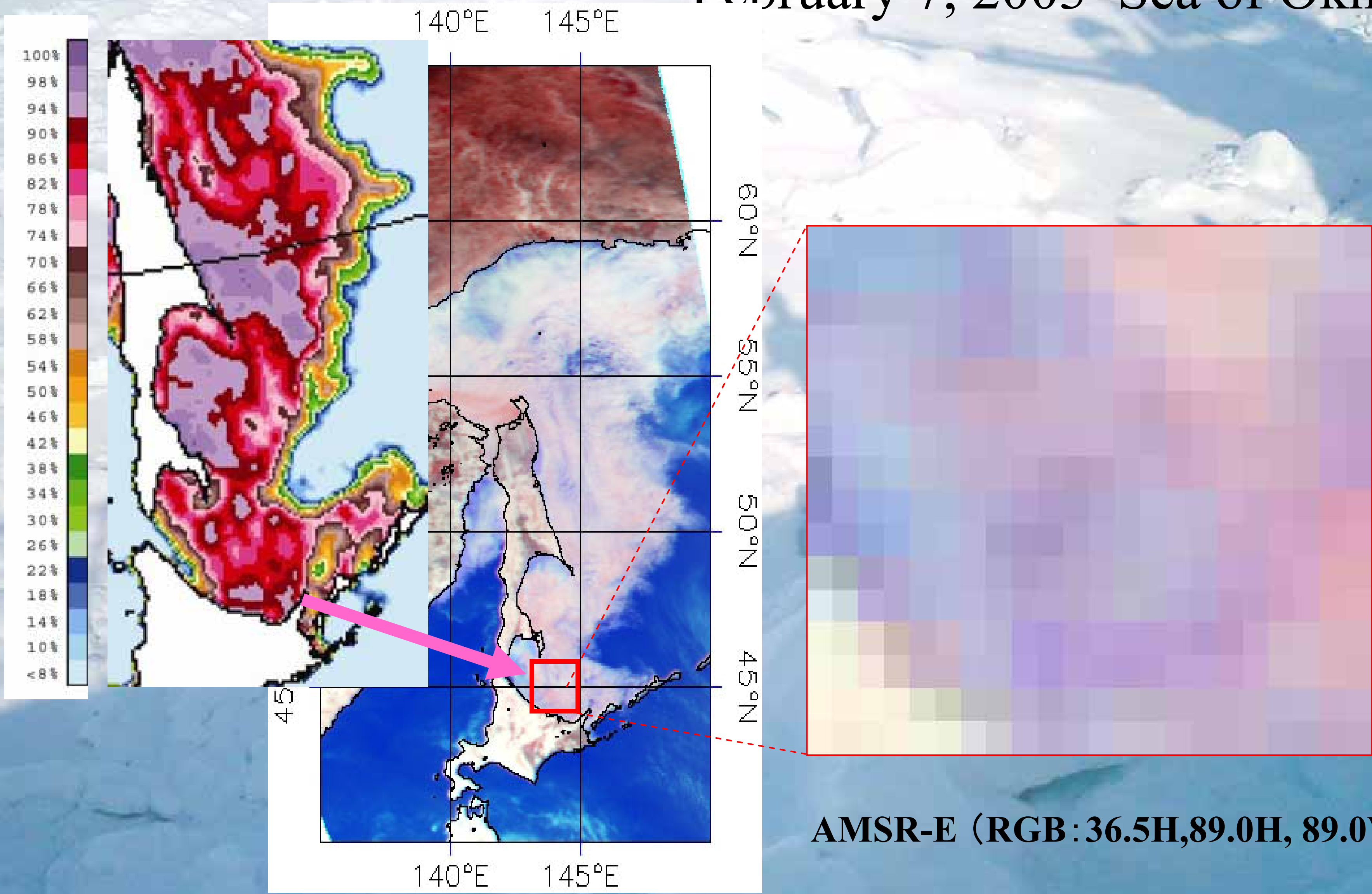

AMSR-E（RGB：36.5H,89.0H, 89.0V)

AMSR-E & Landsat

- **Landsat data provide information that can be very useful in the interpretation of AMSR-E data**
- **The concentration of new ice depends on thickness and stage of growth.**

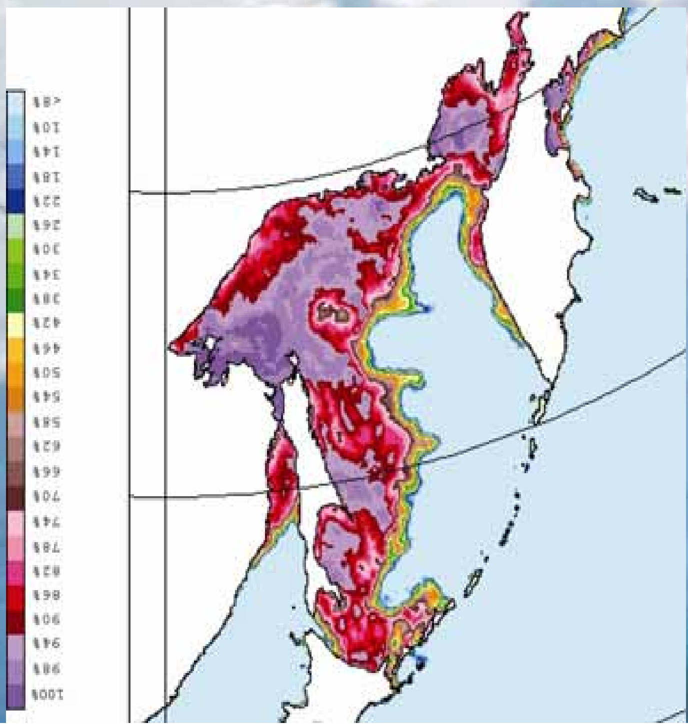

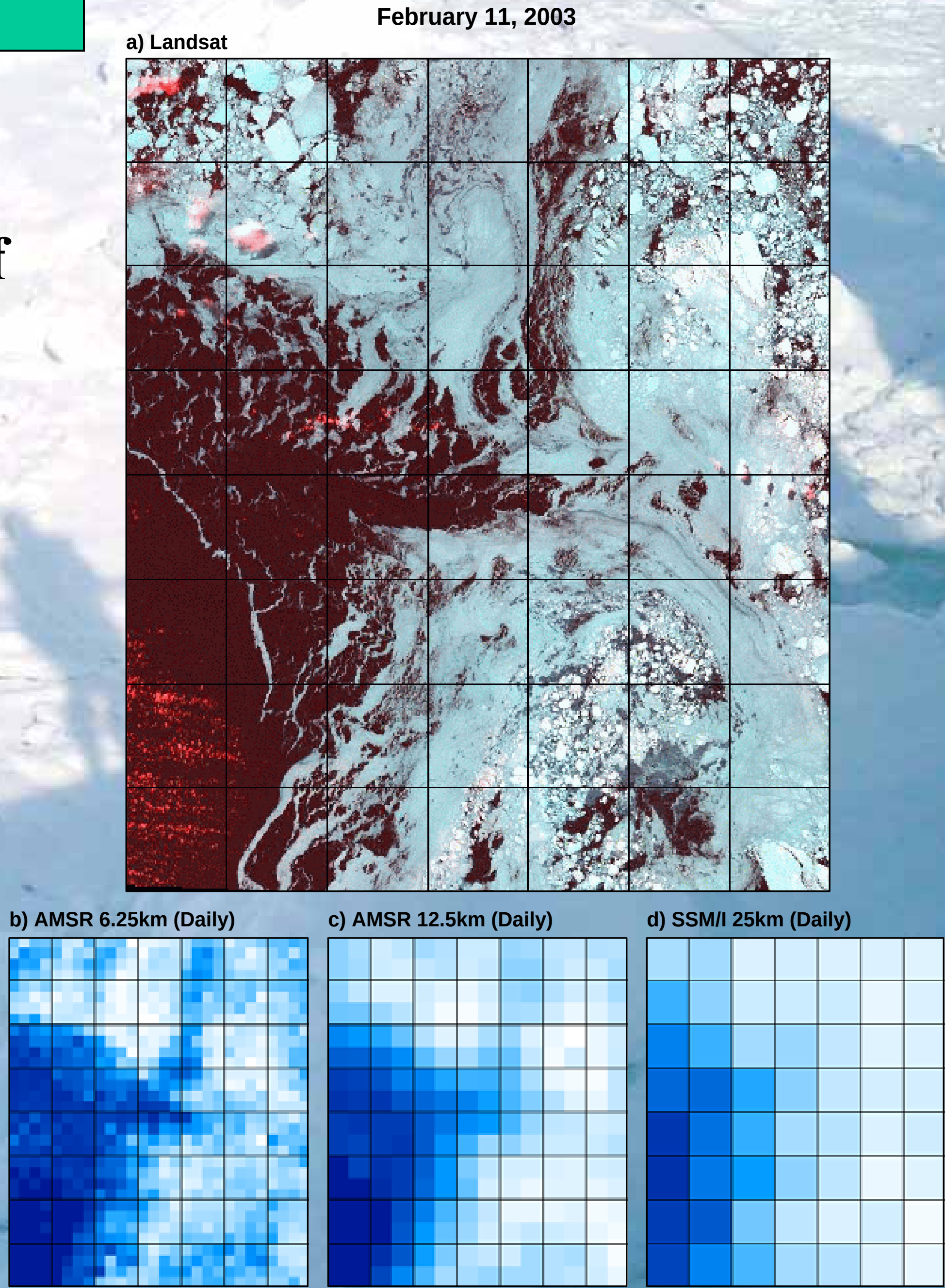

Validation Strategy

- **Aircraft Validation Campaigns**

  Sea of Okhotsk Mission – February 2003

  AASI Campaign – August – September 2003*

  AASI Campaign – October 2004

  PiSAR February 2004 & 05
- **High Resolution Satellite Data**

  MODIS, GLI**

  Landsat

  Quickbird/IKONOS
- **Ship Data/other *in situ* data**
- **Radiative Transfer Modeling**

*Aborted

**Oct. 2003

Validation Tools (2003 & 04))

- P3 Aircraft – coordinate with Aqua & ADEOS2* orbit

  PSR A & C – Sensor calibration and parameter studies

  ATM – ice thickness and topography studies

  THOR – snow thickness and cloud cover studies

  D2P – ice and snow thickness studies

  TAMMS – heat and humidity flux studies
- Ship Observations- in situ data of passive microwave observations and physical characterization of the ice
- High Resolution Satellite Observations – Landsat, ASTER, Ikonos
- PiSAR(2004 & 2005)
- Radiative Transfer Modeling Studies

*Aborted

**Oct. 2003

Aircraft and ship observation

- February 5 – 14, 2003.
  - Sea of Okhotsk
- August 16 – September 4, 2003.
  - Bellingshausen Sea
- September 11 – October 30, 2003.
  - Hobart to Casey station (AUS)
- February 5 – 14, 2004.
  - Sea of Okhotsk

PSR: WBAY03 2003_0207 DF018 Navigation Data - Parsing (bbs: 4/24/03)

PSR flight on Feb. 7, 03

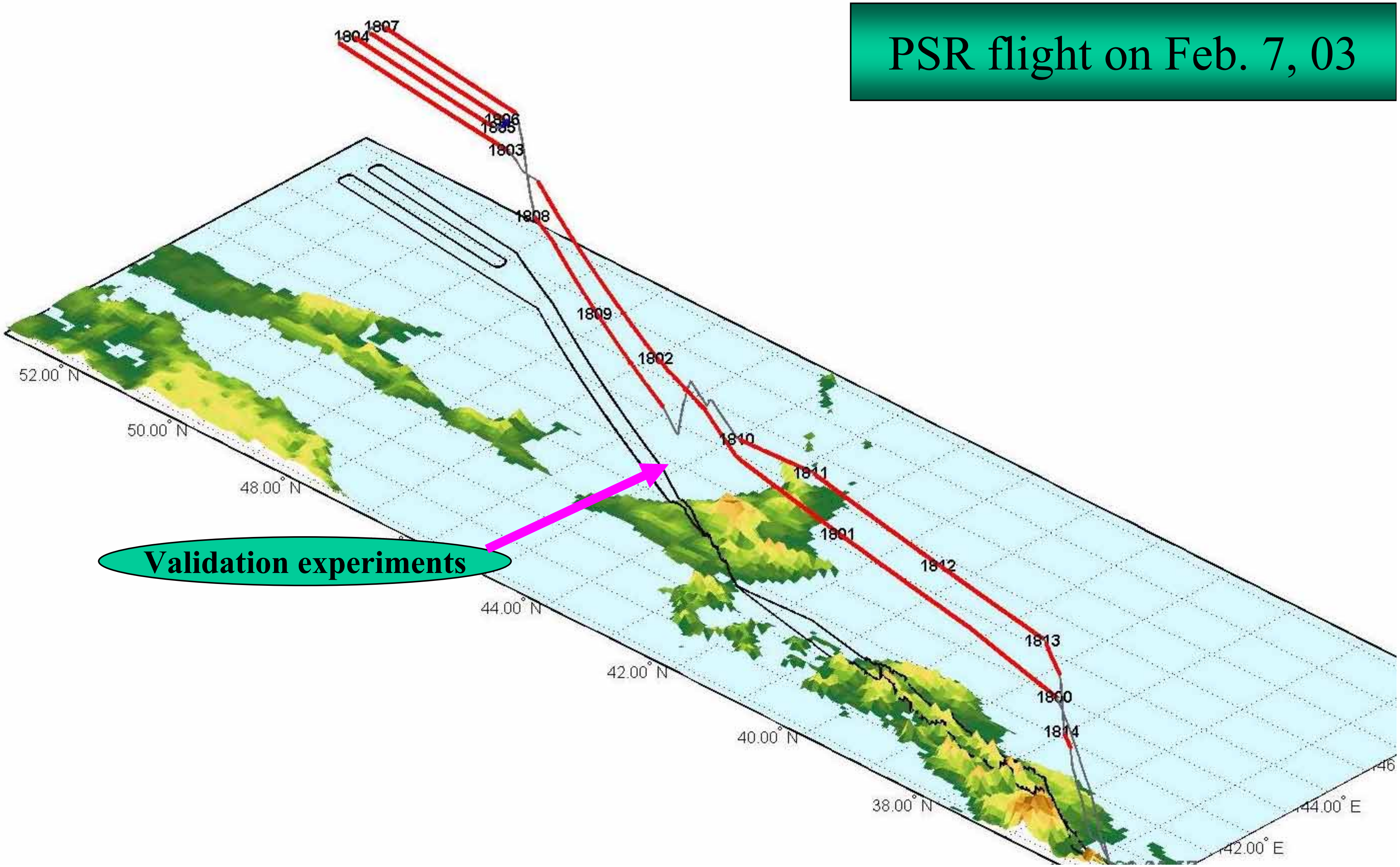

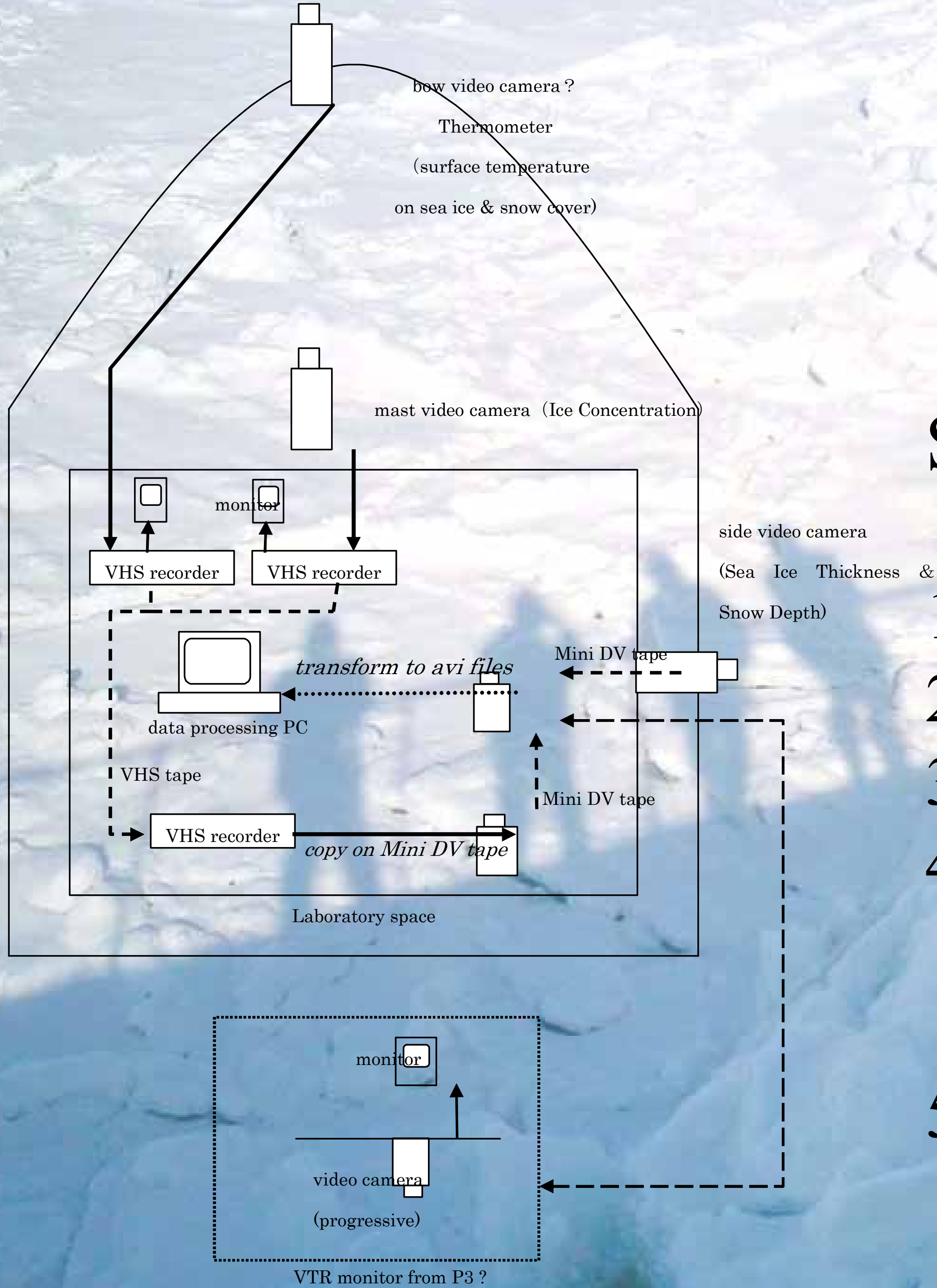

Ship measurements

1) ice concentration
2) sea ice thickness
3) snow depth
4) sea ice classification
(by VTR, IR-VTR, digital camera)
5) Sea surface temperature
(thermometer)

Validation using MODIS

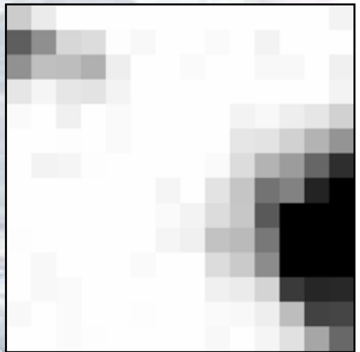

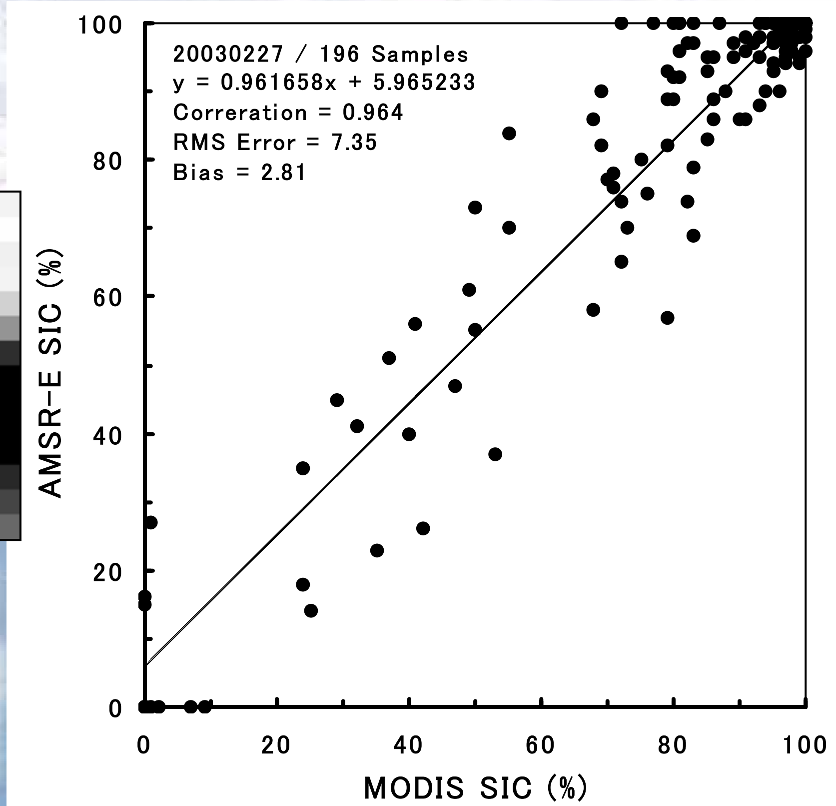

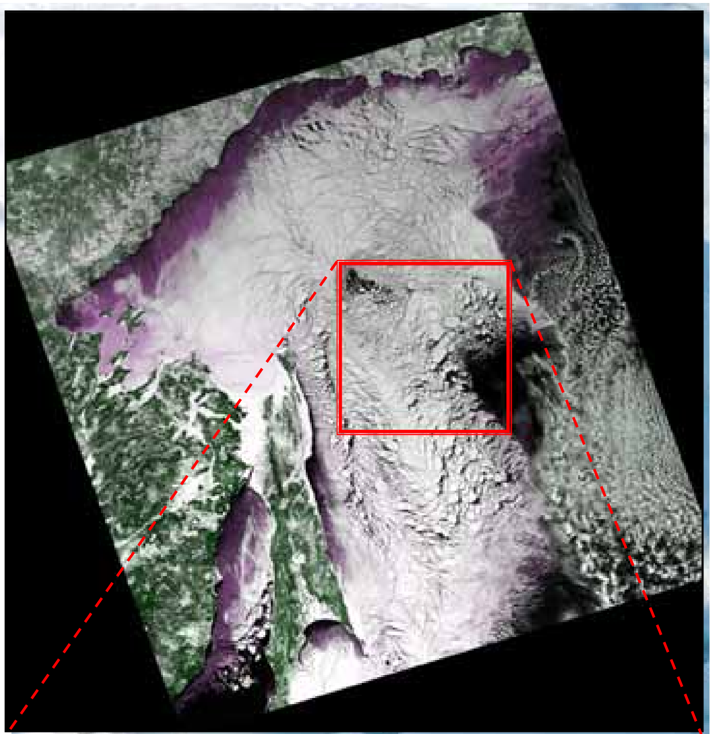

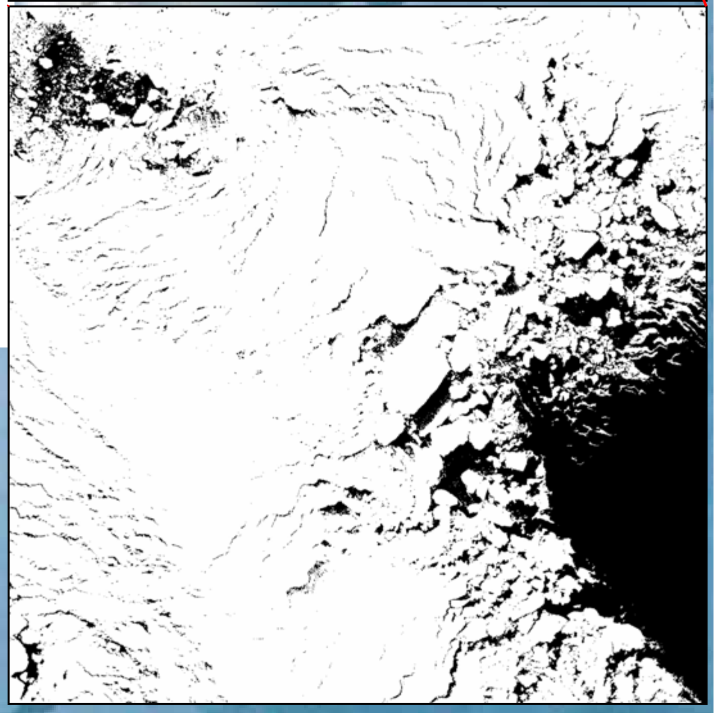

February 27, 2003
Sea of Okhotsk

Modis and AMSR-E at 6 km grid shows basically the same general features of the ice cover. They are also highly correlated.

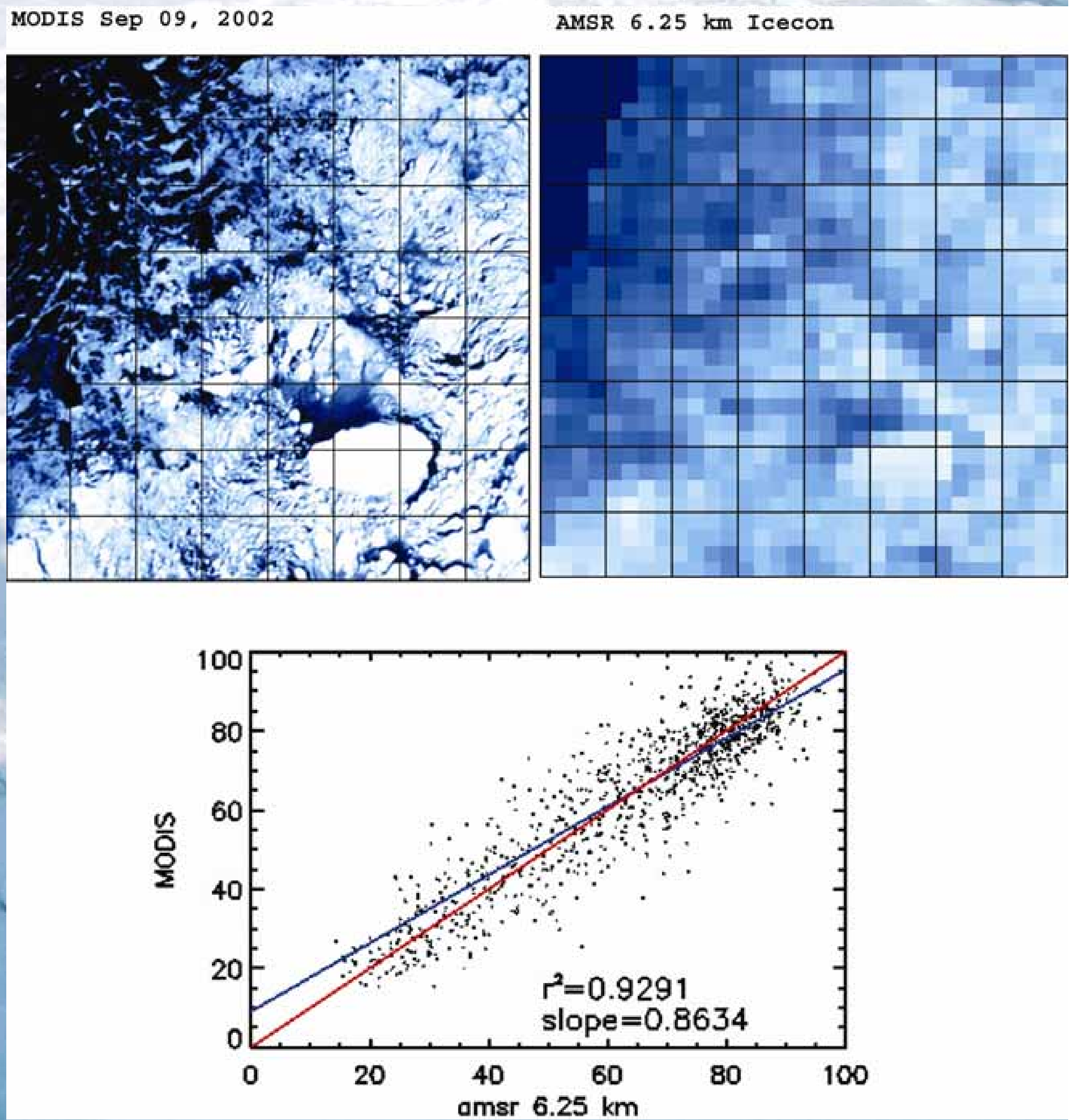

AMSR-E versus Landsat

- Landsat data provide information that can be very useful in the interpretation of AMSR-E data
- The concentration of new ice depends on thickness and stage of growth.

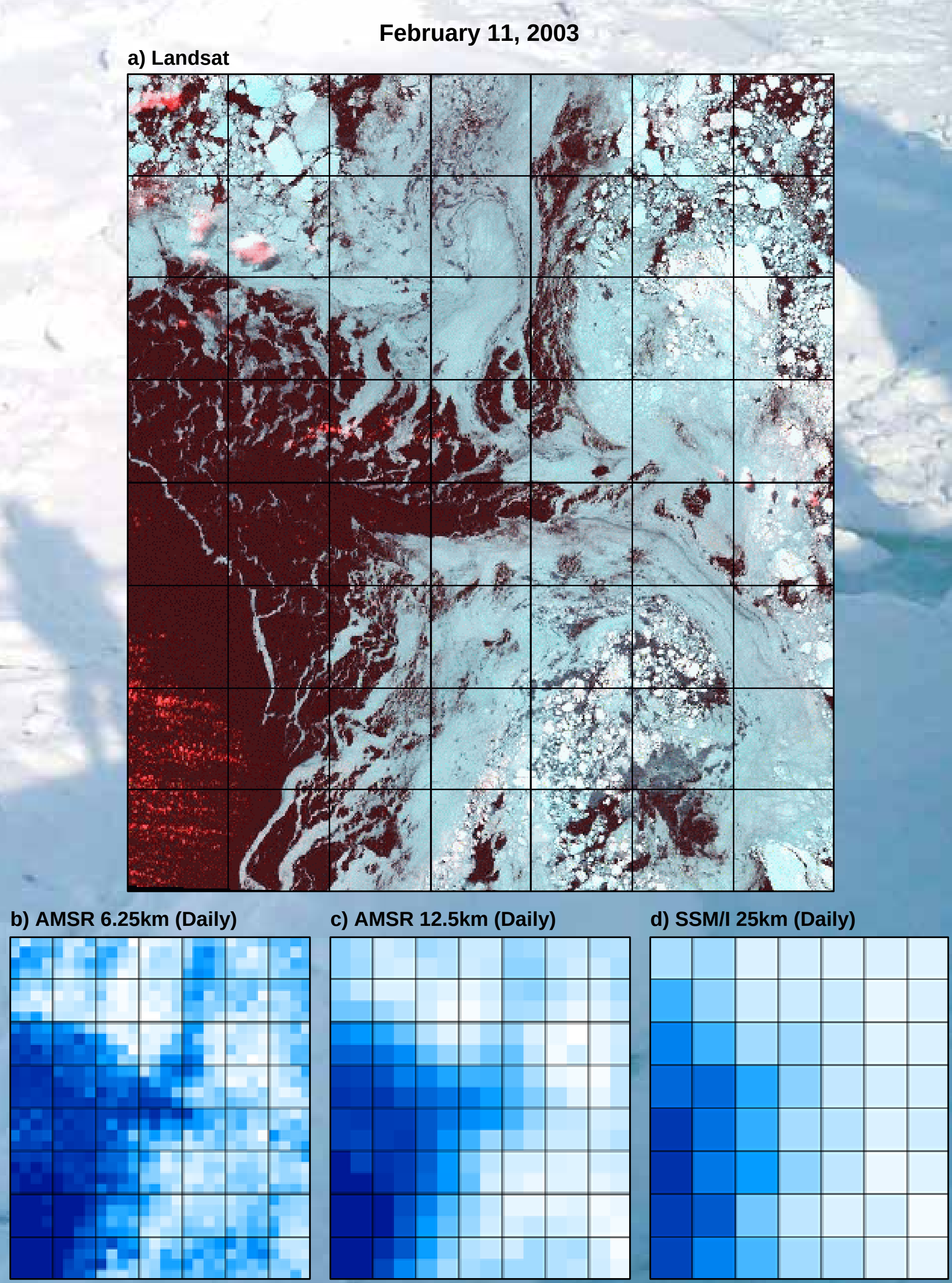

Ice Edge Characterization

- All channels from AMSR are coherent. The ice edge location is almost frequency independent
- Effect of resolution and sidelobes apparent with SSMI
- Error of about 12 km is possible in some locations for SSMI

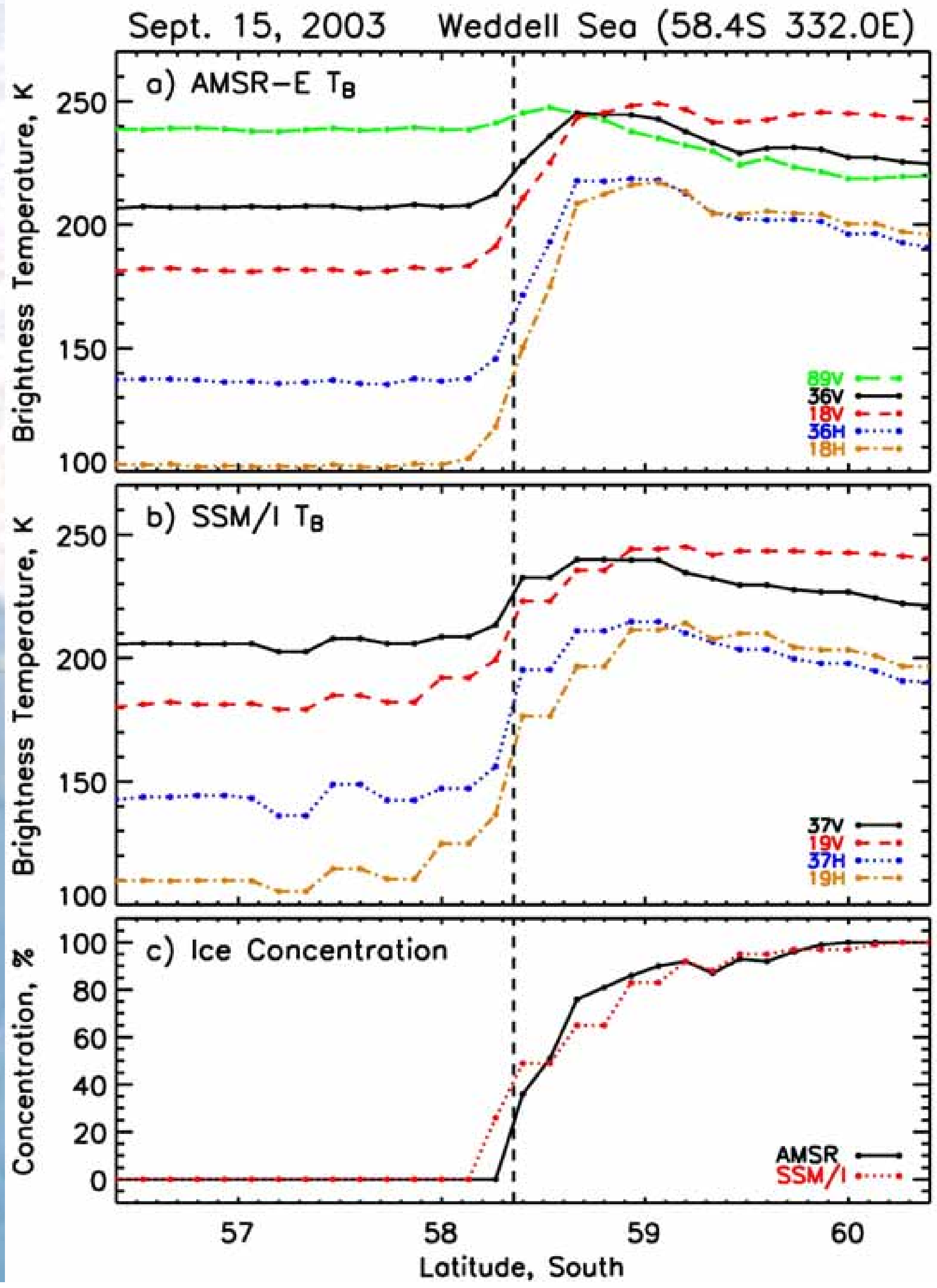

Anomaly/Trend Studies

Northern Hemisphere

- Long term studies requires consistency checks specially during periods of overlap
- Use of AMSR provides a means of improving accuracy in trend analysis but biases should be removed first
- Ice area values are more stable because of less dependency to ice edge location

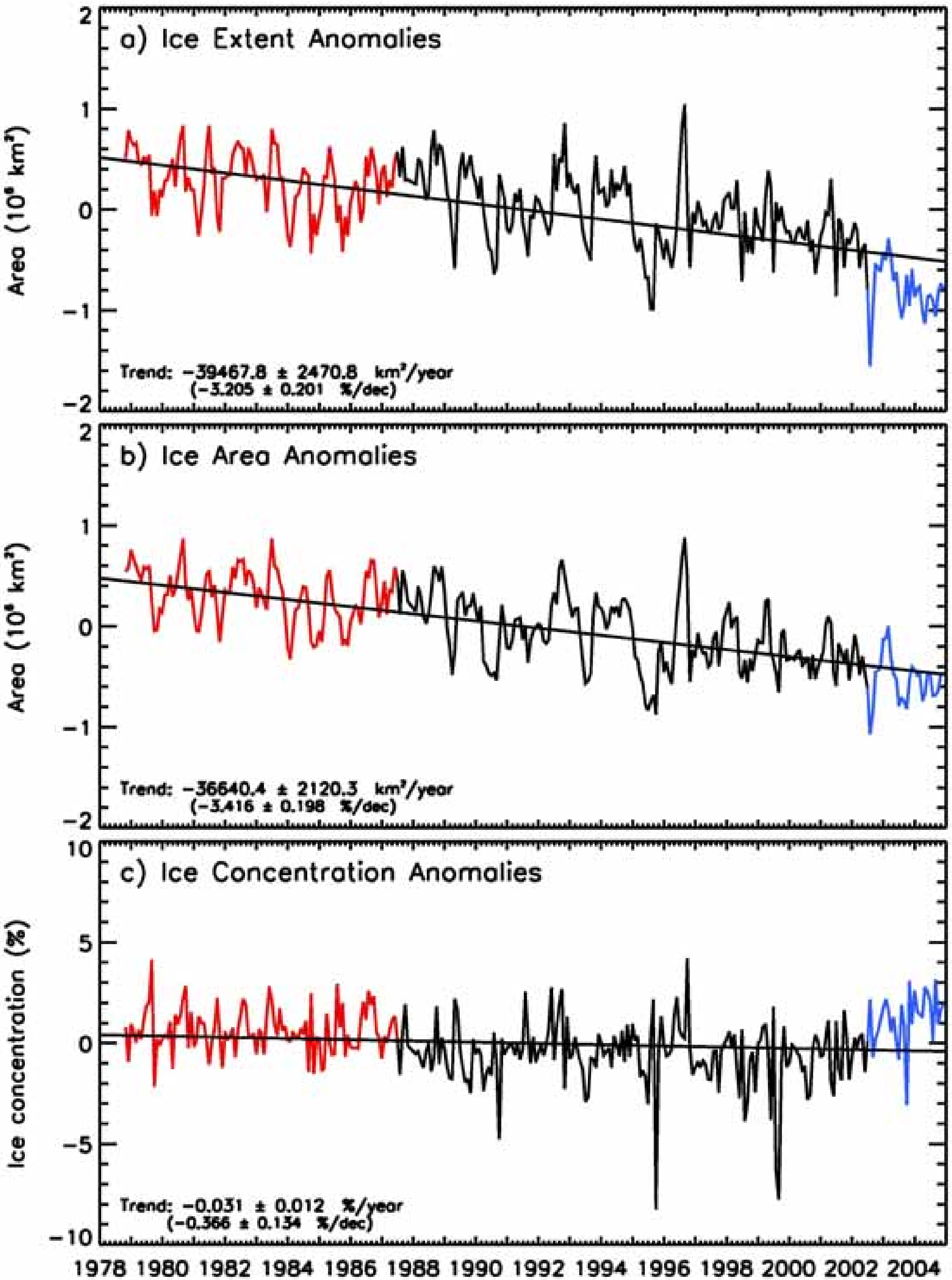

Annomaly/Trend Studies

Southern Hemisphere

- Smaller trend in ice extent is observed with the use of AMSR data vs SSM/I reflecting some bias
- Again, the trends in ice area are almost the same for AMSR and SSMI

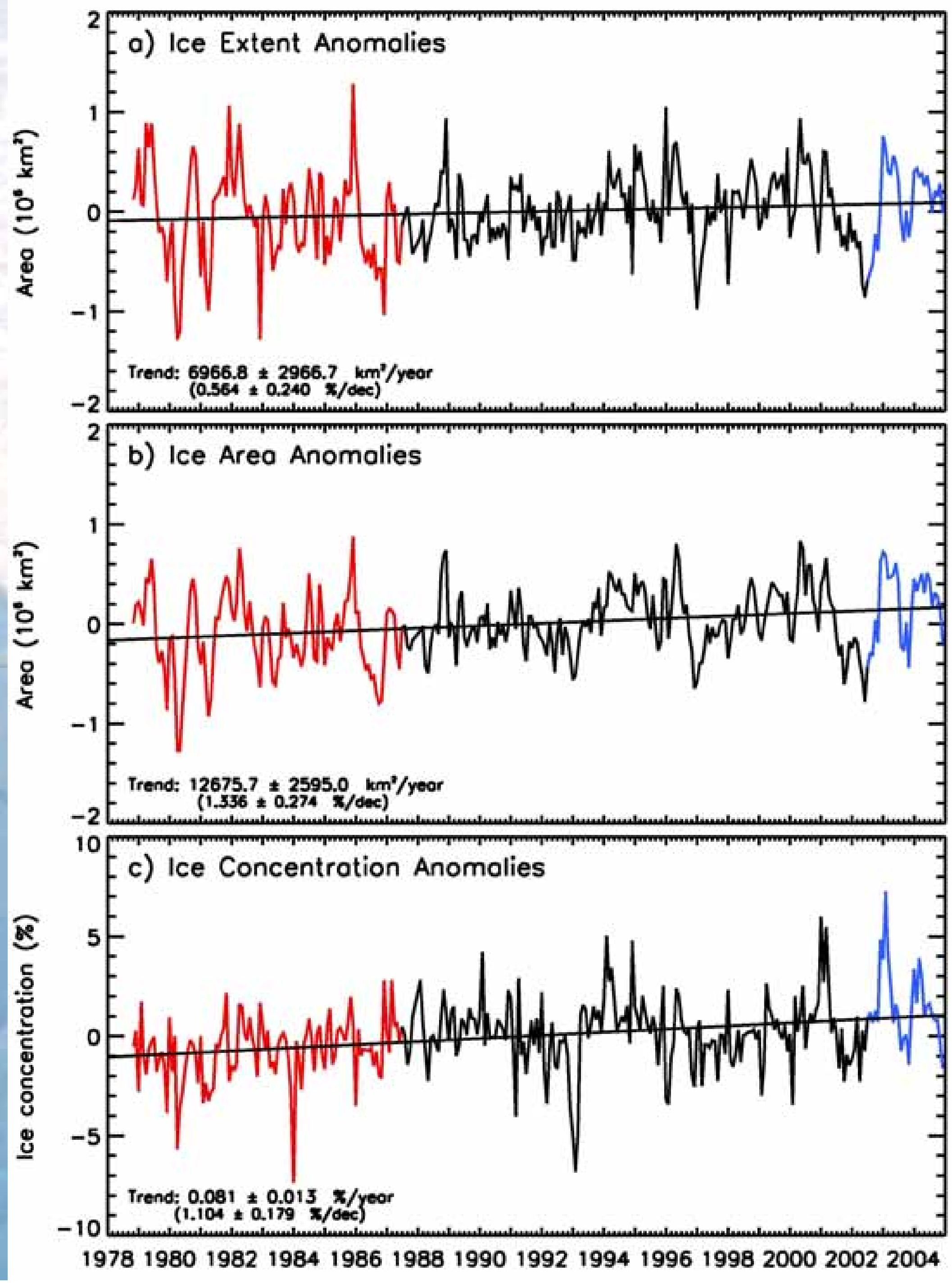

Summary (sea ice concentration)

- High resolution AMSR data are shown to be consistent with MODIS and Landsat data and can be useful for mesoscale studies when atmospheric effects are not critical.
- AMSR/AMSR-E is an excellent successor to SSM/I
- AMSR provides an improved characterization of the ice margin
- AMSR shows spatial details of the ice cover that have never been observed before
- AMSR has the potential of improving the accuracy of long term variability and trend in the ice cover

PSR-A T_B data at 37 GHz (H) and derived ice concentrations Overlayed on MODIS data

(Okhotsk Sea)

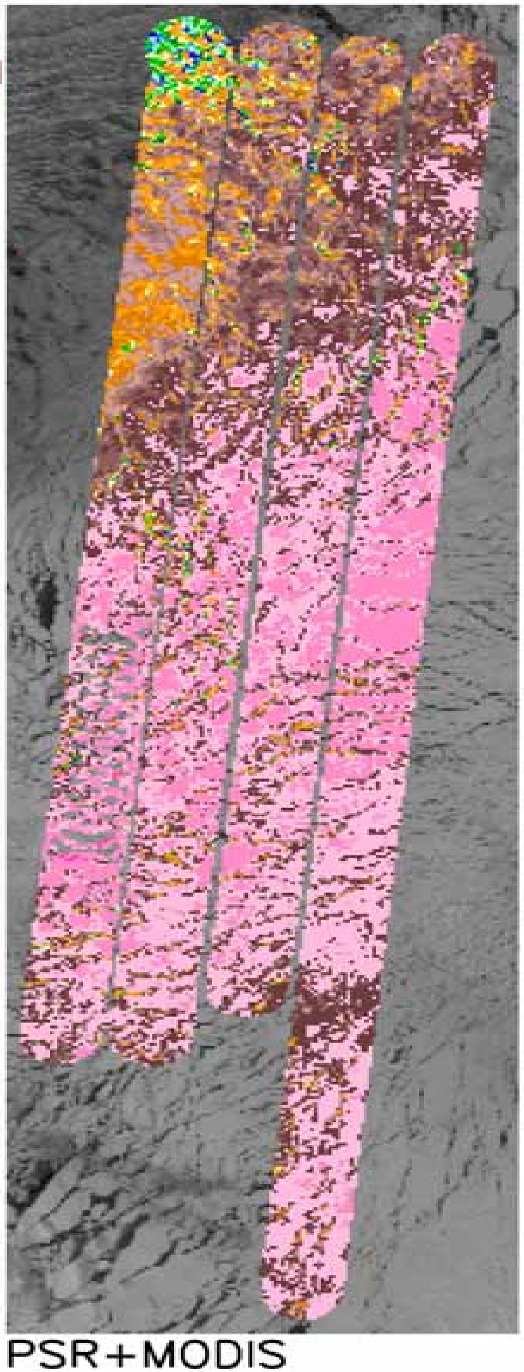

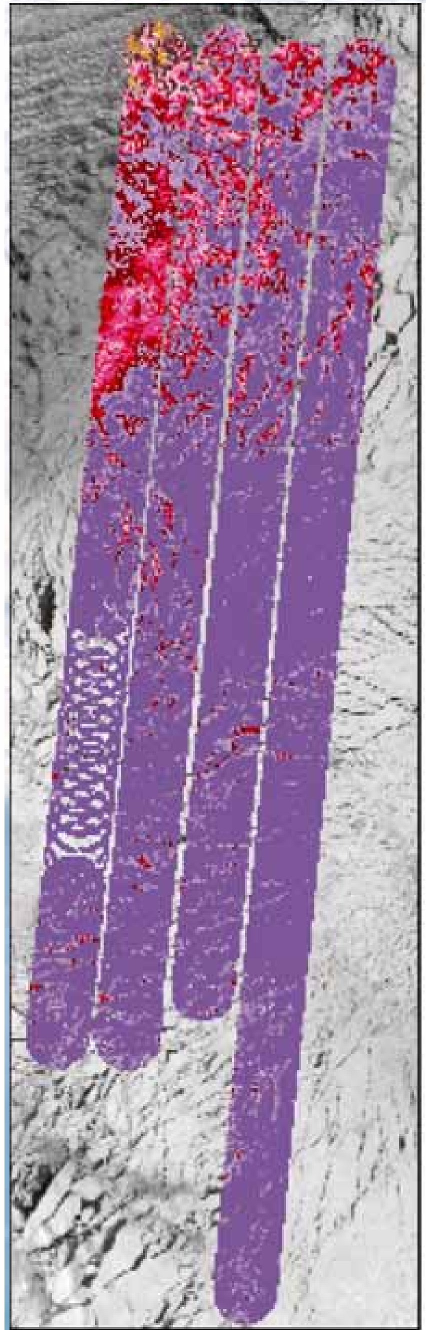

PSR data over P/V "Soya"

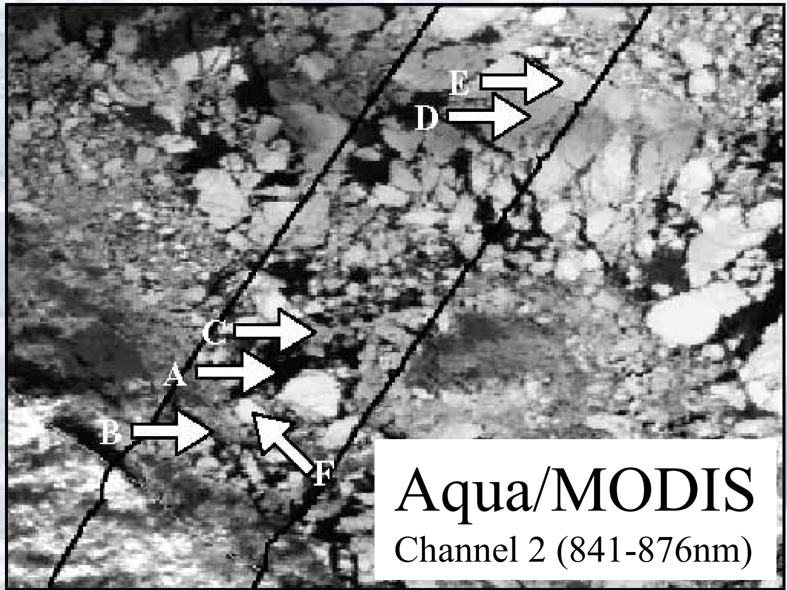

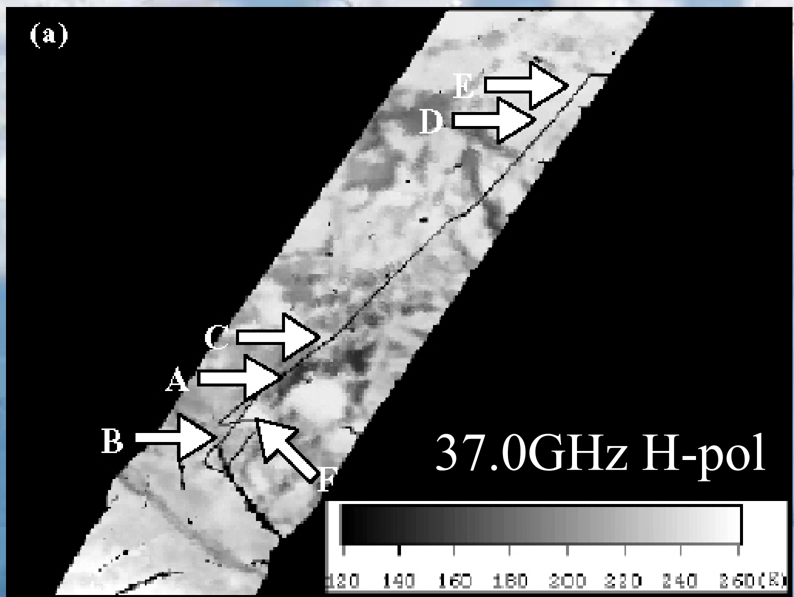

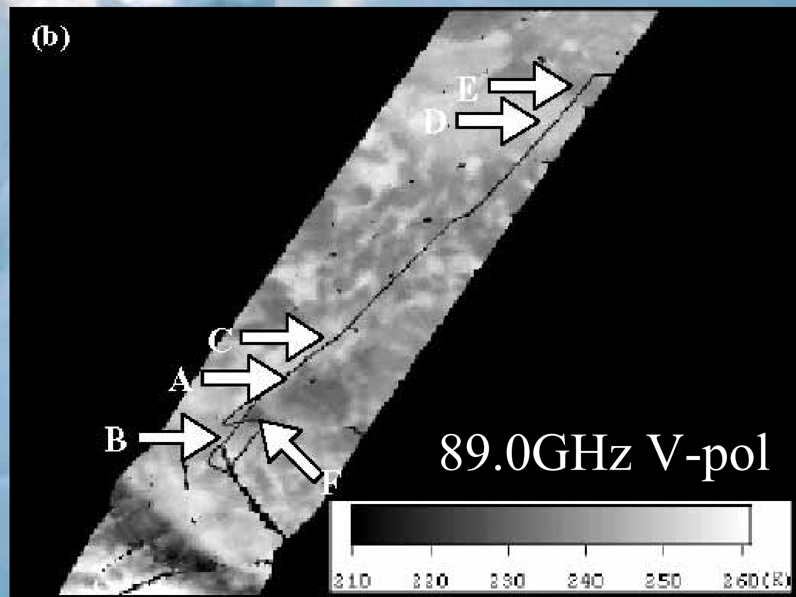

Sea ice thickness observation from ship

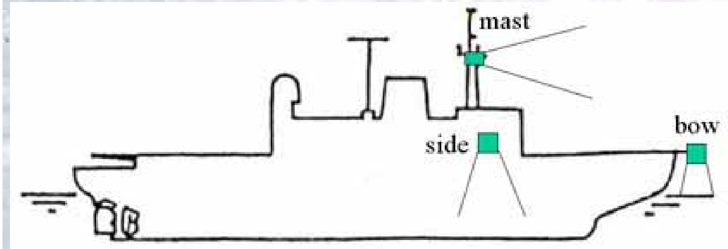

Position of camcorder
on P/V SOYA

Sample images taken by camcorders
a:mast, b:bow, c:broadside

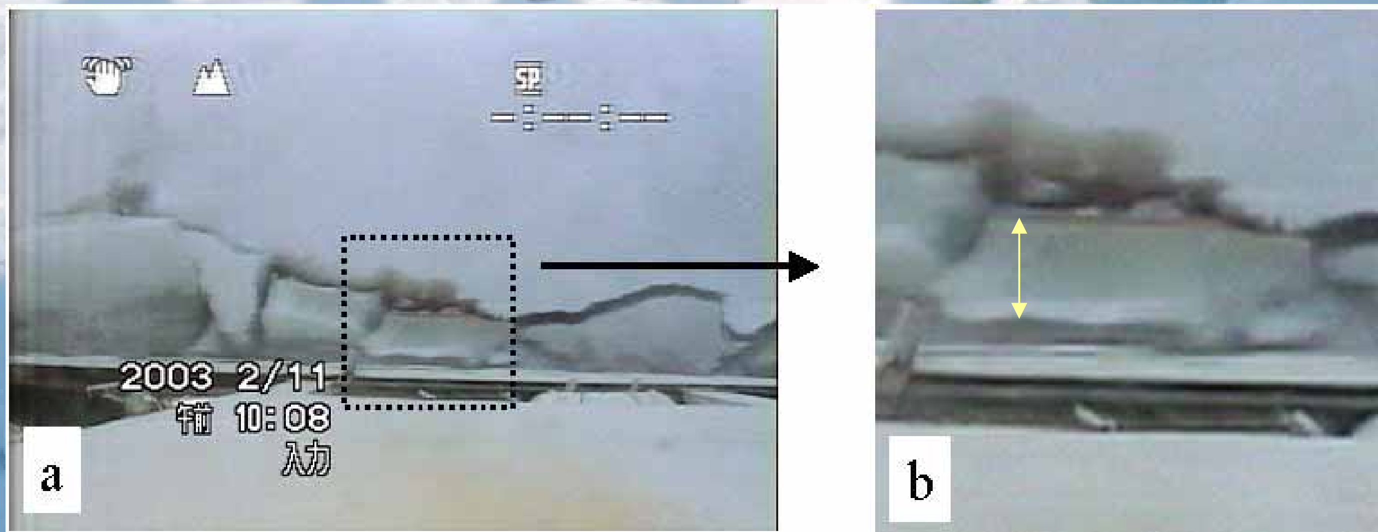

Example image of
measuring sea ice thickness

Average sea ice thickness of area "A" ~ "F" by "Soya"

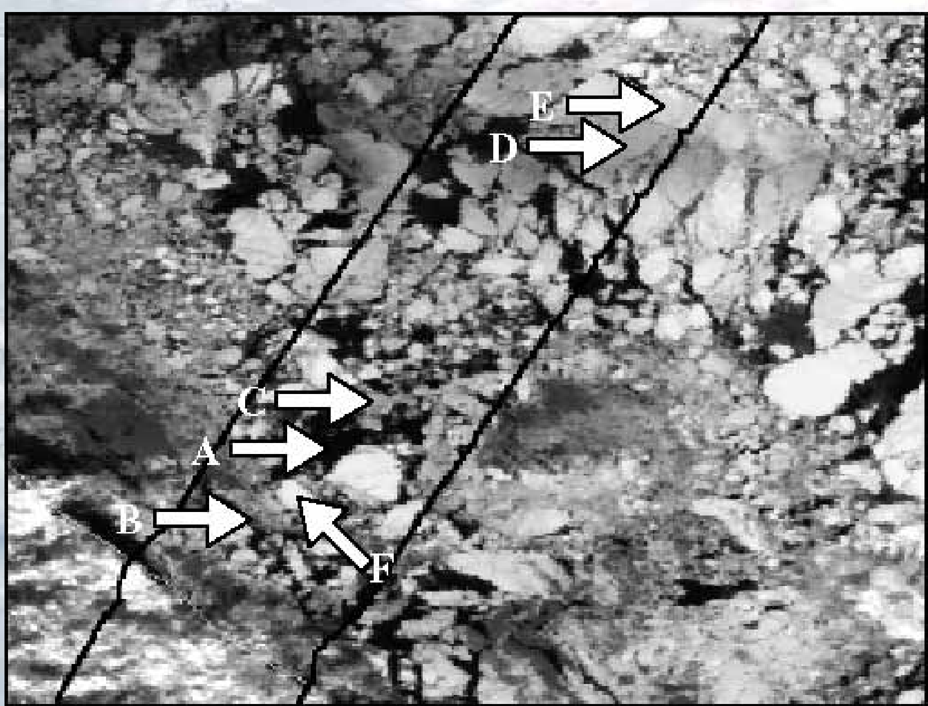

Aqua/MODIS
Channel 2 (841-876nm)

A (>2cm)

B (6.8cm)

C (11.1cm)

D (18.5cm)

E (27.2cm)

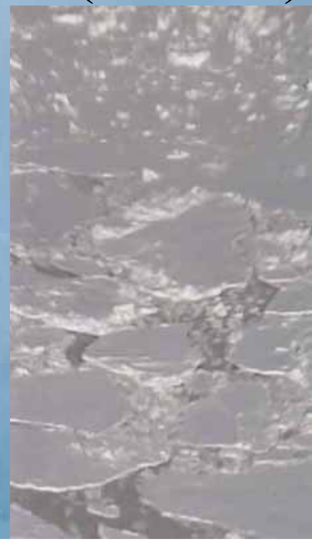

F (32.2cm)

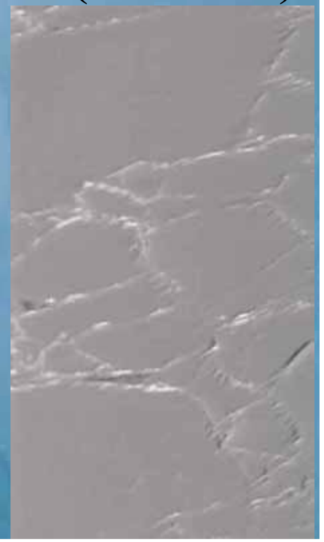

Relationship of brightness temperature to sea ice thickness

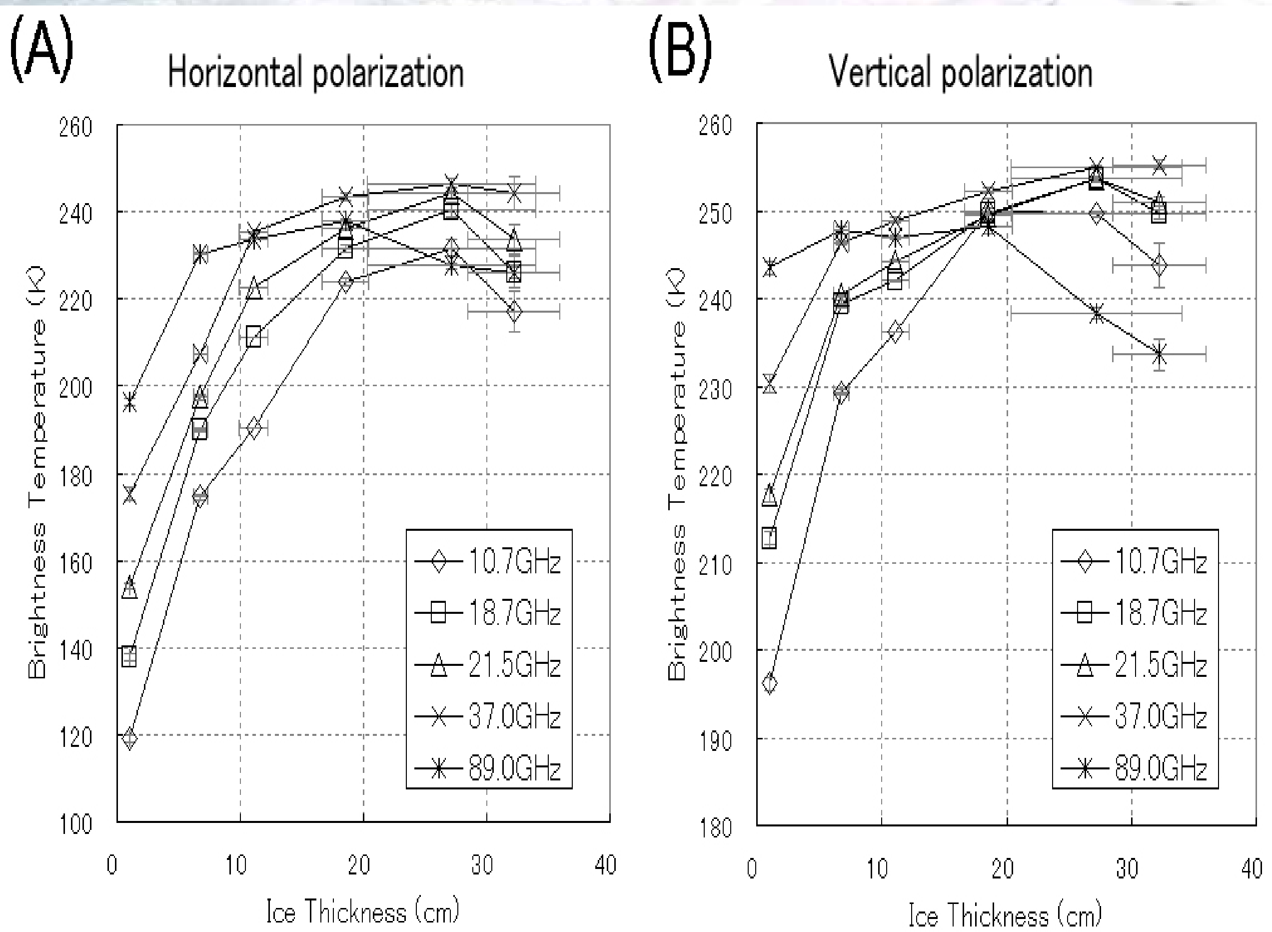

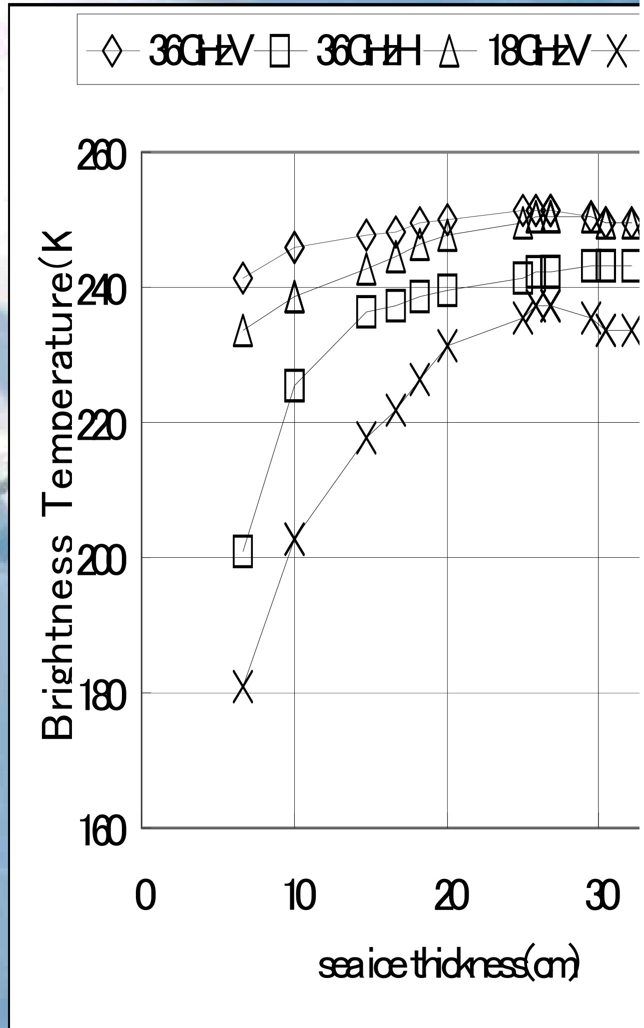

PSR

AMSR/E

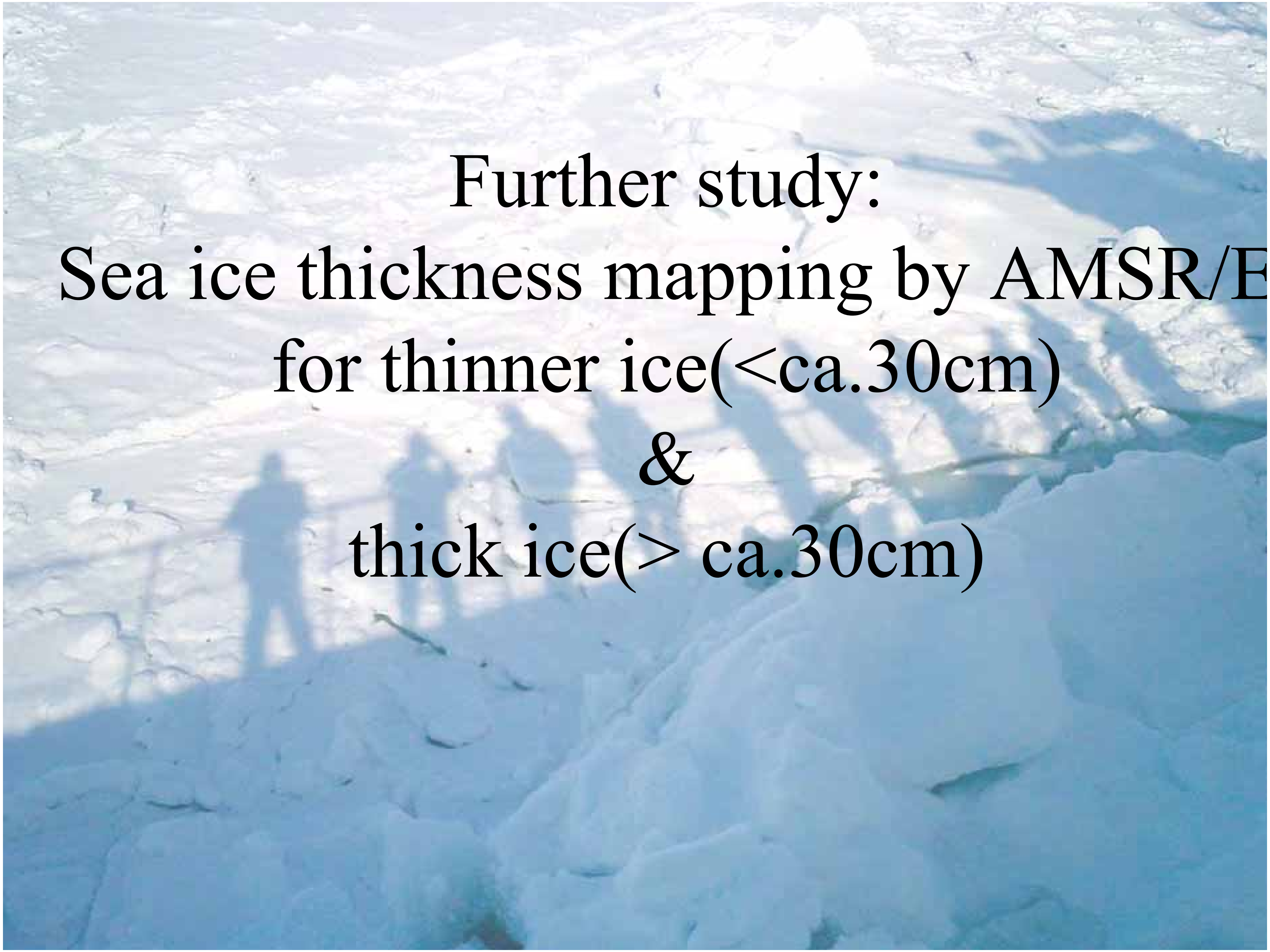
Further study:
Sea ice thickness mapping by AMSR/E
for thinner ice(<ca.30cm)
&
thick ice(> ca.30cm)

in the Sea of Okhotsk by using Dual-Frequency and Fully Polarimetric Airborne SAR (Pi-SAR) D

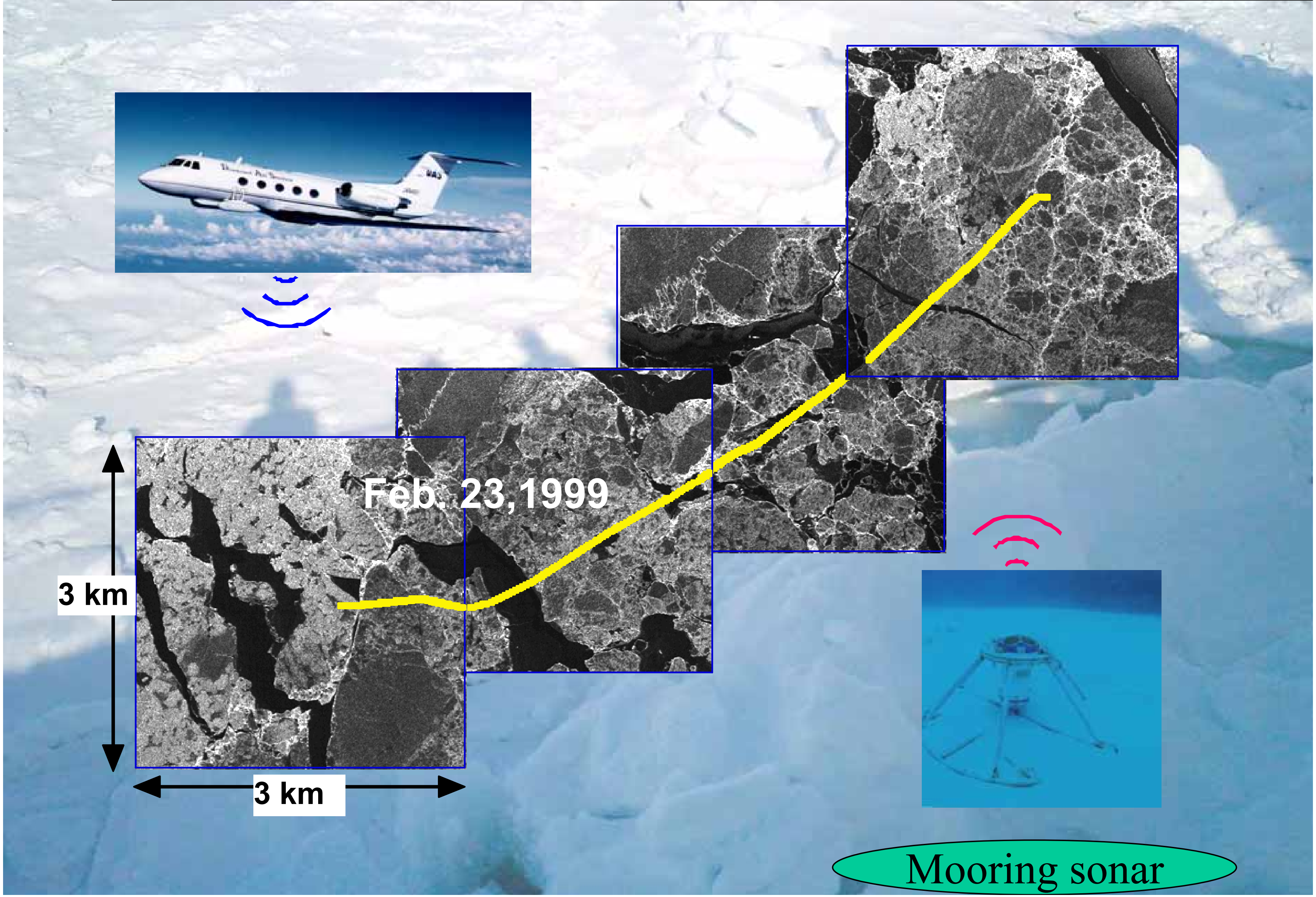

Ice thickness - Backscattering coefficient

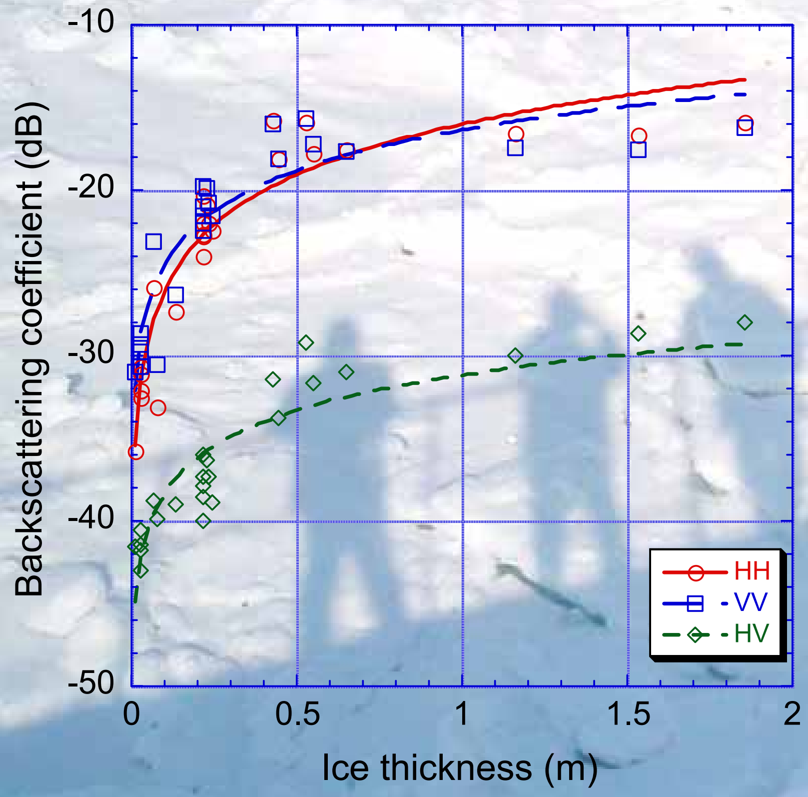

Ice thickness - VV to HH

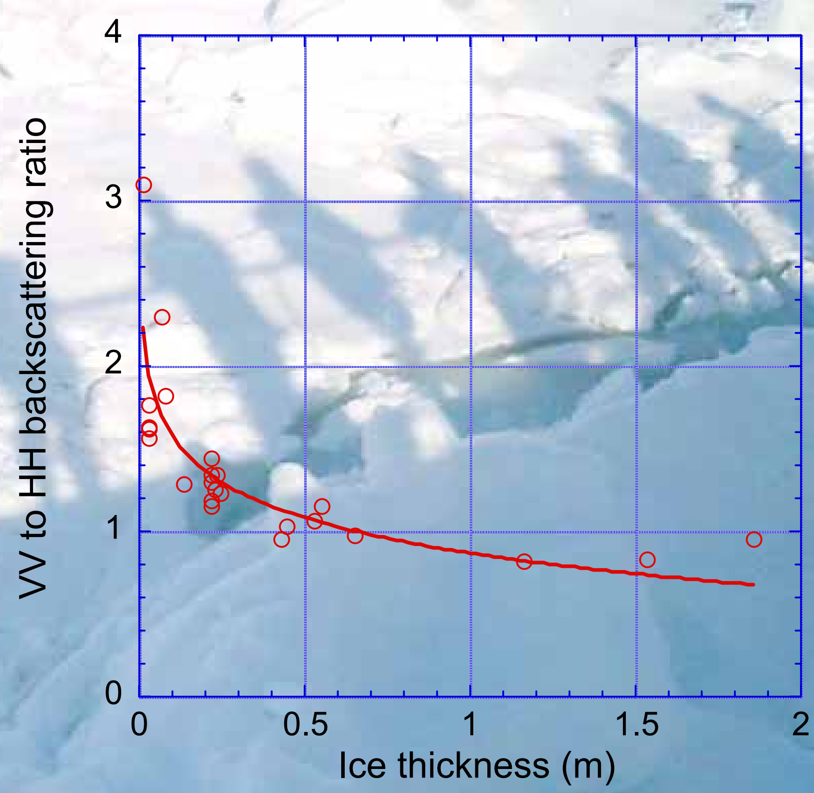

Wakabayashi,H et al., 2003

Ice thickness map

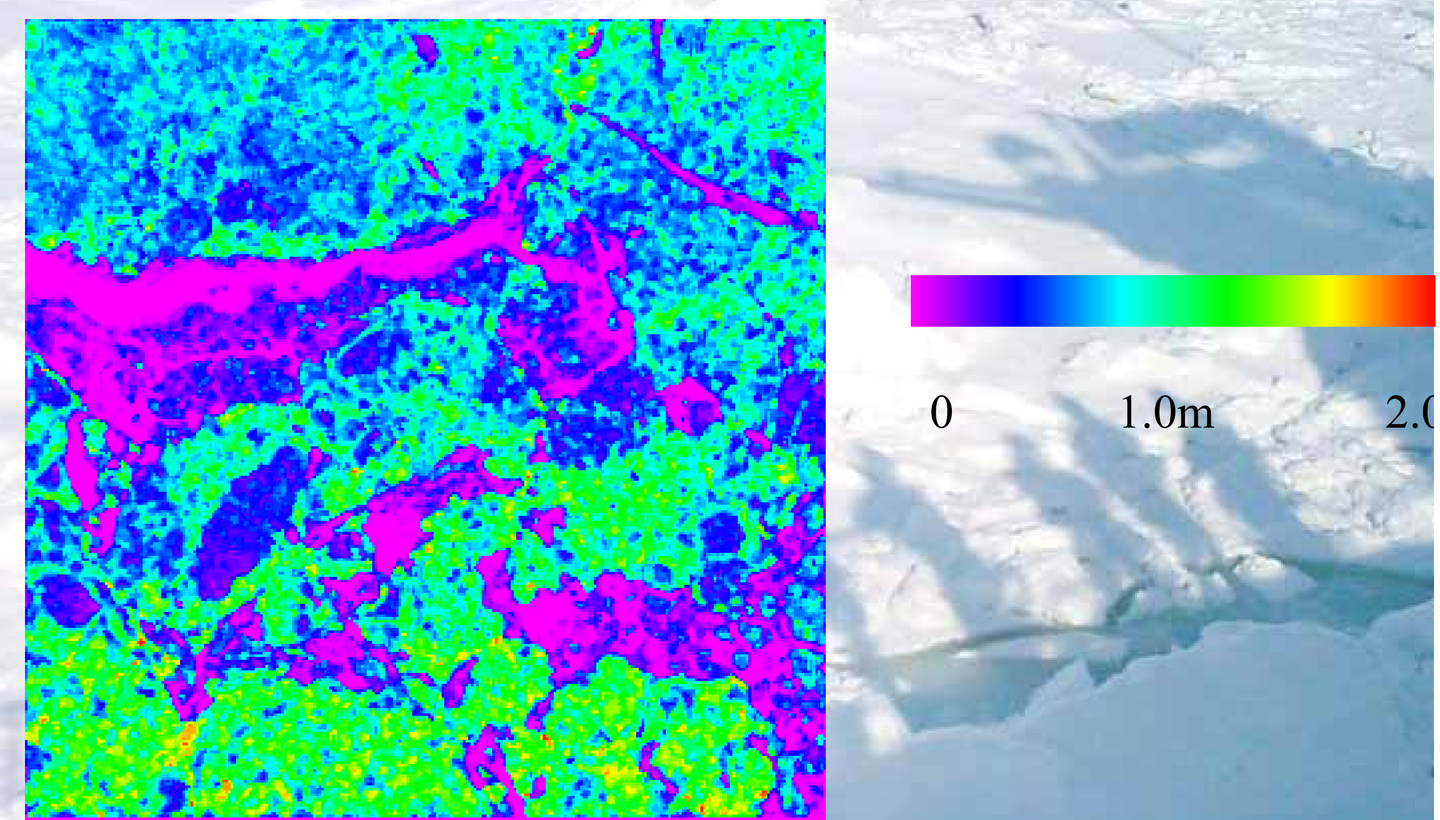

–Ice thickness (presented by Nakamure, et al.:psoter)

- It was possible to estimate the thickness of YI and FYI
- using VV-HH backscattering ratio.

  -> Estimation of ice thickness was possible using both X-band and L-band SAR data.

Summary and Conclusions

- ***AMSR(X) & AMSR/E is an excellent successor to SSM/I.***
- Advantages of AMSR/E includes:
- (a) More accurate ice concentration and better definition of ice edges
  - because of higher resolution and more frequency channels;
- (b) Wider swath and smaller gap around the North Pole;
- (c) Improved masking of ice free ocean; and
- (d) Improved masking of ice free land/ocean boundaries.
- Some disagreements between sensors are apparent but may be largely due to resolution differences and side lobe effects.
- Co-registered and coincident AMSR and MODIS data will provide complemen and more accurate information about the ice cover AMSR(X) can be used to as the accuracy of historical passive microwave data on sea ice.
- The validation of sea ice products from satellite data is very important
- Sea ice thckness could provide the thinner thickness(<30 cm) by passive microwave data
- Acive maicrowave sensor(VV/HH) may provide sea ice thickness(<ca.100cm) maps.
- Sea ice thicckness information & mappins could gives us the changes of ocean-ice-atmosphere, related to global warming


Thank you
ありがとう